Award Number:

W81XWH-09-1-0658

TITLE: New Advanced Technologies in Stem Cell Therapy

PRINCIPAL INVESTIGATOR: Johnny Huard, Ph.D.

CONTRACTING ORGANIZATION: University of Pittsburgh
Pittsburgh, PA 15260

REPORT DATE: November 2014

TYPE OF REPORT: Final

PREPARED FOR:

U.S. Army Medical Research and Materiel Command
Fort Detrick, Maryland 21702-5012

DISTRIBUTION STATEMENT:

Approved for Public Release; Distribution Unlimited

REPORT DOCUMENTATION PAGE

Form Approved
OMB No. 0704-0188

1. REPORT DATE *(DD-MM-YYYY)*	**2. REPORT TYPE**	**3. DATES COVERED** *(From - To)*
November 2014	Final	1 Sep 2009 - 31 Aug 2014

4. TITLE AND SUBTITLE

New Advanced Technologies in Stem Cell Therapy

5a. CONTRACT NUMBER

5b. GRANT NUMBER

W81XWH-09-1-0658

5c. PROGRAM ELEMENT NUMBER

6. AUTHOR(S)

Johnny Huard, Ph.D. – Principle Investigator
PI: SubProject 1
Ira Fox, M.D.
Co-PI: SubProject 2
David Permutter, M.D.
Co-PI: SubProject 2

Email: jhuard@pitt.edu

5d. PROJECT NUMBER

5e. TASK NUMBER

5f. WORK UNIT NUMBER

7. PERFORMING ORGANIZATION NAME(S) AND ADDRESS(ES)

University of Pittsburgh
Bridgeside Point II, Suite 206
450 Technology Drive

8. PERFORMING ORGANIZATION REPORT NUMBER

9. SPONSORING / MONITORING AGENCY NAME(S) AND ADDRESS(ES)

U.S. Army Medical Research and Materiel Command
Fort Detrick, Maryland 21702-5012

10. SPONSOR/MONITOR'S ACRONYM(S)

11. SPONSOR/MONITOR'S REPORT NUMBER(S)

12. DISTRIBUTION / AVAILABILITY STATEMENT
Approved for Public Release; Distribution Unlimited

13. SUPPLEMENTARY NOTES

14. Abstract:

Project 1

Background: We have isolated and characterized a population of skeletal muscle-derived stem cells (MDSCs) that display a greatly improved skeletal and cardiac muscle transplantation capacity when compared to skeletal muscle myoblasts. The MDSCs' ability to withstand oxidative and inflammatory stresses appears to be the single most important factor for their improved transplantation capacity. Although the true origin of MDSCs remains unclear, their high degree of similarity with blood vessel-derived stem cells suggests their potential origin could be from the vascular wall. We have recently isolated two distinct populations of cells from the vasculature of human skeletal muscle known collectively as human skeletal muscle-derived cells (hMDCs). The two populations are myo-endothelial cells and pericytes and both can repair skeletal and cardiac muscles in a more effective manner than myoblasts, as is observed with murine MDSCs.

In the current proposal we intend to evaluate and compare the regeneration capacity of these two hMDC populations after their implantation into the skeletal muscle of immunodeficient/dystrophic (SCID/mdx) mice. We will then investigate the influence that sex has on the regeneration and repair capacity of the hMDCs endowed with the greatest regeneration capacity (either myo-entothelial cells or pericytes). Finally we will investigate the influence that age plays on the regeneration capacity of the cells.

Study Design: We will investigate the effects of cell survival, proliferation, resistance to stress, and neo-angiogenesis on the regeneration capacity of the hMDCs implanted into the skeletal muscle of SCID/mdx mice Since we have observed that female murine MDSCs display an improved transplantation capacity in skeletal muscle when compared to male MDSCs, we will determine the influence that sex has on the hMDCs. Due to the fact that MDSCs isolated from aged mice have a lower skeletal muscle regeneration index than MDSCs isolated from young mice, we will also investigate the influence that donor and host age has on the isolated hMDCs.

Relevance: This project will enable us to further assess the feasibility of using hMDC transplantation to improve the function of skeletal muscle that has been damaged by Duchenne muscular dystrophy (DMD) and other muscle degenerative disorders and injury.

Technical Objective #1: To compare the regeneration capacities of human muscle-derived myo-endo cells and pericytes when implanted in the skeletal muscle of *SCID/mdx* mice and select the optimal cell type to proceed with Technical Objectives 2 and 3.

Hypothesis 1: A differential regeneration capacity will be observed in skeletal muscle of SCID/mdx mice between myo-endo cells and pericytes.

Technical Objective #2: To investigate the influence of sex on the regeneration/repair capacity of the hMDCs implanted in the skeletal muscle of *SCID/mdx* mice.

Hypothesis 2: After implantation into skeletal muscle, the hMDCs cells (myo-endo cells or pericytes) endowed with the highest regenerating potential in skeletal muscle will be influenced by the sex of the donor, due to a differential ability to resist stressful conditions.

Technical Objective #3: To investigate the influence of age on the regeneration/repair capacity of hMDCs implanted in the skeletal muscle of *SCID/mdx* mice.

Hypothesis 3: After implantation into skeletal muscle, the hMDCs cells (myo-endo cells or pericytes) endowed with the highest regenerating potential in skeletal muscle will be influenced by the age of the donor due to a differential ability to induce angiogenesis.

Project 2

Background: Hepatocyte transplantation holds great promise as an alternative to whole organ liver transplantation. Unfortunately, the availability of human hepatocytes is limited. We have shown that functionally normal hepatocytes can be generated from human ES cells (hES). Since human skin fibroblasts can now be genetically modified to produce (iPS) cells with characteristics nearly identical to hES cells, it may be possible to generate hepatocytes from patients using their own cells. We believe the PiZ transgenic mouse model of alpha-1-antitrypsin (AT) deficiency is critical for evaluating the efficacy of stem cell therapies, as hepatocytes without the mutant protein have a selective hepatic repopulation advantage in these mice, and the

PiZ mouse recapitulates the slowly progressing type of disease that affects most patients with chronic liver diseases.

Objective/Hypothesis: Both of the main obstacles to transplantation of stem cells for the treatment of liver disease (the number of livers available and the immunological barrier) might be addressed if liver cells could be generated de novo from precursor cells of the individual to be treated.

Study Design: We will determine the extent to which human patient-specific, inducible pluripotent stem (iPS) cells can be differentiated into primary human hepatocytes. We will then determine the extent to which the PiZ mouse model of AT deficiency can be developed as a platform for pre-clinical testing of hepatic stem cells. Finally, we will identify specific molecules responsible for regenerative and fibrotic signals in the PiZ mouse model of liver disease.

Relevance: This project will determine the extent to which patient-specific hepatic stem cells can be used for regeneration and repair of injuries to the liver and liver failure. A more complete understanding of the mechanisms by which donor stem cells can reduce liver injury and toxin and/or cancer risk should enhance the number of areas where hepatic stem cell transplantation might be effectively applied.

Technical Objective #1: *Determine the extent to which human patient-specific, inducible pluripotent stem (iPS) cells can be differentiated into primary human hepatocytes.*

Hypothesis: Protocols that successfully differentiate mouse and human embryonic stem (ES) cells toward a hepatocyte phenotype will be effective in differentiating human skin cell-derived iPS cells into liver cells.

Technical Objective #2: Determine the extent to which the PiZ mouse model of alpha-1-antitrypsin (AT) deficiency can be developed as a platform for pre-clinical testing of hepatic stem cell transplantation as a treatment for severe liver injury and disease.

Hypothesis: *iPS cells differentiated toward a hepatocyte phenotype can engraft and respond normally to proliferative signals in the livers of PiZ mice.*

Technical Objective #3: Utilize laser-capture microdissection, coupled with high-density oligonucleotide array techniques as well as double-label immunofluorescence techniques to identify specific molecules responsible for regenerative and fibrotic signals in the PiZ mouse model of liver disease.

Hypothesis: *Transplantation of donor stem cells can ameliorate liver injury and cancer risk in liver disease.*

15. SUBJECT TERMS					
Project 1: Duchenne Muscular Dystrophy (DMD), human muscle-derived cells (hMDC), myoendothelial cells, pericytes, hMDC transplantation, angiogenesis Project 2: Hepatacyte transplantation, inducible pluripotent stem (iPS)cells, alpha-1-antitrypsin (AT) deficiency, PiZ mice					
16. SECURITY CLASSIFICATION OF:			**17. LIMITATION OF ABSTRACT**	**18. NUMBER OF PAGES**	**19a. NAME OF RESPONSIBLE PERSON** USAMRMC
a. REPORT	**b. ABSTRACT**	**c. THIS PAGE**			**19b. TELEPHONE NUMBER** *(include area code)*
U	U	U	UU	302	

Standard Form 298 (Rev. 8-98)
Prescribed by ANSI Std. Z39.18

Table of Contents

Final Report
Sub-Project 1: Muscle stem cell transplantation for Duchenne muscular dystrophy
PI: Johnny Huard

INTRODUCTION:

We have isolated and characterized a population of skeletal muscle-derived stem cells (MDSCs) that display an improved skeletal and cardiac muscle repair upon transplantation when compared to skeletal muscle myoblasts. The MDSCs' ability to withstand oxidative and inflammatory stresses appears to be the most important factor for their improved transplantation capacity. Although the true origin of MDSCs remains unclear, their high degree of similarity with blood vessel-derived cells (myo-endothelial and perivascular cells) suggests their potential origin could be from the vascular wall. We have also isolated two distinct populations of cells from the vasculature of human skeletal muscle known collectively as human skeletal muscle-derived cells (hMDCs). The two populations are myoendothelial cells and pericytes and they both can repair skeletal and cardiac muscles in a more effective manner than myoblasts, as is observed with murine MDSCs. In the current proposal we have evaluated and compared the regeneration capacity of these two hMDC populations in vitro and after their implantation into the skeletal muscle of cardiotoxin (ctx) injured immunodeficient mice.

During the last 4 years we were involved with the characterization of 2 populations of hMDCs, myoendothelial cells and pericytes and demonstrated that the myoendothelial cells and pericytes could repair skeletal and cardiac muscle more effectively than myoblasts. As previously reported, several aspects of the first aim of the project were completed, namely the fluorescent-activated cell sorting (FACS) of the myoendothelial cells, pericytes and myoblasts from cryopreserved human progenitor skeletal muscle cells (hPSMCs); comparisons of the *in vitro* myogenic potential of these populations; and the transplantation of the populations into cardiotoxin-injured skeletal muscle of SCID mice to assess their *in vivo* regenerative capacity. The results showed that the myoendothelial cells possessed a better in vitro myogenic differentiation capacity, as well as, a better in vivo engraftment capacity when transplanted into cardiotoxin injured skeletal muscle using an antibody against human spectrin. During the 2nd year of funding we demonstrated on a minimal number of experimental animals that proliferation and myogenic differentiation capacities were greater in the younger experimental animals and that oxidative stress resistance is reduced in MDC's isolated from older individuals. We were also involved with optimizing the media type for MDC expansion and were attempting to identify an optimal dystrophin antibody to use for the in vivo detection of human MDCs in our mouse model of DMD that is also immunocompromised (SCID/mdx). Unfortunately, all but one of the antibodies tested continued to have high levels of background. More importantly was the fact that even after identifying antibodies with reduced background, preliminary studies, where we injected hMDCs into SCID/mdx mice, showed levels of engraftment that were not high. Another tangential study performed during year 3's performance period showed that the immunomodulary properties of MDCs was associated with a reduction in NF-kB/p65 signally and that MDCs with reduced p65 expression could improve the histopathology of a model of DMD that has no dystrophin or utrophin expression, also known as the dKO (double Knock-Out) mouse, when injected IP. The current year's major focus (Year 4) was to continue to determine why we were experiencing the transplantation difficulties with the SCID/mdx mice. It was imperative to determine why the SCID/mdx mice were generating such high levels of background when injected with hMDCs Unfortunately our aged SCID/mdx colony has diminished substantially and we are currently in the process of aging additional mice .We have been aging this colony of mice for 2 years in order to carry out the remaining aims of this grant, which outlined experiments to compare the transplantation efficiency of old and young hMDCs injected into old and young host SCID/mdx animals; however, while continuing to age the mice we will utilize younger SCID/mdx mice and the dKO model that we described in last year's report as well as SCID mice with a ctx injury which we described previously.

Unfortunately, during the extension period in year 5 we still could not acquire reasonable results in the mdx/SCID model. We are not sure if it is the cells, the model or a combination of both that is to blame, the cells simply do not fuse in this xenotransplantation model. Since fusion was our readout on the successful regenerative ability of the cells and fusion was minimal at best with all the cell types tested, we could not

perform the proposed investigations to compare sex and age differences of the cells in vivo. We did however, explore several tangential projects that afforded us with some very interesting results and are described below for our extension in year 5.

BODY:

Statement of Work:
Technical Objective #1: To compare the regeneration capacities of human muscle-derived myoendothelial cells and pericytes when implanted in the skeletal muscle of dystrophic mice and select the optimal cell type to proceed with Technical Objectives 2 and 3.
Hypothesis 1: A differential regeneration capacity will be observed in the skeletal muscle of SCID/mdx mice between myoendothelial cells and pericytes.
Technical Objective #2: To investigate the influence of sex on the regeneration/repair capacity of the hMDCs implanted in the skeletal muscle of dystrophic mice.
Hypothesis 2: After implantation into skeletal muscle, the hMDCs cells endowed with the highest regenerating potential in skeletal muscle will be influenced by the sex of the donor, due to a differential ability to resist stressful conditions.
Technical Objective #3: To investigate the influence of age on the regeneration/repair capacity of hMDCs implanted in the skeletal muscle of dystrophic mice.
Hypothesis 3: After implantation into skeletal muscle, the hMDCs cells endowed with the highest regenerating potential in skeletal muscle will be influenced by the age of the donor due to a differential ability to induce angiogenesis.

Progress made from 9-1-13 to 8-31-14

The role of non-myogenic mesenchymal stem cells (nmMSCs) in the skeletal muscle pathology of muscular dystrophy

Adult skeletal muscle possesses a remarkable regenerative ability which largely depends on satellite cells. However, in severe muscular dystrophies, such as Duchenne muscular dystrophy (DMD), skeletal muscle integrity is debilitated and is often replaced by a mix of fibrous tissue and white adipocytes undergoing a process termed fatty degeneration. In recent publications, it was demonstrated that 6-8 wks old utrophin/dystrophin double knockout (dKO) mice, a severe animal model of DMD, have an excess of ectopic fat, calcium deposits and fibrosis accumulation/infiltration in the skeletal muscle which coincides with progressive muscle wasting and degeneration. These ectopic non-muscle tissues in skeletal muscle alter the tissue environment and induce deregulation of muscle homeostasis; however, the cellular origin of muscle fat formation is still unclear. Based on a previously published preplate technique, we isolated two types of muscle derived cells; PDGFRα+ mesenchymal stem cells (nmMSCs) and Pax7+ myogenic muscle derived stem cells (MDSCs) from the skeletal muscle of dKO mice. Previously, we showed that compared to MDSCs isolated from dKO mice, nmMSCs displayed significantly increased proliferation and adipogenic and osteogenic potentials *in vitro* and suggested nmMSCs as a major contributor to ectopic fat cell, calcium deposits and fibrotic tissue formation within dystrophic muscle. In the current study, we propose that nmMSCs may play an important role in regeneration/degeneration of dKO muscle. We observed significantly increased numbers of endogenous proliferating Ki67+ nmMSCs in the skeletal muscle of the dKO mice compared to age-matched wild-type (WT) mice. We investigated the possibility of cross-talk between the MDSCs and nmMSCs using a co-culture assay and demonstrated that the limited myogenic potential of the dKO-MDSCs was further reduced when they were co-cultured with dKO-nmMSCs. In addition, we observed a reduction in the expression of genes that regulate myogenesis in the dKO-MDSCs co-cultured with nmMSCs. On the other hand, myogenic

differentiation of dKO-MDSCs was significantly enhanced after co-culturing them with WT-nmMSCs. qRT-PCR analysis of secreted frizzled-related protein 1 (sFRP1), a known inhibitor of myoblast differentiation, from 6wks old WT- and dKO –nmMSCs indicated that the sFRP1 expression was significantly increased in dKO-nmMSCs compared to that of WT-nmMSCs. Taken together, we propose the hypothesis that signals originating from nmMSCs may contribute to the micro-environment limiting myogenic differentiation of MDSCs in dKO muscle and sFRP1 may be a soluble mediator of functional interaction between MDSCs and nmMSCs. Results from this study could provide insight into new approaches to alleviate muscle weakness and wasting in DMD patients by inhibiting the proliferation of nmMSCs in dystrophic muscle.

METHODS:

Cell Isolation: Cells were isolated from dKO (dys-/-utro-/-) mice at 6 weeks of age, as previously described via a modified preplate technique [1]. After 2hrs, the nmMSCs were obtained while the MDSCs were obtained after 7 days. Both cells were cultured in proliferation medium (PM, DMEM supplemented with 10% fetal bovine serum, 10% horse serum, 0.5% chicken embryo extract and 1% penicillin-streptomycin).

Immunofluorescence and histology: Cryosections were fixed with 5% formalin for 8 minutes and blocked with 10% donkey serum for 1 hour. Slides were then incubated with rabbit anti-mouse Ki67 (1:200, Abcam) and goat anti PDGFRα (1:100, R&D) in 5% donkey serum. Next, sections were incubated with secondary antibodies including 594-conjugated anti-rabbit IgG (1:300, Invitrogen) and 488-conjugated anti-goat IgG (1:300, Invitrogen) in PBS for 45 minutes.

Co-culture assay: 10,000 dKO-MDSCs were plated in the lower compartment of Transwell Permeable Supports and 10,000 WT/dKO-nmMSCs were seeded into transwell inserts in PM media. To measure the differentiation potential of dKO-MDSCs 48 hours after co-culture, PM media was switched to differentiation media (DMEM medium supplemented with 2% FBS) for 3 days. Three days after differentiation, cells were fixed with 10% formalin for 8 min, and stained for fast myosin heavy chain (fMyHC) using a mouse anti-MyCHf antibody (1:250, M4276, Sigma-Aldrich) with a mouse-on-mouse (M.O.M) staining kit (Vector Labs, Burlingame, CA), according to the manufacturer's protocol.

mRNA analysis was performed via reverse transcriptase, real-time (RT-PCR): Total RNA was obtained from WT- and dKO-nmMSCs using TRizol reagent (Invitrogen) and a RNeasy Mini Kit (Qiagen, Valencia, CA) according to the manufacturer's instructions. Reverse transcription was performed using a Maxima first strand cDNA synthesis kit (Fermentas) according to the manufacturer's protocol. PCR reactions were performed using an iCycler Thermal Cycler (Bio-Rad) as previously described. RT-PCR was carried out using the Maxima Syber Green Assay kit (Thermo Scientific) with an iQ5 thermocycler (Bio Rad).

RESULTS:

Increased in vivo proliferation potential of nmMSCs isolated from old dKO mice. We examined the proliferation of nmMSCs *in vivo* and performed immunohistochemistry for PDGFRα and Ki67 in the gastrocnemius of 6wk old WT and dKO mice. PDGFRα^{+} nmMSCs were localized in the interstitial space between muscle fibers of skeletal muscle. Our results indicated that the number of PDGFRα^{+}Ki67^{+} nmMSCs was about 3 fold higher in the dKO skeletal muscle when compared to age-matched WT muscles (**Figure 1**).

Figure 1

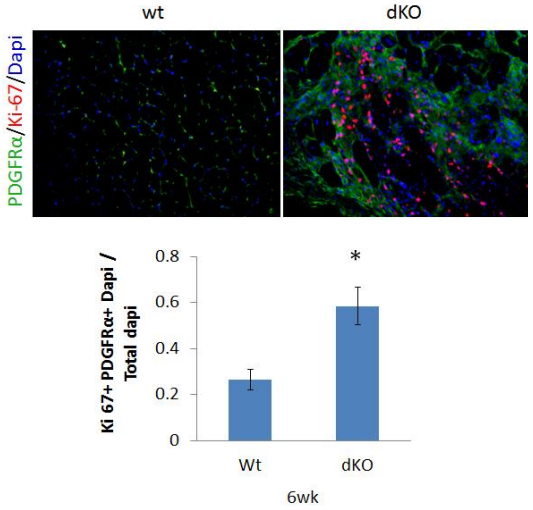

Immunohistochemistry for PDGFRα (green) and Ki-67 (Red) in the skeletal muscle of 6wks old WT and dKO mice (Top). Quantification indicated by the ratio of PDGFRα and Ki67 expressing Dapi to total Dapi counts (Bottom) (* $p<0.005$).

dKO-nmMSCs may inhibit myofiber regeneration of MDSCs in dKO mice. MDSCs isolated from 6-8 wks old dKO mice were co-cultured with age-matched dKO-nmMSCs, using a transwell system and the fusion index of dKO- MDSCs was monitored and compared to that of dKO-MDSCs cultivated alone. We observed that the limited myogenic potential of the dKO-MDSCs was further exacerbated after co-culture with dKO-nmMSCs. fMyHC expressing myotubes were significantly decreased when dKO-MDSCs were cultured in the presence of dKO-nmMSCs compared to dKO-MDSCs alone. When dKO-MDSCs were co-cultured with WT-nmMSCs, the myogenic potential of dKO-MDSCs was significantly enhanced (**Figure 2**).

Figure 2

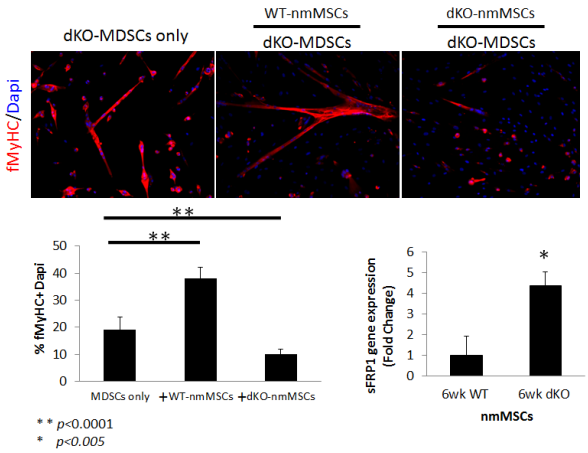

* * $p<0.0001$
* $p<0.005$

dKO-MDSCs and WT-/dKO-nmMSCs were co-cultivated using collagen type 1 coated transwell insert for myogenic differentiation. Immunohistochemistry of fMyHC was performed for detection of myotube formation (Top). Quantification of percentage myotube formation of dKO-MDSCs after 3 days of myogenic differentiation with/without Wt-/dKO-nmMSCs co-cultivation (Bottom left). qRT-PCR analysis was performed and the sFRP1 expression was compared from WT- and dKO-nmMSCs isolated from 6wks old animals (Bottom right).

Increased sFRP1 gene expression in dKO-nmMSCs. Using qRT-PCR, we observed 6 folds increase in the expression of sFRP1 in the dKO-nmMSCs compared to that of WT-nmMSCs.

DISCUSSION:

Previously, we observed accumulation of lipids, ectopic calcium deposits, and fibrotic tissue in skeletal muscle of 6-8 wks old dKO mice[2]. We have suggested that nmMSCs residing in the skeletal muscle may be responsible for these ectopic non-muscle tissues accumulated in dKO muscle since nmMSCs displayed significantly increased proliferation and adipogenic and osteogenic differentiation potentials *in vitro*. In the current study, we showed that the number of endogenous nmMSCs was significantly increased in 6wks old dKO skeletal muscle compared to age-matched WT, suggesting that nmMSCs may have a role in muscle regeneration/degeneration in dKO mice. A co-culture assay demonstrated that dKO-nmMSCs further exacerbate the limited myogenic differentiation potential of dKO-MDSCs, while WT-nmMSCs enhanced myogenesis of dKO-MDSCs. A significantly increased gene expression level of sFRP1, which is known to block myoblast differentiation[3], was observed in dKO-nmMSCs compared to WT-nmMSCs suggested that sFRP1 secreted from dKO-nmMSCs may play a role in limiting the myogenic potential of dKO-MDSCs.

Despite the fact that the underlying pathogenesis in DMD is well studied, DMD remains a very difficult disease to treat. In DMD, the accumulation of intramuscular fat, calcium deposits, and fibrotic tissue represent the hallmarks of advanced disease and the presence of this non-muscle tissue significantly affects muscle structure, function, and recovery. Previously, we showed that nmMSCs may be responsible for the accumulation of lipid, calcium deposits, and fibrotic tissue in dKO mice. In this study, we suggest that cells responsible for forming adipocytes and ectopic bone in dystrophic muscle may also inhibit the myogenic potential of muscle progenitor cells, including MDSCs, hindering muscle regeneration. Results from this study could provide insight into new approaches to alleviate muscle weakness and wasting in DMD patients by inhibiting the proliferation of nmMSCs in dystrophic muscle.

Interaction between myogenic and non-myogenic progenitor cells during muscle regeneration

Efficient muscle regeneration is dependent on the coordinated responses of multiple cell types. During the muscle healing process, muscle progenitor cells (MPCs) are activated and an expanding population of myoblasts interact with inflammatory and stromal cells. It seems likely that these interactions are important for

regulating their activity. The role of inflammatory cells in muscle regeneration has been reported [1]; however, there is little known about the contributions of other tissue-resident cell populations. By using the preplate technique we are able to isolate different populations of cells from skeletal muscle based on their variable adhering capacities. A slowly adhering fraction of cells (PP6) contains a heterogeneous population of stem and progenitor cells that display high myogenic potential [2]. In this study, we characterized a rapidly adhering cell population (PP1) that has a poor myogenic capacity and found that they express markers of fibro/adipogenic progenitor (FAPs) cells and mesenchymal stem cell (MSCs) including: Platelet-Derived Growth Factor Receptors (PDGFR), CD34, CD90, CD105 and Sca-1. Interestingly, when PP6 cells are cultured in PP1 differentiation condition medium (DCM), i.e. medium supplemented with 2%FBS in which the PP1 cells have been allowed to grow in for 3 days, the myogenic potential of the PP6 cells significantly increased. Furthermore the PP1 cells promoted muscle regeneration when transplanted along with the PP6 cells into the dystrophic muscle of MDX/SCID mice. Our results suggested that interactions between resident muscle mesenchymal stem cell like cells (PP1) and muscle progenitor cells (PP6), contribute to efficient muscle regeneration, thus combining both cell types could be used as a potential clinical strategy for the treatment of muscle diseases.

Methods

Cell Isolation: PP1 and PP6 cells were isolated from C57BL/10J at 3-6 week of age, as previously described via a modified preplate technique[3].

DCM collection: $6x10^5$ of PP1cells were cultured with proliferation medium for 3 days, and then, switch to fusion medium (DMEM containing 2% FBS). Three days later the medium was collected.

Myogenic differentiation assay: The myogenic differentiation capacity of the PP6 cells was assessed by switching the proliferation medium into fusion medium. After 3 days, the cells were stained for fast myosin heavy chain (MyHCf). Myogenic differentiation levels were quantified as the percentage of the number of nuclei in MyHC positive myotubes relative to the total number of nuclei.

Pax7 staining and flow cytometry cell analyses: A MOM kit was used for Pax7 staining following the manufacturer's protocol. Flow cytometry was used to analyze the expression of PDGFR and CD34, The cell suspension was divided into equal aliquots and centrifuged, and then re-suspended in a 1:10 dilution of mouse serum in PBS, and incubated for 10 minutes. FITC-conjugated rat anti-CD34, PE-conjugated rat anti-PDGFR was added and incubated an additional 30 minutes. Just before analysis, propidium iodide was added for dead cell exclusion and live cell events were collected and analyzed.

Cell implantation and dystrophin staining*:* A total of 3×10^5 PP6 cells alone were injected into the left gastrocnemius muscles (GM) and 3×10^5 PP1 cells + 3×10^5 PP6 cells were injected into the right GM of 8 week-old MDX/SCID mice. The PP1cells were labeled with red fluorescent dye before injection. Two weeks after implantation, the mice were sacrificed and the GM muscles were harvested and sectioned. Cryosections were fixed with 5% formalin and blocked with 5% donkey serum in PBS for 1 hour, then incubated with rabbit anti-dystrophin (1:300) for 2 hours at RT. The sections were exposed to a secondary 594-conjugated anti-rabbit IgG (1:500) for 30 minutes. The nuclei were revealed by DAPI staining.

Figure 3

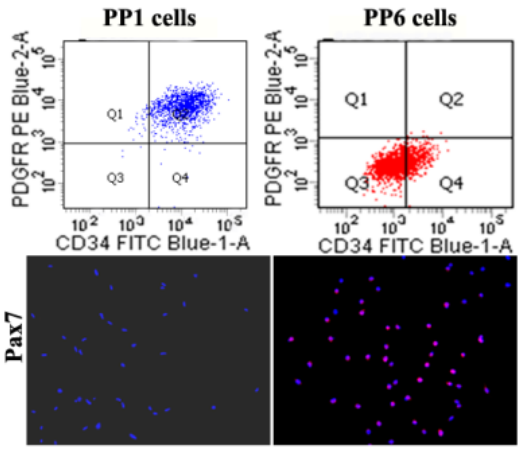

Results ***PP1 and PP6 expressed different cell markers:*** To identify progenitor lineages from dissociated skeletal muscle, we used flow cytometry to detect PDGFR and CD34, which is expressed by FAPs, and immuno-staining to detect the muscle progenitor cell marker Pax7. The data from flow cytometry showed that the PP1 cells are highly PDGFR and CD34 positive while the PP6 cells were PDGFR negative (**Fig. 3**). The PP1 cells also expressed several MSC markers including CD105, CD90 and Sca-1(data not shown). Immuno-staining data showed PP6 cells were highly Pax7 positive, while PP1 cells were Pax7 negative (**Fig. 3**). These

results suggest that the preplate technique is able to prospectively identify myogenic progenitors (PP6) and mesenchymal like cells (PP1).

Figure 4

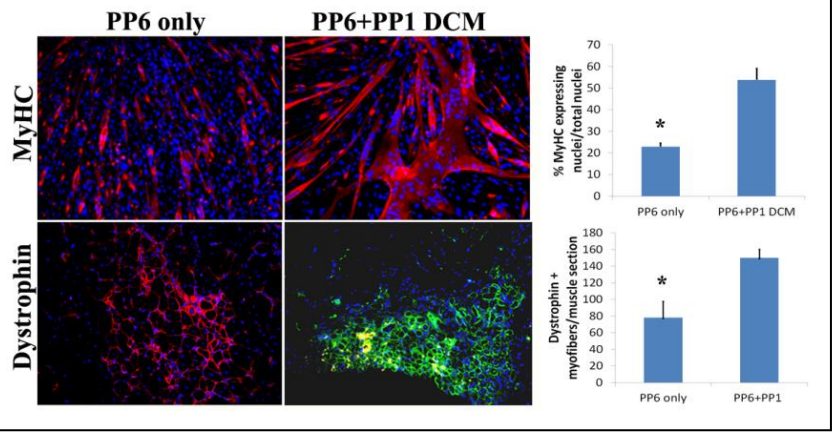

PP1 cells promote the myogenic differentiation of PP6 cells in vitro and muscle regeneration in vivo: After the PP6 cells were cultured in PP1 DCM, MyHC staining demonstrated that a greater number of cells fused and formed significantly larger myotubes in the PP6 cultures grown in the DCM compared to control group that were grown in non-DCM fusion medium **(Fig. 4**). To determine whether combing PP1 and PP6 cells would increase the engraftment and muscle regenerative capacity of PP6 cells, we intramuscularly implanted a combination of both cell populations into an immunocompromised model of Duchenne muscular dystrophy. In this *in vivo* study, we observed that significantly more dystrophin-positive myofibers were detected in the muscles injected with PP1 and PP6 together (dystrophin, green, **Fig. 4**, PP1 cells were labeled with red fluorescent dye) than in the muscles injected with PP6 only (dystrophin, red, **Fig. 4)**, and the injection of PP1 cells resulted in no dystrophin positive fibers, which indicates that PP1 cells enhanced the muscle regenerative potential of the PP6 cells *in vivo*.

Discussion

Muscle regeneration requires the coordinated interaction of multiple cell types. Pax7 expressing MPCs have been implicated as the primary stem cell responsible for regenerating muscle, yet the interaction with other progenitor cells for muscle regeneration has not been evaluated. It has been reported that satellite cells, connective tissue fibroblasts and their interactions are crucial for muscle regeneration[4]. Here we describe that the preplate technique can be used for isolating different populations of muscle-resident progenitor cells. We identified mesenchymal like cells (PP1) and muscle progenitor cells (PP6), based on their specific markers and examined the interaction between these two cell populations. We found *in vitro* that PP6 cells cultured in the presence of PP1 DCM formed larger, more multinucleated myotubes than PP6 cells cultured in unconditioned differentiation medium. In addition, transplantation of PP6 and PP1 together increased dystrophin positive fibers in dystrophic muscle compared to the transplantation of PP6 alone. Our experiments demonstrated that PP1 cells promoted the myogenic differentiation of PP6 cells *in vitro* and muscle regeneration *in vivo*. Future studies will be conducted to further investigate what is being secreted by the PP1 cells that promote the myogenic potential of PP6 cells.

Our findings strongly support a key role for PP1 cells in supporting myogenesis, suggesting that successful muscle regeneration requires the concerted action of multiple cell types.

Mimicking the stem cell niche in diseased muscle by Notch activation

As a follow-up to work performed the previous year we continued our studies regarding the inhibition of stem cell depletion in the skeletal muscle of mdx/SCID mice. The depletion of functional muscle stem cells has been observed in both aged and diseased skeletal muscle (i.e., Duchenne Muscular Dystrophy/DMD) (1-3). Stem cell therapy has been widely studied for the treatment of different muscle diseases, but is still challenged by poor donor cell survival and self-renewal, limited engraftment, frequent fibrogenesis, and importantly, the rapid loss of their stem cell characteristics (stemness) during expansion. The stem cell niche in skeletal muscle is a nest of quiescent stem cells that is critical for maintaining the stemness of stem cells and a key molecular signature of

the stem cell niche is activated Notch signaling, which prevents the early terminal differentiation of muscle stem cells (4-5). Importantly, Notch is critical for the potent regeneration potential of younger skeletal muscle and declines during muscle aging (6).

We hypothesized that the implantation of a biomaterial conjugated with a Notch activator (DLL1, a Notch ligand) could establish an artificial stem cell niche within diseased or aged skeletal muscle that could supply a self-renewable source of stem cells (**Figure 5)**. We posited that the DLL1 (a Notch activating ligand)-conjugated PCL (polycaprolactone, a biodegradable material for tissue engineering (7)) construct would lead to the sustained maintenance of the "stem cell niche-like" microenvironment for the seeded stem cells by improving their self-renewal and survival capacities through the anti-apoptotic effect of Notch, while maintaining the cells' stemness. Thus we believed that the transplanted stem cells would be more capable of migrating from the transplantation site prior to differentiating, which would result in the generation of a larger engraftment area.

Figure 5

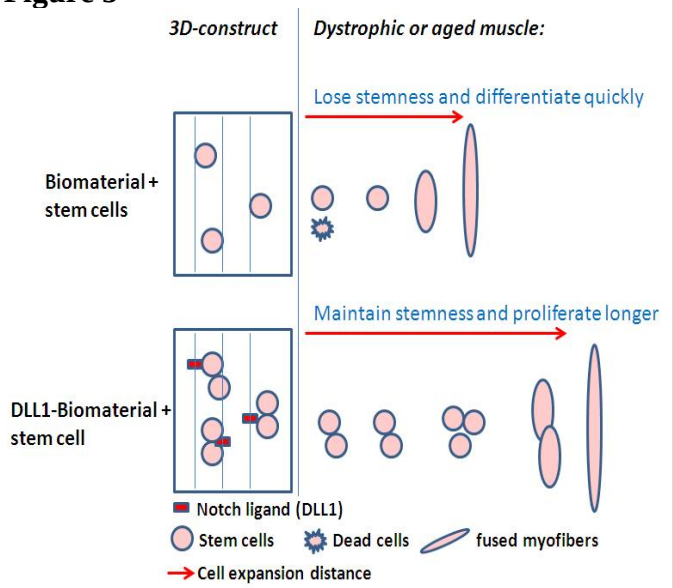

Results:

1. DLL1 treatment of muscle stem cells exhibited increased proliferation and delayed myogenic differentiation. GFP-labeled MDSCs were treated with a recombinant DLL1 protein [DLL1 (mouse): Fc (human), *Adipogen*] (200ng/mL) for 3 days. The proliferation potential of the MDSCs was found to be increased and myogenesis potential of the cells was decreased.

2. MDSCs seeded in DLL1-conjugated PCL showed an accelerated proliferation rate compared to the MDSCs in the control PCL

GFP labeled MDSCs were seeded into the DLL-conjugated PCL or control PCL constructs and cultured in medium. At day 3, after cell seeding, there was a clear increase in the number of GFP-MDSCs observed in the DLL1-conjugated PCL.

3. Implantation of MDSC-seeded DLL1-congugated PCL into mdx/SCID mice resulted in improved muscle engraftment.

Ten days after the implantation of MDSC-seeded DLL1-congugated PCL or MDSC-seeded control PCL, there were more GFP+ cells in the DLL1 group, indicating an improvement in the proliferation of the implanted stem cells. There were also more dystrophin+ myofibers, indicating an improvement in muscle regeneration.

Discussion:

In the current study, the stem cell regulatory mechanism of the stem cell niche in the skeletal muscle was mimicked by conjugating activated Notch signaling into a 3D construct used for stem cell transplantation. With this system, we were able to improve the outcome of stem cell transplantation, in the dystrophic skeletal muscle of dKO mice, through the optimization of the stem cell microenviroment.

Progress made from 9-1-12 to 8-31-13

Below is outlined the progress that we made last year in an attempt to work out the difficulties we have been experiencing with the transplantation of our human MDCs into the SCID/mdx model, which was proposed to be utilized as a DMD model to test the transplantation efficiency of several hMDC populations. Besides the proposed human cell types of pericytes and myo-endo cells we utilized human MDCs isolated via the preplate technique, which is a population of cells that is more heterogeneous in nature and contains both the myo-endo

cell and pericyte sub-populations. We also compared these latter three populations to another human cell population isolated from dental pulp and amniotic fluid to determine if the engraftment problems were related to the stem cell type. Moreover we performed a study to see if we could improve the cells transplantation efficiency by activating the Notch signally pathway, which has been described previously to be necessary for maintaining the stem cell niche in skeletal muscle. Finally, in an attempt to further improve engraftment efficiency we grew the cells on a variety of different substrates with varying degrees of surface elasticity to improve their expansion. Below is a summary of our findings.

Human muscle derived stem cells for muscle regeneration:

Isolation of hMDSCs

Human skeletal muscle tissues obtained from 2 male donors (21 and 23 years old) and 2 female donors (30 and 76 years old) were purchased from the National Disease Research Interchange (NDRI). hMDSCs were isolated using our previously described modified pre-plate technique. Cells were seeded at a density of 1000 cell/cm^2, passaged every 3 days and maintained at less than 50% confluence.

Surface marker expression of the preplate isolated hMDSCs

The marker profile of the cells from each donor was analyzed by flow cytometry using anti-human fluorochrome-conjugated antibodies/ligands: CD45-APC-Cy7, CD56-PE-Cy7, CD90-APC, CD146-FITC, UEA-1R-PE, CD44-PE, CD73-PE, CD105-PE.

Stem cell gene expression by the isolated hMDSCs

The expression of stem cell genes POU class 5 homeobox 1 (POU5F1 or OCT4) and the Nanog homeobox (NANOG) and SRY (sex determining region Y)-box 2 (SOX2) were tested using semiquantitative RT-PCR.

Multipotent differentiation capacities of the hMDSCs

hMDSCs were tested for their myogenic, adipogenic, chondrogenic and osteogenic differentiation capacities in vitro.

Construction of Lenti-GFP and hMDSCs transduction to track the fate of the injected cells

We constructed lenti-GFP vector under the control of CMV promoter. Lenti-GFP virus was packaged in GP293T cells. In order to test whether hMDSCs could efficiently regenerate muscle in vivo, we transduced hMDSCs at passage 10 with lenti-GFP virus. The lenti-GFP transduced cells were then subjected to flow cytometry cell sorting for GFP at passage 3 post transduction and further expanded in proliferation medium for in vivo muscle injection.

In vivo muscle regeneration

SCID/mdx mice at 8 weeks were divided into two groups(n=4): Group 1: MDXSCID injected with hMDSCs-lenti-GFP 5×10^5 cells in the gastrocnemius; Group2, MDXSCID mice were first injured with cardiotoxin 30μl(4μM), 24 hrs later, 5×10^5 hMDSCs-lenti-GFP cells were injected into the same gastrocnemius muscle that was injured with cardiotoxin(CTX). Mice were sacrificed at 14days after injection, gastrocnemius muscle were dissected and snap frozen in 2-methyle-butane that was precooled in liquid nitrogen. Crysections were performed and immunofluorescent staining of dystrophin-GFP and fMHC-GFP were performed.

Results

Characterization of hMDSCshMDSCs isolated by a modified pre-plate technique were characterized by flow cytometry for several cell lineage markers, including CD45 (leukocytes/hematopoietic cells), CD56 (myogenic cells), *Ulex europaeus agglutinin I receptor* (UEA-1R, endothelial cells), CD146 (pericytes/endothelial cells) as well as classic mesenchymal stem/stromal cell (MSC) markers: CD44, CD73, CD90, and CD105. We found that hMDSCs robustly expressed CD56, CD146, and four MSC markers (more than 99% positive) but not CD45 or UEA-1R (**Fig. 1A**). Quantitative analysis revealed a consistent marker expression profile in all the hMDSC populations examined (**Fig.1B**). RT-PCR results revealed that cells from all donors expressed the stem cell markers OCT4 and NANOG, while cells from two of the donors (23 y/o male and 76 y/o female) slightly expressed SOX-2 (**Fig.1C**). In vitro differentiation assays indicated that the hMDSCs could undergo

adipogenic, chondrogenic, osteogenic and myogenic differentiation as shown by oil red O staining, Alcian blue staining, von Kossa staining and fMHC and desmin immunofluorescence respectively (**Fig. 1D**).

Lenti-GFP transduction efficiency

The transduction efficiency of lenti-GFP was approximately 85%. After GFP sorting, the GFP positive cells were approximately 95-99%. Some cells lost GFP over time; however, the majority of the cells maintained GFP transgene expression during cell expansion (Figure 2A).

hMDSCs engrafted in the skeletal muscle of SCID/mdx mice

Our results showed no dystrophin–GFP double positive fibers or fMHC –GFP double positive fibers; however, we did find GFP positive central nucleated muscle fibers along the GFP positive hMDC clusters in both the non-injury and CTX injured groups. There were no statistical differences in the number of central nucleated muscle fibers between the groups. We therefore conclude, as we have in the past experiments, that the hMDCs could engraft in the SCID/mdx mice but only minimal muscle regeneration was observed (**Figure 2B**).

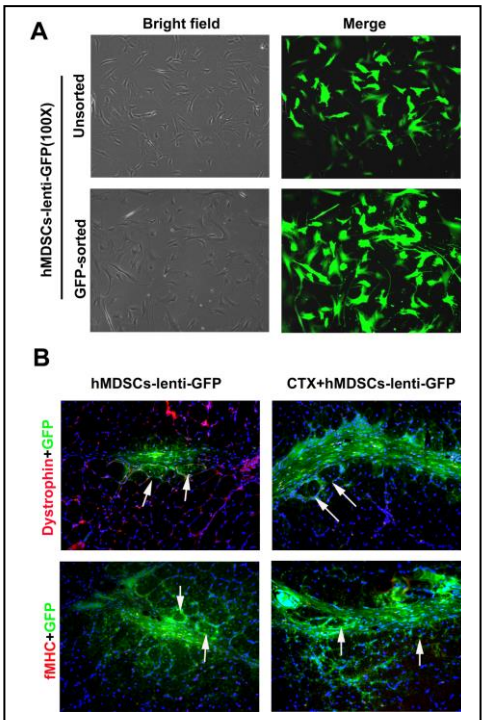

Figure 2: A. Lenti-GFP transduction efficiency. B. hMDSCs fused with very few muscle fibers two weeks after gastrocnemius injection in either non-injured or carditoxin injured dystrophic muscle. We did not find any dystrophin-GFP double positive cells or fast myosin heavy chain double positive cells. We did find very few central nucleated GFP positive cells near the GFP positive cell clusters in the injection site (white arrows). All pictures were taken at 200X magnification.

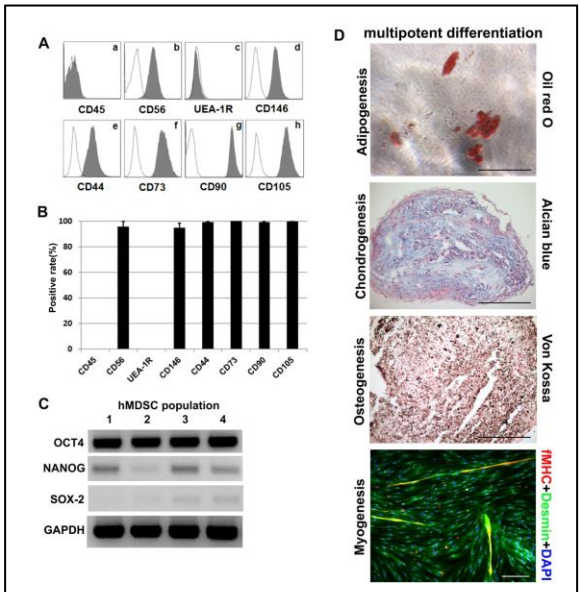

Figure 1: Characterization of the hMDSCs. **A.** Flow cytometry analysis of hMDSC surface markers revealed robust expression of CD56, CD146, CD44, CD73, CD90, CD105 but not CD45 or UEA-1R. **B.** Quantification of cell lineage marker expression in hMDSCs from 4 donors demonstrated consistency in their cell marker expression profiles. **C.** RT-PCR results of stem cell markers. Cells from each donor expressed the stem cell markers OCT4 and NANOG, but only faint expression of SOX-2 was detected in cells from two donors (3 and 4). D. Multipotent differentiation of hMDSCs. hMDSCs undergo adipogenesis(oil red staining), chondrogenesis(Alcian blue staining), osteogenesis (von Kossa staining) and myogenesis as shown by fMHC and desmin immunofluoresence. Scale bars represent 200µm.

Conclusion

We found that the hMDCs isolated by the preplate technique expressed mesenchymal stem cell markers CD73, CD90, CD105 and CD44. They also uniquely expressed the myogenic marker CD56 and the pericyte marker CD146. As they could undergo adipogenic, chondrogenic, osteogenic and myogenic differentiation, we speculate that they are mesenchymal stem cells of muscle origin. The in vivo results indicated that they could engraft within the muscle; however, their regeneration capacities were low. Therefore, the co-injection of myogenic growth factors or ex vivo enhancing myogenic transcription factors or other cellular enhancement protocols are perhaps required to increase the muscle regeneration capacity of the hMDCs within this model of DMD.

Enhanced myogenic potential of human dental pulp and amniotic fluid stem cells by use of a demethylation agent and conditioned media.

Duchenne muscular dystrophy (DMD) is a X-linked genetic disease that is caused by a lack of dystrophin which results in severe muscle degeneration and leads to early death by the mid-twenties. Cell therapy can be used to reintroduce dystrophin to repair damaged muscle fibers. Human dental pulp (hDPSCs) and amniotic fluid stem cells (hAFSCs) may represent alternative cell sources that are less controversial than the use of embryonic stem cells. HDPSCs can be isolated from the adult

human dental pulp of the third molars during routine extraction. HAFSCs, represent 1% of the cells in human amniocentesis specimens and can be isolated by immunoselection of the c-Kit (CD117) antigen positive population via magnetic cell sorting (MACS). HDPSCs and hAFSCs have been shown to possess self-renewal and multipotent capacities (1,2); therefore, they may represent promising cell populations for developing therapies for treating DMD. This study evaluated the myogenic potential of hDPSCs and hAFSCs using different conditions which optimized the most effective protocol to differentiate the cells towards a myogenic lineage.

Human DPSCs were isolated as described by Riccio et al (3). The STRO-1+ DPSC population was obtained by magnetic cell sorting. AFSCs were isolated as previously described by De Coppi et al (2): hAFSCs cultures, from supernumerary amniocentesis specimens, were subjected to c-Kit immuno-selection by MACS technology.
To test the ability of hAFSCs and hDPSCs to form new myotubes, the cells were differentiated in a direct co-culture system with C2C12 myoblasts. Human cells and C2C12 cells, seeded at a 10:1 ratio, were maintained in proliferation medium (PM: DMEM High Glucose + 10% FBS) until confluent, the medium was then replaced with fusion medium (FM: DMEM High Glucose + 1% FBS + 10nM insulin).
To evaluate whether hAFSCs and hDPSCs could be committed to the myogenic lineage, cells were seeded at 3000 cells/cm2 in PM until confluent. Subsequently, the medium was replaced with low serum differentiation medium supplemented with 10µM 5-Aza-2'-deoxycytidine (5-Aza) for 24 hours, to induce DNA demethylation. After removing 5-Aza, medium was replaced with low serum differentiation medium (fusion medium) supplemented with 10 nM insulin. Cells were differentiated in a) low serum medium plus 10 nM insulin and b) pre-filtered conditioned FM from the C2C12 culture + fresh differentiation medium + 10 nM insulin.
To determine myogenic differentiation, staining for human Nuclei (huNu) and myosin heavy chain (MyHC) was performed. Myogenic differentiation after demethylation was verified by myogenin and MyHC immune-fluorescent (IF) staining. Human cells were processed for IF staining as previously described (3).

Figure 3

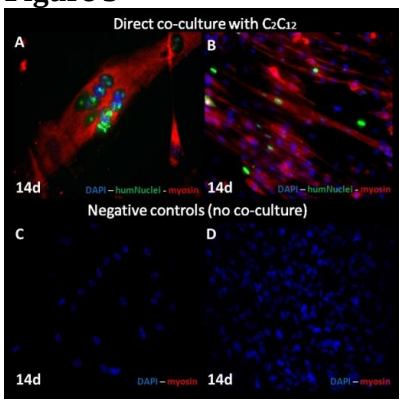

When differentiated in direct co-culture with C2C12 cells, human AFSCs and DPSCs were able to undergo myogenic differentiation, as demonstrated by the positive staining of the myotubes with anti-huNu ab (**Fig. 3A-B**). Human cells which were not co-cultured with C2C12 did not undergo myogenic differentiation and did not fuse in myotubes (**Fig. 3C-D**).

Data from the IF analysis of myogenic differentiation after treatment with 10µM 5-Aza showed that hAFSCs are driven toward a myogenic lineage and express myogenin, a myogenic differentiation marker, after 14 days of differentiation (**Fig. 4A**), while the hDPSCs underwent myogenic differentiation expressing myogenin after 21 days of differentiation under the same conditions (**Fig. 4C**). Moreover, some hAFSCs also showed positive staining for MyHC (**Fig. 4B**).

Immunofluorescence labeling also showed that when conditioned medium from the differentiating C2C12 cells was added to fresh myogenic medium, the human cells pre-treated with 5-Aza started to express myogenin after 14 and 21 days of differentiation (**Fig. 4D-4F**) respectively. Furthermore, some of the hAFSCs also showed positive staining for MyHC (**Fig. 4E**). Cells not

Figure 4

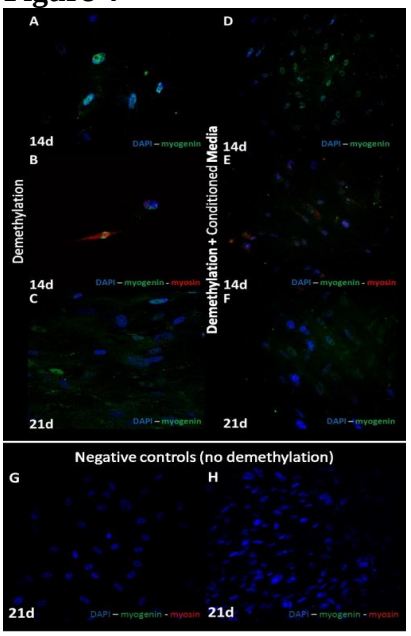

demethylated demonstrated no positive staining for muscle specific markers (**Fig. 4G-H**).

Figure 5

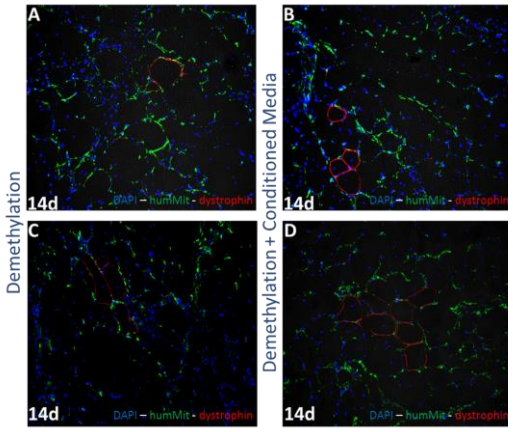

In vitro pre-differentiated hDPSCs and hAFSCs were injected into the gastrocnemius muscles of 8-10 week old SCID/mdx mice. The muscles were harvested 14 days after injection, snap frozen in liquid N2 and cryosectioned. Immunofluorescent labeling of muscle cryosections using an anti-human mitochondrial (humMit) antibody showed engraftment by both the hDPSCs (**Fig.5A-B**) and hAFSCs (**Fig.5C-D**). Interestingly, the double IF staining of humMit and dystrophin revealed the presence of human cells in some dystrophin-positive muscle fibers, as shown in **Fig.5.**

The IF image data in this study demonstrated that the hAFSCs and hDPSCs stem cell populations could actively participate in the formation of myotubes. These human cells were capable of fusing with murine C2C12, as demonstrated by the positive IF staining of the multi-nucleated cells to anti-huNu ab. These results showed the potential of these cells for skeletal muscle repair.

This study demonstrated that demethylation treatment could effectively induce a myogenic commitment of hAFSCs and hDPSCs, in two different conditions, as shown by IF staining: hAFSCs underwent myogenic differentiation earlier than hDPSCs, and reached a more mature differentiation status as shown by their expression of MyHC. The *in vivo* results suggest that hAFSCs and hDPSCs represent a potential, non-controversial sources of stem cells that could be very useful for translational strategies to enhance the repair of injured skeletal muscle in DMD patients; however, these cell population were also very limited in their ability to engraft and produce human dystrophin in the SCID/mdx model as was observed with the myo-endo and pericyte populations indicated that the poor expression of dystrophin is not exclusively a hMDC related phenomenon. This study also demonstrated the utility of demethylation to induce hAFSCs and hDPSCs to differentiate towards the myogenic lineage in vitro and, to a very limited degree, engraft and produce dystrophin. The positive fibers observed were very few and could represent revertant myofibers. We therefore conclude that like the myo-endo, pericytes, and preplate isolated MDCs, the hAFSCs and hDPSCs could engraft but could only participate in myofiber regeneration and dystrophin production to a very limited degree, if at all.

Improving the efficacy of human cell transplantation into dystrophic muscle by activating Notch signaling.

It is believed that optimized mechanisms for the regulation of muscle stem cells are naturally inherent in the stem cell niche in healthy skeletal muscle (7-9). The stem cell niche in skeletal muscle is the nest of quiescent stem cells beneath the basal lamina of myofibers, and is critical for maintaining the stemness and self-renewal of stem cells (7). In diseased or aged skeletal muscle, the proper function of the stem cell niche is impaired, resulting in the loss of the cells' self-renewal and regeneration capacities (7). It is notable that the activation of Notch signaling has been identified as a key molecular signature of the native stem cell niche in skeletal muscle, and is needed for the colonization of stem cells in the niche and asymmetric cell division (10-12). Therefore, we suggested that the transplantation of human muscle cells could be greatly improved by activating Notch signaling in the cells.

Methods:

Mouse model: immune-deficient mdx mice (SCID/mdx, female, 8 weeks old) were used in the study. **Preparation of PCL scaffold:** PCL (polycaprolactone) was prepared and provided by Dr. Jin Gao in Dr. Yadong Wang's lab, according to a procedure described previously.

DLL1 conjugation to PCL: DLL1 (mouse): Fc (human) (rec) (Enzolifesciences) was chemically conjugated with PCL following the procedure previously described by Zhang et al (13). Briefly, aminolysis of PCL was

conducted first and then DLL1 was immobilized to aminated PCL with the help of heterobifunctional crosslinker Sulfosuccinimidyl-4-(*N*-maleimidomethyl) cyclohexane-1-carboxylate (Sulfo-SMCC).

Cell seeding into PCL: Cell seeding was conducted by injecting 0.1 x10^5 human GFP labeled MDCs into the DLL-conjugated PCL or control PCL constructs (a size of around 2 x 2 x1mm) and cultured in medium. Cell suspensions were aspirated in a syringe with a 20G needle and injected into the scaffold once per every 1mm distance. Half of the culture medium was then carefully added to each well and allowed to incubate for 4 hours, prior to adding the remaining half of the medium.

Implantation of Jagged1 treated cells:

Human muscle-derived cells were treated with Jagged1 peptide (CDDYYYGFGCNKFCRPR) (10nM) in proliferation medium for 2 days in vitro, and then injected into the left GM muscles of 8-week old SCID/mdx mice (3x10^5 cells). The same numbers of cells without treatment were injected into the right GM muscles of the same SCID/mdx mice to serve as a control.

Histology and Immunohistochemistry: The frozen skeletal muscles were cryosectioned at a thickness of 10 microns and processed for histological analysis. Expansion and engraftment of muscle stem cells were identified by immuno-staining with antibodies against human lamin A/C and utrophin.

To find out the effect of Notch activation *in vitro*, and to mimick the in vivo growth environment, GFP-labeled human muscle stem cells were seeded in 3D constructs made of PCL (polycaprolactone), which were chemically conjugated with an activating Notch ligand [DLL1 (mouse): Fc (human) (rec)] following a procedure previously described by Zhang et al (13). Specifically, 2 µg DLL1 (mouse): Fc (human) (rec) was dissolved in 50µL of PBS and incubated with Sulf-SMCC treated PCL construct (size: 2 x 2 x 1 mm). Cell seeding was conducted by injecting of 0.2 x10^5 GFP labeled human muscle stem cells into the DLL-conjugated PCL or control PCL constructs and cultured in medium. At day 3 after cell seeding, there was a clearly increased number of GFP labeled human muscle stem cells observed in DLL1-conjugated P CL (**Figure 6**). This observation indicated that the activation of Notch signaling in human muscle stem cells could promote their proliferation.

Figure 6

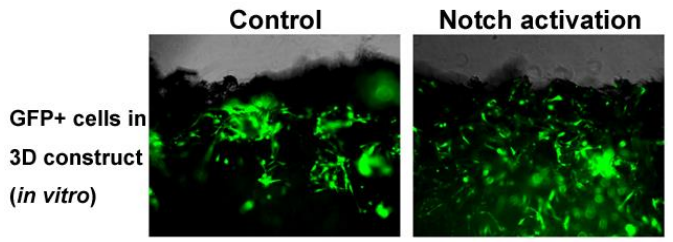

We further tested the effect of Notch activation in human muscle-derived cells *in vivo*, by transplanting the Notch activator (Jagged1) treated cells into the skeletal muscle of SCID/mdx mice. Human muscle-derived cells were treated with Jagged1 peptide (CDDYYYGFGCNKFCRPR) (10nM) in proliferation medium for 2 days in vitro, and then injected into the Gastrocnemius (GM) muscles of 8-week old SCID/mdx mice (3x10^5 cells). Cells without treatment were also injected in to GM muscle of SCID/mdx mice to serve as a control. Ten days after the cell transplantation, muscle tissues were harvested and immuno-stained with antibodies against human lamin A/C and utrophin. Compared to the skeletal muscle transplanted with the untreated control cells, there were more utrophin-positive myofibers and larger cell engraftment observed in the skeletal muscle transplanted with the Notch-activated human muscle cells (**Figure 7**). Our results indicated that the transplantation of human MDCs into dystrophic muscle could potentially be improved by activating Notch signaling prior to their implantation.

Figure 7

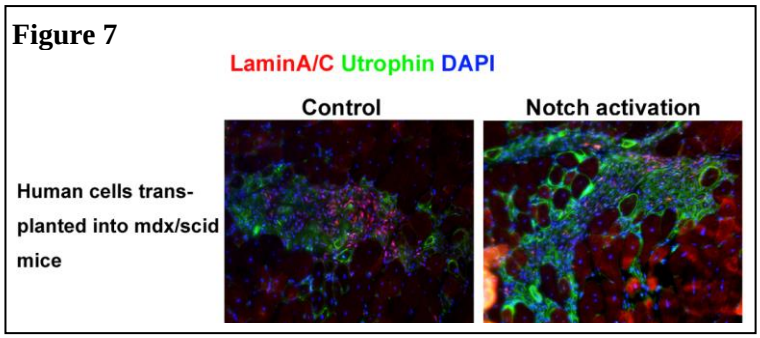

Proliferation and Differentiation Capacities of Muscle Derived Stem/Progenitor Cells Cultured on Polydimethylsiloxane Substrates of Varying Elastic Modulus and Protein Coating

Introduction:

In this proof of concept study we utilized muscle derived stem/progenitor cells (MDSPCs) which are multipotent murine cells that display a capacity for long term proliferation. These cells have been utilized to regenerate bone (14), cartilage (15), skeletal (14) and cardiac muscles[3], as well as ameliorate the effects of aging[4]. MDSPCs are isolated and cultured on collagen I coated polystyrene flasks, but recent publications have shown that culturing progenitor cells on substrates with anatomically relevant elasticities and protein coatings can vastly alter their ability to proliferate and differentiate *in vitro* as well as engraft *in vivo* (18-20). Polydimethylsiloxane (PDMS) blends have shown to be a readily tunable substrate creating reproducible culture surfaces at anatomically relevant elasticities (20). These blends can be adjusted across three orders-of-magnitude, surpassing what is capable with other hydrogel or PDMS systems. This study was designed to observe the effects of altering the culture surface conditions on MDSPCs *in vitro* and determine how to translate these findings to improve tissue regeneration with MDSPCs *in vivo*.

Methods:

Creating variable stiffness PDMS substrates and protein coated culture surfaces: PDMS substrates and protein coatings were prepared using previously defined methods7. Briefly, blends of Sylgard 527 and Sylgard 184 (Dow Corning) were mixed to create PDMS substrates with elastic modulus of 5 kPa, 50 kPa, 830 kPa, and 1.72 MPa. These blends were cured in 12 well plates with one of each protein coating, collagen type I (Col-1), collagen type IV and laminin (Col-4/Lam), or fibronectin (FN).

Proliferation of MDSPCs: MDSPC proliferation was investigated for 3 days on 12-well plates using a Live Cell Imaging (LCI) system. Time-lapse images were acquired every 15 minutes over 72 hours and cell numbers quantified at 6-hour intervals using ImageJ (NIH). Counts were averaged for each time point from at least 6 separate images and experiments were performed in duplicate.

Myogenic differentiation of MDSPCs: Myogenic differentiation potential was assessed by inducing *in vitro* myotubes formation after switching the proliferation medium (Dulbecco's modified Eagle's medium [DMEM] containing 10% fetal bovine serum [FBS], 10% horse serum, 1% Penicillin/Streptomycin, and 0.5% chick embryo extract) to fusion medium (DMEM containing 2% FBS and 1% penicillin/streptomycin). After 2-3 days, cells were fixed in cold methanol and immunostained for skeletal fast myosin heavy chain (f-MyHC)-positive myotubes (1:400, Sigma) and counterstained with DAPI (1:1000, Sigma). Images were taken on a Leica DM-IRB inverted microscope with a 20x objective.

Results:

Culture surfaces with PDMS substrates and protein coatings increase the proliferative capacity of MDSPCs: MDSPCs were observed on 13 separate combinations of protein coating and substrate elastic modulus, including the negative control of tissue culture plastic with no substrate or coating, to evaluate their effects on rate of proliferation (**Figure 8**).

Figure 8

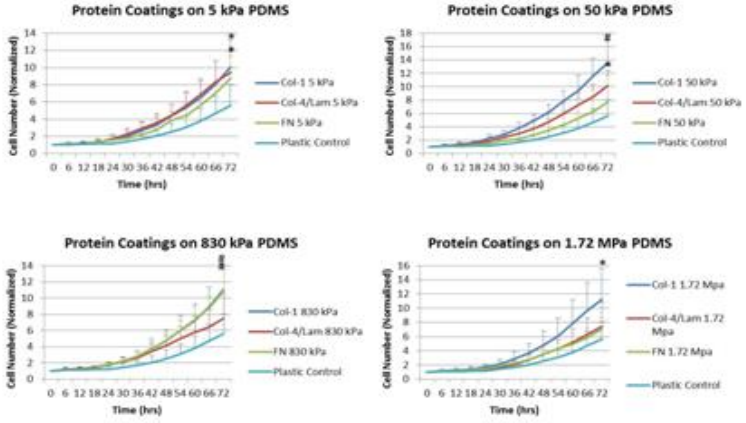

Significance in comparison to the negative control (plastic) is denoted with * ($p < 0.05$) and # ($p<0.001$). The highest proliferation rate from each group of substrate elastic modulus came from the condition including the coating of collagen type I. The combination of collagen type I coating on the 50 kPa PDMS provided the optimal condition for MDSPC proliferation.

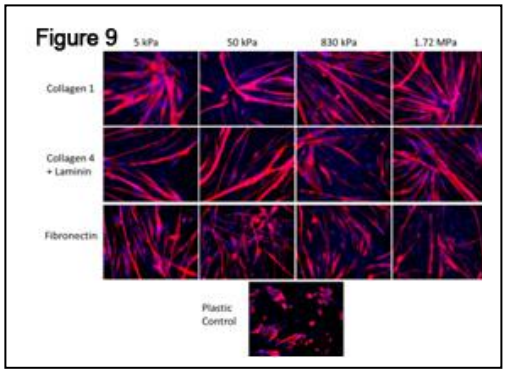

Qualitative differences in myotube formation between substrate elasticities and protein coatings: MDSPCs were differentiated into myotubes on the various PDMS substrates and protein coatings for 2-3 days, displaying a dynamic range of myotube dimensions (**Figure 9**). MDSPCs cultured on collagen type I and collagen type IV/laminin coatings created more robust and elongated myotubes. Myotubes formed on stiffer substrates (830 kPa and 1.72 MPa) were more numerous, but also more slender, than their broader counterparts formed on softer PDMS.

Figure 10

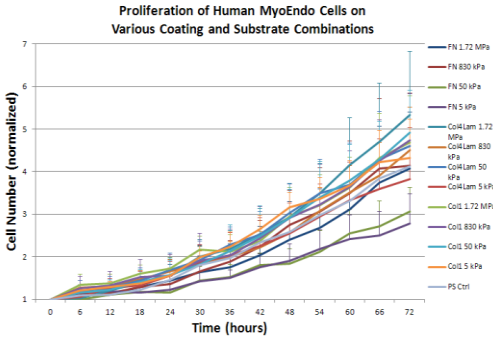

After these initial findings utilizing murine MDSPCs we initiated experiments using human MDCs, specifically human myo-endo cells, employing the same parameters outlined above for the murine MDSPCs. As above, both the proliferation and differentiation (fusion) capacities were analyzed as the endpoint measurement abilities of the cells. In regard to the proliferation capacities of the MDCs we found that the most highly proliferative cells were found in the collagen 4/laminin coated plates with a rigidity of 1.72 MPa and the lowest proliferative capacity was observed in the fibronectin coated plates with a rigidity of 5kPa (**Figure 10**). In regard to the effects on the differentiation (myogenic fusion), the substrate that promoted the highest fusion was seen in the collagen I coated plates with a rigidity of 5kPa and the lowest fusion index was observed with the fibronectin substrate with a rigidity of 50kPa (**Figures 11A and 11B**).

Figure 11

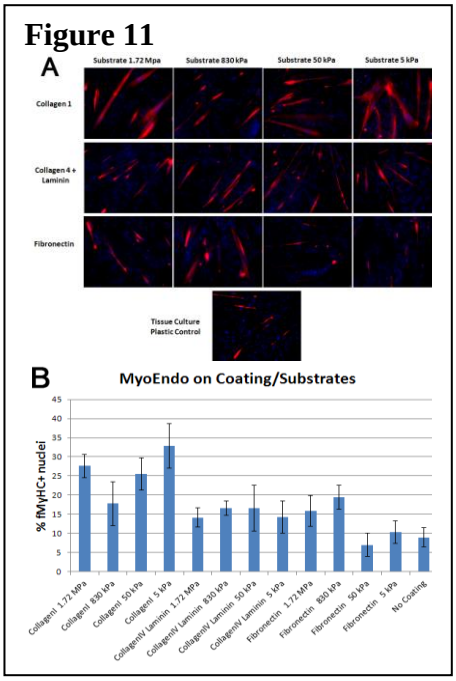

Discussion:

These findings support the view that optimizing the *in vitro* environment, by modulating the surface culture conditions with a variable stiffness PDMS substrate and protein coatings; can augment stem cell proliferation and differentiation capacities. Culture methods such as this may be used to prime MDSPCs towards specific lineages, by simulating tissue conditions of their natural niche, to improve cellular engraftment for therapeutic cell transplantations. The object of proliferating the cells in vitro is to expand the number of cells without promoting their differentiation into more mature lineages; therefore, we suspect that the optimal substrate is probably the fibronectin coated on plates with a 50kPa rigidity. Future cell therapies implemented for tissue repair may significantly benefit from the application of primary cells isolated and expanded on PDMS surfaces with protein coatings. Future in vivo studies are planned to test if modulating the cells in vitro expansion can affect their engraftment and regeneration capacities in injured and diseased skeletal muscle.

Progress made from 9-1-11 to 8-31-12

SCID/mdx mice skeletal muscle generates high levels of background when immunostained with an antibody against "human dystrophin".

An ongoing problem exists with the animal model that we were intending to utilize for our transplantation efficiency experiments on aged and young animals using aged and young hMDCs. It is a mouse model that is both deficient in murine dystrophin (mdx) and is immune-compromised (SCID, lacking both T and B cell functional activity). The purpose of utilizing this model was to demonstrate muscle regeneration in a dystrophic animal without eliciting a cellular immune response. When originally created this model demonstrated excellent grafting capacities and very little immune response, however, over the past year we have been experiencing a problem with this model, in that all the anti-human dystrophin antibodies we have been using have been giving us very high levels of background in the skeletal muscle of these mice. Originally we thought that it was a cross reactivity with the cells injected, but soon discovered the antibody was binding in vivo even when only PBS was being injected. The following is a summary of the work we performed over the past year to try and elucidate and correct this problem.

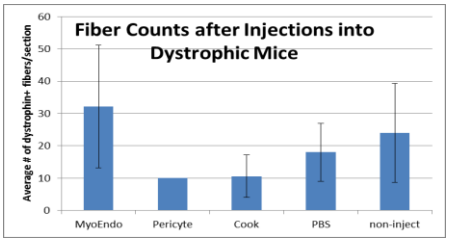

Figure 1 MyoEndo data is taken from 4 separate donor populations injected into 12 separate muscles. Pericyte data is taken from 1 muscle. Cook Myosite data is taken from 1 donor population and 5 muscles. PBS data was taken from 6 separate muscles. Non-injected data was taken from 4 different muscles.

In this 1st set of experiments human myoendothelial (myoendo) cells, pericyte, and preplate cells purchased from Cook Myosite, Inc. were injected into 8 week old SCID/mdx mice and compared with mice injected with vehicle alone (PBS) or not injected at all. The mice were sacrificed 2 weeks post-transplantation. The following is the resulting data which shows very limited engraftment overall and no significance between the groups **Figure 1**.

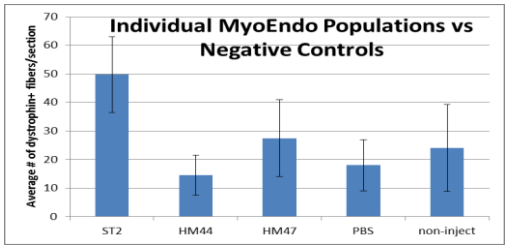

Figure 2: ST2 MyoEndo (69 M) data is taken from 5 separate muscles. HM44 MyoEndo (26 F) data is taken from 4 separate muscle. HM47 MyoEndo (16 M) data is taken from 2 separate muscles. PBS data was taken from 6 separate muscles. Non-injected data was taken from 4 different muscles. Significance between ST2 and PBS ($P > 0.005$); and between ST2 and non-injected ($P > 0.05$) was observed.

Since previous data indicated that the myoendo populations appeared superior to the pericytes and cells 3 separate populations of the myoendo cells were compared. The data can be seen in **Figure 2**. Again even when comparing all the populations of myoendo cells we have isolated, only the ST2 population showed any significance in myofiber regeneration; however the number of regenerated myofibers were barely above that observed for revertancy as seen in the PBS and non-injected muscles

Comparison of "dystrophin-positive" myofibers in SCID/mdx after injecting either STS2 myoendo cells in PBS or PBS alone. As is evident in this figure, positive fibers can be seen **in both muscles indicating cross reactivity of the antibody with some membrane bound molecule** in both the cell injected and PBS injected muscles (**Figure 3**).

Figure 3

ST2 myoendo cells | PBS

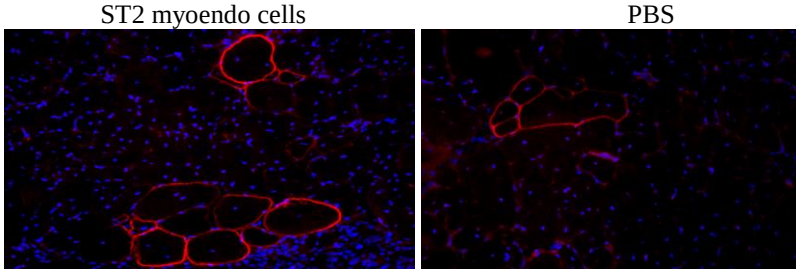

In order to confirm that the cells were actually present in the injected muscle after transplantation we used a retrovirus to label the cells with GFP and 2 days after injecting the cells the mice were sacrificed and the muscles were analyzed for GFP and dystrophin (**Figure 4A**). Some of the transplanted muscles were allowed to go 14 days prior to harvesting the muscles in order to see if additional time was required for the injected cells to fuse and begin expressing

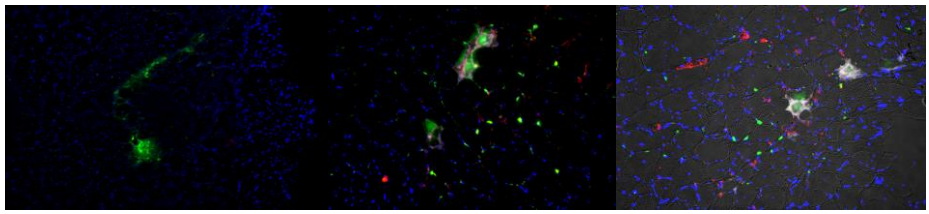

Figure 4: MDCs expressing GFP (green); A and B, anti-GFP (white), C; anti-Dystrophin (red), DAPI (blue)

dystrophin (**Figure 4B**). To confirm that GFP was truly positive in these sections an anti-GFP antibody was used to detect GFP expression (**Figure 4C**, white). We have concluded from these data that the injected cells were engrafting but not producing dystrophin; so what are the cells doing?

In order to observe the regenerative processes, if any, in the SCID/mdx skeletal muscle after hMDC injection, we stained the muscles with an antibody against embryonic skeletal myosin heavy chain. Interestingly all the muscles injected, including the PBS injected control, demonstrated a massive amount of myofiber regeneration and there was no difference in the numbers of eMyHC expressing myofibers between any of the groups as can be seen in **figure 5**.

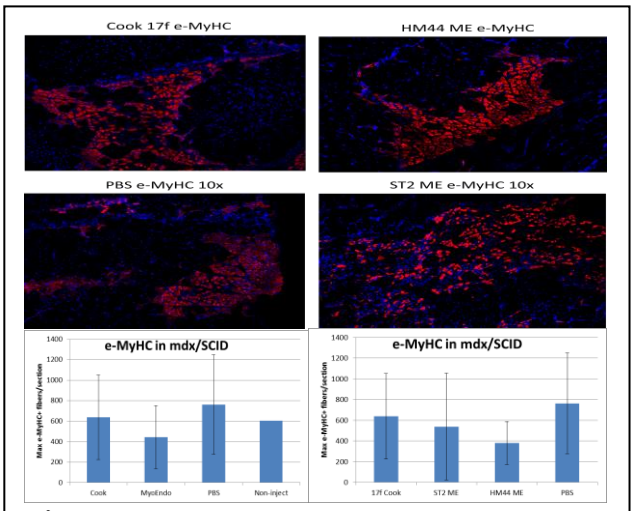

Figure 5: 17f Cook data is taken from 4 separate muscles, ST2 MyoEndo data is taken from 2 separate muscles, HM44, MyoEndo data is taken from 3 separate muscles, PBS data is taken from 4 separate muscles.

In a related set of experiments which confirmed the positive engraftment of the hMDCs and the lack of dystrophin expression, we had injected hMDCs that were being cultured using Platelet-Rich Plasma (PRP) in place of Fetal Bovine Serum (FBS). This experiment was intended to explore the use of an autologously-derived material to expand isolated hMDCs, which would have tremendous benefits for clinical applications of the hMDCs. In this experiment PRP-expanded and FBS-expanded hMDCs were injected into Mdx-SCID mouse muscles damaged with cardiotoxin. 4 weeks after cell injection, human major histocompatability complex I (hMHC-I) positive myofibers (red) could be detected in the injured muscles (**Figure 6**). The human MHC-I (red) expressed both on the membrane and in the cytoplasm of muscle fibers. All populations of hMDCs that were expanded in PRP supplemented medium retained their ability to regenerate myofibers upon extended culture. No significant differences were found between PRP and FBS expanded hMDPCs. From the point of view of SCID/mdx skeletal muscle engraftment, the cells were readily engrafting and producing hMHC-I. This finding supports engraftment occurring, but unfortunately does not explain the lack of dystrophin expression in the transplanted muscles.

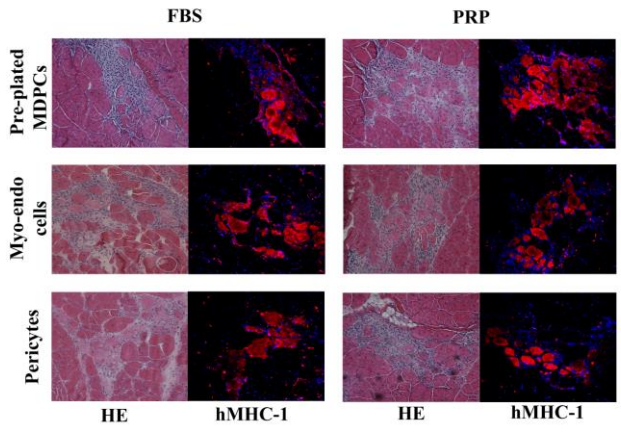

Figure 6. ***In vivo*** **myogenic potential of PRP-expanded hMPDCs.** PRP-expanded and FBS-expanded hMDPCs were also injected into Mdx-SCID mouse muscles damaged with cardiotoxin. 4 weeks after cell injection, HE staining and immuno-fluorescence staining of human MHC-fluorescence staining of human MHC-n MHC-g and immuno-fluorescence staining human MHC- I MHC- MHC myofibers can be detected in the injured muscles. All populations of hMDPCs that were expanded in PRP supplemented medium retained their ability to regenerate myofibers

In addition to the elucidation of why our SCID/mdx model was not exhibiting good engraftment with the human MDCs we have isolated, we have been performing additional tangential experiments on another model of DMD that is deficient for both dystrophin and utrophin known as the double-knock out (dKO) mouse.

This model was being used because its pathophysiology more accurately resembles that of DMD patients and we felt might better accommodate the experiments outline in this grant. The following are results we have obtained using the dKO model.

Progression of muscular dystrophy in dystrophin/utrophin-/- mice is associated with rapid muscle progenitor cell exhaustion

In this study we isolated MPCs from the skeletal muscle of young (2 weeks) and old (6 weeks) dKO (dystrophin/utrophin double knock out) mice, which have a maximum lifespan of 6 to 8 weeks and is a mouse model of DMD that closely recapitulates the disease progression observed in DMD patients. We found that MPCs isolated from old dKO mice have a reduced ability to proliferate and differentiate compared to MPCs isolated from young dKO mice. In addition, Pax7 staining (a muscle progenitor cell marker) indicated that the MPC population significantly decreased during disease progression. These observations suggest that blocking the exhaustion of the MPC pool could be a new approach to improve muscle weakness in DMD patients, despite their continued lack of dystrophin expression.

Figure 1

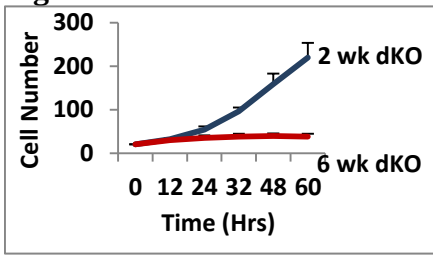

Results:

1. MPCs isolated from aged dKO mice display limited proliferation ability.

We examined the proliferation kinetics of both populations *in vitro* using LCI (3) and we observed a significant reduction in the proliferation capacity of the old dKO MPCs compared to young dKO MPCs (**Figure 1**).

2. Pax7 positive cells undergo a rapid decline in the skeletal muscle of dKO mice during aging and disease progression.

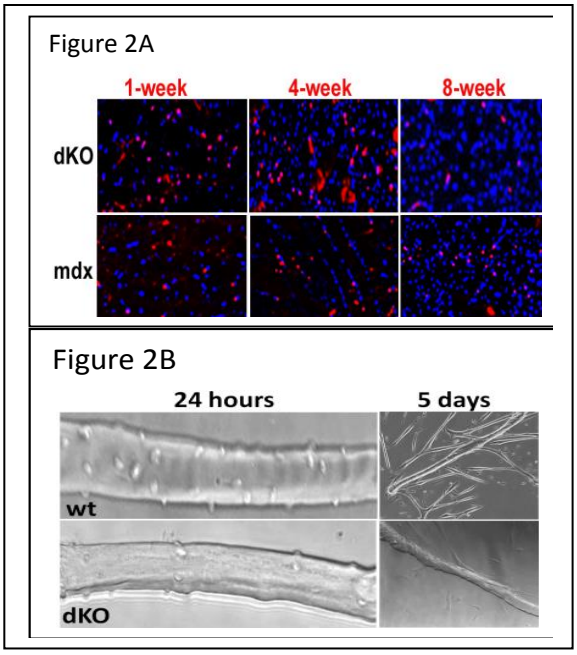

The results from the Pax7 staining showed that there is a rapid statistically significant decline in the population of Pax7 positive cells (red) in the skeletal muscle of dKO mice from 4 to 8 weeks of age in contrast to that observed in *mdx* skeletal muscle ($p<0.05$) (**Figure 2A**).

3. Isolated muscle fibers from dKO mice show a reduction in muscle progenitor cells.

The single muscle fibers were isolated from 6 weeks old dKO and WT control mice. We observed that there were more cell nuclei in the WT muscle fibers compared to the dKO muscle fibers. In addition, 5 days post-culturing, the WT muscle fibers were able to release myogenic progenitor cells forming new myotubes, in contrasts to that observed with the dKO muscle fibers. These results support both a reduction in the number and myogenic potential of the MPCs derived from the dKO mice when compared to the WT MPCs (**Figure 2B**)

4. MPCs isolated from aged dKO mice display a limited myogenic differentiation ability.

We observed that the MPCs isolated from young dKO mice formed numerous, large multi-nucleated myotubes compared to the MPCs isolated from the old dKO mice. The degree of myogenic differentiation was significantly reduced in the old dKO MPCs relative to the MPCs isolated from young dKO mice ($P < 0.001$).(**Figure 3**)

Figure 3

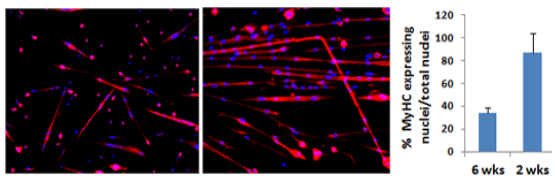

It is interesting to note that despite the lack of dystrophin at birth, the initiation of any signs of muscle weakness does not occur in DMD patients until later in childhood which happens to coincide with the exhaustion of the muscle progenitor cell pool (1). In this study we demonstrated that MPCs isolated from the skeletal muscle of old dKO mice have a reduced ability to proliferate and differentiate compared to MPCs isolated from young mice. Moreover, the numbers of Pax7 positive cells *in vivo* undergo a rapid decline in the skeletal muscle of dKO mice during aging and disease progression. Since dKO mice can only live 6-8 weeks, stem cell exhaustion could represent the main mechanism for the rapid progress of this disease. Blocking the exhaustion of muscle progenitor cells and stem cell-mediated therapy may represent a potential strategy for treating these muscle diseases. This study suggested that the exhaustion of stem cells contributes to the histopathology associated with DMD and that blocking the exhaustion of muscle progenitor cells and stem cell-mediated therapy could be used as a potential clinical strategy to treat muscle disease.

Muscle-derived cells (MDCs) responsible for myogenesis differ from MDCs involved in adipogenesis in dystrophin/utrophin-/- mice

DMD is characterized by progressive weakening of the skeletal and cardiac muscles. The predominant symptoms seen in advanced cases of DMD are sarcopenia and pseudohypertrophy with fatty infiltration in skeletal muscle. Ectopic fat accumulation in skeletal muscle can be seen not only in myopathies but also in several disorders, including obesity and ageing-related sarcopenia; however, the origin of ectopic adipocytes, nor the stimulus that trigger their formation in disease, is known. In our lab, we utilize utrophin/dystrophin double knockout (dys-/-utro-/-, dKO) mice, which better emulates the phenotype seen in DMD patients. Several types of cells, including satellite cells, can be isolated from skeletal muscle and based on a previously published preplate technique we isolated two types of cells; rapidly adhering cells (RACs) ,which are PDGFRα + mesenchymal progenitor cells, and slowly adhering cells (SACs), which are Pax7+ myogenic progenitor cells, from skeletal muscle of dKO and wild type (wt) mice. Previously, we have shown that dKO-SACs have reduced proliferation and myogenic and adipogenic differentiation abilities compared to wt-SACs. These observations suggested that SACs in dKO mice are exhausted and potentially are the main mechanism for the rapid progress of sarcopenia; however, the cells involved in pseudohypertrophy in dKO mice remains unclear. In this study, we examined the proliferation and adipogenic differentiation capabilities of RACs since adipose cells are thought to be derived from mesenchymal stem cells. We observed increased proliferation and adipogenic differentiation capabilities in dKO-RACs compared to wt-RACs. Our results suggest that muscle progenitor cells, SACs, may be more involved in muscle fiber regeneration or degeneration while mesenchymal progenitor cells, RACs, may be the origin of the cell population that is involved in adipogenesis in dKO muscle.

Figure 1. Flow analysis of PDGFRα surface protein expression in RACs and SACs from wt and dKO mice.

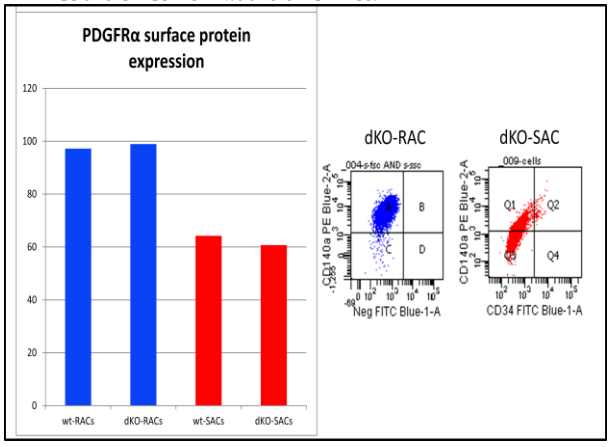

RESULTS:

dKO-RACs had increased PDGFRα expression compared to dKO-SACs. Flow cytometry analysis was used to evaluate the expression of PDGFRα, a marker for mesenchymal cells, of the RACs and SACs from both dKO and wt mice. dKO-RACs were about 98% positive for the PDGFRα surface protein, while much lower expression levels were detected in the SACs (**Figure 1**).

dKO-RACs displayed increased proliferation ability. The proliferation of the RACs and SACs were examined in vitro using an LCI system and MTT assay. We observed a significant increase in the proliferation of the dKO-RACs compared to the wt-RACs.

Increased in vitro adipogenic potential was detected in dKO-RACs. RACs and SACs from both dKO and wt mice were cultured in adipogenic differentiation medium for 21 days. AdipoRed staining was observed in the cytoplasm of the cells, around the nuclei. The degree of adipogenic differentiation was significantly increased in PDGFRα+ dKO-RACs compared to the dKO-SACs (**Figure 2**).

In dKO mice, an animal model of DMD, we observed severe peri-muscular adipose tissue on the surface of the gastrocneminus muscles (GM) as well as lipid accumulation inside of skeletal muscle myofibers. Intramyocellular lipid accumulation could be observed in the cardiac muscle of dKO mice; however, the source of the ectopic fat tissue within the skeletal muscle is unknown. In this study, we provide evidence that the RACs, PDGFRα + mesenchymal progenitor cells, are responsible for increased fat cell formation in the skeletal muscle of dKO mice. We observed that dKO-RACs had increased proliferation and adipogenic differentiation capabilities. This result suggests that dKO-RACs are prone to form adipocytes in skeletal muscle. This study suggests that dKO-RACs, mesenchymal progenitor cells in skeletal muscle, may contribute to adipogenesis and are responsible for ectopic fat cell formation within skeletal muscle in pathological conditions such as DMD. Therefore, targeting RACs to block adipogenesis in skeletal muscle may open new opportunities to treat muscle diseases.

Figure 2. Adipogenesis of RACs and SACs. Bright field pictures and AdipoRed staining. Quantification of AdipoRed assay is shown.

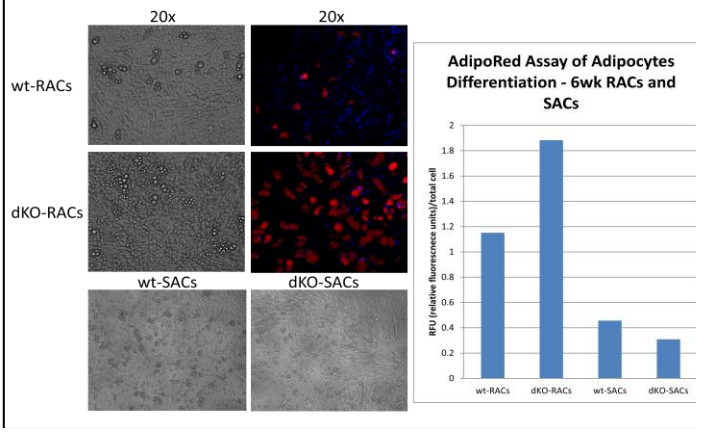

RhoA signaling regulates heterotopic ossification and fatty infiltration in dystrophic skeletal muscle

Frequent heterotopic ossification (HO) or fatty infiltration is observed in the dystrophic muscle of many animal models of human Duchenne muscular dystrophy (DMD); however, little is known about the correlated molecular mechanisms involved in the process. The RhoA-Rho kinase (ROCK) signaling pathway has been shown to function as a commitment switch of the osteogenic and adipogenic differentiation of mesenchymal stem cells (MSCs). Activation of RhoA-ROCK signaling in cultured MSCs in vitro induces their osteogenesis but inhibits the potential of adipogenesis, while the application of Y-27632, a specific inhibitor of ROCK, reversed the process. Inflammation has been shown to be one of main contributors to HO, while the role of RhoA signaling in inflammation reaction has been demonstrated. The objective of the current study is to investigate the potential role of RhoA signaling in regulating HO *and* fatty infiltration in dystrophic skeletal *muscle.*

Figure 1

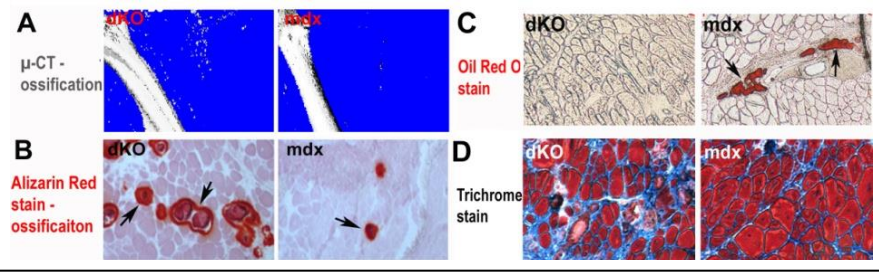

Results:

1.Skeletal muscle of dKO mice features more HO but less fatty infiltration than mdx mice (**Fig. 1**). Both μ-CT scan of animals (**Fig. 1A**) and Alizarn Red stain (**Fig. 1B**) of the muscle tissues revealed greatly enriched HO in the dystrophic muscles of the dKO mice. While, Oil Red O stain (**Fig. 1C**) and Trichrome stain

(**Fig. 1D**) of the muscle tissues revealed reduced fatty infiltration and a number of normal muscle fibers in the muscle of dKO mice.

2. RhoA signaling is more activated in both skeletal muscle and muscle-derived stem cells (MDSCs) from dKO mice. Both semi-quantitative PCR and immunohistochemistry study demonstrated that RhoA signaling is more activated in the muscles of dKO mice, as well as dKO MDSCs.

3. *In vitro* RhoA inactivation of cultured MDSCs from dKO mice decreases the osteogenesis potential and increases adipogenesis and myogenesis potential (**Fig. 2**). Semi-quantitative PCR study showed that Y27632 treatment *(10 μM)* of dKO-MDSCs down-regulated the expression of RhoA, BMP2 and 4, and inflammatory factors such as TNF-α and IL-6 (**Fig. 2A**). Osteogenesis potential was repressed while the adipogenesis and myogenesis potential of the dKO-MDSCs were increased by Y27632 (**Fig. 2B**).

4. RhoA inactivation in the skeletal muscle of dKO mice decreased HO and increased both fatty infiltration and muscle regeneration. GM muscles of 6 dKO mice were injected with Y27632 (5mM in 20μL of DMSO) (left limb) or control (20μL of DMSO) DMSO (right limb). Injections were conducted 3 times a week for 3 weeks. The skeletal muscles that received Y27632 injection demonstrated much slower development of HO and improved muscle regeneration, as well as
reduced fibrosis formation.

Figure 2

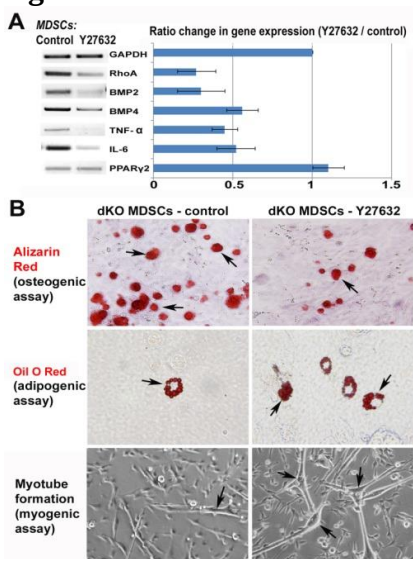

These results revealed that DMD mouse models featuring different severity of muscular dystrophy may have varied potentials for developing HO or fatty infiltration in the dystrophic muscle, and RhoA signaling might be a critical mediator of the determining these differential fates, including the progression towards HO, fatty infiltration, or normal muscle regeneration. RhoA inactivation is shown to have a great potential to repress HO and improve the phenotypes of dystrophic muscle. The status of RhoA activation in the skeletal muscle of human DMD patients and the potential effect of RhoA inactivation in human dystrophic muscle requires further investigation. This data reveals the involvement of RhoA signaling in regulating the process *of* heterotopic ossification, and indicates that RhoA may serve as a potential target for repressing injury-induced and congenital heterotopic ossification in humans.

Suppression of skeletal muscle inflammation by muscle stem cells is associated with hepatocyte growth factor in wild type and mdx;p65$^{+/-}$ mice

Persistent, unresolved inflammation can lead to secondary tissue damage. In a previous study, we reported that intramuscular (i.m.) injection of muscle-derived stem cells (MDSCs) heterozygous for the NF-kB subunit p65 (p65$^{+/-}$) reduced host inflammation and fiber necrosis seven days following muscle injury, relative to wild type (WT) MDSC injection [1]. In this investigation, we looked closer at the role of secreted factors in this observation. Using a murine cardiotoxin muscle injury model, we observed that delivery of p65$^{+/-}$ MDSCs accelerated the resolution of inflammation, relative to WT MDSCs. *In vitro* inflammation assays demonstrated that MDSCs secrete factors that modulate cytokine expression in LPS-activated macrophages, and genetic reduction of p65 enhanced this effect. Finally, deletion of one p65 allele in a murine model of Duchenne muscular dystrophy (mdx) increased the expression of the anti-inflammatory factor hepatocyte growth factor (HGF) and was associated with disease improvement.

RESULTS

Confirming our previous report [1], we found that by 7 days, p65$^{+/-}$ cell engraftments were associated with reduced numbers of F4/80+ cells, compared to WT cell engraftments (**Fig 1A**). This can be further demonstrated histologically by H&E staining, revealing a reduction in mono-nuclear cells at sites of injury one week post injection (**Fig 1B**).

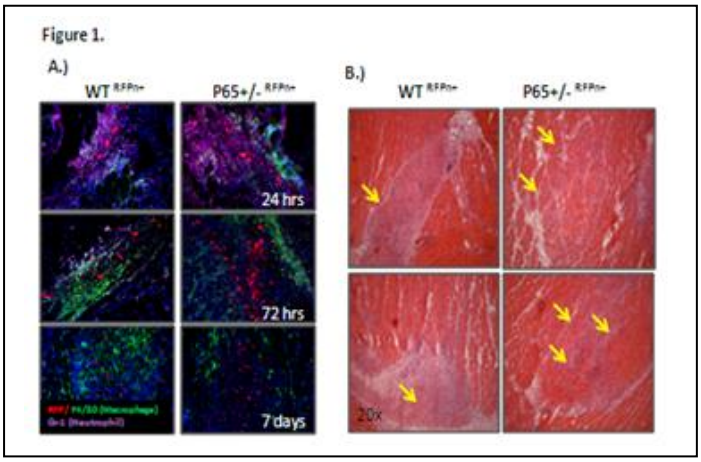

To look at the direct effects of MDSC-secreted factors, we performed *in vitro* inflammation assays. Briefly, RAW264.7 macrophages were activated with LPS (100ng/mL) in normal PM or WT or p65$^{+/-}$ conditioned medium (CM) (**Fig 2A**). The expression of the cytokines IL-1β and IL-6 was determined by real time (RT-PCR). Our results demonstrated that MDSC-CM significantly attenuates cytokine expression (Fig 2B). Although WT and p65$^{+/-}$ CM had a similar effect, we found that p65$^{+/-}$ CM exerted a stronger suppression of IL-6 expression. Previous reports have found that the activation of inflammatory macrophages is attenuated by the phosphorylation and subsequent inactivation of GSK3β [3]. By western blot, we found that upon treatment with LPS in WT-CM, the fraction of pS9-GSK3beta modestly increased within 30mins and was maintained through 24 hours. Furthermore, p65$^{+/-}$-CM demonstrated an even stronger induction of phosphorylation (**Fig 2C**).

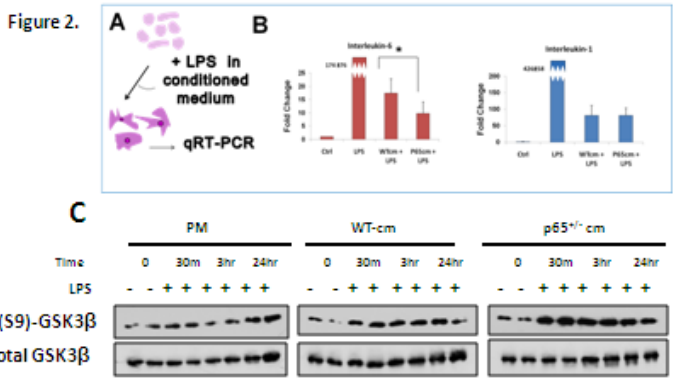

Hepatocyte growth factor (HGF) is one of the factors previously demonstrated to modulate inflammation via pS9-GSK3beta. We examined HGF expression in MDSCs and found elevated levels in p65$^{+/-}$ cells compared to the WT cells (**Fig 3A**). Acharyya and colleagues have reported that haploinsufficiency of p65 in an mdx background improves dystrophic pathology [4]. As we had hypothesized, HGF expression was significantly increased (**Fig 3B**). Based on our *in vitro* and *in vivo* inflammatory studies, HGF could be one of the contributing factors to disease improvement.

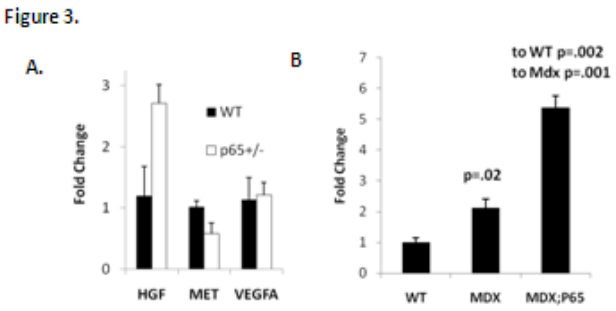

These findings indicate that NF-kB has a broader role in muscle stem and progenitor cells than previously thought, and that the anti-inflammatory molecules secreted by stem cells, such as HGF, could potentially be harnessed to control secondary pathologies of muscle diseases such as DMD.

Progress made from 9-1-10 to 8-31-11

Myogenic and proliferation capacity of young vs. old myoendothelial cells

In vitro assays to look at differences in myogenic capacities of young and old human myoendothelial cells were conducted using two cell populations one from a 30 year old female and the other from a 76 year old female. Both cell populations were derived from human skeletal muscle and isolated using our lab's pre-plate technique for stem cell isolation. Cells isolated from the latest preplate, preplate 3(PP3), were utilized in the current experiments (which means that the isolated cells adhered to the collagenated flasks between 24-48 hours after the initial muscle biopsy isolation and dissociation. For murine cell isolations, PP6 cells are able to be isolated and possess the highest multipotency and engraftment capacities as compared to PP1-PP5. To compare the myogenic capacities of the young and old cells in vitro, the cells were promoted to differentiate by placing them in low (2%) serum media for five days after which the cells were fixed and then stained for their expression of myosin heavy chain (MHC) and DAPI. The myogenic differentiation index (MDI) for each cell type was calculated by counting the number of nuclei inside MHC-stained differentiated myotubes and dividing this number by the total number of nuclei. The results shown in **figure 1** indicated that the older female PP3 cells had a reduction in their myogenic potential (myotube formation) *in vitro* compared the cells isolated from the younger female biopsy. These results are being confirmed and the experiment is being repeated with human male myoendothelial cells, as well.

Figure 1

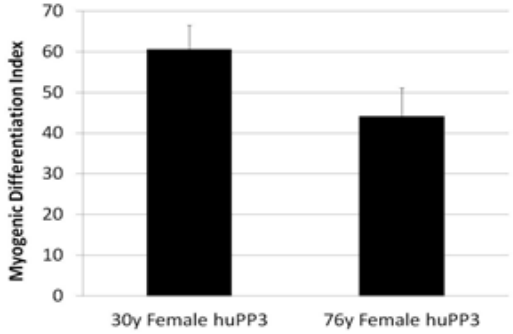

The MDI of two populations of human female myoendothelial cells. The MDI shows the cells isolated from the 30 year old female donor have a greater myogenic capacity than cells isolated from the 76 year old donor ($p < 0.05$).

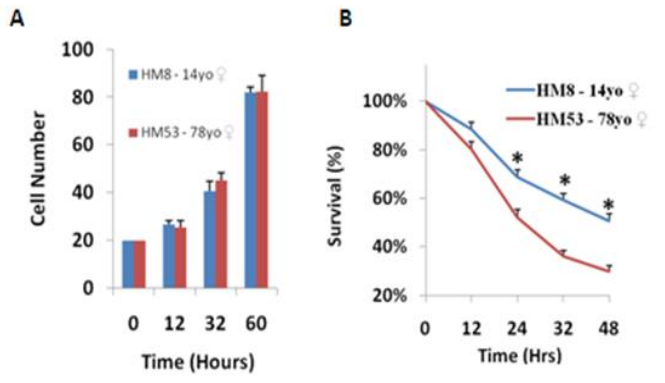

Figure2 Myoendothelial cells isolated from skeletal muscle biopsies taken from 78 year old (HM53) or 14 year old (HM8) female patients exhibit no differences in cell proliferation (A). However, aged cells are significantly less resistant to hydrogen peroxide induced (400uM) oxidative stress (B). ($p<0.05$, data represented as mean +/- s.e.m.)

In another set of experiments we isolated myoendothelial cells via FACS from the skeletal muscle of a 76 year old female (HM53) and a 14 year old female (HM8) patient. The cells were studied for their proliferative and oxidative stress resistance (exposure to 400uM hydrogen peroxide) capacities. In this study the cells were found to not differ in their proliferative capacity between HM53 and HM8 (**Figure 2A**); however there was a significant difference in their resistance to oxidative stress capacities at 24, 32 and 48 hrs post-exposure (**Figure 2B**, older cells displaying a reduction to stress resistance).

Additional studies are currently underway to increase the number of populations of young and old myoendothelial and PP3 cells (and sex) studied for their proliferation, myogenic and their stress resistance capacities.

Optimizing the culture conditions for expanding myoendothelial cells

It is of critical importance that the myoendothelial cells isolated from human skeletal muscle can be maintained in a "stem" like state when expanded in a cell monolayer. A media formulation of 10% fetal bovine serum, 10% horse serum, 1% penicillin/streptomycin and 1% chick embryo extract is normally used to culture the cells. This proliferation media (PRO) was combined with Endothelial Growth Media-2 (EGM2) media (Lonza) at a 1:1 mixture and designated PROe media. A 69 year old, male population of human myoendothelial cells (ST2) isolated via FACS were seeded on a 24-well plate at a density of 2000 cells/cm^2 of growth area. The ST2 cells had been maintained in normal proliferation media or PROe media since the cell isolation and were designated ST2 and ST2e, respectively. The 12-well plate was place on a Live Cell Imaging system (Kairos Instruments) which can capture images at different coordinates in the well and in all the seeded wells at preprogrammed time intervals, which can then be viewed after a set time as a time- lapsed movie. In the current experiment 100x images were captured every 15 minutes for a period of 108 hours. Images were analyzed using ImageJ and the data are presented in **figure 3**. Morphologically, the ST2e cells (**Fig. 3B**) are smaller and less elongated than the ST2 cells and proliferate at a faster rate than ST2 cells (**Fig. 3C**). Next, we wanted to know if the cells were able to differentiate after culture in PROe media and to compare this to cells grown under the usual culture conditions (PRO). A myogenic differentiation assay was performed, as described above, and representative images are shown in **figure 4**. ST2e cells not only form a greater number of myotubes but a greater number of the myotubes contained more nuclei which indicate a higher degree of maturity. These data suggest the PROe media or another variant may be more ideal for culturing human myoendothelial cells and maintaining them in a stem-like state.

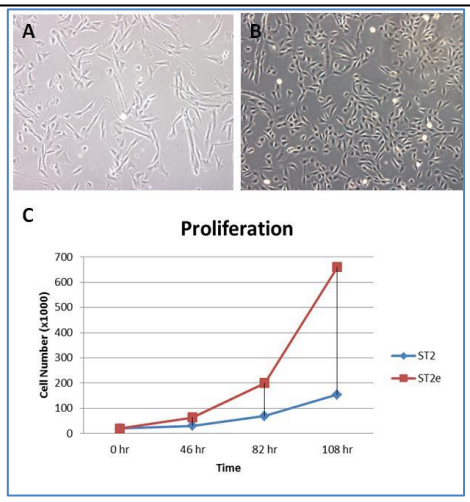

Figure 3: 100x images of human, male myoendothelial cells cultured in PRO media or PROe media. The expected doubling time of 24-36 hours is seen in the ST2 population while the ST2e cells show a doubling time of less than 24 hours (C). The morphologies of the cells are shown in A and B and indicate PROe media maintains the population in a more stem-like morphology.

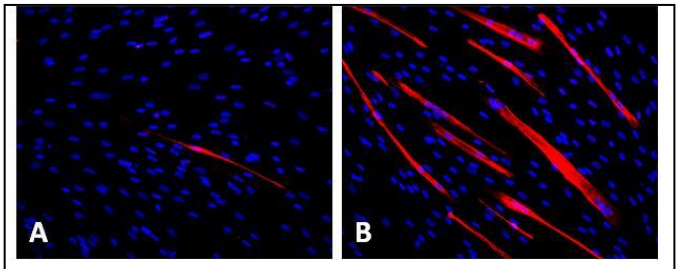

Figure 4: ST2 cells (A) and ST2e cells (B) growth in low (2%) serum media for 5 days. Cells were fixed and stained against DAPI (blue) and myosin heavy chain (red).

Identification of a dystrophin antibody for use in mdx mice

Early analysis of the first SCID/mdx tissues transplanted with human myoendothelial cells revealed a critical problem. Our group was using a polyclonal anti-dystrophin antibody (Abcam #15277) which we use for all our other mouse tissues. The initial staining of the SCID/mdx tissues showed high levels of positive staining in the PBS injected control muscles which should have been completely negative (**figure 5C-D**). Indeed the PBS groups had higher levels of dystrophin staining than some of the tissues tissues injected with myoendothelial cells (**Fig. 5A-B**). It was essential to identify a viable anti-dystrophin antibody to stain *mdx* mouse tissues. Dr. Bing Wang of the Stem Cell Research

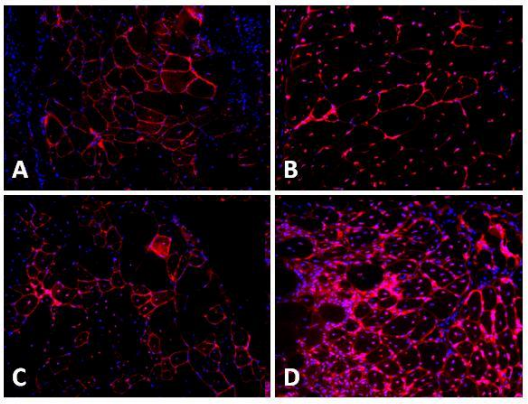

Figure 5: Mdx/SCID muscle sections stained against DAPI (blue) and mammalian dystrophin (red). (A-B) tissue transplanted with human myoendothelial cells. (C-D) tissue injected with PBS.

Center had created four variants (R1R2, R2N, R22R23, R24H4) of a mammalian dystrophin antibody for testing on these tissues. The results shown in figure 5 suggested variant R1R2 was the best antibody to use on the *SCID/mdx muscle* tissues (**Figure 6**).

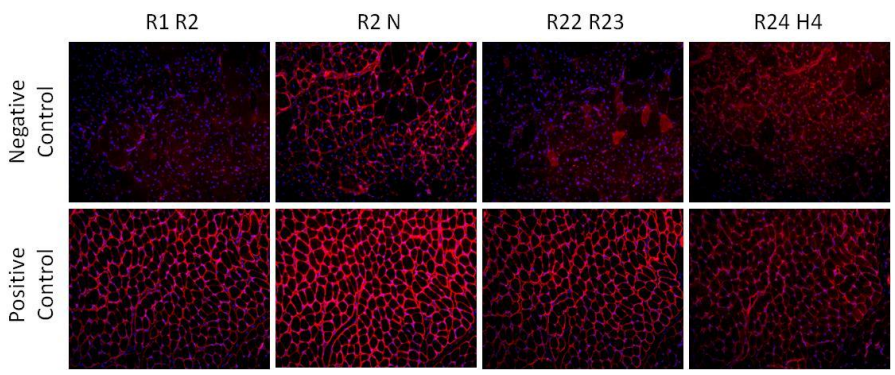

Figure 6: Testing the 4 variants of Dr. Bing Wang's polyclonal dystrophin antibody. Negative control = mdx tissue. Positive control = C57BL6 tissue. Each figure for negative or positive controls shows the identical area of the tissue. Variant R1R2 shows the lowest level of nonspecific staining.

Effect of host sex on the regenerative capacity of old male and female myoendothelial cells

Eight week old SCID/mdx mice, male and female, were randomly assigned to 1 of 5 groups; non-injected (controls), PBS (controls), ST2, ST2e or HM49. All groups, except non-injected controls, received bilateral injections into the gastrocnemius muscles of 20 microliters of PBS or PBS containing $3x10^5$ myoendothelial cells via a 31 gauge insulin syringe. Animals were sacrificed and tissue collected 14 days post-injection. Tissues were cryosectioned and the sectioned tissues stained for dystrophin using the R1R2 variant. Analysis was performed by capturing 100x fluorescent images of the entire stained section and counting the number of positively-stained (for dystrophin) fibers present in the section. The data in **figure 7** are not complete as analysis has just begun on these tissues but early evidence suggests ST2 cells (cultured in PRO media) have a greater regenerative capacity than cells grown in PROe media (ST2e). The ST2 (69 year old, male) cells showed no differences when transplanted into male or female hosts (n=3 for both). The trend for ST2e cells is for better regeneration when transplanted into female hosts but the n is low for both conditions (male host, n=1; female host, n=2). This trend is seen in the HM49 again with the HM49 (75 year old, female) injected tissues as greater regeneration is seen when the cells are transplanted into a male host. Again, the n is small (n=1 for both hosts) making further analysis essential for any conclusions to be drawn. More importantly, the numbers of dystrophin positive fibers in female host tissues are all at near-background levels based on the number of revertant myofibers seen in non-injected controls. Analysis has not been performed on non-injected tissues from male hosts. Also, analysis has not yet been performed on non-injected tissues from male hosts.

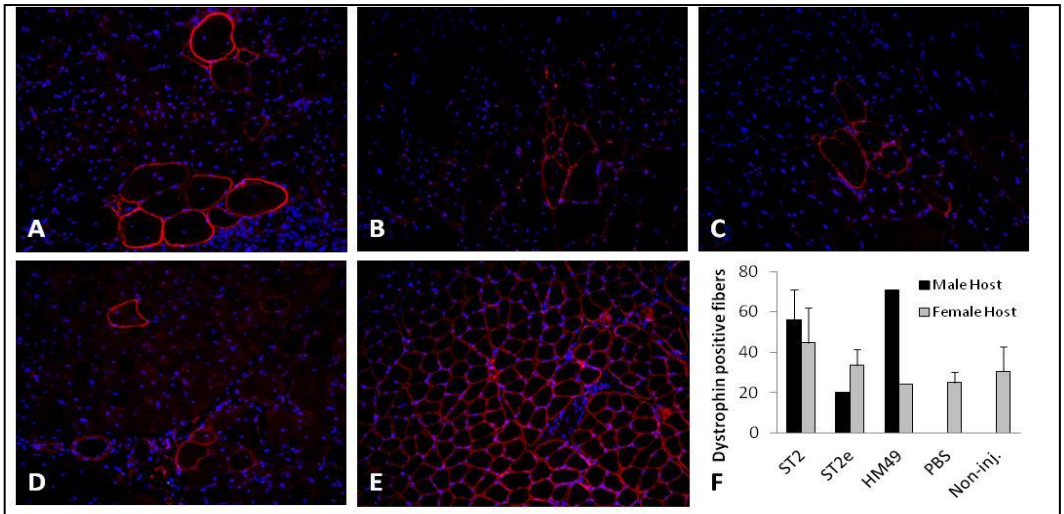

Figure 7: Analysis of tissue cryosections from *mdx/SCID* mice. Dr. Bing Wang's R1R2 dystrophin antibody (red) was used for staining. DAPI (blue) stained for nuclei. A) ST2 injected. B) ST2e injected. C) HM49 injected. D) PBS injected E) wild type (dystrophin positive) control tissue. No significant differences are seen between groups but analysis of tissues is not complete.

Non-invasive behavioral testing to detect functional improvement following stem cell transplantation

Preliminary studies were performed on nine, 12-week old female *SCID/mdx* mice in order to test the potential use of a DigiGait™ system (Mouse Specifics, Inc., Quincy, MA) functional gait analysis system to test the functional improvement of our transplanted mice. The mice received bilateral intramuscular (gastrocnemius) injections of 20uL of PBS or 20uL PBS containing either $3x10^5$ male myoendothelial cells or $3x10^5$ male perivascular cells. This initial experiment was conducted before the determination that myoendothelial cells were the best human cell type for these studies. For non-invasive analysis of muscle function we used the DigiGait™ system (Mouse Specifics, Inc., Quincy, MA). The system consists of a treadmill with a transparent belt which had a high speed digital camera mounted ventral to the test subject. Proprietary software provide by Mouse Specifics used to analyze numerous indices of the animal's gait. A simple schematic of what the software is looking at when calculating these indices is shown in **figure 8A**. For our study animal gaits were examined at a velocity of 20cm/s and the ratio of the stance time to swing time was calculated. The stance and swing phases are shown in **figure 8A** and the analysis for the *SCID/mdx* mice is shown in **figure 8B**. The data suggest that within 2 weeks of transplantation the myoendothelial-injected mice showed a reduced "running" stride compared to the pericyte-injected mice. Since these mice were forced to move at a constant velocity subjects capable of generating more force via plantar flexion could have a ratio of stance/swing greater than 1. Since the gastrocnemious is partially responsible for plantar flexion and this muscle was the target of the transplantation, these data are encouraging and warrant further use with our other experimental animals.

Figure 8

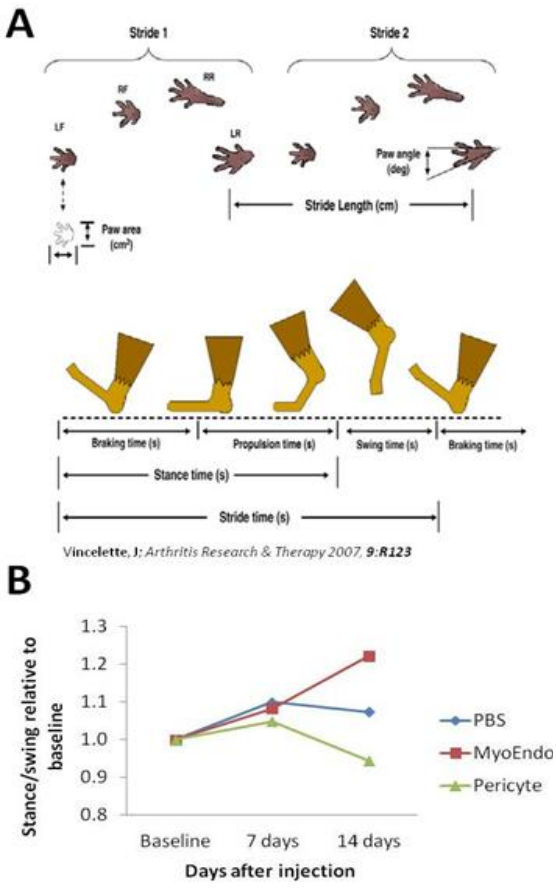

Non-invasive behavioral testing A) schematic of the paw areas detected by the high-speed camera as part of the DigiGait™ system. The diagram below is a visual representation of the 3 phases of a stride; braking, propulsion and swing. B) The stance phase/swing phase ratio for each group at each time point relative to each groups' baseline ratio. An increasing ratio may be indicative of increased muscle function/strength.

Immunomodulatory properties of muscle-derived stem cells associated with reduced NF-κB/p65 signaling

In this study, we examined the role of NF-kB signaling in the regenerative phenotype of muscle-derived stem cells (MDSCs) isolated from the gastrocnemius of p65 deficient mice (heterozygous, *p65+/-*) and wild type littermates (*p65+/+*). We previously found that *p65+/-* MDSCs have enhanced cell proliferation, survival under oxidative stress, differentiation, and muscle regeneration capacity. Furthermore, we have found that *p65+/-* engraftments in wild type skeletal muscle are associated with reduced inflammation and fiber necrosis compared to *p65+/+* MDSC engraftments. *In vitro* and *in vivo* experiments suggest that reduction of p65 signaling enhances the regenerative phenotype of MDSCs, suggesting this pathway as a candidate target to improve stem cell-based therapies for muscle disease and injury. The data presented in this study provides evidence supporting that NF-kB inhibition stimulates MDSC-mediated muscle regeneration through multiple mechanisms, including through the expression of anti-inflammatory factors that attenuate inflammation and necrosis. These experiments identify the NF-κB signaling pathway as a potential therapeutic target to enhance muscle regeneration following injury or disease (**Paper in revision. A. Lu et al. Mol. Therapy, Sept. 2011**).

p65 +/- MDSC transplantation improves muscle histology in dKO mice after IP transplantation

MDSCs were isolated from 5 month old $p65^{+/-}$ and WT mice as previously described via a modified preplate technique. A total of 5-9 $x10^5$ viable cells or 50µl PBS were injected intraperitoneally into 5-7 day old dKO mice. Four to six weeks after transplantation, the muscles were harvested and cryosections were prepared for staining. Our preliminary data suggest that the regeneration of both the gluteus maximus and diaphragm muscles were more greatly improved in their histopathological appearance in the animals injected IP with p65-deficient MDSCs than the nontreated animals at 4 weeks post-implantation. Muscle cryosections were also stained for mouse IgG to determine the extent of muscle fiber necrosis.The results showed that there were less necrotic muscle fibers in the mice injected with $p65^{+/-}$ MDSCs compared to non-treated muscles (**Fig. 9**). Trichrome staining was also preformed according to the manufacturer's instructions and the results showed that there was less muscle fibrosis in the mice injected with $p65^{+/-}$ MDSCs compared to the non-treated muscles (PBS) (**Fig. 9**). An antibody against embryonic muscle heavy chain (E-MyHC) was used to evaluate muscle regeneration and another antibody against F4/80 (macrophage marker) was used to analyze the extent of inflammation in the regenerated area. These results showed less inflammation (red, F4/80) within the regenerated area (E-MyHC (green) positive myofibers) in the muscles of mice injected with $p65^{+/-}$ MDSCs compared to the untreated muscles (**Fig. 9**). The use of NF-kappa blockade may be useful to improve the regeneration index of hMDCs in the skeletal muscle of SCID/MDX mice.

Figure 9

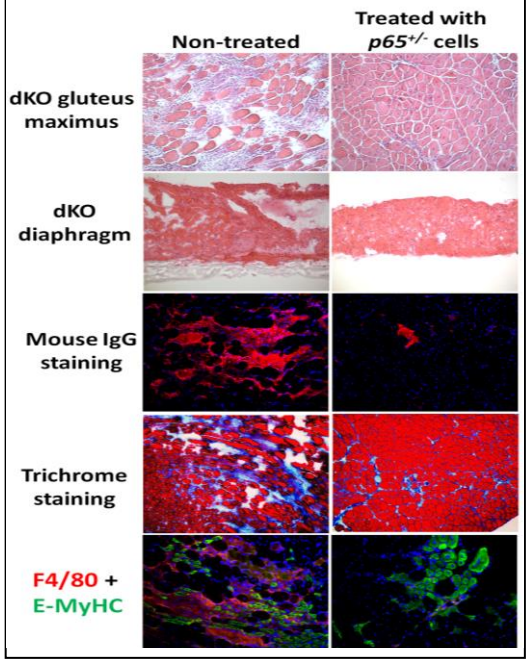

Progress made from 9-1-09 to 8-31-10

The overall goal of Technical Objective 1 is to identify the optimal human muscle derived cell type for skeletal muscle regeneration. We have completed several aspects of Technical Objective 1, namely – 1) isolation of FACS-defined populations of myoblasts, myo-endothelial cells and pericytes, 2) side-by-side comparison of in vitro myogenic differentiation potential of these populations and 3) transplantation of these 3 populations to SCID/mdx animals and in vivo assessment of skeletal muscle regeneration potential of these cells.

After expansion, the cryopreserved human progenitor skeletal muscle cells (cryo-hPSMCs) were examined by immunocytochemistry for cell surface marker expression. The majority of the cryopreserved skeletal muscle cells expressed desmin and CD56, and to a lesser extent, CD146 (**Figure 1**). Only a fraction of cells expressed α-SMA, CD144, vWF or UEA-1R. As expected with cultured human cells, cells lacked CD34 expression. Our flow cytometry analysis quantitatively confirmed the diverse expressions of cell lineage

Figure 1

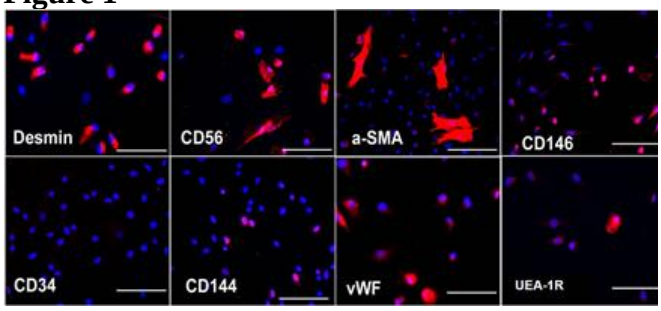

Differential expressions of myogenic and endothelial markers by cryopreserved human skeletal muscle cells. Immunocytochemistry revealed the diverse expressions of various cell lineage markers by cryopreserved skeletal muscle cells after expansion. Nuclei were stained blue with DAPI. (Scale bars = 100µm).

makers by the cells: 77.1±5.7% CD56$^+$, 66.9±8.1% CD146$^+$, 11.2±2.5% UEA-1R$^+$, 0.3±0.1% CD144$^+$, 0.1% vWF$^+$, and no expression of CD34 and KDR (**Figure 2A**). Surprisingly, the number of cryo-hPSMCs positive for CD56, CD146 or UEA-1R decreased dramatically after passage 10 as compared to expression prior to passage 10 (**Figure 2B**).

Figure 2

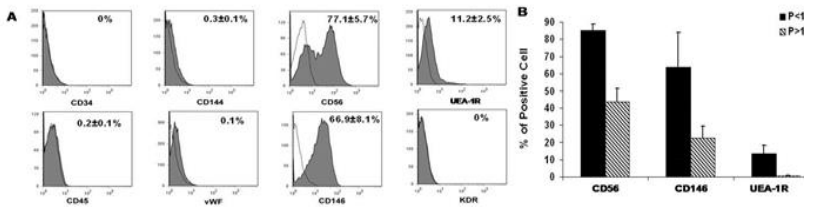

Differential expressions of myogenic and endothelial markers by cryopreserved human skeletal muscle cells. (A) Flow cytometry analysis quantitatively confirmed the diverse cell composition of cryopreserved skeletal muscle cells (B) The number of cryopreserved skeletal muscle cells positive for CD56, CD146, or UEA-1R decreased dramatically when cells were cultured beyond passage 10 (passage>10).

Isolation of myogenic stem/progenitor cells: Using a collection of cell lineage markers, we analyzed cryopreserved cells by flow cytometry for their expression of hematopoietic (CD45), myogenic (CD56), endothelial (UEA-1R), and perivascular (CD146) cell markers. After the exclusion of CD45$^+$ cells, four distinct cell fractions were identified, including myoblasts (Myo) (CD56$^+$/CD45$^-$CD146$^-$UEA-1R$^-$), endothelial cells (ECs) (UEA-1R$^+$/CD45$^-$CD56$^-$CD146$^-$), perivascular stem cells (PSCs) (CD146$^+$/CD45$^-$CD56$^-$UEA-1R$^-$), and myogenic endothelial cells (MECs) which expressed all three cell lineage markers (CD56$^+$UEA-1R$^+$CD146$^+$/CD45$^-$). The composition of long-term cultured cryopreserved muscle cells included 22.58±6.32% Myo, 0.58±0.23 % ECs, 5.92±4.66% PSCs, and 1.16±0.19% MECs (Figure 3). These four cell subsets were subsequently fractionated by FACS (**Figure 3**).

Figure 3

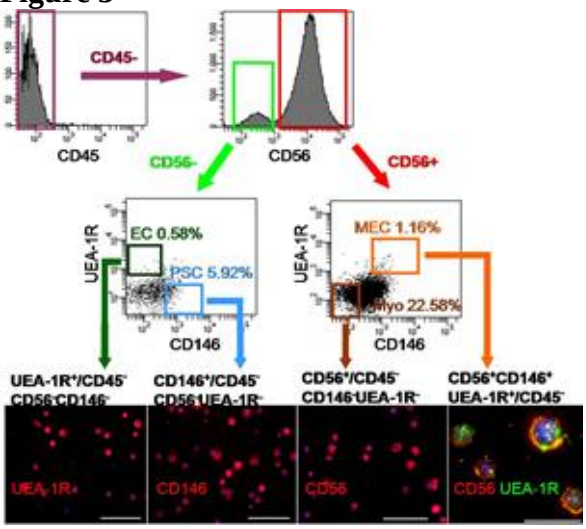

Identification and purification of myogenic stem cells within cryopreserved muscle cell populations. CD45$^-$ cells were separated based on CD56 expression. CD56$^+$ and CD56$^-$ populations were further gated on UEA-1R by CD146 to identify and/or sort four distinct cell populations: myogenic endothelial cells (MEC) (CD56$^+$UEA-1R$^+$CD146$^+$/CD45$^-$), myoblasts (Myo) (CD56$^+$/CD45$^-$CD146$^-$UEA-1R$^-$), perivascular stem cells (PSC) (CD146$^+$/CD45$^-$CD56$^-$UEA-1R$^-$), and endothelial cells (EC) (UEA-1R$^+$/CD45$^-$CD56$^-$CD146$^-$). The purities of the sorted populations were 90.73±4.82%, 92.94±1.23%, 93.86±1.72, and 94.9±0.64, respectively. Immunocytochemistry confirmed the expression of key cell lineage makers by freshly sorted cells: UEA-1R, CD146, and/or CD56. (Scale bars = 100μm except in CD56/UEA-1R double staining = 20μm)

Next, we examined the in vitro differentiation capacity of myoendothelial cells and pericytes. Cells were stimulated for 1 week under conditions of low serum and high density and we observed a marked difference in the ability to undergo myogenic differentiation, as noted by the presence of multinucleated myotubes and positive immunostaining for myosin heavy chain (MHC) and desmin (**Figure 4**).

Finally, to evaluate the myogenic capacities of these purified cell fractions, all freshly sorted cells were immediately transplanted into cardiotoxin-injured skeletal muscles of SCID mice (n=7 per cell fraction). Unpurified muscle cell- and saline-injected muscles were employed as controls. Mouse muscles were harvested 2 weeks post-injection, cryosectioned, and examined by immunohistochemistry to detect muscle fiber regeneration *in vivo*. An antibody

Figure 4

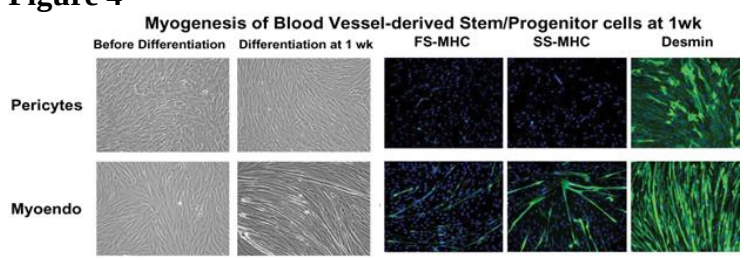

Myoendothelial cells displayed a higher myogenic potential as compared to pericytes. After 1 week in myogenic conditions, we find more myotubes, and greater expression of myosin heavy chain (MHC, green) and desmin (green) in the myoendothelial cell populations as compared to pericytes populations. Nuclei are DAPI stained.

against human spectrin, a myofiber cytoskeletal protein, was used to identify human cell-derived skeletal myofibers in the tissue sections. Quantitative analyses revealed that the myogenic regeneration index, indicated by human spectrin-positive skeletal myofibers per 1×10^3 injected cells, was 71.23±27.15 for MECs, 31.26±11.57 for endothelial cells (ECs), 11.44±3.79 for PSCs, 4.23±1.16 for myoblasts (Myo), and 0.55±0.36 for unsorted muscle cells (Unsort) (**Figure 4**). MECs exhibited the highest regeneration of human skeletal myofibers among all five cell fractions tested (p<0.05) (**Figure 4**). PSCs regenerated more myofibers than the Myo (p>0.05) and the Unsort (p<0.05) (**Figure 5**). Purified myoblasts displayed a higher myogenic capacity than the unsorted cells (p<0.05) (**Figure 5**).

Figure 5

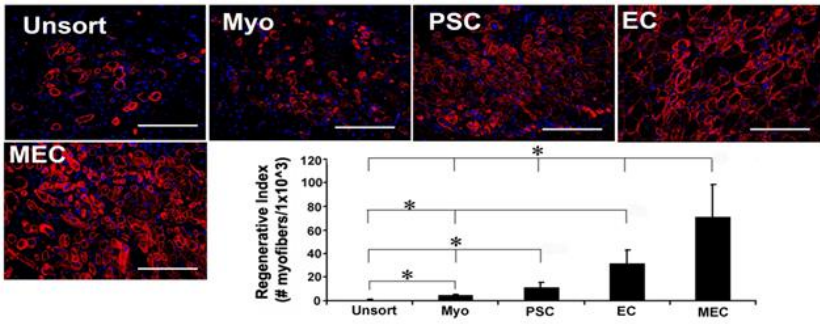

Comparison of myogenic regenerative capacities *in vivo*. Freshly sorted cells were transplanted into the cardiotoxin-injured skeletal muscles of SCID mice. Quantitative analyses of human spectrin-positive skeletal myofibers on tissue sections revealed that myogenic endothelial cells (MEC) mediated the highest myogenic regeneration among all five cell fractions tested (* p<0.05). Injection of perivascular stem cells (PSC) regenerated more human myofibers than injections of myoblasts (Myo) (p>0.05) and unpurified muscle cells (Unsort) (* p<0.05). Finally, myoblasts (Myo) displayed a higher myogenic capacity than unpurified muscle cells (Unsort) (* p<0.05). (Red immunostaining is spectrin, Blue nuclei are DAPI stained)

Similar experiments are currently under way where the cell populations have been transplanted into the gastrocnemius muscles of SCID/mdx mice – a mouse model of Duchenne muscular dystrophy that is dystrophin deficient and also is immune deficient to inhibit the rejection of the injected human cell populations. These in vivo experiments will allow us to compare the myogenic potential of the cells in a DMD model verse the acute muscle injury model used above (i.e., the cardiotoxin injured mice).

KEY RESEARCH ACCOMPLISHMENTS:

Newly acquired accomplishments underlined below.

- Demonstration of prospective isolation of myoblasts, pericytes and myo-endothelial cells derived from human skeletal muscle biopsy, and from both expanded and cryopreserved populations.
- Demonstration that the myo-endothelial cells show a higher level of myogenic potential in vitro as compared to myoblasts and pericytes.
- Demonstration that both expanded and cryopreserved cells continue to show some myogenic potential in vitro.
- Demonstration that the myo-endothelial cells show a significantly higher level of skeletal muscle regeneration in vivo as compared to myoblasts and pericytes.
- Obtained preliminary evidence that PP3 cells isolated from young female skeletal muscle has a higher myogenic capacity than PP3 cells isolated from old skeletal muscle.
- Obtained preliminary evidence that myoendothelial cells isolated from young skeletal muscle is more resistant to the effects of oxidative stress than those isolated from old skeletal muscle.
- Preliminary evidence that young and old myondothelial cells possess a similar proliferation capacity.
- Optimized the growth medium for human myoendothelial cells in order to increase their proliferation rates and reduce their differentiation rates by maintaining their stem-like state in culture.
- Identified an antibody that could be used without significant background staining in our SCID/mdx model of DMD.

- Initiated studies comparing male and female myoendothelial regeneration efficiencies in vitro.
- Identified a physiological testing system (DigiGait system) that could give us excellent physiologic readouts of our transplanted animals.
- Immunomodulatory properties of muscle-derived stem cells are associated with reduced NF-κB/p65 signaling.
- p65 +/- MDSC transplantation can improve muscle histology in dKO mice (mice deficient for both utrophin and dystrophin) after IP transplantation.
- Further preliminary studies have demonstrated human muscle-derived cell engraftment in the SCID/mdx model; however, there is poor to no dystrophin expression in the transplanted muscles of these mice with any of the human population utilized.
- Engraftment has been confirmed with GFP and human MHC-1 antibodies.
- Identification of another potential model of DMD to complete the aims of this grant has led to studies using a dystrophin/utrophin-/- (double knock-out, dKO) model of DMD which has been shown to demonstrate an association between rapid muscle progenitor cell pool exhaustion with the progression of the DMD pathology.
- Further study of the dKO model led us to discover that the MDCs responsible for myogenesis differ from MDCs involved in adipogenesis in the dKO mice.
- We have also demonstrated the role of RhoA signaling in regulating the process *of* heterotopic ossification in the dystrophic muscle of dKO mice which indicates that RhoA may serve as a potential target for repressing injury-induced and congenital heterotopic ossification in humans.
- Found that NF-kB has a broader role in muscle stem and progenitor cells than previously thought, and that the anti-inflammatory molecules secreted by stem cells, such as HGF, could potentially be harnessed to control secondary pathologies of muscle diseases such as DMD.
- Preplate isolated hMDCs also exhibited poor muscle regenerative potentials as was demonstrated by the muscle-derived myo-endo and pericytes in the SCID/mdx model.
- Human dental pulp (hDPSCs) and amniotic fluid stem cells (hAFSCs) also exhibited very poor muscle regenerative potentials as was demonstrated by the muscle-derived myo-endo and pericytes in the SCID/mdx model indicating this was not a muscle stem cell related problem, but probably a problem with the ability of human cells to effectively fuse in vivo.
- We found that Notch-activated human muscle cells demonstrated larger cell engraftment areas in the when transplanted into the skeletal muscle of SCID mdx indicated that the transplantation of human MDCs into dystrophic muscle could potentially be improved by activating Notch signaling prior to their implantation.
- We found that optimizing the *in vitro* environment, by modulating the surface culture conditions with a variable stiffness PDMS substrate and protein coatings; can augment stem cell proliferation and differentiation capacities which could augment the cells transplantation regenerative efficiency.
- Demonstrated that nmMSCs are probably responsible for the accumulation of lipid, calcium deposits, and fibrotic tissue in dKO (dystrophic) mice and suggest that the cells responsible for forming adipocytes and ectopic bone in dystrophic muscle may also inhibit the myogenic potential of muscle progenitor cells, including MDSCs, hindering muscle regeneration. These findings provide insight into potential new approaches to alleviate muscle weakness and wasting in DMD patients by inhibiting the proliferation of nmMSCs in dystrophic muscle.
- We identified mesenchymal-like cells (MLCs) and muscle progenitor cells (MPCs) based on their specific markers and examined the interaction between these two cell populations. We found *in vitro* that MPCs cultured in the presence of MLCs formed larger, more multinucleated myotubes than MPCs cultured alone in differentiation medium. In addition, the transplantation of MPCs and MLCs together increased dystrophin positive fibers in dystrophic muscle compared to the transplantation of PP6 alone, which demonstrated that MLCs promoted the myogenic differentiation of MPCs *in vitro* and muscle regeneration *in vivo*.

- Demonstrated that the stem cell regulatory mechanism of the stem cell niche in the skeletal muscle was mimicked by conjugating activated Notch signaling into a 3D construct used for stem cell transplantation. With this system, we were able to improve the outcome of stem cell transplantation, in the dystrophic skeletal muscle of dKO mice, through the optimization of the stem cell microenviroment.

REPORTABLE OUTCOMES:

Refer to MANUSCRIPTS/REPRINTS, ABSTRACTS Section.

CONCLUSIONS:

Year 1: Our results to date show that even after *in vitro* expansion and cryopreservation, primary human muscle cells harbored various subpopulations of cells. We have identified and purified to homogeneity four distinct cell populations from cryopreserved primary human muscle cells including two stem cell subpopulations: Pericytes (PSCs) ($CD146^+/CD45^-CD56^-UEA\text{-}1R^-$) and myoendothelial cells (MECs) ($CD56^+CD146^+UEA\text{-}1R^+/CD45^-$). Freshly sorted MECs, PSCs, endothelial, and myogenic cells were transplanted into the injured skeletal muscles of SCID mice to examine their myogenic efficacy. MECs displayed the highest muscle regenerative capacity among all cell subsets tested, and PSCs were superior to myoblasts and unpurified cryopreserved primary human muscle cells. These results were consistent with previous observations from the injection of cells isolated from fresh muscle biopsies. Taken together, our results suggest the presence of distinct subpopulations of highly myogenic stem/progenitor cells within expanded cryopreserved primary human muscle cells and support the feasibility of further purifying stem cell fractions from cryopreserved human cells. Most importantly, these findings infer the practicability of prospective isolation of myogenic stem/progenitor cell populations from banked human skeletal muscle cells, highlighting a new technology to further enhance the availability and efficacy of cell-mediated therapies.

Year 2: We have preliminary evidence that there are no differences in the proliferative abilities between old and young human muscle derived cells; however, there appears to be a difference in the MDCs myogenic differentiation capacity and resistance to oxidative stress. We also formulated a medium that optimizes the proliferative capacity of our human MDCs while reducing their premature myogenic differentiation and identified a non-invasive behavioral testing system to detect the functional physiological improvements of the muscles that have been transplanted with our muscle derived stem cells. Moreover, we have demonstrated that NF-κB inhibition stimulates MDSC-mediated muscle regeneration through multiple mechanisms, including through the expression of anti-inflammatory factors that attenuate inflammation and necrosis. These experiments have identified the NF-κB signaling pathway as a potential therapeutic target to enhance muscle regeneration following injury or disease. Our results have demonstrated less inflammation within the regenerating areas of muscles of mice injected with $p65^{+/-}$ MDSCs (MDSCs with ½ the expression of the NF-κB sub unit p65) compared to the untreated muscles; hence the use of NF-kappa blockade may be useful to improve the regeneration index of human muscle-derived stem cells in the skeletal muscle of SCID/MDX mice and potentially in the skeletal muscle to DMD patients.

Year 3: SCID/mdx mice skeletal muscle generates high levels of background when immunostained with an antibody against "human dystrophin", which has been an ongoing problem with this animal model. We have been performing additional tangential experiments on another model of DMD that is deficient for both dystrophin and utrophin known as the double-knock out (dKO) mouse. This model was being used because its pathophysiology more accurately resembles that of DMD patients and we felt might better accommodate the experiments outline in this grant, since we were experiencing the technical problems with the SCID/mdx model. In a set of experiments performed on the dKO mice, we demonstrated that MPCs isolated from the skeletal

muscle of old dKO mice have a reduced ability to proliferate and differentiate compared to MPCs isolated from young mice. Moreover, the numbers of Pax7 positive cells *in vivo* undergo a rapid decline in the skeletal muscle of dKO mice during aging and disease progression. This study suggested that the exhaustion of stem cells contributes to the histopathology associated with DMD and that blocking the exhaustion of muscle progenitor cells and stem cell-mediated therapy could be used as a potential clinical strategy to treat muscle disease. In another set of experiments we found that dKO-RACs, mesenchymal progenitor cells in skeletal muscle, may contribute to adipogenesis and are responsible for ectopic fat cell formation within skeletal muscle in pathological conditions such as DMD. Therefore, targeting RACs to block adipogenesis in skeletal muscle may open new opportunities to treat muscle diseases. We also found that DMD mouse models featuring different severities of muscular dystrophy may have varied potentials for developing HO or fatty infiltration in the dystrophic muscle, and RhoA signaling might be a critical mediator of the determining these differential fates, including the progression towards HO, fatty infiltration, or normal muscle regeneration. In another set of experiments we found that NF-kB has a broader role in muscle stem and progenitor cells than previously thought, and that the anti-inflammatory molecules secreted by stem cells, such as HGF, could potentially be harnessed to control secondary pathologies of muscle diseases such as DMD.

Year 4: This year's major focus was to continue to determine why we were experiencing the transplantation difficulties with the SCID/mdx mice. It was imperative to determine why the SCID/mdx mice were generating such high levels of background when injected with hMDCs and whether the hMDCs were actually engrafting and we continued to try and determine why we were experiencing the problems and to try and identifying potential ways of improving the hMDCs engraftment efficiency in this model. Besides the proposed human cell types of pericytes and myo-endo cells we utilized human MDCs isolated via the preplate technique, which is a population of cells that is more heterogeneous in nature and contains both the myo-endo cell and pericyte sub-populations. We found that the hMDCs isolated by the preplate technique expressed mesenchymal stem cell markers CD73, CD90, CD105 and CD44 and also expressed the myogenic marker CD56 and the pericyte marker CD146. The in vivo results indicated that they could engraft within the muscle; however, their muscle fiber fusion and regeneration capacities were extremely poor and no human dystrophin expression could be detected. We also compared these latter three populations to other human cell populations isolated from dental pulp and amniotic fluid, respectively, to determine if the engraftment problems were related to the stem cell type. This study demonstrated the utility of demethylation to induce hAFSCs and hDPSCs to differentiate towards the myogenic lineage in vitro and, to a very limited degree, engraft and produce dystrophin. The positive fibers observed were very few and could represent revertant myofibers. We therefore conclude that like the myo-endo, pericytes, and preplate isolated MDCs, the hAFSCs and hDPSCs could engraft but could only participate in myofiber regeneration to a very limited degree. Moreover we performed a study to see if we could improve the cells transplantation efficiency by activating the Notch signally pathway, which has been described previously to be necessary for maintaining the stem cell niche in skeletal muscle. We found that compared to the skeletal muscle transplanted with untreated control cells, that there were obviously more regenerating myofibers and larger cell engraftment observed in the skeletal muscle transplanted with the Notch-activated human muscle cells, which indicated that the transplantation of human MDCs into dystrophic muscle could potentially be improved by activating Notch signaling prior to their implantation. Finally, in an attempt to further improve engraftment efficiency we grew the cells on a variety of different substrates with varying degrees of surface elasticity. The findings of this study support the view that optimizing the *in vitro* environment, by modulating the surface culture conditions with a variable stiffness PDMS substrate and protein coatings; can augment stem cell proliferation and differentiation capacities. Future cell therapies implemented for tissue repair may significantly benefit from the application of primary cells isolated and expanded on PDMS surfaces with protein coatings.

Year 5: Unfortunately, during the extension period in year 5 we still could not acquire reasonable results in the mdx/SCID mice. We are not sure if it is the cells, the model or a combination of both that is to blame, the cells

simply do not fuse in this xenotransplantation model. Since fusion was our readout on the successful regenerative ability of the cells and fusion was minimal at best with all the cell types tested, we could not perform the proposed investigations to compare sex and age differences of the cells. We did however, explore several tangential projects that afforded us with some very interesting results and are described below for our extension in year 5. During the last year much effort was put toward completing and submitting the manuscripts that were compiled based on the results we acquired during the funding period of this grant. The following is a list of recent papers and abstracts that we have completed during the last year of the project.

Papers:

1) Pisciotta, A, Riccio M, Gianluca C, Lu A, La Sala G, Bruzzesi G, Ferrari A, **Huard J** and De Pol A. Stem cells isolated from human dental pulp and amniotic fluid improve the dystrophic phenotype of skeletal muscle in mdx/SCID mice. In submission for publication 2014.
2) Xiaodong Mu, Ying Tang, Aiping Lu, Koji Takayama, Bing Wang, Kurt Weiss, and **Johnny Huard**. The Beneficial Effect of Glucocorticoid in Dystrophic Muscle is Mediated Through a Reduction of Stem Cell Exhaustion & Senescence. In submission (J. FASEB). 2014.
3) Xiaodong Mu, Ying Tang, Aiping Lu, Koji Takayama, Arvydas Usas, Bing Wang, Kurt Weiss, and **Johnny Huard**. The role of Notch signaling in muscle progenitor cell exhaustion and the rapid onset of histopathology in muscular dystrophy. In revision. Human. Molecular Genetics. 2014.
4) Lu A, Poddar M, Tang Y, Proto J, Sohn J, Mu X, Oyster N, Wang B, **Huard J**. "*Rapid Depletion of Muscle Progenitor Cells in Dystrophic mdx/utrophin-/- Mice" , Hum Mol Genet*. 2014 Apr 29. pii: ddu194. [Epub ahead of print] PMID:24781208
5) Fox IJ, Daley GQ, Goldman SA, **Huard J**, Kamp TJ, Trucco M Stem cell therapy. Use of differentiated pluripotent stem cells as replacement therapy for treating disease. Science. 2014 Aug 22;345(6199):1247391. doi: 10.1126/science.1247391.

Abstracts:

1) Li H; Lu A; Tang Y; Wang B; **Huard J**. "Dystrophic Systemic Milieu Plays an Important Role in the Muscle and Bone Abnormalities in Duchenne Muscular Dystrophy" ASBMR annual meeting, September 12-15, 2014. Houston, TX.

2) Sohn J, Tang Y, Wang B, Lu A**, Huard J**. "Mesenchymal progenitor cells (MPCs) responsible for ectopic fat accumulation in dystrophic muscle may also impair the myofiber regeneration of muscle progenitors in skeletal muscle of utrophin/dystrophin double knockout mice." ASGCT 17th Annual Meeting, May 21-24, 2014 in Washington, DC, USA.

3) Proto J, Tang Y, Lu A, Poddar M, Chen CW, Beckman S, Imbrogno K, Hannigan T, Mars W, Wang B, **Huard J.** "HGF is critical for the beneficial effect of NF-κB/p65 inhibition in dystrophic muscle" ASGCT 17th Annual Meeting, May 21-24 in Washington, DC, USA.

4) Mu X, Gao, J, Wang Y, Weiss K, **Huard J.** "Mimicking the stem cell niche in diseased muscle by Notch activation" ASGCT 17th Annual Meeting, May 21-24 in Washington, DC, USA.

5) Sohn J, Tang Y, Ascoli A, Lu A, Wang B, **Huard J. "**Isolation and characterization of non-myogenic mesenchymal stem cells (non-MMSCs) that play a role in the skeletal muscle pathology of utrophin/dystrophin double knockout mice." Experimental Biology Annual Meeting, April 26-30, 2014, San Diego, CA.

6) Lu A, Proto J, Niedernhofer L, Robbins P, Wang B, **Huard J**."NF-κB inhibition delays the effects of aging in muscle derived stem cells" 2014 Annual Orthopaedic Research Society Meeting in New

Orleans, LA. March 15-18, 2014.

7) Mu X, "The Beneficial Effect Of Steroid Therapy In DMD Is Mediated Through A Reduction In Stem Cell Exhaustion" 2014 Annual Orthopaedic Research Society Meeting in New Orleans, LA. March 15-18, 2014.

8) Thompson SD, Lavasani M, Ahani B, Reddy P, Sun Y, Jallerat Q, Feinberg AW, **Huard J**. "Proliferation and Differentiation Capacities of Muscle Derived Stem/Progenitor Cells Cultured on Polydimethylsiloxane Substrates of Varying Elastic Modulus and Protein Coating" 2014 Annual Orthopaedic Research Society Meeting in New Orleans, LA. March 15-18, 2014.

9) Sohn J, Tang Y, Wang B, Lu A, **Huard J**. "Mesenchymal progenitor cells (MPCs) involvement in ectopic fat formation in muscular dystrophy" 2014 Annual Orthopaedic Research Society Meeting in New Orleans, LA. March 15-18, 2014.

10) Proto J, Tang Y, Lu A, Poddar M, Chen CW, Beckman S, Imbrogno K, Hannigan T, Mars W, Wang B, **Huard J.** "A novel role for HGF in the beneficial effects of NF-kB blockade on dystrophic muscle" 2014 Annual Orthopaedic Research Society Meeting in New Orleans, LA. March 15-18, 2014.

REFERENCES:

Year 5

1. Gharaibeh, B., et al., Nat Protoc, 2008. 3(9): p. 1501-9.
2. Lu, A., et al., Hum Mol Genet, 2014.
3. Descamps, S., et al., Cell Tissue Res, 2008. 332(2): p. 299-306.
4. Arnold, L., et al., J Exp Med, 2007. 204(5): p. 1057-69.
5. Qu-Petersen, Z., et al., J Cell Biol, 2002. 157(5): p. 851-64.
6. Gharaibeh, B., et al., Nat Protoc, 2008. 3(9): p. 1501-9.
7. Murphy, M.M., et al., Development, 2011. 138(17): p. 3625-37.
8. Sacco A, et al., Cell. 2010;143(7):1059-71. PMCID: 3025608.
9. Song M, et al., Stem Cell Res Ther. 2013;4(2):33. PMCID: 3706820.
10. Lavasani M,et al., Nat Commun. 2012;3:608. PMCID: 3272577.
11. Bjornson CR, etal., Stem Cells. 2012;30(2):232-42. PMCID: 3384696.
12. Brohl D, et al., Dev Cell. 2012;23(3):469-81.
13. Conboy IM, et al., Science. 2003;302(5650):1575-7.
14. Dash TK and Konkimalla VB. J Control Release. 2012;158(1):15-33.

Years 1-4

1. Zhang et al. 2006. Tissue Eng 12, 2813.
2. De Coppi et al. 2007 Nat Biotechnol 25, 100.
3. Riccio et al. 2010. Eur J Histochem 54, 4.
4. N.S. Ye et al. 2006. Stem Cells Dev 15, 665.
5. Antonitsis et al. 2008 Thorac Cardiovasc Surg 56, 77.
6. Duan et al. 2010. Gen Comp Endocrinol 167, 344.
7. Boonen KJ and Post MJ, Tissue Eng Part B Rev. 2008;14(4):419-31.
8. Gopinath SD, et al., 2008;7(4):590-8.
9. Chakkalakal JV, et al., Nature. 2012;490(7420):355-60.
10. Brohl D, et al., Dev Cell. 2012;23(3):469-81.

11. Lepper C, et al., Cell Stem Cell. 2012;11(4):443-4.
12. Kuang S, et al., Cell. 2007;129(5):999-1010. PMCID: 2718740.
13. Zhang H, et al. Tissue Eng Part A. 2010;16(11):3441-8. PMCID: 2965194.
14. Lee JY, et al., *J Cell Bio* 150, 1085-1100 (2000).
15. Kuroda R, et al., *Arthritis Rheum* 54, 433-422 (2006).
16. Oshima H, etl al., *Mol Ther* 12, 1130-1141.
17. Lavasani M, et al., *Nat Comm* 3: e608 (2012).
18. Gilbert PM, et al., *Science* 329, 1078-1081 (2010).
19. Engler AJ, et al., *Cell* 126, 677-689 (2006).
20. Palchesko RN, et al., *PLoS ONE* 7(12): e51499 (2012).

APPENDICES:

Refer to Manuscripts/Reprints, Abstracts Section

MANUSCRIPTS/REPRINTS, ABSTRACTS:

1. Chen C, Okada M, Tobita K, Crisan M, Péault B, Huard J; **Transplantation of Purified Human Skeletal Muscle-Derived Pericytes Reduce Fibrosis in Injured Ischemic Muscle Tissues**. Orthopaedic Research Society; March 6-9, 2010; New Orleans, La **(Appendix 1)**

2. Aiping Lu, Qing Yang, Minakshi Poddar, Bing Wang, Denis C. Guttridge, Paul D. Robbins, Johnny Huard; **Transplantation of p65 Deficient Stem Cells Improved the Histopathology of Skeletal Muscle in Dystrophic Mice.** Orthopaedic Research Society; 2011 ORS Annual Meeting; January 13-16, 2011; Long Beach, CA. **(Appendix 2)**

3. Proto, J., Lu, A., Robbins, P.D., Huard, J; **Immunomodulatory properties of muscle-derived stem cells associated with reduced NF-κB/p65 signaling.** Orthopaedic Research Society; 2011 ORS Annual Meeting; January 13-16, 2011; Long Beach, CA. **(Appendix 3)**

4. Aiping Lu, Jonathan Proto, Lulin Guo, Ying Tang, Mitra Lavasani, Jeremy S. Tilstra, Laura J. Niedernhofer, Bing Wang, Denis C. Guttridge, Paul D. Robbins, Johnny Huard J.H. **NF-κB negatively impacts the myogenic potential of muscle-derived stem cells.** *Molecular Therapy* 2012; 20(3): 661-8. PMID: 22158056 **(Appendix 4)**

5. Zheng B, Chen C, Li G, Thompson S, Poddar M, Peault B, Huard J. **Isolation of myogenic stem cells from cultures of cryopreserved human skeletal muscle.** Cell Transplantation 2012 Apr, 21(6):1087-93. PMID: 22472558 **(Appendix 5)**

6. Bo Zheng, Guangheng Li, William Chen, Bridget M Deasy, Jonathan B Pollett, Bin Sun, Lauren Drowley, Burhan Gharaibeh, Arvydas Usas, Alison Logar, Bruno Peault , Johnny Huard; **Human Myogenic Endothelial Cells Exhibit Chondrogenic and Osteogenic Potentials at the Clonal Level.** *Journal of Orthopaedic Research.* 2013 Jul;31(7):1089-95. PMID: 23553740 (**Appendix 6)**

7. Aiping Lu; Jonathan Proto; Xiaodong Mu; Ying Tang; Minakshi Poddar; Bing Wang; Johnny Huard**. Progression of muscular dystrophy in dystrophin/utrophin-/- mice is associated with rapid muscle progenitor cell exhaustion.** Orthopaedic Research Society; 2013 ORS Annual Meeting; January 26-30, 2013; San Antonio, TX **(Appendix 7)**

8. Jihee Sohn, Ying Tang, Bing Wang, Aiping Lu, Johnny Huard. **Muscle-derived cells (MDCs) responsible for myogenesis differ from MDCs involved in adipogenesis in dystrophin/utrophin-/- mice.** Orthopaedic Research Society; 2013 ORS Annual Meeting; January 26-30, 2013; San Antonio, TX **(Appendix 8)**

9. Xiaodong Mu, Arvydas Usas, Ying Tang, Aiping Lu, Jihee Sohn, Bing Wang, Kurt Weiss, and Johnny Huard. **RhoA signaling regulates heterotopic ossification and *fatty infiltration* in dystrophic skeletal muscle.** Orthopaedic Research Society; 2013 ORS Annual Meeting; January 26-30, 2013; San Antonio, TX **(Appendix 9)**

10. Proto, J., Tang, Y; Lu, A., Robbins, P.D., Wang, B. Huard, J. **Suppression of skeletal muscle inflammation by muscle stem cells is associated with hepatocyte growth factor in wild type and *mdx*;p65$^{+/-}$ mice.** Orthopaedic Research Society; 2013 ORS Annual Meeting; January 26-30, 2013; San Antonio, TX **(Appendix 10)**

11. Chen WC, Park T, Murray R, Zimmerlin L, Lazzari L, Huard J, Peault B. **Cellular Kinetics of Perivascular MSC Precursors**, *Stem Cells International.* Vol. 2013:983059 (18) 2013. (**Appendix11**)

12. Mu X, Usas A, Tang Y, Lu A, Wang B, Weiss K, Huard J**. RhoA mediates defective stem cell function and heterotopic ossification in dystrophic muscle of mice**, Mu X, Usas A, Tang Y, Lu A, Wang B, Weiss K, Huard J. *FASEB J.* 2013 Sep;27(9):3619-31. doi: 10.1096/fj.13-233460. Epub 2013 May 23. PMID:23704088 (**Appendix 12**)

13. Pisciotta, Alessandra; Lu, Aiping; Gharaibeh, Burhan; De Pol, Anto[1]; Huard, Johnny, **Enhanced myogenic potential of human dental pulp and amniotic fluid stem cells by use of a demethylation agent and conditioned media.** Orthopaedic Research Society; 2014 ORS Annual Meeting; March 15-18, 2014; New Orleans, LA (**Appendix13**)

14. Seth David Thompson, Mitra Lavasani, Bahar Ahani, Prerana Reddy, Yan Sun, Quentin, Jallerat, Adam W. Feinberg, Johnny Huard. **Proliferation and Differentiation Capacities of Muscle Derived Stem/Progenitor Cells Cultured on Polydimethylsiloxane Substrates of Varying Elastic Modulus and Protein Coating**. Orthopaedic Research Society; 2014 ORS Annual Meeting; March 15-18, 2014; New Orleans, LA (**Appendix 14**)

15. Jihee Sohn, Ying Tang, Aiping Lu, Bing Wang, Johnny Huard**. The role of non-myogenic mesenchymal stem cells (nmMSCs) in the skeletal muscle pathology of muscular dystrophy.** Orthopaedic Research Society; 2015 ORSAnnual Meeting; March 28-31-2015; Las Veges, NV **(Appendix 15)**

16. Aiping Lu; Jihee Sohn; Berkcan Akpinar; Johnny Huard**. Interaction between myogenic and non-myogenic progenitor cells during muscle regeneration.** Orthopaedic Research Society; 2015 ORSAnnual Meeting; March 28-31-2015; Las Veges, NV **(Appendix 16)**

17. Xiaodong Mu, Jin Gao, Yadong Wang, Kurt Weiss, and Johnny Huard. **Mimicking the stem cell niche in diseased muscle by Notch activation.** American Society of Gene and Cell Therapy. 2014 ASGCT Annual Meeting; May 20-24th; Washington, DC **(Appendix 17)**

18. Lu A, Poddar M, Tang Y, Proto J, Sohn J, Mu X, Oyster N, Wang B, Huard J. **"Rapid Depletion of Muscle Progenitor Cells in Dystrophic mdx/utrophin-/- Mice"** , *Hum Mol Genet*. 2014 Apr 29. pii: ddu194. [Epub ahead of print] PMID:24781208 (**Appendix 18**)

19. Xiaodong Mu, Ying Tang, Aiping Lu, Koji Takayama, Arvydas Usas, Bing Wang, Kurt Weiss, and Johnny Huard. **The role of Notch signaling in muscle progenitor cell exhaustion and the rapid onset of histopathology in muscular dystrophy. (Under revision for *Human Molecular Genetics*) (Appendix 19)**

20. Alessandra Pisciotta, Massimo Riccio, Gianluca Carnevale, Aiping Lu, Giovanni B. La Sala, Giacomo Bruzzesi, Adriano Ferrari, Johnny Huard, Anto De Pol. **Stem cells isolated from human dental pulp and amniotic fluid improves the dystrophic phenotype of skeletal muscle in mdx/SCID mice. (In preparation for submission to *Stem Cells*) (Appendix 20)**

21. Jihee Sohn, Johnny Huard, Anthony Ascoli, Tim Hannigan, Bing Wang, Aiping Lu, Ying Tang. **Isolation and characterization of non-myogenic mesenchymal stem cells that play a role in skeletal muscle pathology of utrophin/dystrophin double knockout mice. (In preparation for submission to *Human Molecular Genetics*) (Appendix 21)**

22. Jihee Sohn and Johnny Huard. **Sexual dimorphism in skeletal muscle and muscle stem cells. (Review paper in preparation) (Appendix 22)**

23. Fox IJ, Daley GQ, Goldman SA, **Huard J**, Kamp TJ, Trucco M. **Stem cell therapy. Use of differentiated pluripotent stem cells as replacement therapy for treating disease.** *Science.* 2014 Aug 22;345(6199):1247391. doi: 10.1126/science.1247391.

Sub-Project 2: Generation of human hepatocytes from patient-specific stem cells for treatment of life-threatening liver injury
PIs: David Perlmutter and Ira J. Fox

INTRODUCTION: (New data is underlined in the text of the Introduction and body.)
These studies are focused on generating human hepatocytes from patient-specific stem cells for the treatment of life-threatening liver injury. Two technical objectives were proposed: 1) Determine the extent to which human patient-specific, induced pluripotent stem (iPS) cells can be differentiated into human hepatocytes, and 2) Determine the extent to which the PiZ mouse model of alpha-1-antitrypsin (AT) deficiency can be developed as a platform for pre-clinical testing of hepatic stem cell transplantation as a treatment for severe liver injury and disease. In order to accomplish these objectives, we have generated 3 human iPS cell lines from normal patients and 12 iPS cell lines from patients with alpha-1-antitrypsin deficiency (ATD). These cell lines have now been characterized and 7 of which have been differentiated into hepatocytes. We have demonstrated that iPS cell-derived hepatocyte-like cells (iHeps) from ATD patients recapitulate the pathobiological defects observed in ATD primary hepatocytes. We show decreased AT secretion and decreased rate of disappearance of intracellular AT in ATD iHeps compared to normal iHeps. We also show that iHeps from ATD patients with severe liver disease have less efficient degradation of intracellular AT compared to ATD patients with no liver disease. More importantly, the presence of intracellular inclusions, which is a hallmark of the disease, was seen only in iHeps from individuals with severe liver disease. We have demonstrated that iPS derived cells can be transplanted in rodents that are models of human disease and that engraftment and expansion of the derived hepatocytes corrects the disease. Finally, we have further determined the ability of donor hepatocytes to expand in the PiZ mouse, and we have generated PiZ mice on an immune-deficient background and have begun studies showing engraftment and expansion of pluripotent stem cell-derived hepatocytes in these mice.

BODY:
Technical Objective #1: Determine the extent to which human patient-specific, inducible pluripotent stem (iPS) cells can be differentiated into primary human hepatocytes.
Hypothesis: *Protocols that successfully differentiate mouse and human embryonic stem (ES) cells toward a hepatocyte phenotype will be effective in differentiating human skin cell-derived iPS cells into liver cells.*

1.1. Generation of human induced pluripotent stem cells (iPS cells).
We hypothesized that patient specific iPS cells could be generated from primary human cells, including hepatocytes, and that under appropriate conditions, the iPS cells could be induced to differentiate back to hepatocytes that could be used as cellular therapy to treat the liver defect. Here, we report the generation of multiple human iPS cell lines from primary human cells following exposure to either lentiviral, excisable lentiviral stem cell cassette or plasmid constructs carrying reprogramming factors. In **Table 1** and **2**, we characterize lines derived from normal controls, and patients with ATD. We have characterized the lines for markers of pluripotency, including alkaline phosphatase activity, nuclear NANOG, OCT3/4 and SOX2 staining, and reactivity to antibodies to the surface markers SSEA-4 and TRA1-60, and confirmed these results by qPCR. In addition, genotyping has been completed on most of the ATD and control iPS cell lines.

Table 1. List of normal iPS cell lines

Source of iPS cell line	Normal human hepatocyte (biopsy)	Normal dermal fibroblast	Normal dermal fibroblast
Vector used for iPS induction	Lentivirus	Excisable Lentiviral Stem Cell Cassette	Non-integrating plasmids
Characterization of Pluripotency			
qPCR	✔	✔	✔
Immunostaining	✔	✔	✔
Teratoma formation	✔	✔	✔
Genotype*	G/G	G/G	G/G
Name of iPS cell line	**HH1591** iPS cells (Wild Type)	**BMC-1** iPS cells (Wild Type)	**NF-IF** iPS cells (Wild Type)

*** G/G: Homozygous for the wild type allele**

Table 2. List of ATD iPS cell lines

Source of iPS cell line	AT deficient human hepatocyte (Biopsy, CHP HH1764 (7/21/2010), 10(Y) M	AT deficient human hepatocyte (Biopsy, Einstein College of Medicine)	AT deficient lung fibroblast (Biopsy)	AT deficient lung fibroblast (Biopsy)	AT deficient lung fibroblast (Biopsy)	AT deficient lung fibroblast (Biopsy)
Vector used for iPS induction	Lentivirus	Non-integrating plasmids	Lentivirus	Excisable Lentiviral Stem Cell Cassette	Excisable Lentiviral Stem Cell Cassette	Excisable Lentiviral Stem Cell Cassette
Characterization of Pluripotency						
qPCR	✔	✔	✔	✔	✔	✔
Immunostaining	✔	✔	✔	✔	✔	✔
Teratoma formation	✔	✔	✔	✔	✔	✔

Genotype	A/A	A/A	A/A	A/A	A/A	A/A
Name of iPS cell line	**ATH-1** iPS cells (Severe LD ATD)	**AAT2** iPS cells (Severe LD ATD)	**AT-10 c1-6** iPS cells (Mild LD ATD) 6 other clones	**100-3-Cr-1** iPS cells (Mild LD ATD)	**102-37B-Cr-2** iPS cells (Mild LD ATD)	**103-3-Cr-1** iPS cells (Mild LD ATD)

*** A/A: Homozygous for the Z allele**

1.2. Differentiation of human iPS cells into hepatocytes.

We have now generated iHeps from normal and ATD iPS cell lines in a manner similar to what we have published[1], and using a variation on the technique described by Si-Tayeb[2]. **Figure 1** illustrates the morphologic changes that occur during differentiation. **Figure 2** shows that the differentiated H1 hES cells and ATD iPS cells exhibit several ultrastructural features seen in primary human hepatocytes.

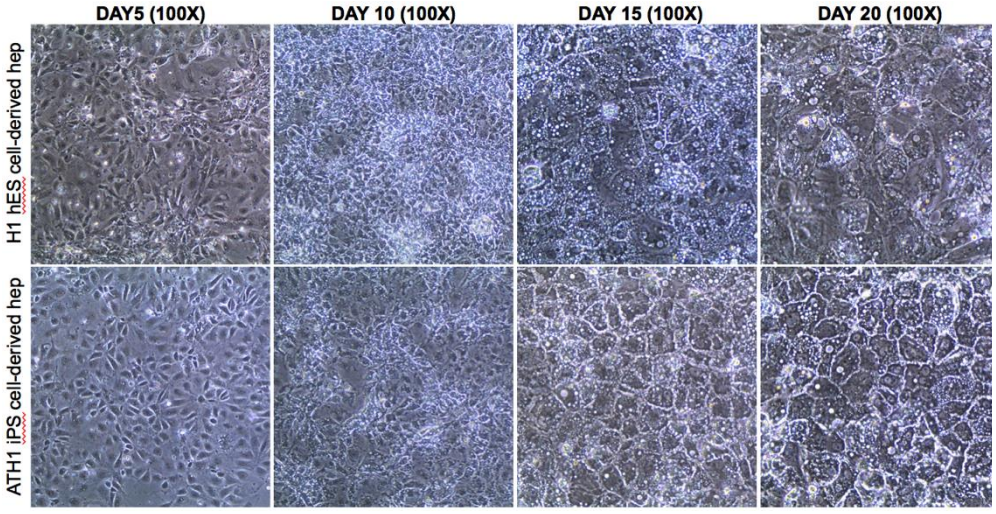

Figure 1. Morphologic changes during hepatocyte differentiation of H1 hES cell and ATD iPS cell after each stage of the differentiation. Morphology of iPS cells after the phase of definitive endoderm (day 5), hepatic specification (day 10), hepatic induction (day 15), and hepatic maturation (day 20).

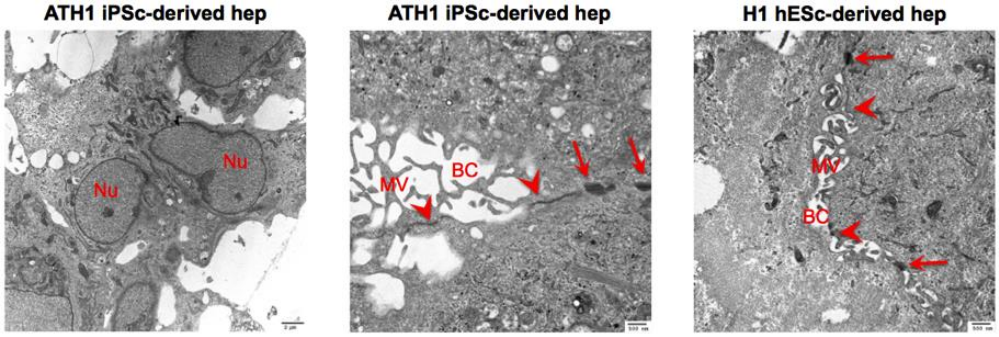

Figure 2. Electron micrograph of H1 hES cells and ATD iPS cells following hepatocyte-specific differentiation. Shown are the nuclei (Nu), bile canaliculi (BC), microvilli (MV), tight junctions (arrowhead), and desmosomes (arrow).

1.3. Analysis of differentiated ATD iPS cells.

We performed several experiments to determine whether ATD iHeps recapitulate the defect observed in primary human hepatocytes from ATD patients. In **Figure 3**, we show that although normal and ATD iHeps secreted equal levels of albumin, ATD iHeps secreted only ~25% of the level of AT secreted by normal wild type (WT) iHeps. We also show using pulse chase analysis that iHeps from patients with ATD accurately model both intracellular accumulation and diminished secretion characteristic of the misfolded ATZ molecule (**Figure 4, A-B**). Using biochemical analysis, we show that ATD iHeps recapitulate the processing of the ATZ molecule which accumulates as a partially glycosylated intermediate (**Figure 4C**). We demonstrate by double label immunofluorescence and 3D reconstruction experiments that AT in ATD iHeps accumulates predominantly in

pre-Golgi secretory compartments, some of which co-localize with calnexin and calreticulin and some that do not (**Figure 5**). We also show that similar to primary human hepatocytes from an ATD patient with severe liver disease (severe LD), electron micrograph of severe LD ATD iHeps showed poorly organized and markedly dilated rER (**Figure 6**). While some severe LD ATD iHeps had normal looking organelles, many cells that contained inclusions had obvious accumulation of autophagosomes, abnormal mitochondrial structures and fragmented Golgi remarkably similar to what was seen in severe LD ATD liver sections (**Figure 7**). We next investigated the fate of ATZ in severe LD and no LD ATD iHeps by pulse-chase labeling. We determined that ATZ is degraded more slowly in severe LD iHeps compared to no LD iHeps (**Figure 8**). In **Figure 9**, we show that while severe LD iHeps exhibited markedly dilated rER and globular inclusions, no LD iHeps only exhibited dilated rER but lacked globular inclusions.

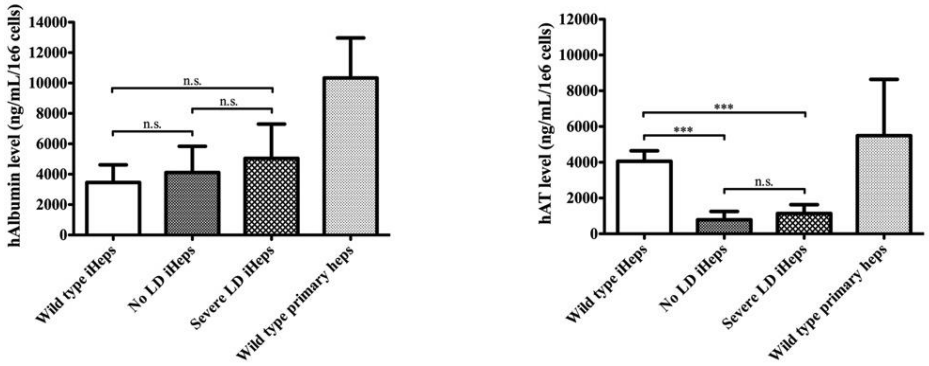

Figure 3. Levels of hAlbumin and hAT secreted *in vitro* over a period of 24 hours. ELISA measuring the amount of hAlbumin and hAT secreted by the wild type iHeps (n=3), no LD iHeps (n=2), severe LD iHeps (n=4), and severe LD primary hepatocytes (n=2) shown as mean ± s.d. ***p<0.001 (one-way ANOVA followed by Bonferroni posttests for each pair of samples).

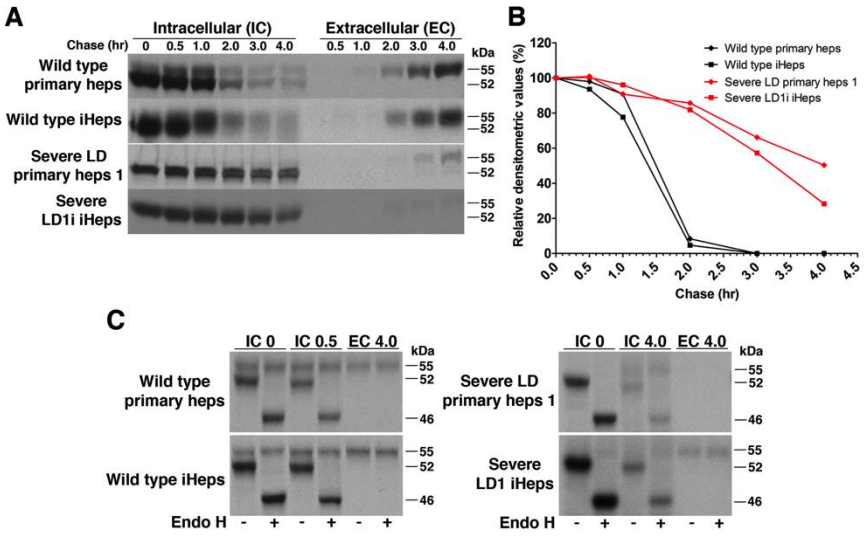

Figure 4. ATD iHeps recapitulate the accumulation and processing of ATZ. (A) Pulse-chase labeling showing intracellular accumulation of AT in severe LD cells but not in wild type cells. (B) Kinetics of the disappearance of AT in severe LD and wild type cells. Values are band densities of IC fractions in (A) relative to IC signal at time 0. Effect of (C) endoglycosidase H digestion on AT in pulse-chase IC and EC fractions of cells at indicated timepoints. (-) mock digestion, (+) endo H digestion.

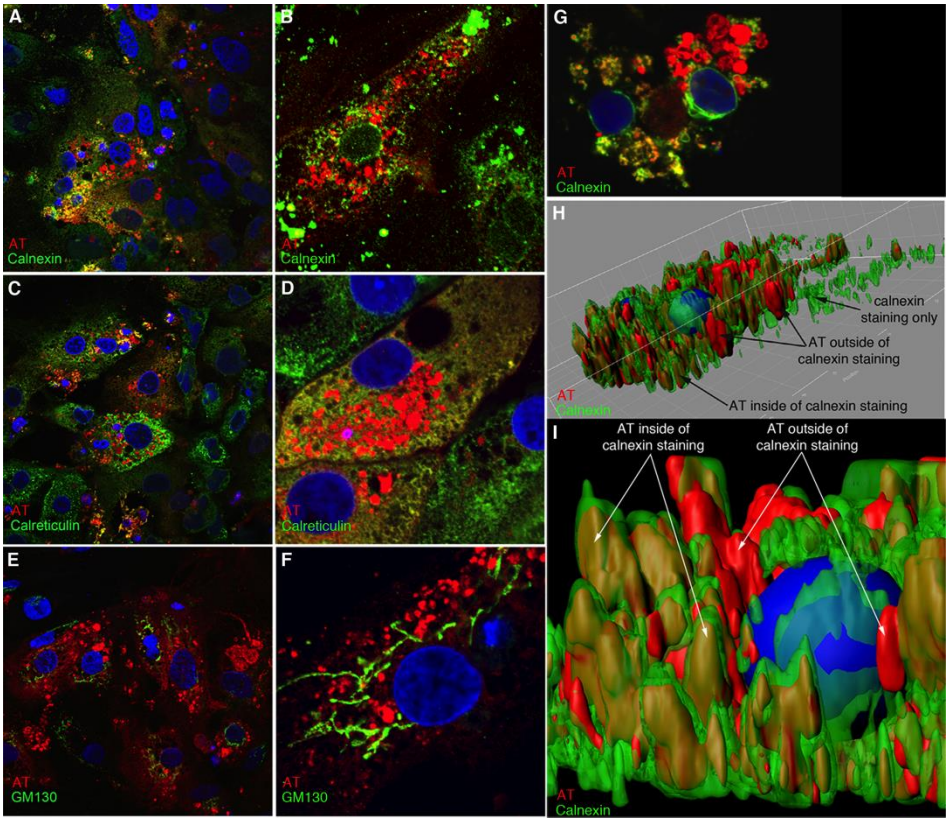

Figure 5. ATZ in severe LD iHeps accumulates in rER and in compartments that are devoid of calnexin, calreticulin, or GM130. Immunofluorescent staining of severe LD iHeps for AT and calnexin (A, B), calreticulin (C, D), or GM130 (E, F). A, C, E (600X), B, D, F (2000X). (G) Single stack image of severe LD iHeps stained for AT and calnexin. (H and I) 3D surface reconstruction of multiple stacks of images of AT/calnexin-stained severe LD iHeps with calnexin signal made partially transparent to reveal AT staining inside calnexin staining. Nuclei are stained blue.

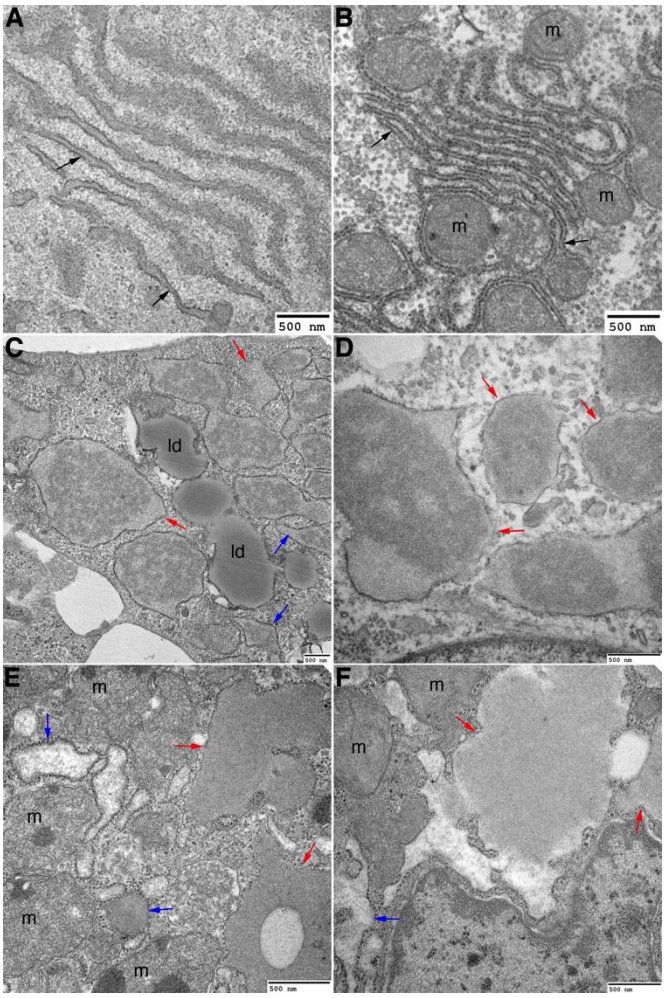

Figure 6. Severe LD iHeps and severe LD liver tissue sections exhibit dilated rER and dilated globular inclusions that are partially covered with ribosomes. Electron micrograph of wild type iHeps (A), wild type liver tissue section (B), severe LD iHeps (C, D), and severe LD liver tissue section (E, F) showing normal rER (black arrows), dilated rER (blue arrows) and dilated globular inclusions that are partially covered with ribosomes (red arrows). m: mitochondria, ld: lipid droplets.

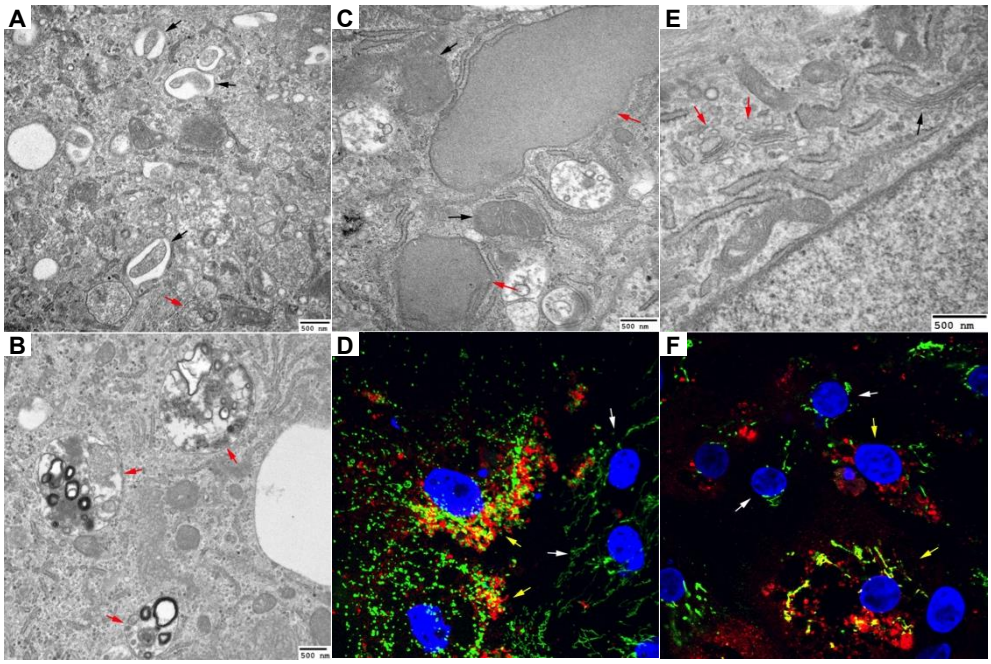

Figure 7. Autophagosomes, abnormal mitochondrial structures and fragmented Golgi are evident severe LD iHeps. (A-B) EM showing the presence of autophagosomes (black arrows) and autophagolysosomes (red arrows). (C) Electron micrograph showing normal mitochondria (black arrows) and enlarged mitochondria (red arrows). (D) Immunofluorescent staining for AT (red), TOM20 (green), and nuclei (blue) showing dilated mitochondria in cells with increased AT accumulation (yellow arrows) compared to cells with minimal AT accumulation (white arrows) (1000X). (E) Electron micrograph of showing normal Golgi (black arrows) and fragmented Golgi (red arrows). (F) Immunofluorescent staining for AT (red), GM130 (green), and nuclei (blue) showing fragmented Golgi in cells with AT accumulation (yellow arrows) compared to cells with minimal AT accumulation (white arrows) (1000X).

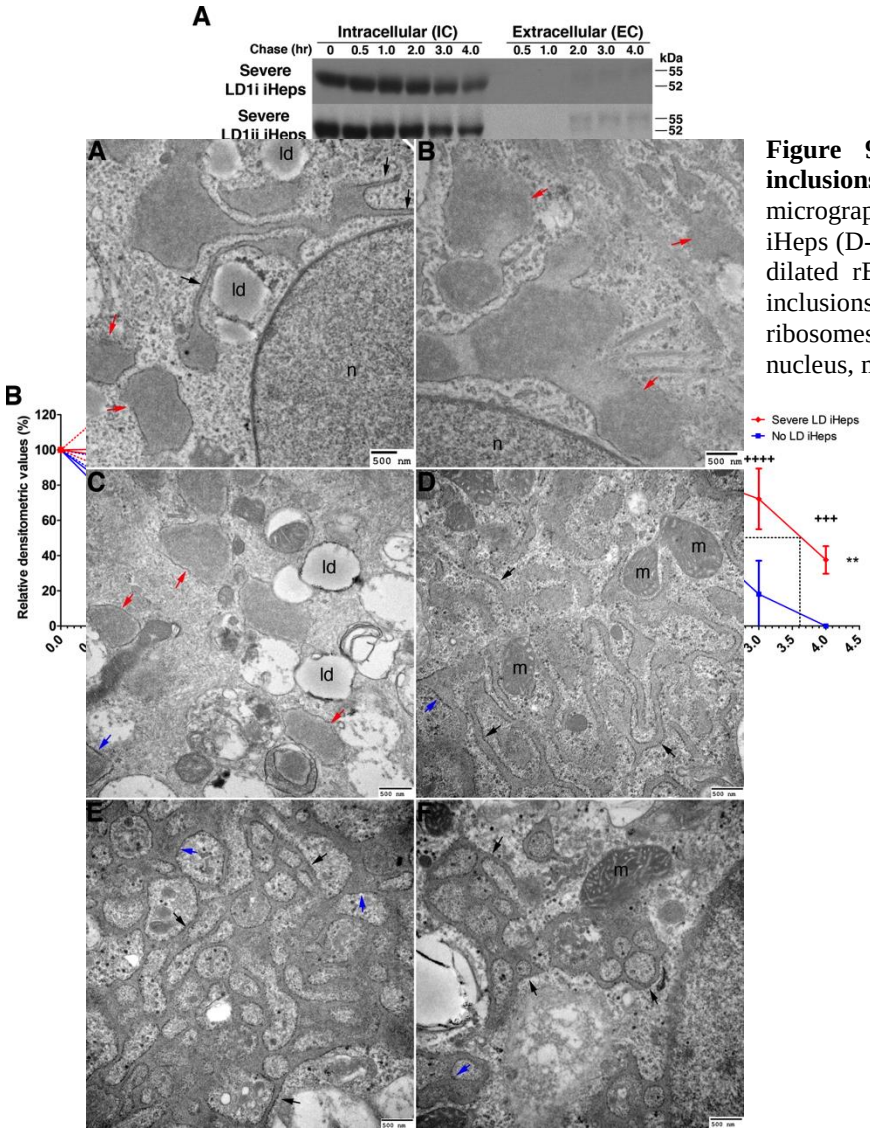

Figure 8. The rate of degradation of intracellular ATZ correlates with liver disease severity in ATD iHeps. (A) Pulse-chase labeling comparing the disappearance of intracellular AT in severe and no LD iHeps. Severe LD1i and LD1ii are replicates from the same iPS cell line. No LD1a and LD1b are different iPS cell clones from the same patient. (B) Kinetics of the degradation of AT in severe and no LD iHeps. Values are band densities of IC fractions in (A), relative to IC signal at time 0. (C) Composite curves of (B) shown as mean ± s.d. Dashed lines represent the half-time for disappearance of intracellular AT. **p<0.005 (two-way repeated measures ANOVA), ++p<0.01, +++p<0.001, ++++p<0.0001 (Bonferroni posttests at each time point). Although densitometric values for the no LD iHeps appear to reach zero, the absolute values are <1% in B and C.

Figure 9. Dilated rER but no globular inclusions are seen in no LD iHeps. Electron micrograph of severe LD iHeps (A-C) and no LD iHeps (D-F) showing normal rER (black arrows), dilated rER (blue arrows) and dilated globular inclusions that are partially covered with ribosomes (red arrows). ld: lipid droplets, n: nucleus, m: mitochondria.

1.4. Transplantation of human iPS cell-derived hepatocytes with correction of hyperbilirubinemia in the Gunn rat model of Crigler-Najjar syndrome type 1.

To determine the extent to which stem cell-derived human hepatocytes could be engrafted in immune suppressed rat hosts, we transplanted iPS cell-derived hepatocytes into Gunn rat livers by intrasplenic injection [3]. To provide a proliferative advantage to the transplanted cells,

Figure 10. Effect of repopulation of the Gunn rat liver by iPS cell-derived hepatocytes. a, Serum bilirubin levels in the four recipient Gunn rats (diamond, square, open and closed triangles) at the indicated time points after transplantation of human iPS cell-derived hepatocytes are shown as percentage of pre-transplantation levels. Bilirubin levels of untreated age-matched controls are also shown (open circles, mean+SEM of 6 rats). The upper limit of serum bilirubin levels in congenic normal Wistar-RHA rats is shown as a dotted line. b and c, Representative liver sections from a recipient Gunn rat 4-6 months after transplantation of human iPS-derived hepatocytes. b, Immunohistochemical staining for human UGT1A1 showing cell clusters derived from the transplanted cells. c, Dual immunofluorescence staining showed that a majority of cells positive for human serum albumin (green) were also positive for human UGT1A1 (red). The nuclei are stained blue (DAPI). A magnified view is shown in the insert. d-f, HPLC analysis of bilirubin species excreted in the bile of a control Gunn rat, a rat receiving iPS-derived hepatocytes and a congeneic normal Wistar RHA rat is shown. sf, solvent front; ucb, unconjugated bilirubin; bdg, bilirubin diglucuronide; bmg, bilirubin monoglucuronide. Note the difference in the absorbance unit scale in panel c from that in panels d and e.

part of the host liver was irradiated (50Gy) and an adenovirus vector expressing hepatocyte growth factor was injected. For immune suppression, Tacrolimus (2mg/kg) was injected daily beginning 7 days before transplantation. After transplantation, serum bilirubin levels declined, as shown in **Figure 10**, and immuno-histochemistry of liver sections showed clusters of human albumin and UGT1A1-positive cells, and bilirubin conjugates appeared in the bile, indicating function by engrafted, UGT1A1-expressing iPS-derived hepatocytes.

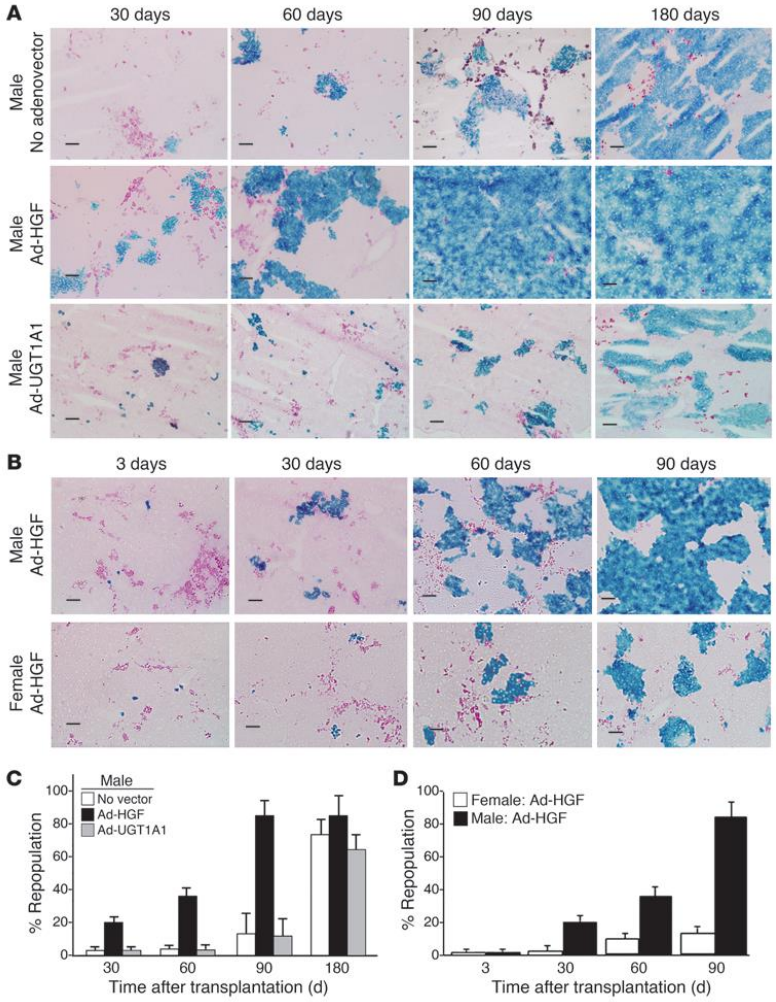

Figure 11. Kinetics of hepatic repopulation in PiZ mice. (A) Ad-HGF administration accelerated repopulation. ROSA26 mouse hepatocytes (1 × 106) were transplanted into male PiZ mice without (upper row) or with (lower row) Ad- HGF (1 × 1011 particles, i.v.). Liver sections were stained for *E. coli* β-gal (blue), and diastase plus PAS (magenta) to visualize AAT-Z globules. Scale bars: 100 μm. Data are from representative mice from each group (n = 6). (B) Repopulation was greater in male recipients. Male and female PiZ mice received Ad-HGF (n = 6). Hepatocyte transplantation and staining of liver sections were as in A. (C and D) Quantitative DNA PCR. Quantitative PCR for the *E. coli lacZ* gene was performed on DNA extracted from livers of recipient mice. Percentage of repopulation was calculated as described in the text. (C) Graphic presentation of data from experimental groups shown in A (mean ± SEM; n = 6 in each group), showing significantly higher repopulation in the Ad-HGF group at all time points ($P < 0.05$). (D) Data are from the experimental groups shown in B (mean ± SEM; n = 6 in each group), showing significantly higher repopulation in males 30, 60, and 90 days after transplantation ($P < 0.05$).

Technical Objective #2: Determine the extent to which the PiZ mouse model of alpha-1-antitrypsin (AT) deficiency can be developed as a platform for pre-clinical testing of hepatic stem cell transplantation as a treatment for severe liver injury and disease.
Hypothesis: *iPS cells differentiated toward a hepatocyte phenotype can engraft and respond normally to proliferative signals in the livers of PiZ mice.*

2.1. Hepatocyte engraftment and proliferation in AT (PiZ) transgenic mice.

In several animal models, transplanted hepatocytes have a proliferation advantage over the host liver cells, and nearly 100% of the native liver can be replaced by the donor cells [4, 5]. In AT deficiency, the abnormal Z protein can aggregate in hepatocytes and these aggregates may damage cells. Through this mechanism, AT deficiency patients may develop liver disease. Since Z protein aggregation leads to hepatocyte apoptosis, it has been hypothesized that PiM hepatocytes transplanted into PiZ livers would have a similar selective advantage and may progressively increase their relative contribution to liver mass. To examine this possibility, hepatocytes isolated from ROSA26 (beta-galactosidase transgenic mice) were transplanted into 6-8 week old human AT (hAT) transgenic mice. Three months after transplantation approximately 20% of the native liver was replaced by ROSA26 hepatocytes, as assessed histologically by lacZ staining **(Figure 11)**. These data provide direct evidence, in an animal model, that PiM hepatocytes have the capacity to progressively replace PiZ-expressing hepatocytes following transplantation. In addition, we have accumulated direct evidence that expansion of donor hepatocytes occurs in association with specific areas in the native liver where high levels of the mutant AT protein can be found as aggregates in the host hepatocytes, presumably leading to apoptosis [6].

We then hypothesized that expression of the mutant AT-Z should reduce the capacity of the host hepatocytes to proliferate in response to mitotic stimuli, which should accelerate repopulation by transplanted wildtype cells. To test this, we examined the extent of hepatic repopulation after hepatocyte transplantation in groups of recipient PiZ mice with administration of Ad-HGF. The extent of repopulation was significantly greater at all time points in the group that received Ad-HGF. A control group that received an adenovector that expressed an irrelevant gene did not exhibit accelerated repopulation. Ninety days after transplantation 40-60% of the hepatocytes were replaced by donor cells, and in occasional PiZ recipients, the repopulation was nearly complete, so that only the bile duct epithelial cells and the non-parenchymal cells remained from the host liver **(Figure 11)**. The increased death rate of host hepatocytes, combined with a greater mitotic activity of the donor cells resulted in progressive repopulation of the host liver by the donor cells, while the liver size remained unaltered.

2.1. Human hepatocyte engraftment and proliferation in AT (PiZ)-NSG transgenic mice.

To determine the extent to which hepatic repopulation by human hepatocytes in immune-deficient PiZ mice, we transplanted 1° human hepatocytes in male PiZ-NSG mice by intrasplenic injection. To accentuate the difference in mitotic capacity, transplanted mice were injected with an adenoviral vector expressing human hepatocyte growth factor (Ad-HGF, 1x1011 pfu/mouse) within 48 hours after transplantation. **Figure 12** shows the changes in the levels of human albumin in the serum of PIZ-NSG mice transplanted with 1° human hepatocytes. Thus, this model did not function as desired. We will need to assess AT copy number and other means to enhance repopulation.

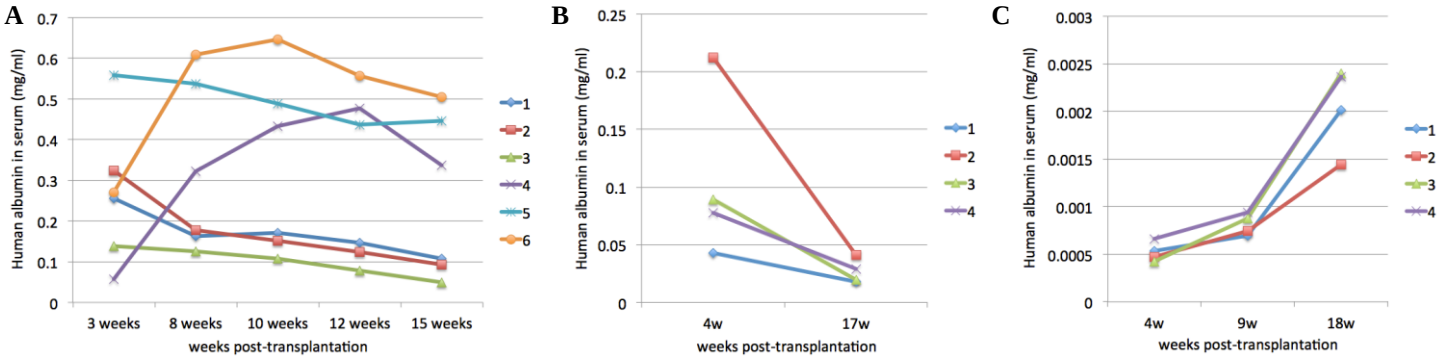

Figure 12. Human serum albumin levels in PiZ-NSG mice transplanted with primary human hepatocytes. Human serum albumin levels in mice transplanted with (A) 1-cycle chemo-treated 1° human hepatocytes (B) normal 1° human hepatocytes from a 6-month old donor and (C) 6-cycle chemo-treated 1° human hepatocytes. $1x10^6$ human hepatocytes were transplanted into each mouse by intra-splenic injection. Ad-HGF ($1x10^{10}$pfu) was injected within 48 hours post transplantation.

2.2. iPS cell-derived human hepatocyte engraftment and proliferation in immune-deficient SCID AT transgenic mice.

In last year's report we examined whether human hES cell-derived hepatocytes could engraft and proliferate spontaneously in the livers of immune deficient PiZ mice. We have now examined whether iPS-derived hepatocytes can engraft in such animals. We generated SCID/PiZ mice, and the PiZ genotype in the offspring and zygosity for the SCID mutation were determined by PCR and pyrosequencing, respectively. Human iPS cells were then differentiated to hepatocytes as described, and one million cells were transplanted into the livers of SCID/PiZ mice by intrasplenic injection. To stimulate mitosis of hepatocytes, $1x10^{11}$ adenovirus vector particles expressing hepatocyte growth factor (Ad-HGF) were injected IV into recipients one day after transplantation. Engrafted hepatocytes were identified by immunofluorescence staining for human serum albumin (HSA). The engrafted human cells had hepatocyte-like morphology and, by three months after transplantation, engrafted iPS-derived hepatocytes were present as large colonies within the host liver **(Figure 13)**. Host cells exhibited diastase/PAS-positive AT-Z globules, but the HSA-positive human hepatocytes did not. These studies indicate that immune deficient PiZ mice are an excellent model for evaluating stem cell-derived human hepatocytes in terms of engraftment, proliferation and function[7].

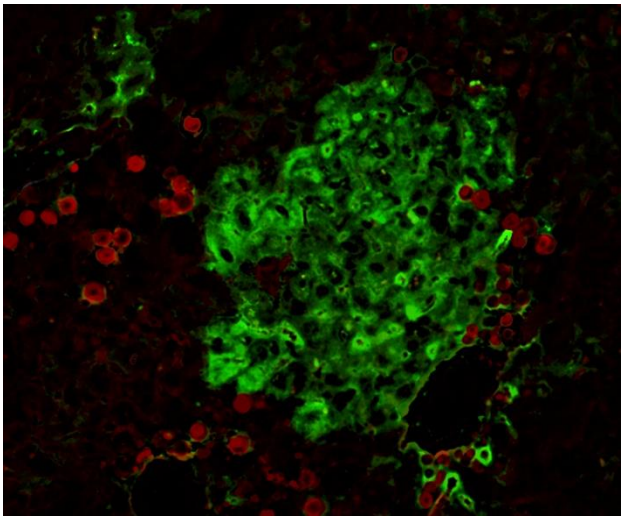

Figure 13. Transplantation of ES-derived human hepatocytes in SCID-PiZ mice. Three-months following transplantation of iPS-derived hepatocytes into immune deficient PiZ mice, immunofluorescence shows large clusters of engrafted iPS-derived hepatocytes stained green for human albumin. Red staining represents hAT globules in host hepatocytes. Nuclei are stained with Dapi (blue).

2.3. iPS cell-derived human hepatocyte engraftment and proliferation in immune-deficient AT-NSG transgenic mice.

To determine the extent to which hepatic repopulation by pluripotent stem cell-derived hepatocytes in immune-deficient PiZ mice, we transplanted normal iPSc-derived hepatocytes in male PiZ-NSG mice by intrasplenic injection. To accentuate the difference in mitotic capacity, transplanted mice were injected with an adenoviral vector expressing human hepatocyte growth factor (Ad-HGF, 1x1011 pfu/mouse) within 48 hours after transplantation. **Figure 14** shows the changes in the levels of human albumin in the serum of PIZ-NSG mice transplanted with normal iPSc-derived hepatocytes. As with transplantation with primary human hepatocytes, engraftment was not sustained in this animal model.

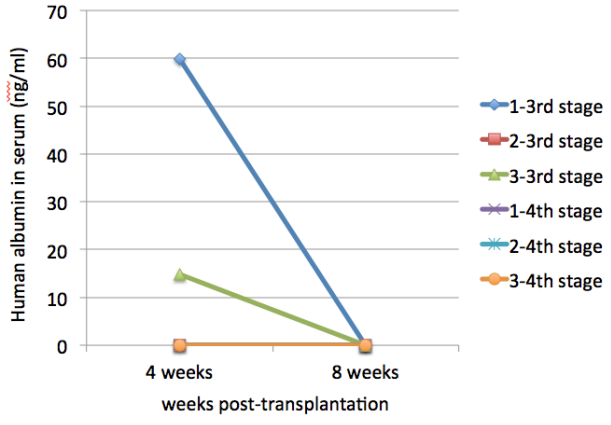

Figure 14. Human albumin levels in PiZ-NSG mouse serum transplanted with normal iPSc-derived hepatocytes. $1x10^{6}$ human hepatocytes were transplanted into each mouse by intra-splenic injection. Ad-HGF ($1x10^{10}$pfu) was injected within 48 hours post transplantation.

2.4. Further development of the PiZ mouse model to optimize its use for liver cell repopulation studies.

We found that accumulation of ATZ in model cell lines and in the liver of transgenic mice elicited marked activation of the transcription factor NFκB. To determine whether NFκB activation protects the liver from inflammation or carcinogenesis we mated our mouse models of AT deficiency to a mouse model in which NFκB activation is conditionally disrupted in hepatocytes during adult life, the IKKβΔhep mouse. Our preliminary results show increased globule-containing hepatocytes, inflammatory nodules and fibrosis in the PiZ x IKKβΔhep mouse. We have also generated 2 other mouse models of AT deficiency with defects in NFκB signaling. In one we used a mouse model with NFκB activation disrupted in both hepatic parenchymal cells and hepatic macrophages, i.e. Kupfer cells. We used the IKKβΔL+H mouse that has been conditional targeted deletion of IKKβ kinase in hepatocytes and Kupfer cells. Second, we used a mouse model with targeted disruption of the NFκB p50 subunit. Our studies have shown that accumulation of ATZ leads to a unique phosphorylation of the p50 subunit and so the p50-null mouse should even more precisely elucidate the role of NFκB activation in the pathobiology of the liver in AT deficiency. Finally, we generated the Z mouse, which provides two unique features to complement the studies in the PiZ mouse: a lower level of expression of ATZ associated with milder hepatocyte necrosis and inflammation; expression of ATZ and the inflammatory reaction can be suppressed by adding doxycycline to the drinking water of the mice. These novel models will be characterized for severity of liver disease and then we will analyze liver repopulation to provide insight into how naturally occurring variation in disease severity influences repopulation of the liver.

KEY RESEARCH ACCOMPLISHMENTS:

1. Generation and characterization of iPS cell lines from control patients and patients with AT-deficiency
2. Further characterization of iPS cells during differentiation into hepatocyte-like cells
3. Determination of AT secretion by ELISA, ultrastructure by electron microscopy and rate of disappearance of intracellular AT by pulse chase analysis in ATD iPS cell-derived hepatocytes compared to controls.
4. Transplantation and expansion of human iPS-derived hepatocytes in rats, with correction of hyperbilirubinemia in the Gunn rat model of Crigler-Najjar syndrome type 1.
5. Complete repopulation of PiZ mouse livers with allogeneic hepatocytes facilitated by the use of hepatocyte growth factor administration after transplantation.
6. Engraftment and proliferation of human pluripotent stem cell-derived hepatocytes in immune-deficient SCID alpha-1-antitrypsin-deficient transgenic mice.
7. Generation of PiZ-NSG mice.
8. Preliminary studies on transplantation of primary human hepatocytes and human iPS-derived hepatocytes in PiZ-NSG mice.
9. **Further development of the PiZ mouse model to optimize its use for liver cell repopulation studies.**

REPORTABLE OUTCOMES:

1. Fox, IJ, Daley GQ, Goldman SA, Huard J, Kamp TJ, Trucco M. Potential for the use of differentiated pluripotent stem cells as replacement therapy in treating disease. Science 2014;345:1247391..
2. Mazariegos G, Shneider B, Burton B, Fox IJ, Hadzic N, Kishnani P, Morton DH, McIntire S, Sokol RJ, Summar M, White D, Chavanon V, Vockley J. Liver transplantation for pediatric metabolic disease. Mol Genet Metab. 2014 Jan 17 [Epub ahead of print]

3. Chen Y, Chang C-J, Li Y, Ding J, Atienza K, Wang X, Avsar Y, Tafaleng E, Strom S, Guha C, Bouhassira EE, Fox IJ, Roy-Chowdhury J, Roy-Chowdhury N. Amelioration of hyperbilirubinemia in Gunn rats after transplantation of human induced pluripotent stem cell-derived hepatocytes. Stem Cell Reports (in revision).
4. Tafaleng E, Han B, Hale P, Chakraborty S, Soto-Gutierrez A, Nagaya M, Duncan S, Stolz D, Strom S, Roy-Chowdhury J, Perlmutter D, Fox I. The rate of disappearance of intracellular α-1-antitrypsin correlates with liver disease severity in iPSc-derived hepatocytes generated from PIZZ α-1-antitrypsin deficiency patients. AASLD Liver Meeting 2013.
5. Tafaleng E, Han B, Hale P, Chakraborty S, Soto-Gutierrez A, Nagaya M, Duncan S, Stolz D, Strom S, Roy-Chowdhury J, Perlmutter D, Fox I. Modeling α-1-antitrypsin deficiency using patient-derived iPSc generated hepatocytes. ISSCR Stem Cell Meeting 2013.
6. Tafaleng, EN, Watson A, Fox IJ. "Normal Hepatocyte Function and Mechanisms of Dysfunction" In: Kleinman RE, Goulet O, Mieli-Vergani G, Sanderson IR, Sherman PM, Shneider BL, eds., Walker's Pediatric Gastrointestinal Disease: Physiology, Diagnosis, Management PMPH—USA. PMPH-USA (People's Medical Publishing House–USA. (in press)
7. Khan Z, Tafaleng EN, Soltys KA, Fox IJ. "Congenital and Acquired Diseases of the Liver" In: Gumucio D and Samuelson L, eds. Translational Gastroenterology. John Wiley & Sons, Inc., 2014
9. Gramignoli R, Tahan V, Dorko K, Skvorak KJ, Hansel MC, Zao W, Venkataramanan R, Ellis ECS, Jorns C, Soltys KA, Mazariegos GV, Fox IJ, Strom SC. New potential cell source for hepatocyte transplantation: discarded livers from metabolic disease liver transplants. Stem Cell Research 2013;11:563-573.
10. Hansel MC, Gramignoli R, Blake W, Davila J, Skvorak K, Dorko K, Tahan V, Lee BR, Tafaleng E, Guzman-Lepe J, Soto-Gutierrez A, Fox IJ, Strom SC. Increased Reprogramming of Human Fetal Hepatocytes Compared With Adult Hepatocytes in Feeder-Free Conditions. Cell Transplant 2013;Feb 4.
11. Fox IJ, Duncan SA. Engineering Liver Tissue from Induced Pluripotent Stem Cells: A first step in generating new organs for transplantation? Hepatology 2013;58(6):2198-2201.
12. Tafaleng E, Han B, Hale P, Soto-Gutierrez A, Nagaya M, Duncan S, Stolz D, Strom S, Roy-Chowdhury J, Perlmutter D, Fox I. In vitro modeling of alpha-1-antitrypsin deficiency using induced pluripotent stem cell-derived hepatocytes from alpha-1-antitrypsin deficient patients. AASLD Liver Meeting 2012.
13. Ding J, Yannam GR, Roy-Chowdhury N, Hidvegi T, Basma H, Rennard SI, Wong RJ, Avsar Y, Guha C, Perlmutter DH, Fox IJ, Roy-Chowdhury J. Spontaneous repopulation of the liver of transgenic mice expressing mutant human alpha 1-anti-trypsin by wildtype donor hepatocytes. J Clin Invest 2011;121(5):1930-1934.
14. Roy-Chowdhury N, Chen Y, Atienza K, Chang C, Wang X, Guha C, Fox IJ, Bouhassira EE, Roy-Chowdhury J. Amelioration of hyperbilirubinemia in Gunn rats after transplantation of human hepatocytes derived from induced pluripotent stem cells. Stem Cell Reports (in revision).
15. Atienza K, Ding J, Chang C-J, Bouhassira E, Chen Y, Wang X, Avsar Y, Liu L, Guha C, Fox IJ, Salido E, Roy-Chowdhury J, Roy-Chowdhury N. Reduction of urinary oxalate excretion after transplantation of human induced pluripotent stem cell-derived hepatocytes in a mouse model of primary hyperoxaluria-1. AASLD 2011.
16. Ding J, Wang X, Neufeld D, Hansel M, Strom S, Fox IJ, Guha C, Roy-Chowdhury N, Roy-Chowdhury J. SCID/PiZ mice: a novel animal model for evaluating engraftment and proliferation of human stem cell-derived hepatocytes. AASLD 2011.
17. Avsar Y, Zhou H, Wang X, Ding J, Guha C, Fox IJ, Roy-Chowdhury N, Roy-Chowdhury J. Pharmacological enhancement of hepatocyte engraftment augments the hypobilirubinemic effect of hepatocyte transplantation in the Gunn rat model of Crigler-Najjar syndrome type 1. AASLD 2011.
18. Ito R, Fong J, Setoyama K, Gramignoli R, Tahan V, Nagaya M, Soto-Gutierrez A, Strom S, Fox IJ. Hepatocyte Xenografts Undergo Stable Long-Term Engraftment in Rats Treated with FK506 but Discordant Xenograft Albumin Secretion is 100-Fold Lower than Allograft Albumin Secretion. AST 2011.

19. Invited Speaker, iPS cell Banking Workshop, California Institute for Regenerative Medicine, San Francisco, CA, November 17-18, 2010.
20. Invited Speaker, Oregon Health and Science University Stem Cell Center, "Use of stem cells to study and treat liver disease" Portland, Oregon, February 7-8, 2011
21. Invited Speaker, AASLD Basic Research Single Topic Conference – Stem Cell in Liver Diseases and Cancer: Discovery and Promise, "Stem cells and the treatment of liver disease: understanding liver failure and cirrhosis, Atlanta, Georgia, March 19-20, 2011.
22. Invited Speaker, Yale University Stem Cell Center Seminar Series, "Stem cells and the liver" New Haven, Connecticut, March 28-29, 2011.
23. Invited Speaker, Medical College of Wisconsin, "Use of hepatocytes and stem cells to study and treat liver disease", Milwaukee, Wisconsin, May 10-11, 2011.
24. Invited Speaker, The 66th General Meeting of the Japanese Society of Gastroenterological Surgery, "Overcoming barriers to the use of hepatocytes and stem cells in treating patients with liver diseases", Nagoya, Japan, July 13-15, 2011.
25. Invited Speaker, Research Seminar Series in Developmental and Regenerative Biology, University of Kansas Medical Center, "Use of hepatocytes and stem cells to study and treat liver disease", Kansas City, Kansas, November 9-10, 2011.
26. Keynote Speaker, ISMRM Workshop on MRI-based cell tracking "Hepatocyte transplantation and the need to track engrafted cells", Miami Beach, Florida, January 29 – February 1, 2012.
27. Invited Speaker, Challenging the Paradigms: Liver Transplantation for Metabolic Disease, Children's Hospital of Pittsburgh, "Hepatocyte transplantation", Pittsburgh, PA, May 4-5, 2012.
28. Invited Speaker, American Society of Gene & Cell Therapy 15th Annual Meeting, "Overcoming barriers to successful cell therapy to treat liver disease", Philadelphia, PA May 16-19, 2012
29. Invited Speaker, 16th Maple Syrup Urine Disease Symposium, "Clinical hepatocyte transplantation for the treatment of metabolic liver diseases", Philadelphia, PA, June 28-30, 2012
30. Moderator, Mid-day Symposium: "Allotransplants, Cellular Transplants, Organ Repair, and Xenotransplants? A Debate about the Future of Organ Transplantation", American Transplant Congress, Boston, MA, June 2-6, 2012.
31. Invited Speaker, Liver Biology: Fundamental Mechanisms & Translational Application, FASEB Summer Research Conference, "Hepatocyte, stem cell transplantation, tissue engineering", Snowmass Village, Colorado, July 29 – August 3, 2012.
32. Invited Speaker, 8th Royan International Congress on Stem Cell Biology and Technology, "Overcoming barriers to the use of hepatocytes and stem cells in treating patients with liver diseases" and "Use of hepatocytes and stem cells in understanding and treating liver failure and cirrhosis", Tehran, Iran, September 5-7, 2012.
33. Invited Speaker, Masters of Surgery lecture series, Montefiore Medical Center, The University Hospital for Albert Einstein College of Medicine, "Bench to bedside: finding alternatives to organ transplantation for patients with life-threatening liver disease", New York, NY, November 4-5, 2012.
34. Faculty Member, American Association for the Study of Liver Diseases 2012 Postgraduate Course, "Tissue engineering and liver cell replacement – liver stem cells on the horizon", Boston, MA, November 10, 2012.
35. Invited Speaker, 23rd Conference of the Asian Pacific Association for the Study of the Liver (APASL 2013), "Future strategies for cellular transplantation", Singapore, June 6-10, 2013.
36. Invited Speaker, 19th Annual International Congress of ILTS, "Liver regeneration and hepatocyte repopulation", Sydney, Australia, June 14, 2013.
37. Invited Speaker, Cell Transplant Society, "Hepatocyte transplantation and regeneration in the treatment of liver disease", Milan, Italy, July 7-10, 2013.
38. Invited Speaker, AASLD/NASPGHAN Pediatric Symposium, The Liver Meeting 2013, "Pros and cons of hepatocyte transplantation for treatment of liver-based metabolic disease", Washington, DC, November 1, 2013.

39. 132. Invited Speaker, Annual meeting – Adult Liver Stem Cell Transplantation Project, University Utrecht, "Bench to bedside: hepatocyte transplantation for the treatment of liver-based metabolic disease", Utrecht, The Netherlands, January 13, 2014.
40. 133. Invited Speaker, Center for Cell and Gene Therapy Seminar Series, Baylor College of Medicine, "Bench to Bedside: Hepatocyte transplantation and regeneration in the treatment of liver disease", Houston, TX, February 4, 2014.
41. 134. Invited Speaker, Whole Liver Replacement State-of-the-Science Summit, Chicago, IL, April 29-30, 2014
42. 135. Invited Speaker, FASEB Summer Research Conference on Liver Biology: Fundamental Mechanisms & Translational Applications, "Modeling alpha-1-antitrypsin deficiency and PFIC using patient-derived pluripotent stem cells", Keystone, Co, July 10, 2014.
43. 136. Invited Speaker, Bridging Biomedical Worlds conference: Turning Obstacles into Opportunities for Stem Cell Therapy, "Translating stem cells to the treatment of life-threatening liver disease." Beijing, China, October 13-15, 2014
44. 137. Invited Speaker, Advances and Applications of Functional Hepatocytes (AAFH), "Treatment of life-threatening liver disease by primary or stem cell-derived hepatocyte transplantation." Shanghai, China, October 29-30, 2014

CONCLUSIONS:

The outcomes of our studies are being accomplished as expected, and there is no change anticipated in the research plan. The intention for future studies is to attain better engraftment and more complete characterization of differentiated cells following transplantation.

REFERENCES

1. Basma H, Soto-Gutierrez A, Yannam GR, et al. Differentiation and transplantation of human embryonic stem cell-derived hepatocytes. Gastroenterology 2009;136:990-9.
2. Si-Tayeb K, Noto FK, Nagaoka M, et al. Highly efficient generation of human hepatocyte-like cells from induced pluripotent stem cells. Hepatology;51:297-305.
3. Roy-Chowdhury N, Chen Y, Atienza K, et al. Amelioration of hyperbilirubinemia in Gunn rats after transplantation of human hepatocytes derived from induced pluripotent stem cells. . AASLD 2010.
4. Overturf K, Al-Dhalimy M, Tanguay R, et al. Hepatocytes corrected by gene therapy are selected in vivo in a murine model of hereditary tyrosinaemia type I. Nat Genet 1996;12:266-73.
5. Rhim JA, Sandgren EP, Degen JL, Palmiter RD, Brinster RL. Replacement of diseased mouse liver by hepatic cell transplantation. Science 1994;263:1149-52.
6. Ding J, Yannam GR, Roy-Chowdhury N, et al. Spontaneous hepatic repopulation in transgenic mice expressing mutant human alpha1-antitrypsin by wild-type donor hepatocytes. The Journal of Clinical Investigation 2011;121:1930-4.
7. Ding J, Wang X, Neufeld DS, et al. SCID/PiZ mice: a novel animal model for evaluating engraftment and proliferation of human stem cell-derived hepatocytes. AASLD 2011.

TRANSPLANTATION OF PURIFIED HUMAN SKELETAL MUSCLE-DERIVED PERICYTES REDUCE FIBROSIS IN INJURED ISCHEMIC MUSCLE TISSUES

[1,2,4]Chien-Wen Chen, [2,4]Masaho Okada, [1,3,4,5]Kimimasa Tobita, [4]Mihaela Crisan, [3,4,5,6]Bruno Péault, [2,4,5]Johnny Huard
Department of Bioengineering[1], Orthopedic Surgery[2], Pediatrics[3], Stem Cell Research Center, Children's Hospital of Pittsburgh[4], and McGowan Institute for Regenerative Medicine[5], University of Pittsburgh and UPMC and [6]David Geffen School of Medicine, University of California at Los Angeles;
jhuard@pitt.edu

INTRODUCTION

Vascular pericytes are the mural cells that tightly encircle capillaries and microvessels throughout the body. In general, pericytes control blood vessel maturation, stability and contractility.

Multi-lineage stem/progenitor cells have been identified within virtually all organs in both human and mouse and are named diversely [1]. However, due to the retrospective discovery of these multi-lineage stem/progenitor cells in culture, the true identity of these cells *in situ* remained obscure. It has been hypothesized that vascular pericytes are indeed, or at least contain, stem/progenitor cells that are able to differentiate into bone, cartilage, fat tissue and odontoblasts [2]. Recently, we and others laboratories have shown that vascular pericytes purified from multiple human organs not only express classic MSC markers but harbor stem cell properties such as myo-, osteo-, chondro- and adipogenic potentials [2]. Consequently, pericytes are assumed to be one of the developmental origins of MSC. Human skeletal muscle-derived pericytes were not only shown to regenerate skeletal muscle fibers in dystrophic as well as cardiotoxin-injured mouse muscle but also sustain impaired cardiac function after myocardial infarction *in vivo* [2]. Nevertheless, whether transplanted vascular pericytes contribute to the reduction of fibrosis at the site of injury remains to be elucidated. Matrix metalloproteinases (MMPs) are proteolytic enzymes responsible for extracellular matrix protein degradation with an important role in tissue remodeling processes. MMP-2 and MMP-9 activities are often implicated in fibrosis [3]. Using the animal model that has been established previously, we commenced to explore whether or not pericytes influences scar tissue formation within the damaged ischemic myocardium and attempt to elucidate the mechanism(s) of action [4].

METHODS

Cell Isolation and Cell Sorting: Fresh specimens of human fetal skeletal muscle were mechanically dissociated and digested with collagenases. After lysis of erythrocytes, single cell suspension was obtained by filtering with 70-μm cell strainer. For cell sorting, cells were incubated with the following directly-conjugated antibodies: anti-CD34-PE, anti-CD45-APC, anti-CD56-PE-Cy7, and anti-CD146-FITC. For dead cell exclusion, 7-amino-actinomycin D (7-AAD) was added to stained cells before running on a FACSAria flow cytometer. Flow cytometry with an identical gating strategy was used to verify the purity of long-term cultured muscle-derived pericytes.

Animal Model of Fibrosis: Permanent ligation of the left coronary artery was performed on NOD/SCID mice under open-chest surgery. Immediately after the ligation, skeletal muscle-derived pericytes from cultures were injected into the ischemic myocardium (3×10^5 cells/heart), while the control groups received saline injections (PBS).

Histology: Masson's trichrome staining was employed to reveal myocardial fibrosis. The ratio of fibrotic area was estimated by total collagen deposition versus total sectional area using Image J software.

Hypoxic Culture: Pericytes were cultured *in vitro* under hypoxic conditions (2.5% oxygen) for 24 hours. Supernatants and cell pellets were subsequently collected for analysis.

Real-time Quantitative PCR: Real-time Quantitative PCR analysis was performed to detect gene expressions of matrix metalloproteinase-2 (MMP-2) and -9 (MMP-9) in total muscle lysates and muscle-derived pericytes cultured under normal and hypoxic conditions.

RESULTS

Purification of Human Muscle-derived Pericytes: $CD34^-45^-56^-146^{high}$ muscle-derived pericytes were sorted and cultured as previously described [2]. To ensure long-term cultured muscle-derived pericytes remain homogeneous and retain their native properties, flow cytometry was employed to examine the expression of cell surface markers used to select these cells plus alkaline phosphatase (ALP), another pericyte marker. The result shows that after long-term culturing (>10 passages), all cells remain negative for CD34, CD45 and CD56, and virtually all pericytes are positive for CD146 and ALP (Figure 1a).

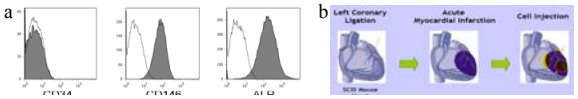

Figure 1. (a) Flow cytometry analysis of long-term cultured $CD34^-CD45^-CD56^-CD146^{high}$ pericytes . (b) Schematic depiction of transplantation of muscle-derived pericytes.

Transplantation of Muscle-derived Pericytes: Immediately after permanent ligation of the left coronary artery, muscle-derived pericytes from cultures were injected into the ischemic myocardium at a density of 3×10^5 cells/heart (Figure 1b) [4].

Scar Tissue Formation: Masson's trichrome staining revealed myocardial fibrosis after infarction with collagen deposition stained in blue (Figure 2a). Quantification at 2 weeks post injection demonstrated a 38% reduction of the fibrotic area in pericyte-injected left ventricles, compared to saline-injection (Figure 2b).

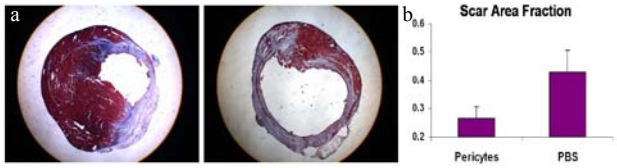

Figure 2. (a) Collagen deposition was stained blue to show the extent of myocardial fibrosis. (b) Pericyte-injected hearts had an average 38% reduction of the scar area.

Expression of MMP-2 by Muscle-derived Pericytes: Real-time quantitative PCR results revealed that cultured muscle pericytes have higher expression of MMP-2 gene than total muscle lysates, but not MMP-9. Under hypoxic culture conditions, muscle pericytes retain high expression of MMP-2 gene, while MMP-9 remained very low (Figure 3).

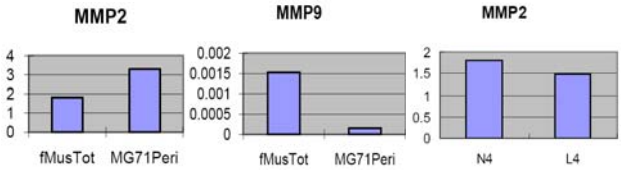

Figure 3. Real-time qPCR results of (a) MMP-2 gene (b) MMP-9 gene expression level of total muscle lysates and long-term cultured muscle pericytes. MMP-2 gene expression level was compared between muscle pericytes cultured under normoxia (N4) and hypoxia (L4).

DISCUSSION

We demonstrated that transplantation of purified skeletal muscle-derived pericytes ameliorate fibrosis in injured ischemic cardiac muscle, possibly exerting a preventative effect. Reduced MMP-2 activity has been shown to contribute to cardiac fibrosis in pathological conditions [5]. We consequently hypothesized that the high expression level of MMP-2 by muscle-derived pericytes, even under hypoxic conditions, may play a key role in pericyte-mediated reduction of fibrosis. We are currently conducting experiments to demonstrate the efficacy of muscle pericyte transplantation in diminishing chronic fibrosis. We are also investigating the influence of increased angiogenesis, a beneficial effect displayed by muscle pericytes, on reduction of fibrosis. Overall, this study will shed light on the therapeutic value of muscle-derived pericytes for the treatment of fibrosis in the injured tissues including musculoskeletal tissues.

ACKNOWLEDGMENTS

This work was partly supported by funding from the National Institutes of Health (1R21 HL083057-01A2 awarded to B.P.) and by the Henry J. Mankin Endowed Chair for Orthopaedic Research at the University of Pittsburgh (held by J.H.).

REFERENCES

1. Péault et al. Mol Ther. 2007 May;15(5):867-77.; **2.** Crisan et al. Cell Stem Cell 2008; 3(3):301-13**.;** 3. Tanriverdi-Akhisaroglu et al. Cell Biochem Funct. 2009 Mar;27(2):81-7.; 4. Okada et al. J Am Coll Cardiol. 2008; 52(23):1869-80.; 5. Van Linthout et al. Basic Res Cardiol. 2008 Jul;103(4):319-27.

Transplantation of p65 Deficient Stem Cells Improved the Histopathology of Skeletal Muscle in Dystrophic Mice

[1]Aiping Lu; [2] Qing Yang; [1]Minakshi Poddar; [1]Bing Wang; [3]Denis C. Guttridge; [4]Paul D. Robbins; [1]+ Johnny Huard
[1]+Stem Cell Research Center and Department of Orthopaedic Surgery, University of Pittsburgh, Pittsburgh, PA
[2]Department of Orthopaedic Surgery, Tongji Hospital, Huazhong University of Science and Technology, Wuhan, China
[3]Department of Molecular Virology, Immunology and Medical Genetics, Ohio State University, Columbus, OH
[4]Department of Microbiogy and Molecular Genetics. University of Pittsburgh, Pittsburgh, PA
jhuard@pitt.edu

INTRODUCTION

Duchenne muscular dystrophy (DMD) is a deadly genetic disease mainly characterized by progressive weakening of the skeletal, cardiac and diaphragmatic muscles. It is critical to find a successful therapy that will improve the histopathology of the muscles of DMD patients and restore their normal function. Recent studies have demonstrated that blocking p65, a subunit of NF-κB, enhances muscle regeneration in injured and diseased skeletal muscle [1, 2], which suggests that the NF-kB signaling pathway is a contributing factor to the dystrophic pathology in DMD patients. Previously we demonstrated that muscle derived stem cells (MDSCs) isolated from the skeletal muscles of heterozygote P65 knock-out (*P65*$^{+/-}$) mice showed better muscle regeneration *in vitro* and *in vivo* compared to the MDSCs isolated from wild-type (WT) mice. We also demonstrated that the transplantation of P65$^{+/-}$ MDSCs could reduce inflammation. Based on these results we performed a set of experiments to determine if these P65$^{+/-}$ MDSCs could alleviate the pathology associated with DMD more efficiently than wild-type MDSCs. When we injected p65$^{+/-}$ MDSCs intraperitoneally into dystrophin/utrophin deficient (dys-/-:utro-/-, dKO) mice, a reliable mouse model of DMD, we found that the histopathology of various skeletal muscles improved and observed a reduction in inflammation, necrosis and pathological muscle regeneration.

MATERIALS AND METHODS

Cell Isolation: MDSCs were isolated from 5 month old P65$^{+/-}$ and WT mice as previously described via a modified preplate technique [3]. The cell suspensions from both P65$^{+/-}$ and WT muscle were plated on collagen coated flasks and cultured in proliferation medium (DMEM supplemented with 10% fetal bovine serum, 10% horse serum, 0.5% chicken embryo extract and 1% Penicillin-streptomycin) until the cell number was sufficient for injection.

***Intraperitoneal injection* (IP):** A total of 5-9 x10^5 viable cells were suspended in 50 µl of PBS and injected IP into 5-7 days old of dKO mice. Four to six weeks after transplantation, the mice were sacrificed and their muscles were harvested and flash frozen in liquid nitrogen-cooled 2-methylbutane. 10µm serial cryosections were prepared from the frozen muscle.

Immunohistocytochemistry

Cryosections were fixed with 5% formalin, blocked with 5% Donkey serum, and then incubated with an antibody against mouse IgG (Biotinlated) to determine the extent of muscle fiber necrosis. An antibody against embryonic muscle heavy chain (E-MyHC) was used to evaluate myogenic regeneration and an antibody against F4/80 (macrophage marker) was used to analyze the extent of inflammation in the muscle tissues. Streptavidin Cy3 conjugate and Alexafluor 488 conjugated anti-mouse IgG were used as secondary antibodies. H&E staining was performed to assess myofiber morphology and fibrosis.

RESULTS

Transplantation of P65+/- MDSCs improved muscle histology

H&E showed histology improvement in various skeletal muscles including the gastrocnemius, diaphragm, thigh and tibialis anterior muscles. We observed many centrally nucleated muscle fibers (new regenerated fibers) and decreased fibrosis in the p65$^{+/-}$ MDSC injection group (**Figure 1,** thigh muscle**)**.

Transplantation of P65+/- MDSCs reduced muscle necrosis

Mouse IgG staining showed that there were less necrotic muscle fibers in the mice injected with p65$^{+/-}$ MDSCs compared to the un-treated muscle **(Figure2)**

Transplantation of P65$^{+/-}$ MDSCs reduced inflammation and pathological muscle regeneration

Less inflammation and E-MyHC positive myofibers were found in the muscles of mice injected with p65$^{+/-}$ MDSCs compared to non-treated muscle **(Figure3).**

Figure1

DKO untreated muscle **DKO muscle treated with MDSCs**

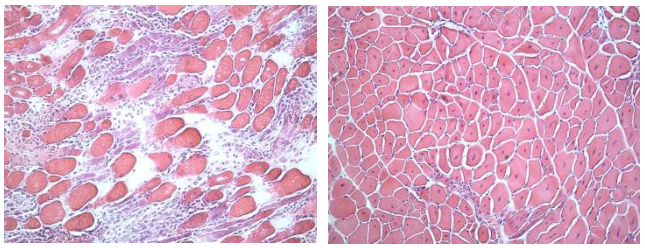

Figure2

DKO untreated muscle **DKO muscle treated with MDSCs**

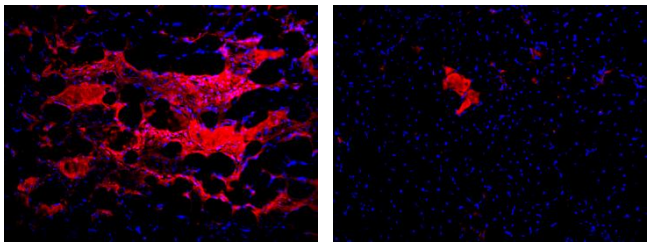

Figure3

DKO muscle nontreated **DKO muscle treated with MDSCs**

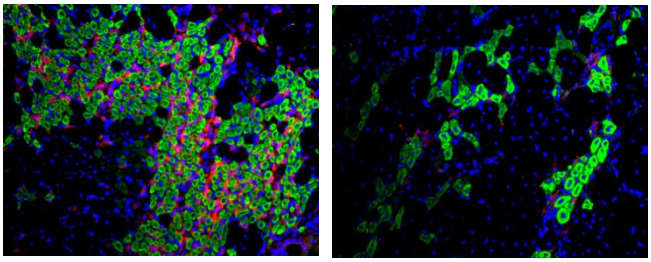

DISCUSSION

In this study we used MDSCs isolated from p65+/- mice to treat dystrophin-/-utrophin-/- mice. The up-regulation of the NF-κB pathway in these mice is associated with chronic inflammation which results in pathologies such as muscle fibrosis, necrosis, and muscle wasting. Our findings indicated that blocking p65, a subunit of NF-κB, can decrease macrophage infiltration, fibrosis formation, necrosis, and diminishes pathologic regeneration in 4 to 6 week dKO mice. We also attempted to inject the WT MDSCs isolated from normal animals; however, the results did not show an improvement in the histopathology of the mice. These results suggest that reducing the activity of the IKK/NF-κB pathway is a potential therapeutic target for the treatment of DMD. These are only preliminary data; however they are very exciting and we are planning to test additional animals in order to further confirm these results.

REFERENCES:

[1] Thaloor, D, et al Am. J.Physiol 1999; 277:C320–C329. [2] Acharyya S et al, J. Clin. Invest 2007 ; 117 :889-901. [3] Gharaibeh, et al. Nat Protoc. 2008; 3:1501-9

Immunomodulatory properties of muscle-derived stem cells associated with reduced NF-κB/p65 signaling

[1]Proto, J.; [1]Lu, A.; [2]Robbins, P.D.; [1]+Huard, J.
[1]+ Stem Cell Research Center, Children's Hospital of Pittsburgh, and Department of Orthopedic Surgery;
[2]Departments of Microbiology and Molecular Genetics, University of Pittsburgh School of Medicine, Pittsburgh, PA
jhuard@pitt.edu

INTRODUCTION

The nuclear factor kappa B (NF-kB) signal pathway has been implicated in both the normal and disease states of many different tissues. In skeletal muscle, for example, constitutive activation of inhibitor of kappa B kinase (IKKβ), a potent activator of NF-kB, leads to muscle wasting[1]. Inversely, muscle specific deletion of IKKβ in a murine model of muscular dystrophy improves dystrophic pathology and is accompanied by an increase in the number of cells fitting a muscle progenitor marker profile ($CD34^+/Sca1^-$), suggesting that NF-kB has a direct effect on muscle stem cells[2]. The NF-kB protein family includes five subunits, two of which, a p65-p50 heterodimer, are thought to play a role in blocking early myogenesis[3]. In this study, we examined the role of NF-kB signaling in the regenerative phenotype of muscle-derived stem cells (MDSCs) isolated from the gastrocnemius of p65 deficient mice (heterozygous, $p65^{+/-}$) and wild type littermates ($p65^{+/+}$). We previously found that $p65^{+/-}$ MDSCs have enhanced cell proliferation, survival under oxidative stress, differentiation, and muscle regeneration capacity. Furthermore, we have found that $p65^{+/-}$ engraftments in wild type skeletal muscle are associated with reduced inflammation and fiber necrosis compared to $p65^{+/+}$ MDSC engraftments. *In vitro* and *in vivo* experiments suggest that reduction of p65 signaling enhances the regenerative phenotype of MDSCs, suggesting this pathway as a candidate target to improve stem cell-based therapies for muscle disease and injury.

MATERIALS AND METHOD

Cell Isolation: MDSCs were isolated from five month old (n=3) $p65^{+/+}$ or $p65^{+/-}$ mice via a preplate technique [4]. A population of slowly adhering cells was obtained and expanded in DMEM containing 10% fetal bovine serum (FBS), 10% horse serum, 1% penicillin-streptomycin, and 0.5% chick embryo extract. Cells were used between passages 15 and 30.

In vivo regeneration assay: Muscle injury was induced in C57Bl/6J mice by cardiotoxin injected into gastrocnemius. One day later, MDSCs were injected into the injured muscles. Six days following transplantation, mice were sacrificed and injected muscles were harvested and snap-frozen. Serial cryosections were prepared and immunohistochemistry was performed to assess inflammation (CD14) and necrosis (IgG). The number of CD14 (+) cells was counted to assess infiltration of macrophages/monocytes. Necrosis was determined by mouse IgG staining and quantified by assessing the percentage of positively stained area.

In vitro Inflammation Model: MDSCs were grown for 24 hours in proliferation medium, after which the medium was collected and sterile filtered. RAW264.7 cells, immortal murine macrophage-like cells, were activated by exposure to 100 ng/mL LPS in either $p65^{+/+}$-, $p65^{+/-}$-, or muscle-derived fibroblast conditioned medium for 24 hours.

***Gene Expression Analysis*:** Cells were washed and RNA collected by Trizol extraction. Total RNA was reverse transcribed with Superscript III reverse transcriptase (Invitrogen) according to manufacturer's protocols. The PCR reaction was carried out with Taq Polymerase (Promega), according to manufacturer's protocols. PCR products were analyzed by electrophoresis on a 1.5% agarose gel

RESULTS

Wild type mice were injected with either $p65^{+/+}$ (Fig 1A) or $p65^{+/-}$ (Fig 1B) MDSCs in the gastrocnemius muscle and sacrificed six days later. Tissues were cryosectioned and immunostained with antibodies against CD14 to identify a monocyte/macrophage infiltrate, indicating inflammation, as well as with antibodies against mouse immunoglobulin G, a marker of necrosis. Injections of $p65^{+/-}$ cells were associated with a decrease in both necrosis and inflammation (Fig 1B-D), compared to $p65^{+/+}$ injections (Fig1A, C-D).

Figure 1.

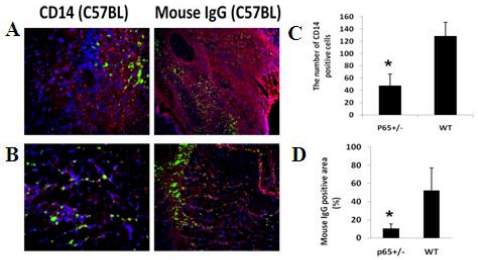

To investigate anti-inflammatory properties of MDSCs, we utilized an *in vitro* inflammation model in which RAW264.7 cells, immortal murine macrophage-like cells, are activated by LPS exposure. We found that RAW264.7 cells exposed to LPS in $p65^{+/-}$ CM expressed less IL-1 compared to controls, suggesting that p65+/- MDSCs secrete immunomodulatory factors that hinder pro-inflammatory macrophage activation.

Figure 2.

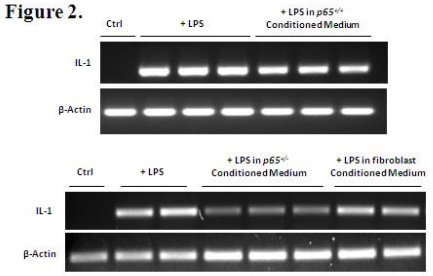

DISCUSSION

The data presented here provides evidence supporting that NF-kB inhibition stimulates MDSC-mediated muscle regeneration through multiple mechanisms, including through the expression of anti-inflammatory factors that attenuate inflammation and necrosis. These experiments identify the NF-κB signaling pathway as a potential therapeutic target to enhance muscle regeneration following injury or disease. Future directions for this project include investigating modulation of the IKK/NF-kB pathway as a means to rejuvenate the phenotype of aged muscle stem and progenitor cells. Clinical research should be conducted to test the efficacy of p65 inhibition therapy in patients suffering from muscle disorders.

REFERENCES

[1]Cai, D., et al. Cell 2004, 119:285-298. [2]Acharyya, S., et al., J Clin Invest 2007, 117:889-901. [3]Bakkar, N., et al. JCB 2008, 180(25): 787-802. [4] Gharaibeh, et al. Nat Protoc. 2008; 3:1501-9

Appendix 4

NF-κB Negatively Impacts the Myogenic Potential of Muscle-derived Stem Cells

Aiping Lu[1], Jonathan D Proto[1], Lulin Guo[1], Ying Tang[1], Mitra Lavasani[1], Jeremy S Tilstra[2], Laura J Niedernhofer[2], Bing Wang[1], Denis C Guttridge[3], Paul D Robbins[2] and Johnny Huard[1]

[1]Stem Cell Research Center, School of Medicine and Department of Orthopedic Surgery, University of Pittsburgh, Pittsburgh, Pennsylvania, USA; [2]Department of Microbiology and Molecular Genetics, University of Pittsburgh, Pittsburgh, Pennsylvania, USA; [3]Department of Molecular Virology, Immunology and Medical Genetics, The Ohio State University, Columbus, Ohio, USA

Inhibition of the inhibitor of kappa B kinase (IKK)/nuclear factor-kappa B (NF-κB) pathway enhances muscle regeneration in injured and diseased skeletal muscle, but it is unclear exactly how this pathway contributes to the regeneration process. In this study, we examined the role of NF-κB in regulating the proliferation and differentiation of muscle-derived stem cells (MDSCs). MDSCs isolated from the skeletal muscles of $p65^{+/-}$ mice (haploinsufficient for the p65 subunit of NF-κB) had enhanced proliferation and myogenic differentiation compared to MDSCs isolated from wild-type (wt) littermates. In addition, selective pharmacological inhibition of IKKβ, an upstream activator of NF-κB, enhanced wt MDSC differentiation into myotubes *in vitro*. The $p65^{+/-}$ MDSCs also displayed a higher muscle regeneration index than wt MDSCs following implantation into adult mice with muscular dystrophy. Additionally, using a muscle injury model, we observed that $p65^{+/-}$ MDSC engraftments were associated with reduced inflammation and necrosis. These results suggest that inhibition of the IKK/NF-κB pathway represents an effective approach to improve the myogenic regenerative potential of MDSCs and possibly other adult stem cell populations. Moreover, our results suggest that the improved muscle regeneration observed following inhibition of IKK/NF-κB, is mediated, at least in part, through enhanced stem cell proliferation and myogenic potential.

Received 15 April 2011; accepted 5 November 2011; published online 13 December 2011. doi:10.1038/mt.2011.261

INTRODUCTION

Nuclear factor-kappa B (NF-κB) is a ubiquitously expressed nuclear transcription factor that is evolutionarily conserved. In mammals, the NF-κB family consists of five subunits, p65 (RelA), c-Rel, RelB, p50, and p52.[1] Transcriptionally active NF-κB exists as a dimer, with the most common form being a p50–p65 heterodimer. Under nonstress conditions, the heterodimer is maintained in an inactive state in the cytoplasm via its interaction with inhibitor of kappa B (IkB) proteins. Classic NF-κB activation is mediated by IkB kinase (IKK), a large, 700–900 kDa complex consisting of two catalytic subunits, IKKα and IKKβ, and a regulatory subunit named IKKγ or NEMO (NF-κB essential modulator). In response to a variety of stimuli, including proinflammatory cytokines, bacterial products, viruses, growth factors, and oxidative stress, the complex is activated. Activated IKKβ phosphorylates IkB, leading to its polyubiquitylation and subsequent degradation by the 26S proteasome. IkB degradation allows NF-κB to translocate to the nucleus where it binds to its cognate DNA site, as well as coactivators such as CBP/p300, to induce gene expression.[2–5] Dysregulation of this pathway can result in chronic activation of IKK or NF-κB, and is seen in several pathophysiological states including cancer, rheumatoid arthritis, sepsis, muscular dystrophy, heart disease, inflammatory bowel disease, bone resorption, and both type I and II diabetes.[6,7]

The NF-κB pathway, long recognized as an important component of innate and adaptive immunity, has also more recently emerged as a key player in the regulation of skeletal muscle homeostasis.[8] Furthermore, activation of NF-κB in skeletal muscle has been linked to cachexia, muscular dystrophies, and inflammatory myopathies.[9–13] Conversely, knockout of p65, but not other subunits of NF-κB, enhances myogenic activity in MyoD-expressing mouse embryonic fibroblasts.[14] Although it is known that genetic depletion of p65 enhances muscle regeneration in both mdx and wild-type (wt) murine skeletal muscle,[13] the mechanism through which reduced of NF-κB activity positively impacts skeletal muscle remains unclear.

Given that the repair of damaged tissues is mediated by adult stem cell populations, we hypothesized that NF-κB activity negatively regulates muscle stem cell function. In this study, we specifically focus on the role of p65 in regulating muscle-derived stem cell (MDSC) growth and differentiation. This population of adult stem cells is capable of restoring muscle function.[15,16] As complete knockout of p65 ($p65^{-/-}$) results in embryonic lethality, we isolated MDSCs from the skeletal muscles (SKM) of $p65^{+/-}$ mice and wt littermates.[17] We observed that, *in vitro*, p65 haploinsuffiency was associated with increased cell proliferation and myogenic differentiation. Pharmacologic inhibition of IKK/NF-κB also enhanced myogenic

The first two authors contributed equally to the work.

Correspondence: *Johnny Huard, Stem Cell Research Center, 2 Bridgeside Point, 450 Technology Drive, Pittsburgh, Pennsylvania 15219, USA. E-mail: jhuard@pitt.edu*

differentiation. We also demonstrated that $p65^{+/-}$ MDSCs have a higher capacity for muscle regeneration after implantation into dystrophic, mdx mouse SKM. Furthermore, we show that muscle inflammation and necrosis post-injury is decreased following $p65^{+/-}$ MDSC implantation into cardiotoxin (CTX) injured SKM. These results suggest that reducing the activity of the IKK/NF-κB pathway is an effective approach to improve the myogenic potential of MDSCs and possibly other adult stem cell populations. Our results provide a novel mechanistic insight as to why the inhibition of this pathway promotes SKM healing.

RESULTS

Isolation and phenotypic characterization of MDSCs from $p65^{+/-}$ and wt mice

To examine the effect of NF-κB activity on MDSC function, we purified populations of muscle stem cells from the SKM of mice heterozygous for the p65 subunit of NF-κB ($p65^{+/-}$) and wt littermates. Using a modified preplate technique,[18] we isolated independent populations of MDSCs from three mice of each genotype. To confirm that p65 haploinsufficiency reduced basal levels of NF-κB activity, nuclear p65 was measured via ArrayScan. Nuclear, or active, p65 was found to be 30% lower in $p65^{+/-}$ than the wt MDSCs (**Figure 1a**). Upon activation, NF-κB subunits undergo post-translational modifications, such as phosphorylation, to enhance their activity.[19] Immunoblot analysis revealed that the level of phosphorylated p65 (P-p65) was also reduced; however, stimulation with tumor necrosis factor-α (TNFα) led to an increased level of P-p65 in both wt and $p65^{+/-}$ MDSCs (**Figure 1b**), demonstrating that basal, but not induced, NF-κB activity is affected by knocking-out one allele of *p65*.

To confirm the MDSC phenotype of $p65^{+/-}$ and wt cells, each population was analyzed for the expression of stem (CD34, Sca-1), myogenic (MyoD, desmin), and endothelial (CD144, CD31) cell markers by reverse transcriptase-PCR. For each of the markers, there was variability in expression between cell populations of a single genotype. However upon quantification, no significant differences were found between the different genotypes, with the exception of CD144, which was elevated in $p65^{+/-}$ MDSCs. (**Figure 2a,c,** $P < 0.05$). Such variability in marker expression has been previously reported and interpreted as evidence that these cell populations contain a mixture of stem and committed progenitor cells.[20,21] We next examined the expression of Pax7 and MyoD protein by immmunostaining, and also found no significant difference between $p65^{+/-}$ and wt cells (**Figure 2b,d**). These results suggest that genetic reduction of p65 does not dramatically alter the phenotype of MDSCs.

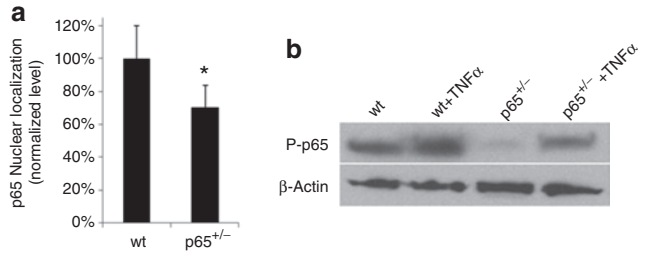

Figure 1 Muscle-derived stem cells (MDSCs) obtained from the skeletal muscles (SKM) of $p65^{+/-}$ mice have a lower level of activated p65 compared to wild-type (wt) MDSCs. (**a**) ArrayScan analysis of nuclear p65 in MDSCs isolated from $p65^{+/-}$ and wt mice. Error bars indicate "mean + SD." (**b**) Immunoblotting for phosphorylated p65 in whole cell lysates of MDSCs before and after tumor necrosis factor-α (TNFα) stimulation for 30 minutes.

$p65^{+/-}$ MDSCs proliferate faster than wt MDSCs

NF-κB is known to regulate cell division, so we investigated whether p65 reduction would alter MDSC proliferation. The three populations of $p65^{+/-}$ and wt MDSCs were plated in collagen-coated flasks and expanded in growth medium for 10–12 passages. Cells were then transferred to 24-well plates and proliferation measured using a previously described Live Cell Imaging system.[22] We observed that $p65^{+/-}$ MDSCs proliferated significantly faster than wt cells (**Figure 3a** and **Supplementary Videos S1–S2**). Equal numbers of cells were also plated on a 96-well plate and grown for three days at which point the differences in cell number were determined using an MTS assay. This assay demonstrated a similar significant increase in cell proliferation in $p65^{+/-}$ MDSCs (**Figure 3b**) suggesting that NF-κB, and in particular p65, limits the proliferation of MDSCs.

$p65^{+/-}$ MDSCs have enhanced myogenic differentiation compared to wt cells

We next measured the ability of the $p65^{+/-}$ and wt MDSCs to undergo myogenic differentiation *in vitro*. Equal numbers of cells were plated in a 24-well plate and switched to differentiation medium once the cells adhered. After 3 days the majority (80%) of the $p65^{+/-}$ cells had differentiated into myotubes, as determined by immunodetection of myosin heavy chain (**Figure 4a**). The differentiation potential of the $p65^{+/-}$ MDSCs was significantly greater than the wt MDSCs (60%; $P < 0.01$; **Figure 4b**). The difference was also demonstrated using the live cell imaging system described above (**Supplementary Videos S3–S4**). These results demonstrate that NF-κB, and in particular p65, represses MDSC differentiation *in vitro*.

Pharmacologic inhibition of IKKβ increases myogenic differentiation *in vitro*

To confirm this finding implicating NF-κB as negatively impacting MDSC differentiation, we tested whether a pharmacologic inhibitor of NF-κB could enhance MDSC myogenic potential *in vitro*. wt MDSCs were exposed to differentiation medium containing various doses of IKK-2 inhibitor IV (IKKi), a specific, reversible inhibitor of IKKβ. Cell lysates were collected at 0, 1, 14, 24, 48, and 72 hours following treatment. Accordingly, myosin heavy chain (MyHC) levels dramatically increased, beginning at 14 hours (**Figure 5a,c**). As expected, we observed a robust time-dependent decrease in P-p65 that was dose-dependent (greater at 3 μmol/l than 1 μmol/l; **Figure 5b**). We next examined NF-κB activity in wt and $p65^{+/-}$ MDSCs at various time points during myogenic differentiation by immunodetection of P-p65 and MyHC. In wt cells, beginning at 48 hours post-transition to differentiation medium, the levels of p-p65 were detectably reduced (**Figure 5d**). This occurred more rapidly (by 24 hours) in $p65^{+/-}$ cells. Similarly, accumulation of MyHC was greater at earlier time points (14 hours) in $p65^{+/-}$ cells than wt. This timeframe for MyHC accumulation is similar

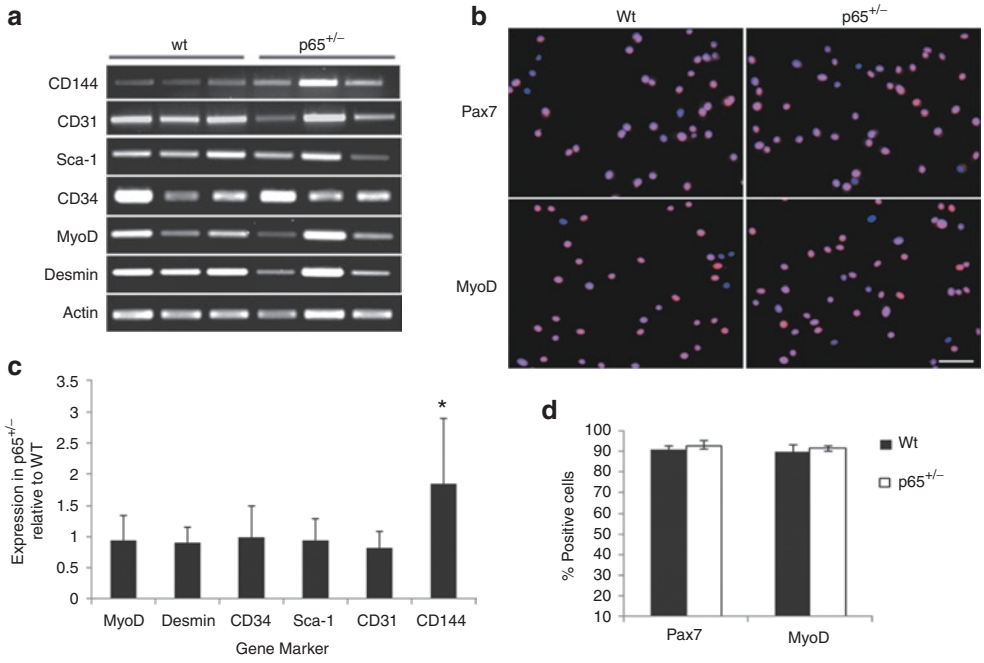

Figure 2 ***p65*$^{+/-}$ and wild-type (wt) muscle-derived stem cells (MDSCs) exhibit a similar molecular marker profile.** (**a**) RNA was isolated from three independent cell populations of each genotype. Reverse transcriptase-PCR (RT-PCR) was performed to characterize the MDSC populations for the expression of stem (CD34 and Sca-1), endothelial (CD31 and CD144) and myogenic (MyoD and desmin) cell markers. (**b**) Immunostaining for the muscle stem cell markers Pax7 and MyoD was also performed (bar = 25 µm). (**c**) Quantification of RT-PCR results. Error bars indicate "mean + SD" (n = 3 independent experiments). (**d**) Quantification of Immunostaining of Pax7 and MyoD.

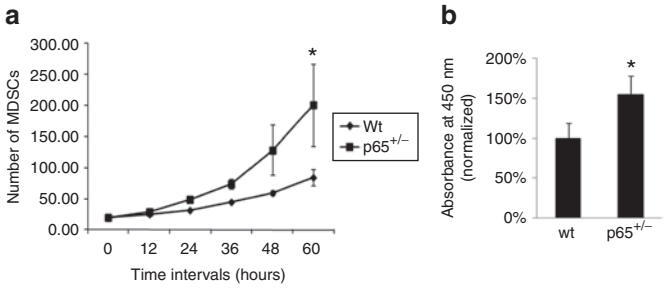

Figure 3 Muscle-derived stem cells (MDSCs) isolated from *p65*$^{+/-}$ mouse skeletal muscles (SKM) have a higher rate of proliferation than wild-type (wt) cells. (**a**) Cell proliferation rate was measured by Live Cell Imaging and (**b**) by an MTS assay ($P < 0.05$).

to that observed in wt cells treated with IKKi (Figure 5a). In order to verify that increased MyHC expression was concomitant with increased myotube formation, we treated wt MDSCs with 5 µmol/l IKKi. After 3 days, differentiation was assessed by immunofluorescence detection of MyHC. As shown in Figure 5e, compared to nontreated controls, the inhibitor caused a significant increase in myotube formation. The level of myogenic differentiation was comparable to that of *p65*$^{+/-}$ MDSCs ($P < 0.01$; Figure 5f). These results provide strong support that MDSC myogenic potential can be improved using NF-κB inhibition *ex vivo*.

p65$^{+/-}$ MDSCs have greater muscle regenerative capacity *in vivo*

To determine whether genetic depletion of p65 increases the engraftment and muscle regenerative capacity of MDSCs *in vivo*, we examined the ability of *p65*$^{+/-}$ and wt MDSCs to regenerate muscle fibers following their intramuscular implantation into an immunocompromised model of Duchenne muscular dystrophy. For these experiments, 3 × 10^5 *p65*$^{+/-}$ and wt MDSCs were injected into the gastrocnemius muscles of 8-week-old dystrophin-deficient SCID (mdx/SCID) mice. Fourteen days after implantation, significantly more dystrophin-positive myofibers were detected in the muscle injected with *p65*$^{+/-}$ MDSCs than in muscle injected with wt MDSCs ($P < 0.01$; Figure 6a,b). These results confirm our *in vitro* observations and may provide a novel mechanism as to why IKK inhibitors have been reported to improve muscle regeneration.[23]

Transplantation of *p65*$^{+/-}$ MDSCs postinjury reduces SKM inflammation and necrosis

The results above suggest that lowering basal levels of NF-κB activity increased the ability of MDSCs to engraft and differentiate following intramuscular injection (Figure 6). However, while it is possible this is mediated through enhanced proliferation and differentiation, the exact mechanism as to why more dystrophin-positive myofibers were found within the *p65*$^{+/-}$ MDSC engraftment sites remains unclear. Surrounding the engraftments of the wt MDSCs, we observed numerous cells positive for the macrophage marker CD14 as detected by immunofluorescent staining (data not shown), whereas the *p65*$^{+/-}$ MDSC engraftment sites were surrounded by fewer numbers of CD14+ cells (data not shown). As the mdx/SCID is an immunocompromised mouse model with a high level of background inflammation, we decided to further investigate this phenomenon using the well-established CTX muscle injury model in immunocompetent wt mice. In order

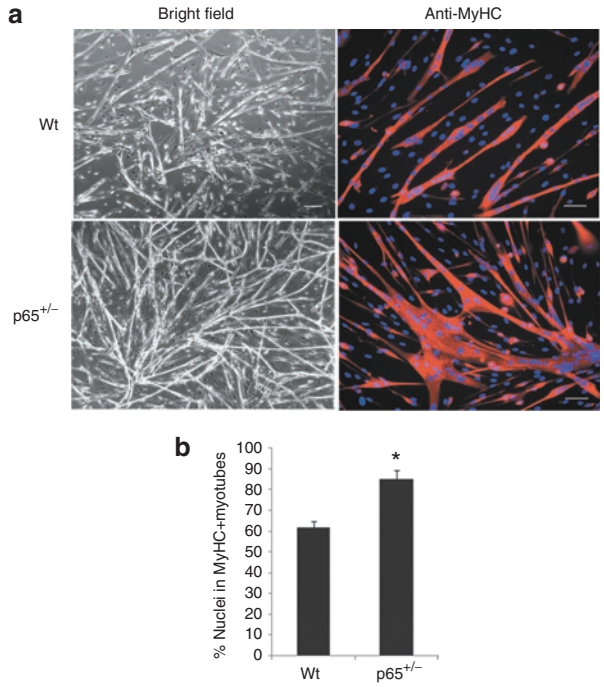

Figure 4 Myogenic differentiation is enhanced in muscle-derived stem cells (MDSCs) isolated from *p65*$^{+/-}$ mouse skeletal muscles (SKM) compared to wild-type (wt) MDSCs *in vitro*. (**a**) MDSCs were cultured in myogenic differentiation medium for 3 days, during which cell fusion into multinucleated myotubes was monitored using bright field microscopy and then confirmed by immunostaining for myosin heavy chain (MyHC-f). (**b**) Quantitation of MyHC-f positive myotubes. The percentage of differentiated myotubes was quantified as the number of nuclei in MyHC-f positive myotubes relative to the total number of nuclei. A total of three populations of *p65*$^{+/-}$ and wild-type (wt) MDSCs were tested ($P < 0.05$). In panel "**a**" all bars = 200 µm on bright field and all bars = 50 µm on MyHC immunostaining.

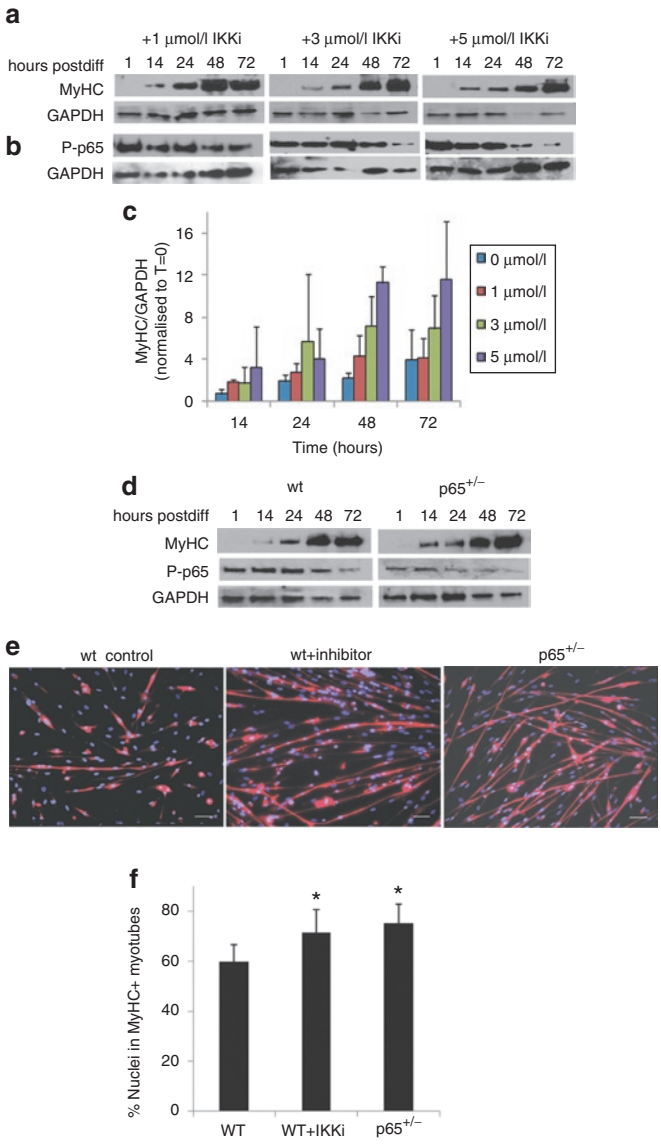

Figure 5 Muscle-derived stem cells (MDSCs) myogenic differentiation is enhanced by pharmacological inhibition of inhibitor of kappa B kinase β (IKKβ). (**a**) Western blot for myosin heavy chain (MyHC) over 72 hours of wild-type (wt) MDSCs treated with 1, 3, or 5 µmol/l IKKi during differentiation. (**b**) Western blot for P-p65 over 72 hours of wt MDSCs treated with 1, 3, or 5 µmol/l IKK inhibitor (IKKi) during differentiation. (**c**) Quantification of **b**, myosin heavy chain (MyHC-f) levels during differentiation ($n = 3$ independent experiments). (**d**) In parallel, wt and *p65*$^{+/-}$ MDSCs were cultured in differentiation medium and lysates were collected at the various time points indicated. Lysates were used for western blot for MyHC and P-p65 levels. (**e**) wt MDSCs, *p65*$^{+/-}$ MDSCs, and wt MDSCs treated with IKKi (5 µmol/l), were grown under fusion conditons for 72 hours and immunostained for MyHC-f expression (**f**) Quantification of MyHC-f staining ($P < 0.05$). In panel "**e**" all bars = 100 µm.

to confirm that transplanted *p65*$^{+/-}$ MDSCs are able to reduce inflammation in host skeletal muscle, we injected *p65*$^{+/-}$ and wt MDSCs into the gastrocnemius muscles of 8-week-old C57BL/6J mice 24 hours post-CTX injury. Six days post-transplantation, the wt MDSC engraftment area demonstrated a greater number of inflammatory cells surrounding the wt donor MDSCs than the *p65*$^{+/-}$ MDSCs. Furthermore, numerous centrally located nuclei, characteristic of regenerating muscle fibers, were found within the *p65*$^{+/-}$ MDSC injection sites. Consistent with observations made in mdx/SCID mice, the *p65*$^{+/-}$ MDSC engraftment area was associated with significantly fewer CD14+ cells than the wt MDSC engraftment area ($P < 0.01$; **Figure 7a,b**). There was also a significant (42%) reduction in tissue necrosis, as determined by quantification of mouse immunoglobulin G (IgG) staining ($P < 0.01$; **Figure 7a,c**). These results suggest that the improved engraftment and differentiation of *p65*$^{+/-}$ MDSCs is potentially due to their ability to attenuate the inflammation and necrosis that typically occurs after muscle injury.

DISCUSSION

NF-κB signaling has been implicated in the regulation of muscle degeneration and regeneration. The five mammalian NF-κB transcription factors are all expressed in skeletal muscle to modulate a variety of processes, including apoptosis, inflammation, and myoblast differentiation. Although there have been conflicting results reported as to whether NF-κB acts as a repressor or promoter of myogenesis,[8,24–29] recent results suggest that the classical NF-κB signaling pathway functions as a negative regulator of myogenesis.[14] In addition, NF-κB activation is associated with the degeneration and/or lack of regeneration of dystrophic

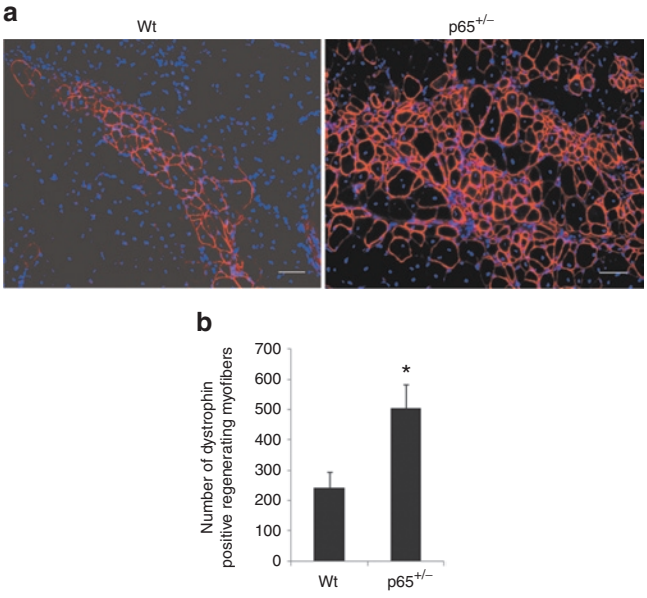

Figure 6 Heterozygous deletion of p65 promotes the regeneration capacity of muscle-derived stem cells (MDSCs). (**a**) Gastrocnemius cryosections from 8-week-old mdx/SCID mice in which $p65^{+/-}$ and wild-type (wt) MDSCs were implanted. Engraftment was determined by immunostaining for dystrophin (red). Three populations of $p65^{+/-}$ and wt MDSCs were transplanted into 12 mice in two independent experiments. (**b**) Quantitation of regenerated dystrophin-positive myofibers ($P < 0.05$). In panel "**a**" all bars = 50 µm. Error bars indicate "mean + SD" ($n = 12$).

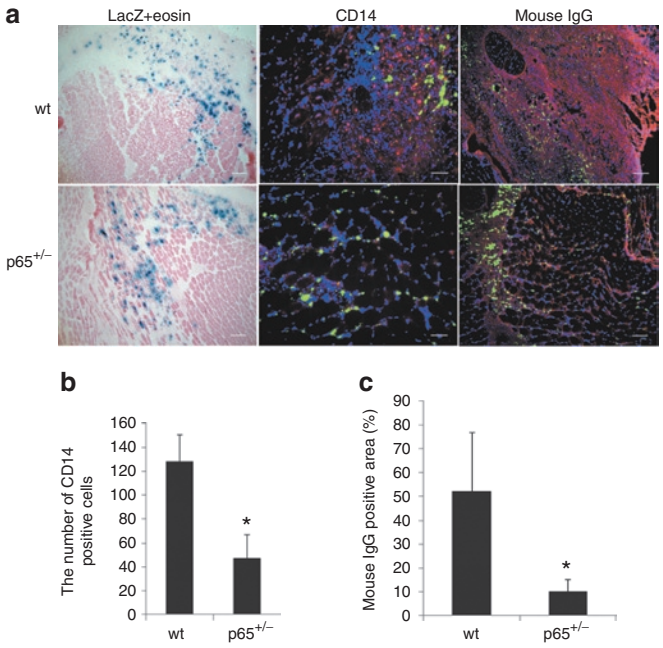

Figure 7 $p65^{+/-}$ muscle-derived stem cells (MDSCs) attenuate muscle inflammation and necrosis. (**a**) Gastrocnemius cryosections from 8-week-old C57BL/6J mice, which were injected with $p65^{+/-}$ or wild-type (wt) MDSCs 24 hours post-CTX injury. LacZ and eosin staining identified the injection area and immunostaining for CD14 (red) and mouse immunoglobulin G (IgG) (red) identified macrophages and necrotic tissue, respectively. In immunological stains, fluorescent green beads in C57BL/6J muscle sections confirmed the location of injection sites. (**b**) Quantitation of $CD14^+$ cells (the data represent six muscles per group). (**c**) Necrotic area in the gastrocnemius muscles was identified by IgG staining and quantified based on the total positive area per image (the data represent six muscles per group). In panel "**a**" all bars = 100 µm on LacZ+eosin and mouse IgG staining. All bars = 50 µm on CD14 staining.

muscle in mdx mice.[13] Thus, in this study, we examined the effect of NF-κB reduction on the proliferation and differentiation of MDSCs isolated from wt mice and mice heterozygous for p65. Although $p65^{+/-}$ MDSCs had more than a 30% reduction in p65/NF-kB levels compared to the wt MDSCs, the two genotypes expressed similar stem (CD34, Sca-1), myogenic (desmin, MyoD) and endothelial (CD144, CD31) cell markers. This result suggests that the reduction in NF-kB did not affect overall expression of MDSC markers, albeit there is some variability in stem cell marker expression between populations of the same genotype.

We observed that MDSCs with reduced p65 levels have improved proliferation compared to wt cells, suggesting that p65/NF-κB activity negatively controls MDSC expansion. More importantly, we also observed that both the rate and extent of myogenic differentiation was accelerated in MDSCs with reduced p65 and in wt MDSCs treated with an IKKβ inhibitor. Together, these data suggest that NF-κB inhibits muscle stem cell differentiation. Our results are in agreement with previous studies showing that regulation of myogenesis is dependent on p65 transcriptional activity, which is able to inhibit myogenesis.[14] It has been suggested previously that the negative effect of NF-κB on differentiation is mediated through the transcriptional activation of cyclin D1 and YinYang1 (YY1).[30,31] Interestingly, we have observed a reduction in the level of cyclin D1 in $p65^{+/-}$ MDSCs compared to wt cells, but found no difference in the level of YY1 expression (data not shown).

Recent genetic evidence supports the role of IKK/NF-κB in driving the pathogenesis of muscular dystrophy, identifying this signaling pathway a potential therapeutic target for the treatment of DMD.[13] The activity of NF-κB in dystrophic muscle is associated with not only immune cells, but also regenerative muscle fibers. Thus, we investigated whether the $p65^{+/-}$ MDSCs have a higher muscle regeneration potential than wt MDSCs after their intramuscular injection into dystrophic mdx/SCID skeletal muscles. Our results demonstrated that $p65^{+/-}$ MDSCs are more efficient at regenerating dystrophin-positive myofibers compared to wt MDSCs, which is consistent with the enhanced ability of the $p65^{+/-}$ MDSCs to differentiate in culture.

We also assessed inflammation around the engrafted site by immunofluorescent staining for CD14, a macrophage marker. While we found very few CD14+ cells within the injection sites of the $p65^{+/-}$ cells, many CD14+ cells were detected within the wt MDSC engraftment areas. As a decreased number of macrophages in the $p65^{+/-}$ cell engraftment area correlated with a reduction in necrosis, it is possible that a reduction in p65 enhances the local anti-inflammatory properties of MDSCs via regulation of paracrine factors. Several cytokines under the control of NF-κB, such as TNFα and interleukin-6 (IL-6), are potent inhibitors of myogenic differentiation.[8] Thus, taken together, these results suggest that inhibition of NF-κB/p65 may enhance myogenesis by reducing inflammation and necrosis.

During regeneration following injury, numerous paracrine factors such as myostatin, hepatocyte growth factor, and basic fibroblast growth factor play critical roles coordinating repair.[32] Other groups have demonstrated the importance of non-NF-kB proteins in muscle development and pathology. For example, myostatin acts independently of the classical TNFα and NF-kB pathway to inhibit MyoD expression and signal cachexia by reversing the IGF-1/PI3K/AKT hypertrophy pathway.[33] However, other factors, such as hepatocyte growth factor and IL-6, have been reported to activate NF-κB.[34] Given the numerous growth factors and cytokines present in damaged and regenerating muscle, the NF-κB pathway likely directs inflammation or regeneration in response to more than one factor. In summary, here we described a negative role for the p65/NF-κB signaling pathway in MDSC growth and differentiation *in vitro*, as well as muscle regeneration *in vivo*. Similarly, pharmacological inhibition of IKKβ identifies the IKK/NF-κB signaling pathway as a potential therapeutic target to improve the myogenic potential of MDSCs and muscle regeneration after injury and diseases.

MATERIALS AND METHODS

Animals. The C57BL/6J mice heterozygous for p65/RelA were originally described by Amer Beg (Cambridge, MA).[17] The mdx/SCID (C57BL/10ScSn DMD^{mdx}/J/CB17-Prkdc^{scid}/J) and C57BL/6J mice were obtained from the Jackson Laboratory (Bar Harbor, ME). All animal protocols used for these experiments were approved by the Children's Hospital of Pittsburgh's Institutional Animal Care and Use Committee.

Isolation of MDSCs from p65$^{+/-}$ mice. The mice were sacrificed at 5 months of age and muscle stem cell isolation was performed as previously described via a modified preplate technique.[18] Briefly, the SKM tissue was minced and processed through a series of enzymatic dissociations: 0.2% of collagenase type XI (Sigma-Aldrich, St Louis, MO) for 1 hour, 2.4 units/ml of dispase (Invitrogen, Carlsbad, CA) for 45 minutes, and 0.1% of trypsin-EDTA (Invitrogen) for 30 minutes at 37°C. After enzymatic dissociation, the muscle cells were centrifuged and resuspended in proliferation medium (Dulbecco's modified Eagle's medium supplemented with 10% fetal bovine serum, 10% horse serum, 0.5% chicken embryo extract, and 1% penicillin-streptomycin), and the resulting cell suspension from both $p65^{+/-}$ and wt muscle were plated in collagen type I coated flasks. Different populations of muscle-derived cells were isolated based on their adhesion characteristics. After 7 days, late preplate populations (slow-adhering cells) were obtained and cultured in proliferation medium. The slowly adhering fraction of muscle cells has been previously shown to contain MDSCs.[18] For all experiments, congenic $p65^{+/-}$ and $p65^{+/+}$ MDSCs of the same passage number were compared.

p65 staining and ArrayScan assay. Cells were fixed with 4% paraformaldehyde for 15 minutes at room temperature (RT), rinsed two times with phosphate-buffered saline (PBS), and the cells' membrane permeabilized for 10 minutes with 0.1% Triton X-100 in PBS. A 10% goat serum blocking solution was used for 1 hour and the cells were incubated with a 1:200 dilution of rabbit polyclonal anti-p65 (Abcam, Cambridge, MA) for 1 hour at RT. After washing three times, the cells were incubated for 30 minutes with Cy3-conjugated anti-rabbit IgG (1:500; Sigma-Aldrich). The nuclei were revealed by 4′,6-Diamidino-2-phenylindole (DAPI) staining. Nuclear localization of the NF-κB subunit p65 was measured via ArrayScan. This technique allows for the rapid, automated quantification of p65 and DAPI colocalization, as identified by immunocytochemistry in cells grown on a 96-well plate. Recordings were taken from multiple fields of view per well, generating data representative of each well.

Western blot assay. The cell populations isolated from $p65^{+/-}$ and wt mice were cultured in proliferation medium and stimulated with TNFα (10 ng/ml) for 30 minutes before harvesting. Cells were then lysed in Laemmli sample buffer (Bio-Rad, Hercules, CA), boiled for 5 minutes, and centrifuged at 4,000 r.p.m. for 5 minutes. Each sample was loaded on a 10% SDS-polyacrylamide gel, which was run for 2 hours and then transferred for 1.5 hours at 100 V while stirring on ice. The membrane was blocked with 5% bovine serum albumin (Sigma-Aldrich, St Louis, MO) in PBS for 1 hour and then incubated with rabbit anti-phospho-NF-κB/p65 monoclonal antibody (1:1,000; Cell Signaling, Danvers, MA) overnight at 4°C. After washing three times with Tris-buffered saline Tween-20, the membrane was incubated with goat anti-rabbit IgG (H+L) (1:5,000; Pierce, Rockford, IL) for 50 minutes at RT. Blots were developed by ECL solution (Pierce).

RT-PCR analysis. Total RNA was extracted from cells using Nucleo Spin RNA II column (Clontech, Mountain View, CA). Following isolation, complementary DNA was synthesized with SuperScript II reverse transcriptase (Invitrogen), according to the manufacturer's instructions. PCR was performed with Taq polymerase (Invitrogen) as per the manufacturer's instructions and PCR products were separated by electrophoresis with 1% agarose gels. The primers used for PCR are listed in **Table 1**. Each set of oligonucleotides was designed to span two different exons to avoid background amplification of genomic DNA. The data were quantified by densitometry using Adobe Photoshop 7.0.

Pax7 and MyoD staining. $P65^{+/-}$ and wt cells were fixed and permeabilized with 2% paraformaldehyde plus 1% Triton X-100 for 30 minutes at 4°C and rinsed two times with PBS. Cells were blocked with 5% horse serum and then incubated with a 1:100 dilution of mouse monoclonal anti-Pax7 (DSHB, Iowa City, IA) or anti-MyoD (Santa Cruz Biotechnology, Santa Cruz, CA) over night at 4°C. After washing three times, the cells were incubated for 1 hour with biotinylated anti-mouse IgG (1:300; Vector Lab, Burlingame, CA), which acted as a secondary antibody. Streptavidin 594 conjugate (1:500; Invitrogen) was added in the last step. The nuclei were revealed by DAPI staining. Negative control staining was performed by an identical procedure, with the exception that the primary antibody was omitted.

In vitro *assessment of cell proliferation.* In order to compare the proliferative potential of $p65^{+/-}$ MDSCs to wt MDSCs, we used a previously

Table 1 Primers used for RT–PCR

Gene	Forward primer	Reverse primer	Location
Sca-1	CCTACTGTGTGCAGAAAGAGC	CAGGAAGTCTTCACGTTGACC	89–331
CD34	GCAGCTTTGAGATGACATCACC	CTCAGCCTCCTCCTTTTCACA	498–715
MyoD1	ACAGTGGCGACTCAGATGCATC	GCTGCAGTCGATCTCTCAAAGC	708–1105
Desmin	AACCTGATAGACGACCTGCAG	GCTTGGACATGTCCATCTCCA	615–873
CD31	AGAGCTACGTCATTCCTCAG	GACCAAGTGTGTCACTTGAAC	474–988
CD144	CACCAACAAAAACCTGGAACA	CCACCACGATCTTGTATTCAG	425–729
β-Actin	TCAGAAGGACTCCTATGTGG	TCTTTGATGTCACGCACGAT	234–722

described Live Cell Imaging system (Kairos Instruments LLC, Pittsburgh, PA).[22] Bright field images were taken at a ×100 magnification at 10 minutes intervals over a 72-hour period in three fields of view per well, with three wells per population. The images were combined to generate a video using ImageJ software (NIH). Proliferation was assessed by counting the number of cells per field of view, over 12 hours. All six populations were also plated in 96-well plates in quadruplicate (500 cells/well) and cultured under normal conditions for 72 hours. At this time, 20 µl of CellTiter96 AQueous One Reagent (Promega, Madison, WI) was added to each well and incubated in 5% CO_2 at 37 °C. Following another 3-hour incubation, absorbance at 490 nm was read with a 96-well plate reader.

Myogenic differentiation assay and fast MyHC (MyHC-f) staining. After 15 passages, cells were plated on 24-well plates (30,000 cells/well) with Dulbecco's modified Eagle's medium supplemented with 2% fetal bovine serum to stimulate myotube formation. Three days later, immunocytochemical staining for fast skeletal MyHC was performed. After rinsing three times with PBS, cells were fixed for 2 minutes in cold methanol, blocked with 10% horse serum for 1 hour and then incubated with a mouse anti-MyHC-f (1:250; Sigma-Aldrich, clone MY-32) antibody for 2 hours at RT. The primary antibody was detected with a secondary anti-mouse IgG antibody conjugated with Cy3 (1:300; Sigma-Aldrich) for 15 minutes. The nuclei were revealed by DAPI staining. The percentage of differentiated myotubes was quantified as the number of nuclei in MyHC-f positive myotubes relative to the total number of nuclei. The myogenic differentiation was also monitored over a period of 5 days using Live Cell Imaging. The images were combined to create a video using ImageJ software (NIH).

Selective inhibition of IKKβ. To determine the effects of IKK/NF-κB inhibition on wt MDSCs during myogenic differentiation, we used IKK-2 inhibitor IV (IKKi), or 2-[(aminocarbonyl)amino]-5-(4-fluorophenyl)-3-thiophenecarboxamide (Calbiochem, San Diego, CA), a reversible competitive inhibitor of IKKβ ATP binding. Cells were plated at 10^5 cells/well in 6-well plates and exposed to IKK inhibitor in differentiation medium. Cells were treated with either 1, 3, or 5 µmol/l IKKi. Lysates were collected at 0 minute, 14, 24, 48, and 72 hours following treatment. NF-kB activity and myogenic differentation was assessed by western blot for phosphorylated NF-kB/p65 (1:1,000; Cell Signaling) and MyHC-f (1:500; Sigma-Aldrich, clone MY-32), as detailed above.

Cell implantation and dystrophin staining. MDSCs from $p65^{+/-}$ and wt muscle were grown in proliferation medium until the cell number was sufficient for injection. A total of 3×10^5 viable cells was suspended in 20 µl of Hank's balanced salts solution and injected into the gastrocnemius muscles of 8–12-week-old mdx/SCID mice using a Hamilton syringe. The same number of cells was injected into the gastrocnemius muscles of 8-week-old wt C57BL/6J mice that had been injured 1 day earlier by a 30 µl intramuscular injection of 2 µmol/l CTX (Sigma-Aldrich) in PBS. The cell suspension was mixed with green fluorescent-labeled beads before injection to detect the injection sites. Six or fourteen days after implantation, the mice were sacrificed and the gastrocnemius muscles were harvested and flash frozen in liquid nitrogen-cooled 2-methylbutane. Serial cryosections 10 µmol/l in thickness were obtained for immunohistochemical analyses. Cryosections were fixed with 5% formalin and blocked with 5% donkey serum in PBS for 1 hour, then incubated with rabbit anti-dystrophin (1:300; Abcam) for 2 hours at RT. The sections were exposed to secondary 594-conjugated anti-rabbit IgG (1:500; Invitrogen) in PBS for 30 minutes. The nuclei were revealed by DAPI staining. Immunostaining was visualized and images were taken by fluorescence microscopy (Nikon Eclipse E800; Nikon, Melville, NY). Northern Eclipse software was used for quantitative analysis of the regenerated dystrophin-positive myofibers. A series of pictures were taken, and Adobe Photoshop 7.0 was used to construct a composite picture of the dystrophin-positive myofibers, which were then manually counted.

Retroviral transduction of MDSCs. MDSCs were plated at an initial confluence of 30–40% and retrovirally transduced [in the presence of Polybrene (8 µg/ml)] to express the β-galactosidase gene (LacZ), as previously described.[35]

LacZ staining. The cryosections were fixed in 1% glutaraldehyde and incubated 3 hours with 5-bromo-4-chloro-3-indolyl β-D-galactopyranoside (X-gal) substrate at 37 °C. Sections were counterstained with Eosin.

CD14 staining. Cryosections were fixed with 5% formalin and blocked with 5% donkey serum in PBS for 1 hour, then incubated with rat anti-CD14 (1:200; Biolegend, San Diego, CA) overnight at 4 °C. This was followed by a 1-hour incubation with biotinylated anti-rat IgG (1:300; Vector Lab). Streptavidin Cy3 conjugate (1:500; Sigma-Aldrich) was added in the last step followed by several rinses in PBS. Following CD14 staining, five random pictures per slide were taken and the number of CD14+ cells was counted manually.

Mouse IgG staining and quantification of necrosis. Muscle sections were fixed with 5% formalin and blocked with 10% horse serum in PBS for 1 hour, then incubated with biotinylated anti mouse IgG (1:300; Vector Lab) for 1 hour at RT. This was followed by a 15-minute incubation with streptavidin Cy3 conjugate (1:500; Sigma-Aldrich). The nuclei were revealed by DAPI staining. The IgG positive area was measured and quantified as the percentage of mouse IgG expressing area per total area using Northern Eclipse software (Cheektowaga, NY).

Statistical analysis. All results are given as the mean ± SD. Means from $p65^{+/-}$ and wt or treated and untreated were compared using Students' *t*-test. Differences were considered statistically significant when the *P* value was < 0.05.

SUPPLEMENTARY MATERIAL

Video S1. $p65^{+/-}$ MDSC proliferation.
Video S2. wt MDSC proliferation.
Video S3. $P65^{+/-}$ MDSC differentiation.
Video S4. wt MDSC differentiation.

ACKNOWLEDGMENTS

The authors thank the members of the Huard Laboratory, especially Jenny Zhu and Bin Sun for discussions and technical advice. Special thanks go to Joseph Feduska and Bridget Deasy for live cell imaging advice. This work was supported in part by the Henry J. Mankin Endowed Chair for Orthopedic Research at the University of Pittsburgh, the William F. and Jean W. Donaldson Chair at Children's Hospital of Pittsburgh. L.J.N. is supported by NIEHS (ES016114) and NIA (AG033907). The authors do not have conflicts of interest to disclose other than the corresponding author who receives consulting fees from Cook MyoSite Inc.

REFERENCES

1. Verma, IM, Stevenson, JK, Schwarz, EM, Van Antwerp, D and Miyamoto, S (1995). Rel/NF-kappa B/I kappa B family: intimate tales of association and dissociation. *Genes Dev* **9**: 2723–2735.
2. Baeuerle, PA and Baltimore, D (1996). NF-kappa B: ten years after. *Cell* **87**: 13–20.
3. Baldwin, AS Jr (1996). The NF-kappa B and I kappa B proteins: new discoveries and insights. *Annu Rev Immunol* **14**: 649–683.
4. Li, Z and Nabel, GJ (1997). A new member of the I kappaB protein family, I kappaB epsilon, inhibits RelA (p65)-mediated NF-kappaB transcription. *Mol Cell Biol* **17**: 6184–6190.
5. Karin, M (1999). How NF-kappaB is activated: the role of the IkappaB kinase (IKK) complex. *Oncogene* **18**: 6867–6874.
6. Hayden, MS and Ghosh, S (2004). Signaling to NF-kappaB. *Genes Dev* **18**: 2195–2224.
7. Karin, M, Cao, Y, Greten, FR and Li, ZW (2002). NF-kappaB in cancer: from innocent bystander to major culprit. *Nat Rev Cancer* **2**: 301–310.
8. Langen, RC, Schols, AM, Kelders, MC, Wouters, EF and Janssen-Heininger, YM (2001). Inflammatory cytokines inhibit myogenic differentiation through activation of nuclear factor-kappaB. *FASEB J* **15**: 1169–1180.
9. Baghdiguian, S, Martin, M, Richard, I, Pons, F, Astier, C, Bourg, N *et al.* (1999). Calpain 3 deficiency is associated with myonuclear apoptosis and profound

perturbation of the IkappaB alpha/NF-kappaB pathway in limb-girdle muscular dystrophy type 2A. *Nat Med* **5**: 503–511.
10. Kumar, A, Lnu, S, Malya, R, Barron, D, Moore, J, Corry, DB *et al.* (2003). Mechanical stretch activates nuclear factor-kappaB, activator protein-1, and mitogen-activated protein kinases in lung parenchyma: implications in asthma. *FASEB J* **17**: 1800–1811.
11. Monici, MC, Aguennouz, M, Mazzeo, A, Messina, C and Vita, G (2003). Activation of nuclear factor-kappaB in inflammatory myopathies and Duchenne muscular dystrophy. *Neurology* **60**: 993–997.
12. Hunter, RB and Kandarian, SC (2004). Disruption of either the Nfkb1 or the Bcl3 gene inhibits skeletal muscle atrophy. *J Clin Invest* **114**: 1504–1511.
13. Acharyya, S, Villalta, SA, Bakkar, N, Bupha-Intr, T, Janssen, PM, Carathers, M *et al.* (2007). Interplay of IKK/NF-kappaB signaling in macrophages and myofibers promotes muscle degeneration in Duchenne muscular dystrophy. *J Clin Invest* **117**: 889–901.
14. Bakkar, N, Wang, J, Ladner, KJ, Wang, H, Dahlman, JM, Carathers, M *et al.* (2008). IKK/NF-kappaB regulates skeletal myogenesis via a signaling switch to inhibit differentiation and promote mitochondrial biogenesis. *J Cell Biol* **180**: 787–802.
15. Payne, TR, Oshima, H, Okada, M, Momoi, N, Tobita, K, Keller, BB *et al.* (2007). A relationship between vascular endothelial growth factor, angiogenesis, and cardiac repair after muscle stem cell transplantation into ischemic hearts. *J Am Coll Cardiol* **50**: 1677–1684.
16. Ambrosio, F, Ferrari, RJ, Distefano, G, Plassmeyer, JM, Carvell, GE, Deasy, BM *et al.* (2010). The synergistic effect of treadmill running on stem-cell transplantation to heal injured skeletal muscle. *Tissue Eng Part A* **16**: 839–849.
17. Beg, AA, Sha, WC, Bronson, RT, Ghosh, S and Baltimore, D (1995). Embryonic lethality and liver degeneration in mice lacking the RelA component of NF-kappa B. *Nature* **376**: 167–170.
18. Gharaibeh, B, Lu, A, Tebbets, J, Zheng, B, Feduska, J, Crisan, M *et al.* (2008). Isolation of a slowly adhering cell fraction containing stem cells from murine skeletal muscle by the preplate technique. *Nat Protoc* **3**: 1501–1509.
19. Wan, F and Lenardo, MJ (2009). Specification of DNA binding activity of NF-kappaB proteins. *Cold Spring Harb Perspect Biol* **1**: a000067.
20. Sacco, A, Doyonnas, R, Kraft, P, Vitorovic, S and Blau, HM (2008). Self-renewal and expansion of single transplanted muscle stem cells. *Nature* **456**: 502–506.
21. Jankowski, RJ, Haluszczak, C, Trucco, M and Huard, J (2001). Flow cytometric characterization of myogenic cell populations obtained via the preplate technique: potential for rapid isolation of muscle-derived stem cells. *Hum Gene Ther* **12**: 619–628.
22. Deasy, BM, Jankowski, RJ, Payne, TR, Cao, B, Goff, JP, Greenberger, JS *et al.* (2003). Modeling stem cell population growth: incorporating terms for proliferative heterogeneity. *Stem Cells* **21**: 536–545.
23. Tang, Y, Reay, DP, Salay, MN, Mi, MY, Clemens, PR, Guttridge, DC *et al.* (2010). Inhibition of the IKK/NF-?B pathway by AAV gene transfer improves muscle regeneration in older mdx mice. *Gene Ther* **17**: 1476–1483.
24. Lehtinen, SK, Rahkila, P, Helenius, M, Korhonen, P and Salminen, A (1996). Down-regulation of transcription factors AP-1, Sp-1, and NF-kappa B precedes myocyte differentiation. *Biochem Biophys Res Commun* **229**: 36–43.
25. Guttridge, DC, Albanese, C, Reuther, JY, Pestell, RG and Baldwin, AS Jr (1999). NF-kappaB controls cell growth and differentiation through transcriptional regulation of cyclin D1. *Mol Cell Biol* **19**: 5785–5799.
26. Kaliman, PA and Barannik, TV (1999). Regulation of delta-aminolevulinate synthase activity during the development of oxidative stress. *Biochemistry Mosc* **64**: 699–704.
27. Canicio, J, Ruiz-Lozano, P, Carrasco, M, Palacin, M, Chien, K, Zorzano, A *et al.* (2001). Nuclear factor kappa B-inducing kinase and Ikappa B kinase-alpha signal skeletal muscle cell differentiation. *J Biol Chem* **276**: 20228–20233.
28. Munz, B, Hildt, E, Springer, ML and Blau, HM (2002). RIP2, a checkpoint in myogenic differentiation. *Mol Cell Biol* **22**: 5879–5886.
29. Baeza-Raja, B and Muñoz-Cánoves, P (2004). p38 MAPK-induced nuclear factor-kappaB activity is required for skeletal muscle differentiation: role of interleukin-6. *Mol Biol Cell* **15**: 2013–2026.
30. Guttridge, DC, Mayo, MW, Madrid, LV, Wang, CY and Baldwin, AS Jr (2000). NF-kappaB-induced loss of MyoD messenger RNA: possible role in muscle decay and cachexia. *Science* **289**: 2363–2366.
31. Wang, H, Hertlein, E, Bakkar, N, Sun, H, Acharyya, S, Wang, J *et al.* (2007). NF-kappaB regulation of YY1 inhibits skeletal myogenesis through transcriptional silencing of myofibrillar genes. *Mol Cell Biol* **27**: 4374–4387.
32. Karalaki, M, Fili, S, Philippou, A and Koutsilieris, M (2009). Muscle regeneration: cellular and molecular events. *In Vivo* **23**: 779–796.
33. McFarlane, C, Plummer, E, Thomas, M, Hennebry, A, Ashby, M, Ling, N *et al.* (2006). Myostatin induces cachexia by activating the ubiquitin proteolytic system through an NF-kappaB-independent, FoxO1-dependent mechanism. *J Cell Physiol* **209**: 501–514.
34. Yao, P, Zhan, Y, Xu, W, Li, C, Yue, P, Xu, C *et al.* (2004). Hepatocyte growth factor-induced proliferation of hepatic stem-like cells depends on activation of NF-kappaB. *J Hepatol* **40**: 391–398.
35. Li, Y and Huard, J (2002). Differentiation of muscle-derived cells into myofibroblasts in injured skeletal muscle. *Am J Pathol* **161**: 895–907.

Appendix 5

Cell Transplantation, Vol. 21, pp. 1087–1093, 2012
Printed in the USA.

0963-6897/12 $90.00 + .00
DOI: http://dx.doi.org/10.3727/096368912X636876
E-ISSN 1555-3892
www.cognizantcommunication.com

Isolation of Myogenic Stem Cells From Cultures of Cryopreserved Human Skeletal Muscle

Bo Zheng,*[1] Chien-Wen Chen,*†[1] Guangheng Li,* Seth D. Thompson,*
Minakshi Poddar,* Bruno Péault,*‡§¶ and Johnny Huard*†

*Stem Cell Research Center, Department of Orthopaedic Surgery,
University of Pittsburgh School of Medicine and Children's Hospital of Pittsburgh of UPMC, Pittsburgh, PA, USA
†Department of Bioengineering, University of Pittsburgh Swanson School of Engineering, Pittsburgh, PA, USA
‡Department of Pediatrics, Children's Hospital of Pittsburgh of UPMC, Pittsburgh, PA, USA
§David Geffen School of Medicine, University of California at Los Angeles, Los Angeles, CA, USA
¶Center for Vascular Science and Center for Regenerative Medicine, University of Edinburgh, Edinburgh, UK

We demonstrate that subpopulations of adult human skeletal muscle-derived stem cells, myogenic endothelial cells (MECs), and perivascular stem cells (PSCs) can be simultaneously purified by fluorescence-activated cell sorting (FACS) from cryopreserved human primary skeletal muscle cell cultures (cryo-hPSMCs). For FACS isolation, we utilized a combination of cell lineage markers: the myogenic cell marker CD56, the endothelial cell marker UEA-1 receptor (UEA-1R), and the perivascular cell marker CD146. MECs expressing all three cell lineage markers ($CD56^+UEA\text{-}1R^+CD146^+/CD45^-$) and PSCs expressing only CD146 ($CD146^+/CD45^-CD56^-UEA\text{-}1R^-$) were isolated by FACS. To evaluate their myogenic capacities, the sorted cells, with and without expansion in culture, were transplanted into the cardiotoxin-injured skeletal muscles of immunodeficient mice. The purified MECs exhibited the highest regenerative capacity in the injured mouse muscles among all cell fractions tested, while PSCs remained superior to myoblasts and the unpurified primary skeletal muscle cells. Our findings show that both MECs and PSCs retain their high myogenic potentials after in vitro expansion, cryopreservation, and FACS sorting. The current study demonstrates that myogenic stem cells are prospectively isolatable from long-term cryopreserved primary skeletal muscle cell cultures. We emphasize the potential application of this new approach to extract therapeutic stem cells from human muscle cells cryogenically banked for clinical purposes.

Key words: Myogenesis; Human skeletal muscle; Myogenic endothelial cells (MECs); Perivascular stem cells (PSCs); Cell therapy

INTRODUCTION

Mammalian skeletal muscle harbors multiple stem/progenitor cell populations, which can repair and/or regenerate injured/defective tissues such as damaged/dystrophic skeletal muscles and ischemic hearts (1,2,5,7,8,10,12–19). In particular, we previously reported the identification of two subpopulations of multipotent stem cells within human skeletal muscle [i.e., myogenic endothelial cells (MECs) ($CD45^-CD34^+CD56^+CD144^+$) and perivascular stem cells (PSCs) ($CD34^-CD45^-CD56^-CD146^+$)], which exhibit multilineage mesodermal developmental potentials (6,20). These stem cell populations were specifically localized in situ within the walls of small blood vessels and can be prospectively purified by fluorescence-activated cell sorting (FACS) from fresh human skeletal muscle biopsies, through the use of a combination of positive and negative cell lineage markers (6,20). In vitro, purified MECs and PSCs displayed osteo-, chondro-, adipo-, and myogenic differentiation competence, and their high repair/regenerative capacities were not only demonstrated in injured mouse skeletal muscles but also in infarcted hearts (3,4,6,11,20). However, it has never been documented whether these stem cell fractions could persist and retain their high myogenic capacities after the cryopreservation of human primary skeletal muscle cell cultures (cryo-hPSMCs). Furthermore, MECs and PSCs have been shown to be superior to myoblasts for muscle regeneration in previously performed studies; however, it has

Received July 12, 2010; final acceptance July 10, 2011. Online prepub date: March 21, 2012.
[1]These authors provided equal contribution to this work.
Address correspondence to Johnny Huard, Ph.D., Stem Cell Research Center, Department of Orthopaedic Surgery, University of Pittsburgh School of Medicine, 206 Bridgeside Point II, 450 Technology Drive, Pittsburgh, PA, USA 15219, USA. Tel: (412) 648-2798; Fax: (412) 648-4066; E-mail: jhuard@pitt.edu

never been determined whether MECs isolated from cryopreserved, culture-expanded hPSMCs possessed the same superior regenerative capacity.

In order to identify and purify MECs and PSCs by FACS from in vitro expanded cryo-hPSMCs, we employed a collection of cell lineage markers reported in our previous studies, including the hematopoietic cell marker CD45, the myogenic cell marker CD56 (neural cell adhesion molecule; N-CAM), the perivascular cell marker CD146 (melanoma cell adhesion molecule; M-CAM/Mel-CAM/MUC18), and the endothelial cell marker UEA-1 receptor (*Ulex europaeus* agglutinin I receptor, UEA-1R) (6,20,21). UEA-1R was chosen as a substitute marker for CD34 and CD144 because these two endothelial cell markers are frequently lost during long-term culture whereas UEA-1 maintains consistent reactivity within endothelial cell lineage cultures (20,21). We hypothesized that MECs and PSCs (with and without culture expansion), purified from cryo-hPSMCs, retain their superior myogenic potential and exhibit a greater regeneration capacity of skeletal myofibers when compared to myoblasts.

MATERIALS AND METHODS

Human Muscle Biopsies and Animal Usage

In total, nine independent human skeletal muscle biopsies, from four female and five male donors (age range 4–75, mean 28), were used to obtain human primary skeletal muscle cells (hPSMCs). The procurement of human skeletal muscle biopsies from the National Disease Research Interchange (NDRI) was approved by the Institutional Review Board at the University of Pittsburgh Medical Center (UPMC). All the animal research experiments performed in this study were approved by the Animal Research and Care Committee at the Children's Hospital of Pittsburgh of UPMC (Protocol #34-05) and the University of Pittsburgh (Protocol #0810310-B2).

Cell Isolation and Cryopreservation

The human skeletal muscle biopsies were placed in Hank's Balanced Salt Solution (HBSS, Invitrogen) and transferred to the laboratory on ice. Briefly, tissues were finely minced and serially digested with 0.2% collagenase type XI, 0.25% dispase, and 0.1% trypsin, as previously described (20,21). Dispersed single cell suspensions were cultured in complete medium containing DMEM supplemented with 10% fetal bovine serum (FBS), 10% horse serum, 1% chicken embryo extract, and 1% penicillin/streptomycin (all from Invitrogen). After expansion, cells were cryopreserved at passages 2–8 in medium consisting of 50% complete culture medium and 50% freezing medium (80% FBS + 20% dimethyl sulfoxide) and stored in liquid nitrogen (21).

Flow Cytometry and Cell Sorting

To culture cryo-hPSMCs, cells were thawed and expanded for 2–6 passages. To perform flow cytometry analysis, cells were trypsinized, washed, and incubated with anti-human monoclonal antibodies/ligands: CD45-allophycocyanin-cyanine 7 (APC-Cy7), CD56-phycoerythrin-Cy7 (PE-Cy7), CD34-APC (all from Becton Dickinson), CD146-fluorescein isothiocyanate (FITC; Serotec), UEA-1-PE (Biomeda), von Willebrand factor (vWF)-FITC (US Biology), kinase insert domain receptor (also known as vascular endothelial growth factor receptor 2; VEGFR2) KDR-APC (R&D Systems), and CD144-PE (Beckman Coulter). Negative control samples received equivalent amounts of isotype-matched fluorophore-conjugated antibodies. For FACS purification, cells were incubated with CD45-APC-Cy7, CD56-PE-Cy7, CD146-FITC, UEA-1-PE, and with 7-amino-actinomycin D for dead cell exclusion. Sorted subpopulations were collected for immediate transplantation or transiently expanded in appropriate conditions as previously described (6,20).

Immunocytochemistry

For immunocytochemistry, cells were cytospun onto glass slides, fixed, and incubated with 10% serum. The following primary antibodies were used to detect cell lineage markers, including myogenic cell markers, CD56 (BD) and desmin (Sigma); perivascular cell markers, α-smooth muscle actin (Abcam) and CD146 (Cayman Chemical); endothelial cell markers/ligands, CD144 (Sigma), vWF (DAKO), CD34 (Novocastra), and biotinylated UEA-1 (Vector), followed by incubation with biotinylated secondary antibodies and/or Cy3-conjugated streptavidin (Sigma). Slides were observed and photographed on an epifluorescence microscope system (Nikon Eclipse E800).

Myogenesis In Vivo

To investigate whether the myogenic capacities of the cells were preserved, after cryopreservation, purified MECs, PSCs, myoblasts (Myos), endothelial cells (ECs), and unpurified muscle cells, without in vitro expansion, from six independent hPSMC samples were used for intramuscular injection. The newly sorted cells, on average, $11.8 \pm 5.8 \times 10^4$ $CD56^+$ Myo cells, $7.3 \pm 4.4 \times 10^4$ $CD146^+$ PSCs, $4.5 \pm 2.6 \times 10^4$ $UEA\text{-}1R^+$ ECs, and $2.9 \pm 1.7 \times 10^4$ $CD56^+UEA\text{-}1R^+CD146^+$ MECs as well as 30×10^4 corresponding unsorted cells, were resuspended in 20 μl of HBSS and used for transplantation.

To precisely measure the myogenic-regenerative capacity of each stem/progenitor cell subpopulation, newly sorted MECs, PSCs, and Myo cells were expanded in culture for 1–2 passages. Fifty thousand cells from each subpopulation as well as 5×10^4 corresponding

unsorted cells were trypsinized, washed, and resuspended in 20 μl of phosphate-buffered saline (PBS). Four individual animal experiments were performed, with each using cell populations purified from a single FACS sort of one independent cryo-hPSMC culture.

Cells were injected into a single site of the gastrocnemius muscles of severe combined immunodeficient (SCID) mice that were injured 24 h before by injecting 1 μg of cardiotoxin in 20 μl of HBSS. The untreated group received sham injections of 20 μl of HBSS or PBS only. Treated muscles were collected 2 weeks postinjection for immunohistochemical analyses. Anti-human spectrin was used to identify human cell-derived skeletal myofibers in the mouse muscles. In order to quantitatively evaluate the myogenic regenerative capacity of each subpopulation, the number of human spectrin-positive skeletal myofibers was averaged from six randomly selected sections at the site of injection in each specimen and presented as the regenerative index (per section).

Statistical Analysis

Data were summarized as average ± SE. Statistical comparison between the groups (purified cells after expansion in vitro) was performed using one-way ANOVA with a 95% confidence interval. Bonferroni pairwise multiple comparison test was performed for ANOVA post hoc analysis. Statistical analyses were performed with SigmaStat software.

RESULTS

Heterogenous Cell Composition of Human Primary Skeletal Muscle Cell Cultures (hPSMCs) After Cryopreservation and Long-Term Expansion

After expansion, the cryopreserved hPSMCs (cryo-hPSMCs) were examined by immunocytochemistry for cell surface marker expression. The majority of cryo-hPSMCs expressed desmin and CD56, and to a lesser extent, CD146 (Fig. 1). Only a fraction of cells expressed α-SMA, CD144, vWF, or UEA-1R. As predicted, the cultured human cryo-hPSMCs lacked CD34 expression. After excluding $CD45^+$ hematopoietic cells ($0.2 \pm 0.1\%$), flow cytometry analysis quantitatively confirmed the presence of cells with diverse expressions of cell lineage makers by cryo-hPSMCs: $77.1 \pm 5.7\%$ $CD56^+$, $66.9 \pm 8.1\%$ $CD146^+$, $11.2 \pm 2.5\%$ UEA-$1R^+$, $0.3 \pm 0.1\%$ $CD144^+$, 0.1% vWF^+, and null expression of CD34 and KDR (Fig. 1B). The number of cryo-hPSMCs positive for CD56, CD146, or UEA-1R decreased dramatically after passage 10 (Fig. 1C).

Isolation of Myogenic Stem/Progenitor Cells From Cryo-hPSMCs

After revealing the heterogeneous nature of cryo-hPSMCs, we analyzed these cells for the existence of previously defined subpopulations by multicolor flow cytometry, based on their expression of hematopoietic (CD45), myogenic (CD56), endothelial (UEA-1R), and perivascular (CD146) cell lineage markers (6,20). After exclusion of $CD45^+$ cells, four distinct cell fractions were identified, including myoblasts (Myo) ($CD56^+$/$CD45^-CD146^-$UEA-$1R^-$), endothelial cells (ECs) (UEA-$1R^+$/$CD45^-CD56^-CD146^-$), perivascular stem cells (PSCs) ($CD146^+$/$CD45^-CD56^-$UEA-$1R^-$), and myogenic endothelial cells (MECs), which expressed all three markers ($CD56^+$UEA-$1R^+CD146^+$/$CD45^-$). Long-term cultured cryo-hPSMCs included $22.58 \pm 6.32\%$ Myo, $0.58 \pm 0.23\%$ ECs, $5.92 \pm 4.66\%$ PSCs, and $1.16 \pm 0.19\%$ MECs (Fig. 2). These four cell subsets were subsequently fractionated by FACS, and on average we were able to recover the following number of each cell type: $25.61 \pm 9.16 \times 10^4$ $CD56^+$ Myo, $13.28 \pm 7.37 \times 10^4$ UEA-$1R^+$ ECs, $33.54 \pm 20.53 \times 10^4$ $CD146^+$ PSCs, and $3.84 \pm 0.96 \times 10^4$ $CD56^+$UEA-$1R^+CD146^+$ MECs (Fig. 2).

Purified Myogenic Stem/Progenitor Cells Retain High Myogenic Potentials In Vivo

To evaluate whether the myogenic capacity was preserved after cryopreservation, all sorted cells were immediately transplanted (without culture expansion) into the cardiotoxin-injured gastrocnemius muscles of SCID mice ($n = 6$ per cell fraction). Unpurified muscle cells and HBSS injections were employed as treated and untreated controls, respectively. Mouse muscles were harvested 2 weeks postinjection, cryosectioned, and examined by immunohistochemistry to detect muscle fiber regeneration. An antibody against human spectrin, a myofiber cytoskeletal protein, was used to identify human cell-derived skeletal myofibers in the tissue sections. All of the newly purified cell fractions regenerated human spectrin-positive myofibers in the injured mouse skeletal muscles; however, the purified fractions appeared to regenerate a greater number of muscle fibers than the unpurified cryo-hPSMCs (Fig. 3A). As expected, a lack of spectrin-expressing muscle fibers was observed in the HBSS-injected muscles (Fig. 3A).

To quantitatively measure the myogenic regenerative capacity of each purified stem/progenitor cell population, newly sorted MECs, PSCs, and Myo cells were transiently expanded in culture for 1–2 passages. Fifty thousand cells from each of the subpopulations as well as 5×10^4 corresponding unsorted cells were transplanted into the same type of muscle injury model described above ($n = 4$ per cell fraction). Phosphate-buffered saline (PBS) injections were used as negative controls. ECs were not included in this experiment due to their unstable phenotype in culture. Quantitative analyses revealed that the myogenic regenerative index,

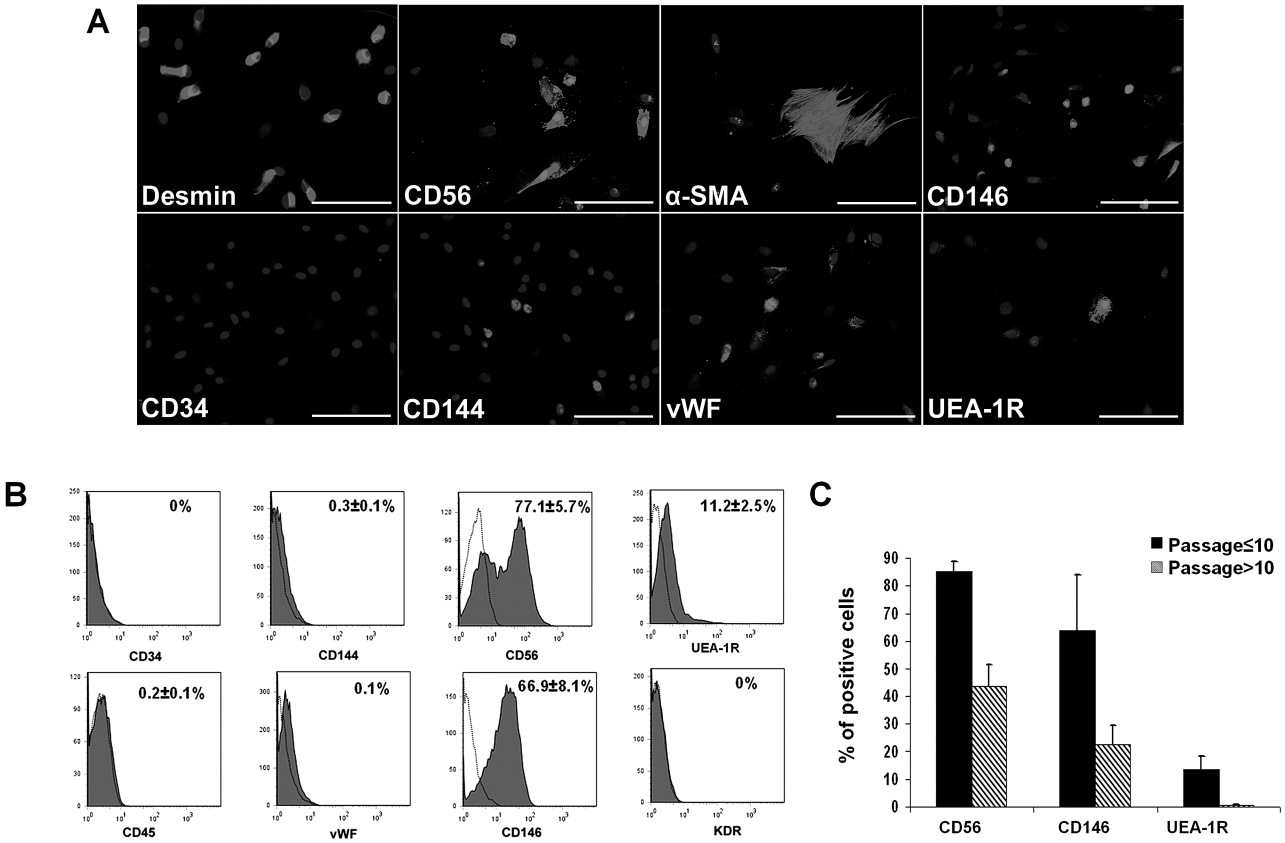

Figure 1. Expression of cell lineage markers by cryopreserved human primary skeletal muscle cells (cryo-hPSMCs). (A) Immunocytochemistry revealed the expression of various cell lineage markers (light gray) by cryo-hPSMCs after expansion. Nuclei were stained with DAPI (dark gray). (B) Flow cytometry analysis quantitatively confirmed the diverse cell composition of cryo-hPSMCs. (C) The number of cryo-hPSMCs positive for CD56, CD146, or UEA-1R decreased when cells were cultured beyond passage 10. Scale bars: 100 μm.

indicated by the average number of human spectrin-positive skeletal myofibers per muscle section, was 166.3 ± 19.2 for the MECs, 90.1 ± 8.0 for the PSCs, 45.7 ± 6.2 for the myoblasts (Myo), and 28.7 ± 8.4 for the unsorted muscle cells (Unsort) (Fig. 3B). The MECs exhibited the highest regeneration index of all four cell fractions tested ($p < 0.005$) (Fig. 3B) and the PSCs regenerated more myofibers than the Myo ($p > 0.05$) and the Unsort ($p = 0.017$) groups (Fig. 3B). Although the purified myoblasts displayed a trend of higher myogenic capacity than the unsorted cells, no statistically significant difference was observed ($p > 0.05$) (Fig. 3B).

DISCUSSION

Skeletal muscle is known to possess multiple stem/progenitor cell populations that are associated with muscle development, maintenance, and regeneration (13,18). Upon purification, muscle stem/progenitor cells in general display more robust myogenic regenerative capacities than unpurified muscle cells in animal disease models, suggesting the advantage of isolating stem cells for therapeutic purposes (6,10,13,20). More recent data have shown that there is a functional heterogeneity in myogenesis even among the muscle precursor cell pool (2).

In the present study, we demonstrated that even after in vitro expansion and cryopreservation, primary human muscle cell cultures include various subpopulations, as indicated by expression of diverse cell lineage markers. Using a modified collection of cell lineage markers (CD45, CD56, CD146, and UEA-1R), we identified and purified to homogeneity four distinct cell populations from cryo-hPSMCs, including two stem cell subpopulations: PSCs ($CD146^+/CD45^-CD56^-UEA\text{-}1R^-$) and MECs ($CD56^+CD146^+UEA\text{-}1R^+/CD45^-$) (6,20,21). Newly sorted MECs, PSCs, ECs, and Myo cells were immediately transplanted into the cardiotoxin-injured skeletal muscles of SCID mice to examine the preservation of their myogenic potential after FACS, all of which regenerated human spectrin-positive myofibers in the injured mouse

skeletal muscles. Quantitative analyses using sorted subpopulations that were minimally expanded in culture showed that the MECs displayed the highest muscle regenerative capacity among all cell subsets tested, and the PSCs were superior to myoblasts and unpurified cryo-hPSMCs.

These results were consistent with our previous observations from injections of cells isolated from fresh skeletal muscle biopsies (6,20). Taken together, our results suggest the presence of distinct subpopulations of highly myogenic stem/progenitor cells within culture-expanded, cryopreserved hPSMCs and support the feasibility of further purifying stem cell fractions from these unpurified cryopreserved human cells. Most importantly, these findings infer the practicability of prospective isolation of myogenic stem/progenitor cell populations from banked human skeletal muscle cells, highlighting a new technology to further enhance the availability and efficacy of cell-mediated therapies (9).

ACKNOWLEDGMENTS: This work was supported in part by grants to J.H from the National Institutes of Health (R01 DE013420-09) and the Department of Defense (W81XWH-09-1-0658) and from the William F. and Jean W. Donaldson Endowed Chair at the Children's Hospital of Pittsburgh, the Henry J. Mankin Endowed Chair for Orthopaedic Research at University of Pittsburgh, and by a grant to B.P. from the National Institutes of Health (R21 HL083057-01A2). The authors also wish to thank Allison Logar for her excellent technical assistance on the flow cytometry and the cell sorting and James H. Cummins for his editorial assistance in the preparation of this manuscript. The following author contributions are recognized: conception and design, collection and/or assembly of data, data analysis and interpretation, manuscript writing (B.Z.); conception and design, collection and/or

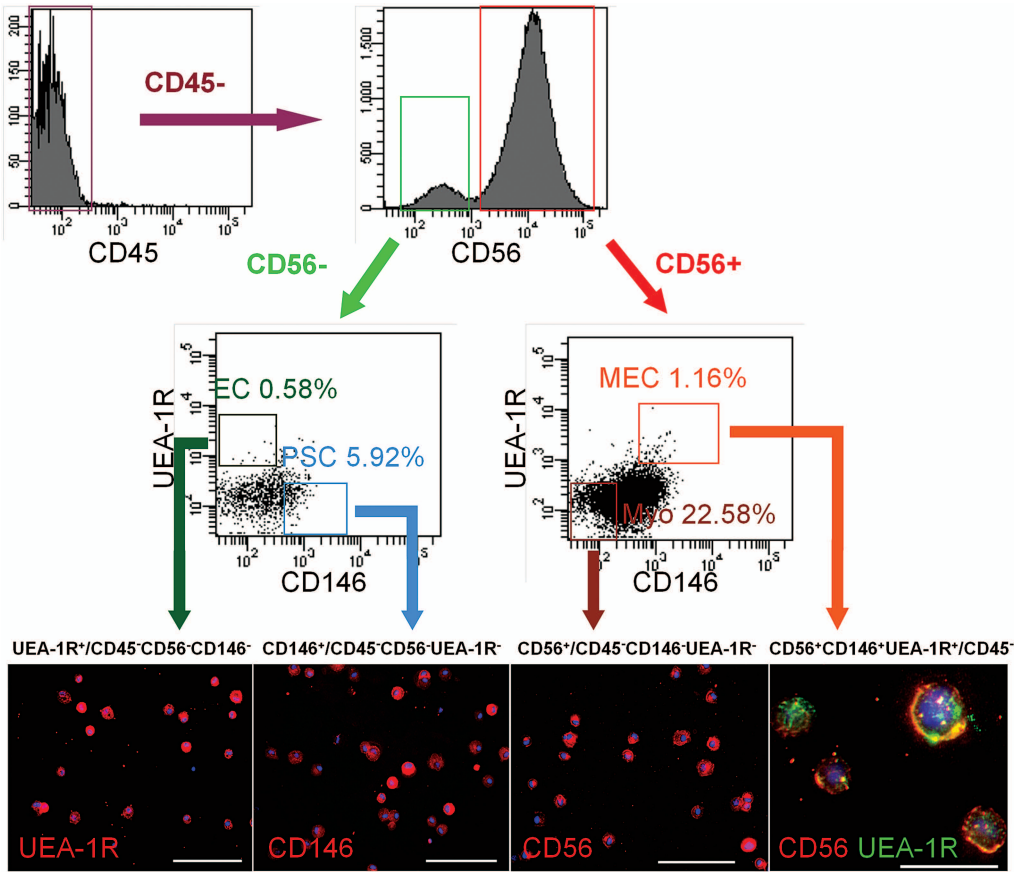

Figure 2. Identification and purification of myogenic stem cells within cryo-hPSMCs. After excluding $CD45^+$ hematopoietic cells, $CD45^-$ cells were separated based on CD56 expression. $CD56^+$ and $CD56^-$ populations were further gated on UEA-1R by CD146 to identify and/or sort four distinct cell populations: myogenic endothelial cells (MECs) ($CD56^+UEA\text{-}1R^+CD146^+/CD45^-$), myoblasts (Myos) ($CD56^+/CD45^-CD146^-UEA\text{-}1R^-$), perivascular stem cells (PSCs) ($CD146^+/CD45^-CD56^-UEA\text{-}1R^-$), and endothelial cells (ECs) ($UEA\text{-}1R^+/CD45^-CD56^-CD146^-$). The purities of the sorted populations were $90.73 \pm 4.82\%$, $92.94 \pm 1.23\%$, 93.86 ± 1.72, and 94.9 ± 0.64, respectively. Immunocytochemistry confirmed the expression of key cell lineage makers by freshly sorted cells: UEA-1R, CD146, and/or CD56. Nuclei were stained blue with DAPI. Scale bars: 100 µm; CD56/UEA-1R double staining: 20 µm.

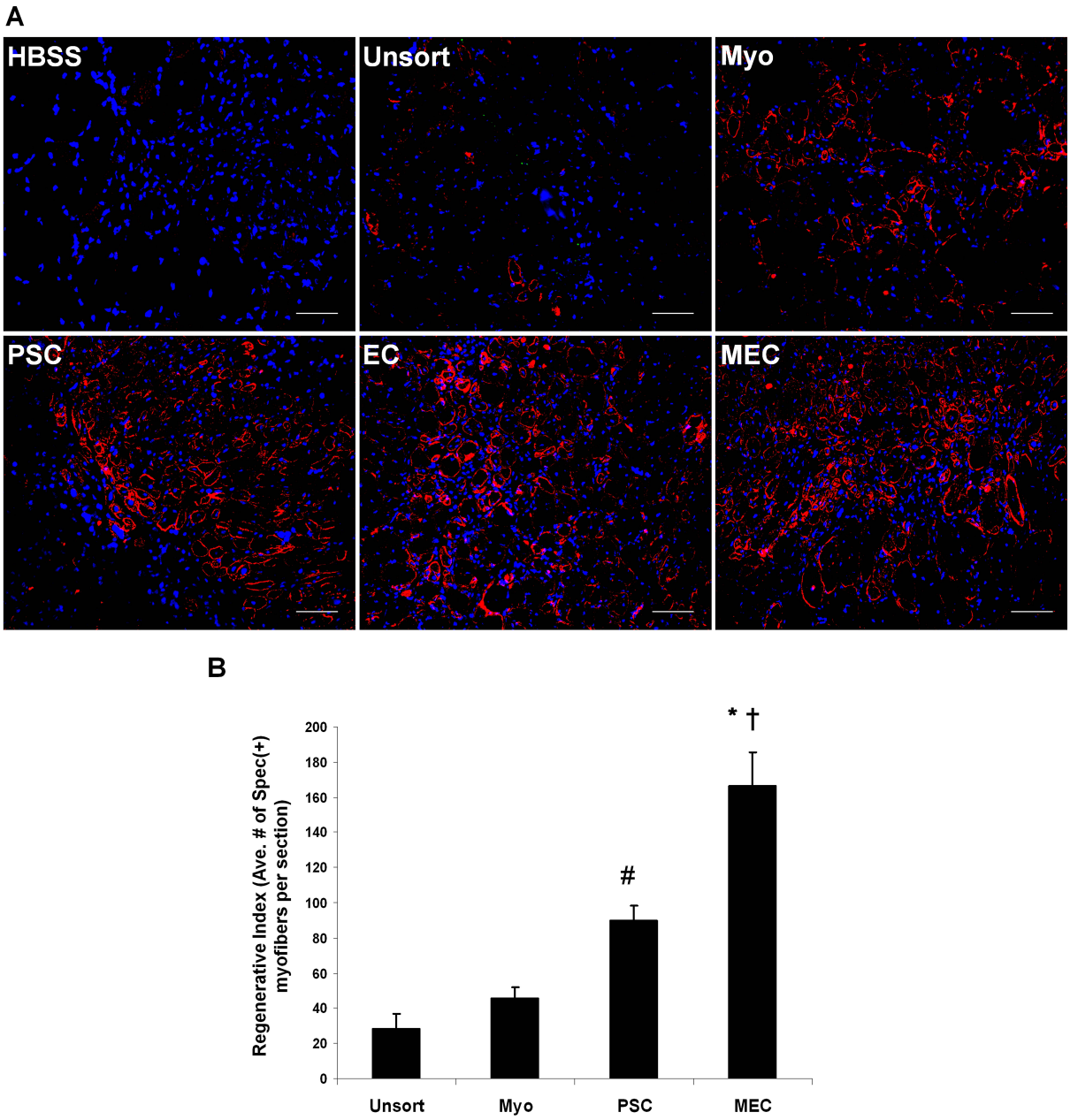

Figure 3. Comparison of myogenic regenerative capacities in vivo. (A) Representative pictures of regenerating human spectrin-positive myofibers in cardiotoxin-injured mouse skeletal muscles transplanted with newly sorted cell fractions from a single donor-derived cryo-hPSMC culture, including myogenic endothelial cells (MECs), perivascular stem cells (PSCs), endothelial cells (ECs), and myoblasts (Myos). Unsorted cryo-hPSMCs (Unsort) and HBSS were injected as treated and untreated controls respectively. Original magnification: 200×; scale bars: 50 µm. (B) Quantitative analyses of the myogenic regenerative capacities of sorted stem/progenitor cell populations. Fifty thousand cells from each cell fraction that was minimally expanded in culture were injected. Quantitative analyses of spectrin-positive human skeletal myofibers on tissue sections revealed that MECs mediated the highest myogenic regeneration among all four cell fractions tested (*$p < 0.001$ vs. Myo and Unsort; †$p = 0.004$ vs. PSC). Injection of PSCs regenerated more human myofibers than injections of Myos ($p > 0.05$) and Unsort (#$p = 0.017$). Finally, Myos displayed a trend of higher myogenic capacity than Unsort, but no significant difference was observed ($p > 0.05$).

assembly of data, data analysis and interpretation, manuscript writing (C.-W.C.); collection and/or assembly of data, data analysis, and interpretation (G.L.); collection and/or assembly of data, data analysis, and interpretation (S.D.T.); collection and/or assembly of data, data analysis and interpretation (M.P.); conception and design, financial support, data analysis and interpretation (B.P.); conception and design, financial support, data analysis and interpretation, manuscript writing, final approval of manuscript (J.H.). Dr. Johnny Huard has received remuneration from Cook Myosite, Inc. for consulting services and for royalties received from technology licensing during the period that the above research was performed. All other authors declare no conflicts of interst.

REFERENCES

1. Carr, L. K.; Steele, D.; Steele, S.; Wagner, D.; Pruchnic, R.; Jankowski, R.; Erickson, J.; Huard, J.; Chancellor, M. B. 1-year follow-up of autologous muscle-derived stem cell injection pilot study to treat stress urinary incontinence. Int. Urogynecol. J. Pelvic Floor Dysfunct. 19(6): 881–883; 2008.
2. Cerletti, M.; Jurga, S.; Witczak, C. A.; Hirshman, M. F.; Shadrach, J. L.; Goodyear, L. J.; Wagers, A. J. Highly efficient, functional engraftment of skeletal muscle stem cells in dystrophic muscles. Cell 134(1):37–47; 2008.
3. Chen, C. W.; Montelatici, E.; Crisan, M.; Corselli, M.; Huard, J.; Lazzari, L.; Péault, B. Perivascular multilineage progenitor cells in human organs: regenerative units, cytokine sources or both? Cytokine Growth Factor Rev. 20(5–6):429–434; 2009.
4. Chen, C. W.; Okada, M.; Tobita, K.; P?ault, B.; Huard, J. Purified human muscle-derived pericytes support formation of vascular structures and promote angiogenesis after myocardial infarction. Circulation 120(18 Suppl.):S1053; 2009.
5. Collins, C. A.; Zammit, P. S.; Ruiz, A. P.; Morgan, J. E.; Partridge, T. A. A population of myogenic stem cells that survives skeletal muscle aging. Stem Cells 25(4):885–894; 2007.
6. Crisan, M.; Yap, S.; Casteilla, L.; Chen, C. W.; Corselli, M.; Park, T. S.; Andriolo, G.; Sun, B.; Zheng, B.; Zhang, L.; Norotte, C.; Teng, P. N.; Traas, J.; Schugar, R.; Deasy, B. M.; Badylak, S.; Buhring, H. J.; Giacobino, J. P.; Lazzari, L.; Huard, J.; Péault, B. A perivascular origin for mesenchymal stem cells in multiple human organs. Cell Stem Cell 3(3):301–313; 2008.
7. Dellavalle, A.; Sampaolesi, M.; Tonlorenzi, R.; Tagliafico, E.; Sacchetti, B.; Perani, L.; Innocenzi, A.; Galvez, B. G.; Messina, G.; Morosetti, R.; Li, S.; Belicchi, M.; Peretti, G.; Chamberlain, J. S.; Wright, W. E.; Torrente, Y.; Ferrari, S.; Bianco, P.; Cossu, G. Pericytes of human skeletal muscle are myogenic precursors distinct from satellite cells. Nat. Cell Biol. 9(3):255–267; 2007.
8. Drowley, L.; Okada, M.; Payne, T. R.; Botta, G. P.; Oshima, H.; Keller, B. B.; Tobita, K.; Huard, J. Sex of muscle stem cells does not influence potency for cardiac cell therapy. Cell Transplant. 18(10):1137–1146; 2009.
9. Hirt-Burri, N.; de Buys Roessingh, A. S.; Scaletta, C.; Gerber, S.; Pioletti, D. P.; Applegate, L. A.; Hohlfeld, J. Human muscular fetal cells: A potential cell source for muscular therapies. Pediatr. Surg. Int. 24(1):37–47; 2008.
10. Jankowski, R. J.; Deasy, B. M.; Huard, J. Muscle-derived stem cells. Gene Ther. 9(10):642–647; 2002.
11. Okada, M.; Payne, T. R.; Zheng, B.; Oshima, H.; Momoi, N.; Tobita, K.; Keller, B. B.; Phillippi, J. A.; Péault, B.; Huard, J. Myogenic endothelial cells purified from human skeletal muscle improve cardiac function after transplantation into infarcted myocardium. J. Am. Coll. Cardiol. 52(23):1869–1880; 2008.
12. Oshima, H.; Payne, T. R.; Urish, K. L.; Sakai, T.; Ling, Y.; Gharaibeh, B.; Tobita, K.; Keller, B. B.; Cummins, J. H.; Huard, J. Differential myocardial infarct repair with muscle stem cells compared to myoblasts. Mol. Ther. 12(6):1130–1141; 2005.
13. Péault, B.; Rudnicki, M.; Torrente, Y.; Cossu, G.; Tremblay, J. P.; Partridge, T.; Gussoni, E.; Kunkel, L. M.; Huard, J. Stem and progenitor cells in skeletal muscle development, maintenance, and therapy. Mol. Ther. 15(5):867–877; 2007.
14. Pisani, D. F.; Dechesne, C. A.; Sacconi, S.; Delplace, S.; Belmonte, N.; Cochet, O.; Clement, N.; Wdziekonski, B.; Villageois, A. P.; Butori, C.; Bagnis, C.; Di Santo, J. P.; Kurzenne, J. Y.; Desnuelle, C.; Dani, C. Isolation of a highly myogenic CD34-negative subset of human skeletal muscle cells free of adipogenic potential. Stem Cells 28(4):753–764; 2010.
15. Rousseau, J.; Dumont, N.; Lebel, C.; Quenneville, S. P.; Côté, C. H.; Frenette, J.; Tremblay, J. P. Dystrophin expression following the transplantation of normal muscle precursor cells protects mdx muscle from contraction-induced damage. Cell Transplant. 19(5):589–596; 2010.
16. Seidel, M.; Borczyńska, A.; Rozwadowska, N.; Kurpisz, M. Cell-based therapy for heart failure: Skeletal myoblasts. Cell Transplant. 18(7):695–707; 2009.
17. Sherman, W.; He, K. L.; Yi, G. H.; Wang, J.; Harvey, J.; Lee, M. J.; Haimes, H.; Lee, P.; Miranda, E.; Kanwal, S.; Burkhoff, D. Myoblast transfer in ischemic heart failure: Effects on rhythm stability. Cell Transplant. 18(3):333–341; 2009.
18. Sherwood, R. I.; Christensen, J. L.; Conboy, I. M.; Conboy, M. J.; Rando, T. A.; Weissman, I. L.; Wagers, A. J. Isolation of adult mouse myogenic progenitors: Functional heterogeneity of cells within and engrafting skeletal muscle. Cell 119(4):543–554; 2004.
19. Torrente, Y.; Belicchi, M.; Marchesi, C.; Dantona, G.; Cogiamanian, F.; Pisati, F.; Gavina, M.; Giordano, R.; Tonlorenzi, R.; Fagiolari, G.; Lamperti, C.; Porretti, L.; Lopa, R.; Sampaolesi, M.; Vicentini, L.; Grimoldi, N.; Tiberio, F.; Songa, V.; Baratta, P.; Prelle, A.; Forzenigo, L.; Guglieri, M.; Pansarasa, O.; Rinaldi, C.; Mouly, V.; Butler-Browne, G. S.; Comi, G. P.; Biondetti, P.; Moggio, M.; Gaini, S. M.; Stocchetti, N.; Priori, A.; D'Angelo, M. G.; Turconi, A.; Bottinelli, R.; Cossu, G.; Rebulla, P.; Bresolin, N. Autologous transplantation of muscle-derived CD133$^+$ stem cells in Duchenne muscle patients. Cell Transplant. 16(6):563–577; 2007.
20. Zheng, B.; Cao, B. H.; Crisan, M.; Sun, B.; Li, G. H.; Logar, A.; Yap, S.; Pollett, J. B.; Drowley, L.; Cassino, T.; Gharaibeh, B.; Deasy, B. M.; Huard, J.; Péault, B. Prospective identification of myogenic endothelial cells in human skeletal muscle. Nat. Biotechnol. 25(9):1025–1034; 2007.
21. Zheng, B.; Li, G. H.; Logar, A.; Péault, B.; Huard, J. Identification of CD56+CD146+UEA-1+ cell population within cryopreserved human skeletal muscle cells which endowed with a high myogenic potential in vivo. The Orthopaedic Research Society (ORS) 54th Annual Meeting, San Francisco, CA; 2008.

Appendix 6

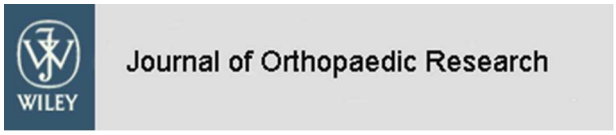

Human Myogenic Endothelial Cells Exhibit Chondrogenic and Osteogenic Potentials at the Clonal Level

Journal:	*Journal of Orthopedic Research*
Manuscript ID:	JOR-12-0639
Wiley - Manuscript type:	Research Article
Date Submitted by the Author:	29-Aug-2012
Complete List of Authors:	Zheng, Bo; Oregon Health & Science University, Li, Guangheng; University of Pittsburgh, Orthopedic Surgery Chen, William; University of Pittsburgh, Orthopedic Surgery; University of Pittsburgh, Bioengineering Deasy, Bridget; University of Pittsburgh, Orthopedic Surgery Pollett, Jonathan; Allegheny General Hospital, Cardiology Sun, Bin; University of Pittsburgh, Vascular Medicine Institute Drowley, Lauren; AstraZeneca, Gharaibeh, Burhan; University of Pittsburgh, Orthopedic Surgery Usas, Arvydas; University of Pittsburgh, Orthopedic Surgery Péault, Bruno; University of Edinburgh, Queens Medical Research Institute Huard, Johnny; Stem Cell Research Center, Dept. of Orthopaedic Surgery;
Keywords:	myogenic endothelial cells , muscle stem cells, clonal analysis, osteogenesis, chondrogenesis

Human Myogenic Endothelial Cells Exhibit Chondrogenic and Osteogenic Potentials at the Clonal Level

Bo Zheng[1,2], Guangheng Li[1,2,*], William CW Chen[1,3,*], Bridget M Deasy[1,2], Jonathan B Pollett[1], Bin Sun[1,4], Lauren Drowley[1], Burhan Gharaibeh[1], Arvydas Usas[1,2], Bruno Péault[1,4,5,6,7], Johnny Huard[1,2,5]

[1]Stem Cell Research Center, University of Pittsburgh School of Medicine

[2]Department of Orthopaedic Surgery, University of Pittsburgh School of Medicine

[3]Department of Bioengineering, University of Pittsburgh Swanson School of Engineering

[4]Department of Pediatrics, Children's Hospital of Pittsburgh of UPMC

[5]McGowan Institute for Regenerative Medicine, University of Pittsburgh

[6]David Geffen School of Medicine, University of California at Los Angeles

[7]Centre for Cardiovascular Science and MRC Centre for Regenerative Medicine, University of Edinburgh, UK

*These authors contributed equally to this work

Correspondence to:

Johnny Huard, PhD

Stem Cell Research Center, Department of Orthopaedic Surgery, School of Medicine, University of Pittsburgh, Bridgeside Point II, Suite 206, 450 Technology Drive, Pittsburgh, PA 15219

TEL: 1-412-648-2798

FAX: 1-412-648-4066

Email: jhuard@pitt.edu

Running Title: Clonal Myogenic Endothelial Cells Exhibit Osteogenic and Chondrogenic Potential

Key words: myogenic endothelial cells, muscle stem cells, clonal analysis, osteogenesis, chondrogenesis

Abstract

We have previously reported the high regenerative potential of murine muscle-derived stem cells (mMDSCs) that are capable of differentiating into multiple mesodermal cell lineages, including myogenic, endothelial, chondrocytic, and osteoblastic cells. Recently we described a putative human counterpart of mMDSCs, the myogenic endothelial cells (MECs), in adult human skeletal muscle, which efficiently repair/regenerate the injured and dystrophic skeletal muscle as well as the ischemic heart in animal disease models. Nevertheless it remained unclear whether human MECs, at the clonal level, preserve mMDSC-like chondrogenic and osteogenic potentials and classic stem cell characteristics including high proliferation and resistance to stress. Herein we demonstrated that MECs, sorted from fresh postnatal human skeletal muscle biopsies, can be grown clonally and exhibit robust resistance to oxidative stress with no tumorigeneity. MEC clones were capable of differentiating into chondrocytes and osteoblasts under inductive conditions in vitro and participated in cartilage and bone formation in vivo. Additionally, adipogenic and angiogenic potentials of clonal MECs (cMECs) were observed. Overall, our study showed that cMECs not only display typical properties of adult stem cells but also exhibit chondrogenic and osteogenic capacities in vitro and in vivo, suggesting their potential applications in articular cartilage and bone repair/regeneration.

INTRODUCTION

Recent studies suggest that stem/progenitor cell populations other than satellite cells repair/regenerate skeletal muscle.[1-7] Our group previously reported that murine muscle-derived stem cells (mMDSCs), a unique population of myogenic stem cells isolated from the slowly adhering fraction of primary muscle cells by the "preplate" technique, proliferate long-term, self-renew, and differentiate into diverse cell lineages.[8-13] mMDSCs express markers typically associated with stem cells, including CD34 and Sca-1. However, expression of these markers in mMDSCs is highly influenced by extended cell culture, leading to the difficulties of finding a valid marker profile for prospective identification and purification of native mMDSCs.

Recently, we have prospectively purified by cell sorting a unique stem cell population associated with the vasculature in the human skeletal muscle.[14] These myogenic endothelial cells (MECs) ($CD34^+/CD56^+/CD144^+/CD45^-$), which presumably represent the human counterpart of mMDSCs, can undergo long-term proliferation, multi-lineage differentiation, and repair skeletal and cardiac muscles with high efficiency, similar to mMDSCs.[14, 15] Although MECs have been characterized in our prior studies,[14, 15] the true capacity of these cells to function as multi-lineage regenerative units has not yet been fully disclosed, especially in chondrogenesis and osteogenesis. One major limitation in characterizing their multipotent potential is the likely heterogeneous nature in stemness. In the present study, we investigated whether MECs, freshly sorted from adult human skeletal muscle based on their unique cell surface marker profile, preserve chondrogenic and osteogenic potentials at the clonal level.

Our results showed that MEC clones possess stem cell characteristics equivalent to mMDSCs, including long-term proliferation with no karyotypic abnormalities and high resistance to stress. The robust ability of clonal MECs (cMECs) to differentiate into

chondrogenic and osteogenic cell lineages in vitro and in vivo was demonstrated. This clonal study of human MECs highlights their regenerative potential for integrated musculoskeletal repair and regeneration.

METHODS

Human Muscle Biopsy Procurement and Animal Research

The procurement of adult human skeletal muscle biopsies from the National Disease Research Interchange (Philadelphia, PA, USA) was approved by the Institutional Review Board at the University of Pittsburgh Medical Center (UPMC). After procurement, biopsies were immediately transported to our laboratory in Hanks' Balanced Salt Solution (HBSS) (Invitrogen, Grand Island, NY, USA) on ice. Animal experiments were approved by the Animal Research and Care Committee of the Children's Hospital of Pittsburgh of UPMC (Protocol #42-04).

Cell Isolation and Cloning

Muscle biopsies were finely minced and digested with collagenases and dispase to obtain single cell suspension as previously described.[14] Cells were immunofluorescently labeled and subject to cell sorting.[14] Details are documented in Supplementary Material.

Gene Expression Profiling

Total RNA was extracted from the 1×10^6 cells using Nucleospin RNA kit (Clontech, Mountain View, CA, USA). Details are listed in Supplementary Material. Primer sequences used for PCR are listed in Supplemental Table 1.

Cell Proliferation Analysis and Cell Survival under Oxidative Stress

For the single cell proliferation assay, cMECs were transduced with lentiviral eGFP reporter and further sorted to homogeny by FACS as previously reported.[16] To test the capacity of cMECs against oxidative stress, MEC clones were plated onto collagen-coated plates and

cultured with proliferation medium containing 400μM hydrogen peroxide (H_2O_2) and 2μl propidium iodide (1:500, PI, Sigma-Aldrich). Bright-field and fluorescent images were taken in a time-lapsed microscopic imaging system. Details are summarized in Supplementary Material.

Tumorigenesis Assay and Karyotype Analysis

To examine the tumorigenic property of cMECs in vitro, we monitored the growth of cMECs plated at different densities on 1% agar in proliferation medium. For karyotype analysis, cMEC clones were cultured for 8 weeks and harvested. The cell pellets were processed for chromosome analysis. Detail procedures are listed in Supplementary Material.

Chondrogenic and Osteogenic Differentiation in Culture and in Vivo

The details of in vitro chondrogenesis and osteogenesis are documented in Supplementary Material. To track donor cells after implantation, cMECs and unsorted cells were co-transduced with retroviral nuclear LacZ (nLacZ) reporter and subsequently with retroviral BMP4 gene as previously reported.[17] After expansion, 5×10^6 cells were seeded onto a 6×6-mm piece of Gelfoam, incubated overnight, and implanted into the gluteofemoral muscle pockets of SCID mice (8-week-old male; The Jackson Laboratory, Bar Harbor, ME, USA).

Adipogenesis in Culture and Angiogenesis in Vitro/in Vivo

The details of in vitro adipogenesis and angiogenesis as well as in vivo angiogenesis are summarized in Supplementary Material.

RESULTS

Isolation and characterization of myogenic endothelial cell clones

MECs ($CD34^+CD56^+CD144^+CD45^-$) were isolated by fluorescence activated cell sorting (FACS) from dissociated muscle biopsies as previously reported.[18] Single sorted MEC was then automatically seeded by the autoclone system of the FACSAria sorter into each well of a

collagen-coated 96-well plate (seeding density: 1 cell/well). Wells that did not contain exactly 1 cell/well were excluded from the study. A total of six MEC clones from 2 distinct muscle biopsies were obtained from 576 single-cell seeded wells. The average cloning efficiency was 1.04 %, with MECs of donor #1 and #2 having the cloning efficiency of 0.69% and 1.39% respectively. Clonal MECs (cMECs) at passage 6-15 were analyzed for their phenotypes, single cell proliferation, and multi-lineage differentiation capacity and subsequently used for transplantation experiments. Six MEC clones were individually analyzed for gene expression by RT-PCR. The results showed that genes of the lineage-specific markers were expressed in all clones at similar levels (**Figure 1A**). Notably, in addition to the late myogenic markers: desmin, m-cadherin, and CD56, we also detected expression of the early myogenic transcription factors, Pax3, Pax7, and Myf5 in all 6 clones (**Figure 1A**).

Single cells derived from MEC clones undergo clonogenic proliferation

To precisely quantitate the clonogenic potential and long-term proliferation of cMECs in culture, we performed sub-cloning analysis. MEC clones were lentivirally transduced at passage 15 to express enhanced green fluorescence protein (eGFP). Sub-cloning analysis was performed with eGFP+ cMECs individually sorted into each well of a 384-well plate by the FACSAria autoclone system (**Supplemental Figure 1**). Approximately 1/3 of all wells received exactly one cell per well; the remaining 2/3 received none. Proliferation of sub-cloned cMECs was monitored by a time-lapsed microscopic imaging system. The results showed that 73% of sub-cloned cMECs expanded to more than 8 cells, 14% divided into 2-4 cells, 12% did not divide, and 1% eventually died (**Figure 1B**). Cell doubling time and averaged cell division time were 28.1 ± 5.5 hours and 16.8 ± 2.1 hours respectively (mean±SD, n=4) (**Figure 1C**). A video of single sub-cloned cMEC proliferation was presented (**Supplemental Video**).

Gene expression, tumorigenesis, karyotype analysis, and resistance to oxidative stress

Gene expression analyses revealed that cMECs express genes associated with undifferentiated cells (GABRB3 and DNMT3B), and the stemness gene, IL6ST when compared to the unsorted human primary skeletal muscle cells (hPSMCs) (**Supplemental Table 2**). In contrast, hPSMCs expressed genes associated with myogenic differentiation including: Runx-2, Noggin, MYF5, MyoD1, Des and Actc (**Supplemental Table 2**). To assess their tumorigenesis, cMECs cultured for 2 months were analyzed for anchorage independent growth, a hallmark of transformed tumor cells. Cells were plated on a layer of 1% agar at different densities, and colony growth was scored at 2 and 3 weeks post-seeding. Non-adherent cell growth was only observed when cMECs were plated at a very high density of 2.5×10^4 cells/cm^2. Cells plated at low densities (25 and 250 cells/cm^2) and regular culture density (2,500 cells/cm^2) did not grow in an anchorage-independent manner and eventually died (**Supplemental Figure 2**). Furthermore, tumorigenesis in vivo was examined by implanting expanded cMECs into skeletal muscle pockets in the hind limbs of SCID mice. No evidence of tumor growth at 12 weeks post-transplantation was observed physically and histologically (data not shown). Finally, karyotype analyses revealed little-to-no structural (data not shown) and numerical (**Figure 1D**) abnormalities in the chromosome of all long-term cultured MEC clones.

Non-clonal MECs displayed a superior regenerative capacity in both skeletal and cardiac muscles when compared to myoblasts and/or endothelial cells, a behavior hypothesized to be associated with MECs' ability to withstand oxidative stress.[18, 19] Whether cMECs retain the resistance to oxidative stress was examined by culturing the cells in 400μM H_2O_2 and analyzing their survival every 12 hours over a 72-hour period.[20] Among five MEC clones tested, four withstood the oxidative stress to a similar or better level as non-clonal MECs, which had a

survival rate of 30.6% at 72 hours (**Supplemental Table 3**). This result suggested that cMECs in general have high resistance to extended exposure of oxidative stress.

cMECs undergo chondrogenic differentiation in vitro and in vivo

To induce chondrogenic differentiation, cMECs and hPSMCs were pellet-cultured in chondrogenic induction medium supplemented with BMP4 and TGF-β3 for up to 3 weeks. Gross morphology of pellets was compared (**Figure 2A**). The average volume of the pellets formed by cMECs was significantly larger than those formed by hPSMCs at day 7 and 21 (n=3 per group, $p<0.01$, two-tailed unpaired t test) (**Figure 2B**). Pellets were then sectioned and stained specifically for the cartilaginous matrix with Alcian blue (pH=1). cMEC pellets displayed denser blue staining when compared to hPSMC ones at all 3 time points, suggesting a robust chondrogenic potential of cMECs (**Figure 2C**). To investigate their chondrogenic potential in vivo, we co-transduced cMECs with retroviruses encoding BMP4 and nuclear LacZ (nLacZ) genes. The transduction efficiency was near 80%, revealed by the positive β-gal staining (blue) localized to the nuclei of cMECs (**Figure 2D.a**). The presence of round chondrocytes with LacZ+ nuclei (**Figure 2D.b**) and positive immunostaining for collagen type II (**Figure 2D.c**) were observed within the implanted scaffold. A few collagen type II-positive cells co-expressed β-galactosidase, confirming the presence of functional chondrogenic cells originated from donor cMECs (**Figure 2D.d**). Together these data suggest that cMECs were able to differentiate into chondrocytes in vitro and in vivo, albeit to a different extent.

cMECs undergo osteogenic differentiation in vitro and in vivo

To assay the production of mineralized extracellular matrix, cMECs were pellet-cultured in osteogenic induction medium supplemented with BMP4. Osteogenic differentiation was revealed by von Kossa staining after 7 and 21 days in culture. Compared with hPSMCs, pellets

formed by cMECs exhibited more intense mineralization (**Figure 3A**). cMEC pellets maintained in control proliferation medium with no BMP4 remained negative for von Kossa staining, suggesting no spontaneous osteogenic differentiation of cMECs without a proper inductive signal (**Figure 3A**). Mineralization within the pellet was detected by micro-computerized tomography (μCT) at 7 and 21 days (**Figure 3B**). μCT images showed that cMECs produced a significantly higher volume (**Figure 3C**) and density (**Figure 3D**) of mineralized matrix when compared to hPSMCs at both time points (n=3 per group, both $p<0.01$, two-tailed unpaired t test).

To evaluate their osteogenic potential in vivo, cMECs or hPSMCs were co-transduced with retroviruses encoding nLacZ and BMP4 genes and seeded onto a gelatin sponge (5×10^6 cells), followed by implantation into an intramuscular pocket of SCID mice. μCT imaging revealed that transduced cMECs form dense ectopic bone consistently at 2, 4, 8 and 16 weeks post-implantation while transduced hPSMCs fail to form any organized structure (**Figure 3E**). A significant difference in mineralized tissue volume between the two groups was observed at all time points (n=3 per group, all $p<0.01$, two-tailed unpaired t test) (**Figure 3F**). To track donor cMECs undergoing osteogenic differentiation, β-gal/eosin co-staining was performed on the sections of the cMEC-formed ectopic bone structure (**Figure 3G.a**). Osteogenic differentiation of donor cMECs was also confirmed by co-localization of the positive immunohistochemical signals of nLacZ and osteocalcin (**Figure 3G.b**) as well as the positive immunofluorescent signals of β-galactosidase and osteocalcin (**Figure 3G.c)**. Collectively, cMECs exhibited robust osteogenic differentiation capacity under appropriate inductive signals in vitro and in vivo.

cMECs differentiate into adipocytes and remain angiogenic in vitro and in vivo

To understand whether cMECs are able to differentiate into other mesodermal cell lineages, we examined their adipogenic potential in vitro. cMECs cultured in adipogenic induction medium were subsequently stained positive by Oil Red O, revealing the accumulated cytoplasmic lipid droplets **(Supplemental Figure 3A)**. cMECs maintained in control medium were not adipogenic **(Supplemental Figure 3B)**.

To investigate the angiogenic capacity of cMECs, Matrigel culture was used to observe the formation of capillary-like structures.[21] After incubation for 16 hours, cMECs cultured in Matrigel formed capillary-like network **(Supplemental Figure 3C)** while hPSMCs failed to form similar structures under the same condition **(Supplemental Figure 3D)**. Next we subcutaneously implanted Matrigel plugs encapsulating 1.0×10^6 cMECs, hPSMCs, or no cells into the back of SCID mice (n=4 per group). Capillary formation within the implanted plug was determined by anti-CD31 immunostaining **(Supplemental Figure 3E-G)**. The cMEC-plugs displayed significantly higher capillary density than the hPSMC-plugs ($p<0.01$, two-tailed unpaired t test) **(Supplemental Figure 3H)**. Implants with no cells exhibited no presence of CD31-positive structures. To confirm the human origin of the newly formed microvessels within the Matrigel plugs, Lamin A/C, a human nuclear specific antigen, was used to identify donor cMECs. A fraction of microvascular endothelial cells within the cMEC plugs indeed co-expressed CD31 and Lamin A/C, indicative of their human origin **(Supplemental Figure 3I-L).** These results suggest that human cMECs are not only capable of differentiating into major mesenchymal cell lineages but also retain their angiogenic capacity and participate in neovascularization in vivo after long-term culture.

DISCUSSION

Our group has previously demonstrated that mMDSCs differentiate into diverse cell lineages including bone, cartilage, muscle, endothelial, and blood cells.[8-11, 13, 22] mMDSCs repair skeletal and cardiac muscles more efficiently than myoblasts and vascular endothelial cells.[9, 11] Recently we have purified myogenic endothelial cells (MECs) from adult human skeletal muscle that co-express cell surface markers of both myogenic and endothelial cell lineages and exhibit superior regenerative capacities in injured skeletal and cardiac muscle, similar to mMDSCs.[14, 15] Nevertheless, the osteogenic and chondrogenic potentials of MECs were not fully examined at the clonal level. The present study employed the clonogenic assay to evaluate the osteogenic and chondrogenic capacities of single MEC and further characterize their stem cell properties.

We herein established a protocol that enable us to prospectively purify MEC clones from fresh human muscle biopsies directly by FACS sorting, using the previously reported combination of cell surface markers for MEC isolation.[14] RT-PCR analysis revealed that all of the MEC clones expressed genes of myogenic (desmin, CD56, Pax3, Pax7, m-cadherin and MYf5), endothelial (CD34, CD144 and vWF), smooth muscle/vascular mural (α-smooth muscle actin, PDGFR-β, NG2 and CD146), and mesenchymal stem/stromal (CD90 and CD105) cell lineages, showing consistency between clones from the two donor sources. cMECs displayed robust multipotency in vitro and in vivo, including chondrogenesis, osteogenesis, adipogenesis and angiogenesis/vasculogenesis, in addition to myogenesis reported previously.[14] Nevertheless, cMECs could not differentiate into hematopoietic cells in vitro under inductive conditions, even with the presence of OP9 stromal cells (data not shown).

MEC clones were shown to resist oxidative stress efficiently, to a similar or better level of that of non-clonal MECs. cMECs up-regulated genes associated with early progenitor cells, GABRB3 and DNMT3B, and a gene correlated to stemness, IL6ST. When compared to hPSMC,

cMECs expressed much lower level of genes associated with advanced myogenic differentiation, including Runx-2, Noggin, MyoD1, MYF5, Desmin and α-actin. The tumorigenic assay and karyotype analysis revealed no tumorigeneity in long-term expanded cMECs, suggesting the safety of this novel multi-lineage stem cell population in regenerative applications.

Our previous studies of mMDSCs indicated that these cells reside in areas that are normally occupied by capillaries running alongside myofibers.[8, 9] Similarly, MECs are associated with the vasculature in human skeletal muscle, specifically the capillaries located within the interstitial space between myofibers. The hypothesis that MECs represent a developmental intermediate between myogenic and endothelial cells was further supported by the evidence suggesting that muscle satellite cells and endothelial cells are close neighbors and privileged developmental partners.[23] Despite the unclear developmental relationship between MECs and other blood-vessel-associated stem/progenitor cells such as mesoangioblasts[24-26] and pericytes[16, 27], our data suggest that cMECs are indeed one of the multi-lineage mesodermal stem cell populations residing in a vascular niche within the adult skeletal muscle[1, 28, 29] and likely represent a human counterpart of mMDSCs.[30] Overall, these cells not only represent a promising cell source for an integrative application in musculoskeletal repair but also provide more evidence to the involvement of vasculature in post-natal musculoskeletal regeneration.

ACKNOWLEDGEMENTS

The authors wish to thank Alison Logar for her expert assistance in flow cytometry and James H. Cummins for his editorial assistance. This work was supported in part by grants from the National Institutes of Health (R01-AR049684; RO1-DE13420-06; IU54AR050733-01) and the Department of Defense (AFIRM grant W81XWH-08-2-0032) and by the William F. and Jean W. Donaldson Endowed Chair at the Children's Hospital of Pittsburgh, the Henry J. Mankin

Endowed Chair at the University of Pittsburgh, the Orris C. Hirtzel and Beatrice Dewey Hirtzel Memorial Foundation, and the Lemieux Foundation at the University of Pittsburgh. Johnny Huard received remuneration as a consultant for Cook MyoSite, Inc. during the period of this investigation. No other authors have any conflict of interest to disclose.

REFERENCES

1. Peault B, Rudnicki M, Torrente Y, Cossu G, Tremblay JP, Partridge T, et al. Stem and Progenitor Cells in Skeletal Muscle Development, Maintenance, and Therapy. Mol Ther. 2007; **15**(5): 867-77.
2. De Angelis L, Berghella L, Coletta M, Lattanzi L, Zanchi M, Cusella-De Angelis MG, et al. Skeletal myogenic progenitors originating from embryonic dorsal aorta coexpress endothelial and myogenic markers and contribute to postnatal muscle growth and regeneration. J Cell Biol. 1999; **147**(4): 869-78.
3. Ferrari G, Cusella-De Angelis G, Coletta M, Paolucci E, Stornaiuolo A, Cossu G, et al. Muscle regeneration by bone marrow-derived myogenic progenitors. Science. 1998; **279**(5356): 1528-30.
4. Sampaolesi M, Torrente Y, Innocenzi A, Tonlorenzi R, D'Antona G, Pellegrino MA, et al. Cell therapy of alpha-sarcoglycan null dystrophic mice through intra-arterial delivery of mesoangioblasts. Science. 2003; **301**(5632): 487-92.
5. Dellavalle A, Sampaolesi M, Tonlorenzi R, Tagliafico E, Sacchetti B, Perani L, et al. Pericytes of human skeletal muscle are myogenic precursors distinct from satellite cells. Nat Cell Biol. 2007; **9**(3): 255-67.
6. Crisan M, Yap S, Casteilla L, Chen C-W, Corselli M, Park TS, et al. A Perivascular Origin for Mesenchymal Stem Cells in Multiple Human Organs. Cell Stem Cell. 2008; **3**(3): 301-13.
7. Dellavalle A, Maroli G, Covarello D, Azzoni E, Innocenzi A, Perani L, et al. Pericytes resident in postnatal skeletal muscle differentiate into muscle fibres and generate satellite cells. Nat Commun. 2011; **2**: 499.
8. Lee JY, Qu-Petersen Z, Cao B, Kimura S, Jankowski R, Cummins J, et al. Clonal isolation of muscle-derived cells capable of enhancing muscle regeneration and bone healing. J Cell Biol. 2000; **150**(5): 1085-100.
9. Qu-Petersen Z, Deasy B, Jankowski R, Ikezawa M, Cummins J, Pruchnic R, et al. Identification of a novel population of muscle stem cells in mice: potential for muscle regeneration. J Cell Biol. 2002; **157**(5): 851-64.
10. Cao B, Zheng B, Jankowski RJ, Kimura S, Ikezawa M, Deasy B, et al. Muscle stem cells differentiate into haematopoietic lineages but retain myogenic potential. Nat Cell Biol. 2003; **5**(7): 640-6.
11. Payne TR, Oshima H, Sakai T, Ling Y, Gharaibeh B, Cummins J, et al. Regeneration of dystrophin-expressing myocytes in the mdx heart by skeletal muscle stem cells. Gene Ther. 2005; **12**(16): 1264-74.

12. Gharaibeh B, Lu A, Tebbets J, Zheng B, Feduska J, Crisan M, et al. Isolation of a slowly adhering cell fraction containing stem cells from murine skeletal muscle by the preplate technique. Nat Protocols. 2008; **3**(9): 1501-9.
13. Kuroda R, Usas A, Kubo S, Corsi K, Peng H, Rose T, et al. Cartilage repair using bone morphogenetic protein 4 and muscle-derived stem cells. Arthritis Rheum. 2006; **54**(2): 433-42.
14. Zheng B, Cao B, Crisan M, Sun B, Li G, Logar A, et al. Prospective identification of myogenic endothelial cells in human skeletal muscle. Nat Biotech. 2007; **25**(9): 1025-34.
15. Okada M, Payne TR, Zheng B, Oshima H, Momoi N, Tobita K, et al. Myogenic Endothelial Cells Purified From Human Skeletal Muscle Improve Cardiac Function After Transplantation Into Infarcted Myocardium. Journal of the American College of Cardiology. 2008; **52**(23): 1869-80.
16. Crisan M, Yap S, Casteilla L, Chen CW, Corselli M, Park TS, et al. A perivascular origin for mesenchymal stem cells in multiple human organs. Cell Stem Cell. 2008; **3**(3): 301-13.
17. Zheng B, Cao B, Li G, Huard J. Mouse adipose-derived stem cells undergo multilineage differentiation in vitro but primarily osteogenic and chondrogenic differentiation in vivo. Tissue Eng. 2006; **12**(7): 1891-901.
18. Zheng B, Cao B, Crisan M, Sun B, Li G, Logar A, et al. Prospective identification of myogenic endothelial cells in human skeletal muscle. Nat Biotechnol. 2007; **25**(9): 1025-34.
19. Okada M, Payne TR, Zheng B, Oshima H, Momoi N, Tobita K, et al. Myogenic endothelial cells purified from human skeletal muscle improve cardiac function after transplantation into infarcted myocardium. J Am Coll Cardiol. 2008; **52**(23): 1869-80.
20. Drowley L, Okada M, Payne TR, Botta GP, Oshima H, Keller BB, et al. Sex of muscle stem cells does not influence potency for cardiac cell therapy. Cell Transplant. 2009; **18**(10): 1137-46.
21. Wang ZZ, Au P, Chen T, Shao Y, Daheron LM, Bai H, et al. Endothelial cells derived from human embryonic stem cells form durable blood vessels in vivo. Nat Biotechnol. 2007; **25**(3): 317-8.
22. Gharaibeh B, Lu A, Tebbets J, Zheng B, Feduska J, Crisan M, et al. Isolation of a slowly adhering cell fraction containing stem cells from murine skeletal muscle by the preplate technique. Nat Protoc. 2008; **3**(9): 1501-9.
23. Christov C, Chretien F, Abou-Khalil R, Bassez G, Vallet G, Authier FJ, et al. Muscle satellite cells and endothelial cells: close neighbors and privileged partners. Mol Biol Cell. 2007; **18**(4): 1397-409.
24. Minasi MG, Riminucci M, De Angelis L, Borello U, Berarducci B, Innocenzi A, et al. The meso-angioblast: a multipotent, self-renewing cell that originates from the dorsal aorta and differentiates into most mesodermal tissues. Development. 2002; **129**(11): 2773-83.
25. Cossu G, Bianco P. Mesoangioblasts--vascular progenitors for extravascular mesodermal tissues. Curr Opin Genet Dev. 2003; **13**(5): 537-42.
26. Sampaolesi M, Blot S, D'Antona G, Granger N, Tonlorenzi R, Innocenzi A, et al. Mesoangioblast stem cells ameliorate muscle function in dystrophic dogs. Nature. 2006; **444**(7119): 574-9.
27. Dellavalle A, Sampaolesi M, Tonlorenzi R, Tagliafico E, Sacchetti B, Perani L, et al. Pericytes of human skeletal muscle are myogenic precursors distinct from satellite cells. Nat Cell Biol. 2007; **9**(3): 255-67.
28. Kuang S, Gillespie MA, Rudnicki MA. Niche regulation of muscle satellite cell self-renewal and differentiation. Cell Stem Cell. 2008; **2**(1): 22-31.

29. Voog J, Jones DL. Stem cells and the niche: a dynamic duo. Cell Stem Cell. **6**(2): 103-15.
30. Chen C-W, Corselli M, Péault B, Huard J. Human Blood-Vessel-Derived Stem Cells for Tissue Repair and Regeneration. Journal of Biomedicine and Biotechnology. 2012: Epub Feb 2.

FIGURE LEGENDS

Figure 1. Characterization of clonal myogenic endothelial cells (cMECs) in culture. (A) RT-PCR analysis was performed on all six FACS-sorted MEC clones and compared with HUVECs, cultured unsorted hPSMCs (Unsorted), and fresh skeletal muscle cell lysate (Fresh total cells). All MEC clones consistently expressed myogenic (desmin, CD56, Pax7, m-cadherin, Pax3 Myf5), endothelial (CD34, VE-cadherin, vWF), smooth muscle/vascular mural (α-smooth muscle actin, PDGFR-β, NG2, CD146), and mesenchymal stem/stromal (CD90 and CD105) cell markers. **(B)** Analysis of cMEC clonogenic proliferation capacity by sub-cloning single cells from GFP-transduced MEC clones. A total of 80 sub-cloned single GFP-positive cMEC cells (31% of 258 seeded wells) were tracked. Among them, 1% died, 12% did not divide, 14% divided to 2-4 cells, and 73% were able to form colonies (> 8 cells). **(C)** Colony growth rate (n=4) after 17 days in culture showed that the population doubling time was 28.1±5.5 hours, and the cell division time was 16.8 ±2.1 hours. **(D)** After 10 passages in culture, the majority of cMEC metaphases analyzed possess an euploid number (46) of chromosomes.

Figure 2. Chondrogenic differentiation in vitro and in vivo. (A) Gross morphology of cartilage-like pellets formed by cMECs and unsorted muscle cells after being pellet-cultured in chondrogenic medium for 3 weeks. **(B)** cMEC pellets had significantly larger volume than unsorted hPSMC pellets at day 7 and 21 (**p<0.01, Student's t-test). Data were shown as mean ± SD (n=3). **(C)** Chondrogenic differentiation is revealed by Alcian blue/nuclear fast red staining

of pellets cultured in chondrogenic medium supplemented with BMP4 and TGFβ3 at different time points (day 7, 14 and 21) (10X magnification, scale bar represents 25μm). **(D.a)** cMECs were genetically engineered to express nLacZ reporter gene. Positive staining (blue) is localized to the nuclei of the cells (scale bar represents 25μm). **(D.b)** Three weeks after transplantation, chondrogenesis in vivo by cMECs was demonstrated by co-localization of round chondrocytes with blue nuclei (arrow) after staining for β-galactosidase/eosin (scale bar represents 50μm) **(D.c)** Chondrogenesis of cMECs was also revealed by positive immunostaining for collagen type-II (red) (scale bar represents 25μm), and (**D.d**) Co-localization of collagen type-II (red) and β-galactosidase (green, arrow) signals was also detected (scale bar represents 50μm).

Figure 3. Osteogenic differentiation in vitro and in vivo. (A) von Kossa staining of cell pellets cultured in the osteogenic inductive conditions at different time points. Compared to unsorted cell pellets, cMEC pellets cultured in the osteogenic inductive medium containing BMP4 appear to display more extensive mineralization at day 7 and 21. Nevertheless, control cMEC pellets maintained in proliferation medium exhibited no mineralization (scale bar represents 250μm). **(B)** MicroCT images showed that cMEC pellets have a significantly higher **(C)** mineralized matrix volume and (**D)** mineralized matrix density when compared with unsorted cell pellets at day 7 and 21 (**$p<0.01$, Student t-test). Data were shown as mean ± SD (n=3). **(E)** cMECs or unsorted hPSMCs were retrovirally transduced to express BMP4, seeded onto Gelfoam, and implanted into the intramuscular pocket of SCID mice. MicroCT imaging demonstrated that cMEC implants appear to give rise to larger and more organized ectopic mineralized tissue than unsorted cells at all time points. **(F)** There is a significant difference of mineralized tissue volume between the two groups ($p<0.01$ at all time points, Student's t-test). Data were shown as mean ± SEM (n=3). Osteogenesis in vivo by cMECs was also confirmed by co-localization of

(G.a) β-galactosidase-positive nuclei (blue) within eosin-positive cells and **(G.b)** positive immunohistochemical staining for β-galactosidase (blue) and osteocalcin (brown) in the newly formed mineralized tissue as well as **(G.c)** co-localized immunofluorescent staining of osteocalcin (red) and β-galactosidase (green, arrow) (scale bar represents 50μm).

Figure 1

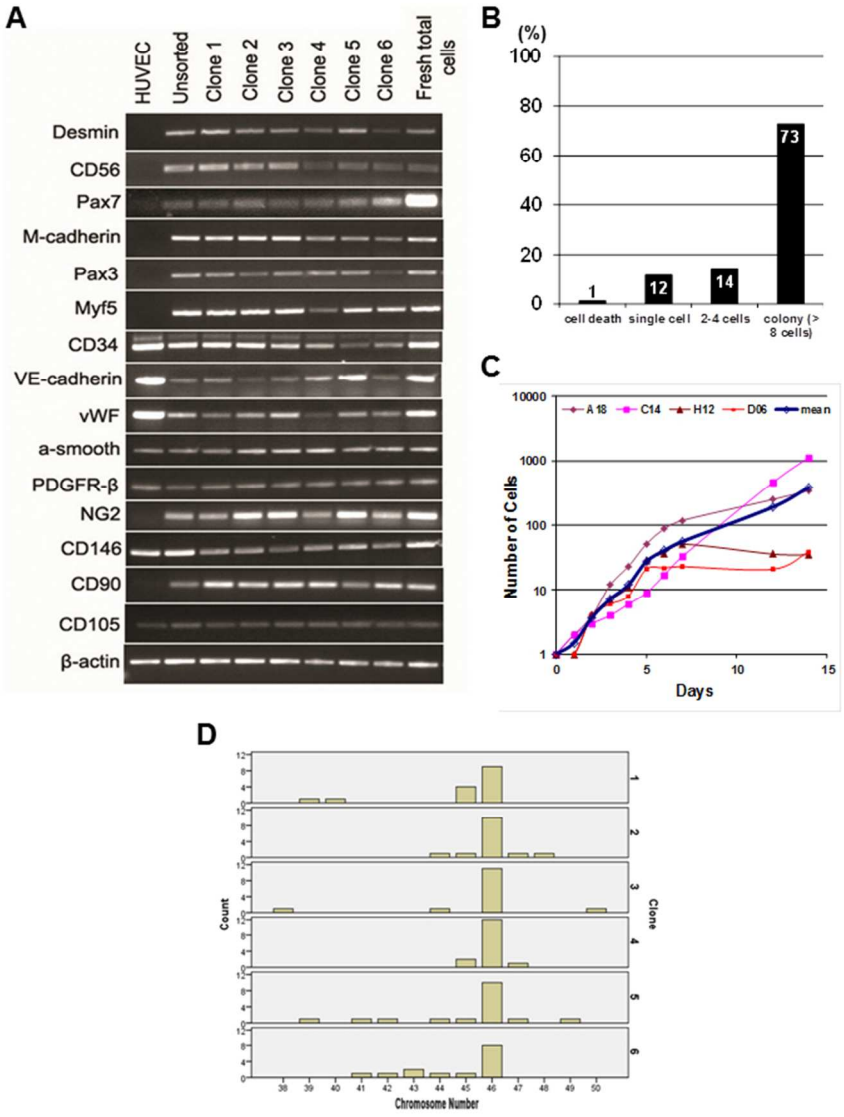

190x254mm (96 x 96 DPI)

Figure 2

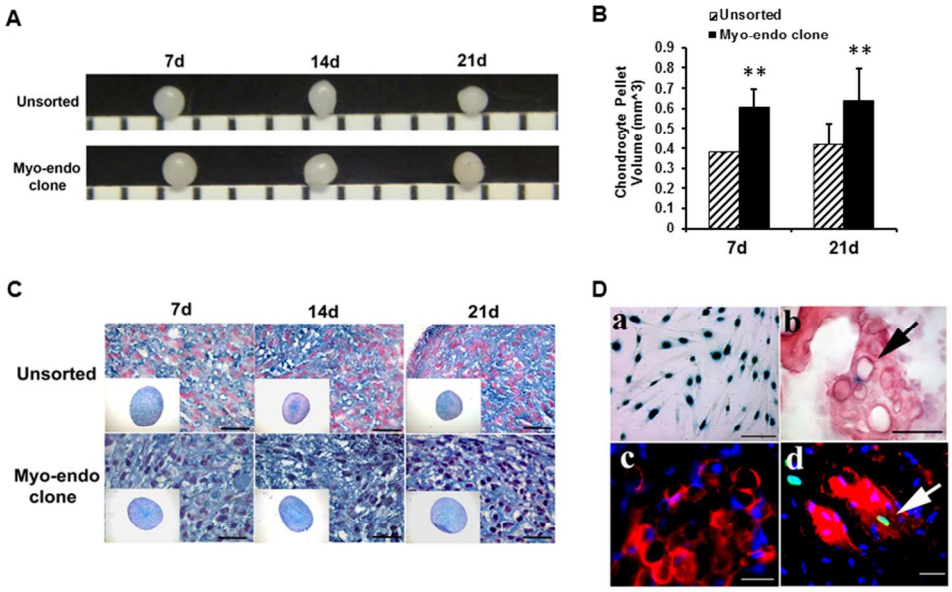

246x168mm (96 x 96 DPI)

Figure 3

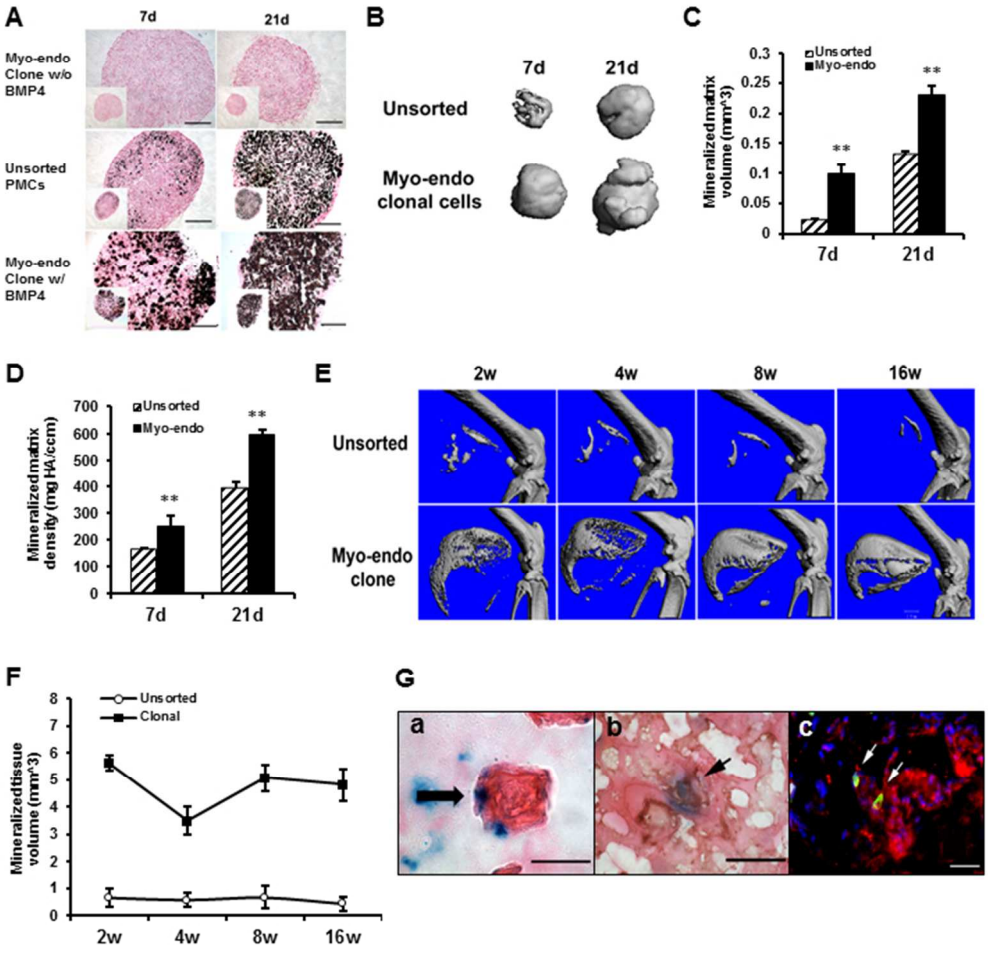

190x194mm (96 x 96 DPI)

Progression of muscular dystrophy in dystrophin/utrophin-/- mice is associated with rapid muscle progenitor cell exhaustion

Aiping Lu; Jonathan Proto; Xiaodong Mu; Ying Tang; Minakshi Poddar; Bing Wang; Johnny Huard
Stem Cell Research Center, Department of Orthopaedic Surgery, University of Pittsburgh, Pittsburgh, PA

Introduction

Duchenne muscular dystrophy (DMD) is a deadly genetic disease characterized by a lack of dystrophin expression and progressive weakening and wasting of the skeletal muscles. Researchers have observed that despite the lack of dystrophin at birth, the histopathological signs of muscle weakness do not become apparent until 4-8 years of age, which happens to coincide with the exhaustion of the muscle progenitor cell (MPC) pool (1).In this study we isolated MPCs from the skeletal muscle of young (2 weeks) and old (6 weeks) dKO (dystrophin/utrophin double knock out) mice, which have a maximum lifespan of 6 to 8 weeks and is a mouse model of DMD that closely recapitulates the disease progression observed in DMD patients. We found that MPCs isolated from old dKO mice have a reduced ability to proliferate and differentiate compared to MPCs isolated from young dKO mice. In addition, Pax7 staining (a muscle progenitor cell marker) indicated that the MPC population significantly decreased during disease progression. These observations suggest that blocking the exhaustion of the MPC pool could be a new approach to improve muscle weakness in DMD patients, despite their continued lack of dystrophin expression.

Methods

1. Cell Isolation: MPCs were isolated from dKO mice at 2 and 6 weeks of age, as previously described via a modified preplate technique (2).

2. Cell proliferation: Proliferation behavior of the MPCs isolated from the skeletal muscle of dKO mice was examined and compared by using a robotic time-lapsed live-cell imaging system (LCI).

3. ***Immunohistocytochemistry:***

Cryosections were stained for mouse Pax7 and the nuclei were revealed by DAPI staining.

4. Myogenic differentiation assay: Myogenic differentiation capacity of the MPCs was assessed by switching the proliferation medium to fusion medium (DMEM containing 2% fetal bovine serum). After 3 days, the cells were stained for fast myosin heavy chain (MyHCf), which is a marker of terminal myogenic differentiation. Myogenic differentiation levels were quantified as the percentage of the number of nuclei in MyHCf positive myotubes relative to the total number of nuclei.

5. Single fiber isolation: Skeletal muscle tissue isolated from 6 week old dKO and 9 week old WT control mice were incubated in a solution of 0.2% collagenase type I for 40 minutes at 37°C. When the muscle was sufficiently digested the muscles were triturated with heat polished glass pipettes to liberate single fibers and then transferred to a matrigel coated 12 well plate with proliferation medium.

Results

1. MPCs isolated from aged dKO mice display limited proliferation ability.

We examined the proliferation kinetics of both populations *in vitro* using LCI (3) and we observed a significant reduction in the proliferation capacity of the old dKO MPCs compared to young dKO MPCs (**Figure 1**)

2. Pax7 positive cells undergo a rapid decline in the skeletal muscle of dKO mice during aging and disease progression.

The results from the Pax7 staining showed that there is a rapid statistically significant decline in the population of Pax7 positive cells in the skeletal muscle of dKO mice from 4 to 8 weeks of age in contrast to that observed in *mdx* skeletal muscle ($p<0.05$) (**Figure 2A**).

3. Isolated muscle fibers from dKO mice show a reduction in muscle progenitor cells.

The single muscle fibers were isolated from 6 weeks old dKO and WT control mice. We observed that there were more cell nuclei in the WT muscle fibers compared to the dKO muscle fibers. In addition, 5 days post-culturing, the WT muscle fibers were able to release myogenic progenitor cells forming new myotubes, in contrasts to that observed with the dKO muscle fibers. These results support both a reduction in the number and myogenic potential of the MPCs derived from the dKO mice when compared to the WT MPCs (**Figure 2B**)

***4. MPCs isolated from aged dKO mice display a limited myogenic differentiation ability*.**
We observed that the MPCs isolated from young dKO mice formed numerous, large multi-nucleated myotubes compared to the MPCs isolated from the old dKO mice. The degree of myogenic differentiation was significantly reduced in the old dKO MPCs relative to the MPCs isolated from young dKO mice ($P < 0.001$).(**Figure 3**)

Discussion:
It is interesting to note that despite the lack of dystrophin at birth, the initiation of any signs of muscle weakness does not occur in DMD patients until later in childhood which happens to coincide with the exhaustion of the muscle progenitor cell pool (1). In this study we demonstrated that MPCs isolated from the skeletal muscle of old dKO mice have a reduced ability to proliferate and differentiate compared to MPCs isolated from young mice. Moreover, the numbers of Pax7 positive cells *in vivo* undergo a rapid decline in the skeletal muscle of dKO mice during aging and disease progression. Since dKO mice can only live 6-8 weeks, stem cell exhaustion could represent the main mechanism for the rapid progress of this disease. Blocking the exhaustion of muscle progenitor cells and stem cell-mediated therapy may represent a potential strategy for treating these muscle diseases.

Significance:
This study suggested that the exhaustion of stem cells contributes to the histopathology associated with DMD and that blocking the exhaustion of muscle progenitor cells and stem cell-mediated therapy could be used as a potential clinical strategy to treat muscle disease.

Figure 1

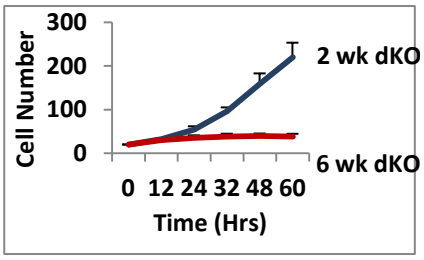

Figure 2A

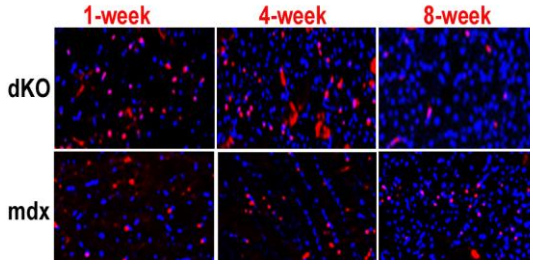

Figure 2B

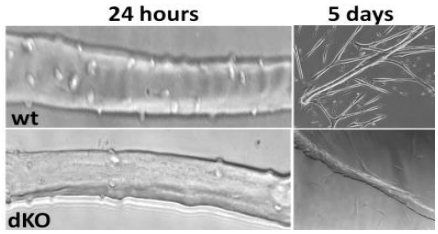

Figure 3

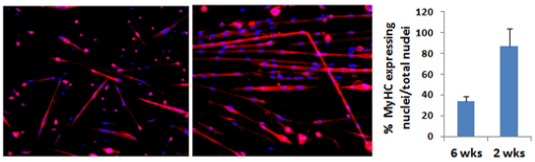

Reference

1. McLoon LK. Focusing on fibrosis: halofuginone-induced functional improvement in the mdx mouse model of Duchenne muscular dystrophy. Am J Physiol Heart Circ Physiol. 2008;294(4):H1505-7.
2. Gharaibeh B, Lu A, Tebbets J, Zheng B, Feduska J, Crisan M, et al. Isolation of a slowly adhering cell fraction containing stem cells from murine skeletal muscle by the preplate technique. Nat Protoc. 2008;3(9):1501-9.
3. Deasy BM, Jankowski RJ, Payne TR, Cao B, Goff JP, Greenberger JS, et al. Modeling stem cell population growth: incorporating terms for proliferative heterogeneity. Stem Cells. 2003;21(5):536-45.

TITLE:
Muscle-derived cells (MDCs) responsible for myogenesis differ from MDCs involved in adipogenesis in dystrophin/utrophin-/- mice

AUTHORS:
Jihee Sohn, Ying Tang, Bing Wang, Aiping Lu, +Johnny Huard
Department of Orthopaedic Surgery, University of Pittsburgh, Pittsburgh, Pennsylvania, United States, 15260 and [2]Department of Bioengineering and McGowan Institute for Regenerative Medicine, University of Pittsburgh, Pittsburgh, Pennsylvania, United States, 15260.
jhuard@pitt.edu

ABSTRACT BODY:
INTRODUCTION: Duchenne muscular dystrophy (DMD) is a genetic disease characterized by progressive weakening of the skeletal and cardiac muscles. The predominant symptoms seen in advanced cases of DMD are sarcopenia and pseudohypertrophy with fatty infiltration in skeletal muscle. Ectopic fat accumulation in skeletal muscle can be seen not only in myopathies but also in several disorders, including obesity and ageing-related sarcopenia; however, the origin of ectopic adipocytes, nor the stimulus that trigger their formation in disease, is known. In our lab, we utilize utrophin/dystrophin double knockout (dys-/-utro-/-, dKO) mice, which better emulates the phenotype seen in DMD patients. Several types of cells, including satellite cells, can be isolated from skeletal muscle and based on a previously published preplate technique (1) we isolated two types of cells; rapidly adhering cells (RACs) ,which are PDGFRα + mesenchymal progenitor cells, and slowly adhering cells (SACs), which are Pax7+ myogenic progenitor cells, from skeletal muscle of dKO and wild type (wt) mice. Previously, we have shown that dKO-SACs have reduced proliferation and myogenic and adipogenic differentiation abilities compared to wt-SACs. These observations suggested that SACs in dKO mice are exhausted and potentially are the main mechanism for the rapid progress of sarcopenia; however, the cells involved in pseudohypertrophy in dKO mice remains unclear. In this study, we examined the proliferation and adipogenic differentiation capabilities of RACs since adipose cells are thought to be derived from mesenchymal stem cells. We observed increased proliferation and adipogenic differentiation capabilities in dKO-RACs compared to wt-RACs. Our results suggest that muscle progenitor cells, SACs, may be more involved in muscle fiber regeneration or degeneration while mesenchymal progenitor cells, RACs, may be the origin of the cell population that is involved in adipogenesis in dKO muscle.

METHODS:

Cell Isolation: Cells were isolated from dKO (dys-/-utro-/-) and wild type (wt) mice at 6 weeks of age, as previously described via a modified preplate technique [1]. After 24hrs, the RACs were obtained and after 7 days, the SACs were obtained. Both cells were cultured in proliferation medium (DMEM supplemented with 10% fetal bovine serum, 10% horse serum, 0.5% chicken embryo extract and 1% penicillin-streptomycin).

Cell proliferation: Proliferation behavior of the dKO-SACs, dKO-RACs, wt-SACs, and wt-RACs were examined by using a robotic time-lapsed microscopic live-cell imaging system (LCI) and MTT assay.

Flow cytometry analysis and Immunofluorescent staining: 100,000 RACs and SACs were used to analyze their PDGFRα expressions. Cells were harvested and stained with PDGFRα-PE (eBioscience) antibody. 10,000 cells/well RACs and SACs were seeded on 24 well collagen type-1 coated plates and stained with mouse-monoclonal primary Pax7 antibody (1:400).

Multi-lineage Differentiation:

Adipogenic: 25,000 cells were cultured on 24 well plates for 21days in adipogenic induction media (Lonza) and then tested for adipogenesis with an AdipoRed reagent.

Myogenic: Myogenic differentiation capacity of the MDSCs was assessed by switching the proliferation medium into fusion medium (DMEM containing 2% fetal bovine serum). After 3 days, we analyzed myotube formation.

RESULTS:

dKO-RACs had increased PDGFRα expression compared to dKO-SACs. Flow cytometry analysis was used to evaluate the expression of PDGFRα, a marker for mesenchymal cells, of the RACs and SACs from both dKO and wt mice. dKO-RACs were about 98% positive for the PDGFRα surface protein, while much lower expression levels were detected in the SACs (Figure 1).

dKO-RACs displayed increased proliferation ability. The proliferation of the RACs and SACs were examined in vitro using an LCI system and MTT assay. We observed a significant increase in the proliferation of the dKO-RACs compared to the wt-RACs.

Increased in vitro adipogenic potential was detected in dKO-RACs. RACs and SACs from both dKO and wt mice were cultured in adipogenic differentiation medium for 21 days. AdipoRed staining was observed in the cytoplasm of the cells, around the nuclei. The degree of adipogenic differentiation was significantly increased in PDGFRα+ dKO-RACs compared to the dKO-SACs (Figure 2).

DISCUSSION: In dKO mice, an animal model of DMD, we observed severe peri-muscular adipose tissue on the surface of the gastrocneminus muscles (GM) as well as lipid accumulation inside of skeletal muscle myofibers. Intramyocellular lipid accumulation could be observed in the cardiac muscle of dKO mice; however, the source of the ectopic fat tissue within the skeletal muscle is unknown. In this study, we provide evidence that the RACs, PDGFRα + mesenchymal progenitor cells, are responsible for increased fat cell formation in the skeletal muscle of dKO mice. We observed that dKO-RACs had increased proliferation and adipogenic differentiation capabilities. This result suggests that dKO-RACs are prone to form adipocytes in skeletal muscle.

SIGNIFICANCE: This study suggests that dKO-RACs, mesenchymal progenitor cells in skeletal muscle, may contribute to adipogenesis and are responsible for ectopic fat cell formation within skeletal muscle in pathological conditions such as DMD. Therefore, targeting RACs to block adipogenesis in skeletal muscle may open new opportunities to treat muscle diseases.

REFERENCE:
[1] Gharaibeh, et al. Nat Protoc. 2008; 3:1501-9
[2] Uezumi, et al. Nat Cell biology. 2010; 2:143-152

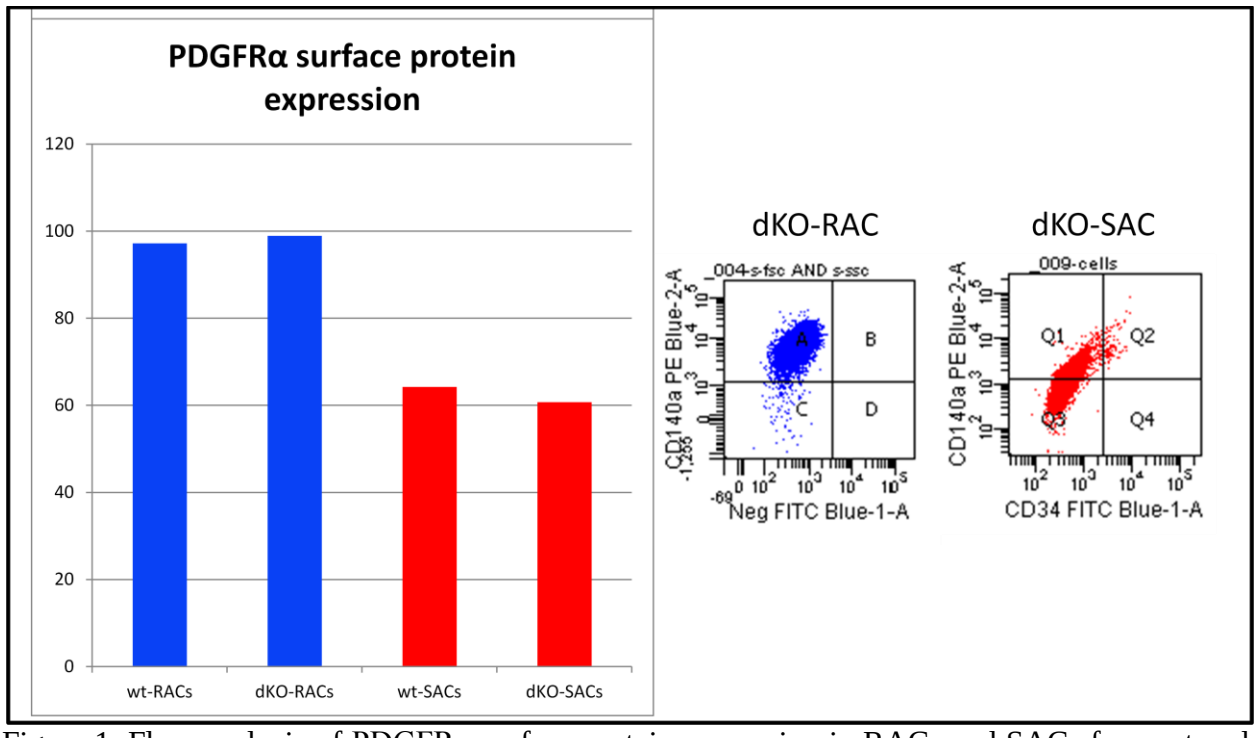

Figure 1. Flow analysis of PDGFRα surface protein expression in RACs and SACs from wt and dKO mice.

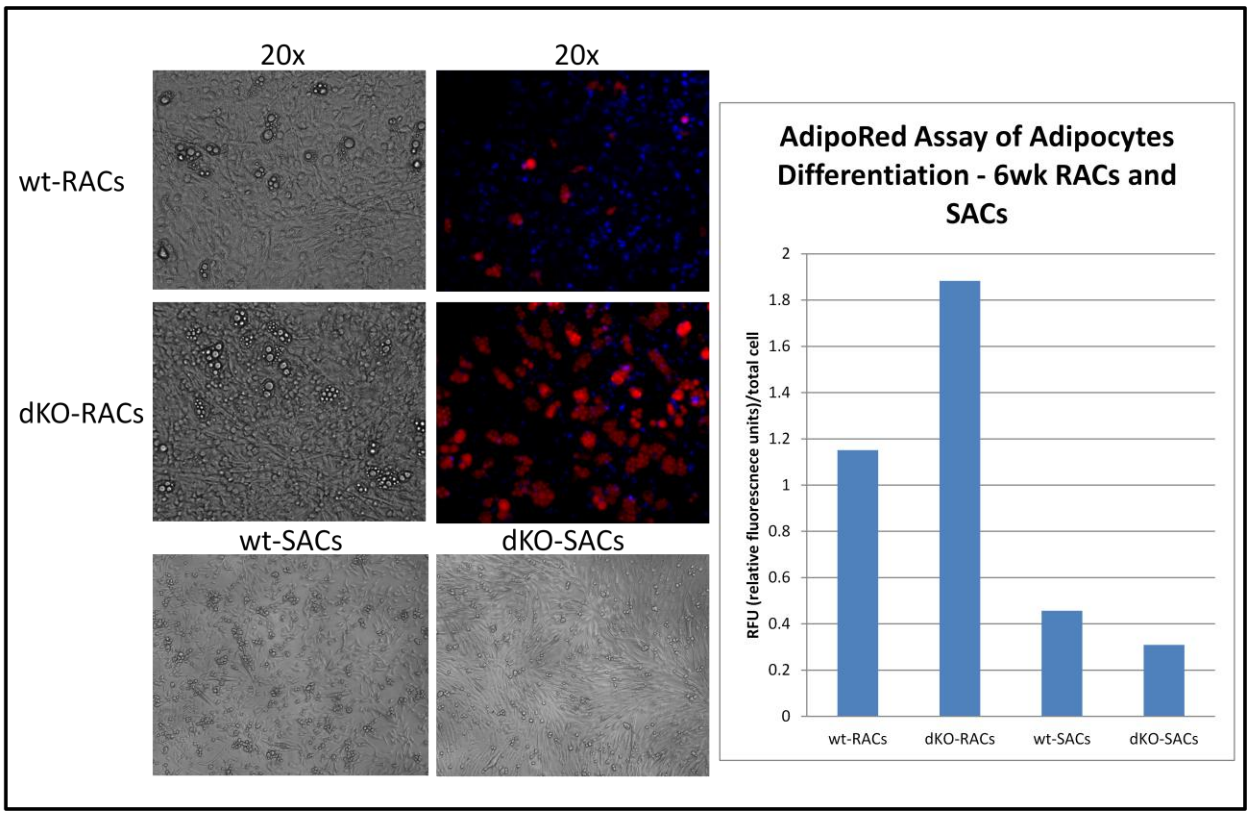

Figure 2. Adipogenesis of RACs and SACs. Bright field pictures and AdipoRed staining. Quantification of AdipoRed assay is shown.

RhoA signaling regulates heterotopic ossification and fatty infiltration in dystrophic skeletal muscle

Xiaodong Mu, Arvydas Usas, Ying Tang, Aiping Lu, Jihee Sohn, Bing Wang, Kurt Weiss, and Johnny Huard
Stem Cell Research Center, Department of Orthopaedic Surgery, University of Pittsburgh

Introduction: Frequent heterotopic ossification (HO) or fatty infiltration is observed in the dystrophic muscle of many animal models of human Duchenne muscular dystrophy (DMD); however, little is known about the correlated molecular mechanisms involved in the process. The RhoA-Rho kinase (ROCK) signaling pathway has been shown to function as a commitment switch of the osteogenic and adipogenic differentiation of mesenchymal stem cells (MSCs). Activation of RhoA-ROCK signaling in cultured MSCs *in vitro* induces their osteogenesis but inhibits the potential of adipogenesis, while the application of Y-27632, a specific inhibitor of ROCK, reversed the process. Inflammation has been shown to be one of main contributors to HO, while the role of RhoA signaling in inflammation reaction has been demonstrated. The objective of the current study is to investigate the potential role of RhoA signaling in regulating HO and fatty infiltration in dystrophic skeletal muscle.

Methods: 1.Mice models**:** Animal experiments were approved by IACUC of University of Pittsburgh. mdx mice (dystrophin-deficient) and dKO (Dystrophin/Utrophin double knockout) mice are both important mouse models of DMD; however, in contrast to the mild phenotype of mdx mice, dKO mice display a far more severe phenotype as is observed in human DMD patients, including a much shorter life span (~ 8 weeks compared to 2 years), more necrosis and fibrosis in the skeletal muscle, etc. 2. Tissue histological analysis: The gastrocnemius muscles (GM) of the mice were used for histological analysis. Alizarin red stain shows calcium deposition caused by HO or during osteogenic differentiation, Oil Red O stain shows fatty infiltration in muscle or fat cells, and Trichrome stain shows fibrosis. 3. Statistics: N >=6 for each group in animal study. Student's T-test was used to evaluate the significance.

Results: 1. Skeletal muscle of dKO mice features more HO but less fatty infiltration than mdx mice (Fig. 1). Both μ-CT scan of animals (**Fig. 1A**) and Alizarn Red stain (**Fig. 1B**) of the muscle tissues revealed greatly enriched HO in the dystrophic muscles of the dKO mice. While, Oil Red O stain (**Fig. 1C**) and Trichrome stain **(Fig. 1D)** of the muscle tissues revealed reduced fatty infiltration and a number of normal muscle fibers in the muscle of dKO mice.

2. RhoA signaling is more activated in both skeletal muscle and muscle-derived stem cells (MDSCs) from dKO mice. Both semi-quantitative PCR and immunohistochemistry study demonstrated that RhoA signaling is more activated in the muscles of dKO mice, as well as dKO MDSCs.

3. *In vitro* RhoA inactivation of cultured MDSCs from dKO mice decreases the osteogenesis potential and increases adipogenesis and myogenesis potential (Fig. 2). Semi-quantitative PCR study showed that Y27632 treatment *(*10 μM) of dKO-MDSCs down-regulated the expression of RhoA, BMP2 and 4, and inflammatory factors such as TNF-α and IL-6 (**Fig. 2A**). Osteogenesis potential was repressed while the adipogenesis and myogenesis potential of the dKO-MDSCs were increased by Y27632 (**Fig. 2B**).

4. RhoA inactivation in the skeletal muscle of dKO mice decreased HO and increased both fatty infiltration and muscle regeneration. GM muscles of 6 dKO mice were injected with Y27632 (5mM in 20μL of DMSO) (left limb) or control (20μL of DMSO) DMSO (right limb). Injections were conducted 3 times a week for 3 weeks. The skeletal muscles that received Y27632 injection demonstrated much slower development of HO and improved muscle regeneration, as well as reduced fibrosis formation.

Discussion: Our current results revealed that DMD mouse models featuring different severity of muscular dystrophy may have varied potentials for developing HO or fatty infiltration in the dystrophic muscle, and RhoA signaling might be a critical mediator of the determining these differential fates, including the progression towards HO, fatty infiltration, or normal muscle regeneration. RhoA inactivation is shown to have a great potential to repress HO and improve the phenotypes of dystrophic muscle. The status of RhoA activation in the skeletal muscle of human DMD patients and the potential effect of RhoA inactivation in human dystrophic muscle requires further investigation.

Significance: Our data reveals the involvement of RhoA signaling in regulating the process of heterotopic ossification, and indicates that RhoA may serve as a potential target for repressing injury-induced and congenital heterotopic ossification in humans.

Fig 1

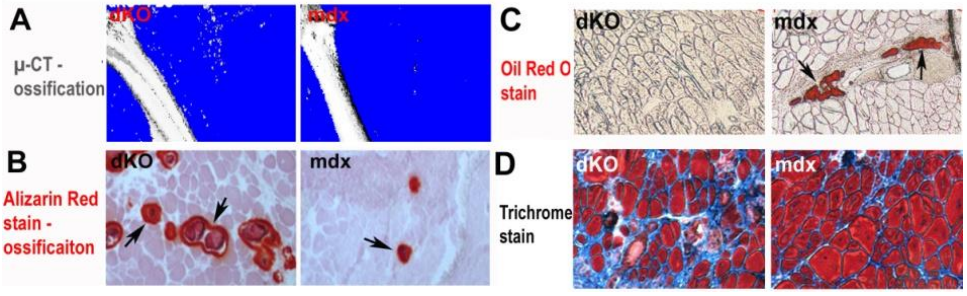

Fig 2

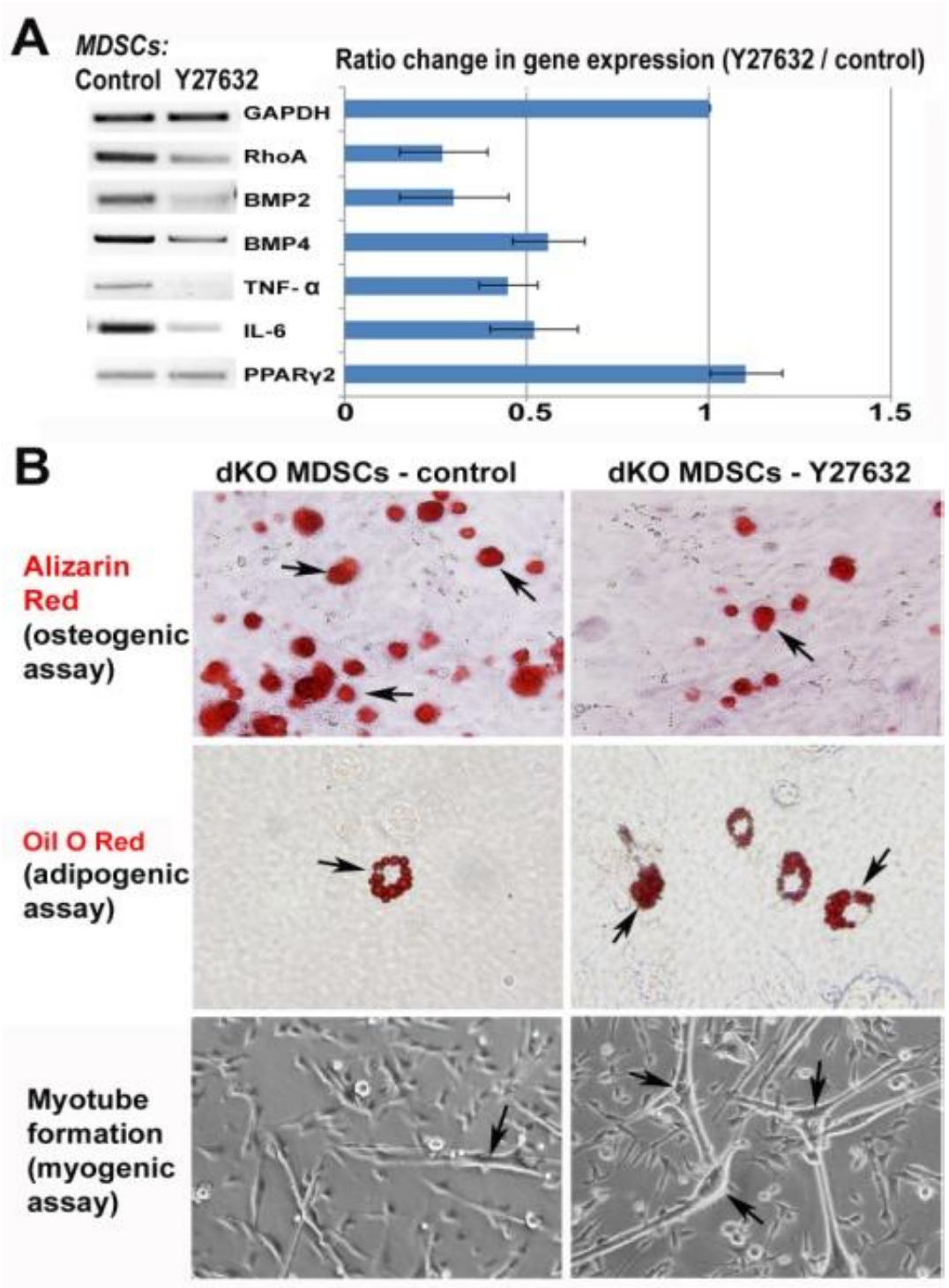
A
MDSCs:
Control Y27632
GAPDH
RhoA
BMP2
BMP4
TNF-α
IL-6
PPARγ2
Ratio change in gene expression (Y27632 / control)
0
0.5
1
1.5
B
dKO MDSCs - control
dKO MDSCs - Y27632
Alizarin Red (osteogenic assay)
Oil O Red (adipogenic assay)
Myotube formation (myogenic assay)

Suppression of skeletal muscle inflammation by muscle stem cells is associated with hepatocyte growth factor in wild type and *mdx*;p65$^{+/-}$ mice

[1]Proto, J.; [1]Tang, Y; [1]Lu, A.; [2]Robbins, P.D.; [1]Wang, B. [1]+Huard, J.
[1]+ Stem Cell Research Center, Children's Hospital of Pittsburgh, and Department of Orthopedic Surgery;
[2]Department of Metabolism and Aging, The Scripps Research Institute, Jupiter, FLA
jhuard@pitt.edu

INTRODUCTION

Persistent, unresolved inflammation can lead to secondary tissue damage. Recently, we reported that intramuscular (i.m.) injection of muscle-derived stem cells (MDSCs) heterozygous for the NF-kB subunit p65 (p65$^{+/-}$) reduced host inflammation and fiber necrosis seven days following muscle injury, relative to wild type (WT) MDSC injection [1]. In this investigation, we looked closer at the role of secreted factors in this observation. Using a murine cardiotoxin muscle injury model, we observed that delivery of p65$^{+/-}$ MDSCs accelerated the resolution of inflammation, relative to WT MDSCs. *In vitro* inflammation assays demonstrated that MDSCs secrete factors that modulate cytokine expression in LPS-activated macrophages, and genetic reduction of p65 enhanced this effect. Finally, deletion of one p65 allele in a murine model of Duchenne muscular dystrophy (mdx) increased the expression of the anti-inflammatory factor hepatocyte growth factor (HGF) and was associated with disease improvement.

MATERIALS AND METHODS

Mice: C57Bl/6 (WT) mice were purchased from the Jackson Laboratory (Bar Harbor, ME). P65$^{+/-}$ mice were bred with *mdx* mice to produce mdx/p65$^{+/-}$ and mdx/p65$^{+/+}$ mice. PCR analysis of tail samples was used for genotyping.

Cell Isolation: MDSCs were isolated from five month old (n=3) *p65*$^{+/+}$ or *p65*$^{+/-}$ mice via a modified preplate technique [2]. A population of slowly adhering cells was obtained and expanded in proliferation medium (PM, DMEM containing 10% fetal bovine serum (FBS), 10% horse serum, 1% penicillin-streptomycin, and 0.5% chick embryo extract).

In vivo regeneration assay: Muscle injury was induced in C57Bl/6J mice by the injection of cardiotoxin (4uM) into the gastrocnemius muscle. One day later, MDSCs were injected into the injured muscles. Muscles were harvested 1, 3, and 7 days post-injury. Serial cryosections were prepared and immunohistochemistry was performed to assess inflammation (F480, Gr-1). Gross tissue histology was performed by hematoxylin and eosin (H&E) staining.

In vitro Inflammation Model: MDSCs were grown for 24 hours in proliferation medium, after which the medium was collected and sterile filtered. RAW264.7 cells, immortal murine macrophage-like cells, were activated by exposure to 100 ng/mL LPS in either PM, *p65*$^{+/+}$-, or *p65*$^{+/-}$- conditioned medium for 30 min, 3 hours, and 24 hours. At each time point, RNA was collected for real time RT-PCR analysis or lysates were collected for western blot.

RESULTS

Confirming our previous report [1], we found that by 7 days, p65$^{+/-}$ cell engraftments were associated with reduced numbers of F4/80+ cells, compared to WT cell engraftments (Fig 1A). This can be further demonstrated histologically by H&E staining, revealing a reduction in mono-nuclear cells at sites of injury one week post injection (Fig 1B).

To look at the direct effects of MDSC-secreted factors, we performed *in vitro* inflammation assays. Briefly, RAW264.7 macrophages were activated with LPS (100ng/mL) in normal PM or WT or p65$^{+/-}$ conditioned medium (CM) (Fig 2A). The expression of the cytokines IL-1β and IL-6 was determined by real time (RT-PCR). Our results demonstrated that MDSC-CM significantly attenuates cytokine expression (Fig 2B).

Figure 1.

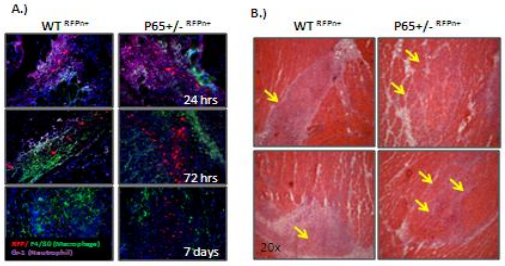

Although WT and p65$^{+/-}$ CM had a similar effect, we found that p65$^{+/-}$ CM exerted a stronger suppression of IL-6 expression. Previous reports have found that the activation of inflammatory macrophages is attenuated by the phosphorylation and subsequent inactivation of GSK3β [3]. By western blot, we found that upon treatment with LPS in WT-CM, the fraction of pS9-GSK3beta modestly increased within 30mins and was maintained through 24 hours. Furthermore, p65$^{+/-}$-CM demonstrated an even stronger induction of phosphorylation.

Figure 2.

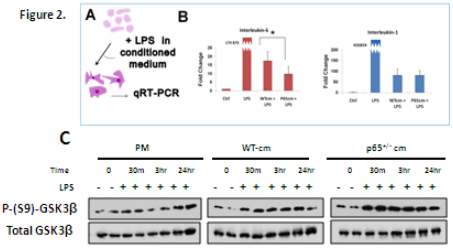

Hepatocyte growth factor (HGF) is one of the factors previously demonstrated to modulate inflammation via pS9-GSK3beta. We examined HGF expression in MDSCs and found elevated levels in p65$^{+/-}$ cells compared to the WT cells. Acharyya and colleagues have reported that haploinsufficiency of p65 in an mdx background improves dystrophic pathology [4]. As we had hypothesized, HGF expression was significantly increased. Based on our *in vitro* and *in vivo* inflammatory studies, HGF could be one of the contributing factors to disease improvement.

Figure 3.

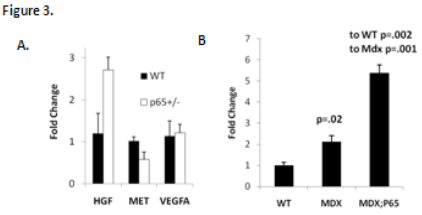

DISCUSSION

These findings indicate that NF-kB has a broader role in muscle stem and progenitor cells than previously thought, and that the anti-inflammatory molecules secreted by stem cells, such as HGF, could potentially be harnessed to control secondary pathologies of muscle diseases such as DMD.

REFERENCES

[1]Lu, A., et al, Mol Ther 2012, 20(3);661-68. [2] Gharaibeh, et al. Nat Protoc. 2008; 3:1501-9. [3] Beurel, E., et al, Trends Immunol 2010; 3-(1):24-31 [4]Acharyya, S., et al., J Clin Invest 2007, 117:889-901.

Hindawi Publishing Corporation
Stem Cells International
Volume 2013, Article ID 983059, 18 pages
http://dx.doi.org/10.1155/2013/983059

Review Article

Cellular Kinetics of Perivascular MSC Precursors

William C. W. Chen,[1,2] Tea Soon Park,[3] Iain R. Murray,[4,5] Ludovic Zimmerlin,[3] Lorenza Lazzari,[6] Johnny Huard,[1,7] and Bruno Péault[4,5,8]

[1] *Stem Cell Research Center, Department of Orthopaedic Surgery, School of Medicine, University of Pittsburgh, Pittsburgh, PA 15219, USA*
[2] *Department of Bioengineering, University of Pittsburgh, Pittsburgh, PA 15260, USA*
[3] *Institute for Cell Engineering and Department of Pediatric Oncology, School of Medicine, Johns Hopkins University, Baltimore, MD 21205, USA*
[4] *Centre for Regenerative Medicine, University of Edinburgh, Edinburgh, EH16 4TJ, UK*
[5] *Orthopaedic Hospital Research Center and David Geffen School of Medicine at UCLA, University of California at Los Angeles, 615 Charles E. Young Drive South, Los Angeles, CA 90095-7358, USA*
[6] *Cell Factory, Fondazione Ospedale Maggiore Policlinico, 20122 Milan, Italy*
[7] *McGowan Institute for Regenerative Medicine, Pittsburgh, PA 15219, USA*
[8] *Centre for Cardiovascular Science, University of Edinburgh, Queen's Medical Research Institute, 47 Little France Crescent, Edinburgh EH16 4TJ, UK*

Correspondence should be addressed to Bruno Péault; bpeault@mednet.ucla.edu

Received 14 May 2013; Accepted 13 July 2013

Academic Editor: Donald G. Phinney

Mesenchymal stem/stromal cells (MSCs) and MSC-like multipotent stem/progenitor cells have been widely investigated for regenerative medicine and deemed promising in clinical applications. In order to further improve MSC-based stem cell therapeutics, it is important to understand the cellular kinetics and functional roles of MSCs in the dynamic regenerative processes. However, due to the heterogeneous nature of typical MSC cultures, their native identity and anatomical localization in the body have remained unclear, making it difficult to decipher the existence of distinct cell subsets within the MSC entity. Recent studies have shown that several blood-vessel-derived precursor cell populations, purified by flow cytometry from multiple human organs, give rise to *bona fide* MSCs, suggesting that the vasculature serves as a systemic reservoir of MSC-like stem/progenitor cells. Using individually purified MSC-like precursor cell subsets, we and other researchers have been able to investigate the differential phenotypes and regenerative capacities of these contributing cellular constituents in the MSC pool. In this review, we will discuss the identification and characterization of perivascular MSC precursors, including pericytes and adventitial cells, and focus on their cellular kinetics: cell adhesion, migration, engraftment, homing, and intercellular cross-talk during tissue repair and regeneration.

1. Introduction

The availability of mesenchymal stem/stromal cells (MSCs) and MSC-like multipotent stem/progenitor cells marked a major milestone in stem cell therapies [1, 2]. For more than a decade, MSC has been a highly promising stem cell source and extensively investigated for its therapeutic potentials [3, 4]. Unlike embryonic stem cells (ESCs) or induced pluripotent stem cells (iPSCs), MSCs are inherently more relevant to clinical applications due to the lack of ethical and safety issues, despite lower developmental versatility [5]. MSCs and similar mesodermal stem/progenitor cells have been shown to repair and/or regenerate a wide variety of damaged/defective organs, including bone, cartilage, muscle, heart, and skin [6–10]. MSCs have also been reported to support hematopoiesis and suppress immune reaction after cell/organ transplantation [11–14].

Nevertheless, owing to the nature of MSC isolation by plastic adherence in tissue culture, the native identity and anatomical localization of MSCs have remained unclear for

years [15]. Recently, several studies have indicated that MSCs represent a heterogeneous entity in culture, and a number of multipotent precursor cells potentially contributing to the MSC pool have been identified *in vivo* [16, 17]. Increasing evidence further suggests that MSCs and some tissue-specific progenitor cells are anatomically and functionally associated with vascular/perivascular niches in various tissues [18–21]. Following the hypothesis that blood vessels throughout the body serve as a systemic reservoir of multipotent stem/progenitor cells, we and other researchers have identified, purified, and characterized distinct populations of MSC-like multilineage precursors from the vasculature of multiple human organs [17, 22]. These human blood vessel-derived precursor cell subsets, including pericytes (PCs) [23], adventitial cells (ACs) [24], and myogenic endothelial cells (MECs) [25], can be isolated via fluorescence-activated cell sorting (FACS) based on their unique expression of cell surface antigens. Purified PCs, ACs, and MECs not only exhibit typical mesodermal multipotency in culture but also demonstrate robust regenerative capacities in animal disease models. Consequently these precursor cell subsets, particularly PCs and ACs that can be universally derived from definitive structures of blood vessel walls, represent active contributors to the MSC entity [17].

In this review, we will discuss the identification and characterization of perivascular MSC precursors (i.e., PCs and ACs) from multiple organs and focus on their cellular kinetics during regenerative events, including cell adhesion, migration, engraftment, homing, and intercellular cross-talk.

2. Native Distribution of MSCs and MSC-Like Multipotent Stem/Progenitor Cells

MSCs and MSC-like stem/progenitor cells have been found in nearly all organs in the human body. Despite slight differences in phenotypes and cellular functions, MSCs and MSC-like cells from various ontogenies share basic features in general, including selective plastic adherence, expression of typical MSC surface markers, and mesenchymal multipotency such as osteogenesis, chondrogenesis, and adipogenesis. Some of the most common MSCs and MSC-like multilineage cells are briefly introduced here.

2.1. Bone Marrow-Derived MSCs (BM-MSCs). Bone marrow (BM) harbors multiple types of stem/progenitor cells, including hematopoietic stem cells (HSCs), endothelial progenitor cells (EPCs), and BM-MSCs [26, 27]. As a standard MSC population, BM-MSCs are defined as nonhematopoietic, plastic adherent progenitor cells that self-renew, differentiate into typical mesodermal cell lineages including osteogenic, chondrogenic, and adipogenic lineages, and express CD73, CD90, and CD105 but are negative for CD11b, CD14, CD19, CD34, CD45, CD79α, and HLA-DR1 [28]. Estimated by the colony forming unit fibroblasts assay (CFU-F) *in vitro,* BM-MSCs typically exist at a very low frequency within the BM mononucleated cell population (0.01%–0.1% of total BM cells) but can be efficiently expanded in culture, making them one of the most investigated autologous stem/progenitor cell populations. Interestingly, multipotent BM-MSC clones retain approximately twofold higher CD146 expression level than unipotent clones [29].

2.2. Adipose-Derived Stem/Stromal Cells (ASCs). The stromal vascular fraction (SVF) of adipose can be isolated via enzymatic digestion of intact fat tissue or lipoaspirate, followed by the depletion of mature adipocytes through centrifugation. The SVF embodies a broad and heterogeneous cellular compartment, including vascular cells (endothelial and perivascular populations), hematopoietic cells (resident and circulating cells), and stromal fibroblasts. In 1976, human adipogenic progenitors (aka preadipocytes) were successfully isolated by two independent groups from the adipose SVF by selective adherence to culture plastics [30, 31]. The adherent fraction of the adipose SVF was later identified as a source of mesenchymogenic progenitors [32], termed adipose-derived stem/stromal cells (ASC) [33]. ASCs are defined *in vitro* using the same criteria as *bona fide* BM-MSCs [34], including their selective plastic adherence, mesenchymal differentiation capacities and immunophenotypes [32], although ASCs only resemble BM-MSCs at subsequent passages in culture [35]. Unlike BM-MSCs, early-passage ASCs temporarily retain expression of mucosialin (CD34) [35], a well-established marker for stem/progenitor cells in both hematopoietic [36] and endothelial [37] cell lineages. On another note, the temporary retention of CD34 expression in primary ASCs led to confusion regarding their origin *in situ*. This misperception was accentuated in light of the recent characterization of CD34-negative PCs as a source of MSCs in a variety of mesodermal tissues, including fat [23]. While the adipogenic activity is mainly exhibited by the prevalent CD34+/CD31− subset of the adipose SVF [38], the CD34-negative fraction can also generate ASCs *in vitro* [24, 39, 40]. Immunohistochemical studies have confined these mesenchymogenic subpopulations to the adipose microvasculature where they coexist, respectively, in the media and adventitia in an annular fashion [24, 39, 41, 42]. Both PCs and an outer supra-adventitial layer of CD34-positive cells (adventitial cells/supra-adventitial stromal cells, ACs) possess high adipogenic potential *in vitro* [39, 43] and may contribute together to replenish the pool of adipocytes essential to sustain the high fat turnover *in vivo* [44].

2.3. Umbilical Cord-Derived Mesenchymal Stem/Stromal Cells (UC-MSCs). Stem/progenitor cells isolated from disposable perinatal tissues, including amnion/amniotic fluid, umbilical cord blood, placental tissue, umbilical cord blood vessels, and the Wharton's jelly, have been deemed promising for clinical applications because of the minimal safety and ethical concerns [45, 46]. MSCs and MSC-like cells have been isolated from different compartments of the umbilical cord, including umbilical vein subendothelial zone, umbilical cord blood, and specifically, Wharton's jelly [45, 47]. Wharton's jelly is the parenchyma within the umbilical cord, a mucoid connective tissue surrounding umbilical cord arteries and vein [45]. The Wharton's jelly can be further divided into three anatomical regions where MSCs can be derived from the perivascular

zone, the intervascular zone, and the subamnion [47]. Similar to BM-MSCs, MSCs derived from Wharton's jelly exhibit plastic adherence, mesenchymal multipotency, and expression of CD10, CD13, CD29, CD44, CD73, CD90, CD105, and HLA-class I but are negative for CD11b, CD14, CD19, CD31, CD34, CD45, CD56, CD79, and HLA class II [45–47].

3. Blood Vessels as a Source of MSC Precursors

The similarities between MSCs derived from many different tissues aroused the idea that a common reservoir of MSCs may exist in the body. The blood vessel, which typically consists of three structural layers: *tunica intima*, *tunica media*, and *tunica adventitia* [48], is distributed throughout nearly all human organs and therefore represents a favorable candidate. Early evidence supporting the hypothesis that the vascular wall serves as a systemic source of stem cells came from a study of the emerging hematopoietic system in the embryo and fetus, where hematopoietic cells emerged in close vicinity to vascular endothelial cells (ECs) in both intra- and extraembryonic blood-forming tissues [22]. Recently, several studies have indicated the possibility that blood vessels in different organs contain multilineage precursors that possess MSC-like features and contribute to tissue repair/regeneration [49, 50]. New evidence further pointed out that tissue-specific multipotent stem/progenitor cells, including osteogenic, neural, odontoblastic, and adipogenic progenitors, may originate from and/or associate with vascular/perivascular niches *in vivo* [18–21].

Microvascular pericytes (PCs), a set of perivascular mural cells surrounding *the intima* of microvessels and capillaries, are traditionally regarded as a structural component of blood vessels, regulating vascular contractility, stability, and integrity [51, 52]. Intimate interactions between PCs and ECs tightly regulate vascular growth, maturation, and remodeling [51, 53–55]. Recently, PCs have been implicated in a number of pathological conditions, making them potential targets for therapeutic interventions [55, 56]. On the other hand, the *tunica adventitia*, the outermost layer of large blood vessels, has long been considered as a structural bystander, consisting of loosely structured collagen-rich extracellular matrix (ECM), which embeds stromal cells/fibroblasts, the *vasa vasorum*, and perivascular nerves [57]. The importance of the *tunica adventitia* was recently reevaluated due to a number of studies reporting its active role in vascular remodeling, immune response mediation, cell trafficking, and atherosclerosis [57–59]. In a vascular remodeling setting following an injury, it has been shown that adventitial cells (ACs) start a process of proliferation, migration into the tunicae media and intima, and differentiation into smooth muscle cells [60–62]. Recently, we and several other groups reported new strategies for the identification and purification of the elusive PCs and ACs [23, 24, 39, 63–65]. Using immunohistochemistry and flow cytometry, we identified human PCs and ACs *in situ* and purified these cells to homogeneity based on their unique expressions of cell surface antigens. Details of the isolation and characterization of PCs and ACs will be described in the following sections.

Unlike the *tunicae media* and *adventitia*, the subendothelial zone of *tunica intima* has previously been suggested as one of the sources of EPCs [66, 67]. Apart from PCs and ACs, some of us have also reported a rare but distinct subset of blood-vessel-derived stem cells, that is, myogenic endothelial cells (MECs), residing within the intima of microvasculature in human skeletal muscle [25]. MECs, presumably the human counterpart of murine muscle derived stem cells (MDSCs), not only express the myogenic cell marker, CD56, but also display endothelial cell markers, CD34 and CD144. Following purification by FACS, MECs (CD34+/CD56+/CD144+/CD45−) can be clonally expanded and exhibited osteo-, chondro-, adipo-, and myogenic differentiation capacities *in vitro* [25]. Furthermore, MECs exhibited superior cardiac repair capacity in ischemic hearts and myogenic regeneration in injured skeletal muscle than conventional CD56+ myoblasts and ECs [25, 68, 69]. Nevertheless, despite their MSC-like features and tissue reparative/regenerative capability, whether MECs contribute significantly to the MSC entity remains to be clarified due to their restricted presence in skeletal muscle.

4. Identification and Purification of Perivascular MSC Precursors

4.1. Placenta. While placenta and umbilical cord are often discarded at birth, these extraembryonic tissues contain large numbers of stem/progenitor cells, making them attractive sources of donor cells for regenerative medicine. We and others have isolated multipotent PCs (CD146+/CD34−/CD45−/CD56−) from these tissues and utilized them toward multiple tissue repair/regeneration, including skeletal muscle [70], lung [71], dermal [72], and nervous tissues [73].

Placenta is a highly vascularized extraembryonic tissue, which serves as fetomaternal interface to sustain proper oxygen transportation, waste disposal, and nutrient delivery. The placental vasculature has been thoroughly characterized throughout fetal development previously and consists of all sizes/types of blood vessels and both pericytes/perivascular cells and ECs at all stages [74, 75]. Placenta PCs are critical to maintain blood vessel homeostasis and promote angiogenesis [76, 77]. PC abnormity in placenta capillaries leads to defects in sinusoidal integrity, a phenotype often observed during pregnancy complications due to diabetes, postmaturity, or preeclampsia [78]. In addition to their supportive role in the fetal vasculature, placental PCs have also been identified as a source of MSCs [23, 70, 79]. Our previous studies have discriminated mesenchymogenic placental PCs based on the expression of the cell adhesion molecule CD146 and lack of EC markers: CD34, CD144, and vWF [23, 70]. Similarly, Castrechini et al. described a perivascular population residing in human fetal and term placenta, which coexpressed MSC/PC markers (Stro-1, 3G5, CD105, CD106, CD146, CD49a, α-SMA) but not hematovascular markers (CD117, CD34, vWF) and were competent for trilineage mesenchymal differentiation [79]. In our hands, human fetal and term chorionic villi

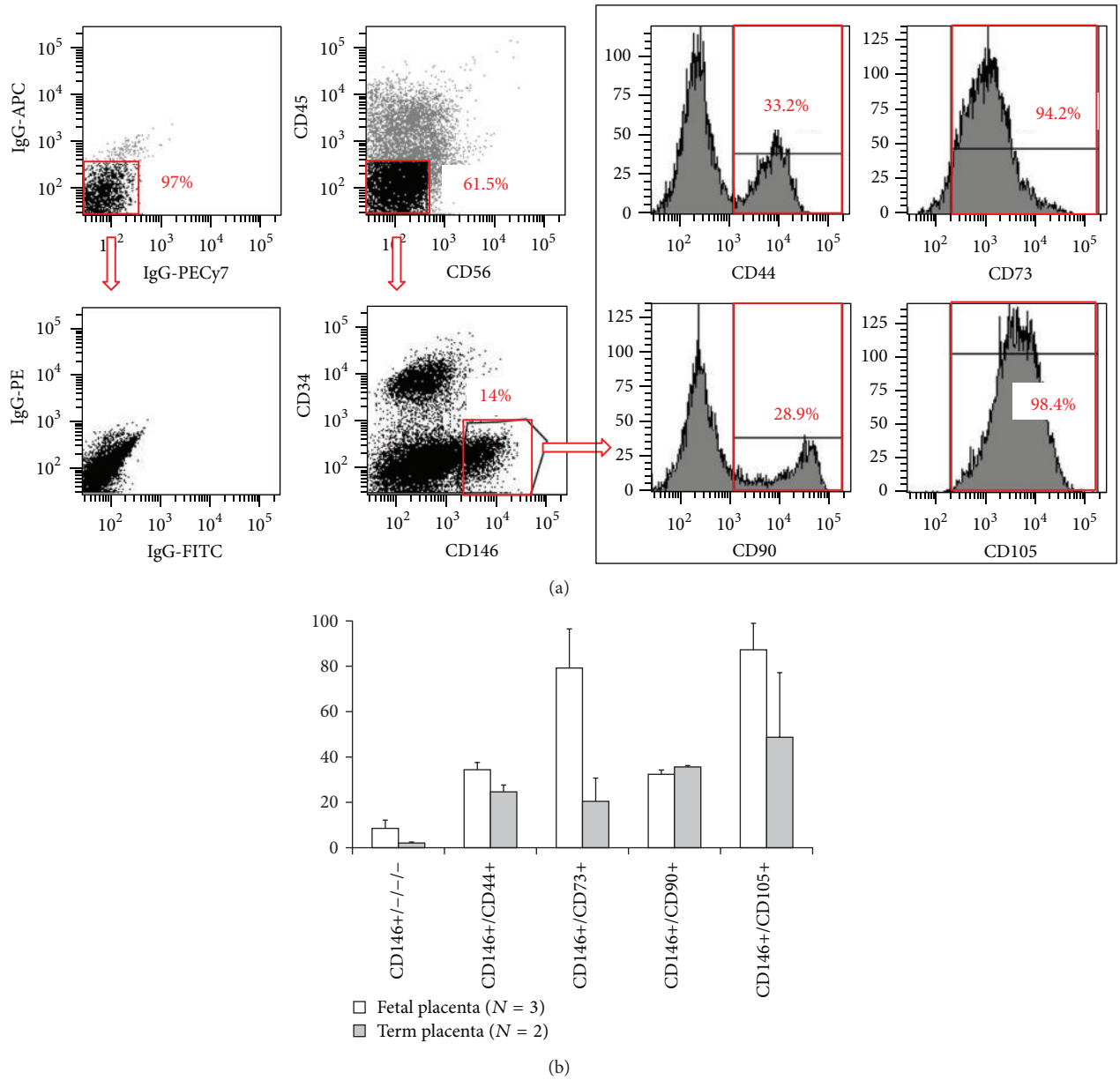

Figure 1: Flow cytometry analysis of mesenchymal stem cell marker expression in freshly isolated fetal and term placental pericytes. (a) Representative flow cytometry analysis of human placenta that was mechanically dissociated and enzymatically digested and subsequently stained for CD45, CD56, CD34, and CD146 along with CD44, CD73, CD90, or CD105. Matching isotype controls were shown in the left column. (b) Human fetal placenta ($N = 3$, average 20 weeks of gestation) and term placenta ($N = 2$, average 39 weeks of gestation) were used to isolate subsets of pericytes using surface expression of CD146+/CD34−/CD45−/CD56− (CD146+/−/−/−) and colabeled with one of the mesenchymal stem cell markers (CD146+/CD44+, CD146+/CD73+, CD146+/CD90+, CD146+/CD105+) as shown in (a). Values are mean ± standard error.

of placentas included 8.5 ± 3.66% ($N = 3$, 19 to 21 weeks of gestation) and 2.1 ± 0.43% ($N = 2$, 39 weeks of gestation) of PCs (CD146+/CD34−/CD45−/CD56−), respectively (Figure 1).

The native expression of CD146 by mesenchymogenic PCs in many tissues including bone marrow, fetal and term placentas has been reported [23, 70]. Using FACS, we purified PCs from mechanically and enzymatically dissociated placental chorionic villi [23, 70]. Freshly isolated placenta PCs natively expressed MSC markers (CD44, CD73, CD90, and CD105) at varying levels (30 to 87% of fetal and 20 to 48% of term placental CD146+/CD34−/CD45−/CD56− PCs) (Figure 1). We have previously demonstrated that when placed onto ECM-coated plates, dissected fetal placental villi release a population of vascular cells, which possess high migratory activity and robust capacity to regenerate skeletal muscle fibers in dystrophic mice [70]. The cells migrating out of placental villi included predominantly CD146+ cells

which coexpressed PC (NG2 and PDGFRβ) and MSC (CD44, CD73, CD90, and CD105) surface antigens and were deprived of EC antigens (CD31, CD34, CD144, and vWF) [70]. Maier et al. employed a similar approach to isolate PCs from the cellular outgrowth of human term placenta explants [80]. Consistently with fetal placenta, term placenta PCs expressed high levels of PC/MSC markers (CD146, PDGFRβ, NG2, CD90, and calponin), including 65 transcripts that are highly expressed in undifferentiated MSCs, and lacked endothelial/hematopoietic cell marker expression (CD31, CD34, and CD45) [80].

4.2. Umbilical Cord. Human umbilical cord (HUC) has been known as an abundant source of ECs as well as MSCs derived from the Wharton's jelly. Recently some of us demonstrated that human full-term UCs and, at a higher frequency, fetal (preterm) UCs contain perivascular cells that exhibit features of MSCs. These perivascular smooth muscle-like cells present in the HUC co-expressed CD146 and alpha-smooth muscle actin (αSMA) but did not express the established EC markers: CD144, CD34, CD31, and Ulex europaeus agglutinin (UEA-1) receptor. Using FACS, Montemurro et al. isolated a population of PCs (CD146+/NG2+/PDGFRβ+) from umbilical cords of preterm newborns [71]. These HUC-derived perivascular cells (HUCPCs) can be maintained in long-term culture, exhibiting classical spindle-shape PC morphology. When characterized by flow cytometry during subsequent passages, they maintained the expression of CD44, CD90, CD73, CD105, HLA class I, CD146, NG2, αSMA, and PDGFRβ as well as retained their multipotency to differentiate towards different cell types, including osteogenic, adipogenic, and myogenic cell lineages [71].

4.3. Skeletal Muscle. Skeletal muscle has been shown to harbor several adult stem/progenitor cell populations in mammals including humans, in addition to the typical muscle stem cells, that is, satellite cells [81–83]. Many studies have demonstrated that muscle derived stem/progenitor cells are capable of differentiating into a variety of cell lineages *in vitro* and *in vivo*, including blood cells and fat [25, 81, 84–86]. Using similar immunohistochemical and flow cytometry strategies, we first identified microvascular PCs *in situ* within human skeletal muscle and subsequently purified them from mechanically and enzymatically dissociated muscle biopsies via FACS [23]. Similar to PCs sorted from other tissues, muscle PCs (CD146+/CD34−/CD45−/CD56−) expressed typical PC markers: CD146, NG2, PDGFR-β, alkaline phosphatase (ALP), and α-smooth muscle actin (α-SMA), with the absence of EC markers: CD31, CD34, CD144, and vWF as well as the hematopoietic cell marker CD45 and myogenic cell marker CD56. Muscle PCs can be efficiently expanded in culture, at the clonal level, while maintaining robust mesodermal developmental potentials. Freshly isolated and long-term cultured muscle PCs both displayed robust myogenic capacity *in vitro* and *in vivo*. Moreover, muscle PCs natively and in culture expressed classic MSC markers: CD44, CD73, CD90, and CD105, indicating their developmental status as MSC ancestors [23].

4.4. Adipose. Vasculogenic CD34+/CD31− cell populations have been described in the adventitial *vasa vasorum* of large blood vessels such as the vena saphena [65] and the thoracic aorta [67], but microvascular CD34+ ACs seem to be a specific feature of the adipose and subcutaneous tissue [87]. Apart from CD34 expression and their adjacent anatomical localization within the blood vessel wall, ACs can be discriminated from adipose PCs due to the lack of native expression of PC markers (αSMA, CD146, NG2, PDGFRβ) [24, 39, 42]. The high prevalence (~50%) of CD34+/CD146− progenitor cells in the nonhematopoietic adipose SVF [39, 88, 89] and their limited clonogenicity and heterogeneous proliferative capacity [24] do not preclude the possibility that distinct CD34+ stem/progenitor cells exist within adult adipose tissue. Using a peroxisome proliferator-activated receptor gamma (PPARγ) reporter mouse model, Tang et al. demonstrated that adipogenic progenitors emerge from CD34+ cells which later adopt a perivascular niche and express PC markers (αSMA, NG2, PDGFRβ) [21]. Similarly, human adipose CD34+/CD146− ACs can acquire PC markers (αSMA, CD146, NG2, PDGFRβ) *in vitro*, following treatment with angiotensin II or angiopoietin-2 [24].

While developmentally mesenchymogenic PCs may arise from transient CD34+ cell population(s), the persistence of such CD34+ precursors in the adult and their ontological relationship to the bulk of CD34+ ACs in human fat will require further investigation. Indeed, rare CD34+ mesenchymogenic cells have been reported in fetal [24, 90, 91] and adult [92, 93] bone marrow, as well as in fetal muscle and fetal lung [24]. A multipotent CD34+ cell population residing in the wall of dorsal aorta, the mesoangioblast, has been proposed to be an ancestor of adult mesenchymogenic PCs in the mouse [49, 81]. Some groups have reported the direct derivation of CD34+ primitive MSCs from human embryonic stem cells (hESC) [94, 95], while Vodyanik et al. described the emergence of a multipotent MSC precursor, the mesenchymoangioblast, from hESC-derived CD34+ cells in a stepwise differentiation system [96]. Furthermore, Dar et al. recently reported successful derivation of CD105+/CD90+/CD73+/CD31− multipotent mesodermal precursors from embryoid bodies of either human ESCs or iPSCs that exhibit clonogenicity, mesenchymal differentiation potentials, and *bona fide* pericyte features, including angiogenic/vasculogenic capacity and expression of CD146, NG2, and PDGFRβ but not αSMA, CD56, CD34, or EC markers [97]. These hPSC-derived PCs significantly facilitated vascular and muscle regeneration when transplanted into the ischemic limb of immunodeficient mice, with the presence of hPSC-PCs in both recovered vasculature and myofibers, indicating robust vasculogenic and myogenic capacities *in vivo* similar to their adult counterparts [97]. Yet, the reciprocity of all these fetal populations to all or part of adult MSC precursors remains to be clarified.

A rare CD34+/CD146+/CD31−/CD45− population of adipose PCs has also been characterized in the SVF [39, 98–103] and may represent a developmental intermediate between PCs and some or all ACs [102]. This elusive CD34+ PC population is not easily detected within the vascular wall by immunohistochemistry [24, 42] and requires

stringent rare-event strategies for its detection and isolation by flow cytometry [100, 103]. Traktuev et al. suggested the existence of CD34+ cells exhibiting a native pericytic phenotype [98]. They demonstrated that primary cultures of AC-like CD34+CD144−CD45− SVF cells can express PC markers (NG2, PDGFRα, PDGFRβ) without requirement of blood vessel remodeling growth factors in contrast to CD34+CD146− cells [24]. Though these disparities may be related to culture conditions, SVF isolation techniques, and cell sorting strategies, the intricacy and anatomical proximity of these distinct subpopulations highlight the necessity to use multidimensional strategies for their isolation via exclusion of hematopoietic (CD45) and endothelial (CD31, CD144) lineages and combinatory positive selection of pericytic (i.e., CD146, NG2, PDGFRβ), adventitial (CD34), or MSC (CD44, CD73, CD90, CD105) cell subsets. A number of studies have employed preliminary sorting strategies relying on single markers, such as CD146 [104, 105] or CD34 [40, 106, 107], which may be inadequate in regard to the overlapping phenotypes of the vascular/perivascular cell subsets populating the adipose tissue.

Recently, using a combination of above-mentioned positive and negative selection antigens, we performed advanced flow cytometry analyses and FACS in the adipose SVF in order to identify and simultaneously purify these MSC precursor subpopulations [23, 24, 39, 101]. Both CD146+/CD34−/CD45− PCs and CD34+/CD31−/CD45−/CD146− ACs purified from adipose SVF have been shown to express MSC markers *in vivo* and in culture [23, 24, 101]. Furthermore, our quantitative multiparameter studies showed that only a third of adipose PCs (CD146+/CD34−/CD31−/Lineage−/CD45−) natively coexpress the MSC markers CD73, CD90, and CD105, which reveals the cellular heterogeneity of the pericyte compartment [101]. In contrast, both CD146+ (putative PC-AC intermediates) and CD146− (ACs) subsets of CD34+/CD31−/Lineage−/CD45− SVF cells homogenously co-express MSC markers [101]. On the other hand, among these MSC-like perivascular cells, two subpopulations in the adipose SVF can be discerned on the basis of CD34 expression and further distinguished by their proliferation pattern: a low proliferative CD34− subset and a high proliferative CD34+ subset. While CD34− is a typical phenotype of multipotent mesenchymogenic PCs in adipose and most other tissues [23], the CD34+ phenotype may represent transit-amplifying intermediates between stem-like adipose PCs and highly prevalent ACs *in vivo* but require prudent interpretations in culture due to its instability.

5. Adhesion and Migration of Perivascular MSC Precursors

In view of future stem cell-based approaches and therapies, it is crucial to identify predictive parameters that allow the researchers and clinicians to foresee the *in vivo* action of stem/progenitor cells. Since cell adhesion and migration capacities are tightly correlated with *in vivo* cell trafficking and homing, these parameters represent potential predictors for the clinical outcome of stem cell-treated patients and require further investigation [108–110]. Herein we discuss recent progresses in the understanding of perivascular MSC precursors in regard to cell adhesion, migration, and response to hypoxia.

5.1. Cell Adhesion. Anatomically, PCs closely surround ECs populating the vascular intima with specific adhesion and migration properties that allow them to regulate the blood vessel stability/integrity as well as the proliferation and motility of adjacent ECs [51]. Up to 1000 contacts can be secured by peg-sockets to a juxtaposing EC via cytoplasmic fingers inserted into endothelial invaginations [111]. Pericytic elongated terminal arms include adhesion plaques that strongly embed into the basement membrane and EC body to secure their location [111]. Different molecules and pathways have been involved in mural cell motility and adhesion. Notably, ephB/ephrin-B interactions mediate human MSC/PC adhesion, migration, and differentiation [112, 113]. The eph/ephrin family of tyrosine kinase receptors has been identified as an important factor contributing to bone homeostasis and regulating MSC adhesion. Inhibition of ephrin-B signaling prevents MSC attachment and spreading by activation of Src-, PI3 Kinase-, and JNK-dependent signaling pathways [112]. Ephrin-B2-deficient mural cells display major defects in spreading, focal-adhesion formation, and polarized migration as well as exhibiting increased motility [113]. Our group investigated adhesion molecules and proteins involved in PC migratory capacity. We demonstrated that CD146+/NG2+/PDGFRβ+/CD144− PCs exhibited more robust adherence to extracellular matrix substrates (e.g., collagen type-I, gelatin, and fibronectin) and greater migratory capacity than the CD146− population. Enhanced adherence and migratory capacities may result from high expression levels of alpha and beta subunits of integrin and matrix metalloproteinase (MMP)-2, respectively [70]. On the other hand, PCs express intercellular adhesion molecule 1 (ICAM-1) and upregulate its expression in response to tumor necrosis factor (TNF) and pattern-recognition receptor (PRR) ligands. ICAM-1 also regulates interactions of neutrophils and monocytes with PCs *in vitro* [114]. Moreover, it has been suggested that arteriolar and capillary PCs can detect inflammatory stimuli and increase their adhesive interactions with innate leukocytes, implicating their role in the regulation of inflammatory responses [114, 115].

5.2. Cell Migration. PC recruitment and migration occur frequently in response to pathophysiological events such as wound healing, inflammation, or angiogenesis. During vascular development, ECs release PDGF-BB to recruit PCs and stabilize the newly formed blood vessels [116, 117]. Increase of PC density by activation of PDGF-BB/ PDGFRβ signaling pathways has also been detected during wound healing and tumor vascular remodeling [56, 111, 118]. Inversely, disruption of PDGF-BB/PDGFRβ pathways may occur during pathologic conditions (e.g., diabetic retinopathy), resulting in PC apoptosis and augmented permeability of the vascular wall [111, 119]. Upon inflammatory events, PCs control the pattern and efficiency of leukocyte interstitial migration *in vivo* [114,

120]. A recent study highlighted the constitutive expression of chemoattractants by NG2+ PCs: CSC-chemokine ligand-1 (CXCL1) and -8 (CXCL8), macrophage migration inhibitory factor (MIF), CC-chemokine ligand 2 (CCL2), and interleukin-6 (IL-6). PCs further upregulated the expression of these chemo-attractants following stimulation by PRR ligands [114, 115]. Therefore, PCs not only chemotactically migrate to the site of angiogenesis, injury, or inflammation but also actively recruit other proinflammatory participants, including myeloid leukocytes, neutrophils, and macrophages.

Using an *in vitro* model of tissue damage, some of us previously mimicked the ability of HUCPCs to migrate towards the injury site *in vivo* and predicted their capacity to secrete cytokines and trophic factors [71]. Envisioning a possible clinical application of stem cells in the context of extremely immature newborns with an acute lung injury, where alveolar type II cells crucial for producing surfactant and regulating alveolar fluid levels and host defense are damaged, HUC can be readily considered as a convenient source of stem cells. Consequently, a coculture model of pulmonary tissue damage was set up, where an alveolar type II cell line was damaged with bleomycin, an anticancer drug with known pulmonary toxicity [71]. Dye-labeled HUCPCs in coculture were mobilized and migrated towards the damaged alveolar type II cells. HUCPCs showed a great ability to secrete angiogenic/antiapoptotic cytokines and trophic factors compared to the control, in particular high level of keratinocyte growth factor (KGF) [71]. KGF appears to play a crucial role mediating tissue improvement in a range of experimental lung injuries, presumably due to its versatile effects including cellular repair, cytoprotection, and alveolar fluid clearance modulation and immunomodulation [121, 122]. Similarly, skeletal muscle-derived PCs secrete high levels (superior to those of BM-MSCs) of KGF and vascular endothelial growth factor (VEGF) as well as heparin binding-epidermal growth factor (HB-EGF) and basic-fibroblast growth factor (bFGF), which are all considered playing critical roles during wound healing [123, 124].

The abundance of mesenchymogenic progenitors in the SVF of adipose tissue (5,000 CFU-F per gram) [125] provides a great advantage for the development of clinical applications without any *in vitro* expansion requirements [126, 127]. ASC-based therapeutic strategies have been proposed for either regenerative or targeted therapies and often rely on native tropism of ASCs for wound healing, inflammation, or cancer. Although investigations of cell adhesion and migration in purified ACs are currently ongoing, much can be learned from the unfractionated ASCs which have been shown to home to sites of injury and promote tissue repair following systemic injections in animal models of myocardial infarction [128, 129], liver injury [130, 131], olfactory dysfunction [132], hypoxia-ischemia induced brain damage [133], allergic rhinitis [134], inflammatory neuropathy [135], sciatic crush [136], cranial injury [137], and muscular dystrophy [138, 139]. The migratory activity of early-passage ASCs can be modulated by a set of chemokines and growth factors, including PDGF-AB, TGF-β1, and TNFα [140]. These soluble factors can stimulate ASCs via activation of an array of migration-associated receptors such as C-C chemokine receptor types 1 and 7 (CCR1, CCR7), C-X-C chemokine receptor types 4, 5, and 6 (CXCR4, CXCR5, CXCR6), EGF receptor, fibroblast growth factor receptor 1, TGF-β receptor 2, TNF receptor superfamily member 1A, and PDGF receptors α and β [140–142].

ASCs have been proposed to affect various neighboring cells within the subcutaneous tissue via paracrine signals during active remodeling processes such as wound healing [143–145]. In a recent study, ASC-conditioned medium promoted *in vitro* migration of vascular ECs, fibroblasts, and keratinocytes [146]. These data support the impact of ASCs on the proliferation and recruitment of these distinct cell subsets during wound healing via secretion of high levels of promigratory cytokines, including angiopoietin-like-1, EGF, FGF, HGF, TGFβ, SDF-1, and VEGF [145–149].

Similarly to BM-MSCs [150, 151], ASCs have been associated with enhanced migratory activities during tumorigenesis. ASC tropism towards various tumors such as glioma [152, 153], colon cancer [154], and prostate cancer [155] has been exploited to develop targeted therapies. On the other hand, ASCs can modulate the migration of cancer cells, promoting metastasis of breast cancer cells [156, 157] via CCR5/CCL5 signaling in animal models despite the inhibition of breast cancer metastasis in a different model [158]. An antimetastatic result was also observed with pancreas cancer cells [159].

5.3. Cellular Response to Hypoxia. Hypoxia has been shown to promote proliferation and migration of both PCs and MSCs [160, 161]. A recent study highlighted the involvement of the ERK signaling pathway during the modulation of mitogenic and chemotactic responses of human muscle PCs to a low oxygen concentration (6% O_2). This activation of ERK signaling and associated integrins occurred without any detectable alteration on the cell phenotypes or differentiation potentials [160, 162]. A number of growth factors, including PDGF, EGF, and FGF, can activate the Ras-Raf-MEK1/2-ERK signaling axis [163], which controls the adhesion dynamics and cell migratory properties via formation of protrusions within cell membrane and enhancement of the focal adhesion turnover [164]. Culture of MSCs in hypoxic conditions also resulted in higher survival and migration in a hind-limb ischemia model, presumably through Akt signaling [165]. The activation of the Akt pathway has been linked to the cell migratory ability and can be mediated by hepatocyte growth factor (HGF). MSCs under hypoxia exhibited higher expression of cMet, a critical HGF receptor [165, 166], and two receptors of the chemokine stromal-derived factor-1 (SDF-1), CXCR4 and CXCR7, whose expression can also be mediated by hypoxia via the hypoxia-inducible factor-1 alpha (HIF-1α) and Akt phosphorylation [167]. Additionally, even under a 2.5% O_2 hypoxia, the paracrine function of PCs remained highly active when compared to 21% O_2 normoxic culture, with increased expression of VEGF-A, PDGF-B, and TGFβ1 and decreased expression of angiopoietin-1, bFGF, EGF, HGF, and MCP-1, and similar levels of leukemia inhibitory factor (LIF), cyclooxygenase-2 (COX-2/PTGS-2, prostaglandin endoperoxide synthase-2), heme oxygenase-1

(HMOX-1), IL-6, HIF-1α, and MMP-2 [168]. Understanding cellular responses of perivascular MSC precursors and MSCs to hypoxia would help researchers and clinicians to develop better approaches to improve the efficacy of MSC-based cell therapy, including genetic modification, cellular preconditioning, and pharmacological adjunct therapy [9].

6. Migratory and Homing Characteristics of Perivascular MSC Precursors during Tissue Repair/Regeneration

Perivascular MSC precursors have recently been demonstrated as efficient regenerative/supportive units for tissue repair and regeneration. In particular, human muscle PCs and saphenous vein-derived ACs exhibited superior angiogenic, paracrine, and cardioprotective capacities and augmented functional recovery in murine myocardial infarction and hind-limb ischemia models when compared to myoblasts or unfractionated MSCs [65, 168, 169]. Additionally, muscle and placental PCs were shown to repair/regenerate injured and dystrophic muscles in animal disease models as well as contribute to the muscle stem cell (satellite cell) pool [23, 64, 70, 170]. Some of us also showed that HUCPCs prevented/rescued the oxygen-induced arrest in alveolar growth and restored lung function and architecture, primarily through their paracrine function [171]. Interestingly, CD146+ PCs extracted from adipose tissue were shown to support the long-term persistence of human hematopoietic stem/progenitor cells in coculture [172]. Moreover, purified human PCs and ACs exhibited bone formation or healing when implanted into animal models of ectopic bone formation or critical-sized calvarial bone injury, respectively [88, 89, 173]. In this section, we will discuss the current understanding of the cell engraftment, migration, and homing of transplanted perivascular MSC precursors during some of these regenerative events.

6.1. Cardiac Repair. When intramyocardially transplanted into a mouse model of acute myocardial infarction (AMI), purified human muscle PCs contributed to cardiac functional and anatomic recovery after infarction, presumably through multiple cardioprotective and regenerative mechanisms: reversal of ventricular remodeling, reduction of cardiac fibrosis, diminution of chronic inflammation, promotion of host angiogenesis, and small-scale myocardial regenerative events [168]. The engraftment ratio of intramyocardially injected GFP-labeled PCs was approximately 9% at the first week, decreasing to roughly 3% at 8 weeks after infarction. Above all, a fraction of donor PCs was identified in perivascular positions, juxtaposing host CD31+ ECs (Figure 2). In contrast to the engraftment ratio, the vessel-homing ratio of transplanted PCs slightly increased over time, implicating the potential benefit of niche-homing for long-term donor cell survival. Moreover, cellular interactions between donor PCs and host ECs were demonstrated by the expression of human-specific ephrin type-B receptor 2 (EphB2) in some GFP+ PCs adjacent to ECs as well as the formation of connexin 43 gap junctions with ECs [168]. Additionally, immune cells

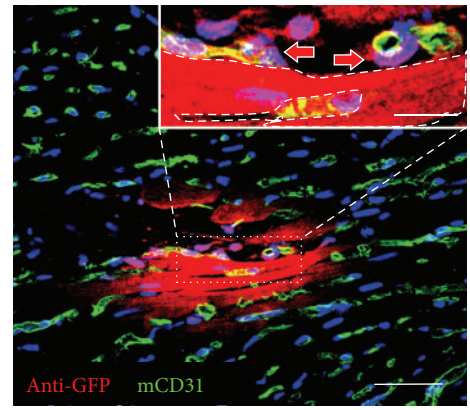

Figure 2: Human pericytes home to perivascular locations. Confocal microscopy showed that GFP+ human pericytes (red), identified by anti-GFP immunostaining, can be located at the interstitial space where host CD31+ capillaries (green) reside (main, scale bar = 50 μm). Some GFP+ donor cells (inset, red arrows) are in close contact with mouse CD31+ endothelial cells (green). Dash line in the inset picture delineates a putative GFP+ cardiomyocyte (inset, scale bar = 10 μm).

in the ischemic tissue release chemokines such as interleukins and monocyte chemoattractant protein-1 (MCP-1), which are involved in the homing of MSCs to the ischemic heart [174]. Moreover, the paracrine anti-inflammatory function of human MSCs was also demonstrated by the high expression of anti-inflammatory protein TSG-6 from MSCs embolized in lung, which led to decreased inflammatory responses, reduced infarct size, and improved cardiac function [175].

Similarly, Katare et al. reported that transplantation of human saphenous vein-derived ACs (hSV-ACs), a putative PC progenitor population, promoted functional improvement in a mouse model of MI, primarily through angiocrine activities and neovascularization via both donor and recipient cells as well as other cardioprotective mechanisms including improved myocardial blood flow, attenuated vascular permeability, and reduction of myocardial remodeling, cardiomyocyte apoptosis, and interstitial fibrosis [169]. hSV-ACs produced and released microRNA-132 (miR-132) as a paracrine agent, which exerts proangiogenic, prosurvival, and antifibrotic activities and likely plays a key role as an activator of cardiac healing. While retaining their original antigenic and perivascular phenotype, homing of hSV-ACs to perivascular locations was confirmed by Dil-labeled hSV-ACs juxtaposing isolectin-positive capillary ECs [169].

6.2. Muscle Regeneration. As mentioned previously, we have demonstrated that intramuscular injection of freshly sorted or cultured PCs derived from human adipose or skeletal muscle regenerated human myofibers efficiently in the mouse dystrophic or injured muscle [23]. In another study, we showed that intramuscular implantation of dissected human placental villi resulted in crude outgrowth of human cells in dystrophic mice [70]. Ample amount of cells of human origin released from placental villi fragments participated in host muscle regeneration, revealed by the

detection of human dystrophin-positive (hDys3t) and/or human spectrin-positive myofibers. Many of these human myofibers coexpressed human lamin A/C, indicating their sole human origin and not intermediate products of cell fusion. Surprisingly, human myofibers were located not only close to the implantation area (500 μm to 2 mm) but also in far more distant regions (up to 2 cm), suggesting active migration of outgrown human myogenic precursors over long distances. Similarly, freshly isolated placental PCs possessed high migratory activity and actively contributed to host skeletal muscle regeneration [70].

6.3. Pulmonary Repair. As mentioned previously, PCs isolated from umbilical cords migrated efficiently *in vitro* toward alveolar type II cells damaged by bleomycin, with an elevated secretion of KGF and VEGF [71]. Using a preclinical animal model of oxygen-arrested lung growth (exposure to 95% oxygen, i.e., hyperoxia), which mimics bronchopulmonary dysplasia (BPD), Pierro et al. tested the *in vivo* therapeutic potential of HUCPCs [171]. To examine suitable approaches for future clinical applications, two different administration strategies, prophylactic or therapeutic, as well as two different therapeutic modalities, direct cell transplantation or HUCPC-conditioned medium injection, were investigated. Intratracheal transplantation of HUCPCs prevented/rescued oxygen-induced arrested alveolar growth and restored normal alveolar architecture. However, immunofluorescence and qPCR revealed very few donor cells localized within the lung. This low cell engraftment suggested that cell replacement is not the primary mechanism of the observed therapeutic effects. Indeed similar therapeutic benefits can be achieved by daily intraperitoneal administration of conditioned medium, resulting in improved alveolar architecture and lung function. In both administration strategies, long-term efficacy and safety were demonstrated till 6 months with an improved exercise capacity and normal alveolar architecture. No suspicious tumor formation was noted by total body CT scans. In conclusion, the therapeutic potential of HUCPCs for pulmonary repair can be exploited by either direct cell therapy or the production of trophic factors, expanding new clinical perspectives for HUCPCs and other perivascular MSC precursors.

6.4. Skeletal Regeneration. To investigate their skeletal regenerative capacity, human PCs and ACs purified from lipoaspirate SVF have been seeded onto osteoinductive scaffolds and implanted into animal models of ectopic bone formation or critical-sized calvarial bone injury, respectively [88, 89, 176]. Significantly greater osteogenesis or bone healing by PCs and ACs in murine muscle pockets or calvarial defects than control SVF cells was observed, respectively. Additionally, the high osteogenic capability of human ACs and PCs can be further enhanced by Nel-like molecule-1 (NELL-1), an osteoinductive growth factor that is a direct transcriptional target of Runx2 [89, 173, 176, 177]. On the other hand, the role of the SDF-1/CXCR4 pathway in MSCs/PCs recruitment during the injury response has been established in a murine model of femoral bone graft, where SDF-1 deficient mice were unable to recruit MSCs at bone fracture sites and consequently limited their participation to local bone repair [178]. The role of the SDF-1/CXCR4 axis in PC recruitment has also been revealed during tumorigenesis [179]. Overexpression of PDGF-BB increased malignant PC growth via activation of the SDF-1/CXCR4 axis and induced expression of SDF-1 in ECs. The upregulation of SDF-1 was directly mediated by inhibition of the Akt/mTOR pathway or HIF-1α. Accordingly, both donor and host stem cell homing can be further enhanced by MSCs genetically modified to overexpress SDF-1 [180].

7. Angiogenic Capacities of Perivascular MSC Precursors and Cellular Interactions with ECs

7.1. Pericyte-EC Cellular Interactions: A Perivascular Niche for MSC Precursors. PCs are ubiquitously present in microvasculature where they extend primary cytoplasmic processes along the abluminal surface of the endothelial tube. They are enveloped in a basement membrane that is continuous with the EC basement membrane to which both cells contribute [181, 182]. The majority of the PC-EC interface is separated by basement membrane, with the two cell types contacting each other at discrete points through peg-socket type interactions, occluding contacts, gap junctions, and adhesion plaques [183, 184]. The intimate anatomical relationship between ECs and PCs suggests close interactions involving not only direct contact but also paracrine or juxtacrine signaling. EC-to-PC ratios in normal tissues vary between 1 : 1 to 10 : 1 and may be up to 100 : 1 (in skeletal muscle), while PC coverage of the endothelial abluminal surface ranges between 10% and 70% [185, 186]. PC density and coverage appear to correlate with endothelial barrier properties (i.e., brain > lungs > muscle) [111], EC turnover (large turnover leading to less coverage) [184], and orthostatic blood pressure (larger coverage in lower body parts) [185], in keeping with a role of PCs in regulating capillary barriers, endothelial proliferation, and capillary diameter [111]. Genetically modified mouse models have demonstrated that these two vascular cell types are interdependent: primary defects in one cell type have obligated consequences for the other. There is growing evidence to suggest that ECs can manipulate the migratory and angiogenic properties of PCs, while *in vitro* data highlighting EC influence on mesenchymal differentiation potential of PCs points to a possible role of ECs as gatekeepers within the context of an adult stem cell niche.

7.2. EC Interactions Regulate Pericyte Recruitment and Angiogenesis. The formation of new capillaries during angiogenesis requires a series of well-orchestrated cellular events allowing ECs and PCs to migrate into the perivascular space. In vessel sprouting, angiogenic factors (e.g., VEGF) stimulate ECs, which in turn secrete proteases that degrade basement membrane and allow EC invasion. An endothelial column, guided by a migrating EC at the very tip, then moves toward a VEGF gradient [183]. Studies of the *corpus luteum* indicate that PCs are also capable of guiding sprouting processes by migrating

Table 1: The influence of ECs on the multipotency of tissue-specific MSCs.

Niche Component	Model	Stem cell surrogate	Niche surrogate	Lineage assessed	Effect on differentiation	Context	Proposed mechanism	Investigator
Endothelial cell	3D	ASC	HUVEC	Osteogenesis	↓	Paracrine	↑Wnt	Rajashekhar et al. [203]
Endothelial cell	3D	ASC	HUVEC	Osteogenesis	↓	Juxtacrine	↑Wnt	Rajashekhar et al. [203]
Endothelial cell	2D	BMSC	HUVEC	Osteogenesis	↑	Paracrine	(Dkk1-Wnt, FGF, PDGF, BMP, TGFβ, Notch)	Saleh et al. [204]
Endothelial cell	2D	BMSC	HUVEC	Adipogenesis	—	Paracrine	—	Saleh et al. [205]
Endothelial cell	2D	BMSC	HUVEC	Osteogenesis	↑	Juxtacrine	—	Xue et al. [206]
Endothelial cell	2D	BMSC	HDMEC	Osteogenesis	↑	Juxtacrine	BMP-2	Kaigler et al. [207]
Endothelial cell	2D	BMSC	HDMEC	osteogenesis	—	Paracrine	—	Kaigler et al. [207]
Endothelial cell	2D	BMSC	HDMEC	Osteogenesis	↑	Juxtacrine	N-cadherin	Li et al. [208]
Endothelial cell	2D	BMSC	HDMEC	Osteogenesis	↑	Paracrine	VEGF	Grellier et al. [209]
Endothelial cell	2D	BMSC	HDMEC	Osteogenesis	↓	Paracrine	Osterix/OSX	Meury et al. [210]
Endothelial cell	2D	BMSC	HUVEC	Osteogenesis	↑	Juxtacrine	Cx43/gap junctions	Villars et al. [211]
Endothelial cell	2D	BMSC	HUVEC	Osteogenesis	↑	Juxtacrine	—	Villars et al. [212]
Endothelial cell	2D	HOP	HUVEC	Osteogenesis	↑	Juxtacrine	—	Guillotin et al. [213]
Endothelial cell	2D	HOP	EPC, HSVEC	Osteogenesis	↑	Juxtacrine	Cx43/gap junctions	Guillotin et al. [213]

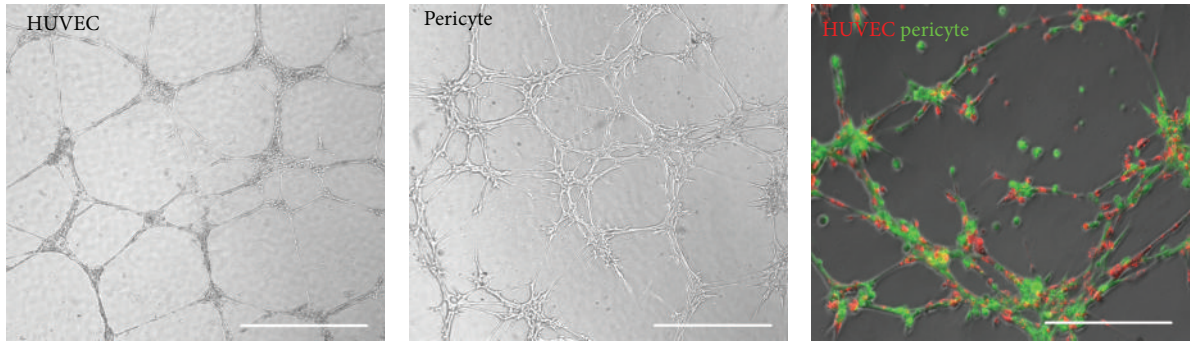

(a) (b) (c)

Figure 3: Human pericytes support formation of microvascular structures. (a) HUVECs seeded onto Matrigel-coated wells formed typical capillary-like structures after 24 hours (scale bar = 1 mm). (b) Human muscle pericytes formed morphologically similar network structures within 6–8 hours (scale bar = 1 mm). (c) Cocultured dye-labeled HUVECs (red) and pericytes (green) at 1 : 1 ratio on Matrigel showed coformation of capillary-like networks within 6–8 hours (scale bars = 500 μm).

ahead of ECs and expressing VEGF [187–189]. Emerging endothelial tubes then secrete growth factors, partly to attract PCs that envelop the vessel wall, and promote vessel maturation. Key pathways implicated in PC-EC signaling include PDGF/PDGFRβ, angiopoietins and Tie receptors, sphingosine-1-phosphate signaling, TGF-β signaling, Notch and Wnt [116, 186, 190, 191]. It is believed that PCs, because of their vessel-embracing position, are able to transfer angiogenic signals along the vessel length by contacting numerous ECs. The recruitment and contribution of PCs to developing endothelial tubes and angiogenic process can be observed *in vitro* through Matrigel culture. Human muscle PCs alone can form network structures in Matrigel culture that were morphologically similar to networks formed by ECs but at an accelerated fashion (Figures 3(a) and 3(b)). Coculture of dye-labeled PCs and ECs at 1 : 1 ratio in Matrigel showed network formation by both cell types, facilitated by the presence of PCs (Figure 3(c)). Blocki et al. further demonstrated that while the capacity to colocalize and/or coform network structures with endothelial tubules on Matrigel is not restricted to PCs, only PCs (CD146+/CD34−) effectively stabilize endothelial networks and improve endothelial sprout integrity [192]. Nevertheless, it is noteworthy that the EC-to-PC ratio may play an important role in the formation of vascular networks and PC functionality *in vitro*.

7.3. ECs: The Gatekeepers of Pericyte Mesenchymal Activation? A growing number of studies demonstrate that tissue resident stem cells reside in vascular niches, including neural, hematopoietic, and MSCs [19, 193–195]. Adult stem cell niche components provide signals that control the balance between quiescence, self-renewal, and differentiation [194]. A significant obstacle in identification of the perivascular origin of

MSCs was the reluctance of PCs to express mesenchymal phenotypes in their native microenvironment [196]. Although it is feasible that PCs acquire MSC potentials upon exiting the microvasculature, it is intuitive that MSC features are expressed by PCs *in situ* but environmentally downregulated. Studies using unfractionated SVF have demonstrated poor and unreliable tissue formation [197] or lower regeneration efficacy relative to prospectively isolated and purified MSCs [197], lending further support to a hypothesis that certain cellular component(s) of SVF have an inhibitory/adverse effect on differentiating MSCs. As such, the influence of ECs on the multipotency of tissue-specific MSCs is now under investigation even though preliminary results to date have been divergent (Table 1). Osteogenic and adipogenic differentiation is not seen within the perivasculature of healthy tissues where the PC-EC relationship is undisturbed. However, disturbed PC-EC interactions have been observed in conditions associated with pathological mineralization and adipogenesis, for example, heterotopic ossification and atherosclerosis [198, 199]. In addition, the ECM proteins, also present within a perivascular niche, have been shown to modify growth and differentiation of MSCs, with collagen type I-, fibronectin-, and vitronectin-treated plates enhancing mineralization *in vitro* [200]. The secretome and proteome of human MSCs have now been extensively documented [201] with studies identifying numerous transcription factors and multiple extracellular and intracellular signaling pathways that regulate adipogenesis and osteogenesis. Interestingly, inducers of differentiation along one lineage often inhibit differentiation along another. For example, the transcription factor PPARγ is a prime inducer of adipogenesis that inhibits osteogenesis, highlighting the mutual exclusivity of these lineages [202]. It is therefore likely that signaling mechanisms responsible for the mesenchymal fate of PCs will be multifactorial and distinct for different lineages.

8. Conclusion

In this review, we described the identification and characterization of perivascular MSC precursors with regard to their adhesion, migration, engraftment/homing, and intercellular cross-talk in culture and in experimental animal models. Although PCs and ACs both exhibit multilineage mesenchymogenic capacities and are derived from adjacent perivascular structural layers, further investigations are required to clarify their developmental relationship as well as the involvement of an ontogenic intermediate. Through the understanding of their unique cellular kinetics and regenerative potential, we will be able to define the pathophysiological role and therapeutic value of the individual blood-vessel-derived MSC precursor population under a particular pathological circumstance. Ultimately, through the purification and/or recombination of these distinct subsets of MSC precursors, it is feasible to further enhance stem cell therapy by eliminating cells with none or limited regenerative potentials in a specific disorder, creating a customized therapeutic modality for the personalized medicine.

Authors' Contribution

Iain R. Murray and Ludovic Zimmerlin contributed equally to this work.

References

[1] S. P. Bruder, D. Gazit, L. Passi-Even, I. Bab, and A. I. Caplan, "Osteochondral differentiation and the emergence of stage-specific osteogenic cell-surface molecules by bone marrow cells in diffusion chambers," *Bone and Mineral*, vol. 11, no. 2, pp. 141–151, 1990.

[2] P. A. Zuk, M. Zhu, H. Mizuno et al., "Multilineage cells from human adipose tissue: implications for cell-based therapies," *Tissue Engineering*, vol. 7, no. 2, pp. 211–228, 2001.

[3] A. I. Caplan and J. E. Dennis, "Mesenchymal stem cells as trophic mediators," *Journal of Cellular Biochemistry*, vol. 98, no. 5, pp. 1076–1084, 2006.

[4] J. García-Castro, C. Trigueros, J. Madrenas, J. A. Pérez-Simón, R. Rodriguez, and P. Menendez, "Mesenchymal stem cells and their use as cell replacement therapy and disease modelling tool," *Journal of Cellular and Molecular Medicine*, vol. 12, no. 6B, pp. 2552–2565, 2008.

[5] W. Prasongchean and P. Ferretti, "Autologous stem cells for personalised medicine," *New Biotechnology*, vol. 29, no. 6, pp. 641–650, 2012.

[6] A. F. Steinert, L. Rackwitz, F. Gilbert, U. Noth, and R. S. Tuan, "Concise review: the clinical application of mesenchymal stem cells for musculoskeletal regeneration: current status and perspectives," *Stem Cells Translational Medicine*, vol. 1, no. 3, pp. 237–247, 2012.

[7] L. Wu, X. Cai, S. Zhang, M. Karperien, and Y. Lin, "Regeneration of articular cartilage by adipose tissue derived mesenchymal stem cells: perspectives from stem cell biology and molecular medicine," *Journal of Cellular Physiology*, vol. 228, no. 5, pp. 938–944, 2013.

[8] W. M. Jackson, L. J. Nesti, and R. S. Tuan, "Potential therapeutic applications of muscle-derived mesenchymal stem and progenitor cells," *Expert Opinion on Biological Therapy*, vol. 10, no. 4, pp. 505–517, 2010.

[9] C. W. Chen, J. Huard, and B. Péault, "Mesenchymal stem cells and cardiovascular repair," in *Mesenchymal Stem Sells*, Y. Xiao, Ed., Nova Science Publishers, New York, NY, USA, 2011.

[10] W. M. Jackson, L. J. Nesti, and R. S. Tuan, "Concise review: clinical translation of wound healing therapies based on mesenchymal stem cells," *Stem Cells Translational Medicine*, vol. 1, no. 1, pp. 44–50, 2012.

[11] C. Pontikoglou, F. Deschaseaux, L. Sensebé, and H. A. Papadaki, "Bone marrow mesenchymal stem cells: biological properties and their role in hematopoiesis and hematopoietic stem cell transplantation," *Stem Cell Reviews and Reports*, vol. 7, no. 3, pp. 569–589, 2011.

[12] M. E. J. Reinders, T. J. Rabelink, and J. W. de Fijter, "The role of mesenchymal stromal cells in chronic transplant rejection after solid organ transplantation," *Current Opinion in Organ Transplantation*, vol. 18, no. 1, pp. 44–50, 2013.

[13] L. Wang, Y. Zhao, and S. Shi, "Interplay between mesenchymal stem cells and lymphocytes: implications for immunotherapy and tissue regeneration," *Journal of Dental Research*, vol. 91, no. 11, pp. 1003–1010, 2012.

[14] M. E. Bernardo and W. E. Fibbe, "Safety and efficacy of mesenchymal stromal cell therapy in autoimmune disorders,"

Annals of the New York Academy of Sciences, vol. 1266, no. 1, pp. 107–117, 2012.

[15] L. D. S. Meirelles, A. I. Caplan, and N. B. Nardi, "In search of the in vivo identity of mesenchymal stem cells," *Stem Cells*, vol. 26, no. 9, pp. 2287–2299, 2008.

[16] M. Pevsner-Fischer, S. Levin, and D. Zipori, "The origins of mesenchymal stromal cell heterogeneity," *Stem Cell Reviews and Reports*, vol. 7, no. 3, pp. 560–568, 2011.

[17] C.-W. Chen, M. Corselli, B. Péault, and J. Huard, "Human blood-vessel-derived stem cells for tissue repair and regeneration," *Journal of Biomedicine and Biotechnology*, vol. 2012, Article ID 597439, 9 pages, 2012.

[18] B. Sacchetti, A. Funari, S. Michienzi et al., "Self-renewing osteoprogenitors in bone marrow sinusoids can organize a hematopoietic microenvironment," *Cell*, vol. 131, no. 2, pp. 324–336, 2007.

[19] M. Tavazoie, L. van der Veken, V. Silva-Vargas et al., "A specialized vascular niche for adult neural stem cells," *Cell Stem Cell*, vol. 3, no. 3, pp. 279–288, 2008.

[20] S. Shi and S. Gronthos, "Perivascular niche of postnatal mesenchymal stem cells in human bone marrow and dental pulp," *Journal of Bone and Mineral Research*, vol. 18, no. 4, pp. 696–704, 2003.

[21] W. Tang, D. Zeve, J. M. Suh et al., "White fat progenitor cells reside in the adipose vasculature," *Science*, vol. 322, no. 5901, pp. 583–586, 2008.

[22] M. Tavian, B. Zheng, E. Oberlin et al., "The vascular wall as a source of stem cells," *Annals of the New York Academy of Sciences*, vol. 1044, pp. 41–50, 2005.

[23] M. Crisan, S. Yap, L. Casteilla et al., "A perivascular origin for mesenchymal stem cells in multiple human organs," *Cell Stem Cell*, vol. 3, no. 3, pp. 301–313, 2008.

[24] M. Corselli, C. W. Chen, B. Sun, S. Yap, J. P. Rubin, and B. Péault, "The tunica adventitia of human arteries and veins as a source of mesenchymal stem cells," *Stem Cells and Development*, vol. 21, no. 8, pp. 1299–1308, 2012.

[25] B. Zheng, B. Cao, M. Crisan et al., "Prospective identification of myogenic endothelial cells in human skeletal muscle," *Nature Biotechnology*, vol. 25, no. 9, pp. 1025–1034, 2007.

[26] C. B. Ballas, S. P. Zielske, and S. L. Gerson, "Adult bone marrow stem cells for cell and gene therapies: implications for greater use," *Journal of Cellular Biochemistry*, vol. 38, pp. 20–28, 2002.

[27] H. Chao and K. K. Hirschi, "Hemato-vascular origins of endothelial progenitor cells?" *Microvascular Research*, vol. 79, no. 3, pp. 169–173, 2010.

[28] Y.-H. Choi, A. Kurtz, and C. Stamm, "Mesenchymal stem cells for cardiac cell therapy," *Human Gene Therapy*, vol. 22, no. 1, pp. 3–17, 2011.

[29] K. C. Russell, D. G. Phinney, M. R. Lacey, B. L. Barrilleaux, K. E. Meyertholen, and K. C. O'Connor, "In vitro high-capacity assay to quantify the clonal heterogeneity in trilineage potential of mesenchymal stem cells reveals a complex hierarchy of lineage commitment," *Stem Cells*, vol. 28, no. 4, pp. 788–798, 2010.

[30] R. L. R. Van, C. E. Bayliss, and D. A. K. Roncari, "Cytological and enzymological characterization of adult human adipocyte precursors in culture," *Journal of Clinical Investigation*, vol. 58, no. 3, pp. 699–704, 1976.

[31] I. Dardick, W. J. Poznanski, I. Waheed, and G. Setterfield, "Ultrastructural observations on differentiating human preadipocytes cultured in vitro," *Tissue and Cell*, vol. 8, no. 3, pp. 561–571, 1976.

[32] P. A. Zuk, M. Zhu, P. Ashjian et al., "Human adipose tissue is a source of multipotent stem cells," *Molecular Biology of the Cell*, vol. 13, no. 12, pp. 4279–4295, 2002.

[33] S. R. Daher, B. H. Johnstone, D. G. Phinney, and K. L. March, "Adipose stromal/stem cells: basic and translational advances: the IFATS collection," *Stem Cells*, vol. 26, no. 10, pp. 2664–2665, 2008.

[34] M. Dominici, K. Le Blanc, I. Mueller et al., "Minimal criteria for defining multipotent mesenchymal stromal cells. The International Society for Cellular Therapy position statement," *Cytotherapy*, vol. 8, no. 4, pp. 315–317, 2006.

[35] J. B. Mitchell, K. McIntosh, S. Zvonic et al., "Immunophenotype of human adipose-derived cells: temporal changes in stromal-associated and stem cell-associated markers," *Stem Cells*, vol. 24, no. 2, pp. 376–385, 2006.

[36] C. I. Civin, L. C. Strauss, and C. Brovall, "Antigenic analysis of hematopoiesis. III. A hematopoietic progenitor cell surface antigen defined by a monoclonal antibody raised against KG-1a cells," *Journal of Immunology*, vol. 133, no. 1, pp. 157–165, 1984.

[37] T. Asahara, T. Murohara, A. Sullivan et al., "Isolation of putative progenitor endothelial cells for angiogenesis," *Science*, vol. 275, no. 5302, pp. 964–967, 1997.

[38] C. Sengenès, K. Lolmède, A. Zakaroff-Girard, R. Busse, and A. Bouloumié, "Preadipocytes in the human subcutaneous adipose tissue display distinct features from the adult mesenchymal and hematopoietic stem cells," *Journal of Cellular Physiology*, vol. 205, no. 1, pp. 114–122, 2005.

[39] L. Zimmerlin, V. S. Donnenberg, M. E. Pfeifer et al., "Stromal vascular progenitors in adult human adipose tissue," *Cytometry A*, vol. 77, no. 1, pp. 22–30, 2010.

[40] H. Suga, D. Matsumoto, H. Eto et al., "Functional implications of CD34 expression in human adipose-derived stem/progenitor cells," *Stem Cells and Development*, vol. 18, no. 8, pp. 1201–1209, 2009.

[41] C.-S. Lin, Z.-C. Xin, C.-H. Deng, H. Ning, G. Lin, and T. F. Lue, "Defining adipose tissue-derived stem cells in tissue and in culture," *Histology and Histopathology*, vol. 25, no. 6, pp. 807–815, 2010.

[42] G. Lin, M. Garcia, H. Ning et al., "Defining stem and progenitor cells within adipose tissue," *Stem Cells and Development*, vol. 17, no. 6, pp. 1053–1063, 2008.

[43] H. Li, L. Zimmerlin, K. G. Marra, V. S. Donnenberg, A. D. Donnenberg, and J. P. Rubin, "Adipogenic potential of adipose stem cell subpopulations," *Plastic and Reconstructive Surgery*, vol. 128, no. 3, pp. 663–672, 2011.

[44] K. L. Spalding, E. Arner, P. O. Westermark et al., "Dynamics of fat cell turnover in humans," *Nature*, vol. 453, no. 7196, pp. 783–787, 2008.

[45] M. Witkowska-Zimny and E. Wrobel, "Perinatal sources of mesenchymal stem cells: wharton's jelly, amnion and chorion," *Cellular and Molecular Biology Letters*, vol. 16, no. 3, pp. 493–514, 2011.

[46] R. R. Taghizadeh, K. J. Cetrulo, and C. L. Cetrulo, "Wharton's Jelly stem cells: future clinical applications," *Placenta*, vol. 32, no. 4, pp. S311–S315, 2011.

[47] D. L. Troyer and M. L. Weiss, "Concise review: wharton's Jelly-derived cells are a primitive stromal cell population," *Stem Cells*, vol. 26, no. 3, pp. 591–599, 2008.

[48] V. Kumar, N. Fausto, and A. Abbas, "Robbins and cotran pathologic basis of disease," in *Blood Vessels*, chapter 11, Saunders, Philadelphia, Pa, USA, 7th edition, 2004.

[49] G. Cossu and P. Bianco, "Mesoangioblasts: vascular progenitors for extravascular mesodermal tissues," *Current Opinion in Genetics and Development*, vol. 13, no. 5, pp. 537–542, 2003.

[50] D. Galli, A. Innocenzi, L. Staszewsky et al., "Mesoangioblasts, vessel-associated multipotent stem cells, repair the infarcted heart by multiple cellular mechanisms: a comparison with bone marrow progenitors, fibroblasts, and endothelial cells," *Arteriosclerosis, Thrombosis, and Vascular Biology*, vol. 25, no. 4, pp. 692–697, 2005.

[51] A. Armulik, A. Abramsson, and C. Betsholtz, "Endothelial/pericyte interactions," *Circulation Research*, vol. 97, no. 6, pp. 512–523, 2005.

[52] D. von Tell, A. Armulik, and C. Betsholtz, "Pericytes and vascular stability," *Experimental Cell Research*, vol. 312, no. 5, pp. 623–629, 2006.

[53] H. K. Rucker, H. J. Wynder, and W. E. Thomas, "Cellular mechanisms of CNS pericytes," *Brain Research Bulletin*, vol. 51, no. 5, pp. 363–369, 2000.

[54] P. Dore-Duffy and J. C. LaManna, "Physiologic angiodynamics in the brain," *Antioxidants and Redox Signaling*, vol. 9, no. 9, pp. 1363–1371, 2007.

[55] F. Kuhnert, B. Y. Y. Tam, B. Sennino et al., "Soluble receptor-mediated selective inhibition of VEGFR and PDGFRβ signaling during physiologic and tumor angiogenesis," *Proceedings of the National Academy of Sciences of the United States of America*, vol. 105, no. 29, pp. 10185–10190, 2008.

[56] P. Lindahl, B. R. Johansson, P. Levéen, and C. Betsholtz, "Pericyte loss and microaneurysm formation in PDGF-B-deficient mice," *Science*, vol. 277, no. 5323, pp. 242–245, 1997.

[57] M. W. Majesky, X. R. Dong, V. Hoglund, W. M. Mahoney Jr., and G. Daum, "The adventitia: a dynamic interface containing resident progenitor cells," *Arteriosclerosis, Thrombosis, and Vascular Biology*, vol. 31, no. 7, pp. 1530–1539, 2011.

[58] Y. Hu and Q. Xu, "Adventitial biology: differentiation and function," *Arteriosclerosis, Thrombosis, and Vascular Biology*, vol. 31, no. 7, pp. 1523–1529, 2011.

[59] Z. Tang, A. Wang, F. Yuan et al., "Differentiation of multipotent vascular stem cells contributes to vascular diseases," *Nature Communications*, vol. 3, article 875, 2012.

[60] Y. Hu, Z. Zhang, E. Torsney et al., "Abundant progenitor cells in the adventitia contribute to atherosclerosis of vein grafts in ApoE-deficient mice," *Journal of Clinical Investigation*, vol. 113, no. 9, pp. 1258–1265, 2004.

[61] Y. Shi, J. E. O'Brien Jr., A. Fard, J. D. Mannion, D. Wang, and A. Zalewski, "Adventitial myofibroblasts contribute to neointimal formation in injured porcine coronary arteries," *Circulation*, vol. 94, no. 7, pp. 1655–1664, 1996.

[62] S. Oparil, S.-J. Chen, Y.-F. Chen, J. N. Durand, L. Allen, and J. A. Thompson, "Estrogen attenuates the adventitial contribution to neointima formation in injured rat carotid arteries," *Cardiovascular Research*, vol. 44, no. 3, pp. 608–614, 1999.

[63] M. Crisan, J. Huard, B. Zheng et al., "Purification and culture of human blood vessel-associated progenitor cells," in *Current Protocols in Stem Cell Biology*, John Wiley and Sons, 2007.

[64] A. Dellavalle, M. Sampaolesi, R. Tonlorenzi et al., "Pericytes of human skeletal muscle are myogenic precursors distinct from satellite cells," *Nature Cell Biology*, vol. 9, no. 3, pp. 255–267, 2007.

[65] P. Campagnolo, D. Cesselli, A. Al Haj Zen et al., "Human adult vena saphena contains perivascular progenitor cells endowed with clonogenic and proangiogenic potential," *Circulation*, vol. 121, no. 15, pp. 1735–1745, 2010.

[66] D. Tilki, H.-P. Hohn, B. Ergün, S. Rafii, and S. Ergün, "Emerging biology of vascular wall progenitor cells in health and disease," *Trends in Molecular Medicine*, vol. 15, no. 11, pp. 501–509, 2009.

[67] E. Zengin, F. Chalajour, U. M. Gehling et al., "Vascular wall resident progenitor cells: a source for postnatal vasculogenesis," *Development*, vol. 133, no. 8, pp. 1543–1551, 2006.

[68] M. Okada, T. R. Payne, B. Zheng et al., "Myogenic endothelial cells purified from human skeletal muscle improve cardiac function after transplantation into infarcted myocardium," *Journal of the American College of Cardiology*, vol. 52, no. 23, pp. 1869–1880, 2008.

[69] B. Zheng, C. W. Chen, G. Li et al., "Isolation of myogenic stem cells from cultures of cryopreserved human skeletal muscle," *Cell transplantation*, vol. 21, no. 6, pp. 1087–1093, 2012.

[70] T. S. Park, M. Gavina, C.-W. Chen et al., "Placental perivascular cells for human muscle regeneration," *Stem Cells and Development*, vol. 20, no. 3, pp. 451–463, 2011.

[71] T. Montemurro, G. Andriolo, E. Montelatici et al., "Differentiation and migration properties of human foetal umbilical cord perivascular cells: potential for lung repair," *Journal of Cellular and Molecular Medicine*, vol. 15, no. 4, pp. 796–808, 2011.

[72] N. Zebardast, D. Lickorish, and J. E. Davies, "Human umbilical cord perivascular cells (HUCPVC): a mesenchymal cell source for dermal wound healing," *Organogenesis*, vol. 6, no. 4, pp. 197–203, 2010.

[73] M. M. Carvalho, F. G. Teixeira, R. L. Reis, N. Sousa, and A. J. Salgado, "Mesenchymal stem cells in the umbilical cord: phenotypic characterization, secretome and applications in central nervous system regenerative medicine," *Current Stem Cell Research and Therapy*, vol. 6, no. 3, pp. 221–228, 2011.

[74] E. Jauniaux, G. J. Burton, G. J. Moscoso, and J. Hustin, "Development of the early human placenta: a morphometric study," *Placenta*, vol. 12, no. 3, pp. 269–276, 1991.

[75] A. Bárcena, M. Kapidzic, M. O. Muench et al., "The human placenta is a hematopoietic organ during the embryonic and fetal periods of development," *Developmental Biology*, vol. 327, no. 1, pp. 24–33, 2009.

[76] R. Demir, P. Kaufmann, M. Castellucci, T. Erbengi, and A. Kotowski, "Fetal vasculogenesis and angiogenesis in human placental villi1," *Acta Anatomica*, vol. 136, no. 3, pp. 190–203, 1989.

[77] M. Wareing, "Effects of oxygenation and luminal flow on human placenta chorionic plate blood vessel function," *Journal of Obstetrics and Gynaecology Research*, vol. 38, no. 1, pp. 185–191, 2012.

[78] C. J. P. Jones and G. Desoye, "A new possible function for placental pericytes," *Cells Tissues Organs*, vol. 194, no. 1, pp. 76–84, 2011.

[79] N. M. Castrechini, P. Murthi, N. M. Gude et al., "Mesenchymal stem cells in human placental chorionic villi reside in a vascular Niche," *Placenta*, vol. 31, no. 3, pp. 203–212, 2010.

[80] C. L. Maier, B. R. Shepherd, T. Yi, and J. S. Pober, "Explant outgrowth, propagation and characterization of human pericytes," *Microcirculation*, vol. 17, no. 5, pp. 367–380, 2010.

[81] B. Péault, M. Rudnicki, Y. Torrente et al., "Stem and progenitor cells in skeletal muscle development, maintenance, and therapy," *Molecular Therapy*, vol. 15, no. 5, pp. 867–877, 2007.

[82] B. M. Deasy, Y. Li, and J. Huard, "Tissue engineering with muscle-derived stem cells," *Current Opinion in Biotechnology*, vol. 15, no. 5, pp. 419–423, 2004.

[83] M. Sampaolesi, S. Blot, G. D'Antona et al., "Mesoangioblast stem cells ameliorate muscle function in dystrophic dogs," *Nature*, vol. 444, no. 7119, pp. 574–579, 2006.

[84] B. Cao, B. Zheng, R. J. Jankowski et al., "Muscle stem cells differentiate into haematopoietic lineages but retain myogenic potential," *Nature Cell Biology*, vol. 5, no. 7, pp. 640–646, 2003.

[85] H. Oshima, T. R. Payne, K. L. Urish et al., "Differential myocardial infarct repair with muscle stem cells compared to myoblasts," *Molecular Therapy*, vol. 12, no. 6, pp. 1130–1141, 2005.

[86] A. Uezumi, S.-I. Fukada, N. Yamamoto, S. Takeda, and K. Tsuchida, "Mesenchymal progenitors distinct from satellite cells contribute to ectopic fat cell formation in skeletal muscle," *Nature Cell Biology*, vol. 12, no. 2, pp. 143–152, 2010.

[87] M. P. Pusztaszeri, W. Seelentag, and F. T. Bosman, "Immunohistochemical expression of endothelial markers CD31, CD34, von Willebrand factor, and Fli-1 in normal human tissues," *Journal of Histochemistry and Cytochemistry*, vol. 54, no. 4, pp. 385–395, 2006.

[88] A. W. James, J. N. Zara, M. Corselli et al., "An abundant perivascular source of stem cells for bone tissue engineering," *Stem Cells Translational Medicine*, vol. 1, no. 9, pp. 673–684, 2012.

[89] A. W. James, J. N. Zara, X. Zhang et al., "Perivascular stem cells: a prospectively purified mesenchymal stem cell population for bone tissue engineering," *Stem Cells Translational Medicine*, vol. 1, no. 6, pp. 510–519, 2012.

[90] E. K. Waller, J. Olweus, F. Lund-Johansen et al., "The "common stem cell" hypothesis reevaluated: human fetal bone marrow contains separate populations of hematopoietic and stromal progenitors," *Blood*, vol. 85, no. 9, pp. 2422–2435, 1995.

[91] E. K. Waller, S. Huang, and L. Terstappen, "Changes in the growth properties of CD34+, CD38– bone marrow progenitors during human fetal development," *Blood*, vol. 86, no. 2, pp. 710–718, 1995.

[92] D. J. Simmons, P. Seitz, L. Kidder et al., "Partial characterization of rat marrow stromal cells," *Calcified Tissue International*, vol. 48, no. 5, pp. 326–334, 1991.

[93] S. Kaiser, B. Hackanson, M. Follo et al., "BM cells giving rise to MSC in culture have a heterogeneous CD34 and CD45 phenotype," *Cytotherapy*, vol. 9, no. 5, pp. 439–450, 2007.

[94] R. A. Kopher, V. R. Penchev, M. S. Islam, K. L. Hill, S. Khosla, and D. S. Kaufman, "Human embryonic stem cell-derived CD34+ cells function as MSC progenitor cells," *Bone*, vol. 47, no. 4, pp. 718–728, 2010.

[95] R. Barbet, I. Peiffer, A. Hatzfeld, P. Charbord, and J. A. Hatzfeld, "Comparison of gene expression in human embryonic stem cells, hESC-derived mesenchymal stem cells and human mesenchymal stem cells," *Stem Cells International*, vol. 2011, Article ID 368192, 9 pages, 2011.

[96] M. A. Vodyanik, J. Yu, X. Zhang et al., "A mesoderm-derived precursor for mesenchymal stem and endothelial cells," *Cell Stem Cell*, vol. 7, no. 6, pp. 718–729, 2010.

[97] A. Dar, H. Domev, O. Ben-Yosef et al., "Multipotent vasculogenic pericytes from human pluripotent stem cells promote recovery of murine ischemic limb," *Circulation*, vol. 125, no. 1, pp. 87–99, 2012.

[98] D. O. Traktuev, S. Merfeld-Clauss, J. Li et al., "A population of multipotent CD34-positive adipose stromal cells share pericyte and mesenchymal surface markers, reside in a periendothelial location, and stabilize endothelial networks," *Circulation Research*, vol. 102, no. 1, pp. 77–85, 2008.

[99] H. Yamanishi, S. Fujiwara, and T. Soma, "Perivascular localization of dermal stem cells in human scalp," *Experimental Dermatology*, vol. 21, no. 1, pp. 78–80, 2012.

[100] L. Zimmerlin, V. S. Donnenberg, and A. D. Donnenberg, "Rare event detection and analysis in flow cytometry: bone marrow mesenchymal stem cells, breast cancer stem/progenitor cells in malignant effusions, and pericytes in disaggregated adipose tissue," *Methods in Molecular Biology*, vol. 699, pp. 251–273, 2011.

[101] L. Zimmerlin, V. S. Donnenberg, J. P. Rubin, and A. D. Donnenberg, "Mesenchymal markers on human adipose stem/progenitor cells," *Cytometry A*, vol. 83, no. 1, pp. 134–140, 2012.

[102] L. Zimmerlin, V. S. Donnenberg, and A. D. Donnenberg, "Pericytes: a universal adult tissue stem cell?" *Cytometry A*, vol. 81, no. 1, pp. 12–14, 2012.

[103] K. Yoshimura, T. Shigeura, D. Matsumoto et al., "Characterization of freshly isolated and cultured cells derived from the fatty and fluid portions of liposuction aspirates," *Journal of Cellular Physiology*, vol. 208, no. 1, pp. 64–76, 2006.

[104] D. T. Covas, R. A. Panepucci, A. M. Fontes et al., "Multipotent mesenchymal stromal cells obtained from diverse human tissues share functional properties and gene-expression profile with CD146+ perivascular cells and fibroblasts," *Experimental Hematology*, vol. 36, no. 5, pp. 642–654, 2008.

[105] A. C. W. Zannettino, S. Paton, A. Arthur et al., "Multipotential human adipose-derived stromal stem cells exhibit a perivascular phenotype in vitro and in vivo," *Journal of Cellular Physiology*, vol. 214, no. 2, pp. 413–421, 2008.

[106] M. Maumus, J.-A. Peyrafitte, R. D'Angelo et al., "Native human adipose stromal cells: localization, morphology and phenotype," *International Journal of Obesity*, vol. 35, no. 9, pp. 1141–1153, 2011.

[107] G. Astori, F. Vignati, S. Bardelli et al., "'In vitro' and multicolor phenotypic characterization of cell subpopulations identified in fresh human adipose tissue stromal vascular fraction and in the derived mesenchymal stem cells," *Journal of Translational Medicine*, vol. 5, article 55, 2007.

[108] A. O. Sahin and M. Buitenhuis, "Molecular mechanisms underlying adhesion and migration of hematopoietic stem cells," *Cell Adhesion and Migration*, vol. 6, no. 1, pp. 39–48, 2012.

[109] A. Augello, T. B. Kurth, and C. de Bari, "Mesenchymal stem cells: a perspective from in vitro cultures to in vivo migration and niches," *European Cells and Materials*, vol. 20, pp. 121–133, 2010.

[110] S. K. Kang, I. S. Shin, M. S. Ko, J. Y. Jo, and J. C. Ra, "Journey of mesenchymal stem cells for homing: atrategies to enhance efficacy and safety of stem cell therapy," *Stem Cells International*, vol. 2012, Article ID 342968, 11 pages, 2012.

[111] A. Armulik, G. Genové, and C. Betsholtz, "Pericytes: developmental, physiological, and pathological perspectives, problems, and promises," *Developmental Cell*, vol. 21, no. 2, pp. 193–215, 2011.

[112] A. Arthur, A. Zannettino, R. Panagopoulos et al., "EphB/ephrin-B interactions mediate human MSC attachment, migration and osteochondral differentiation," *Bone*, vol. 48, no. 3, pp. 533–542, 2011.

[113] S. S. Foo, C. J. Turner, S. Adams et al., "Ephrin-B2 controls cell motility and adhesion during blood-vessel-wall assembly," *Cell*, vol. 124, no. 1, pp. 161–173, 2006.

[114] K. Stark, A. Eckart, S. Haidari et al., "Capillary and arteriolar pericytes attract innate leukocytes exiting through venules and "instruct" them with pattern-recognition and motility programs," *Nature Immunology*, vol. 14, no. 1, pp. 41–51, 2013.

[115] Y. Bordon, "Cell migration: pericytes: route planners," *Nature Reviews Immunology*, vol. 13, no. 1, p. 5, 2013.

[116] M. Hellström, M. Kalén, P. Lindahl, A. Abramsson, and C. Betsholtz, "Role of PDGF-B and PDGFR-β in recruitment of vascular smooth muscle cells and pericytes during embryonic blood vessel formation in the mouse," *Development*, vol. 126, no. 14, pp. 3047–3055, 1999.

[117] M. Enge, M. Bjarnegård, H. Gerhardt et al., "Endothelium-specific platelet-derived growth factor-B ablation mimics diabetic retinopathy," *EMBO Journal*, vol. 21, no. 16, pp. 4307–4316, 2002.

[118] A. Abramsson, P. Lindblom, and C. Betsholtz, "Endothelial and nonendothelial sources of PDGF-B regulate pericyte recruitment and influence vascular pattern formation in tumors," *Journal of Clinical Investigation*, vol. 112, no. 8, pp. 1142–1151, 2003.

[119] S. Ejaz, "Importance of pericytes and mechanisms of pericyte loss during diabetes retinopathy," *Diabetes, Obesity and Metabolism*, vol. 10, no. 1, pp. 53–63, 2008.

[120] K. le Blanc, "Immunomodulatory effects of fetal and adult mesenchymal stem cells," *Cytotherapy*, vol. 5, no. 6, pp. 485–489, 2003.

[121] L. B. Ware and M. A. Matthay, "Keratinocyte and hepatocyte growth factors in the lung: roles in lung development, inflammation, and repair," *The American Journal of Physiology*, vol. 282, no. 5, pp. L924–L940, 2002.

[122] G. F. Curley, M. Hayes, B. Ansari et al., "Mesenchymal stem cells enhance recovery and repair following ventilator-induced lung injury in the rat," *Thorax*, vol. 67, no. 6, pp. 496–501, 2012.

[123] C.-W. Chen, E. Montelatici, M. Crisan et al., "Perivascular multi-lineage progenitor cells in human organs: regenerative units, cytokine sources or both?" *Cytokine and Growth Factor Reviews*, vol. 20, no. 5-6, pp. 429–434, 2009.

[124] M. Takeoka, W. F. Ward, H. Pollack, D. W. Kamp, and R. J. Panos, "KGF facilitates repair of radiation-induced DNA damage in alveolar epithelial cells," *The American Journal of Physiology*, vol. 272, no. 6, pp. L1174–L1180, 1997.

[125] B. M. Strem, K. C. Hicok, M. Zhu et al., "Multipotential differentiation of adipose tissue-derived stem cells," *Keio Journal of Medicine*, vol. 54, no. 3, pp. 132–141, 2005.

[126] D. Matsumoto, K. Sato, K. Gonda et al., "Cell-assisted lipotransfer: supportive use of human adipose-derived cells for soft tissue augmentation with lipoinjection," *Tissue Engineering*, vol. 12, no. 12, pp. 3375–3382, 2006.

[127] P. van Pham, K. H.-T. Bui, D. Q. Ngo, L. T. Khuat, and N. K. Phan, "Transplantation of nonexpanded adipose stromal vascular fraction and platelet-rich plasma for articular cartilage injury treatment in mice model," *Journal of Medical Engineering*, vol. 2013, Article ID 832396, 7 pages, 2013.

[128] L. Cai, B. H. Johnstone, T. G. Cook et al., "IFATS collection: human adipose tissue-derived stem cells induce angiogenesis and nerve sprouting following myocardial infarction, in conjunction with potent preservation of cardiac function," *Stem Cells*, vol. 27, no. 1, pp. 230–237, 2009.

[129] U. Kim, D.-G. Shin, J.-S. Park et al., "Homing of adipose-derived stem cells to radiofrequency catheter ablated canine atrium and differentiation into cardiomyocyte-like cells," *International Journal of Cardiology*, vol. 146, no. 3, pp. 371–378, 2011.

[130] A. Banas, T. Teratani, Y. Yamamoto et al., "IFATS collection: in vivo therapeutic potential of human adipose tissue mesenchymal stem cells after transplantation into mice with liver injury," *Stem Cells*, vol. 26, no. 10, pp. 2705–2712, 2008.

[131] D. H. Kim, C. M. Je, J. Y. Sin, and J. S. Jung, "Effect of partial hepatectomy on in vivo engraftment after intravenous administration of human adipose tissue stromal cells in mouse," *Microsurgery*, vol. 23, no. 5, pp. 424–431, 2003.

[132] Y. M. Kim, Y. S. Choi, J. W. Choi et al., "Effects of systemic transplantation of adipose tissue-derived stem cells on olfactory epithelium regeneration," *Laryngoscope*, vol. 119, no. 5, pp. 993–999, 2009.

[133] W. Xing, D. Zhimei, Z. Liming et al., "IFATS collection: the conditioned media of adipose stromal cells protect against hypoxia-ischemia-induced brain damage in neonatal rats," *Stem Cells*, vol. 27, no. 2, pp. 478–488, 2009.

[134] K.-S. Cho, H.-K. Park, H.-Y. Park et al., "IFATS collection: immunomodulatory effects of adipose tissue-derived stem cells in an allergic rhinitis mouse model," *Stem Cells*, vol. 27, no. 1, pp. 259–265, 2009.

[135] P. Sacerdote, S. Niada, S. Franchi et al., "Systemic administration of human adipose-derived stem cells reverts nociceptive hypersensitivity in an experimental model of neuropathy," *Stem Cells and Development*, vol. 22, no. 8, pp. 1252–1263, 2013.

[136] S. Marconi, G. Castiglione, E. Turano et al., "Human adipose-derived mesenchymal stem cells systemically injected promote peripheral nerve regeneration in the mouse model of sciatic crush," *Tissue Engineering A*, vol. 18, no. 11-12, pp. 1264–1272, 2012.

[137] B. Levi, A. W. James, E. R. Nelson et al., "Studies in adipose-derived stromal cells: migration and participation in repair of cranial injury after systemic injection," *Plastic and Reconstructive Surgery*, vol. 127, no. 3, pp. 1130–1140, 2011.

[138] N. M. Vieira, M. Valadares, E. Zucconi et al., "Human adipose-derived mesenchymal stromal cells injected systemically into GRMD dogs without immunosuppression are able to reach the host muscle and express human dystrophin," *Cell Transplantation*, vol. 21, no. 7, pp. 1407–1417, 2012.

[139] N. M. Vieira, C. R. Bueno Jr., V. Brandalise et al., "SJL dystrophic mice express a significant amount of human muscle proteins following systemic delivery of human adipose-derived stromal cells without immunosuppression," *Stem Cells*, vol. 26, no. 9, pp. 2391–2398, 2008.

[140] S. J. Baek, S. K. Kang, and J. C. Ra, "In vitro migration capacity of human adipose tissue-derived mesenchymal stem cells reflects their expression of receptors for chemokines and growth factors," *Experimental and Molecular Medicine*, vol. 43, no. 10, pp. 596–603, 2011.

[141] C. Garrovo, N. Bergamin, D. Bates et al., "In vivo tracking of murine adipose tissue-derived multipotent adult stem cells and ex vivo cross-validation," *International Journal of Molecular Imaging*, vol. 2013, Article ID 426961, 13 pages, 2013.

[142] N. Kakudo, S. Kushida, K. Suzuki et al., "Effects of transforming growth factor-beta1 on cell motility, collagen gel contraction, myofibroblastic differentiation, and extracellular matrix expression of human adipose-derived stem cell," *Human Cell*, vol. 25, no. 4, pp. 87–95, 2012.

[143] P. R. Baraniak and T. C. McDevitt, "Stem cell paracrine actions and tissue regeneration," *Regenerative Medicine*, vol. 5, no. 1, pp. 121–143, 2010.

[144] L. Casteilla, V. Planat-Benard, P. Laharrague, and B. Cousin, "Adipose-derived stromal cells: their identity and uses in clinical trials, an update," *World Journal of Stem Cells*, vol. 3, no. 4, pp. 25–33, 2011.

[145] S. H. Lee, S. Y. Jin, J. S. Song, K. K. Seo, and K. H. Cho, "Paracrine effects of adipose-derived stem cells on keratinocytes and

dermal fibroblasts," *Annals of Dermatology*, vol. 24, no. 2, pp. 136–143, 2012.

[146] L. Hu, J. Zhao, J. Liu, N. Gong, and L. Chen, "Effects of adipose stem cell-conditioned medium on the migration of vascular endothelial cells, fibroblasts and keratinocytes," *Experimental and Therapeutic Medicine*, vol. 5, no. 3, pp. 701–706, 2013.

[147] S. S. Collawn, N. Sanjib Banerjee, J. de la Torre, L. Vasconez, and L. T. Chow, "Adipose-derived stromal cells accelerate wound healing in an organotypic raft culture model," *Annals of Plastic Surgery*, vol. 68, no. 5, pp. 501–504, 2012.

[148] K. M. Moon, Y. H. Park, J. S. Lee et al., "The effect of secretory factors of adipose-derived stem cells on human keratinocytes," *International Journal of Molecular Sciences*, vol. 13, no. 1, pp. 1239–1257, 2012.

[149] X. Fu, L. Fang, H. Li, X. Li, B. Cheng, and Z. Sheng, "Adipose tissue extract enhances skin wound healing," *Wound Repair and Regeneration*, vol. 15, no. 4, pp. 540–548, 2007.

[150] A. E. Karnoub, A. B. Dash, A. P. Vo et al., "Mesenchymal stem cells within tumour stroma promote breast cancer metastasis," *Nature*, vol. 449, no. 7162, pp. 557–563, 2007.

[151] A. Nakamizo, F. Marini, T. Amano et al., "Human bone marrow-derived mesenchymal stem cells in the treatment of gliomas," *Cancer Research*, vol. 65, pp. 3307–3318, 2005.

[152] C. Pendleton, Q. Li, D. A. Chesler, K. Yuan, H. Guerrero-Cazares, and A. Quinones-Hinojosa, "Mesenchymal stem cells derived from adipose tissue vs bone marrow: in vitro comparison of their tropism towards gliomas," *PLoS ONE*, vol. 8, no. 3, Article ID e58198, 2013.

[153] M. Lamfers, S. Idema, F. van Milligen et al., "Homing properties of adipose-derived stem cells to intracerebral glioma and the effects of adenovirus infection," *Cancer Letters*, vol. 274, no. 1, pp. 78–87, 2009.

[154] L. Kucerova, V. Altanerova, M. Matuskova, S. Tyciakova, and C. Altaner, "Adipose tissue-derived human mesenchymal stem cells mediated prodrug cancer gene therapy," *Cancer Research*, vol. 67, no. 13, pp. 6304–6313, 2007.

[155] I. T. Cavarretta, V. Altanerova, M. Matuskova, L. Kucerova, Z. Culig, and C. Altaner, "Adipose tissue-derived mesenchymal stem cells expressing prodrug-converting enzyme inhibit human prostate tumor growth," *Molecular Therapy*, vol. 18, no. 1, pp. 223–231, 2010.

[156] F. L. Muehlberg, Y.-H. Song, A. Krohn et al., "Tissue-resident stem cells promote breast cancer growth and metastasis," *Carcinogenesis*, vol. 30, no. 4, pp. 589–597, 2009.

[157] S. Pinilla, E. Alt, F. J. Abdul Khalek et al., "Tissue resident stem cells produce CCL5 under the influence of cancer cells and thereby promote breast cancer cell invasion," *Cancer Letters*, vol. 284, no. 1, pp. 80–85, 2009.

[158] B. Sun, K.-H. Roh, J.-R. Park et al., "Therapeutic potential of mesenchymal stromal cells in a mouse breast cancer metastasis model," *Cytotherapy*, vol. 11, no. 3, pp. 289–298, 2009.

[159] B. Cousin, E. Ravet, S. Poglio et al., "Adult stromal cells derived from human adipose tissue provoke pancreatic cancer cell death both in vitro and in vivo," *PLoS ONE*, vol. 4, no. 7, Article ID e6278, 2009.

[160] S. Tottey, M. Corselli, E. M. Jeffries, R. Londono, B. Peault, and S. F. Badylak, "Extracellular matrix degradation products and low-oxygen conditions enhance the regenerative potential of perivascular stem cells," *Tissue Engineering A*, vol. 17, no. 1-2, pp. 37–44, 2011.

[161] B. Annabi, Y.-T. Lee, S. Turcotte et al., "Hypoxia promotes murine bone-marrow-derived stromal cell migration and tube formation," *Stem Cells*, vol. 21, no. 3, pp. 337–347, 2003.

[162] R. K. Assoian and M. A. Schwartz, "Coordinate signaling by integrins and receptor tyrosine kinases in the regulation of G1 phase cell-cycle progression," *Current Opinion in Genetics and Development*, vol. 11, no. 1, pp. 48–53, 2001.

[163] I. Hunger-Glaser, R. S. Fan, E. Perez-Salazar, and E. Rozengurt, "PDGF and FGF induce focal adhesion kinase (FAK) phosphorylation at Ser-910: dissociation from Tyr-397 phosphorylation and requirement for ERK activation," *Journal of Cellular Physiology*, vol. 200, no. 2, pp. 213–222, 2004.

[164] C. Huang, K. Jacobson, and M. D. Schaller, "MAP kinases and cell migration," *Journal of Cell Science*, vol. 117, no. 20, pp. 4619–4628, 2004.

[165] I. Rosová, M. Dao, B. Capoccia, D. Link, and J. A. Nolta, "Hypoxic preconditioning results in increased motility and improved therapeutic potential of human mesenchymal stem cells," *Stem Cells*, vol. 26, no. 8, pp. 2173–2182, 2008.

[166] S. Neuss, E. Becher, M. Wöltje, L. Tietze, and W. Jahnen-Dechent, "Functional expression of HGF and HGF receptor/c-met in adult human mesenchymal stem cells suggests a role in cell mobilization, tissue repair, and wound healing," *Stem Cells*, vol. 22, no. 3, pp. 405–414, 2004.

[167] H. Liu, W. Xue, G. Ge et al., "Hypoxic preconditioning advances CXCR4 and CXCR7 expression by activating HIF-1α in MSCs," *Biochemical and Biophysical Research Communications*, vol. 401, no. 4, pp. 509–515, 2010.

[168] C. W. Chen, M. Okada, J. D. Proto, X. Gao et al., "Human pericytes for ischemic heart repair," *Stem Cells*, vol. 31, no. 2, pp. 305–316, 2013.

[169] R. Katare, F. Riu, K. Mitchell et al., "Transplantation of human pericyte progenitor cells improves the repair of infarcted heart through activation of an angiogenic program involving micro-RNA-132," *Circulation Research*, vol. 109, no. 8, pp. 894–906, 2011.

[170] A. Dellavalle, G. Maroli, D. Covarello et al., "Pericytes resident in postnatal skeletal muscle differentiate into muscle fibres and generate satellite cells," *Nature Communications*, vol. 2, no. 1, article 499, 2011.

[171] M. Pierro, L. Ionescu, T. Montemurro, A. Vadivel et al., "Short-term, long-term and paracrine effect of human umbilical cord-derived stem cells in lung injury prevention and repair in experimental bronchopulmonary dysplasia," *Thorax*, vol. 68, no. 5, pp. 475–484, 2013.

[172] M. Corselli, C. J. Chin, C. Parekh, A. Sahaghian et al., "Perivascular support of human hematopoietic stem/progenitor cells," *Blood*, vol. 121, no. 15, pp. 2891–2901, 2013.

[173] X. Zhang, B. Péault, W. Chen et al., "The nell-1 growth factor stimulates bone formation by purified human perivascular cells," *Tissue Engineering A*, vol. 17, no. 19-20, pp. 2497–2509, 2011.

[174] E. Chavakis, C. Urbich, and S. Dimmeler, "Homing and engraftment of progenitor cells: a prerequisite for cell therapy," *Journal of Molecular and Cellular Cardiology*, vol. 45, no. 4, pp. 514–522, 2008.

[175] R. H. Lee, A. A. Pulin, M. J. Seo et al., "Intravenous hMSCs improve myocardial infarction in mice because cells embolized in lung are activated to secrete the anti-inflammatory protein TSG-6," *Cell Stem Cell*, vol. 5, no. 1, pp. 54–63, 2009.

[176] A. Askarinam, A. W. James, J. N. Zara et al., "Human perivascular stem cells show enhanced osteogenesis and vasculogenesis

with nel-like molecule I protein," *Tissue Engineering A*, vol. 19, no. 11-12, pp. 1386–1397, 2013.

[177] X. Zhang, K. Ting, C. M. Bessette et al., "Nell-1, a key functional mediator of Runx2, partially rescues calvarial defects in Runx2+/– mice," *Journal of Bone and Mineral Research*, vol. 26, no. 4, pp. 777–791, 2011.

[178] T. Kitaori, H. Ito, E. M. Schwarz et al., "Stromal cell-derived factor 1/CXCR4 signaling is critical for the recruitment of mesenchymal stem cells to the fracture site during skeletal repair in a mouse model," *Arthritis and Rheumatism*, vol. 60, no. 3, pp. 813–823, 2009.

[179] N. Song, Y. Huang, H. Shi et al., "Overexpression of platelet-derived growth factor-BB increases tumor pericyte content via stromal-derived factor-1α/CXCR4 axis," *Cancer Research*, vol. 69, no. 15, pp. 6057–6064, 2009.

[180] E. Chavakis, M. Koyanagi, and S. Dimmeler, "Enhancing the outcome of cell therapy for cardiac repair: progress from bench to bedside and back," *Circulation*, vol. 121, no. 2, pp. 325–335, 2010.

[181] A. N. Stratman, A. E. Schwindt, K. M. Malotte, and G. E. Davis, "Endothelial-derived PDGF-BB and HB-EGF coordinately regulate pericyte recruitment during vasculogenic tube assembly and stabilization," *Blood*, vol. 116, no. 22, pp. 4720–4730, 2010.

[182] A. N. Stratman, K. M. Malotte, R. D. Mahan, M. J. Davis, and G. E. Davis, "Pericyte recruitment during vasculogenic tube assembly stimulates endothelial basement membrane matrix formation," *Blood*, vol. 114, no. 24, pp. 5091–5101, 2009.

[183] H. Gerhardt and C. Betsholtz, "Endothelial-pericyte interactions in angiogenesis," *Cell and Tissue Research*, vol. 314, no. 1, pp. 15–23, 2003.

[184] L. Díaz-Flores, R. Gutiérrez, J. F. Madrid et al., "Pericytes. Morphofunction, interactions and pathology in a quiescent and activated mesenchymal cell niche," *Histology and Histopathology*, vol. 24, no. 7, pp. 909–969, 2009.

[185] D. E. Sims, "The pericyte-A review," *Tissue and Cell*, vol. 18, no. 2, pp. 153–174, 1986.

[186] K. Gaengel, G. Genové, A. Armulik, and C. Betsholtz, "Endothelial-mural cell signaling in vascular development and angiogenesis," *Arteriosclerosis, Thrombosis, and Vascular Biology*, vol. 29, no. 5, pp. 630–638, 2009.

[187] G. Rajashekhar, D. O. Traktuev, W. C. Roell, B. H. Johnstone, S. Merfeld-Clauss, B. van Natta et al., "IFATS collection: adipose stromal cell differentiation is reduced by endothelial cell contact and paracrine communication: role of canonical Wnt signaling," *Stem Cells*, vol. 26, no. 10, pp. 2674–2681, 2008.

[188] F. A. Saleh, M. Whyte, P. Ashton, and P. G. Genever, "Regulation of mesenchymal stem cell activity by endothelial cells," *Stem Cells and Development*, vol. 20, no. 3, pp. 391–403, 2011.

[189] F. A. Saleh, M. Whyte, and P. G. Genever, "Effects of endothelial cells on human mesenchymal stem cell activity in a three-dimensional in vitro model," *Journal of European Cells and Materials*, vol. 22, pp. 242–257, 2011.

[190] Y. Xue, Z. Xing, S. Hellem, K. Arvidson, and K. Mustafa, "Endothelial cells influence the osteogenic potential of bone marrow stromal cells," *BioMedical Engineering Online*, vol. 8, article 34, 2009.

[191] D. Kaigler, P. H. Krebsbach, E. R. West, K. Horger, Y. C. Huang, and D. J. Mooney, "Endothelial cell modulation of bone marrow stromal cell osteogenic potential," *FASEB Journal*, vol. 19, no. 6, pp. 665–667, 2005.

[192] H. Li, R. Daculsi, M. Grellier, R. Bareille, C. Bourget, and J. Amedee, "Role of neural-cadherin in early osteoblastic differentiation of human bone marrow stromal cells cocultured with human umbilical vein endothelial cells," *The American Journal of Physiology*, vol. 299, no. 2, pp. 422–430, 2010.

[193] M. Grellier, N. Ferreira-Tojais, C. Bourget, R. Bareille, F. Guillemot, and J. Amedee, "Role of vascular endothelial growth factor in the communication between human osteoprogenitors and endothelial cells," *Journal of Cellular Biochemistry*, vol. 106, no. 3, pp. 390–398, 2009.

[194] T. Meury, S. Verrier, and M. Alini, "Human endothelial cells inhibit BMSC differentiation into mature osteoblasts in vitro by interfering with osterix expression," *Journal of Cellular Biochemistry*, vol. 98, no. 4, pp. 992–1006, 2006.

[195] F. Villars, B. Guillotin, T. Amedee, S. Dutoya, L. Bordenave, R. Bareille et al., "Effect of HUVEC on human osteoprogenitor cell differentiation needs heterotypic gap junction communication," *The American Journal of Physiology*, vol. 282, no. 4, pp. 775–785, 2002.

[196] F. Villars, L. Bordenave, R. Bareille, and J. Amedee, "Effect of human endothelial cells on human bone marrow stromal cell phenotype: role of VEGF?" *Journal of Cellular Biochemistry*, vol. 79, no. 4, pp. 672–685, 2000.

[197] B. Guillotin, C. Bourget, M. Remy-Zolgadri, R. Bareille, P. Fernandez, V. Conrad et al., "Human primary endothelial cells stimulate human osteoprogenitor cell differentiation," *Cellular Physiology and Biochemistry*, vol. 14, no. 4–6, pp. 325–332, 2004.

[198] U. Ozerdem and W. B. Stallcup, "Early contribution of pericytes to angiogenic sprouting and tube formation," *Angiogenesis*, vol. 6, no. 3, pp. 241–249, 2003.

[199] U. Ozerdem, K. A. Grako, K. Dahlin-Huppe, E. Monosov, and W. B. Stallcup, "NG2 proteoglycan is expressed exclusively by mural cells during vascular morphogenesis," *Developmental Dynamics*, vol. 222, no. 2, pp. 218–227, 2001.

[200] L. P. Reynolds, A. T. Grazul-Bilska, and D. A. Redmer, "Angiogenesis in the corpus luteum," *Endocrine*, vol. 12, no. 1, pp. 1–9, 2000.

[201] M. Enge, M. Bjarnegård, H. Gerhardt et al., "Endothelium-specific platelet-derived growth factor-B ablation mimics diabetic retinopathy," *EMBO Journal*, vol. 21, no. 16, pp. 4307–4316, 2002.

[202] K. K. Hirschi, S. A. Rohovsky, L. H. Beck, S. R. Smith, and P. A. D'Amore, "Endothelial cells modulate the proliferation of mural cell precursors via platelet-derived growth factor-BB and heterotypic cell contact," *Circulation Research*, vol. 84, no. 3, pp. 298–305, 1999.

[203] A. Blocki, Y. Wang, M. Koch et al., "Not all MSCs can act as pericytes: functional in vitro assays to distinguish pericytes from other mesenchymal stem cells in angiogenesis," *Stem Cells and Development*, vol. 22, no. 17, 2013.

[204] M. Corselli, C.-W. Chen, M. Crisan, L. Lazzari, and B. Péault, "Perivascular ancestors of adult multipotent stem cells," *Arteriosclerosis, Thrombosis, and Vascular Biology*, vol. 30, no. 6, pp. 1104–1109, 2010.

[205] A. Ehninger and A. Trumpp, "The bone marrow stem cell niche grows up: mesenchymal stem cells and macrophages move in," *Journal of Experimental Medicine*, vol. 208, no. 3, pp. 421–428, 2011.

[206] S. Ergün, D. Tilki, and D. Klein, "Vascular wall as a reservoir for different types of stem and progenitor cells," *Antioxidants and Redox Signaling*, vol. 15, no. 4, pp. 981–995, 2011.

[207] A. I. Caplan, "All MSCs are pericytes?" *Cell Stem Cell*, vol. 3, no. 3, pp. 229–230, 2008.

[208] A. M. Müller, A. Mehrkens, D. J. Schäfer et al., "Towards an intraoperative engineering of osteogenic and vasculogenic grafts from the stromal vascular fraction of human adipose tissue," *European Cells and Materials*, vol. 19, pp. 127–135, 2010.

[209] V. Marthiens, I. Kazanis, L. Moss, K. Long, and C. Ffrench-Constant, "Adhesion molecules in the stem cell niche: more than just staying in shape?" *Journal of Cell Science*, vol. 123, no. 10, pp. 1613–1622, 2010.

[210] J. P. Kirton, F. L. Wilkinson, A. E. Canfield, and M. Y. Alexander, "Dexamethasone downregulates calcification-inhibitor molecules and accelerates osteogenic differentiation of vascular pericytes: implications for vascular calcification," *Circulation Research*, vol. 98, no. 10, pp. 1264–1272, 2006.

[211] S. Mathews, R. Bhonde, P. K. Gupta, and S. Totey, "Extracellular matrix protein mediated regulation of the osteoblast differentiation of bone marrow derived human mesenchymal stem cells," *Differentiation*, vol. 84, no. 2, pp. 185–192, 2012.

[212] S. H. Ranganath, O. Levy, M. S. Inamdar, and J. M. Karp, "Harnessing the mesenchymal stem cell secretome for the treatment of cardiovascular disease," *Cell Stem Cell*, vol. 10, no. 3, pp. 244–258, 2012.

[213] I. Takada, A. P. Kouzmenko, and S. Kato, "PPAR-γ signaling crosstalk in mesenchymal stem cells," *PPAR Research*, vol. 2010, Article ID 341671, 6 pages, 2010.

The FASEB Journal article fj.13-233460. Published online May 23, 2013.

Appendix 12

RhoA mediates defective stem cell function and heterotopic ossification in dystrophic muscle of mice

Xiaodong Mu, Arvydas Usas, Ying Tang, Aiping Lu, Bing Wang, Kurt Weiss, and Johnny Huard[1]

Stem Cell Research Center, Department of Orthopaedic Surgery, University of Pittsburgh, Pittsburgh, Pennsylvania, USA

ABSTRACT **Heterotopic ossification (HO) and fatty infiltration (FI) often occur in diseased skeletal muscle and have been previously described in various animal models of Duchenne muscular dystrophy (DMD); however, the pathological mechanisms remain largely unknown. Dystrophin-deficient *mdx* mice and dystrophin/utrophin double-knockout (dKO) mice are mouse models of DMD; however, *mdx* mice display a strong muscle regeneration capacity, while dKO mice exhibit a much more severe phenotype, which is similar to patients with DMD. Our results revealed that more extensive HO, but not FI, occurred in the skeletal muscle of dKO mice versus *mdx* mice, and RhoA activation specifically occurred at the sites of HO. Moreover, the gene expression of RhoA, BMPs, and several inflammatory factors were significantly up-regulated in muscle stem cells isolated from dKO mice; while inactivation of RhoA in the cells with RhoA/ROCK inhibitor Y-27632 led to reduced osteogenic potential and improved myogenic potential. Finally, inactivation of RhoA signaling in the dKO mice with Y-27632 improved muscle regeneration and reduced the expression of BMPs, inflammation, HO, and intramyocellular lipid accumulation in both skeletal and cardiac muscle. Our results revealed that RhoA represents a major molecular switch in the regulation of HO and muscle regeneration in dystrophic skeletal muscle of mice.—Mu, X., Usas, A., Tang, Y., Lu, A., Wang, B., Weiss, K., Huard, J. RhoA mediates defective stem cell function and heterotopic ossification in dystrophic muscle of mice. *FASEB J.* 27, 000–000 (2013). www.fasebj.org**

Key Words: ROCK · mdx · utrophin$^{-/-}$ *· intramyocellular lipid accumulation*

HETEROTOPIC OSSIFICATION (HO) and/or fatty infiltration (FI) are two distinct histological processes that often occur in diseased muscle tissues. HO refers to the formation of bone in the soft tissues of the body and can occur as a result of trauma, surgery, neurological injury, or genetic abnormalities (1). FI has been reported to be associated with aging, inactivity, obesity, and various diseases, such as diabetes, and results in the accumulation of fat cells outside the typical fat stores (2–3). FI located within skeletal muscle is often the result of disordered lipid metabolism (3); however, abnormal lipid metabolism can also cause another type of abnormal lipid deposition in skeletal muscle, known as intramyocellular lipid accumulation (IMCL; refs. 4–5). Notably, IMCL in cardiac muscle, (intramyocardial lipid accumulation) can be caused by lipid overload, which has the potential to lead to lipotoxicity and progressive cardiac dysfunction (6–9). However, the pathological mechanisms regulating these distinct processes in diseased muscles remain largely unknown.

Duchenne muscular dystrophy (DMD) features progressive muscle degeneration and has no cure yet. Obesity occurs in >50% of patients wtih DMD after 14 yr of age, and a reduction in myocardial fatty acid metabolism has been observed in ~50% of patients wtih DMD (10, 11). FI is commonly observed in the skeletal muscles of patients wtih DMD, and it is one of the main factors responsible for patients' decline in muscular strength (12). Lipid mapping analysis of the hearts and skeletal muscles of patients wtih DMD revealed IMCL within the most damaged areas of the dystrophic muscles (11, 13); however, there are very few studies on the mechanisms and prevention of IMCL in patients wtih DMD. Although less documented in human patients wtih DMD, the presence of HO has been reported in the skeletal muscles of various animal models of human DMD, including *mdx* mice and golden retriever muscular dystrophy (GRMD) dogs

Abbreviations: BMP, bone morphogenetic protein; dKO, dystrophin/utrophin double knockout; DMD, Duchenne muscular dystrophy; FBS, fetal bovine serum; FI, fatty infiltration; GM, gastrocnemius muscle; GRMD, golden retriever muscular dystrophy; HO, heterotopic ossification; IMCL, intramyocellular lipid accumulation; MDSC, muscle-derived stem cell; *mdx*, dystrophin-deficient; micro-CT, micro-computed tomography; MSC, mesenchymal stem cell; NF-κB, nuclear factor-κB; PPARγ, peroxisome proliferator-activated receptor γ

[1] Correspondence: Stem Cell Research Center, Department of Orthopaedic Surgery, University of Pittsburgh, Bridgeside Point 2, Ste. 206, 450 Technology Dr., Pittsburgh, PA 15219, USA. E-mail: jhuard@pitt.edu

doi: 10.1096/fj.13-233460

This article includes supplemental data. Please visit *http://www.fasebj.org* to obtain this information.

(14–16). *In vitro* studies with muscle stem cells showed that bone morphogenetic protein (BMPs) or adipogenic media can promote the differentiation of muscle stem cells into osteogenic and adipogenic cells, respectively (17), suggesting that muscle stem cells may represent a cell source of HO and/or FI in skeletal muscle.

The experiments described in this article were conducted using two animal models of human DMD, dystrophin-deficient (*mdx*) mice and dystrophin/utrophin double-knockout (dKO) mice (14, 18–20). Compared with *mdx* mice, which actually feature potent muscle regeneration capacity, the phenotype of dKO mice is more severe and more closely resembles the phenotype seen in patients wtih DMD (19–20). For example, dKO mice feature a much shorter life span (~8 wk compared with ~2 yr), more necrosis and fibrosis in their skeletal muscles, scoliosis/kyphosis of the spine, and severe cardiac involvement and eventual cardiac failure (14, 19, 20). The occurrence of FI and HO in the skeletal muscles of *mdx* mice has been previously described (15), and more extensive HO in dKO mice has also been recently reported by our group (21). IMCL, on the other hand, has not been studied in either *mdx* or dKO mice or in any other DMD animal models. It is also clear that the knowledge about the molecular regulation of HO, fatty infiltration, and IMCL in dystrophic muscle remains limited.

Inflammation is directly involved in the dystrophic process and represents an important therapeutic target to treat DMD. For example, corticosteroids are capable of repressing systematic inflammation and are the only known effective drugs that can provide relief of the symptoms of DMD (22). Inflammation has been identified as a main contributor of HO (23); hence, the administrations of various anti-inflammatory medications have been used to prevent HO (24–25). For example, Cox-2 inhibitors were found to be effective at preventing HO after total hip arthroplasty (THA) and following spinal cord injury (26–27). Although inflammation and FI often occur simultaneously in diseased or injured skeletal muscles, inflammation has not been directly linked to FI (28–29). On the other hand, it has been well established, in studies of diabetes and obesity, that there is a close association between the occurrence of IMCL and chronic systematic inflammation during the progression of cardiac disease (30, 31). Similarly, lipid peroxidation has been shown to activate nuclear factor-κB (NF-κB), and consequently, has contributed to the histopathological cascade observed in *mdx* muscles (32). Finally, inflammatory cytokines have been shown to inhibit myogenic differentiation through the activation of NF-κB (33–34), and the activation of NF-κB signaling in skeletal muscle has been correlated with muscular dystrophies and inflammatory myopathies (34, 35).

In the current study, we examined the role that RhoA signaling pathway plays in regulating HO, FI, and IMCL in these models of DMD (dKO and *mdx* mice), due to the fact that RhoA signaling has been shown to play an important role in regulating osteogenesis, adipogenesis, myogenesis, and inflammation. RhoA is a small G protein in the Rho family that regulates cell morphology and migration by reorganizing the actin cytoskeleton in response to extracellular signaling (36). The RhoA signaling pathway is involved in the commitment of mesenchymal stem cells (MSCs) toward their osteogenic or adipogenic differentiation (37). RhoA signaling activation in MSCs *in vitro* induces osteogenesis potential and inhibits adipogenic potential of the cells; however, the application of Y-27632, a specific inhibitor of RhoA/Rho kinase (ROCK), reverses this process (37–39). RhoA also mediates BMP-induced signaling in MSCs and promotes osteoblastic cell survival (40, 41). Moreover, the inhibition of RhoA with Y-27632 was found to induce the adipogenic differentiation of muscle-derived cells *in vitro*, and resulted in the manifestation of FI in skeletal muscle (42). RhoA is also activated by Wnt5a, which results in the induction of osteogenic differentiation of human adipose stem cells (ASCs) and the repression of adipogenic differentiation (43). RhoA's role in the inflammatory process has been previously described, where TNF-α induces the activation of RhoA signaling in smooth muscle cells (44), RhoA regulates Cox-2 activity in fibroblasts (45), and RhoA induces the expression of inflammatory cytokines in adipocytes (46). Moreover, involvement of RhoA in mediating myocardial and pulmonary fibrosis has been described (47–48). In addition, previous studies have indicated that the sustained activation of the RhoA pathway can block the differentiation of muscle cells by inhibiting myoblast fusion (49–51).

Because of RhoA's potential involvement in the regulation of osteogenesis, adipogenesis, and myogenesis of stem cells and inflammation, we hypothesized that RhoA may act as a critical regulator of these processes in dystrophic muscle. In the current study, we investigated the status of HO, FI, IMCL, and muscle regeneration in the skeletal muscle of *mdx* and dKO mice, as well as the potential role that RhoA signaling plays in regulating these processes.

MATERIALS AND METHODS

Animals

Wild-type (C57BL/10J) mice were obtained from the Jackson Laboratory (Bar Harbor, ME, USA). The *mdx* and dKO (*mdx*; *utrn*$^{-/-}$) mice were derived from our in-house colony. Mice were housed in groups of 4 on a 12:12-h light-dark cycle at 20–23°C. At least 6 mice were used in each experimental sample group. All procedures were approved by the Institutional Animal Care and Use Committee (IACUC) at the University of Pittsburgh.

Stem cell isolation from skeletal muscle

Muscle-derived stem cells (MDSCs) were isolated from the skeletal muscle of dKO and *mdx* mice (4 wk old) *via* a modified preplate technique (52). Mice were sacrificed in a carbon dioxide chamber, as described in the IACUC proto-

col. Cells were cultured in proliferation medium [DMEM supplemented with 20% fetal bovine serum (FBS), 1% penicillin-streptomycin antibiotics, and 0.5% chicken embryo extract (CEE)].

Micro-computed tomography (micro-CT)

To observe HO in the soft tissues of *mdx* and dKO mice, 8-wk-old mice were anesthetized with 3% isoflurane in O_2 gas (1.5 L/min), and the lower extremities, including the pelvis, were scanned using the Viva CT 40 (Scanco, Wangen-Brüttisellen, Switzerland) with the following settings: energy, 70 kVp; intensity, 114 μA; integration time, 200 ms; isotropic voxel size, 35 μm; threshold, 163.

In vitro RhoA inactivation with Y-27632 and multipotent differentiation assays

dKO MDSCs cultured *in vitro* were treated with the RhoA/Rock inhibitor Y-27632 (10 μM; EMD Millipore, Billerica, MA, USA) in proliferation medium for 2 d, before being plated in 12-well flasks and set up for osteogenesis, adipogenesis, or myogenesis assays. The osteogenesis assay was conducted with osteogenic medium (DMEM supplemented with 110 μg/ml sodium pyruvate, 584 μg/ml L-glutamine, 10% FBS, 1% penicillin/streptomycin, 10^{-7} μM dexamethasone, 50 μg/ml ascorbic-acid-2-phosphate, and 10^{-2} μM β-glycerophosphate), supplemented with BMP2 (50 ng/ml for 7 d). Calcium deposition was assessed with alizarin red stain. Adipogenesis assay was conducted with adipogenic induction medium (Lonza, Basel, Switzerland) for 10 d and tested for lipid droplets with Oil red O stain (Sigma, St. Louis, MO, USA). The myogenesis assay was conducted by switching the proliferation medium into myogenic differentiation medium (DMEM containing 2% horse serum). Myotube formation was tracked during the following 4 d. 10 μM of Y-27632 was continuously present in the differentiation medium.

mRNA analysis with reverse transcriptase-PCR

Total RNA was obtained from MDSCs or the skeletal muscles of mice using a RNeasy Mini Kit (Qiagen, Valencia, CA, USA), according to the manufacturer's instructions. Reverse transcription was performed using the iScript cDNA synthesis kit (Bio-Rad, Hercules, CA, USA). PCR reactions were performed using an iCycler Thermal Cycler (Bio-Rad). The cycling parameters used for all primers were as follows: 95°C for 10 min; PCR, 40 cycles of 30 s at 95°C for denaturation, 1 min at 54°C for annealing, and 30 s at 72°C for extension. Products were separated by size, and they were visualized on 1.5% agarose gels stained with ethidium bromide. All data were normalized to the expression of *GAPDH*. Genes and primers used in the study included *GAPDH*: TCCATGACAACTTTGGCATTG (sense) and TCACGCCACAGCTTTCCA (antisense); *RhoA*: GTAGAGTTGGCTTTATGGGACAC (sense), and TGGAGTCCATTTTTCTGGGATG (antisense); BMP2: TCTTCCGGGAACAGATACAGG (sense), and TGGTGTCCAATAGTCTGGTCA (antisense); *BMP4*: ATTCCTGGTAACCGAATGCTG (sense), and CCGGTCTCAGGTATCAAACTAGC (antisense); *TNF-α*: GATTATGGCTCAGGGTCCAA (sense), and CTCCCTTTGCAGAACTCAGG (antisense); *IL6*: GGAAATCGTGGAAATGAG (sense), and GCTTAGGCATAACGCACT (antisense); *Klotho*: CCCAAACCATCTATGAAAC (sense), and CTACCGTATTCTATGCCTTC (antisense); and peroxisome proliferator-activated receptor γ (*PPARγ*): CCACCAACTTCGGAATCAGCT (sense) and TTTGTGGATCCGGCAGTTAAGA (antisense).

In vivo RhoA inactivation with Y-27632

Intramuscular injections into the gastrocnemius muscles (GMs) of dKO mice were conducted with Y-27632 (5 mM in 30 μl of PBS solution; left limb) or control (30 μl of PBS; right limb), starting from 4 wk of age. Intramuscular injections were conducted 3×/wk for 4 wk. Differential HO formation in the skeletal muscle with or without Y-27632 treatment was assessed by micro-CT scan or alizarin red stain. Systematic inhibition of RhoA signaling was conducted by intraperitoneal injection of Y-27632 (5 mM in PBS, 10 mg/kg/mouse) or control (PBS only) into dKO mice from 3 wk of age. Intraperitoneal injections into dKO mice were conducted 3×/wk for 4 wk.

Histology

Cryostat sections (10 μm) were prepared using standard techniques from GMs of mice. HO in muscle tissue was assessed by alizarin red stain: tissue sections of skeletal muscle were fixed with 4% formalin (10 min) and rinsed with ddH_2O; slides were then incubated with alizarin red working solution for 10 min before being washed with ddH_2O. FI was detected by Oil red O stain: fixed tissue sections were rinsed with ddH_2O and 60% isopropanol; slides were then incubated with Oil red O working solution for 15 min before being rinsed with 60% isopropanol and ddH_2O. The IMCL was detected by AdipoRed assay reagent (Lonza): fixed tissue sections were rinsed with PBS and incubated with AdipoRed assay reagent for 15 min before being washed with PBS. For immunofluorescent staining of tissue sections, the sections were blocked with horse serum (10%) for 1 h, and the primary antibodies RhoA (Santa Cruz Biotechnology, Santa Cruz, CA, USA), CD68 (Abcam, Cambridge, MA, USA), or MyoD (Santa Cruz Biotechnology) were applied at 1:100–1:200. Negative controls were performed concurrently with all immunohistochemical staining. Necrosis with damaged myofibers in muscle was assayed by incubating with biotinylated anti-mouse IgG (1:300; Vector Laboratory, Burlingame, CA, USA) for 1 h at room temperature, which was followed by a 15-min incubation with streptavidin Cy3 conjugate (1:500; Sigma-Aldrich). All incubations were performed at room temperature. All slides were analyzed using fluorescent microscopy (Leica Microsystemic, Buffalo Grove, IL, USA) and photographed at ×4–40 view.

Measurement of results and statistical analysis

The measurement of results from images was performed using commercially available software (Northern Eclipse 6.0; Empix Imaging, Mississauga, ON, Canada) and ImageJ 1.32j (U.S. National Institutes of Health, Bethesda, MD, USA). Data from ≥3 samples from each subject were pooled for statistical analysis. Results are given as means ± SD. Statistical significance of any difference was calculated using Student's t test. Values of $P < 0.05$ were considered statistically significant.

RESULTS

Extensive intramuscular HO and IMCL occurred in the skeletal muscle of dKO mice

Micro-CT scan and alizarin red staining revealed extensive HO in the hind-limb muscles (*i.e.*, GMs) of dKO mice at 8 wk of age (**Fig. 1*A*, *B***), while in age-matched *mdx* mice, only mild HO was observed (Fig. 1*A*, *B*). Oil

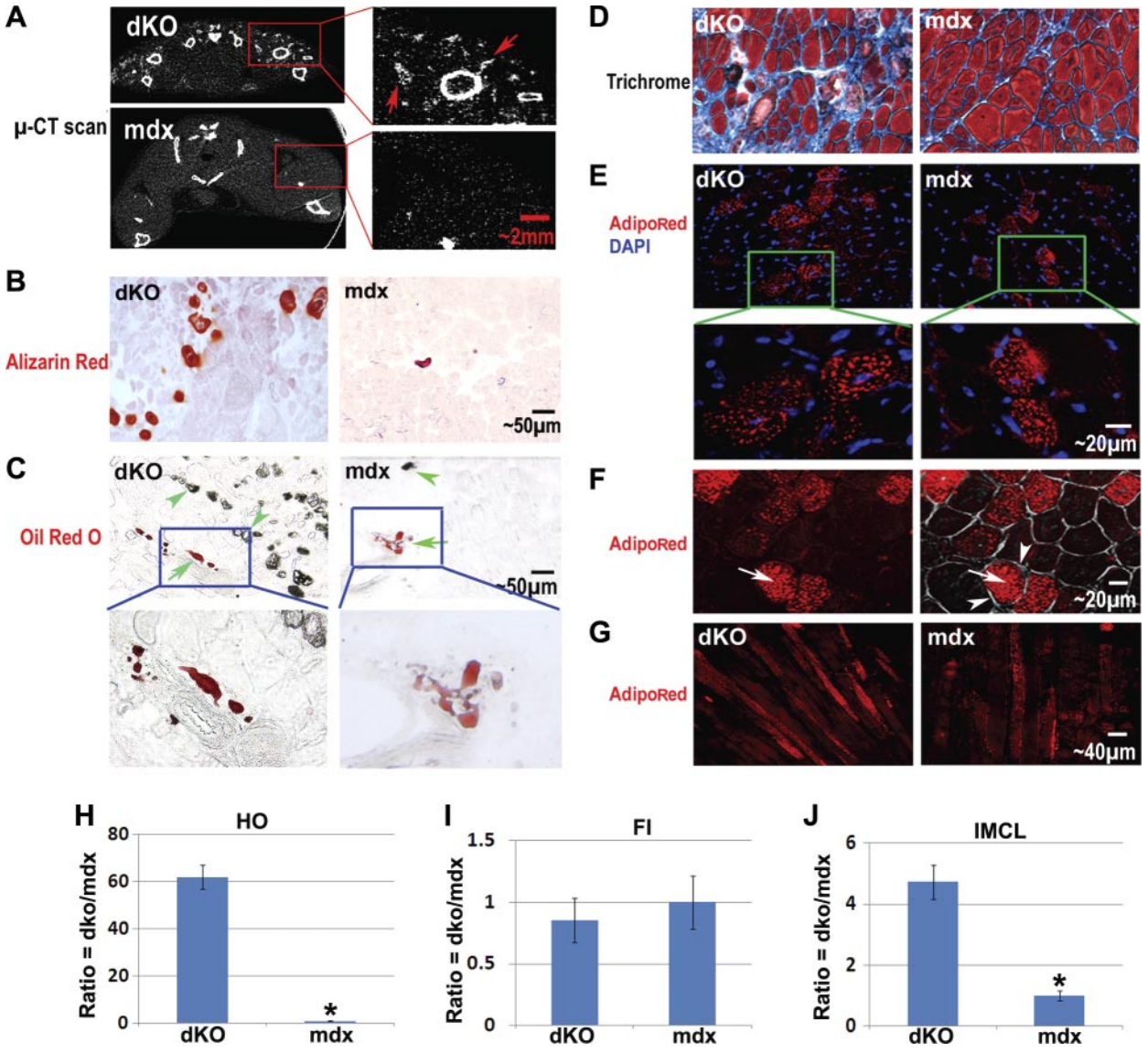

Figure 1. Differential formation of HO, FI, fibrosis, and IMCL in the skeletal muscle of dKO mice and *mdx* mice. *A*) Micro-CT scan revealed extensive HO formation (arrows) in the hind-limb skeletal muscles of dKO mice (8 wk of age), especially in the thigh and GM. Much less HO was observed in *mdx* mice (8 wk of age). *B*) Alizarin red stain of muscle tissue sections also showed more extensive HO formation in the GMs of the dKO mice. *C*) Oil red O stain revealed comparable amounts of intramuscular FI in dKO and *mdx* mice (but a much lower ratio of fat/HO), and the distinct localization of fat and HO (HO is visible with brightfield light). Arrows denote FI; arrowheads denote HO. *D*) Trichrome stain showed more fibrotic tissue (blue) and less normal myofibers in the skeletal muscle of dKO mice. *E*) AdipoRed stain indicated that IMCL occurred in the skeletal muscle of both *mdx* and dKO mice but was more extensive in the dKO mice. *F*) Representative images showing the localization of lipids (arrows) inside the membrane (arrowheads) of myofibers. Left panel: fluorescent image showing AdipoRed signal. Right panel: overlay of fluorescent and brightfield images. *G*) AdipoRed stain of longitudinal sections of GMs, verifying that the identity of the cells with positive signals were myofibers and not fat cells. *H*) Statistics of HO in GMs of dKO mice compared to *mdx* mice. *I*) Statistics of FI in GMs of dKO mice compared to *mdx* mice. *J*) Statistics of IMCL in GMs of dKO mice compared to *mdx* mice. $*P < 0.05$.

red O stain revealed mild intramuscular FI in the GMs of both 8-wk-old *mdx* and dKO mice (Fig. 1*C*). Notably, the FI/HO ratio was much lower in the dKO mice, and the sites of intramuscular HO and FI did not colocalize (Fig. 1*C* and Supplemental Fig. S1*A*). The fact that HO and FI never colocalized in the muscle suggests that these two processes are mutually exclusive and could implicate different cell types and/or niches involved in the two processes. In addition, trichrome staining of the skeletal muscle tissue further revealed more fibrosis in the skeletal muscle of dKO mice when compared with skeletal muscle of the *mdx* mice (Fig. 1*D*). These observations suggest that the microenvironment differs between dKO and *mdx* skeletal muscle, and the micromilieu in the dKO skeletal muscle is more conductive to osteogenesis or fibrogenesis processes. Much like our observation in the dKO mice, other important animal models of human DMD, including the GRMD dog and the canine X-linked muscular dystrophy (CXMD) dog, feature extensive HO and mild FI in their skeletal

muscle, especially before the age of 4–6 mo (16, 53–54).

Interestingly, contrary to the mild FI observed in the skeletal muscles of dKO mice, extensive IMCL was observed; while in the skeletal muscle of *mdx* mice, less extensive amounts of IMCL were noted (Fig. 1*E–G*). This severe lipid accumulation in the mature muscle cells (myofibers) of dKO muscle is indicative of disordered lipid metabolism in their skeletal muscle (55).

In addition, intramuscular HO and FI development was compared between the dKO and *mdx* mice at different ages (dKO mice at 4 or 8 wk and *mdx* mice at 4 wk or 24 mo). Eight weeks and 24 mo represent ~100% of the life span of the dKO and *mdx* mice, respectively. Results showed that HO increased with age in the dKO mice within their very short life span, but it remained mild in the *mdx* mice across their entire life span (**Fig. 2*A*, *C*, *D***). Meanwhile, FI increased with age in both the *mdx* and dKO mice and became quite excessive in aged *mdx* mice but not in the 8-wk-old dKO mice (Fig. 2*B–D*). Notably, in both the 4- and 8-wk-old dKO mice, the presence of FI was much less extensive than HO (Fig. 2*C*), while in *mdx* mice, FI became more extensive than HO with aging (Fig. 2*D*).

HO localizes at the sites of necrosis and fibrosis in the skeletal muscle of dKO mice

Alizarin red or hematoxylin and eosin staining was performed on serial sections of the skeletal muscle of 8-wk-old dKO mice, and HO generally localized at the sites enriched with damaged myofibers, but not in areas where normal myofibers existed (Fig. 2*E*). Also, Trichrome stain and IgG stain further indicated that localization of HO is generally surrounded by fibrotic tissues (Supplemental Fig. S1*B*) or necrotic tissues (Supplemental Fig. S1*C*). Therefore, it appears that

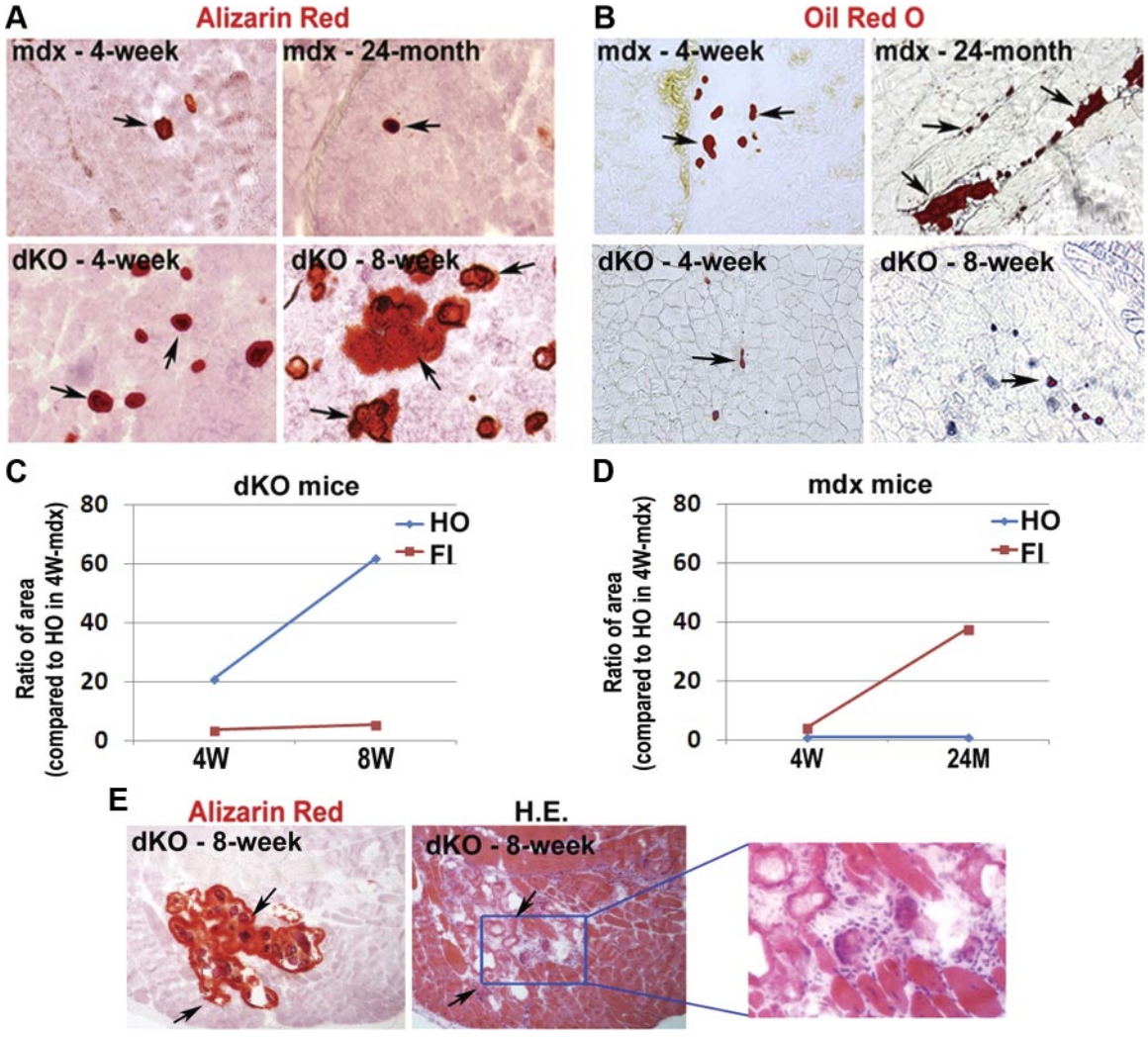

Figure 2. Development of HO and FI in the skeletal muscle of "younger" and "older" dKO mice (4 and 8 wk) and *mdx* mice (4 wk and 24 mo). *A*) HO (arrows) increased significantly with age in dKO mice but not in *mdx* mice. *B*) FI (arrows) increased with age in both *mdx* mice and dKO mice, but to a lesser extent in the dKO mice. *C*) Statistics on the change of HO and FI with aging in dKO mice. *D*) Statistics on the change of HO and FI with aging in *mdx* mice. *E*) Serial sections of the skeletal muscle of 8-wk-old dKO mice were stained with either alizarin red or hematoxylin and eosin (H.E.); it shows that HO was generally localized at the sites enriched with damaged myofibers and fibrosis (arrows) but not at the sites possessing normal myofibers.

HO formation in the skeletal muscle of dKO mice is concurrent with necrosis and fibrosis.

RhoA signaling was activated in the skeletal muscle of dKO mice and RhoA$^+$ cells specifically localized at the sites of necrosis and HO

Semiquantitative RT-PCR analyses revealed that the expression of the inflammatory factor TNF-α, and osteogenesis-related factors BMP2, BMP4, and RhoA were all up-regulated in the dKO skeletal muscle, when compared to the age-matched *mdx* skeletal muscle (**Fig. 3*A***). BMPs are known to induce HO in damaged skeletal muscle, and elevated BMP signaling has been observed in satellite cells of patients wtih DMD (56). We also found that the expression of Klotho, an antiinflammatory and antiaging factor (57), was down-regulated in the dKO skeletal muscle when compared to the *mdx* skeletal muscle (Fig. 3*A*). Because inflammation has been implicated as an important contributor to HO (1, 27, 58), it is possible that highly activated inflammation signaling in the dKO skeletal muscle is involved with the extensive HO observed in this animal model. A similar differential expression of these genes was found in MDSCs isolated from dKO and *mdx* mice.

Furthermore, immunofluorescent staining for the RhoA protein revealed an increased number of RhoA$^+$ cells in the skeletal muscle of dKO mice when compared to *mdx* mice (Fig. 3*B, C*), further confirming elevated RhoA signaling in the dKO skeletal muscle. Notably, it was noted that RhoA$^+$ cells were usually localized at the sites of excessive necrosis and HO (Fig. 3*B* and Supplemental Fig. S2), but not in area of FI, indicating potential involvement of RhoA$^+$ cells in the progression of HO.

In addition, through colocalization analyses, it was demonstrated that RhoA$^+$ cells do not colocalize with CD68$^+$ inflammatory cells (Fig. 3*D*) and MyoD$^+$ myogenic cells (Fig. 3*E*), indicating that the RhoA$^+$ cells did not represent inflammatory or myogenic cells.

RhoA inactivation of dKO MDSCs decreased their osteogenic potential, while it increased their adipogenic and myogenic potentials

Similar to what was observed with skeletal muscle tissues, immunofluorescent staining of MDSCs isolated from dKO and *mdx* mice for MyoD and RhoA also demonstrated a greater number of RhoA$^+$ cells in the MDSCs isolated from the dKO mice than the *mdx* mice (**Fig. 4*A***). Therefore, we hypothesized that the inactiva-

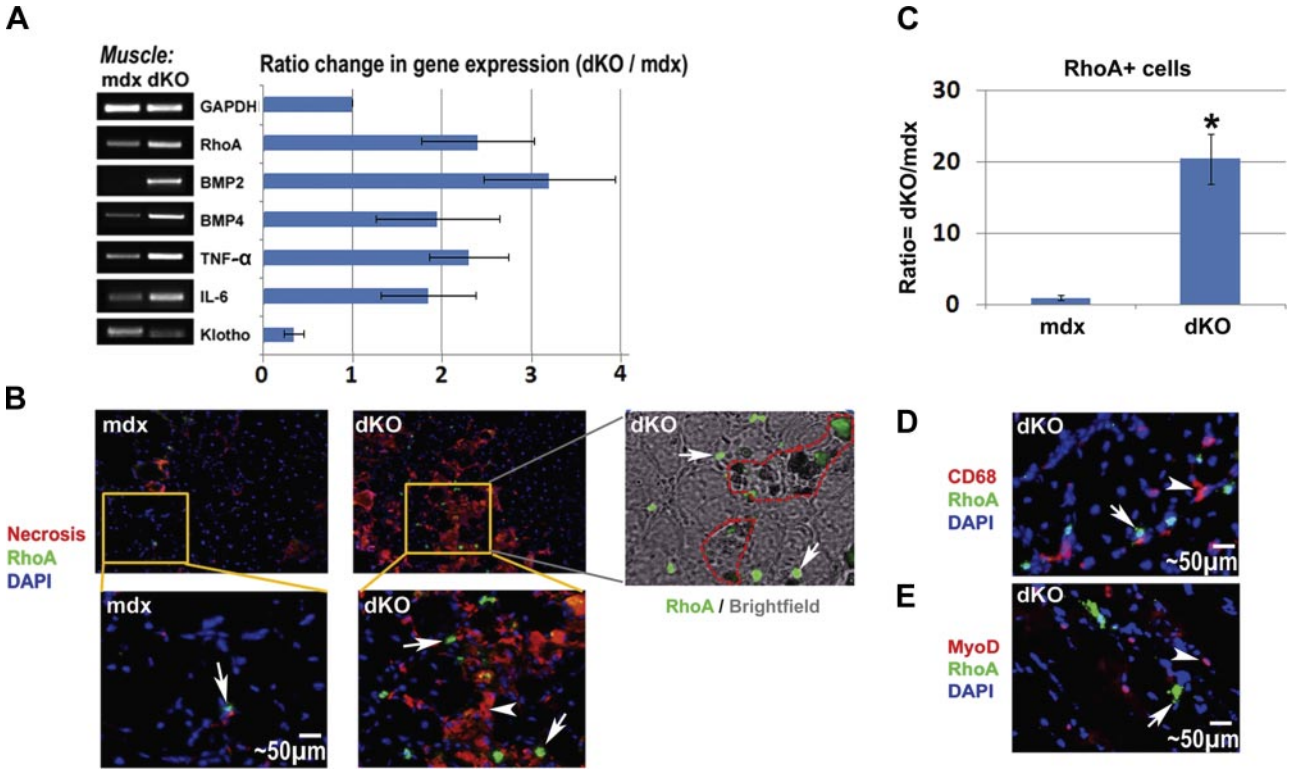

Figure 3. RhoA$^+$ cells in the skeletal muscle of dKO and *mdx* mice. *A*) RT-PCR of mRNA isolated from the skeletal muscle of dKO and *mdx* mice (8 wk of age) showed that the expression of RhoA, BMP2/4, TNF-α, IL-6 was up-regulated in dKO mice, and the expression of the anti-inflammation factor Klotho was down-regulated. *B*) Immunofluorescent staining of RhoA demonstrated a greater number of RhoA$^+$ cells (arrows) in the skeletal muscle of dKO mice. Necrotic areas (arrowheads) were localized by staining with fluorescent anti-mouse IgG, and RhoA$^+$ cells were found to localize at or around the necrotic areas; overlay of images of brightfield and immunofluorescent staining of RhoA further revealed that the same areas enriched with RhoA$^+$ cells (arrows) are the area of HO (circled) too. *C*) Statistics of RhoA$^+$ cells in *mdx* and dKO skeletal muscle. *D*) Representative image of immunofluorescent staining of CD68 and RhoA in the dKO muscle demonstrated that CD68$^+$ cells (arrowheads) and RhoA$^+$ cells (arrows) were two different cell populations. *E*) Representative image of immunofluorescent staining of MyoD and RhoA in the dKO muscle demonstrated that MyoD$^+$ cells (arrowheads) and RhoA$^+$ cells (arrows) were two different cell populations. *$P < 0.05$.

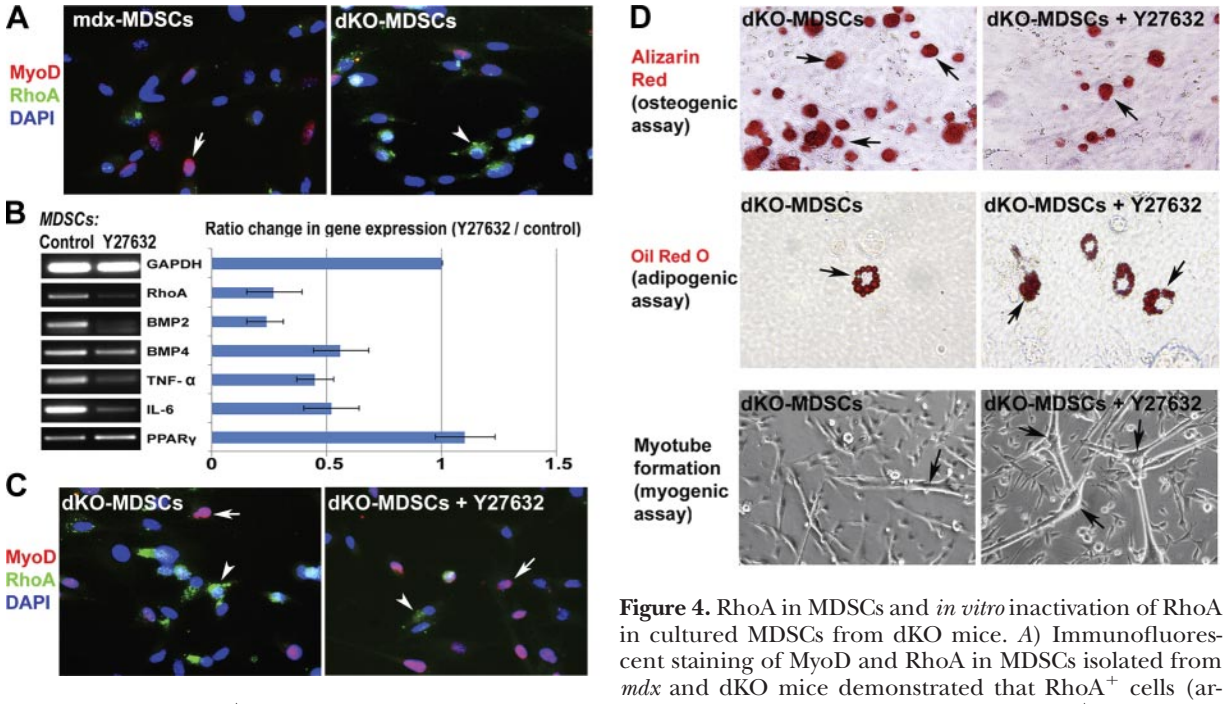

Figure 4. RhoA in MDSCs and *in vitro* inactivation of RhoA in cultured MDSCs from dKO mice. *A*) Immunofluorescent staining of MyoD and RhoA in MDSCs isolated from *mdx* and dKO mice demonstrated that RhoA$^+$ cells (arrowhead) and MyoD$^+$ cells (arrow) were two distinct cell populations, and there were more RhoA$^+$ cells in the MDSCs isolated from dKO mice than *mdx* mice. *B*) Pretreatment of dKO-MDSCs with the RhoA/Rock inhibitor Y-27632 in proliferation medium for 2 d down-regulated the expression of RhoA, BMP2/4, TNF-α, and IL-6, and up-regulated the expression of PPARγ. *C*) Y-27632 treatment decreased the number of RhoA$^+$ cells (arrowheads) and increased the number of MyoD$^+$ cells (arrows). *D*) *In vitro* osteogenesis, adipogenesis, and myogenesis assays indicated that, Y-27632 pretreated dKO-MDSCs demonstrated decreased osteogenic potential (less cells with positive alizarin red signal) in osteogenic medium and increased adipogenesis potential (more cells with positive Oil red O signal) in adipogenic medium, as well as increased myogenic potential (more myotube formation) in the myogenic medium.

tion of RhoA signaling in the MDSCs may change the osteogenic, adipogenic, and myogenic potentials of the cells because RhoA is a proosteogenic and antiadipogenic/myogenic signaling pathway. To test the hypothesis, dKO MDSCs were cultured in proliferation medium and pretreated with the RhoA/Rock inhibitor, Y-27632, for 2 d before undergoing osteogenic, adipogenic, and myogenic assays. Y-27632 pretreatment of dKO MDSCs significantly down-regulated the expression of the inflammation-related genes (TNF-α and IL-6), BMPs, and RhoA (Fig. 4*B*). Also, Y-27632 pretreatment up-regulated the expression of the key adipogenic factor, PPARγ, which is known to have anti-inflammatory activities (59). Immunostaining of RhoA and MyoD showed that RhoA$^+$ cells and MyoD$^+$ cells were 2 distinct cell populations, and the number of RhoA$^+$ cells was decreased, while the number of MyoD$^+$ cells was increased with Y-27632 treatment (Fig. 4*C*), indicating decreased osteogenic but increased myogenic potentials of the treated cell population. Osteogenesis and adipogenesis assays revealed a decreased osteogenic potential and increased adipogenic potential of the MDSCs treated with Y-27632 (Fig. 4*D*). Meanwhile, the dKO MDSCs treated with Y-27632 showed an increase in their myogenic potential (Fig. 4*D*).

RhoA inactivation in dKO skeletal muscle decreased HO and IMCL, while it increased muscle regeneration

The RhoA/Rock inhibitor Y-27632 was injected intramuscularly into the GM muscles of 4-wk-old dKO mice to determine the effect of RhoA inactivation on the development of HO, FI, IMCL, and muscle regeneration. Four weeks after the administration of Y-27632, we observed slower development of HO in the dKO skeletal muscle, as determined by micro-CT scanning and histological staining (**Fig. 5*A, B***). At the same time, skeletal muscle regeneration was enhanced in the treated dKO skeletal muscle (Fig. 5*C*) despite slightly increased FI (Fig. 5*D*). Notably, the increase of FI in the dKO muscle with Y-27632 administration was mild compared to the increase of muscle regeneration, and the overall phenotype of the dystrophic muscle was greatly improved (Fig. 5). Finally, IMCL was decreased (Fig. 5*E*), indicating improved fatty acid metabolism in the skeletal muscle with RhoA inactivation. Immunofluorescent staining of RhoA revealed that the number of RhoA$^+$ cells decreased with the administration of Y-27632 (Fig. 5*F*), which may correlate with the reduced number of osteogenic cells in the skeletal muscle. Furthermore, the number of CD68$^+$ inflammatory cells (mainly macrophages; ref. 60) was also reduced after the administration of Y-27632 (Fig. 5*G*). In addition, semiquantitative RT-PCR showed that the expression of RhoA, BMPs, and inflammation-related factors were down-regulated in skeletal muscle treated with Y-27632, while the expression of PPARγ was up-regulated (Fig. 5*H*). PPARγ activation may have improved fatty acid metabolism and reduced the accumulation of lipid within the muscle cells (61–62). The overall pheno-

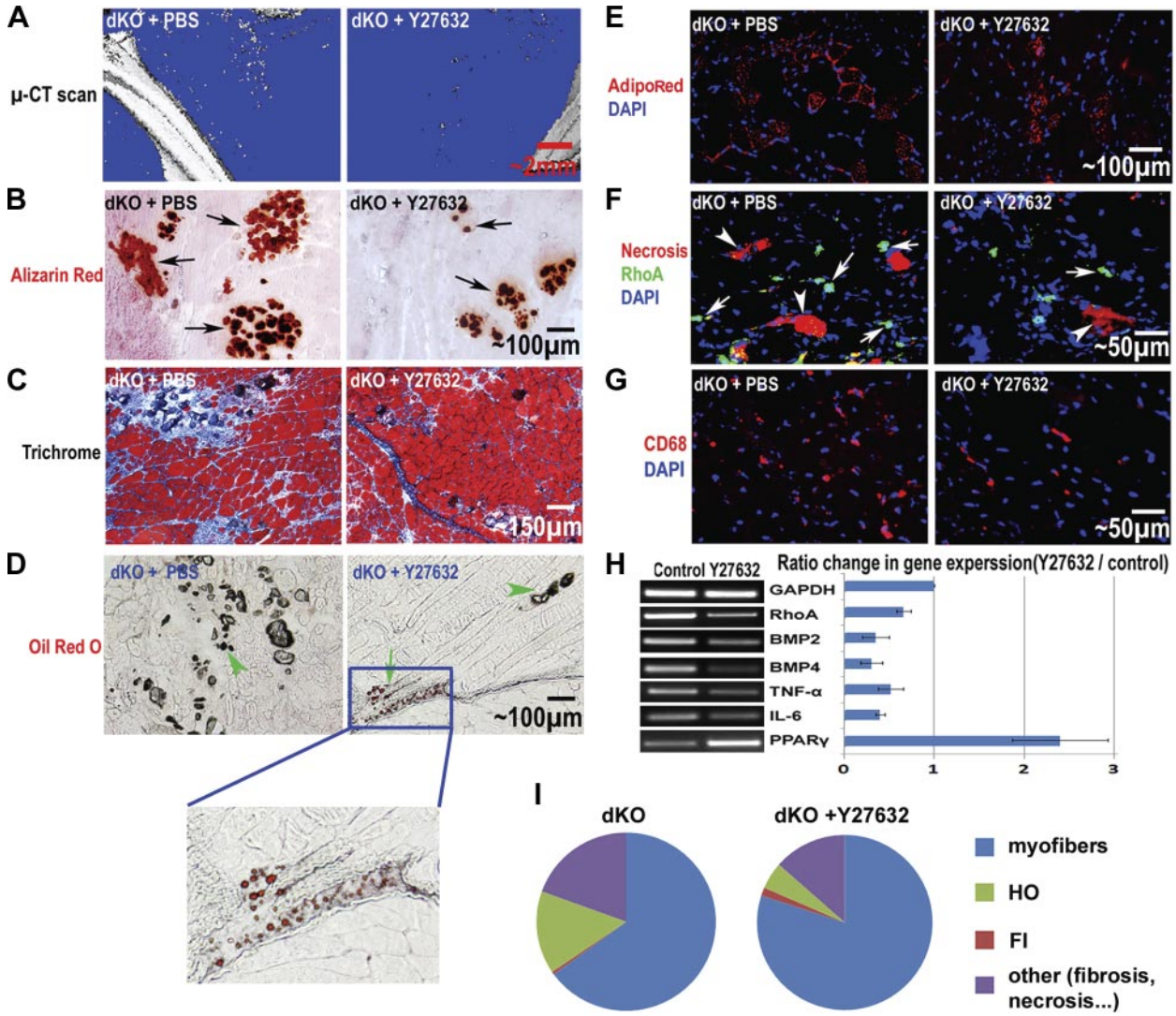

Figure 5. *In vivo* inactivation of RhoA in the skeletal muscle of dKO mice. *A*) Micro-CT scan of the hind-limb skeletal muscles, including the GM, 4 wk after beginning the administration of the RhoA/Rock inhibitor Y-27632 in dKO mice (from 4 to 8 wk of age) showed a reduction in HO. *B*) Alizarin red stain of muscle tissues also revealed greatly reduced HO (arrows) in the GM muscles with Y-27632 treatment. *C*) Hematoxylin and eosin stain showed improved muscle regeneration with Y-27632 treatment. *D*) Oil red O stain showed slightly increased FI (arrows) with Y-27632 treatment. HO is also visible with brightfield microscopy (arrowheads). *E*) AdipoRed stain showed reduced IMCL in dKO mice with Y-27632 treatment. *F*) Immunofluorescent stain showed reduced numbers of $RhoA^+$ cells (arrows) and necrotic myofibers (arrowheads) with Y-27632 treatment. *G*) Immunofluorescent stain showed reduced numbers of $CD68^+$ inflammatory cells with Y-27632 treatment. *H*) RT-PCR of the muscle tissues revealed down-regulated expression of RhoA, BMP2/4, TNF-α, and IL-6, and up-regulated expression of PPARγ with Y-27632 treatment. *I*) The overall phenotypic change of the muscle treated with Y-27632 is summarized in the pie graph, including myofibers, HO, FI, and other (fibrosis and necrosis). It is clear that HO, fibrosis, and necrosis were reduced with Y-27632 treatment, while muscle regeneration was improved; FI was also increased, but only very slightly.

typic change in the dKO skeletal muscle treated with Y-27632 is summarized in Fig. 5*I*.

dKO cardiac muscle featured increased IMCL, fibrosis, and HO when compared to *mdx* mice

Cardiac involvement is the leading cause of early death in patients wtih DMD (63), and intramyocardial lipid accumulation in cardiac muscle has been observed in patients wtih DMD, especially in the most damaged areas of the hearts (11, 13). We hypothesized that IMCL observed in the *mdx* and dKO mice was not limited to the skeletal muscle but would also be found in cardiac muscle and could be related to the formation of fibrosis observed in the dystrophic hearts (cardiomyopathy) of the mice.

Trichrome staining of cardiac muscles from 8-wk-old WT, *mdx*, and dKO mice was conducted to characterize ECM collagen deposition, and it revealed that fibrosis formation is generally severe in dKO mice, mild in *mdx* mice, and absent in WT mice (**Fig. 6*A***). Alizarin red staining of the cardiac muscle revealed occurrences of HO in the dKO mice (Fig. 6*B*), but not in the WT or *mdx* mice (data not shown). Meanwhile, we did not observe any FI in the cardiac muscles in these three

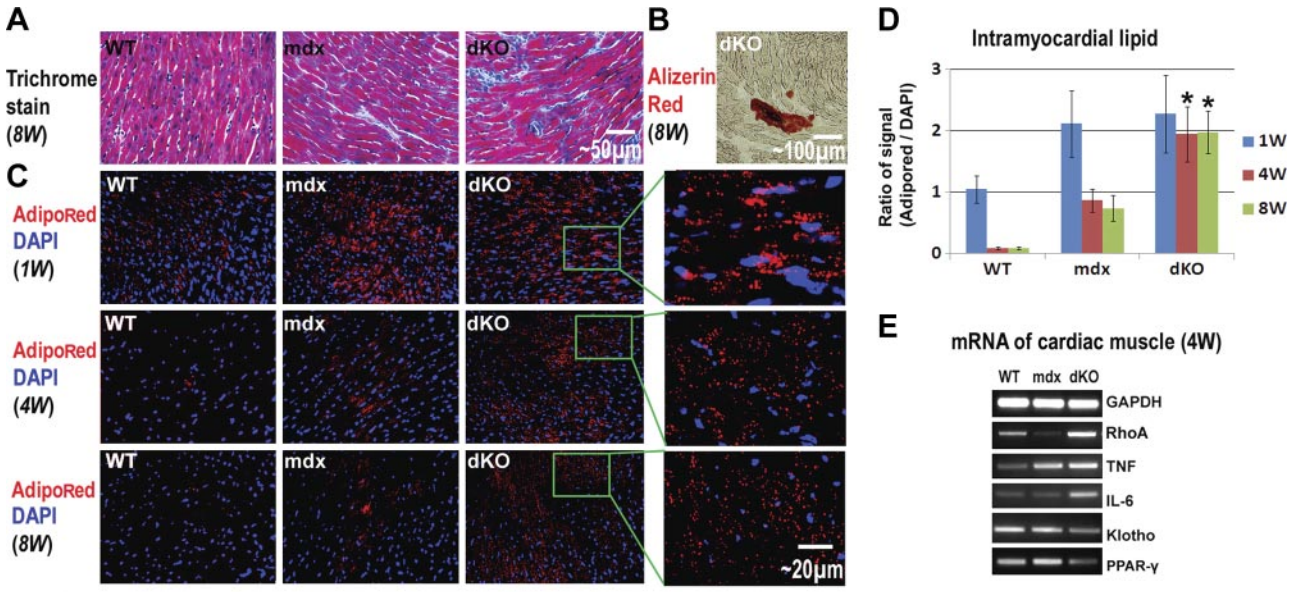

Figure 6. Fibrosis formation and intramyocardial lipid accumulation in the cardiac muscles of WT, *mdx*, and dKO mice. *A*) Trichrome stain showed the progression of fibrosis formation (collagen deposition, blue) in the cardiac muscles as dKO > *mdx* > WT. *B*) Alizarin red stain revealed HO (although mild) in the cardiac muscle of dKO mice. *C*) High levels of intramyocardial lipids were observed in all three mouse models at 1 wk after birth. At 4 and 8 wk after birth, intramyocardial lipid accumulation decreased to an undetectable level in WT mice and decreased to a moderate level in *mdx* mice but still maintained a very high level in the dKO mice. *D*) Statistical analysis of the percentage of area positive for lipid accumulation in WT, *mdx*, and dKO mice of different ages. *E*) RT-PCR results showed that the expression of inflammatory factors (TNF-α and IL-6) were up-regulated in the cardiac muscles of *mdx* and dKO mice, compared with WT mice. The strongest up-regulation of TNF-α and IL-6 occurred to the dKO mice. The expression of the anti-inflammatory factor Klotho was down-regulated in the cardiac muscle of mdx and dKO mice, compared to WT mice. $*P < 0.05$.

mouse models (data not shown), but we did observe intramyocardial lipid accumulation in both the *mdx* and dKO mice (Fig. 6*C*, *D*).

Extensive intramyocardial lipid accumulation at 1 wk of age was observed in all 3 mouse models (Fig. 6*C*). Intramyocardial lipid accumulation in fetal WT mice is a common occurrence because, unlike adult hearts, the fetal hearts use glucose instead of fatty acids as a source of energy (64). Intramyocardial lipid accumulation was found to decrease rapidly in WT mice 1 wk after birth and became nearly undetectable at 4 wk of age (Fig. 6*C*); however, in both *mdx* and dKO mice, intramyocardial lipid accumulation was still observed at 4 wk of age, and the dKO mice exhibited more intramyocardial lipid accumulation than the *mdx* mice (Fig. 6*C*, *D*). Compared to the WT and *mdx* mice, the expression of RhoA and inflammation related factors (TNF-α and IL-6) were also found to be up-regulated in the dKO cardiac muscle, while the expression of the *Klotho* gene was down-regulated (Fig. 6*E*). We suggest that the activation of RhoA and inflammation signaling in dKO cardiac muscle may account for higher levels of HO, intramyocardial lipid accumulation, and fibrosis.

Systemic RhoA inactivation *via* intraperitoneal injection (IP) of Y-27632 reduced IMCL, fibrosis, and HO in dKO cardiac muscle

We hypothesized that RhoA inactivation could reduce HO, IMCL, and fibrosis in the dKO cardiac muscle. To confirm this hypothesis, Y-27632 was injected intraperitoneally (IP) to achieve the systemic inhibition of RhoA signaling in 3-wk-old dKO mice. As expected, after 4 wk of continuous injection. IMCL, fibrosis, and HO in the cardiac muscle decreased compared to nontreated mice (**Fig. 7*A–F***). Actually, involvement of RhoA/ROCK in mediating myocardial fibrosis in type 2 diabetes has been previously demonstrated (48). Semiquantitative PCR further revealed that the expression of RhoA and inflammatory factors were down-regulated with Y-27632 administration, while the expression of Klotho and PPARγ was up-regulated (Fig. 7*G*).

DISCUSSION

Heterotopic ossification (HO) and ectopic fatty infiltration (FI) have been reported in the dystrophic muscle of patients wtih DMD and related animal models (12, 14–16, 65). Our results revealed that mouse models of DMD featuring differing severities of muscular dystrophy have varied potentials for developing HO and FI, and that RhoA signaling could represent a critical mediator in the process, including progression toward HO, FI, and normal muscle regeneration. We noted that the inactivation of RhoA repressed the development of HO and IMCL and improved muscle regeneration in dKO mice. RhoA signaling was previously demonstrated to promote the osteogenic potential of MSCs, while preventing their adipogenic and myogenic potentials (37, 40). Here, we further identified a similar

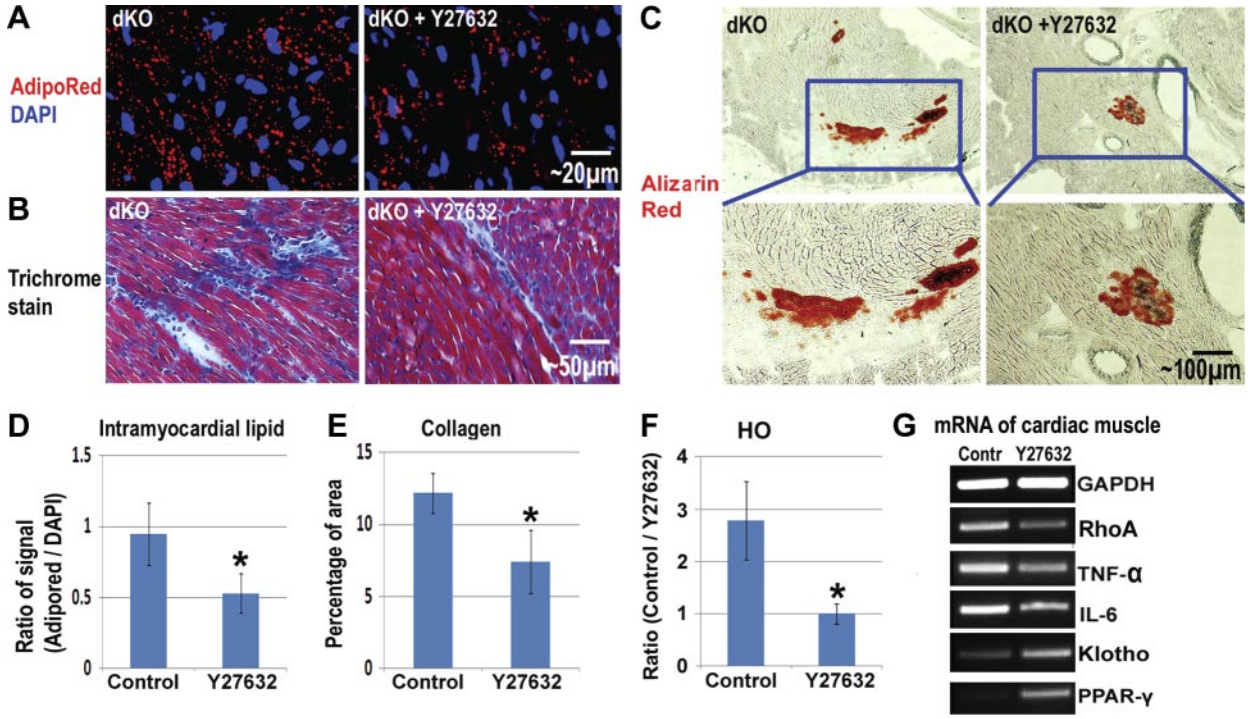

Figure 7. Reduction of intramyocardial lipid accumulation and fibrosis in the cardiac muscles of dKO mice with inactivated RhoA. *A*) AdipoRed stain showed that intramyocardial lipid accumulation in dKO mice was reduced 4 wk after the initiation of Y-27632 administration. *B*) Trichrome stain showed that fibrosis formation was reduced with Y-27632 administration. *C*) Alizarin red stain showed that HO formation in the cardiac muscles of dKO mice was reduced with Y-27632 administration. *D*) Statistical analysis of the percentage of areas positive for IMCL in dKO mice, with and without Y-27632 administration. *E*) Statistical analysis of the percentage of dKO mice positive for HO in their cardiac muscles, with and without Y-27632 administration. *F*) RT-PCR of mRNA from the cardiac muscles showed that the expression of RhoA and inflammatory factors (TNF-α and IL-6) were down-regulated with Y-27632 administration, while the expressions of Klotho and PPAR-γ were up-regulated. *Significant difference, $P < 0.05$.

role of RhoA signaling in muscle stem cells. We suggest that HO in skeletal muscle could be a cell-mediated process involving the transdifferentiation of myogenic cells into osteogenic cells in a stressful microenvironment. The potential mechanisms underlying our current results are proposed in **Fig. 8**.

Muscle stem cells from normal mice are known to possess multipotent differentiation potentials and can

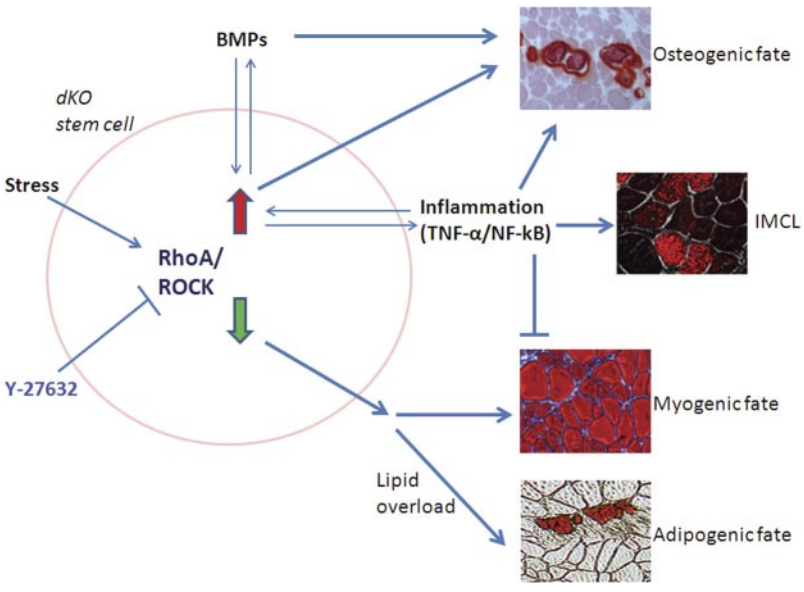

Figure 8. Schematic diagram of the potential mechanism involving RhoA/ROCK signaling in regulating HO, FI, and muscle regeneration in the dystrophic muscle of dKO mice. RhoA/ROCK is responsive to a variety of stresses. Multipotent stem cells, either local stem cells in the dystrophic muscle, bone-marrow-derived stem cells mobilized to the dystrophic muscle of dKO mice, or stem cells of other origins, may be stimulated to differentiate into an osteogenic lineage and may participate in HO formation by highly activated RhoA/Rock signaling, whereas normal myogenic differentiation or potential adipogenic differentiation in dKO mice were repressed by RhoA/Rock signaling. Critical HO-inducing factors, such as BMPs and inflammatory signaling, are interactive with RhoA/Rock signaling, and contribute to HO formation by stem cells or other progenitor cells. RhoA/Rock inactivation with Y-27632 has the potential to reverse the progression of differentiation of the stem cells toward HO, and improve myogenic or adipogenic differentiation. Inflammation-induced IMCL may be directly responsible for HO formation in the muscle (72).

differentiate into osteogenic, chrondrogenic, adipogenic, and myogenic lineages with appropriate induction stimuli (66). In the current study, we observed that the osteogenic potential of muscle stem cells appeared to be promoted, while adipogenic and myogenic potentials appeared to be repressed in the severely dystrophic muscle of dKO mice, a process likely mediated, at least in part, by RhoA activation. RhoA activation was shown to occur in response to stresses, including mechanical stress and oxidative stress (67, 68), suggesting that RhoA activation in the dystrophic muscle of dKO mice could be related to the multiple stresses to which the skeletal muscle of dKO mice is exposed. Compared to *mdx* mice, stresses in the dystrophic muscle of dKO mice may include more myofiber damage and abnormal neuromuscular junctions created by the absence of utrophin; stronger production of profibrotic factors, such as TGF-β1; and severe inflammation caused by extensive muscle degeneration and an abnormally high fat-to-skeletal muscle ratio.

Inactivation of RhoA signaling could be beneficial for improving the severe myopathological phenotype present in dKO mice. Interestingly, RhoA signaling was found to be increased in the spinal cord of an intermediate spinal muscular atrophy (SMA) mouse model, and the inactivation of RhoA signaling with Y-27632 improved the survival of these SMA mice (69). Our results showed that RhoA inactivation in dKO mice led to a less severe dystrophic muscle phenotype that more closely resembled the phenotype observed in *mdx* mice. RhoA signaling has been found to interact with inflammatory signaling and acts as a proinflammatory factor (46, 70). In our current study, we found the level of inflammation to be higher in dKO mice compared to *mdx* mice. By inactivating RhoA with Y-27632, we observed that TNF-α and IL-6 were down-regulated, while Klotho and PPAR-γ were up-regulated in both dKO muscle stem cells and skeletal muscle tissues, indicating a repression of inflammation (59). Therefore, we suggest that the improved muscle phenotype of dKO mice with RhoA inactivation is at least partially due to a reduction in inflammation. Moreover, the up-regulation of PPARγ expression *via* RhoA inactivation could also improve the metabolism of fatty acids in dystrophic muscle since PPARγ was previously reported to increase free fatty acid (FFA) disposal in skeletal muscle through oxidation augmentation, resulting in the reduction of IMCL (71). PPARγ activation in muscle has also been reported to prevent IMCL normally observed in both fat-fed wild-type mice, as well as in the muscles of obese diabetic patients (61, 62). Thus, the up-regulation of PPARγ *via* RhoA inactivation in dKO muscle improved fat metabolism by promoting the uptake of lipids by fat cells and not by muscle cells. Since obesity, inflammation, and IMCL have also been commonly observed in human DMD, we suggest that DMD should also be investigated for the prevention of IMCL by reducing obesity, inflammation, and metabolic abnormalities.

Previous researchers have demonstrated that intramyocardial lipid accumulation is potentially involved with cardiac dysfunction in the dystrophic heart. Cardiac failure is the leading cause for early death of patients wtih DMD (63), and it has been reported that intramyocardial lipid accumulation occurs in the damaged areas of cardiac muscle in patients wtih DMD (11); however, research is sparse regarding the mechanisms and prevention of intramyocardial lipid accumulation. Compared with *mdx* mice, the dKO mouse model exhibits a more severe abnormal cardiac phenotype (*i.e.*, fibrosis formation) and is considered to be an important model for studying DMD-associated cardiomyopathy (14, 19, 20). Our results showed that, when comparing the cardiac muscles of WT, *mdx*, and dKO mice, the severity of intramyocardial lipid accumulation appeared to be closely related to progressive cardiac muscle degeneration. More importantly, our results indicate that intramyocardial lipid accumulation can be reduced by inactivating RhoA, an effect potentially associated with repressed systematic inflammation.

In summary, our results indicated that RhoA signaling could play a major role in regulating the processes of HO, FI, IMCL, and muscle regeneration in the dystrophic skeletal muscle of mice, and consequently, RhoA inactivation may represent a therapeutic target to improve the muscle histopathology associated with DMD. Moreover, RhoA signaling may also serve as a potential target for repressing the development of HO in cases of trauma, neurological injury, and genetic abnormalities. The status of RhoA activation in human patients wtih DMD and the potential effect of RhoA inactivation are, therefore, very promising but require further investigation. FJ

This research was supported, in part, by the Henry J. Mankin endowed chair at the University of Pittsburgh, and the William F. and Jean W. Donaldson endowed chair at the Children's Hospital of Pittsburgh. The authors also thank Ms. Bria King and Mr. James Cummins for their editorial assistance in completing this manuscript.

REFERENCES

1. Cipriano, C. A., Pill, S. G., and Keenan, M. A. (2009) Heterotopic ossification following traumatic brain injury and spinal cord injury. *J. Am. Acad. Orthop. Surg.* **17,** 689–697
2. Marcus, R. L., Addison, O., Kidde, J. P., Dibble, L. E., and Lastayo, P. C. (2010) Skeletal muscle fat infiltration: impact of age, inactivity, and exercise. *J. Nutr. Health Aging* **14,** 362–366
3. Miljkovic-Gacic, I., Wang, X., Kammerer, C. M., Gordon, C. L., Bunker, C. H., Kuller, L. H., Patrick, A. L., Wheeler, V. W., Evans, R. W., and Zmuda, J. M. (2008) Fat infiltration in muscle: new evidence for familial clustering and associations with diabetes. *Obesity* **16,** 1854–1860
4. Savage, D. B., Petersen, K. F., and Shulman, G. I. (2007) Disordered lipid metabolism and the pathogenesis of insulin resistance. *Physiol. Rev.* **87,** 507–520
5. Hulver, M. W., and Dohm, G. L. (2004) The molecular mechanism linking muscle fat accumulation to insulin resistance. *Proc. Nutr. Soc.* **63,** 375–380
6. Schulze, P. C. (2009) Myocardial lipid accumulation and lipotoxicity in heart failure. *J. Lipid Res.* **50,** 2137–2138
7. Axelsen, L. N., Lademann, J. B., Petersen, J. S., Holstein-Rathlou, N. H., Ploug, T., Prats, C., Pedersen, H. D., and Kjolbye, A. L. (2010) Cardiac and metabolic changes in long-term high fructose-fat fed rats with severe obesity and extensive

intramyocardial lipid accumulation. *Am. J. Physiol. Regul. Integr. Comp. Physiol.* **298,** R1560–R1570
8. Ruberg, F. L. (2007) Myocardial lipid accumulation in the diabetic heart. *Circulation* **116,** 1110–1112
9. Sharma, S., Adrogue, J. V., Golfman, L., Uray, I., Lemm, J., Youker, K., Noon, G. P., Frazier, O. H., and Taegtmeyer, H. (2004) Intramyocardial lipid accumulation in the failing human heart resembles the lipotoxic rat heart. *FASEB J.* **18,** 1692–1700
10. Momose, M., Iguchi, N., Imamura, K., Usui, H., Ueda, T., Miyamoto, K., and Inaba, S. (2001) Depressed myocardial fatty acid metabolism in patients with muscular dystrophy. *Neuromusc. Disord.* **11,** 464–469
11. Saini-Chohan, H. K., Mitchell, R. W., Vaz, F. M., Zelinski, T., and Hatch, G. M. (2012) Delineating the role of alterations in lipid metabolism to the pathogenesis of inherited skeletal and cardiac muscle disorders: Thematic Review Series: Genetics of Human Lipid Diseases. *J. Lipid Res.* **53,** 4–27
12. Ionasescu, V., Monaco, L., Sandra, A., Ionasescu, R., Burmeister, L., Deprosse, C., and Stern, L. Z. (1981) Alterations in lipid incorporation in Duchenne muscular dystrophy. Studies of fresh and cultured muscle. *J. Neurol. Sci.* **50,** 249–251
13. Tahallah, N., Brunelle, A., De La Porte, S., and Laprevote, O. (2008) Lipid mapping in human dystrophic muscle by cluster-time-of-flight secondary ion mass spectrometry imaging. *J. Lipid Res.* **49,** 438–454
14. Duan, D. (2006) Challenges and opportunities in dystrophin-deficient cardiomyopathy gene therapy. *Hum. Mol. Genet.* **15**(Spec. 2), R253–R261
15. Kikkawa, N., Ohno, T., Nagata, Y., Shiozuka, M., Kogure, T., and Matsuda, R. (2009) Ectopic calcification is caused by elevated levels of serum inorganic phosphate in *mdx* mice. *Cell Struct. Funct.* **34,** 77–88
16. Nguyen, F., Cherel, Y., Guigand, L., Goubault-Leroux, I., and Wyers, M. (2002) Muscle lesions associated with dystrophin deficiency in neonatal golden retriever puppies. *J. Comp. Pathol.* **126,** 100–108
17. Starkey, J. D., Yamamoto, M., Yamamoto, S., and Goldhamer, D. J. (2011) Skeletal muscle satellite cells are committed to myogenesis and do not spontaneously adopt nonmyogenic fates. *J. Histochem. Cytochem.* **59,** 33–46
18. Sicinski, P., Geng, Y., Ryder-Cook, A. S., Barnard, E. A., Darlison, M. G., and Barnard, P. J. (1989) The molecular basis of muscular dystrophy in the *mdx* mouse: a point mutation. *Science* **244,** 1578–1580
19. Grady, R. M., Teng, H., Nichol, M. C., Cunningham, J. C., Wilkinson, R. S., and Sanes, J. R. (1997) Skeletal and cardiac myopathies in mice lacking utrophin and dystrophin: a model for Duchenne muscular dystrophy. *Cell* **90,** 729–738
20. Deconinck, A. E., Rafael, J. A., Skinner, J. A., Brown, S. C., Potter, A. C., Metzinger, L., Watt, D. J., Dickson, J. G., Tinsley, J. M., and Davies, K. E. (1997) Utrophin-dystrophin-deficient mice as a model for Duchenne muscular dystrophy. *Cell* **90,** 717–727
21. Isaac, C., Wright, A., Usas, A., Li, H., Tang, Y., Mu, X., Greco, N., Dong, Q., Vo, N., Kang, J., Wang, B., and Huard, J. (2013) Dystrophin and utrophin "double knockout" dystrophic mice exhibit a spectrum of degenerative musculoskeletal abnormalities. *J. Orthop. Res.* **31,** 343–349
22. Muntoni, F., Fisher, I., Morgan, J. E., and Abraham, D. (2002) Steroids in Duchenne muscular dystrophy: from clinical trials to genomic research. *Neuromusc. Disord.* **12**(Suppl. 1), S162–S165
23. Mavrogenis, A. F., Soucacos, P. N., and Papagelopoulos, P. J. (2011) Heterotopic ossification revisited. *Orthopedics* **34,** 177
24. Neal, B., Rodgers, A., Dunn, L., and Fransen, M. (2000) Non-steroidal anti-inflammatory drugs for preventing heterotopic bone formation after hip arthroplasty. *Cochrane Database Syst. Rev.*, CD001160
25. Dahners, L. E., and Mullis, B. H. (2004) Effects of nonsteroidal anti-inflammatory drugs on bone formation and soft-tissue healing. *J. Am. Acad. Orthop. Surg.* **12,** 139–143
26. Vasileiadis, G. I., Sioutis, I. C., Mavrogenis, A. F., Vlasis, K., Babis, G. C., and Papagelopoulos, P. J. (2011) COX-2 inhibitors for the prevention of heterotopic ossification after THA. *Orthopedics* **34,** 467
27. Banovac, K., Williams, J. M., Patrick, L. D., and Levi, A. (2004) Prevention of heterotopic ossification after spinal cord injury with COX-2 selective inhibitor (rofecoxib). *Spinal Cord* **42,** 707–710
28. Joe, A. W., Yi, L., Natarajan, A., Le Grand, F., So, L., Wang, J., Rudnicki, M. A., and Rossi, F. M. (2010) Muscle injury activates resident fibro/adipogenic progenitors that facilitate myogenesis. *Nat. Cell Biol.* **12,** 153–163
29. Cox, F. M., Reijnierse, M., van Rijswijk, C. S., Wintzen, A. R., Verschuuren, J. J., and Badrising, U. A. (2011) Magnetic resonance imaging of skeletal muscles in sporadic inclusion body myositis. *Rheumatology* **50,** 1153–1161
30. Mei, M., Zhao, L., Li, Q., Chen, Y., Huang, A., Varghese, Z., Moorhead, J. F., Zhang, S., Powis, S. H., and Ruan, X. Z. (2011) Inflammatory stress exacerbates ectopic lipid deposition in C57BL/6J mice. *Lipids Health Dis.* **10,** 110
31. Hotamisligil, G. S., Shargill, N. S., and Spiegelman, B. M. (1993) Adipose expression of tumor necrosis factor-alpha: direct role in obesity-linked insulin resistance. *Science* **259,** 87–91
32. Messina, S., Altavilla, D., Aguennouz, M., Seminara, P., Minutoli, L., Monici, M. C., Bitto, A., Mazzeo, A., Marini, H., Squadrito, F., and Vita, G. (2006) Lipid peroxidation inhibition blunts nuclear factor-kappaB activation, reduces skeletal muscle degeneration, and enhances muscle function in *mdx* mice. *Am. J. Pathol.* **168,** 918–926
33. Langen, R. C., Schols, A. M., Kelders, M. C., Wouters, E. F., and Janssen-Heininger, Y. M. (2001) Inflammatory cytokines inhibit myogenic differentiation through activation of nuclear factor-κB. *FASEB J.* **15,** 1169–1180
34. Lu, A., Proto, J. D., Guo, L., Tang, Y., Lavasani, M., Tilstra, J. S., Niedernhofer, L. J., Wang, B., Guttridge, D. C., Robbins, P. D., and Huard, J. (2012) NF-κB negatively impacts the myogenic potential of muscle-derived stem cells. *Mol. Ther.* **20,** 661–668
35. Monici, M. C., Aguennouz, M., Mazzeo, A., Messina, C., and Vita, G. (2003) Activation of nuclear factor-κB in inflammatory myopathies and Duchenne muscular dystrophy. *Neurology* **60,** 993–997
36. Ridley, A. J. (2001) Rho GTPases and cell migration. *J. Cell Sci.* **114,** 2713–2722
37. McBeath, R., Pirone, D. M., Nelson, C. M., Bhadriraju, K., and Chen, C. S. (2004) Cell shape, cytoskeletal tension, and RhoA regulate stem cell lineage commitment. *Dev. Cell.* **6,** 483–495
38. Khatiwala, C. B., Kim, P. D., Peyton, S. R., and Putnam, A. J. (2009) ECM compliance regulates osteogenesis by influencing MAPK signaling downstream of RhoA and ROCK. *J. Bone. Miner. Res.* **24,** 886–898
39. Meyers, V. E., Zayzafoon, M., Douglas, J. T., and McDonald, J. M. (2005) RhoA and cytoskeletal disruption mediate reduced osteoblastogenesis and enhanced adipogenesis of human mesenchymal stem cells in modeled microgravity. *J. Bone Miner. Res.* **20,** 1858–1866
40. Wang, Y. K., Yu, X., Cohen, D. M., Wozniak, M. A., Yang, M. T., Gao, L., Eyckmans, J., and Chen, C. S. (2012) Bone morphogenetic protein-2-induced signaling and osteogenesis is regulated by cell shape, RhoA/ROCK, and cytoskeletal tension. *Stem Cells Dev.* **21,** 1176–1186
41. Fromigue, O., Hay, E., Modrowski, D., Bouvet, S., Jacquel, A., Auberger, P., and Marie, P. J. (2006) RhoA GTPase inactivation by statins induces osteosarcoma cell apoptosis by inhibiting p42/p44-MAPKs-Bcl-2 signaling independently of BMP-2 and cell differentiation. *Cell Death Differ.* **13,** 1845–1856
42. Hosoyama, T., Ishiguro, N., Yamanouchi, K., and Nishihara, M. (2009) Degenerative muscle fiber accelerates adipogenesis of intramuscular cells via RhoA signaling pathway. *Differentiation* **77,** 350–359
43. Santos, A., Bakker, A. D., de Blieck-Hogervorst, J. M., and Klein-Nulend, J. (2010) WNT5A induces osteogenic differentiation of human adipose stem cells via rho-associated kinase ROCK. *Cytotherapy* **12,** 924–932
44. Goto, K., Chiba, Y., Sakai, H., and Misawa, M. (2009) Tumor necrosis factor-alpha (TNF-alpha) induces upregulation of RhoA via NF-κB activation in cultured human bronchial smooth muscle cells. *J. Pharmacol. Sci.* **110,** 437–444
45. Slice, L. W., Bui, L., Mak, C., and Walsh, J. H. (2000) Differential regulation of COX-2 transcription by Ras- and Rho-family of GTPases. *Biochem. Biophys. Res. Commun.* **276,** 406–410
46. Nakayama, Y., Komuro, R., Yamamoto, A., Miyata, Y., Tanaka, M., Matsuda, M., Fukuhara, A., and Shimomura, I. (2009) RhoA

induces expression of inflammatory cytokine in adipocytes. *Biochem. Biophys. Res. Commun.* **379,** 288–292
47. Zhou, Y., Huang, X., Hecker, L., Kurundkar, D., Kurundkar, A., Liu, H., Jin, T. H., Desai, L., Bernard, K., and Thannickal, V. J. (2013) Inhibition of mechanosensitive signaling in myofibroblasts ameliorates experimental pulmonary fibrosis. *J. Clin. Invest.* **123,** 1096–1108
48. Zhou, H., Li, Y. J., Wang, M., Zhang, L. H., Guo, B. Y., Zhao, Z. S., Meng, F. L., Deng, Y. G., and Wang, R. Y. (2011) Involvement of RhoA/ROCK in myocardial fibrosis in a rat model of type 2 diabetes. *Acta Pharmacol. Sin.* **32,** 999–1008
49. Charrasse, S., Comunale, F., Grumbach, Y., Poulat, F., Blangy, A., and Gauthier-Rouviere, C. (2006) RhoA GTPase regulates M-cadherin activity and myoblast fusion. *Mol. Biol. Cell* **17,** 749–759
50. Castellani, L., Salvati, E., Alema, S., and Falcone, G. (2006) Fine regulation of RhoA and Rock is required for skeletal muscle differentiation. *J. Biol. Chem.* **281,** 15249–15257
51. Beqaj, S., Jakkaraju, S., Mattingly, R. R., Pan, D., and Schuger, L. (2002) High RhoA activity maintains the undifferentiated mesenchymal cell phenotype, whereas RhoA down-regulation by laminin-2 induces smooth muscle myogenesis. *J. Cell Biol.* **156,** 893–903
52. Gharaibeh, B., Lu, A., Tebbets, J., Zheng, B., Feduska, J., Crisan, M., Peault, B., Cummins, J., and Huard, J. (2008) Isolation of a slowly adhering cell fraction containing stem cells from murine skeletal muscle by the preplate technique. *Nat. Protoc.* **3,** 1501–1509
53. Thibaud, J. L., Monnet, A., Bertoldi, D., Barthelemy, I., Blot, S., and Carlier, P. G. (2007) Characterization of dystrophic muscle in golden retriever muscular dystrophy dogs by nuclear magnetic resonance imaging. *Neuromusc. Disord.* **17,** 575–584
54. Valentine, B. A., Cooper, B. J., Cummings, J. F., and de Lahunta, A. (1990) Canine X-linked muscular dystrophy: morphologic lesions. *J. Neurol. Sci.* **97,** 1–23
55. Greenberg, A. S., Coleman, R. A., Kraemer, F. B., McManaman, J. L., Obin, M. S., Puri, V., Yan, Q. W., Miyoshi, H., and Mashek, D. G. (2011) The role of lipid droplets in metabolic disease in rodents and humans. *J. Clin. Invest.* **121,** 2102–2110
56. Lounev, V. Y., Ramachandran, R., Wosczyna, M. N., Yamamoto, M., Maidment, A. D., Shore, E. M., Glaser, D. L., Goldhamer, D. J., and Kaplan, F. S. (2009) Identification of progenitor cells that contribute to heterotopic skeletogenesis. *J. Bone Joint Surg. Am.* **91,** 652–663
57. Arking, D. E., Krebsova, A., Macek, M., Sr., Macek, M., Jr., Arking, A., Mian, I. S., Fried, L., Hamosh, A., Dey, S., McIntosh, I., and Dietz, H. C. (2002) Association of human aging with a functional variant of klotho. *Proc. Natl. Acad. Sci. U. S. A.* **99,** 856–861
58. Salisbury, E., Rodenberg, E., Sonnet, C., Hipp, J., Gannon, F. H., Vadakkan, T. J., Dickinson, M. E., Olmsted-Davis, E. A., and Davis, A. R. (2011) Sensory nerve induced inflammation contributes to heterotopic ossification. *J. Cell. Biochem.* **112,** 2748–2758
59. Straus, D. S., and Glass, C. K. (2007) Anti-inflammatory actions of PPAR ligands: new insights on cellular and molecular mechanisms. *Trends Immunol.* **28,** 551–558
60. Holness, C. L., and Simmons, D. L. (1993) Molecular cloning of CD68, a human macrophage marker related to lysosomal glycoproteins. *Blood* **81,** 1607–1613
61. Amin, R. H., Mathews, S. T., Camp, H. S., Ding, L., and Leff, T. (2010) Selective activation of PPARgamma in skeletal muscle induces endogenous production of adiponectin and protects mice from diet-induced insulin resistance. *Am. J. Physiol. Endocrinol. Metab.* **298,** E28–E37
62. Ye, J. M., Doyle, P. J., Iglesias, M. A., Watson, D. G., Cooney, G. J., and Kraegen, E. W. (2001) Peroxisome proliferator-activated receptor (PPAR)-α activation lowers muscle lipids and improves insulin sensitivity in high fat-fed rats: comparison with PPAR-γ activation. *Diabetes* **50,** 411–417
63. Finsterer, J., and Stollberger, C. (2003) The heart in human dystrophinopathies. *Cardiology* **99,** 1–19
64. Lehman, J. J., and Kelly, D. P. (2002) Transcriptional activation of energy metabolic switches in the developing and hypertrophied heart. *Clin. Exp. Pharmacol. Physiol.* **29,** 339–345
65. Ahmad, N., Bygrave, M., De Zordo, T., Fenster, A., and Lee, T. Y. (2010) Detecting degenerative changes in myotonic murine models of Duchenne muscular dystrophy using high-frequency ultrasound. *J. Ultrasound. Med.* **29,** 367–375
66. Qu-Petersen, Z., Deasy, B., Jankowski, R., Ikezawa, M., Cummins, J., Pruchnic, R., Mytinger, J., Cao, B., Gates, C., Wernig, A., and Huard, J. (2002) Identification of a novel population of muscle stem cells in mice: potential for muscle regeneration. *J. Cell Biol.* **157,** 851–864
67. Smith, P. G., Roy, C., Zhang, Y. N., and Chauduri, S. (2003) Mechanical stress increases RhoA activation in airway smooth muscle cells. *Am. J. Respir. Cell Mol. Biol.* **28,** 436–442
68. Aghajanian, A., Wittchen, E. S., Campbell, S. L., and Burridge, K. (2009) Direct activation of RhoA by reactive oxygen species requires a redox-sensitive motif. *PLoS One* **4,** e8045
69. Bowerman, M., Beauvais, A., Anderson, C. L., and Kothary, R. (2010) Rho-kinase inactivation prolongs survival of an intermediate SMA mouse model. *Hum. Mol. Genet.* **19,** 1468–1478
70. Segain, J. P., Raingeard de la Bletiere, D., Sauzeau, V., Bourreille, A., Hilaret, G., Cario-Toumaniantz, C., Pacaud, P., Galmiche, J. P., and Loirand, G. (2003) Rho kinase blockade prevents inflammation via nuclear factor κB inhibition: evidence in Crohn's disease and experimental colitis. *Gastroenterology* **124,** 1180–1187
71. Ciaraldi, T. P., Cha, B. S., Park, K. S., Carter, L., Mudaliar, S. R., and Henry, R. R. (2002) Free fatty acid metabolism in human skeletal muscle is regulated by PPARγ and RXR agonists. *Ann. N. Y. Acad. Sci.* **967,** 66–70
72. Demer, L. L. (2002) Vascular calcification and osteoporosis: inflammatory responses to oxidized lipids. *Int. J. Epidemiol.* **31,** 737–741

Received for publication April 18, 2013.
Accepted for publication May 14, 2013.

CONTROL ID: 1473466

TITLE: Enhanced myogenic potential of human dental pulp and amniotic fluid stem cells by use of a demethylation agent and conditioned media.

AUTHORS (LAST NAME, FIRST NAME): Pisciotta, Alessandra[1, 2]; Lu, Aiping[2]; Gharaibeh, Burhan[2,]; De Pol, Anto[1]; Huard, Johnny[2]

INSTITUTIONS (ALL): 1. Department of Surgical, Medical, Dental and Morphological Sciences with interest in Transplant, Oncology and Regenerative Medicine, University of Modena and Reggio Emilia, Modena, Italy.
2. Stem Cell Research Center, Department of Orthopaedic Surgery, University of Pittsburgh, Pittsburgh, PA, United States.

CURRENT PRIMARY CATEGORY: Muscle

AWARDS:

KEYWORDS: Muscle, Cell and Molecular Imaging, Orthopaedic Pathology.

ABSTRACT BODY:

Introduction: Duchenne muscular dystrophy (DMD) is a genetic mutation resulting in muscle degeneration that leads to death by the mid-twenties. Cell therapy can be used to reintroduce dystrophin to repair damaged muscle fibers. Human dental pulp (hDPSCs) and amniotic fluid stem cells (hAFSCs) may represent an alternative, less controversial source to embryonic stem cells. HDPSCs can be isolated from adult human dental pulp of the third molars during routine extraction. HAFSCs, which represent 1% of the cells in human amniocentesis specimens, can be obtained by immunoselecting the antigen c-Kit (CD117) positive population, via magnetic cell sorting. HDPSCs and hAFSCs have been shown to be self-renewing and multipotent (1, 2), therefore they may represent promising tools for muscular dystrophy therapies.
This study evaluated the myogenic potential of hDPSCs and hAFSCs using different conditions which optimized the most effective protocol to differentiate the cells towards a myogenic lineage by means of demethylation. The results of the current study provide the basis for subsequent in vivo uses of hDPSCs and hAFSCs to enhance skeletal muscle repair in animal models and human DMD patients.

Methods: Human DPSCs were isolated as described by Riccio et al (3). The STRO-1+ DPSC population was obtained by magnetic cell sorting. AFSCs were isolated as previously described by De Coppi et al (2): hAFSCs cultures, from supernumerary amniocentesis specimens, were subjected to c-Kit immuno-selection by MACS technology. The STRO-1+ DPSC and the c-kit+

AFSC populations were used in this study.
Direct co-culture: To test the ability of hAFSCs and hDPSCs to form new myotubes, the cells were differentiated in a direct co-culture system with C2C12 myoblasts. Human cells and C2C12 cells, seeded at a 10:1 ratio, were maintained in proliferation medium (PM: DMEM High Glucose + 10% FBS) until confluent, the medium was then replaced with fusion medium (FM: DMEM High Glucose + 1% FBS + 10nM insulin).
Demethylation and differentiation: To evaluate whether hAFSCs and hDPSCs can be committed to the myogenic lineage, cells were seeded at 3000 cells/cm2 in PM until confluent. Subsequently, the medium was replaced with low serum differentiation medium supplemented with 10µM 5-Aza-2'-deoxycytidine (5-Aza) for 24 hours, to induce DNA demethylation. After removing 5-Aza, medium was replaced with low serum differentiation medium supplemented with 10 nM insulin. Cells were differentiated in a) low serum medium plus 10 nM insulin and b) pre-filtered conditioned FM from the C2C12 culture + fresh differentiation medium + 10 nM insulin.
To verify myogenic differentiation, staining for human Nuclei (huNu) and myosin heavy chain (MyHC) was performed. Myogenic differentiation after demethylation was verified by myogenin and MyHC immune-fluorescent (IF) staining. Human cells were processed for IF staining as previously described (3).

Results: When differentiated in a direct co-culture with C2C12 cells, human AFSCs and DPSCs were able to undergo myogenic differentiation, as demonstrated by the positive staining of the myotubes with anti-huNu ab (Fig. 1A-B). Human cells which were not co-cultured with C2C12 did not undergo myogenic differentiation and did not fuse in myotubes (Fig. 1C-D).
Data from the IF analysis of myogenic differentiation after treatment with 10µM 5-Aza showed that hAFSCs are driven to the myogenic lineage and express myogenin, a myogenic differentiation marker, after 14 days of differentiation (Fig. 2A), while the hDPSCs underwent myogenic differentiation expressing myogenin after 21 days of differentiation under the same conditions (Fig. 2C). Moreover, some hAFSCs also showed positive staining for MyHC (Fig. 2B). Immunofluorescence labeling also showed that when conditioned medium from the differentiating C2C12 cells was added to fresh myogenic medium, the human cells pre-treated with 5-Aza started to express myogenin after 14 and 21 days of differentiation (Fig. 2D-2F) respectively. Furthermore, some of the hAFSCs also showed positive staining for MyHC (Fig. 2E). Cells not demethylated demonstrated no positive staining for muscle specific markers (Fig. 2G-H).

Discussion: The IF image data in this study demonstrated the ability of the hAFSCs and hDPSCs stem cell populations to actively participate in the formation of myotubes. These human cells were capable of fusing with murine C2C12, as demonstrated by the positive IF staining of the

multi-nucleated cells to anti-huNu ab. These results showed the potential of these cells for skeletal muscle repair.
Previous studies have demonstrated that the genes related to skeletal myogenic differentiation are controlled by DNA methylation and that the use of the demethylation agent, 5-Aza, was able to induce adult human bone marrow stem cells to differentiate towards a cardiomyogenic lineage (4, 5).
This study demonstrated that demethylation treatment could effectively induce a myogenic commitment of hAFSCs and hDPSCs, in two different conditions, as shown by IF staining: hAFSCs underwent myogenic differentiation earlier than hDPSCs, and reached a more mature differentiation status as shown by their expression of MyHC.
These results demonstrate that hAFSCs and hDPSCs can be induced to differentiate towards a myogenic lineage in vitro, and suggests that modulating the myogenic potential of these stem cells can be achieved by combining demethylation treatment, which increases the expression of muscle regulatory factors (MRFs), with the addition of a conditioned medium from differentiating C2C12 cells, which contains numerous soluble factors, such as IGF-II that promotes the myogenic differentiation process (6).

Significance: This study demonstrated the utility of demethylation to induce hAFSCs and hDPSCs to differentiate towards the myogenic lineage in vitro. Human AFSCs and DPSCs are suitable, non-controversial sources of stem cells that could be very useful for translational strategies to enhance the repair of injured skeletal muscle in DMD or trauma patients.

References: 1. Zhang et al. 2006. Tissue Eng 12, 2813. 2. De Coppi et al. 2007 Nat Biotechnol 25, 100. 3. Riccio et al. 2010. Eur J Histochem 54, 4. 4. N.S. Ye et al. 2006. Stem Cells Dev 15, 665. 5. Antonitsis et al. 2008 Thorac Cardiovasc Surg 56, 77. 6. Duan et al. 2010. Gen Comp Endocrinol 167, 344.

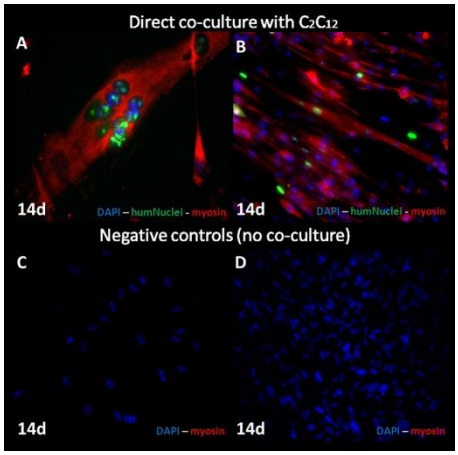

Analysis of co-culture of hAFSCs (A) and hDPSCs (B) with C2C12 cells after14 days of inducing

differentiation. Incorporation of hAFSCs and hDPSCs into myotubes stained against huNu (green), and MyHC (red). C, D. hAFSCs and hDPSCs not co-cultured with C2C12. Nuclei were stained with DAPI (blue).

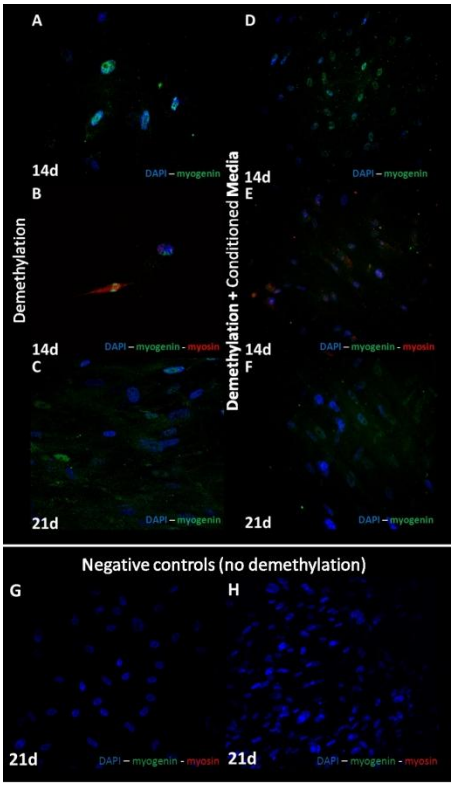

Analysis of myogenic differentiation of hAFSCs and hDPSCs after demethylation (A-C), and after demethylation plus conditioned medium from differentiating C2C12 (D-F). A-B, D-E. hAFSCs at day 14, positively stained with: myogenin (green) (A, D); myogenin (green) and MyHC (red) (B, E). C, F: hDPSCs at day 21, positive stained against myogenin (green).
G, H: hAFSCs and hDPSCs not demethylated. Nuclei were stained with DAPI.

IMAGE CAPTION:
Analysis of co-culture of hAFSCs (A) and hDPSCs (B) with C2C12 cells at 14 days of differentiation. Incorporation of hAFSCs and hDPSCs into myotubes stained against huNu (green), and MyHC (red). C, D. hAFSCs and hDPSCs not co-cultured with C2C12. Nuclei were stained with DAPI (blue).

Analysis of myogenic differentiation of hAFSCs and hDPSCs after demethylation (A-C), and after demethylation plus conditioned medium from differentiating C2C12 (D-F). A-B, D-E. hAFSCs at day 14, positive stained against: myogenin (green) (A, D); myogenin (green) and MyHC (red) (B, E). C, F: hDPSCs at day 21, positive stained against myogenin (green).
G, H: hAFSCs and hDPSCs not demethylated. Nuclei were stained with DAPI.

Proliferation and Differentiation Capacities of Muscle Derived Stem/Progenitor Cells Cultured on Polydimethylsiloxane Substrates of Varying Elastic Modulus and Protein Coating

Seth David Thompson[1], Mitra Lavasani[1,2], Bahar Ahani[1], Prerana Reddy[3], Yan Sun[4], Quentin Jallerat[4], Adam W. Feinberg[4,5], Johnny Huard[1,2].

[1]Stem Cell Research Center, Department of Orthopaedic Surgery, University of Pittsburgh, Pittsburgh, PA, USA,
[2]Department of Bioengineering, University of Pittsburgh, Pittsburgh, PA, USA,
[3]Department of Biological Sciences, Carnegie Mellon University, Pittsburgh, PA, USA,
[4]Department of Biomedical Engineering, Carnegie Mellon University, Pittsburgh, PA, USA,
[5]Department of Materials Science and Engineering, Carnegie Mellon University, Pittsburgh, PA, USA.

Abstract:

Introduction:

Muscle derived stem/progenitor cells (MDSPCs) are multipotent murine cells that display a capacity for long term proliferation. They have been utilized to regenerate bone[1], cartilage[2], skeletal[1] and cardiac muscles[3], as well as ameliorate the effects of aging[4]. MDSPCs are isolated and cultured on collagen I coated polystyrene flasks, but recent publications have shown that culturing progenitor cells on substrates with anatomically relevant elasticities and protein coatings can vastly alter their ability to proliferate and differentiate *in vitro* as well as engraft *in vivo*[5,6,7]. PDMS (polydimethylsiloxane) blends have shown to be a readily tunable substrate creating reproducible culture surfaces at anatomically relevant elasticities[7]. These blends can be adjusted across three orders-of-magnitude, surpassing what is capable with other hydrogel or PDMS systems. This study was designed to observe the effects of altering the culture surface conditions on MDSPCs *in vitro* and determine how to translate these findings to improve tissue regeneration with MDSPCs *in vivo*.

Methods:

Creating variable stiffness PDMS substrates and protein coated culture surfaces: PDMS substrates and protein coatings were prepared using previously defined methods7. Briefly, blends of Sylgard 527 and Sylgard 184 (Dow Corning) were mixed to create PDMS substrates with elastic modulus of 5 kPa, 50 kPa, 830 kPa, and 1.72 MPa. These blends were cured in 12 well plates with one of each protein coating, collagen type I (Col-1), collagen type IV and laminin (Col-4/Lam), or fibronectin (FN).

Proliferation of MDSPCs: MDSPC proliferation was investigated for 3 days on 12-well plates using a Live Cell Imaging (LCI) system. Time-lapse images were acquired every 15 minutes over 72 hours and cell numbers quantified at 6-hour intervals using ImageJ (NIH). Counts were averaged for each time point from at least 6 separate images and experiments were performed in duplicate.

Myogenic differentiation of MDSPCs: Myogenic differentiation potential was assessed by inducing *in vitro* myotubes formation after switching the proliferation medium (Dulbecco's modified Eagle's medium [DMEM] containing 10% fetal bovine serum [FBS], 10% horse serum, 1% Penicillin/Streptomycin, and 0.5% chick embryo extract) to fusion medium (DMEM containing 2% FBS and 1% penicillin/streptomycin). After 2-3 days, cells were fixed in cold methanol and immunostained for skeletal fast myosin heavy chain (f-MyHC)-positive myotubes (1:400, Sigma) and counterstained with DAPI (1:1000, Sigma). Images were taken on a Leica DM-IRB inverted microscope with a 20x objective.

Results:

Culture surfaces with PDMS substrates and protein coatings increase the proliferative capacity of MDSPCs: MDSPCs were observed on 13 separate combinations of protein coating and substrate elastic modulus, including the negative control of tissue culture plastic with no substrate or coating, to evaluate their effects on rate of proliferation (**Figure 1**). Significance in comparison to the negative control (plastic) is denoted with * ($p< 0.05$) and # ($p<0.001$). The highest proliferation rate from each group of substrate elastic modulus came from the condition including the coating of collagen type I. The combination of collagen type I coating on the 50 kPa PDMS provided the optimal condition for MDSPC proliferation.

Qualitative differences in myotube formation between substrate elasticities and protein coatings: MDSPCs were differentiated into myotubes on the various PDMS substrates and protein coatings for 2-3 days, displaying a dynamic range of myotube dimensions (**Figure 2**). MDSPCs cultured on collagen type I and collagen type IV/laminin coatings created more robust and elongated myotubes. Myotubes formed on stiffer substrates (830 kPa and 1.72 MPa) were more numerous, but also more slender, than their broader counterparts formed on softer PDMS.

Discussion:

These findings support the view that optimizing the *in vitro* environment, by modulating the surface culture conditions with a variable stiffness PDMS substrate and protein coating, can augment stem cell proliferation and differentiation capacities. Culture methods such as this may be used to prime MDSPCs towards specific lineages, by simulating tissue conditions of their natural niche, to improve cellular engraftment for therapeutic cell transplantations.

Significance:

Future cell therapies implemented for tissue repair may significantly benefit from the application of primary cells isolated and expanded on PDMS surfaces with protein coatings.

Acknowledgments:

This work was supported in part by the NIH, the Henry J. Mankin Endowed Chair at the University of Pittsburgh, and the Dowd-ICES Fellowship from Carnegie Mellon University.

References:

[1] Lee JY, et al., *J Cell Bio* 150, 1085-1100 (2000). [2] Kuroda R, et al., *Arthritis Rheum* 54, 433-422 (2006). [3] Oshima H, etl al., *Mol Ther* 12, 1130-1141. [4] Lavasani M, et al., *Nat Comm* 3: e608 (2012). [5] Gilbert PM, et al., *Science* 329, 1078-1081 (2010). [6] Engler AJ, et al., *Cell* 126, 677-689 (2006). [7] Palchesko RN, et al., *PLoS ONE* 7(12): e51499 (2012).

Figure 1

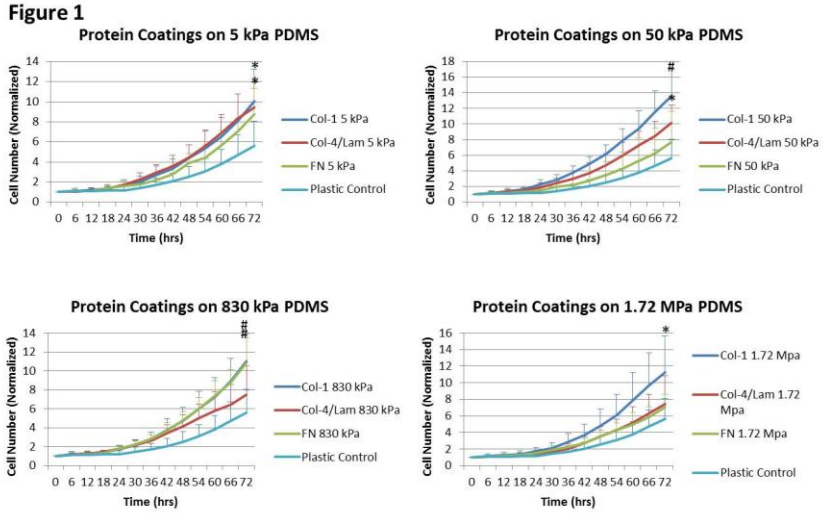

Figure 2

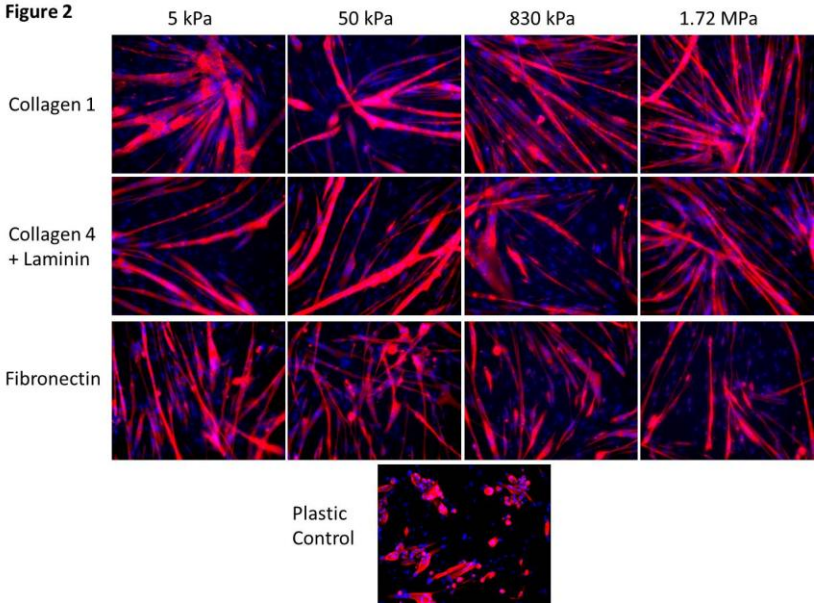

TITLE:
The role of non-myogenic mesenchymal stem cells (nmMSCs) in the skeletal muscle pathology of muscular dystrophy

AUTHORS:
Jihee Sohn, Ying Tang, Aiping Lu, Bing Wang, Johnny Huard
Department of Orthopaedic Surgery, University of Pittsburgh, Pittsburgh, Pennsylvania, United States, 15260 and Department of Bioengineering and McGowan Institute for Regenerative Medicine, University of Pittsburgh, Pittsburgh, Pennsylvania, United States, 15260. jhuard@pitt.edu

INTRODUCTION:
Adult skeletal muscle possesses a remarkable regenerative ability which largely depends on satellite cells. However, in severe muscular dystrophies, such as Duchenne muscular dystrophy (DMD), skeletal muscle integrity is debilitated and is often replaced by a mix of fibrous tissue and white adipocytes undergoing a process termed fatty degeneration. In recent publications, we demonstrated that in 6-8 wks old utrohpin/dystorhpin double knockout (dKO) mice, a severe animal model of DMD, the occurrence of ectopic fat, calcium deposits and fibrosis accumulation/infiltration in the skeletal muscle coincides with progressive muscle wasting and degeneration. These ectopic non-muscle tissues in skeletal muscle alter the tissue environment and induce deregulation of muscle homeostasis; however, the cellular origin of muscle fat formation is still unclear. Based on a previously published preplate technique, we isolated two types of muscle derived cells; PDGFRα+ mesenchymal stem cells (nmMSCs) and Pax7+ myogenic muscle derived stem cells (MDSCs) from the skeletal muscle of dKO mice. Previously, we showed that compared to MDSCs isolated from dKO mice, nmMSCs displayed significantly increased proliferation and adipogenic and osteogenic potentials *in vitro* and suggested nmMSCs as a major contributor to ectopic fat cell, calcium deposits and fibrotic tissue formation within dystrophic muscle. In the current study, we propose that nmMSCs may play an important role in regeneration/degeneration of dKO muscle. We observed significantly increased numbers of endogenous proliferating Ki67+ nmMSCs in the skeletal muscle of the dKO mice compared to age-matched wild-type (WT) mice. We investigated the possibility of cross-talk between the MDSCs and nmMSCs using a co-culture assay and demonstrated that the limited myogenic potential of the dKO-MDSCs was further reduced when they were co-cultured with dKO-nmMSCs. In addition, we observed a reduction in the expression of genes that regulate myogenesis in the dKO-MDSCs co-cultured with nmMSCs. On the other hand, myogenic differentiation of dKO-MDSCs was significantly enhanced after co-culturing them with WT-nmMSCs. qRT-PCR analysis of secreted frizzled-related protein 1 (sFRP1), a known inhibitor of myoblast differentiation, from 6wks old WT- and dKO –nmMSCs indicated that the sFRP1 expression was significantly increased in dKO-nmMSCs compared to that of WT-nmMSCs. Taken together, we propose the hypothesis that signals originating from nmMSCs may contribute to the micro-environment limiting myogenic differentiation of MDSCs in dKO muscle and sFRP1 may be soluble mediator of functional interaction between MDSCs and nmMSCs. Results from this study could provide insight into new approaches to alleviate muscle weakness and wasting in DMD patients by inhibiting the proliferation of nmMSCs in dystrophic muscle.

METHODS:

Cell Isolation: Cells were isolated from dKO (dys-/-utro-/-) mice at 6 weeks of age, as previously described via a modified preplate technique [1]. After 2hrs, the nmMSCs were obtained while the MDSCs were obtained after 7 days. Both cells were cultured in proliferation medium (PM, DMEM supplemented with 10% fetal bovine serum, 10% horse serum, 0.5% chicken embryo extract and 1% penicillin-streptomycin).

Immunofluorescence and histology: Cryosections were fixed with 5% formalin for 8 minutes and blocked with 10% donkey serum for 1 hour. Slides were then incubated with rabbit anti-mouse Ki67 (1:200, Abcam) and goat anti PDGFRα (1:100, R&D) in 5% donkey serum. Next, sections were incubated with secondary antibodies including 594-conjugated anti-rabbit IgG (1:300, Invitrogen) and 488-conjugated anti-goat IgG (1:300, Invitrogen) in PBS for 45 minutes.

Co-culture assay: 10,000 dKO-MDSCs were plated in the lower compartment of Transwell Permeable Supports and 10,000 WT/dKO-nmMSCs were seeded into transwell inserts in PM media. To measure the differentiation potential of dKO-MDSCs 48 hours after co-culture, PM media was switched to differentiation media (DMEM medium supplemented with 2% FBS) for 3 days. Three days after differentiation, cells were fixed with 10% formalin for 8 min, and stained for fast myosin heavy chain (fMyHC) using a mouse anti-MyCHf antibody (1:250, M4276, Sigma-Aldrich) with a mouse-on-mouse (M.O.M) staining kit (Vector Labs, Burlingame, CA), according to manufacturer's directions.

mRNA analysis was performed via reverse transcriptase, real-time (RT-PCR): Total RNA was obtained from WT- and dKO-nmMSCs using TRizol reagent (Invitrogen) and a RNeasy Mini Kit (Qiagen, Valencia, CA) according to the manufacturer's instructions. Reverse transcription was performed using a Maxima first strand cDNA synthesis kit (Fermentas) according to the manufacturer's protocol. PCR reactions were performed using an iCycler Thermal Cycler (Bio-Rad) as previously described. RT-PCR was carried out using the Maxima Syber Green Assay kit (Thermo Scientific) with an iQ5 thermocycler (Bio Rad).

RESULTS:

Increased in vivo proliferation potential of nmMSCs isolated from old dKO mice. We examined the proliferation of nmMSCs *in vivo* and performed immunohistochemistry for PDGFRα and Ki67 in the gastrocnemius of 6wk old WT and dKO mice. PDGFRα^{+} nmMSCs were localized in the interstitial space between muscle fibers of skeletal muscle. Our results indicated that the number of PDGFRα^{+}Ki67^{+} nmMSCs was about 3 fold higher in the dKO skeletal muscle when compared to age-matched WT muscles (Figure 1).

dKO-nmMSCs may inhibit myofiber regeneration of MDSCs in dKO mice. MDSCs isolated from 6-8 wks old dKO mice were co-cultured with age-matched dKO-nmMSCs, using a transwell system and the fusion index of dKO- MDSCs was monitored and compared to that of dKO-MDSCs cultivated alone. We observed that the limited myogenic potential of the dKO-MDSCs was further exacerbated after co-culture with dKO-nmMSCs. fMyHC expressing myotubes were significantly decreased when dKO-MDSCs were cultured in the presence of dKO-nmMSCs compared to dKO-MDSCs alone. When dKO-MDSCs were co-cultured with WT-nmMSCs, the myogenic potential of dKO-MDSCs was significantly enhanced (Figure 2).

Increased sFRP1 gene expression in dKO-nmMSCs. Using qRT-PCR, we observed 6 folds increase in the expression of sFRP1 in the dKO-nmMSCs compared to that of WT-nmMSCs.

DISCUSSION:

Previously, we observed accumulation of lipids, ectopic calcium deposits, and fibrotic tissue in skeletal muscle of 6-8 wks old dKO mice[2]. We have suggested that nmMSCs residing in the skeletal muscle may be responsible for these ectopic non-muscle tissues accumulated in dKO muscle since nmMSCs displayed significantly increased proliferation and adipogenic and osteogenic differentiation potentials *in vitro*. In the current study, we showed that the number of endogenous nmMSCs was significantly increased in 6wks old dKO skeletal muscle compared to age-matched WT, suggesting that nmMSCs may have a role in muscle regeneration/degeneration in dKO mice. Co-culture assay indicated that dKO-nmMSCs further exacerbate the limited myogenic differentiation potential of dKO-MDSCs, while WT-nmMSCs enhance myogenesis of dKO-MDSCs. A significantly increased gene expression level of sFRP1, which is known to block myoblast differentiation [3], was observed in dKO-nmMSCs compared to WT-nmMSCs suggested that sFRP1 secreted from dKO-nmMSCs may play a role in limiting the myogenic potential of dKO-MDSCs.

SIGNIFICANCE:

Despite the underlying pathogenesis is well studied, DMD is among the most difficult disease to treat. In DMD, the accumulation of intramuscular fat, calcium deposits, and fibrotic tissue represent the hallmarks of advanced disease and the presence of this non-muscle tissue significantly affects muscle structure, function, and recovery. Previously, we showed that nmMSCs may be responsible for accumulation of lipid, calcium deposits, and fibrotic tissue in dKO mice. In this study, we suggest that cells responsible for forming adipocytes and ectopic bone in dystrophic muscle may also inhibit the myogenic potential of muscle progenitor cells, including MDSCs, hindering muscle regeneration. Results from this project could provide insight into new approaches to alleviate muscle weakness and wasting in DMD patients by inhibiting the proliferation of nmMSCs in dystrophic muscle.

REFERENCE:

1. Gharaibeh, B., et al., *Isolation of a slowly adhering cell fraction containing stem cells from murine skeletal muscle by the preplate technique.* Nat Protoc, 2008. **3**(9): p. 1501-9.
2. Lu, A., et al., *Rapid depletion of muscle progenitor cells in dystrophic mdx/utrophin-/- mice.* Hum Mol Genet, 2014.
3. Descamps, S., et al., *Inhibition of myoblast differentiation by Sfrp1 and Sfrp2.* Cell Tissue Res, 2008. **332**(2): p. 299-306.

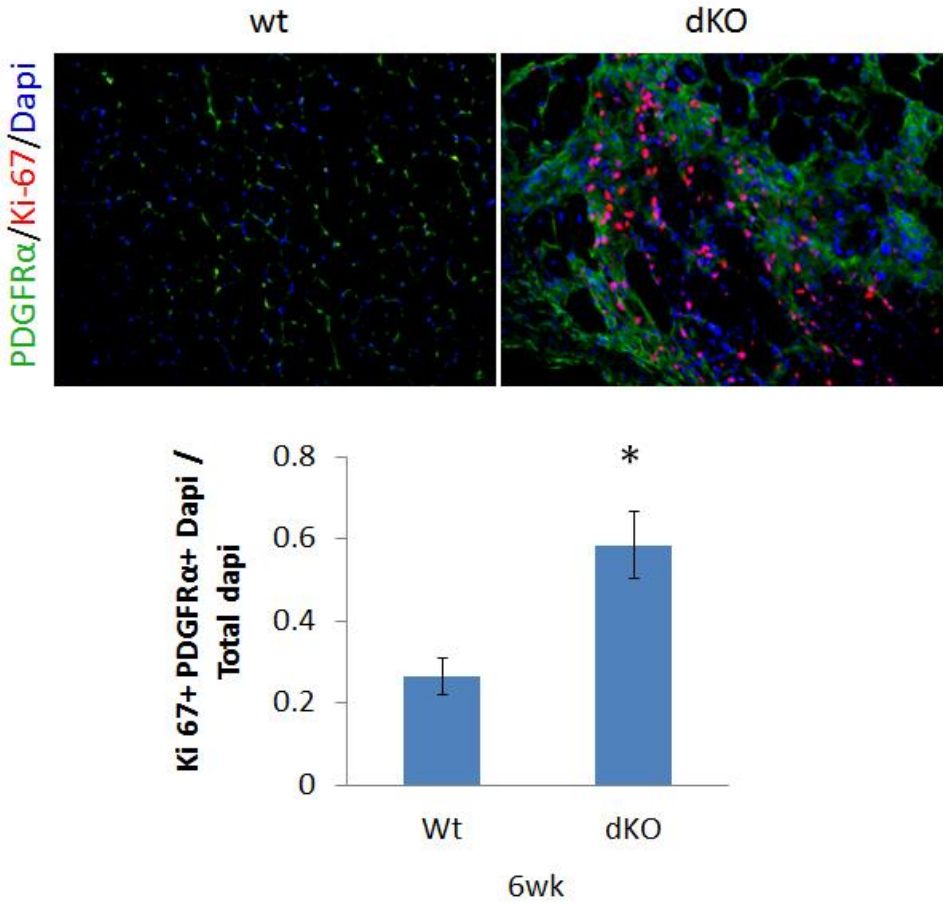

Figure 1. Immunohistochemistry for PDGFRα (green) and Ki-67 (Red) in the skeletal muscle of 6wks old WT and dKO mice (Top). Quantification indicated by the ratio of PDGFRα and Ki67 expressing Dapi to total Dapi counts (Bottom). (* $p<0.005$)

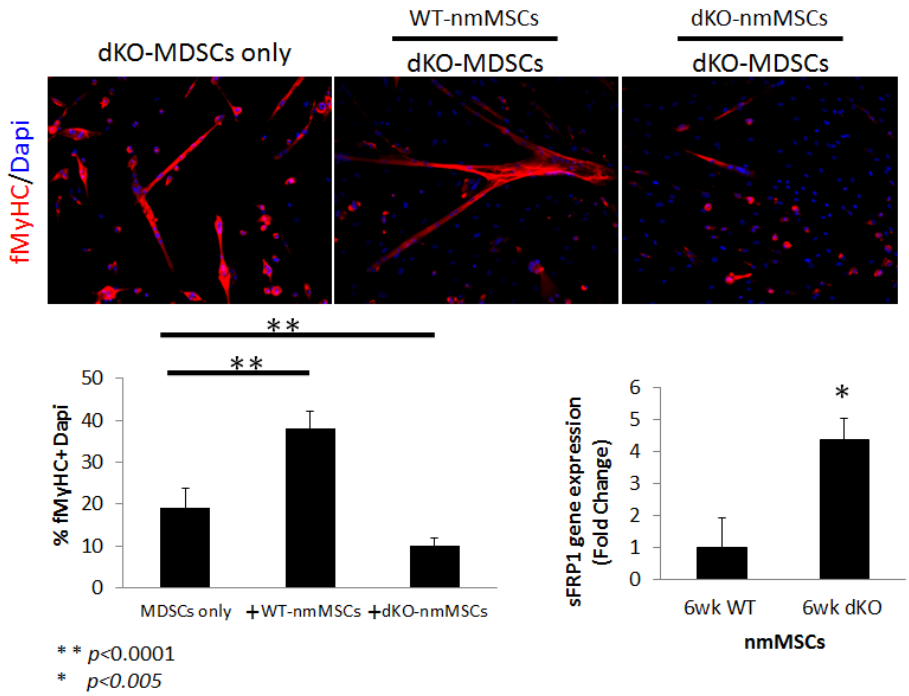

Figure 2. dKO-MDSCs and WT-/dKO-nmMSCs were co-cultivated using collagen type 1 coated transwell insert for myogenic differentiation. Immunohistochemistry of fMyHC was performed for detection of myotube formation (Top). Quantification of percentage myotube formation of dKO-MDSCs after 3 days of myogenic differentiation with/without Wt-/dKO-nmMSCs co-cultivation (Bottom left). qRT-PCR analysis was performed and the sFRP1 expression was compared from WT- and dKO-nmMSCs isolated from 6wks old animals (Bottom right).

1. Gharaibeh, B., et al., *Isolation of a slowly adhering cell fraction containing stem cells from murine skeletal muscle by the preplate technique.* Nat Protoc, 2008. **3**(9): p. 1501-9.
2. Lu, A., et al., *Rapid depletion of muscle progenitor cells in dystrophic mdx/utrophin-/- mice.* Hum Mol Genet, 2014.
3. Descamps, S., et al., *Inhibition of myoblast differentiation by Sfrp1 and Sfrp2.* Cell Tissue Res, 2008. **332**(2): p. 299-306.

Appendix 16

Interaction between myogenic and non-myogenic progenitor cells during muscle regeneration

Aiping Lu; Jihee Sohn; Berkcan Akpinar; Johnny Huard[1*]
Department of Orthopaedic Surgery, University of Pittsburgh, Pittsburgh, PA 15219, USA

Introduction

Efficient muscle regeneration is dependent on the coordinated responses of multiple cell types. During the muscle healing process, muscle progenitor cells (MPCs) are activated and an expanding population of myoblasts interact with inflammatory and stromal cells. It seems likely that these interactions are important for regulating their activity. The role of inflammatory cells in muscle regeneration has been reported [1]; however, there is little known about the contributions of other tissue-resident cell populations. By using the preplate technique we are able to isolate different populations of cells from skeletal muscle based on their variable adhering capacities. A slowly adhering fraction of cells (PP6) contains a heterogeneous population of stem and progenitor cells that display high myogenic potential [2]. In this study, we characterized a rapidly adhering cell population (PP1) that has a poor myogenic capacity and found that they express markers of fibro/adipogenic progenitor (FAPs) cells and mesenchymal stem cell (MSCs) including: Platelet-Derived Growth Factor Receptors (PDGFR), CD34, CD90, CD105 and Sca-1. Interestingly, when PP6 cells are cultured in PP1 differentiation condition medium (DCM), i.e. medium supplemented with 2%FBS in which the PP1 cells have been allowed to grow in for 3 days, the myogenic potential of the PP6 cells significantly increased. Furthermore the PP1 cells promoted muscle regeneration when transplanted along with the PP6 cells into the dystrophic muscle of MDX/SCID mice. Our results suggested that interactions between resident muscle mesenchymal stem cell like cells (PP1) and muscle progenitor cells (PP6), contribute to efficient muscle regeneration, thus combining both cell types could be used as a potential clinical strategy for the treatment of muscle diseases.

Methods

Cell Isolation: PP1 and PP6 cells were isolated from C57BL/10J at 3-6 week of age, as previously described via a modified preplate technique[3].

DCM collection: $6x10^5$ of PP1cells were cultured with proliferation medium for 3 days, and then, switch to fusion medium (DMEM containing 2% FBS). Three days later the medium was collected.

Myogenic differentiation assay: The myogenic differentiation capacity of the PP6 cells was assessed by switching the proliferation medium into fusion medium. After 3 days, the cells were stained for fast myosin heavy chain (MyHCf). Myogenic differentiation levels were quantified as the percentage of the number of nuclei in MyHC positive myotubes relative to the total number of nuclei.

Pax7 staining and flow cytometry cell analyses: A MOM kit was used for Pax7 staining following the manufacturer's protocol. Flow cytometry was used to analyze the expression of PDGFR and CD34, The cell suspension was divided into equal aliquots and centrifuged, and then re-suspended in a 1:10 dilution of mouse serum in PBS, and incubated for 10 minutes. FITC-conjugated rat anti-CD34, PE-conjugated rat anti-PDGFR was added and incubated an additional 30 minutes. Just before analysis, propidium iodide was added for dead cell exclusion and live cell events were collected and analyzed.

Cell implantation and dystrophin staining*:* A total of 3×10^5 PP6 cells alone were injected into the left gastrocnemius muscles (GM) and 3×10^5 PP1 cells + 3×10^5 PP6 cells were injected into the right GM of 8 week-old MDX/SCID mice. The PP1cells were labeled with red fluorescent dye before injection. Two weeks after implantation, the mice were sacrificed and the GM muscles were harvested and sectioned. Cryosections were fixed with 5% formalin and blocked with 5% donkey serum in PBS for 1 hour, then incubated with rabbit anti-dystrophin (1:300) for 2 hours at RT. The sections were exposed to a secondary 594- conjugated anti-rabbit IgG (1:500) for 30 minutes. The nuclei were revealed by DAPI staining.

Results

PP1 and PP6 expressed different cell markers: To identify progenitor lineages from dissociated skeletal muscle, we used flow cytometry to detect PDGFR and CD34, which is expressed by FAPs, and immuno-staining to detect the muscle progenitor cell marker Pax7. The data from flow cytometry showed that the PP1 cells are highly PDGFR and CD34 positive while the PP6 cells were PDGFR negative (**Fig.1**). The PP1 cells also expressed several MSC markers including CD105, CD90 and Sca-1(data not shown). Immuno-staining data showed PP6 cells were highly Pax7 positive, while PP1 cells were Pax7 negative (**Fig.1**). These results suggest that the preplate technique is able to prospectively identify myogenic progenitors (PP6) and mesenchymal like cells (PP1).

PP1 cells promote the myogenic differentiation of PP6 cells in vitro and muscle regeneration in vivo: After the PP6 cells were cultured in PP1 DCM, MyHC staining demonstrated that a greater number of cells fused and formed significantly larger myotubes in the PP6 cultures grown in the DCM compared to control group that were grown in non-DCM fusion medium **(Fig.2**). To determine whether combing PP1 and PP6 cells would increase the engraftment and muscle regenerative capacity of PP6 cells, we intramuscularly implanted a combination of both cell populations into an immunocompromised model of Duchenne muscular dystrophy. In this *in vivo* study, we observed that significantly more dystrophin-positive myofibers were detected in the muscles injected with PP1 and PP6 together (dystrophin, green, **Fig.2**, PP1 cells were labeled with red fluorescent dye) than in the muscles injected with PP6 only (dystrophin, red, **Fig. 2)**, and the injection of PP1 cells resulted in no dystrophin positive fibers, which indicates that PP1 cells enhanced the muscle regenerative potential of the PP6 cells *in vivo*.

Discussion

Muscle regeneration requires the coordinated interaction of multiple cell types. Pax7 expressing MPCs have been implicated as the primary stem cell responsible for regenerating muscle, yet the interaction with other progenitor cells for muscle regeneration has not been evaluated. It has been reported that satellite cells, connective tissue fibroblasts and their interactions are crucial for muscle regeneration[4]. Here we describe that the preplate technique can be used for isolating different populations of muscle-resident progenitor cells. We identified mesenchymal like cells (PP1) and muscle progenitor cells (PP6), based on their specific markers and examined the interaction between these two cell populations. We found *in vitro* that PP6 cells cultured in the presence of PP1 DCM formed larger, more multinucleated myotubes than PP6 cells cultured in unconditioned differentiation medium. In addition, transplantation of PP6 and PP1 together increased dystrophin positive fibers in dystrophic muscle compared to the transplantation of PP6 alone. Our experiments demonstrated that PP1 cells promoted the myogenic differentiation of PP6 cells *in vitro* and muscle regeneration *in vivo*. Future studies will be conducted to further investigate what is being secreted by the PP1 cells that promote the myogenic potential of PP6 cells.

Significance:

Our findings strongly support a key role for PP1 cells in supporting myogenesis, suggesting that successful muscle regeneration requires the concerted action of multiple cell types.

Acknowledgements

This work was supported by grants from the National Institute of Health (NIH 1P01AG043376-01A1)

References:

1. **Arnold, L., et al., J Exp Med, 2007. 204(5): p. 1057-69.**
2. **Qu-Petersen, Z., et al., J Cell Biol, 2002. 157(5): p. 851-64.**
3. **Gharaibeh, B., et al., Nat Protoc, 2008. 3(9): p. 1501-9.**
4. **Murphy, M.M., et al., Development, 2011. 138(17): p. 3625-37.**

Mimicking the stem cell niche in diseased muscle by Notch activation

[1]Xiaodong Mu, [2]Jin Gao, [2]Yadong Wang, [1]Kurt Weiss, and [1]Johnny Huard
[1]Department of Orthopaedic Surgery, University of Pittsburgh;
[2]Department of Bioengineering, University of Pittsburgh

Introduction:

Exhaustion of functional muscle stem cells has been observed in both aged and diseased skeletal muscle (i.e., Duchenne Muscular Dystrophy/DMD) (1-3). Stem cell therapy has been widely studied for the treatment of different muscle diseases, but is still challenged by poor donor cell survival and self-renewal, limited engraftment, frequent fibrogenesis, and importantly, the rapid loss of their stem cell characteristics (stemness) during expansion. The stem cell niche in skeletal muscle is a nest of quiescent stem cells that is critical for maintaining the stemness of stem cells and a key molecular signature of the stem cell niche is activated Notch signaling, which prevents the early terminal differentiation of muscle stem cells (4-5). Importantly, Notch is critical for the potent regeneration potential of younger skeletal muscle and declines during muscle aging (6).

We hypothesized that the implantation of a biomaterial conjugated with a Notch activator (DLL1, a Notch ligand) could establish an artificial stem cell niche within diseased or aged skeletal muscle that could supply a self-renewable source of stem cells (**Figure 1)**. We posited that the DLL1 (a Notch activating ligand)-conjugated PCL (polycaprolactone, a biodegradable material for tissue engineering (7)) construct would lead to the sustained maintenance of the "stem cell niche-like" microenvironment for the seeded stem cells by improving their self-renewal and survival capacities through the anti-apoptotic effect of Notch, while maintaining the cells' stemness. Thus we believed that the transplanted stem cells would be more capable of migrating from the transplantation site prior to differentiating, which would result in the generation of a larger engraftment area.

Results:

1. DLL1 treatment of muscle stem cells exhibited increased proliferation and delayed myogenic differentiation. GFP-labeled MDSCs were treated with DLL1 (mouse): Fc (human) (rec) (200ng/mL) for 3 days. The proliferation potential of the MDSCs was found to be increased and myogenesis potential of the cells was decreased. <<Not sure I understand highlights…define Fc>>

2. MDSCs seeded in DLL1-conjugated PCL showed an accelerated proliferation rate compared to the MDSCs in the control PCL

GFP labeled MDSCs were seeded into the DLL-conjugated PCL or control PCL constructs and cultured in medium. At day 3, after cell seeding, there was a clear increase in the number of GFP-MDSCs observed in the DLL1-conjugated PCL.

3. Implantation of MDSC-seeded DLL1-congugated PCL into mdx mice resulted in improved muscle engraftment.

Ten days after the implantation of MDSC-seeded DLL1-congugated PCL or MDSC-seeded control PCL, there were more GFP+ cells in the DLL1 group, indicating an improvement in the proliferation of the implanted stem cells. There were also more dystrophin+ myofibers, indicating an improvement in muscle regeneration.

Figure 1

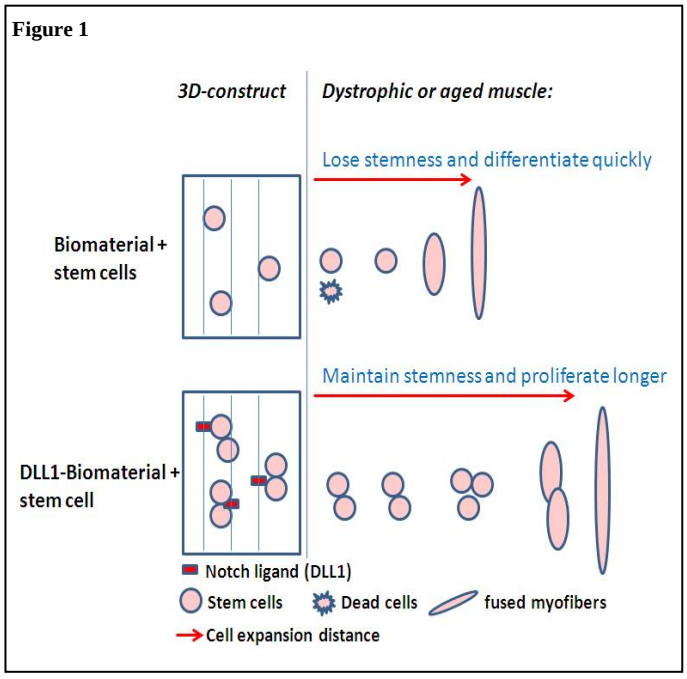

Discussion:

In the current study, the stem cell regulatory mechanism of the stem cell niche in the skeletal muscle was mimicked by conjugating activated Notch signaling to a 3D construct used for stem cell transplantation. With this system, we able to improve the outcome of stem cell transplantation, in the dystrophic skeletal muscle of dKO mice, through the optimization of the stem cell niche.

References:

1. Sacco A, Mourkioti F, Tran R, Choi J, Llewellyn M, Kraft P, et al. Short telomeres and stem cell exhaustion model Duchenne muscular dystrophy in mdx/mTR mice. Cell. 2010;143(7):1059-71. PMCID: 3025608.
2. Song M, Lavasani M, Thompson SD, Lu A, Ahani B, Huard J. Muscle-derived stem/progenitor cell dysfunction in Zmpste24-deficient progeroid mice limits muscle regeneration. Stem Cell Res Ther. 2013;4(2):33. PMCID: 3706820.
3. Lavasani M, Robinson AR, Lu A, Song M, Feduska JM, Ahani B, et al. Muscle-derived stem/progenitor cell dysfunction limits healthspan and lifespan in a murine progeria model. Nat Commun. 2012;3:608. PMCID: 3272577.
4. Bjornson CR, Cheung TH, Liu L, Tripathi PV, Steeper KM, Rando TA. Notch signaling is necessary to maintain quiescence in adult muscle stem cells. Stem Cells. 2012;30(2):232-42. PMCID: 3384696.
5. Brohl D, Vasyutina E, Czajkowski MT, Griger J, Rassek C, Rahn HP, et al. Colonization of the satellite cell niche by skeletal muscle progenitor cells depends on Notch signals. Dev Cell. 2012;23(3):469-81.
6. Conboy IM, Conboy MJ, Smythe GM, Rando TA. Notch-mediated restoration of regenerative potential to aged muscle. Science. 2003;302(5650):1575-7.
7. Dash TK, Konkimalla VB. Poly-small je, Ukrainian-caprolactone based formulations for drug delivery and tissue engineering: A review. J Control Release. 2012;158(1):15-33.

The Role of Muscle Progenitor Cell Exhaustion in the Rapid Disease Progression Observed in Dystrophic *mdx/utrophin*$^{-/-}$ Mice

Aiping Lu; Minakshi Poddar; Ying Tang; Jonathan D. Proto; Jihee Sohn; Xiaodong Mu; Nicholas Oyster; Bing Wang; Johnny Huard*

Department of Orthopaedic Surgery, University of Pittsburgh, Pittsburgh, PA 15219, USA

*To whom correspondence should be addressed: Department of Orthopaedic Surgery, University of Pittsburgh, Pittsburgh, Bridgeside Point 2, 450 Technology Dr. Pittsburgh, PA, 15219, USA. Tel: +1 412-648-2641; Fax: +1 412-648-4066; Email: jhuard@pitt.edu

Abstract

Duchenne muscular dystrophy (DMD) patients lack dystrophin from the time of birth; however, the muscle weakness only becomes apparent at 4-8 years of age, which happens to coincide with the exhaustion of the muscle progenitor cell (MPC) pool. Several lines of evidence support this observation including the gradual impairment of the myogenic potential of MPCs isolated from DMD patients as they age, which likely accounts for the reduction of muscle regeneration potential in older patients. In order to investigate whether the progression of muscular dystrophy is due to MPC exhaustion, we investigated two animal models of DMD, 1) dystrophin/utrophin double Knock-Out (dKO) mice, which display a similar histopathological phenotype to DMD patients, and 2) dystrophin deficient *mdx* mice, the most commonly utilized model of DMD, with a relatively mild dystrophic phenotype. In contrast to age-matched *mdx* mice, we observed that the number and regeneration potential of MPCs, including early and late stage of MPCs in dKO mice, rapidly decline during the rapid progression of the disease. In fact, early MPCs isolated from 6 week old dKO mice have reduced proliferation, resistance to oxidative stress, and multilineage differentiation capacities compared to MPCs isolated from age-matched *mdx* mice, an effect potentially mediated by fibroblast growth factor over expression and/or a reduction in telomerase activity. Our results demonstrate that the rapid disease progression in the dKO model is associated, at least in part; to MPC exhaustion. Preventing MPC exhaustion could represent an approach to delay the onset of the histopathologies in DMD patients.

Introduction

Duchenne muscular dystrophy (DMD), an X-linked progressive muscle wasting disease is caused by a deficiency of dystrophin, a cytoskeletal protein that is essential for the stability of the membrane of multinucleated myofibers in skeletal muscle (1). DMD is the most common form of muscular dystrophy, occurring in approximately 1 out of 3,300 boys (2). In DMD patients, the loss of sarcolemmal dystrophin promotes muscle fiber damage during muscle contraction (3-8). This process results in an efflux of creatine kinase (CK), an influx of calcium ions, and the recruitment of T cells, macrophages, and mast cells to the damaged muscle, causing progressive myofiber necrosis, fibrosis, and muscle weakness (8). An absence of dystrophin leads to the patient losing the ability to independently ambulate by the middle of their second decade of life, and the patient's death, due to cardiac or respiratory failure, by their third decade (9). Normally, skeletal muscle possesses a robust regenerative capacity due to the presence of adult muscle progenitor cells (MPCs), which play an important role in postnatal muscle growth and repair.

Many MPC populations have been reported with various myogenic potentials; however, their origin and relationship to each other remains unclear. Satellite cells, which are located between the basal lamina and muscle fiber plasma membrane (10), were first defined as the major source of MPCs that regulate most of postnatal skeletal muscle growth and regeneration (10-12); however, other myogenic progenitors, such as bone marrow-derived circulating stem cells and cell populations residing in the muscle interstitium and blood vessel walls have also been identified as potential cell populations for muscle repair (13-18). These non-satellite cell progenitors are capable of adopting a skeletal myogenic fate following engraftment into damaged or diseased muscle. Researchers have isolated MPCs utilizing a variety of different methods including cell culture selection techniques, flow cytometry-based sorting using cell surface markers, and Hoechst dye exclusion (19-23). Our research group has reported the isolation of muscle derived stem cells (MDSCs), based on their adhesion characteristics, through the use of the preplate technique (24). These MDSCs are capable of undergoing multiple lineage differentiation (22, 25-27) and have been shown to be superior for muscle regeneration than myoblasts (24). Myoblasts are more committed toward a myogenic lineage (late muscle progenitors) and readily fuse together or with injured mature myofibers to regenerate injured muscle.

In DMD, recurrent myofiber damage elicits a constant need for regeneration, thus giving way to the exhaustion of the MPC pool and the loss of functional muscle regeneration. Eventually, muscle tissue is replaced by fibrotic tissue, calcium deposits, and adipose tissue accumulation that plays a critical role in the wasting process observed in DMD (28). Notably, despite the lack of dystrophin at birth, the onset of muscle weakness in DMD patients does not occur until 4-8 years of age, which happens to coincide with the exhaustion of the MPC pool. Previous studies have shown that myoblasts in DMD patients are impaired and exhibit a severe proliferation deficit *in vitro* which becomes more pronounced with patient age (29, 30); hence, we can theorize that DMD represents a form of accelerated aging that occurs primarily in skeletal muscle.

The *mdx* mouse is the most widely used animal model of DMD, and like DMD patients, the *mdx* mouse lacks dystrophin due to a point mutation in the dystrophin gene (9, 31, 32); however, these mice only exhibit a mild dystrophic phenotype, in contrast to DMD patients. In fact, these mice often live up to 2 years of age, which is comparable to the life span of normal wild type (WT) mice. Furthermore, *mdx* mice do not exhibit the rapid loss of muscle strength and early death observed in DMD patients (33, 34). In addition, various features such as, pseudohypertrophy, scoliosis, and cardiomyopathy, typical of DMD patients, are not observed in young *mdx* mice (35-37). Although the reason by which the mdx mice do not recapitulate the DMD phenotype is still unclear, it has been suggested that *mdx* mice compensate for the lack of dystrophin by up-regulating utrophin, a protein structurally similar to dystrophin (38-40). Utrophin localizes to the sarcolemma of skeletal muscle fibers during fetal development, but after birth, dystrophin replaces utrophin at the myofiber sarcolemma; while, utrophin persists at neuromuscular and myotendinous junctions (NMJ and MTJ) under homeostatic conditions (41, 42). The utrophin expression around the sarcolemma of regenerating myofibers in adult *mdx* skeletal muscle is believed to compensate for the dystrophin deficiency (39, 40, 43). Previous studies have reported that dystrophin and utrophin double-Knock Out (dKO) mice (*dystrophin*$^{-/-}$ */utrophin*$^{-/-}$) share many more of the histopathological symptoms of DMD patients, than do the *mdx* mice (44).

In this study, we tested the hypothesis that the rapid progression of muscular dystrophy seen in DMD patients is associated with a rapid exhaustion of muscle progenitor cells. In support of this contention, it has been recently reported that *mdx* mice lacking the RNA component

telomerase in specifically targeted muscle cells (*mdx*/mTR) have shortened telomeres in their MPCs and develop a more severe form of the muscular dystrophy phenotype that progressively worsens with age, when compared to standard *mdx* mice, which was shown to be due to the rapid exhaustion of the MPCs (45).

For our investigation, we used the dKO mouse model, and compared this model to *mdx* mice in order to further investigate whether the rapid progression of the disease in the dKO mice is associated, at least in part, with an exhaustion of MPCs. Our results indicated that the dKO mice show a much more severe muscle histopathology than *mdx* mice, including the accumulation of muscle necrosis, fibrosis, as well as calcium deposits within their skeletal muscle tissues. Following weaning, dKO mice experience weight loss, progressive loss of muscle force, kyphosis, and a shortened life span. Importantly, we show here that the severity of the phenotype in dKO mice progressively worsens with age and is associated with the exhaustion of MPCs including early and late myogenic progenitors (MDSCs, satellite cells and myoblasts) (24, 46). In addition, we also observed that Fibroblast Growth Factor 2 (FGF2) expression increased and telomerase activity decreased in the muscles of the dKO mice compared to muscles of age-matched *mdx* mice. These results suggest that high FGF expression may promote a decline in stem cell number and function during disease progression, and insufficient telomerase activity can result in progressive telomere shortening which ultimately can lead to cellular senescence. This finding supports our hypothesis that the pathology associated with the dKO phenotype is initiated by both dystrophin and utrophin deficiency, but the rapid progression of the disease is associated with stem cell exhaustion which results in a severe dystrophic phenotype. Taken together, these observations suggest that preventing the exhaustion of the MPC pool could be a novel approach to delay the muscle histopathological symptoms in DMD patients.

Materials and methods

Animals

dKO mice are generated by crossing (utr+/−, dys−/−) mice, which have been obtained by crossing utr−/− mice with *mdx* mice (44) in our lab (36, 47). Wild type mice (C57BL/10J) were ordered from Jackson Laboratories. All animal protocol used for these experiments were approved by the University of Pittsburgh's Animal Care and Use Committee.

Isolation of MDSCs from wild type, mdx and dKO mice

The mice were sacrificed at 6-8 weeks of age, and MDSC isolation was performed as previously described via a modified preplate technique (48, 49). Briefly, the skeletal muscle tissue was minced and processed through a series of enzymatic dissociations: 0.2% of collagenase type XI (C7657, Sigma-Aldrich) for 1 hour, 2.4 units/ml of dispase (17105-041, Invitrogen) for 45 minutes, and 0.1% of trypsin-EDTA (15400-054, Invitrogen) for 30 minutes at 37°C. After enzymatic dissociation, the muscle cells were centrifuged and resuspended in proliferation medium (Dulbecco's modified Eagle's medium (DMEM, 11995-073, Invitrogen) supplemented with 10% fetal bovine serum (FBS, 10437-028, Invitrogen), 10% horse serum (HS, 26050-088, Invitrogen), 0.5% chicken embryo extract (CEE, CE650T-10, Accurate Chemical Co.), and 1% penicillin-streptomycin (15140-122, Invitrogen). The cells were then plated on collagen type I (C9791, Sigma-Aldrich) coated flasks. Different populations of muscle-derived cells were isolated based on their variable adhesion characteristics. After 7 days, late preplate populations (slow-adhering cells) were obtained and cultured in proliferation medium, which have previously been described to contain the MDSC fraction of cells (24).

Immunostaining flow cytometry and cell sorting analyses

Fluorescence-activated cell sorting (FACS Aria II SORP; BD) was used to analyze the expression of CD34, Sca-1 (stem cell antigen-1), and CD45. The mice were sacrificed at 6-8 weeks of age and muscle cell isolation was performed as previously described via a modified preplate technique (48, 49). After enzymatic dissociation, the muscle cells were centrifuged and resuspended in proliferation medium, and then plated on collagen type I coated flasks. After 24 hours, the floating cells were collected, which contain the myogenic progenitor cells, centrifuged, washed with PBS containing 2% FBS, and counted. The cell suspension was divided into equal

aliquots and centrifuged, and then placed on ice and re-suspended in a 1:10 dilution of mouse serum (M5905, Sigma-Aldrich) in PBS. The suspensions were incubated for 10 min. FITC-conjugated rat anti-CD34 (553733, BD), PE-conjugated rat anti-Sca-1(553108, BD), and APC-conjugated rat anti-CD45 (729744, Invitrogen) rat anti-mouse monoclonal antibodies were added to each tube for an additional 30min incubation. Just before analysis, propidium iodide (PI, 556463, BD) was added to each tube for dead cell exclusion and live cell events were collected and analyzed. CD34+/Sca-1-/CD45- cells were sorted after analysis. A single color antibody was used to optimize fluorescence compensation settings for multi-color analyses and sorts.

Single fiber isolation

Mice were sacrificed at 6-8 weeks of age and the extensor digitorum longus (EDL) muscles were isolated from dKO and *mdx* mice and incubated in a solution of 0.2% collagenase type I (C5894, Sigma-Aldrich) for 50 minutes at 35°C while shaking the mixture at 40rpm. When the muscles were sufficiently digested they were triturated with heat polished glass pipettes to liberate single fibers. The muscle fibers were then transferred to a matri-gel (354234, Fisher) coated 24 well plate with proliferation medium.

In vitro assessment of cell proliferation

In order to compare the proliferative potential of the dKO MDSCs to wild type (WT) and *mdx* MDSCs, we used a previously described Live Cell Imaging system (Kairos Instruments LLC)(50, 51). Bright field images were taken at 100× magnification at 10min intervals over a 72-hour period in three fields of view per well, with three wells per population. Proliferation was assessed by manually counting the number of cells per field of view over 60 hours.

Myogenic differentiation assay and fast myosin heavy chain staining

The cells were plated on 24 well plates (30,000 cells/well) with DMEM supplemented with 2% FBS to stimulate myotube formation. Three days after plating, immunocytochemical staining for fast myosin heavy chain (MyHCf) was performed. After rinsing two times with PBS, cells were fixed for 2 minutes in cold methanol (-20°C), blocked with 10% horse serum (S2000, Vector) for 1 hour and then incubated with a mouse anti-MyHCf (M4276, 1:250; Sigma-Aldrich) antibody for 2 hours at RT. The primary antibody was detected with a 594-conjugated anti-mouse IgG

antibody (A21203, 1:500; Molecular probes) for 30 minutes. The nuclei were revealed by 4, 6-diamidino-2- phenylindole (DAPI, D9542, 100ng/ml, Sigma-Aldrich) staining. The percentage of differentiated myotubes was quantified as the number of nuclei in MyHCf positive myotubes relative to the total number of nuclei. This method was also used for analyzing myotube formation from single muscle fibers.

Survival analyses of MDSCs

Cells were exposed to oxidative stress by treating them with 400uM hydrogen peroxide. In order to visualize cell death, propidium iodide (PI), a DNA-binding dye, was added to the culture medium according to manufacturer's protocol (BD Bioscience). Using the LCI system described above, 100x bright field and fluorescence images were taken at 10 minute intervals over 24 hours. Identifying the number of PI+ cells per field of view out of the total cell number determined the percentage of cell death over time.

Histochemistry & Immunocytochemistry

In vitro: MPCs migrating off of the single myofibers were stained for the myogenic marker desmin at 96 hours after the single fibers attached to the matri-gel coated 24 well plates. The myofibers and cells were fixed in 5% formalin for 5min and blocked with 10% donkey serum (017-000-121, Jackson ImmunoResearch) in PBS for 1h at room temperature (RT). Rabbit anti-desmin (D8281, 1:200; Sigma-Aldrich) was incubated for 3h at RT, followed by PBS washes and incubation with a secondary antibody, donkey anti rabbit IgG conjugated with Alexa Fluor 488 (A21206, 1:500, Molecular probes), for 30min. Nuclei were revealed with DAPI staining. Following desmin staining, the total number of desmin positive cells derived from each of the analyzed fibers was counted manually.

In vivo: Muscle samples were frozen in 2-methylbutane pre-cooled in liquid nitrogen and stored at –80°C. H&E, alizarin red, and trichrome staining were performed on ten micrometer cryosections from the gastrocnemius and diaphragm, according to the manufacturer's instructions. Cryosections from the gastrocnemius and diaphragm were also fixed in a 1:1 cold (–20°C) acetone/methanol mixture for 5min and pre-incubated in 10% donkey serum (017-000-121, Jackson ImmunoResearch) in PBS for 1h at RT. Primary antibodies and their dilutions in PBS are listed below: rat anti-F4/80 (MCA497R, 1:500; Secrotec); rabbit anti-FGF (500-P152, 1:200;

PeproTech); and rat anti mouse IgG (BA-2000, 1:300; Vector,). Fixed tissue sections were incubated with the primary antibodies for 3h at RT, followed by PBS washes and incubation with secondary antibodies, 594-conjugated donkey anti-rat IgG (A21209, 1:500; Molecular probes), 594-conjugated donkey anti-rabbit IgG (A21207, 1:500; Molecular probes), and 594-conjugated streptavidin (S-32356, 1:500; Molecular probes) for 30min at RT. A MOM kit (Vector, Inc.) was used for Pax7 and embryonic myosin heavy chain (eMyHC) staining following the manufacturers protocol. The Pax7 and eMyHC primary abs and their PBS dilutions are listed below: Mouse anti-eMyHC (F1.652C, 1:50; Developmental Studies Hybridoma Bank) and mouse anti-Pax7 (1:100, Developmental Studies Hybridoma Bank). Cy3-streptavidin (GEPA43001, 1:500, Sigma-Aldrich) was added to act as the tertiary antibody and the nuclei were stained with DAPI. All the stained sections were visualized on a Nikon Eclipse E800 fluorescence microscope. Ten random pictures per slide were taken and the number of Pax7+ cells and eMyHC+ myofibers were counted manually. The F4/80+ areas were measured and quantified as the percentage of F4/80+ macrophage infiltration area per image using Northern Eclipse software.

Adipogenesis assay

A total of 60,000 MDSCs were cultured on 24 well collagen type I coated plates for 21 days in adipogenic differentiation medium (PT-3004, Lonza). At 100% confluence, 3 cycles of induction/maintenance stimulated optimal adipogenic differentiation. Each cycle consisted of feeding the MDSCs with supplemented adipogenesis induction medium and cultured for 3 days followed by 1-3 days of culture in supplemented adipogenic maintenance medium. Then, MDSCs were tested for adipogenesis with AdipoRed reagent (NC9049267, 30ul/ml, Fisher) following the manufacturer's protocols.

Osteogenesis assay

A total of 50,000 cells were cultured in osteogenic medium (OM: control medium supplemented with dexamethasone (D2915, 0.1 µM, Sigma-Aldrich), abscorbic-acid-2-phosphate (A8960, 50 µg/ml, Sigma-Aldrich), and 10mM B-glycerophosphate (BMP2, G6251, 100ng/ml, Sigma-Aldrich). Cells were stained for calcium deposition (Alizarin Red) after 7 and 10 days of culture, respectively.

Chondrogenesis assay

MDSCs were centrifuged into pellets (250,000 cells/pellet) and cultured for 4 weeks in chondrogenic induction media (PT3003, 200ul/pellet, Lonza) supplemented with 100ng/ml BMP2 and 20ng/ml TGFβ3 (PHG9305, 20ng/ml, Invitrogen). Pellets were frozen in embedding medium and cryosectioned. The sections were then stained with alcian blue to confirm chondrogenesis. To further confirm that the pellets chondrogenecity, a GAG assay was performed to verify the presence proteoglycans.

Real-time PCR

Total RNA was isolated using TRizol Reagent (Invitrogen) and reverse transcribed using a Maxima first strand cDNA synthesis kit (Fermentas) according to the manufacturer's protocol. Real-time PCR was carried out using the Maxima SYBR® Green Assay kit (Fermentas) with an iQ5 thermocycler (Biorad). Primers were designed using PRIMER-Blast (NCBI) and can be found in Table 1.

Detection of telomerase activity in MDSCs

Telomerase activity in MDSCs was detected with a TeloTAGGG Telomerase PCR ELISA kit (11854666910, Roche) according the manufacturer's instructions. Briefly, MDSCs from 4-week old mdx and dKO mice were processed with the lysis reagent provided in the kit to prepare cell extracts. Cell extracts were then used to conduct the telomeric repeat amplification protocol (TRAP reaction), generating PCR products with telomerase-specific 6 nucleotide increments (TTAGGG). The amount of these PCR products depends on the telomerase activity in the cell extracts. The PCR products were then denatured and hybridized to a digoxigenin-(DIG)-labeled, telomeric repeat-specific detection probe. The PCR products were then detected with an antibody against digoxigenin (anti-DIG-POD). The signal intensity of the antibody was then read with an ELISA plate reader (Infinite M200, TECAN, Inc.).

Skeletal muscle functional measurements

Animals were anesthetized with 2-3% isoflurane and maintained in a surgical plane during the procedure with 1.5% isoflurane. The lower hind limbs were shaved and the animal was placed on

an *in situ* muscle physiology test apparatus (Model 806-B, Aurora Scientific) with only the right hind limb being tested. The animal was laid in a supine position and the foot was secured to the force plate with adhesive tape. The knee was positioned and secured at 90 degrees of flexion and the ankle was at 0 degrees of flexion. Twenty-seven gauge needle electrodes were placed intramuscularly into the tibialis anterior. Force-frequency curves were generated by stimulating the muscles with 9 volts at varying frequencies from 1Hz up to 200Hz with a 2 minute rest between each of the frequency stimulations. Data were recorded and analyzed with DMC software (Aurora Scientific).

Statistical analysis

All results are given as the mean ± standard deviation (SD). Means from dKO, *mdx*, or WT were compared using Student's *t*-test. Differences were considered statistically significant when the *P* value was < 0.05.

Results

Severe muscle histopathology in dKO mice

In order to assess the severity of muscular dystrophy in the dKO mice, we first characterized the histopathology that developed in the skeletal muscles of dKO mice (6-8 week old) and the results were compared to age-matched *mdx* and WT mice. H&E staining revealed large areas of necrotic fibers, massive cellular infiltration, and deposition of connective tissue with little evidence of regeneration (centrally nucleated fibers) in the dKO muscles, compared to WT and *mdx* muscle cross sections (**Fig. 1A**). Mouse IgG positive muscle fibers, which indicate necrotic muscle fibers, were markedly increased in the dKO muscles compared to the *mdx* and WT muscles (**Fig. 1B**). Aggregates of calcium deposition (**Fig. 1C**) and fibrosis (**Fig. 1D**) were substantially increased in the dKO muscles compared to the WT and *mdx* muscles. Together, these results indicate that, in contrast to age-match WT and *mdx* mice, the dKO mice rapidly developed a muscle histopathological phenotype similar to DMD patients.

We also observed that the dKO mice rapidly developed muscle histopathology similar to DMD patients, with marked kyphosis, weight loss (**Fig. 1E**), and shortened life span (**Fig. 1F**). These mice begin to die at 4-6 weeks of age, and very few dKO mice can live up to 9 weeks of age, whereas *mdx* mice do not show a life span difference compared to normal WT animals. To assess muscle performance, we measured the isometric torque of the anterior crural muscles and our results indicated that muscle function significantly decreased in the dKO mice in contrast to age matched WT and *mdx* mice (**Fig. 1G**). In order to account for the smaller size of the dKO mice, muscle function was normalized for body weight. This result provides direct evidence for severe muscle weakness of the dKO muscles. In contrast, the function of the anterior crural muscles from *mdx* mice were greater than the muscles from the WT control mice, which is consistent with a previous study that showed that young *mdx* mice have higher muscle mass and greater muscle function compared to age matched WT mice (52).

Muscle progenitor cells from dKO skeletal muscles are exhausted

To test whether the severe skeletal muscle damage seen in the dKO mice is associated with rapid muscle progenitor cell exhaustion, MPCs were isolated from the limb muscles of 6-8 week old dKO, *mdx*, and WT mice. Following a series of enzymatic digestions the muscle cells were seeded on collagen type I-coated flasks. The next day, the floating cells, which contain most of

the myogenic cells, were labeled with antibodies against CD34, Sca-1, and CD45, and subsequently analyzed by flow cytometry. The CD34+/Sca-1-/CD45- cells were classified as myogenic progenitor cells (53). Our analysis found that the percentage of CD34+/Sca-1-/CD45- cells from the dKO mice was significantly reduced when compared to age matched mdx and WT mice indicating that the number of myogenic progenitor cells are reduced in dKO skeletal muscle (**Fig. 2A, 2B**). The myogenic potential of the CD34+/Sca-1-/CD45- cell fractions were further confirmed for their ability to differentiate into myotubes (**Fig. 2C**).

Pax7 positive muscle satellite cells represent a population of myogenic progenitors responsible for postnatal growth, repair, and maintenance of skeletal muscle. We hypothesized that the severe muscle phenotype observed in dKO mice might be caused by defects in muscle satellite cell function. To test this possibility, we first analyzed the number of Pax7 positive cells in the diaphragm muscles from these animal models. The results showed that the number of Pax7 positive cells was significantly reduced in the diaphragm muscles of 8 week old dKO mice (**Fig. 2D**, **2E**) when compared to age matched mdx and WT mice. Moreover, the results from real-time PCR confirmed that there was a rapid, significant decline in Pax7 mRNA in the diaphragm muscles of dKO mice isolated from 4 to 8 week old mice when compared to that observed in the *mdx* and WT diaphragm muscles (**Fig. 2F**). Our results taken together demonstrated that myogenic progenitor cells including CD34+/Sca-1-/CD45- cells and Pax7 positive satellite cells undergo a rapid decline in the skeletal muscles of dKO mice during the progression of the disease. These data highlight that dKO muscle (6-8 weeks old) becomes more severely affected compared to age matched WT and *mdx* mice and the reduction of muscle progenitor cells correlates with the severe dystrophic phenotype observed in the dKO mice.

Impaired proliferation and differentiation of MPCs isolated from dKO single muscle fibers

To further determine whether the rapid progression of muscular dystrophy in dKO mice is caused by a reduction in their MPCs proliferation and differentiation potentials, we assessed the myogenic potential of cells derived from dKO single isolated muscle fibers. Single myofibers were isolated from the EDL muscles of 6-8 weeks old animals. First, we observed more damaged muscle fibers in the dKO muscles (53%±12%) compared to the *mdx* muscles (34%±8%) 24 hours after the single fibers attached to the matri-gel coated plates (**Fig. 3A**). The proliferative potential of the MPCs migrating from the isolated myofibers were analyzed after 4 days of

culture. Satellite cell derived cells were immunostained for desmin, an established myogenic marker. We observed the number of desmin positive cells from the single fibers was significantly decreased in the dKO mice compared to the *mdx* mice (**Fig. 3B, 3C**), indicating that the MPCs derived from the single myofibers of dKO muscle exhibited a reduced proliferative potential compared to the *mdx* MPCs. In addition, 7 days post-culturing, immunostaining for fast myosin heavy chain (MyHCf), a myogenic differentiation marker, was performed to determine the myogenic differentiation capacity of the MPCs. We observed that the MPCs released from the *mdx* muscle fibers formed more MyHCf+ multinucleated myotubes in contrast to those migrating from the dKO muscle fibers (**Fig. 3D, 3E, 3F**). These results support both a reduction in the proliferation and differentiation potentials of the MPCs derived from the dKO mice. The data shown here provides more evidence to suggest that defective proliferation and differentiation capacities of MPCs in dKO mice leads to a reduction in muscle repair, which is similar to DMD patients (29).

The function of myoblasts is also impaired in dKO mice

Next, we asked whether the severe muscle phenotype observed in the dKO mice was related to myoblast dysfunction. Utilizing the previously described preplate technique we isolated the different populations of MPCs including myoblasts from 6 week old WT, *mdx,* and dKO mice. We observed that the number of preplate (PP) 5 and PP6 cell populations isolated from the dKO muscle, which contain muscle stem cells (24, 54), was decreased (**Fig. 4A**). We further tested the rapidly adhering cell populations (PP3 and PP4), which contain mostly satellite cell-derived myoblasts (24, 54), for assessing their differentiation capacity *in vitro*. PP3 and PP4 cells were cultured in proliferation medium until the cells reached 80% confluence, at which point the culture medium was changed to differentiation medium (2% FBS). Three days later, immunofluorescent staining for fast skeletal myosin heavy chain was performed. In comparison with the PP3 and PP4 cells isolated from WT and *mdx* mice, which formed numerous, large multi-nucleated myotubes, the PP3 and PP4 populations isolated from the dKO mice formed fewer and smaller myotubes (**Fig. 4B**), which indicated that the myogenic differentiation potential of the dKO myoblasts was also significantly reduced relative to the myoblasts isolated from the *mdx* and WT mice ($P<0.05$) (**Fig. 4C**). This result demonstrated that myoblasts isolated

from dKO mice are also impaired in their differentiation capacity, which is similar to what is observed in myoblasts isolated from DMD patients.

The function of muscle derived stem cells isolated from dKO mice is defective

We next assessed slowly adhering cell populations which contain a heterogeneous population of stem and progenitor cells that we refer to as muscle derived stem cells (MDSCs) (24, 46). MDSCs display unique characteristics that are associated with non-committed progenitor cells. We have previously shown that MDSCs express markers associated with stem cells and are capable of self-renewing *in vitro* (24). Furthermore, MDSCs have been shown to be capable of replenishing myogenic progenitors when injected into dystrophic murine muscle and contribute to the persistent restoration of dystrophin within the transplanted muscles (24, 55). MDSCs were isolated from 6-8 week old dKO, *mdx*, and WT mice and their function was examined by measuring relative differences in their capacities for proliferation, myogenic differentiation, resistance to oxidative stress, and multiple lineage differentiation capacities. We examined the proliferation kinetics of cell populations *in vitro* using the LCI system described above (51) and observed a significant reduction in the proliferation capacity of the dKO MDSCs when compared to the *mdx* and WT MDSCs (**Fig. 5A**). In order to determine the myogenic differentiation capacity of the MDSCs isolated from the dKO, *mdx*, and WT mice *in vitro*, equal numbers of cells from each group were plated in a 24-well plate and switched to differentiation medium once the cells adhered. After 3 days, the majority of the WT (69%) and *mdx* cells (80%) had differentiated into myotubes, as determined by immunodetection of MyHCf (**Fig. 5B**). The differentiation potential of the dKO MDSCs was observed to be significantly lower, compared to the WT and *mdx* MDSCs ($P < 0.01$; **Fig. 5C)**. Next, we examined cellular resistance to hydrogen peroxide-induced oxidative stress. Each of the populations (dKO, *mdx*, and WT) were exposed to 400μM hydrogen peroxide in proliferation medium containing PI, and the LCI system was used to identify the number of PI+ cells in order to determine the percentage of cell death. In comparison with MDSCs isolated from the *mdx* and WT mice, the dKO MDSCs displayed a reduced resistance to oxidative stress (**Fig. 5D**). Furthermore, the ability of the MDSCs to undergo multi-lineage differentiation was examined, and the results indicated that there was a reduction in the adipogenic, osteogenic, and chondrogenic differentiation capacities of the MDSCs isolated from the dKO mice compared to the MDSCs isolated from the *mdx* and WT

mice (**Fig. 5E**). Together, these data suggest that the functionality of the MDSCs isolated from the dKO mice was severely affected when compared to WT and *mdx* mice.

Impaired muscle regeneration potential of MPCs in dKO mice

Next *in vivo* muscle regeneration and inflammation was determined by assessing embryonic myosin heavy chain (eMyHC) and F4/80 (macrophage marker) expression in young and old dKO muscle. eMyHC is expressed almost exclusively in newly regenerated muscle fibers, which is usually found after acute muscle injury or disease. eMyHC is typically expressed for approximately one week within the newly regenerated muscle fibers. Normally in dystrophic muscle, eMyHC positive fibers are surrounded by F4/80 positive macrophages, during muscle regeneration.

The gastrocnemius muscle sections from young (4 week old) and old (6-8 weeks old) dKO mice were examined for eMyHC and F4/80 expression. Our results indicated that the number of eMyHC positive fibers (green) significantly declined in the dKO muscles from 4 to 8 weeks (**Fig. 6A, 6B**), but macrophage infiltration (red) increased with age and correlated with the progression of the disease state (**Fig. 6A, 6C**). Meanwhile, to further confirm this observation, real-time PCR for F4/80 and eMyHC from 6-8 week old dKO mice was performed. In support of the immunohistochemical findings, the level of inflammation (F4/80 positive macrophage infiltration) increased, whereas the muscle regeneration (eMyHC positive fibers) decreased during the progression of the disease (4W to 8 W). These data indicate that the dKO MPCs have a reduced ability to efficiently regenerate new myofibers during the progression of the disease, a process likely related to the increased inflammatory processes.

Higher FGF expression in dKO skeletal muscle

The above data have provided strong evidence suggesting that the progression of muscular dystrophy in dKO mice is associated with rapid muscle progenitor cell exhaustion, similar to that seen in DMD patients (29), but the mechanism responsible for stem cell exhaustion is still unclear. A study from a recent paper demonstrated that increased FGF2 signaling is a major contributor to the loss of stem cell quiescence and possibly stem cell depletion during aging under homeostatic conditions (56). We questioned whether FGF2 may be a contributing factor involved in the exhaustion of MPCs during the progression of muscular dystrophy in dKO mice.

Therefore, FGF2 expression was examined in dKO and age matched *mdx* muscle tissue sections. FGF2 expression was observed in dKO muscle as early as 6 weeks, whereas FGF2 was not detected in *mdx* muscle until 24 months of age (**Fig. 7A**). Real-time PCR confirmed this observation (**Fig. 7B**). These results indicated that increased levels of FGF signaling may play a role in the decline of the resident muscle progenitor cells, which eventually diminishes the regenerative capacity of the skeletal muscle.

Lower telomerase activity in muscle derived stem cells isolated from dKO mice

In addition, recent studies have reported that the impaired replicative potential of myoblasts from DMD patients is related, at least in part, to telomere shortening, a common feature of dystrophic human muscle cells with increasing age (57). Indeed, it has also been reported that both muscle stem cell exhaustion and cell senescence could be a result of impaired telomerase activity (45, 58, 59). Therefore, we also assessed telomerase activity in MDSCs isolated from *mdx* and dKO mice using the Telomerase PCR ELISA kit. In comparison with age-matched mdx MDSCs (4 weeks), the telomerase activity of the dKO MDSCs was significantly reduced (**Fig. 7C**). These results suggest that the decreased telomerase activity observed in the dKO MDSCs may play a major role in the rapid progression of the muscle histopathology in dKO mice, when compared to age matched mdx MDSCs.

Discussion

Although various mouse models for DMD have been investigated, we are still lacking a reliable mouse model that fully mimics the DMD pathology that could be consequently be used to test potential therapies to treat DMD. *Mdx* mice are the most widely used animal model of DMD because they are deficient in dystrophin; however, they exhibit only a mild dystrophic phenotype (60). It is believed that *mdx* mice compensate for the lack of dystrophin through the up-regulation of other proteins, such as utrophin (61). In this study, we demonstrated that the dystrophin/utrophin double knock-out mouse more closely recapitulates the DMD phenotype than the *mdx* model as evidenced by their severe, progressive loss of muscle function. Histopathological analysis of dKO muscle sections show many of the characteristic features described in DMD biopsies, including a reduction in muscle force, variations in muscle fiber size, infiltration of inflammatory cells, presence of necrotic fibers, calcium deposits, and replacement of functional tissue with fibrotic tissue. Many of the features seen in the dKO mice such as marked myopathy, joint contractures, kyphosis, loss of body weight, muscle function, as well as premature death (6-8weeks) are all similar to what is observed in DMD patients. This is similar to what is seen in mdx/mTRG2 mice, a recently reported DMD model with shortened telomeres in their MPCs, which results in rapid stem cell exhaustion and a severe dystrophic phenotype(45). However, these mdx/mTRG2 mice have a much longer lifespan than the dKO mice (45). As utrophin has been knocked out in this dKO animal model, the genotype is obviously not the same as DMD, which only lacks dystrophin, yet the dKO mice show all of the clinical features of DMD. Since, many studies have shown that the utrophin deficient mice are healthy and show no signs of weakness, living up to 2 years of age (62), it is unlikely that dKO abnormalities is caused primarily by utrophin deficiency.

We have proposed that the severe muscle wasting phenotype observed in this dKO mouse model is due to the impaired function of the muscle progenitor cell pool. Here we determined, both *in vitro* and *in vivo,* that the MPCs, including satellite cells, early myogenic progenitors (MDSCs), and myoblasts from aged dKO mice, are defective. *In vivo* we confirmed that there is a rapid decline of satellite cells during disease progression in dKO mouse muscles from 4 to 8 weeks of age in contrast to that observed in *mdx* skeletal muscle. *In vitro*, the proliferation and differentiation defects were marked by a reduction in the number of satellite cells capable of being derived from the dKO single muscle fibers, and also a reduction in the formation of

MyHCf positive myotubes in culture. MDSCs isolated from dKO mice also exhibited deficiencies in their proliferation and differentiation capacities including deficiencies in their myogenic, adipogenic, osteogenic and chondrogenic differentiation capacities, and a reduction in their oxidative stress resistance. These data obtained from the dKO mouse model differ from the data obtained from the mdx/mTRG2 mouse model which shows no alterations in satellite cell number per myofiber at 8 weeks of age (45), but demonstrates a markedly reduced number of satellite cells when the mice reach 60 weeks of age, indicating that MPC exhaustion appears at a much earlier age in the dKO mice than the mdx/mTRG2 mouse model.

Further *in vivo* histological analysis revealed that the amount of inflammatory infiltration was substantially increased in the muscles of the dKO mice from 4 to 8 weeks of age, while the number of newly regenerated muscle fibers was significantly reduced, during the same period, indicating an inability of the muscle to efficiently regenerate after injury. Similar to DMD patients, we observed a large amount of variability between the dKO mice; however, the occurrence of severe muscle histopathology in the dKO mice was always associated with the exhaustion of the MPC pool. When taken together this study demonstrated both *in vitro* and *in vivo* that MPCs isolated from dKO mice suffer from severe functional defects and that the progressive loss of MPCs plays a major role in determining the severity of the dystrophic phenotype. Indeed, the concept of stem cell exhaustion as a potential cause for the rapid progression of muscle weakness in DMD has been recently reported (29). Thus, we believe that the dKO model represents an excellent murine model of muscle stem cell exhaustion, allowing for the study of potential therapies for treating DMD patients.

Interestingly, we observed that the percentage of Sca-1 and PDGFRα positive mesenchymal interstitial cells was significantly higher in aged dKO muscle compared to WT and *mdx* muscle (data not shown), suggesting that their severe dystrophic phenotype is muscle specific and not the result of a functional defect in other cell types. Moreover, the increase in muscle-derived mesenchymal stem cells within the skeletal muscle of the dKO mice may be responsible for the heterotopic ossification and fibrotic tissue formation observed in the dystrophic muscle of dKO mice. There are several papers to support our hypothesis showing that mesenchymal progenitor cells are a major contributor of ectopic fat cell formation (63) in skeletal muscle and are a predominant source of progenitors that drive heterotopic ossification (64); however further investigation is required.

There are several mechanisms that may contribute to the severe phenotype observed in the dKO mice which are associated with muscle progenitor cell exhaustion. A study from the group of Andrew S. Brack demonstrated that increased FGF signaling is a major contributor to the loss of stem cell quiescence and possibly to the process of stem cell depletion during aging under homeostatic conditions (56). Both PCR and immunostaining showed that an up-regulation of FGF expression is observed as early as 6 weeks of age in the dKO mice, whereas age-matched WT and *mdx* muscles did express FGF until the mice reached 2 years of age. The reason for the increase in FGF expression is unknown, but this may contribute to the rapid muscle stem cell exhaustion observed in the dKO mice. Strategies to prevent chronic FGF production or repress FGF signaling may reduce stem cell loss during normal aging, but may not have beneficial effects on progressive muscle diseases since FGF expression is also required for myoblasts proliferation, differentiation, and muscle regeneration following skeletal muscle injury (65, 66).

Recent studies have shown that muscle cells isolated from DMD patients have shorter telomeres than cells isolated from healthy individuals (57, 67). In addition, Helen M. Blau's group generated *mdx* mice lacking telomerase activity and showed that dystrophin deficiency, coupled with telomere dysfunction, recapitulated the severe dystrophic phenotype characteristic of muscular dystrophy in humans (45). This study provided evidence that telomere shortening, specifically in MPCs, leads to muscle stem cell exhaustion and the occurrence of the dystrophic histopathology. Moreover, it has also been reported that both muscle stem cell exhaustion and senescence could be the result of impaired telomerase activity (45, 58, 59). Because of these findings, we tested the hypothesis that the muscle stem cell defect present in the dKO mice is also associated with a reduction in telomerase activity, and indeed found that the telomerase activity in dKO MDSCs was significantly reduced, when compared to MDSCs isolated from age matched WT and *mdx* mice. Reduced telomerase activity in dKO MDSCs could lead to defective cell proliferation, resistance to stress, and muscle regeneration potentials. Taken together, we believe that both increased FGF over-expression in the dKO muscles and a reduction in telomerase activity in the dKO MDSCs all play a role in the rapid exhaustion of the MPC pool in dKO mice, which ultimately results in the severe dystrophic phenotype observed in this model of DMD. The data presented in the current study demonstrates that the dKO mouse model more closely recapitulates the severe phenotype observed in DMD patients compared to the *mdx* mouse model. Moreover, the causative mechanism for the rapid occurrence of the dystrophic

phenotype in the dKO mice and DMD patients might be related to the exhaustion of the MPC pool.

In summary, we provided evidence that dKO mice that lack both utrophin and dystrophin exhibit a progressive exhaustion of their MPC pool and have a severe reduction in their muscle regenerative potential. The dKO animal model more readily recapitulates the disease progression seen in human DMD patients in comparison to the *mdx* mouse model, which is the most commonly utilized mouse model of DMD. Hence, the dKO model may prove useful for elucidating the pathophysiology of DMD and for testing potential therapeutic approaches to treat DMD patients.

Acknowledgements

We wish to thank James Cummins and Bria King for their editorial assistance. This work was supported in part by the Department of Defense (W81-XWH-09-1-0658) awarded to Johnny Huard and the Henry J. Mankin Endowed Chair at the University of Pittsburgh.

The authors do not have conflicts of interest to disclose other than the corresponding author who receives consulting fees from Cook MyoSite Inc.

Table 1 Primers used for real time PCR

Gene	Forward primers	Reverse primers	Location
Pax7	GTGCCCTCAGTGAGTTCGAT	CCACATCTGAGCCCTCATCC	499-667
FGF2	GGCTGCTGGCTTCTAAGTGT	GTCCCGTTTTGGATCCGAGT	463-615
eMyHC	GGAGGCTGATGAACAAGCCA	GCTAGAGGTGAAGTCACGGG	5696-5897
F4/80	CGGGGCTATGGGATGCATAA	TCAGCAACCTCGTGTCCTTG	2375-2564
β-Actin	TCAGAAGGACTCCTATGTGG	TCTTTGATGTCACGCACGAT	234–722

References

1 Durbeej, M. and Campbell, K.P. (2002) Muscular dystrophies involving the dystrophin-glycoprotein complex: an overview of current mouse models. *Current opinion in genetics & development*, **12**, 349-361.

2 Tinsley, J.M., Blake, D.J., Zuellig, R.A. and Davies, K.E. (1994) Increasing complexity of the dystrophin-associated protein complex. *Proc Natl Acad Sci U S A*, **91**, 8307-8313.

3 Bonilla, E., Samitt, C.E., Miranda, A.F., Hays, A.P., Salviati, G., DiMauro, S., Kunkel, L.M., Hoffman, E.P. and Rowland, L.P. (1988) Duchenne muscular dystrophy: deficiency of dystrophin at the muscle cell surface. *Cell*, **54**, 447-452.

4 Koenig, M. and Kunkel, L.M. (1990) Detailed analysis of the repeat domain of dystrophin reveals four potential hinge segments that may confer flexibility. *J Biol Chem*, **265**, 4560-4566.

5 Koenig, M., Monaco, A.P. and Kunkel, L.M. (1988) The complete sequence of dystrophin predicts a rod-shaped cytoskeletal protein. *Cell*, **53**, 219-228.

6 Miranda, A.F., Francke, U., Bonilla, E., Martucci, G., Schmidt, B., Salviati, G. and Rubin, M. (1989) Dystrophin immunocytochemistry in muscle culture: detection of a carrier of Duchenne muscular dystrophy. *Am J Med Genet*, **32**, 268-273.

7 Senter, L., Luise, M., Presotto, C., Betto, R., Teresi, A., Ceoldo, S. and Salviati, G. (1993) Interaction of dystrophin with cytoskeletal proteins: binding to talin and actin. *Biochem Biophys Res Commun*, **192**, 899-904.

8 Lapidos, K.A., Kakkar, R. and McNally, E.M. (2004) The dystrophin glycoprotein complex: signaling strength and integrity for the sarcolemma. *Circ Res*, **94**, 1023-1031.

9 Hoffman, E.P., Brown, R.H., Jr. and Kunkel, L.M. (1987) Dystrophin: the protein product of the Duchenne muscular dystrophy locus. *Cell*, **51**, 919-928.

10 Mauro, A. (1961) Satellite cell of skeletal muscle fibers. *The Journal of biophysical and biochemical cytology*, **9**, 493-495.

11 Montarras, D., Morgan, J., Collins, C., Relaix, F., Zaffran, S., Cumano, A., Partridge, T. and Buckingham, M. (2005) Direct isolation of satellite cells for skeletal muscle regeneration. *Science*, **309**, 2064-2067.

12 Zammit, P.S., Relaix, F., Nagata, Y., Ruiz, A.P., Collins, C.A., Partridge, T.A. and Beauchamp, J.R. (2006) Pax7 and myogenic progression in skeletal muscle satellite cells. *Journal of cell science*, **119**, 1824-1832.

13 Benchaouir, R., Rameau, P., Decraene, C., Dreyfus, P., Israeli, D., Pietu, G., Danos, O. and Garcia, L. (2004) Evidence for a resident subset of cells with SP phenotype in the C2C12 myogenic line: a tool to explore muscle stem cell biology. *Experimental cell research*, **294**, 254-268.

14 Dellavalle, A., Sampaolesi, M., Tonlorenzi, R., Tagliafico, E., Sacchetti, B., Perani, L., Innocenzi, A., Galvez, B.G., Messina, G., Morosetti, R. *et al.* (2007) Pericytes of human skeletal muscle are myogenic precursors distinct from satellite cells. *Nat Cell Biol*, **9**, 255-267.

15 Dellavalle, A., Maroli, G., Covarello, D., Azzoni, E., Innocenzi, A., Perani, L., Antonini, S., Sambasivan, R., Brunelli, S., Tajbakhsh, S. *et al.* (2011) Pericytes resident in postnatal skeletal muscle differentiate into muscle fibres and generate satellite cells. *Nat Commun*, **2**, 499.

16 Mitchell, K.J., Pannerec, A., Cadot, B., Parlakian, A., Besson, V., Gomes, E.R., Marazzi, G. and Sassoon, D.A. (2010) Identification and characterization of a non-satellite cell muscle resident progenitor during postnatal development. *Nat Cell Biol*, **12**, 257-266.

17 Pannerec, A., Marazzi, G. and Sassoon, D. (2012) Stem cells in the hood: the skeletal muscle niche. *Trends in molecular medicine*, **18**, 599-606.

18 Pannerec, A., Formicola, L., Besson, V., Marazzi, G. and Sassoon, D.A. (2013) Defining skeletal muscle resident progenitors and their cell fate potentials. *Development*, **140**, 2879-2891.

19 Asakura, A., Seale, P., Girgis-Gabardo, A. and Rudnicki, M.A. (2002) Myogenic specification of side population cells in skeletal muscle. *J Cell Biol*, **159**, 123-134.
20 De Angelis, L., Berghella, L., Coletta, M., Lattanzi, L., Zanchi, M., Cusella-De Angelis, M.G., Ponzetto, C. and Cossu, G. (1999) Skeletal myogenic progenitors originating from embryonic dorsal aorta coexpress endothelial and myogenic markers and contribute to postnatal muscle growth and regeneration. *J Cell Biol*, **147**, 869-878.
21 Tamaki, T., Okada, Y., Uchiyama, Y., Tono, K., Masuda, M., Nitta, M., Hoshi, A. and Akatsuka, A. (2008) Skeletal muscle-derived CD34+/45- and CD34-/45- stem cells are situated hierarchically upstream of Pax7+ cells. *Stem cells and development*, **17**, 653-667.
22 Lee, J.Y., Qu-Petersen, Z., Cao, B., Kimura, S., Jankowski, R., Cummins, J., Usas, A., Gates, C., Robbins, P., Wernig, A. *et al.* (2000) Clonal isolation of muscle-derived cells capable of enhancing muscle regeneration and bone healing. *J Cell Biol*, **150**, 1085-1100.
23 Torrente, Y., Tremblay, J.P., Pisati, F., Belicchi, M., Rossi, B., Sironi, M., Fortunato, F., El Fahime, M., D'Angelo, M.G., Caron, N.J. *et al.* (2001) Intraarterial injection of muscle-derived CD34(+)Sca-1(+) stem cells restores dystrophin in mdx mice. *J Cell Biol*, **152**, 335-348.
24 Qu-Petersen, Z., Deasy, B., Jankowski, R., Ikezawa, M., Cummins, J., Pruchnic, R., Mytinger, J., Cao, B., Gates, C., Wernig, A. *et al.* (2002) Identification of a novel population of muscle stem cells in mice: potential for muscle regeneration. *J Cell Biol*, **157**, 851-864.
25 Usas, A. and Huard, J. (2007) Muscle-derived stem cells for tissue engineering and regenerative therapy. *Biomaterials*, **28**, 5401-5406.
26 Kuroda, R., Usas, A., Kubo, S., Corsi, K., Peng, H., Rose, T., Cummins, J., Fu, F.H. and Huard, J. (2006) Cartilage repair using bone morphogenetic protein 4 and muscle-derived stem cells. *Arthritis Rheum*, **54**, 433-442.
27 Cao, B., Zheng, B., Jankowski, R.J., Kimura, S., Ikezawa, M., Deasy, B., Cummins, J., Epperly, M., Qu-Petersen, Z. and Huard, J. (2003) Muscle stem cells differentiate into haematopoietic lineages but retain myogenic potential. *Nat Cell Biol*, **5**, 640-646.
28 McLoon, L.K. (2008) Focusing on fibrosis: halofuginone-induced functional improvement in the mdx mouse model of Duchenne muscular dystrophy. *Am J Physiol Heart Circ Physiol*, **294**, H1505-1507.
29 Blau, H.M., Webster, C. and Pavlath, G.K. (1983) Defective myoblasts identified in Duchenne muscular dystrophy. *Proc Natl Acad Sci U S A*, **80**, 4856-4860.
30 Webster, C. and Blau, H.M. (1990) Accelerated age-related decline in replicative life-span of Duchenne muscular dystrophy myoblasts: implications for cell and gene therapy. *Somatic cell and molecular genetics*, **16**, 557-565.
31 Bulfield, G., Siller, W.G., Wight, P.A. and Moore, K.J. (1984) X chromosome-linked muscular dystrophy (mdx) in the mouse. *Proceedings of the National Academy of Sciences of the United States of America*, **81**, 1189-1192.
32 Ryder-Cook, A.S., Sicinski, P., Thomas, K., Davies, K.E., Worton, R.G., Barnard, E.A., Darlison, M.G. and Barnard, P.J. (1988) Localization of the mdx mutation within the mouse dystrophin gene. *The EMBO journal*, **7**, 3017-3021.
33 DiMario, J.X., Uzman, A. and Strohman, R.C. (1991) Fiber regeneration is not persistent in dystrophic (MDX) mouse skeletal muscle. *Developmental biology*, **148**, 314-321.
34 Straub, V., Rafael, J.A., Chamberlain, J.S. and Campbell, K.P. (1997) Animal models for muscular dystrophy show different patterns of sarcolemmal disruption. *The Journal of cell biology*, **139**, 375-385.
35 Khouzami, L., Bourin, M.C., Christov, C., Damy, T., Escoubet, B., Caramelle, P., Perier, M., Wahbi, K., Meune, C., Pavoine, C. *et al.* (2010) Delayed cardiomyopathy in dystrophin deficient mdx mice relies on intrinsic glutathione resource. *Am J Pathol*, **177**, 1356-1364.
36 Isaac, C., Wright, A., Usas, A., Li, H., Tang, Y., Mu, X., Greco, N., Dong, Q., Vo, N., Kang, J. *et al.* (2013) Dystrophin and utrophin "double knockout" dystrophic mice exhibit a spectrum of degenerative

musculoskeletal abnormalities. *Journal of orthopaedic research : official publication of the Orthopaedic Research Society*, **31**, 343-349.
37 Kornegay, J.N., Childers, M.K., Bogan, D.J., Bogan, J.R., Nghiem, P., Wang, J., Fan, Z., Howard, J.F., Jr., Schatzberg, S.J., Dow, J.L. *et al.* (2012) The paradox of muscle hypertrophy in muscular dystrophy. *Physical medicine and rehabilitation clinics of North America*, **23**, 149-172, xii.
38 Nguyen, T.M., Le, T.T., Blake, D.J., Davies, K.E. and Morris, G.E. (1992) Utrophin, the autosomal homologue of dystrophin, is widely-expressed and membrane-associated in cultured cell lines. *FEBS Lett*, **313**, 19-22.
39 Ferretti, R., Neto, H.S. and Marques, M.J. (2011) Expression of utrophin at dystrophin-deficient neuromuscular synapses of mdx mice: a study of protected and affected muscles. *Anat Rec (Hoboken)*, **294**, 283-286.
40 Baban, D. and Davies, K.E. (2008) Microarray analysis of mdx mice expressing high levels of utrophin: therapeutic implications for dystrophin deficiency. *Neuromuscul Disord*, **18**, 239-247.
41 Bewick, G.S., Nicholson, L.V., Young, C., O'Donnell, E. and Slater, C.R. (1992) Different distributions of dystrophin and related proteins at nerve-muscle junctions. *Neuroreport*, **3**, 857-860.
42 Law, D.J., Allen, D.L. and Tidball, J.G. (1994) Talin, vinculin and DRP (utrophin) concentrations are increased at mdx myotendinous junctions following onset of necrosis. *Journal of cell science*, **107 (Pt 6)**, 1477-1483.
43 Deol, J.R., Danialou, G., Larochelle, N., Bourget, M., Moon, J.S., Liu, A.B., Gilbert, R., Petrof, B.J., Nalbantoglu, J. and Karpati, G. (2007) Successful compensation for dystrophin deficiency by a helper-dependent adenovirus expressing full-length utrophin. *Mol Ther*, **15**, 1767-1774.
44 Deconinck, A.E., Rafael, J.A., Skinner, J.A., Brown, S.C., Potter, A.C., Metzinger, L., Watt, D.J., Dickson, J.G., Tinsley, J.M. and Davies, K.E. (1997) Utrophin-dystrophin-deficient mice as a model for Duchenne muscular dystrophy. *Cell*, **90**, 717-727.
45 Sacco, A., Mourkioti, F., Tran, R., Choi, J., Llewellyn, M., Kraft, P., Shkreli, M., Delp, S., Pomerantz, J.H., Artandi, S.E. *et al.* (2010) Short telomeres and stem cell exhaustion model Duchenne muscular dystrophy in mdx/mTR mice. *Cell*, **143**, 1059-1071.
46 Lu, A., Cummins, J.H., Pollett, J.B., Cao, B., Sun, B., Rudnicki, M.A. and Huard, J. (2008) Isolation of myogenic progenitor populations from Pax7-deficient skeletal muscle based on adhesion characteristics. *Gene therapy*, **15**, 1116-1125.
47 Wang, B., Li, J., Fu, F.H. and Xiao, X. (2009) Systemic human minidystrophin gene transfer improves functions and life span of dystrophin and dystrophin/utrophin-deficient mice. *J Orthop Res*, **27**, 421-426.
48 Lavasani, M., Lu, A., Thompson, S.D., Robbins, P.D., Huard, J. and Niedernhofer, L.J. (2013) Isolation of muscle-derived stem/progenitor cells based on adhesion characteristics to collagen-coated surfaces. *Methods Mol Biol*, **976**, 53-65.
49 Gharaibeh, B., Lu, A., Tebbets, J., Zheng, B., Feduska, J., Crisan, M., Peault, B., Cummins, J. and Huard, J. (2008) Isolation of a slowly adhering cell fraction containing stem cells from murine skeletal muscle by the preplate technique. *Nat Protoc*, **3**, 1501-1509.
50 Deasy, B.M., Jankowski, R.J., Payne, T.R., Cao, B., Goff, J.P., Greenberger, J.S. and Huard, J. (2003) Modeling stem cell population growth: incorporating terms for proliferative heterogeneity. *Stem Cells*, **21**, 536-545.
51 Chirieleison, S.M., Bissell, T.A., Scelfo, C.C., Anderson, J.E., Li, Y., Koebler, D.J. and Deasy, B.M. (2011) Automated live cell imaging systems reveal dynamic cell behavior. *Biotechnology progress*, **27**, 913-924.
52 Dellorusso, C., Crawford, R.W., Chamberlain, J.S. and Brooks, S.V. (2001) Tibialis anterior muscles in mdx mice are highly susceptible to contraction-induced injury. *J Muscle Res Cell Motil*, **22**, 467-475.

53 Kallestad, K.M., Hebert, S.L., McDonald, A.A., Daniel, M.L., Cu, S.R. and McLoon, L.K. (2011) Sparing of extraocular muscle in aging and muscular dystrophies: a myogenic precursor cell hypothesis. *Exp Cell Res*, **317**, 873-885.
54 Jankowski, R.J., Haluszczak, C., Trucco, M. and Huard, J. (2001) Flow cytometric characterization of myogenic cell populations obtained via the preplate technique: potential for rapid isolation of muscle-derived stem cells. *Hum Gene Ther*, **12**, 619-628.
55 Deasy, B.M., Gharaibeh, B.M., Pollett, J.B., Jones, M.M., Lucas, M.A., Kanda, Y. and Huard, J. (2005) Long-term self-renewal of postnatal muscle-derived stem cells. *Molecular biology of the cell*, **16**, 3323-3333.
56 Chakkalakal, J.V., Jones, K.M., Basson, M.A. and Brack, A.S. (2012) The aged niche disrupts muscle stem cell quiescence. *Nature*, **490**, 355-360.
57 Mouly, V., Aamiri, A., Bigot, A., Cooper, R.N., Di Donna, S., Furling, D., Gidaro, T., Jacquemin, V., Mamchaoui, K., Negroni, E. *et al.* (2005) The mitotic clock in skeletal muscle regeneration, disease and cell mediated gene therapy. *Acta physiologica Scandinavica*, **184**, 3-15.
58 Zhu, C.H., Mouly, V., Cooper, R.N., Mamchaoui, K., Bigot, A., Shay, J.W., Di Santo, J.P., Butler-Browne, G.S. and Wright, W.E. (2007) Cellular senescence in human myoblasts is overcome by human telomerase reverse transcriptase and cyclin-dependent kinase 4: consequences in aging muscle and therapeutic strategies for muscular dystrophies. *Aging Cell*, **6**, 515-523.
59 Wootton, M., Steeghs, K., Watt, D., Munro, J., Gordon, K., Ireland, H., Morrison, V., Behan, W. and Parkinson, E.K. (2003) Telomerase alone extends the replicative life span of human skeletal muscle cells without compromising genomic stability. *Hum Gene Ther*, **14**, 1473-1487.
60 Lefaucheur, J.P., Pastoret, C. and Sebille, A. (1995) Phenotype of dystrophinopathy in old mdx mice. *Anat Rec*, **242**, 70-76.
61 Matsumura, K., Ervasti, J.M., Ohlendieck, K., Kahl, S.D. and Campbell, K.P. (1992) Association of dystrophin-related protein with dystrophin-associated proteins in mdx mouse muscle. *Nature*, **360**, 588-591.
62 Deconinck, A.E., Potter, A.C., Tinsley, J.M., Wood, S.J., Vater, R., Young, C., Metzinger, L., Vincent, A., Slater, C.R. and Davies, K.E. (1997) Postsynaptic abnormalities at the neuromuscular junctions of utrophin-deficient mice. *J Cell Biol*, **136**, 883-894.
63 Uezumi, A., Fukada, S., Yamamoto, N., Takeda, S. and Tsuchida, K. (2010) Mesenchymal progenitors distinct from satellite cells contribute to ectopic fat cell formation in skeletal muscle. *Nat Cell Biol*, **12**, 143-152.
64 Wosczyna, M.N., Biswas, A.A., Cogswell, C.A. and Goldhamer, D.J. (2012) Multipotent progenitors resident in the skeletal muscle interstitium exhibit robust BMP-dependent osteogenic activity and mediate heterotopic ossification. *J Bone Miner Res*, **27**, 1004-1017.
65 Stratos, I., Madry, H., Rotter, R., Weimer, A., Graff, J., Cucchiarini, M., Mittlmeier, T. and Vollmar, B. (2011) Fibroblast growth factor-2-overexpressing myoblasts encapsulated in alginate spheres increase proliferation, reduce apoptosis, induce adipogenesis, and enhance regeneration following skeletal muscle injury in rats. *Tissue Eng Part A*, **17**, 2867-2877.
66 Neuhaus, P., Oustanina, S., Loch, T., Kruger, M., Bober, E., Dono, R., Zeller, R. and Braun, T. (2003) Reduced mobility of fibroblast growth factor (FGF)-deficient myoblasts might contribute to dystrophic changes in the musculature of FGF2/FGF6/mdx triple-mutant mice. *Mol Cell Biol*, **23**, 6037-6048.
67 Decary, S., Hamida, C.B., Mouly, V., Barbet, J.P., Hentati, F. and Butler-Browne, G.S. (2000) Shorter telomeres in dystrophic muscle consistent with extensive regeneration in young children. *Neuromuscular disorders : NMD*, **10**, 113-120.

Blank Page

The role of Notch signaling in muscle progenitor cell exhaustion and the rapid onset of histopathology in muscular dystrophy

Running title: Notch signaling involvement in muscular dystrophy

Xiaodong Mu, Ying Tang, Aiping Lu, Koji Takayama, Arvydas Usas, Bing Wang, Kurt Weiss, and Johnny Huard

Stem Cell Research Center, Department of Orthopaedic Surgery, University of Pittsburgh, Pittsburgh, PA 15219

Corresponding author:

Johnny Huard, Ph. D, Stem Cell Research Center, Department of Orthopaedic Surgery, University of Pittsburgh, Bridgeside Point 2, Suite 206, 450 Technology Drive, Pittsburgh, PA 15219, 412-648-2798 (Phone); 412-648-4066 (Fax); Email: jhuard@pitt.edu

Acknowledgements:

This research was supported in part by a grant from the NIH (PO1AG043376-01-A1) and the Henry J. Mankin endowed chair at the University of Pittsburgh.

Keywords: Notch; mdx mice, utrophin deficient, muscle stem cells, stem cell exhaustion, senescence, dystrophic muscle, heterotopic ossification, fatty infiltration

Abstract

Although it has been speculated that stem cell exhaustion play a role in the rapid progression of the muscle histopathology associated with Duchenne Muscular Dystrophy (DMD), the molecular and cellular mechanisms responsible for the stem cell exhaustion remain poorly understood. The rapid exhaustion of muscle stem cells has not been observed in the dystrophin-deficient model of DMD (mdx mouse), which may explain the relatively mild dystrophic phenotype observed in this animal model. In contrast, we have observed a rapid occurrence of stem cell exhaustion in the dystrophin/utrophin double knockout (dKO) mouse model, which exhibits histopathological features that more closely recapitulate the phenotype observed in DMD patients than mdx mice. Notch signaling has been found to be a the key regulator of stem cell self-renewal and myogenesis in normal skeletal muscles; however, little is known about the role that Notch plays in the development of dystrophic histopathology. Our results revealed an over-activation of Notch in the skeletal muscles of dKO mice, which correlated with sustained inflammation, impaired muscle regeneration and the rapid exhaustion and senescence of the Muscle Progenitor Cells (MPCs). Consequently, repression of Notch in dKO skeletal muscle delays/reduces exhaustion and senescence of MPCs, and restores myogenesis while reducing inflammation and fibrosis. We suggest that the down-regulation of Notch could represent a viable approach to reduce the dystrophic histopathologies associated with DMD.

Introduction

The rapid onset of muscle histopathology observed in DMD patients has been related, at least in part, to the exhaustion of functional muscle stem cells as a result of the continuous muscle regeneration/degeneration cycle due to the lack of dystrophin (1-3). The widely utilized mdx mouse model of DMD is also deficient for dystrophin, but in contrast to DMD, the muscle regeneration capacity of the mdx mouse is un-altered and muscle histopathology is very mild, which is potentially attributed to the lack of muscle stem cell exhaustion (2, 4-5). In support of this contention, mdx/mTR mice that are dystrophin-deficient and have a telomere dysfunction/shortening, specifically in their Muscle Progenitor Cells (MPCs), develop a more severe dystrophic phenotype than mdx mice, which rapidly worsens with age, due to the rapid exhaustion of their MPCs (2). Hence, treatments directed exclusively at restoring dystrophin within the mdx muscle fibers may not be sufficient for treating DMD patients, especially the older patients (2, 6-7); therefore, therapeutic modulation of muscle stem cell activities could represent a viable approach for alleviating muscle weakness in DMD (7). To achieve that goal, many questions remain unanswered about the molecular pathway involved in the regulation of muscle stem cell activity in dystrophic muscle.

The mdx and dystrophin/utrophin double knockout (dKO) mice are both important mouse models of DMD (5, 8-10); however, in contrast to the mild phenotype observed in mdx mice, dKO mice exhibit a similar phenotype to that observed in human DMD patients including a shorter life span (~8 weeks compared to 2 years), increased necrosis and fibrosis in their skeletal muscles, severe scoliosis/kyphosis of the spine, and severe cardiac involvement (cardiomyopathy) (8-9). Although utrophin is lacking in dKO mice, in contrast to DMD patients, the dKO mouse model represents an additional animal model that more closely recapitulates DMD (4, 8, 11-12). It is important to note that utrophin-/- mice are not developing major histopathological signs, suggesting that utrophin deletion only

does not lead to major skeletal muscle histopathologies (13). Our group has recently verified that the exhaustion of MPCs occurs in dKO mice, which correlates with impaired muscle regeneration capacity (14).

The reports on the role that Notch plays in normal muscle regeneration and muscle stem cell activation remain controversial. Notch has been shown to be involved in the maintenance of stem cell quiescence and the stem cell pool in skeletal muscle (15-17) and declines in Notch signaling during the aging process correlates with an impairment in muscle regeneration capacity (18-20); however, Notch signaling has also been shown to be a repressor of myogenesis and hence has an adverse effect on muscle regeneration (21-25). Moreover, constitutively activated Notch1 Intracellular Domain (NICD) has been shown to result in an impairment in skeletal muscle regeneration and an increase in the number of undifferentiated Pax7 expressing cells present in the muscle (26). Elevated Notch signaling was also found in Stra13−/− mice that have a defect in muscle regeneration which leads to the development of fibrosis (27). Conversely, delta-like 1 (Dlk1), a non-canonical Notch ligand that inhibits Notch signaling, was found to be required for proper skeletal muscle development and regeneration (23). It was suggested that the continuous activation of Notch signaling impairs muscle regeneration and that a temporal decline in Notch signaling in muscle stem cells is required for proper muscle regeneration and repair (28).

Several lines of evidence have suggested that activated Notch signaling may also play an important role in the histopathologies observed with DMD disease, including increases in: 1) muscle atrophy, 2) premature cellular senescence, 3) inflammation, and 4) fibrosis formation (29-30) (31-41). **1) Muscle Atrophy**: Increased Notch1 activation has been observed in denervation-induced skeletal muscle atrophy (29-30), while both DMD patients (42) and dKO mice (9-10) experience massive muscle atrophy. **2) Premature Cellular Senescence:** dKO mice show multiple phenotypic similarities

to progeroid animals (animals with premature aging), including premature death, stem cell defects, and skeletal muscle histopathologies; notably, Notch activation has been observed to mediate the premature senescence of various cell types in progeroid animals (35-37, 43-45). **3) Inflammation:** The skeletal muscle of dKO mice shows much greater inflammation than mdx mice (9-10) and Notch is often co-activated with pro-inflammatory signaling involving TNF-α and NF-κB (31-33). In fact, recent studies showed that the canonical NF-κB DNA-binding motif 5-GGRRNNYYCC-3 exists in the promoters of Notch genes in human cells (46) and the treatment of porcine satellite cells with recombinant NF-κB enhances Notch1 expression (47). Additionally, Notch signaling has also been shown to mediate inflammatory responses in cardiovascular disorders (48). Finally, both Notch signaling and TNF-α/NF-κB signaling are known to repress the myogenic potential of muscle stem cells by down-regulating MyoD (21, 49-51). **4) Fibrosis:** Extensive fibrosis has been observed in the skeletal muscle of both DMD patients and dKO mice (9-10); while the co-activation of TGF-β1 and Notch signaling pathways has been reported in various tissues and cell types (including C2C12 myoblasts) during fibrogenesis, supporting the fact that Notch signaling represents a potential target to block fibrosis (38-41).

Taken together, these observations suggest that Notch signaling may play an important role in the histopathology of dystrophic muscle of dKO mice, and the exhaustion and senescence of MPCs. Therefore, the current study was conducted to determine whether the MPC exhaustion and senescence that occurs in severely affected dystrophic muscle in dKO mice correlates with the over-activation of Notch signaling, and the results was compared to mdx mice (mild phenotype). In addition, Notch inactivation experiments were conducted in MPCs isolated from dKO mice (*in vitro*) and in dKO skeletal muscle (*in vivo*) to determine whether MPC exhaustion and senescence of and impaired muscle regeneration could be alleviated by Notch inactivation. Our results not only reveal that over-activation of Notch signaling occurs in MPCs and skeletal muscle of dKO mice, but more importantly that

inhibition of Notch signaling delays MPC exhaustion and senescence, and restores myogenesis while reducing inflammation and fibrosis in the severely affected dystrophic muscle in dKO mice.

Results

1. The exhaustion and senescence of MPCs rapidly occurs in skeletal muscle of dKO mice.

Through Pax7 immunostaining, we observed that the number of Pax7 positive (Pax7+) cells (satellite cells/MPCs) generally remains unchanged in the Gastrocnemius (GM) muscles of 1- to 8-week old mdx mice (**Figure 1A, B**). Although the number of Pax7+ cells was enriched from 1- to 4-week old in dKO mice, a significant decrease in the number of Pax7+ cells was observed in 8-week old dKO mice (**Figure 1A, B**). Notably, Pax7+ cells in the "younger" dKO mice (1- or 4-week old) were generally more enriched than that of the age-matched mdx mice (**Figure 1A, B**). In support of the observations *in vivo*, when examining single myofibers isolated from the 4- or 8-week old dKO mice, fewer Pax7+ cells were observed to reside at the myofibers of the 8-week old dKO mice, compared to the 4-week old dKO mice (**Figure 1C**).

We next investigated whether the rapid exhaustion of muscle stem cells in dKO skeletal muscles correlate with a reduction in the proliferation of Pax7+ satellite cells. Co-immunostaining of Ki67 (a proliferation marker) and Pax7 in the skeletal muscle of 4- and 8-week old dKO mice revealed a reduction in cells co-expressing Ki67 and Pax7 (Ki67+/Pax7+) in the 8-week old dKO mice compared to the 4-week old dKO mice (**Figure 1D, E**), indicating a progressive reduction in Pax-7+ cells proliferation in dKO skeletal muscle with age. During skeletal muscle regeneration, MyoD activation occurs for proper myogenesis, and Pax7+ cells remain at an undifferentiated status without MyoD activation (52). Although Pax7+ cells were more enriched in the skeletal muscle of 4-week old dKO mice than 4-week old mdx mice, the number of MyoD+ myogenic cells was greatly reduced in the 4-week old dKO mice, when compared to age matched mdx mice (**Figure 1F, G**), suggesting the reduced myogenesis potential of the muscle cells in dKO mice.

Furthermore, the cell senescence assay revealed that there were also more β-Galactosidase + (β-gal+) senescent cells in the skeletal muscle of 8-week old dKO mice, compared to 8-week old mdx mice, suggesting that the exhaustion of the MPCs in dKO mice could be contributed by accelerated cell senescence.

2. Increased non-muscle tissues [heterotopic ossification (HO), adipose tissue, and fibrosis] and up-regulation of Notch and pro-inflammatory signaling molecules in the skeletal muscle of dKO mice.

HO has been described in the limb muscles of mdx mice previously (53-54), and our recent study demonstrated much more extensive HO in the limb muscles of dKO mice, compared to mdx and WT mice (55-56). Our current observation further revealed that, in comparison with mdx mice, 8-week old dKO mice featured not only extensive intramuscular HO, but also much more peri-muscular adipose tissue (**Figure 2A**). Meanwhile, Trichrome staining showed extensive formation of fibrosis in the skeletal muscle of dKO mice (**Figure 2A**) (8-9). The presence of extensive HO, adipose tissue, and fibrosis in the skeletal muscle of dKO mice may suggest that the exhaustion of muscle stem cells (Pax7+ cells) and myogenic cells (MyoD+ cells) could have been accelerated by the trans-differentiation of the cells into non-muscle tissues.

The expression of a group of genes directly regulating muscle stem cell activity was compared among skeletal muscle tissues of 4-week old mdx, dKO, and wild-type (WT) mice. A semi-quantitative PCR study showed that, in comparison with mdx mice, the expression of the Notch genes (Notch1-3, Hes1, Hey1, and Jagged2) (57), TGF-β genes (myostatin/MSTN, BMP4 and TGF-β1), pro-inflammatory factors (TNF-α, IL-1β and IL-6), and Pax3 (a marker of quiescent/undifferentiated muscle

stem cells) (28) were up-regulated in the skeletal muscle of dKO mice, while the expressions of Klotho (an anti-inflammatory factor) (58) and MyoD were down-regulated (**Figure 2B**).

The expression of Notch genes in the dKO skeletal muscle was also higher than that of age-matched WT mice (**Figure 2B**), indicating an "over-activated" status of Notch signaling in dKO mice. In comparison with WT mice, the skeletal muscle of mdx mice also showed an up-regulation of pro-inflammatory factors, but to a lesser extent than dKO mice (**Figure 2B**). Also, co-immunostaining of Notch3 and Pax7 in the skeletal muscle of 4-week old dKO and mdx mice demonstrated a higher number of Notch3+ cells or Pax7+/Notch3+ cells in the skeletal muscle of dKO mice (**Figure 2C, D**). Immunostaining of Notch1 also revealed increased number of Notch1+ cells in the skeletal muscle of 4-week old dKO mice, compared to mdx mice (**Figure 2C**). Furthermore, western blot analysis revealed an increase in Hes1 protein (a key down-stream mediator of Notch activation) in the skeletal muscle of 4-week old dKO mice, compared to mdx mice (**Figure 2E**).

In addition, we found that the expression of the Notch genes was up-regulated in dKO mice of different ages (1-, 4-, and 8-week old mice) (**Supplemental Figure 1A**), compared to aged-matched mdx mice, indicating a chronic activation of Notch signaling in the skeletal muscle of dKO mice. Similarly, the expressions of Notch, TGF-β, and pro-inflammatory factors in MPCs isolated from mdx and dKO (4- or 6-week old) were also compared, and the expression of these genes was also found to be generally higher in dKO mice (**Supplemental Figure 1B**).

3. The role of Notch activation in MPCs and skeletal muscle of mdx mice.

In addition to the role of Notch in repressing myogenesis [9], previous observations have shown a positive effect of Notch activation on the proliferation of muscle stem cells (34, 59). We suggest that lower Notch activity observed in the mdx MPCs may influence their proliferation and myogenic

potential. To verify this possibility, the effect of Notch activation on the proliferation and myogenic potential of the mdx MPCs was studied by treating the *in vitro* cultured mdx MPCs from 4-week old mdx mice with the peptide of Jagged1 (60-62), a Notch ligand known to activate Notch signaling in skeletal muscle (19). Results showed that the proliferation of mdx MPCs was promoted, while the myogenic differentiation was reduced with Jagged1 treatment (**Figure 3A**). Meanwhile, the percentage of Pax7+ cells in the mdx MPCs was increased after 2 days of Jagged1 treatment (**Figure 3B, C**). In addition, the expression of the pro-inflammatory factors TNF-α and IL-6 in the mdx MPCs was up-regulated with Jagged1 treatment, suggesting an increased activation of inflammatory signaling (**Figure 3D**); meanwhile, the expression of MyoD was down-regulated with Jagged1 treatment mdx MPCs (**Figure 3D**). This result is consistent with previous observations that TNF-α/NF-κB signaling represses the myogenic potential of muscle stem cells via a potential down-regulation of MyoD (49-51).

To further investigate the potential effect of Notch activation in the skeletal muscle of mdx mice *in vivo,* we conducted intramuscular injections of the Jagged1 peptide into the GM muscle of mdx mice 4 days after cardiotoxin-induced injury. Three days after peptide injection (7 days after muscle injury), we observed a higher number of Pax7+ cells and a lower number of MyoD+ cells in the injected muscle, compared to the control muscles injected with the scrambled peptide (**Figure 3E, F**)**.** Also, the size of the regenerating myofibers was smaller 3 days after the injection in the Jagged1 treated muscles compared to the control muscles (**Figure 3G**), which is indicative of delayed muscle regeneration.

Previous studies have shown that pro-inflammatory TNF-α/NF-κB signaling reduces the myogenic potential of muscle stem cells, via the down-regulation of MyoD (49-51). As expected, here we observed that the myogenic potential of mdx MPCs was reduced through exposure to TNF-α (20 ng/mL), and this effect was able to be prevented by co-treatment of the cells with the Notch inhibitor DAPT (γ-secretase inhibitor) (10 μM) (**Figure 3H**). This observation indicates that Notch signaling

interacts with the pro-inflammatory signaling pathway in repressing myogenesis of muscle stem cells, and Notch inhibition could rescue the pro-inflammatory factor-induced reduction in myogenesis.

4. The beneficial effect of Notch inactivation in dKO MPCs.

Since Notch over-activation was observed in dKO MPCs, we suggest that repression of Notch signaling may influence their proliferation and myogenic potential of dKO MPCs. MPCs isolated from 4-week old dKO mice were cultured in proliferation medium containing DAPT (10 μM) to inhibit Notch activity (63). A reduction in proliferation and an increased in myogenic differentiation was observed in dKO MPCs with DAPT treatment (**Figure 4A**). Meanwhile, the expression of TNF-α and IL-6 was down-regulated, and the expression of MyoD was up-regulated in DAPT treated dKO MPCs (**Figure 4B**). In addition, an increase in the percentage of MyoD+ cells after 2 days of DAPT treatment was also observed in dKO MPCs (**Figure 4C**).

Notch activation is also known to promote the osteogenic potential of human bone marrow stromal cells or vascular smooth muscle cells (64-65). Because MPCs are known to have osteogenic potential (56, 66), and extensive HO was observed in the dKO mice (56), we suggest that the over-activation of Notch signaling in dKO MPCs may be related to the potent osteogenic potential of dKO MPCs. To verify this hypothesis, an osteogenesis assay was performed with dKO MPCs (from 4-week old dKO mice) with and without DAPT treatment (10 μM), and our results indicate a reduction in osteogenic potential of the dKO MPCs with DAPT treatment (**Figure 4C**). Finally, the increased myofibroblastic differentiation (a-SMA positive cells) of dKO MPCs with TGF-β1 stimulation, was reduced with DAPT treatment (**Figure 4C**). Compared to the dKO MPCs treated with TGF-β1 stimulation only, Collagen type I and TGF-β1 was also down-regulated when the cells were co-treated

with DAPT **(Supplemental Figure 1C).** Therefore, the osteogenic or myofibroblastic differentiation potential of the dKO MPCs is reduced by Notch inhibition.

5. Beneficial effects of Notch inactivation in dKO skeletal muscle on stem cell exhaustion, senescence and histopathologies.

In vivo inactivation of Notch signaling in dKO mice was conducted with the intraperitoneal (IP) injection of DAPT dissolved in 95% corn oil/5% ethanol (67-69). The disolving vehicle without DAPT served as a control. The DAPT injections were performed in the dKO mice (3-week to 8-week of age), 3 times per week. Results showed that DAPT injections significantly altered the expression profile of stem cell regulating genes in the dKO skeletal muscle toward that of the mdx skeletal muscle: the expression of Notch, TGF-βs, pro-inflammatory factors, and Pax3 was down-regulated, and the expression of Pax7 and MyoD was up-regulated with DAPT treatment (**Figure 5A**). Western blot analysis confirmed a decrease in Hes1 protein in the skeletal musle of the dKO mice receiving DAPT injection (**Figure 5B**).

Pax7 Immunostaining in the skeletal muscle of 8-week old dKO mice injected with DAPT revealed a significant increased in the number of Pax7+ cells (**Figure 5C**). Co-immunostaining of Notch3 and Pax7 revealed that the number of Notch3+ cells was decreased and the number of Pax7+/Notch3- cells was increased in the dKO mice injected with DAPT (**Figure 5D, E)**. Also, there was an increase in the number of Pax7+ cells residing in the isolated single myofibers of DAPT treated dKO mice (**Figure 5F, G**). Meanwhile, the number of MyoD+ cells in the skeletal muscle of dKO mice was also increased with DAPT treatment (**Figure 5H**), indicating an improvement in the myogenic potential of muscle stem cells. Moreover, the number of β-gal+ senescent cells in the skeletal muscle of dKO mice was decreased with DAPT treatemnt (**Figure 5I**).

Notch inhibition by DAPT also improved the histopathologies of the dystrophic skeletal muscle including an increase in the number of regenerating myofibers expressing embryonic-Myosin Heavy Chain (E-MHC+), and a reduction in the number of inflammatory cells (CD68+) and necrotic myofibers (mouse IgG+) (**Figure 6A**); also, the formation of HO and fibrosis was reduced in DAPT treated dKO mice (**Figure 6B**). In addtion, the intramyocellular lipid accumulation (IMCL) that we reported previously to be enriched in the myofibers of dKO mice (70), was also reduced with DAPT treatment (**Figure 6B**).

A schematic diagram of the potential role of Notch in the histopathology and the regulation of muscle stem cells in dKO skeletal muscle, is outlined in **Figure 6C**.

Discussion

Our results demonstrated that chronic over-activation of Notch signaling occurs in the severely dystrophic muscles of dKO mice which correlates with accelerated stem cell senescence, exhaustion, and impaired muscle regeneration. Repression of Notch signaling was found to be beneficial for rescuing stem cell senescence and exhaustion, and it reduced the histopathological features of the dKO mice by controlling stem cell proliferation, repressing pro-inflammatory signaling, and reducing fibrosis and HO in their skeletal muscle. Decreased Notch activity appears to be necessary for improving muscle regeneration in severely dystrophic muscle, and we suggest that the therapeutic modulation of stem cell activity by regulating Notch could represent a viable therapeutic target for treating DMD patients.

The adverse role of Notch in muscle regeneration has been previously demonstrated by many studies, and constant activation of Notch has been found to impair muscle regeneration (21-27). A temporal decline of Notch in muscle stem cells has been found necessary for proper muscle regeneration and repair (28). Dystrophic muscle undergoes repeated cycles of degeneration and regeneration (71), and our results revealed that this "decline of Notch" during muscle regeneration is more properly regulated in the skeletal muscle of mdx mice but exacerbated in the dKO mice. It is well known that stem cell exhaustion does not occur in the skeletal muscle of mdx mice during most of their lives (2); however, mdx mice lacking the RNA component of telomerase (mdx/mTR) develop stem cell exhaustion and severe muscular dystrophy (2), which has a phenotype very similar to the dKO mouse. Whether telomerase could be involved in the exhausted proliferation capacity of muscle stem cells in dKO mice is still unclear.

It has been reported that Notch promotes stem cell proliferation in normal muscle and maintains muscle stem cells in an undifferentiated state (20, 26). Injection of the Jagged1 peptide into mdx mice in our study also revealed a similar function of Notch activation at promoting the proliferation of Pax7+

cells and repressing myogenic differentiation (**Figure 3**). Meanwhile, Notch activation is also known to promote osteogenesis and calcification processes (64-65, 72), and our results support that notion since Notch inactivation *in vitro* and *in vivo* repress the osteogenic differentiation of dKO MPCs and HO formation in the skeletal muscle of dKO mice (**Figure 4, 6**). Therefore, we suggest that the rapid exhaustion of Pax7+ muscle stem cells in dKO mice (6~8-week) could be explained in 2 ways: 1) Notch-mediated increased in proliferation of stem cells at an early age in dKO mice (before 4-weeks of age) could have exhausted the stem cell compartment and accelerated their senescence; and 2) Notch- and inflammation-mediated excessive formation of HO, fibrotic tissue, and adipose tissue in the skeletal muscle of dKO mice could promote the differentiation of muscle stem cells toward non-myogenic cells (i.e. osteogenic cells, myofibroblasts, or adipogenic cells) (66, 73-74).

Based on our observations, we also suggest that "stem cell exhaustion" in dKO mice is not restricted to early myogenic progenitor (i.e., Pax7+ cells) since an exhaustion of MyoD+ myogenic cells were also observed at 4 weeks of age (**Figure 2A, B**), which occurs earlier than the exhaustion of Pax7+ cells. MyoD+ cells are generally more differentiated than Pax7+ cells and are responsible for muscle regeneration. Therefore, the exhaustion of functional myogenic cells (MyoD+ cells) could be the reason for the impaired muscle regeneration observed in the dKO mice. One recent study demonstrated that Notch activation promoted the proliferation of Pax7+ cells while it inhibited the proliferation of primary myoblasts (MyoD+ cells) (26). Based on this report and our observations, we suggest that increased Notch activity in the dKO mice promote the proliferation of Pax7+ cells but not MyoD+ cells, and prevents Pax7+ cells from differentiating into MyoD+ cells. Thus in order to improve muscle regeneration, both properly controlled stem cell proliferation and myogenic differentiation are required. The micro-environment in the dKO muscles, which is hypoxic, necrotic, fibrotic, and inflammatory, is

not conducive for myogenic differentiation; although Notch over-activation stimulate the proliferation of Pax7+ stem cells, the impaired myogenic differentiation lead to a reduced muscle regeneration.

Notch often acts as a pro-inflammatory signal in mouse cells (48, 75), and recently the canonical NF-κB DNA-binding motif was found in the Notch promoter of human cells (46). Notch and TNF-α/NF-κB signaling have both been reported to repress muscle stem cell differentiation by down-regulating MyoD (21, 49-51), suggesting that these two signaling pathways likely interact in regulating myogenesis and are therefore probably involved in mediating the formation of a dystrophic histopathology; however, such a correlation of Notch and TNF-α/NF-κB signaling in either normal muscle or diseased muscle has never been described. Our current results suggest that Notch signaling maybe interactive with pro-inflammatory TNF-α/NF-κB signaling in the severely affected dystrophic muscle. Co-activation of Notch signaling and pro-inflammatory signaling was observed in the skeletal muscle and muscle stem cells of dKO mice, which is consistent with previous observations of the interactive correlation of Notch and TNF-α/NF-κB in pathologies of various tissues (31-33).

Our results also revealed that the over-activation of Notch signaling in the dKO skeletal muscle appears to interact with TGF-β signaling, and contributes to the formation of fibrosis, muscle atrophy, and HO in the dystrophic muscles. Interaction between Notch signaling and TGF-β family members (TGF-β1, myostatin, and BMP2/4) has been previously demonstrated in a variety of tissue related events (39, 76) including TGF-β1-mediated fibrosis formation (38, 77-79), myostatin-mediated muscle atrophy (80), and BMP-mediated osteogenesis (65, 81). Our *in vitro* and *in vivo* results further validate a correlation between the Notch and TGF-β signaling pathways in mediating the histopathology observed in the dKO muscle including fibrosis, muscle atrophy, and HO.

Notch inhibition with γ-secretase inhibitors (ex. DAPT) has previously been studied for their ability to prevent a variety of different types of organ fibrogenesis and cancers (41, 82-83). Several

phase I and II clinical trials are currently underway to investigate the therapeutic efficacy of various γ-secretases, which has revealed some promising results (84-85). Our study demonstrated that the γ-secretase inhibitor DAPT was effective for improving the myogenic potential of dKO MSDCs *in vitro*, and for improving the muscle regenerative potential of dKO mice *in vivo*. Importantly, the life span of the DAPT treated dKO mice was also slightly increased (data not shown). Our results suggest that Notch inhibition with a γ-secretase inhibitor could potentially be beneficial for treating DMD patients. Gene expression profiles early on in the disease process of DMD have shown a progressive down-regulation of DLK1 (an inhibitory ligand for Notch) from 5 to 24 months after birth (86), indicating a potential increase in Notch activation during disease progression; however, the activation status and the role of Notch signaling in the skeletal muscles of DMD patients requires further investigation.

In summary, our results revealed that the over-activation of Notch signaling plays a role, at least in part, in leading to the severe muscle histopathologies observed in dKO mice. Notch inactivation in severely dystrophic muscle helps repress cell senescence and delays/reduces stem cell exhaustion. In addition, Notch inactivation can reduce inflammation, necrosis, HO, and fibrosis, while improving muscle regeneration. We suggest that the Notch signaling pathway can represent a target for the development of therapeutic approach to alleviate the muscle weakness observed in DMD patients.

Methods and materials

Animals:

Wild-type (C57BL/10J) mice were obtained from Jackson Laboratories (Bar Harbor, ME). The mdx (dys-/-) and dKO (dys-/-; utrn$^{-/-}$) mice were derived from our in house colony. At least 8 mice were used in each experimental sample group. All procedures were approved by the Institutional Animal Care and Use Committee (IACUC) at the University of Pittsburgh.

Stem cell isolation from skeletal muscle:

The muscle derived stem cells (MPCs) were isolated from the skeletal muscle of dKO and mdx mice (4- or 6-weeks old) using the modified preplate technique (87). Mice were sacrificed in a carbon dioxide chamber according to the IACUC protocol. The cells were cultured in the proliferation medium [PM, DMEM supplemented with 20% Fetal Bovine Serum (FBS), 1% Penicillin-Streptomycin antibiotics, and 0.5% chicken essential extract (CEE)] at 37^{o}C in 5% CO_2.

Single myofiber isolation: Skeletal muscle tissue isolated from 4- and 8-week old dKO mice were incubated in a solution of 0.2% collagenase type I for 150 minutes at 37°C, using a protocol previously described (88-89). When the muscles were sufficiently digested they were triturated with heat polished glass pipettes to liberate single fibers. Single intact myofibers were maintained in matrigel coated 12-well plates in PM at 37°C in 5% CO_2.

In vitro Notch activation or inactivation:

MPCs from 4-week old mdx mice (mdx MPCs) were treated with the Jagged1 peptide (CDDYYYGFGCNKFCRPR) or a control scrambled peptide (RCGPDCFDNYGRYKYCF) (60-62) (GenScript USA, Inc.) (20 µg/mL) in myogenic differentiation medium (DMEM with 2% horse serum) for 3 days to compare their myogenic potentials. MPCs from 4-week old dKO mice (dKO MPCs) were

treated with DAPT (N-[N-(3,5-Difluorophenacetyl-L-alanyl)]-S-phenylglycine t-Butyl Ester; Calbiochem) (γ-secretase inhibitor) (10 μM) in myogenic differentiation medium for 3 days to compare their myogenic potentials, or in osteogenic differentiation medium to compare their osteogenic potentials. Control cells were treated with carrier (DMSO) only.

***In vivo* Notch activation or inactivation:**

In order to observe the effect of Notch activation on muscle regeneration in mdx mice, cardiotoxin (Calbiochem) (10μM in 40μL of PBS) was intramuscularly injected into the GM muscles of 8-week old mdx mice to generate muscle injury, followed by intramuscular injection of the Jagged1 peptide or the control scrambled peptide (5 mg/ml in 15 μL of PBS) twice, on days 3 and 5 post-muscle injury. Peptides were prepared and injected as previously reported (60-62). Four days after the injection of the Jagged1 peptide (7 days after cardiotoxin injection), the muscle tissues were harvested for analysis. In order to observe the effect of Notch inactivation on muscle regeneration in the dKO mice, DAPT solution (10 mg/ml in 95% corn oil/5% ethanol, 30 mg/kg per mouse) (67-69) was injected into dKO mice via intraperitoneal (IP) injection 3 times per week from the age of 3-weeks old, and continued until the mice reached 8 weeks of age. dKO mice receiving the vehicle (95% corn oil/5% ethanol) served as a control.

***In vitro* myogenic, osteogenic and myofibroblastic diffferentiation assays:**

For the myogenesis assay, MPCs from 4-week old dKO mice were cultured in myogenic differentiation medium (2% horse serum/HS in DMEM) for 4 days, with or without DAPT (10 μM) supplementation. The myogenic potential was then tracked by observing myotube formation. The osteogenesis assay was conducted with osteogenic medium (DMEM supplemented with 110 mg/L sodium pyruvate, 584 mg/L L-glutamine, 10% FBS, 1% penicillin/streptomycin, 10^{-7} M dexamethasone, 50 μg/ml ascorbic-acid-2-phosphate, and 10^{-2} M β-glycerophosphate), supplemented with BMP2 (50 ng/ml for 7 days). Calcium

deposition assessed with Alizarin Red staining was used to determine the osteogenic potential. The fibrogenesis assay was conducted by supplementing growth medium with TGF-β1 (10 ng/ml). Cells positive for α-smooth muscle actin (SMA) were monitored to determine the myofibroblastic differentiation potential.

Cell senescence assay:

A cell senescence assay was performed on muscle cells and muscle tissues using a Senescence β-Galactosidase (β-gal) Staining Kit (Cell Signaling Technology) following the manufacturer's protocol. The number of cells positive for β-gal activity at pH6, a known characteristic of senescent cells not found in pre-senescent, quiescent, or immortal cells, was determined.

mRNA analysis with semi-quantitative Reverse Transcriptase-PCR:

Total RNA was obtained from MPCs or the skeletal muscles of mice using the RNeasy Mini Kit (Qiagen, Inc., Valencia, CA) according to the manufacturer's instructions. Reverse transcription was performed using the iScript cDNA Synthesis Kit (Bio-Rad Laboratories, Inc., Hercules, CA). The primer sequences are listed in **Table 1**. PCR reactions were performed using an iCycler Thermal Cycler (Bio-Rad Laboratories, Inc.). The cycling parameters used for all primers were as follows: 95°C for 10 minutes; PCR, 40 cycles of 30 seconds at 95°C for denaturation, 1 minute at 54°C for annealing, and 30 seconds at 72°C for extension. Products were separated and visualized on a 1.5% agarose gel stained with ethidium bromide. All data were normalized to the expression of GAPDH (glyceraldehydes 3-phosphate dehydrogenase).

Western blot:

Frozen muscle tissues were lysed with a lysate buffer [ratio of β-mercaptoethanol to sample buffer (62.5 mM Tris-HCl, pH 6.8, 2% SDS, 25% glycerol) = 1:20], as previously reported (90). After being boiled, the whole tissue lysates were centrifuged at 3,000 *g* for 5min, and the supernatant was collected and

stored at 4°C. The samples were analyzed on a 12% SDS-polyacrylamide gel. Protein concentrations were determined by using the Bradford method (91). Four micrograms of protein from each sample were loaded onto the gel and electrophoresed at 80V for 3h. We then transferred the total protein to a nitrocellulose membrane (Bio-Rad, Hercules, CA) via electroblot transfer at 60V for 50 min. Membranes were washed in PBS for 5min and blocked with 1% nonfat dry milk and 2% horse serum in Triton-PBS (T-PBS; 0.01%) for 1h at room temperature (shaken at 60 cycles/min). A primary antibody of Notch1 (Abcam) or Hes1 (Abcam) was applied 1: 1,000 and incubated overnight at 4^{o}C. The blots were then washed four times in T-PBS (15 min/wash). A secondary antibody of anti-Rabbit IgG conjugated with horseradish peroxidase (1:5,000, Pierce, Rockford, IL) was applied for 1h, at which time the blots again were washed 4 times in T-PBS (15 min/wash). After the blots were washed, they were developed using enhanced chemiluminescence (Supersignal West Pico Chemilluminescent Substrate, Pierce), and the positive bands were identified using X-ray film. Protein levels of GAPDH were also analyzed to serve as a control.

Histology:

HO in the muscle tissues was assessed by Alizarin Red staining: Tissue sections of skeletal muscle were fixed with 4% formalin (10 min), and rinsed with double-distilled (dd) H_2O; slides were then incubated with alizarin red working solution for 10 min before they were washed with ddH2O. Fatty infiltration was detected by Oil Red O staining: tissue sections of skeletal muscle were fixed with 4% formalin (10 min), and rinsed with ddH_2O and 60% isopropanol; slides were then incubated with Oil Red O working solution for 15 min, before being rinsed with 60% isopropanol and ddH_2O. The IMCL was detected by AdipoRed assay reagent (Lonza): tissue sections of skeletal muscle were fixed with 4% formalin (10 min), and rinsed with PBS; slides were than incubated with AdipoRed assay reagent for 15min, before being washed with PBS. Slides were rinsed and dehydrated prior to coverslip mounting using permanent

mounting medium. For Masson Trichrome staining, sections were incubated in Weigert's iron hematoxylin working solution for 10 min, and rinsed under running water for 10 min. Slides were transferred to Biebrich scarlet-acid fuchsin solution for 15min before incubation in aniline blue solution for another 5 min. Slides were then rinsed, dehydrated, and mounted as above. Muscle tissue was sectioned and slides were incubated for 5 min in alizarin red solution prior to counterstaining with eosin. Slides were rinsed, dehydrated, and mounted. All incubations were performed at room temperature. Immunofluorescent staining of tissue sections: The frozen tissue sections were fixed with 4% formalin. The primary antibodies Pax7 (DHSB), MyoD (Santa Cruz), Collagen IV (Abcam), Ki67 (Santa Cruz), Notch1 (Abcam), and α-SMA (Abcam) were applied at 1:100 ~ 1:200. It is notable that Pax7 antibody from DHSB was developed in mouse, and in addition to specifically binding to Pax7+ cells, it non-specifically binds to the necrotic myofibers; such necrotic tissue revealed by the Pax7 antibody was verified by staining with mouse IgG, which has been traditionally used to identify necrotic tissue. All slides were analyzed under fluorescence microscopy (Leica Microsystemic Inc., IL) and photographed at 4-40X magnification.

Measurements of results and statistical analysis:

The quantitation of the results from images was performed using the software Northern Eclipse (version 6.0; Empix Imaging, Inc., Mississauga, ON, Canada) and Image J software (version 1.32j; National Institutes of Health, Bethesda, MD). Data from at least four samples from each subject were pooled for statistical analyses. Results are given as the mean ± standard deviation (SD). Statistical significance of any difference was calculated using Student's *t*-test. When p values were less than 0.05 the difference was considered statistically significant.

References:

1. Carnio, S., Serena, E., Rossi, C.A., De Coppi, P., Elvassore, N., and Vitiello, L. 2011. Three-dimensional porous scaffold allows long-term wild-type cell delivery in dystrophic muscle. *J Tissue Eng Regen Med* 5:1-10.
2. Sacco, A., Mourkioti, F., Tran, R., Choi, J., Llewellyn, M., Kraft, P., Shkreli, M., Delp, S., Pomerantz, J.H., Artandi, S.E., et al. 2010. Short telomeres and stem cell exhaustion model Duchenne muscular dystrophy in mdx/mTR mice. *Cell* 143:1059-1071.
3. Zhu, C.H., Mouly, V., Cooper, R.N., Mamchaoui, K., Bigot, A., Shay, J.W., Di Santo, J.P., Butler-Browne, G.S., and Wright, W.E. 2007. Cellular senescence in human myoblasts is overcome by human telomerase reverse transcriptase and cyclin-dependent kinase 4: consequences in aging muscle and therapeutic strategies for muscular dystrophies. *Aging Cell* 6:515-523.
4. Janssen, P.M., Hiranandani, N., Mays, T.A., and Rafael-Fortney, J.A. 2005. Utrophin deficiency worsens cardiac contractile dysfunction present in dystrophin-deficient mdx mice. *Am J Physiol Heart Circ Physiol* 289:H2373-2378.
5. Bulfield, G., Siller, W.G., Wight, P.A., and Moore, K.J. 1984. X chromosome-linked muscular dystrophy (mdx) in the mouse. *Proc Natl Acad Sci U S A* 81:1189-1192.
6. Shadrach, J.L., and Wagers, A.J. 2011. Stem cells for skeletal muscle repair. *Philos Trans R Soc Lond B Biol Sci* 366:2297-2306.
7. Dilworth, F.J., and Blais, A. 2011. Epigenetic regulation of satellite cell activation during muscle regeneration. *Stem Cell Res Ther* 2:18.
8. Duan, D. 2006. Challenges and opportunities in dystrophin-deficient cardiomyopathy gene therapy. *Hum Mol Genet* 15 Spec No 2:R253-261.
9. Grady, R.M., Teng, H., Nichol, M.C., Cunningham, J.C., Wilkinson, R.S., and Sanes, J.R. 1997. Skeletal and cardiac myopathies in mice lacking utrophin and dystrophin: a model for Duchenne muscular dystrophy. *Cell* 90:729-738.
10. Deconinck, A.E., Rafael, J.A., Skinner, J.A., Brown, S.C., Potter, A.C., Metzinger, L., Watt, D.J., Dickson, J.G., Tinsley, J.M., and Davies, K.E. 1997. Utrophin-dystrophin-deficient mice as a model for Duchenne muscular dystrophy. *Cell* 90:717-727.
11. Gehrig, S.M., van der Poel, C., Sayer, T.A., Schertzer, J.D., Henstridge, D.C., Church, J.E., Lamon, S., Russell, A.P., Davies, K.E., Febbraio, M.A., et al. 2012. Hsp72 preserves muscle function and slows progression of severe muscular dystrophy. *Nature* 484:394-398.
12. Chun, J.L., O'Brien, R., and Berry, S.E. 2012. Cardiac dysfunction and pathology in the dystrophin and utrophin-deficient mouse during development of dilated cardiomyopathy. *Neuromuscul Disord* 22:368-379.
13. Deconinck, A.E., Potter, A.C., Tinsley, J.M., Wood, S.J., Vater, R., Young, C., Metzinger, L., Vincent, A., Slater, C.R., and Davies, K.E. 1997. Postsynaptic abnormalities at the neuromuscular junctions of utrophin-deficient mice. *J Cell Biol* 136:883-894.
14. Huard, A.L.M.P.Y.T.J.D.P.J.S.X.M.N.O.B.W.J. 2014. Rapid depletion of Muscle Progenitor Cells in the Dystrophic mdx/utrophin-/- mice. *Human Molecular Genetics*.
15. Bjornson, C.R., Cheung, T.H., Liu, L., Tripathi, P.V., Steeper, K.M., and Rando, T.A. 2012. Notch signaling is necessary to maintain quiescence in adult muscle stem cells. *Stem Cells* 30:232-242.
16. Mourikis, P., Sambasivan, R., Castel, D., Rocheteau, P., Bizzarro, V., and Tajbakhsh, S. 2012. A critical requirement for notch signaling in maintenance of the quiescent skeletal muscle stem cell state. *Stem Cells* 30:243-252.
17. Fukada, S., Yamaguchi, M., Kokubo, H., Ogawa, R., Uezumi, A., Yoneda, T., Matev, M.M., Motohashi, N., Ito, T., Zolkiewska, A., et al. 2011. Hesr1 and Hesr3 are essential to generate undifferentiated quiescent satellite cells and to maintain satellite cell numbers. *Development* 138:4609-4619.

18. Mayeuf, A., and Relaix, F. 2011. [Notch pathway: from development to regeneration of skeletal muscle]. *Med Sci (Paris)* 27:521-526.
19. Carey, K.A., Farnfield, M.M., Tarquinio, S.D., and Cameron-Smith, D. 2007. Impaired expression of Notch signaling genes in aged human skeletal muscle. *J Gerontol A Biol Sci Med Sci* 62:9-17.
20. Conboy, I.M., and Rando, T.A. 2002. The regulation of Notch signaling controls satellite cell activation and cell fate determination in postnatal myogenesis. *Dev Cell* 3:397-409.
21. Kopan, R., Nye, J.S., and Weintraub, H. 1994. The intracellular domain of mouse Notch: a constitutively activated repressor of myogenesis directed at the basic helix-loop-helix region of MyoD. *Development* 120:2385-2396.
22. Kuroda, K., Tani, S., Tamura, K., Minoguchi, S., Kurooka, H., and Honjo, T. 1999. Delta-induced Notch signaling mediated by RBP-J inhibits MyoD expression and myogenesis. *J Biol Chem* 274:7238-7244.
23. Waddell, J.N., Zhang, P., Wen, Y., Gupta, S.K., Yevtodiyenko, A., Schmidt, J.V., Bidwell, C.A., Kumar, A., and Kuang, S. 2010. Dlk1 is necessary for proper skeletal muscle development and regeneration. *PLoS One* 5:e15055.
24. Buas, M.F., Kabak, S., and Kadesch, T. 2009. Inhibition of myogenesis by Notch: evidence for multiple pathways. *J Cell Physiol* 218:84-93.
25. Kitamoto, T., and Hanaoka, K. 2010. Notch3 null mutation in mice causes muscle hyperplasia by repetitive muscle regeneration. *Stem Cells* 28:2205-2216.
26. Wen, Y., Bi, P., Liu, W., Asakura, A., Keller, C., and Kuang, S. 2012. Constitutive Notch activation upregulates Pax7 and promotes the self-renewal of skeletal muscle satellite cells. *Mol Cell Biol* 32:2300-2311.
27. Sun, H., Li, L., Vercherat, C., Gulbagci, N.T., Acharjee, S., Li, J., Chung, T.K., Thin, T.H., and Taneja, R. 2007. Stra13 regulates satellite cell activation by antagonizing Notch signaling. *J Cell Biol* 177:647-657.
28. Brack, A.S., Conboy, I.M., Conboy, M.J., Shen, J., and Rando, T.A. 2008. A temporal switch from notch to Wnt signaling in muscle stem cells is necessary for normal adult myogenesis. *Cell Stem Cell* 2:50-59.
29. Liu, X.H., Yao, S., Qiao, R.F., Levine, A.C., Kirschenbaum, A., Pan, J., Wu, Y., Qin, W., Bauman, W.A., and Cardozo, C.P. 2011. Nandrolone reduces activation of Notch signaling in denervated muscle associated with increased Numb expression. *Biochem Biophys Res Commun* 414:165-169.
30. Nagpal, P., Plant, P.J., Correa, J., Bain, A., Takeda, M., Kawabe, H., Rotin, D., Bain, J.R., and Batt, J.A. 2012. The ubiquitin ligase Nedd4-1 participates in denervation-induced skeletal muscle atrophy in mice. *PLoS One* 7:e46427.
31. Yang, Y., Duan, W., Jin, Z., Bi, S., Yan, J., Jin, Y., Lu, J., Yang, J., and Yi, D. 2011. New role of Notch-mediated signaling pathway in myocardial ischemic preconditioning. *Med Hypotheses* 76:427-428.
32. Osipo, C., Golde, T.E., Osborne, B.A., and Miele, L.A. 2008. Off the beaten pathway: the complex cross talk between Notch and NF-kappaB. *Lab Invest* 88:11-17.
33. Bash, J., Zong, W.X., Banga, S., Rivera, A., Ballard, D.W., Ron, Y., and Gelinas, C. 1999. Rel/NF-kappaB can trigger the Notch signaling pathway by inducing the expression of Jagged1, a ligand for Notch receptors. *EMBO J* 18:2803-2811.
34. Liu, W., Wen, Y., Bi, P., Lai, X., Liu, X.S., Liu, X., and Kuang, S. 2012. Hypoxia promotes satellite cell self-renewal and enhances the efficiency of myoblast transplantation. *Development* 139:2857-2865.
35. Zhang, K.J., Huang, L.F., Sun, H.Y., Zhu, Y., Xiao, Y., Huang, M., and Liu, W.L. 2010. [Relation of notch pathway to senescence of murine bone marrow stromal cells]. *Zhongguo Shi Yan Xue Ye Xue Za Zhi* 18:410-415.
36. Noseda, M., Chang, L., McLean, G., Grim, J.E., Clurman, B.E., Smith, L.L., and Karsan, A. 2004. Notch activation induces endothelial cell cycle arrest and participates in contact inhibition: role of p21Cip1 repression. *Mol Cell Biol* 24:8813-8822.
37. Liu, Z.J., Tan, Y., Beecham, G.W., Seo, D.M., Tian, R., Li, Y., Vazquez-Padron, R.I., Pericak-Vance, M., Vance, J.M., Goldschmidt-Clermont, P.J., et al. 2012. Notch activation induces endothelial cell

senescence and pro-inflammatory response: implication of Notch signaling in atherosclerosis. *Atherosclerosis* 225:296-303.
38. Aoyagi-Ikeda, K., Maeno, T., Matsui, H., Ueno, M., Hara, K., Aoki, Y., Aoki, F., Shimizu, T., Doi, H., Kawai-Kowase, K., et al. 2011. Notch induces myofibroblast differentiation of alveolar epithelial cells via transforming growth factor-{beta}-Smad3 pathway. *Am J Respir Cell Mol Biol* 45:136-144.
39. Blokzijl, A., Dahlqvist, C., Reissmann, E., Falk, A., Moliner, A., Lendahl, U., and Ibanez, C.F. 2003. Cross-talk between the Notch and TGF-beta signaling pathways mediated by interaction of the Notch intracellular domain with Smad3. *J Cell Biol* 163:723-728.
40. Leask, A. 2010. Targeting the jagged/notch pathway: a new treatment for fibrosis? *J Cell Commun Signal* 4:197-198.
41. Kavian, N., Servettaz, A., Weill, B., and Batteux, F. 2012. New insights into the mechanism of notch signalling in fibrosis. *Open Rheumatol J* 6:96-102.
42. Theroux, M.C., Olivant, A., and Akins, R.E. 2008. C Histomorphology of neuromuscular junction in Duchenne muscular dystrophy. *Paediatr Anaesth* 18:256-259.
43. Scaffidi, P., and Misteli, T. 2008. Lamin A-dependent misregulation of adult stem cells associated with accelerated ageing. *Nat Cell Biol* 10:452-459.
44. Meshorer, E., and Gruenbaum, Y. 2008. Gone with the Wnt/Notch: stem cells in laminopathies, progeria, and aging. *J Cell Biol* 181:9-13.
45. Guarani, V., Deflorian, G., Franco, C.A., Kruger, M., Phng, L.K., Bentley, K., Toussaint, L., Dequiedt, F., Mostoslavsky, R., Schmidt, M.H., et al. 2011. Acetylation-dependent regulation of endothelial Notch signalling by the SIRT1 deacetylase. *Nature* 473:234-238.
46. Li, J., Tang, Y., and Cai, D. 2012. IKKbeta/NF-kappaB disrupts adult hypothalamic neural stem cells to mediate a neurodegenerative mechanism of dietary obesity and pre-diabetes. *Nat Cell Biol* 14:999-1012.
47. Qin, L., Xu, J., Wu, Z., Zhang, Z., Li, J., Wang, C., and Long, Q. 2013. Notch1-mediated signaling regulates proliferation of porcine satellite cells (PSCs). *Cell Signal* 25:561-569.
48. Quillard, T., and Charreau, B. 2013. Impact of notch signaling on inflammatory responses in cardiovascular disorders. *Int J Mol Sci* 14:6863-6888.
49. Langen, R.C., Van Der Velden, J.L., Schols, A.M., Kelders, M.C., Wouters, E.F., and Janssen-Heininger, Y.M. 2004. Tumor necrosis factor-alpha inhibits myogenic differentiation through MyoD protein destabilization. *FASEB J* 18:227-237.
50. Szalay, K., Razga, Z., and Duda, E. 1997. TNF inhibits myogenesis and downregulates the expression of myogenic regulatory factors myoD and myogenin. *Eur J Cell Biol* 74:391-398.
51. Lu, A., Proto, J.D., Guo, L., Tang, Y., Lavasani, M., Tilstra, J.S., Niedernhofer, L.J., Wang, B., Guttridge, D.C., Robbins, P.D., et al. 2012. NF-kappaB negatively impacts the myogenic potential of muscle-derived stem cells. *Mol Ther* 20:661-668.
52. Megeney, L.A., Kablar, B., Garrett, K., Anderson, J.E., and Rudnicki, M.A. 1996. MyoD is required for myogenic stem cell function in adult skeletal muscle. *Genes Dev* 10:1173-1183.
53. Kikkawa, N., Ohno, T., Nagata, Y., Shiozuka, M., Kogure, T., and Matsuda, R. 2009. Ectopic calcification is caused by elevated levels of serum inorganic phosphate in mdx mice. *Cell Struct Funct* 34:77-88.
54. LaRusso, J., Jiang, Q., Li, Q., and Uitto, J. 2008. Ectopic mineralization of connective tissue in Abcc6-/- mice: effects of dietary modifications and a phosphate binder--a preliminary study. *Exp Dermatol* 17:203-207.
55. Isaac, C., Wright, A., Usas, A., Li, H., Tang, Y., Mu, X., Greco, N., Dong, Q., Vo, N., Kang, J., et al. 2012. Dystrophin and utrophin "double knockout" dystrophic mice exhibit a spectrum of degenerative musculoskeletal abnormalities. *J Orthop Res*.
56. Mu, X., Usas, A., Tang, Y., Lu, A., Wang, B., Weiss, K., and Huard, J. 2013. RhoA mediates defective stem cell function and heterotopic ossification in dystrophic muscle of mice. *FASEB J*.
57. Chiba, S. 2006. Notch signaling in stem cell systems. *Stem Cells* 24:2437-2447.

58. Zhao, Y., Banerjee, S., Dey, N., LeJeune, W.S., Sarkar, P.S., Brobey, R., Rosenblatt, K.P., Tilton, R.G., and Choudhary, S. 2011. Klotho depletion contributes to increased inflammation in kidney of the db/db mouse model of diabetes via RelA (serine)536 phosphorylation. *Diabetes* 60:1907-1916.
59. Luo, D., Renault, V.M., and Rando, T.A. 2005. The regulation of Notch signaling in muscle stem cell activation and postnatal myogenesis. *Semin Cell Dev Biol* 16:612-622.
60. Nickoloff, B.J., Qin, J.Z., Chaturvedi, V., Denning, M.F., Bonish, B., and Miele, L. 2002. Jagged-1 mediated activation of notch signaling induces complete maturation of human keratinocytes through NF-kappaB and PPARgamma. *Cell Death Differ* 9:842-855.
61. Sainson, R.C., Aoto, J., Nakatsu, M.N., Holderfield, M., Conn, E., Koller, E., and Hughes, C.C. 2005. Cell-autonomous notch signaling regulates endothelial cell branching and proliferation during vascular tubulogenesis. *FASEB J* 19:1027-1029.
62. Hellstrom, M., Phng, L.K., Hofmann, J.J., Wallgard, E., Coultas, L., Lindblom, P., Alva, J., Nilsson, A.K., Karlsson, L., Gaiano, N., et al. 2007. Dll4 signalling through Notch1 regulates formation of tip cells during angiogenesis. *Nature* 445:776-780.
63. Engin, F., Bertin, T., Ma, O., Jiang, M.M., Wang, L., Sutton, R.E., Donehower, L.A., and Lee, B. 2009. Notch signaling contributes to the pathogenesis of human osteosarcomas. *Hum Mol Genet* 18:1464-1470.
64. Ugarte, F., Ryser, M., Thieme, S., Fierro, F.A., Navratiel, K., Bornhauser, M., and Brenner, S. 2009. Notch signaling enhances osteogenic differentiation while inhibiting adipogenesis in primary human bone marrow stromal cells. *Exp Hematol* 37:867-875 e861.
65. Shimizu, T., Tanaka, T., Iso, T., Doi, H., Sato, H., Kawai-Kowase, K., Arai, M., and Kurabayashi, M. 2009. Notch signaling induces osteogenic differentiation and mineralization of vascular smooth muscle cells: role of Msx2 gene induction via Notch-RBP-Jk signaling. *Arterioscler Thromb Vasc Biol* 29:1104-1111.
66. Corsi, K.A., Pollett, J.B., Phillippi, J.A., Usas, A., Li, G., and Huard, J. 2007. Osteogenic potential of postnatal skeletal muscle-derived stem cells is influenced by donor sex. *J Bone Miner Res* 22:1592-1602.
67. Teachey, D.T., Seif, A.E., Brown, V.I., Bruno, M., Bunte, R.M., Chang, Y.J., Choi, J.K., Fish, J.D., Hall, J., Reid, G.S., et al. 2008. Targeting Notch signaling in autoimmune and lymphoproliferative disease. *Blood* 111:705-714.
68. Zhang, W., Xu, W., and Xiong, S. 2010. Blockade of Notch1 signaling alleviates murine lupus via blunting macrophage activation and M2b polarization. *J Immunol* 184:6465-6478.
69. McGowan, P.M., Simedrea, C., Ribot, E.J., Foster, P.J., Palmieri, D., Steeg, P.S., Allan, A.L., and Chambers, A.F. 2011. Notch1 inhibition alters the CD44hi/CD24lo population and reduces the formation of brain metastases from breast cancer. *Mol Cancer Res* 9:834-844.
70. Mu, X., Usas, A., Tang, Y., Lu, A., Wang, B., Weiss, K., and Huard, J. 2013. RhoA mediates defective stem cell function and heterotopic ossification in dystrophic muscle of mice. *FASEB J* 27:3619-3631.
71. Carlson, B.M. 1973. The regeneration of skeletal muscle. A review. *Am J Anat* 137:119-149.
72. Rusanescu, G., Weissleder, R., and Aikawa, E. 2008. Notch signaling in cardiovascular disease and calcification. *Curr Cardiol Rev* 4:148-156.
73. Usas, A., Maciulaitis, J., Maciulaitis, R., Jakuboniene, N., Milasius, A., and Huard, J. 2011. Skeletal muscle-derived stem cells: implications for cell-mediated therapies. *Medicina (Kaunas)* 47:469-479.
74. Li, Y., and Huard, J. 2002. Differentiation of muscle-derived cells into myofibroblasts in injured skeletal muscle. *Am J Pathol* 161:895-907.
75. Maniati, E., Bossard, M., Cook, N., Candido, J.B., Emami-Shahri, N., Nedospasov, S.A., Balkwill, F.R., Tuveson, D.A., and Hagemann, T. 2011. Crosstalk between the canonical NF-kappaB and Notch signaling pathways inhibits Ppargamma expression and promotes pancreatic cancer progression in mice. *J Clin Invest* 121:4685-4699.
76. Tang, Y., Urs, S., Boucher, J., Bernaiche, T., Venkatesh, D., Spicer, D.B., Vary, C.P., and Liaw, L. 2010. Notch and transforming growth factor-beta (TGFbeta) signaling pathways cooperatively regulate vascular smooth muscle cell differentiation. *J Biol Chem* 285:17556-17563.

77. Higgins, D.F., Kimura, K., Bernhardt, W.M., Shrimanker, N., Akai, Y., Hohenstein, B., Saito, Y., Johnson, R.S., Kretzler, M., Cohen, C.D., et al. 2007. Hypoxia promotes fibrogenesis in vivo via HIF-1 stimulation of epithelial-to-mesenchymal transition. *J Clin Invest* 117:3810-3820.
78. Matsuno, Y., Coelho, A.L., Jarai, G., Westwick, J., and Hogaboam, C.M. 2012. Notch signaling mediates TGF-beta1-induced epithelial-mesenchymal transition through the induction of Snai1. *Int J Biochem Cell Biol* 44:776-789.
79. Chen, Y., Zheng, S., Qi, D., Guo, J., Zhang, S., and Weng, Z. 2012. Inhibition of Notch signaling by a gamma-secretase inhibitor attenuates hepatic fibrosis in rats. *PLoS One* 7:e46512.
80. McFarlane, C., Hui, G.Z., Amanda, W.Z., Lau, H.Y., Lokireddy, S., Xiaojia, G., Mouly, V., Butler-Browne, G., Gluckman, P.D., Sharma, M., et al. 2011. Human myostatin negatively regulates human myoblast growth and differentiation. *Am J Physiol Cell Physiol* 301:C195-203.
81. Lin, G.L., and Hankenson, K.D. 2011. Integration of BMP, Wnt, and notch signaling pathways in osteoblast differentiation. *J Cell Biochem* 112:3491-3501.
82. Dees, C., Zerr, P., Tomcik, M., Beyer, C., Horn, A., Akhmetshina, A., Palumbo, K., Reich, N., Zwerina, J., Sticherling, M., et al. 2011. Inhibition of Notch signaling prevents experimental fibrosis and induces regression of established fibrosis. *Arthritis Rheum* 63:1396-1404.
83. Shih Ie, M., and Wang, T.L. 2007. Notch signaling, gamma-secretase inhibitors, and cancer therapy. *Cancer Res* 67:1879-1882.
84. Takebe, N., Nguyen, D., and Yang, S.X. 2014. Targeting notch signaling pathway in cancer: clinical development advances and challenges. *Pharmacol Ther* 141:140-149.
85. Purow, B. 2012. Notch inhibition as a promising new approach to cancer therapy. *Adv Exp Med Biol* 727:305-319.
86. Pescatori, M., Broccolini, A., Minetti, C., Bertini, E., Bruno, C., D'Amico, A., Bernardini, C., Mirabella, M., Silvestri, G., Giglio, V., et al. 2007. Gene expression profiling in the early phases of DMD: a constant molecular signature characterizes DMD muscle from early postnatal life throughout disease progression. *FASEB J* 21:1210-1226.
87. Gharaibeh, B., Lu, A., Tebbets, J., Zheng, B., Feduska, J., Crisan, M., Peault, B., Cummins, J., and Huard, J. 2008. Isolation of a slowly adhering cell fraction containing stem cells from murine skeletal muscle by the preplate technique. *Nat Protoc* 3:1501-1509.
88. Mu, X., Brown, L.D., Liu, Y., and Schneider, M.F. 2007. Roles of the calcineurin and CaMK signaling pathways in fast-to-slow fiber type transformation of cultured adult mouse skeletal muscle fibers. *Physiol Genomics* 30:300-312.
89. Shefer, G., and Yablonka-Reuveni, Z. 2005. Isolation and culture of skeletal muscle myofibers as a means to analyze satellite cells. *Methods Mol Biol* 290:281-304.
90. Chan, Y.S., Li, Y., Foster, W., Horaguchi, T., Somogyi, G., Fu, F.H., and Huard, J. 2003. Antifibrotic effects of suramin in injured skeletal muscle after laceration. *J Appl Physiol* 95:771-780.
91. Bradford, M.M. 1976. A rapid and sensitive method for the quantitation of microgram quantities of protein utilizing the principle of protein-dye binding. *Anal Biochem* 72:248-254.

Figures and legends:

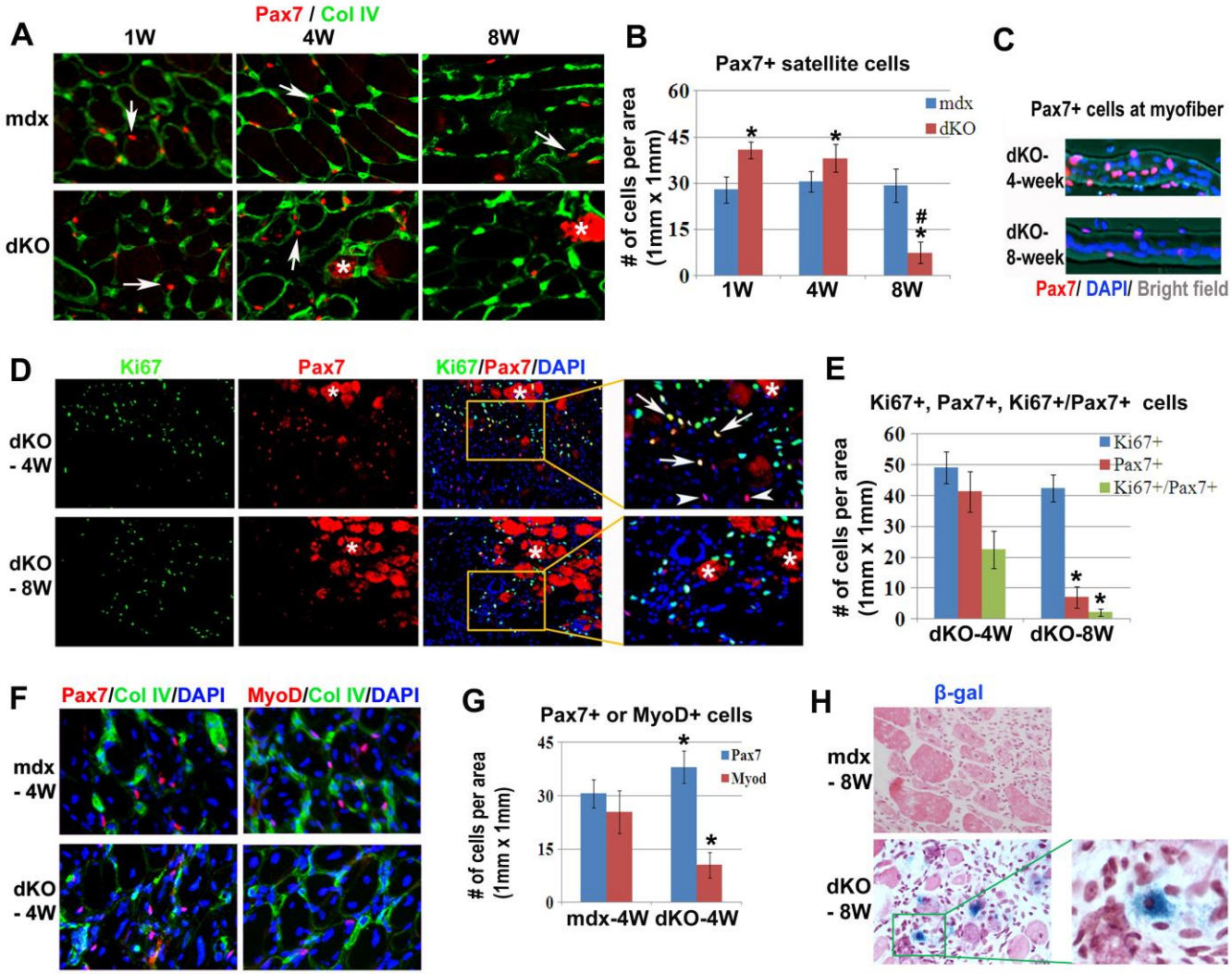

Figure 1. MPC exhaustion and senescence occurs in dKO mice but not in mdx mice, and involves both Pax7+ cells and MyoD+ cells.

A. Representative images showing that in comparison with mdx mice**,** the number of Pax7+ cells (muscle stem cells) (red, arrows) was enriched in the skeletal muscle (Gastrocnemius muscle/GM) of 1-week and 4-week old dKO mice and decreased in the skeletal muscle of 8-week old dKO mice. Red: Pax7; green: Collagen type IV (Col IV). Non-specific staining of necrotic structures (degenerated myofibers) by the mouse-anti-mouse Pax7 antibody is marked with asterisks "*****", and it shows dKO mice developed more necrosis in muscle. ***B***. Statistics of the number of Pax7+ cells in the GM muscle of mdx and dKO mice at 1, 4, and 8-weeks of age. "*****" indicates $p < 0.05$ comparing skeletal muscles of the dKO and mdx mice, "**#**' indicates $p < 0.05$ comparing muscle of 8-week old dKO mice and 1-week (or 4-week) old dKO mice. ***C.*** *In vitro* cultured single myofibers isolated from 4- and 8-week old dKO mice show a different numbers of Pax7+ satellite cells. ***D.*** representative images of cells positive for Ki67, Pax7 or both in the GMs of 4- and 8-week old dKO mice; the number of Ki67+/Pax7+ cells decreased with age. Red: Pax7; green: Ki67; blue: DAPI. Arrows: Ki67+/Pax7+ cells (proliferating satellite cells); arrowheads: Pax7+/Ki67- cells (non-proliferating satellite cells); asterisks: necrotic myofibers. ***E.*** Statistics of the number of Ki67+, Pax7+, or Ki67+/Pax7+ satellite cells in the GM muscle of mdx and dKO mice at 1, 4, and 8-week old. "*****" indicates the p value is < 0.05. ***F.*** Representative images of

immunostaining of cells positive for Pax7+ or MyoD in the skeletal muscle of mdx or dKO mice at 4-week age: the number of Pax7+ cells in dKO skeletal muscle was higher, but the number of MyoD+ cells was lower than that in mdx skeletal muscle. Red: Pax7; green: Col IV; blue: DAPI. ***G.*** Statistics of the number of Pax7+ and MyoD+ cells in mdx and dKO mice. "*****" indicates $p < 0.05$ compared to mdx mice. ***H.*** Cell senescence assay revealed more β-gal+ cells in the skeletal muscle of 8-week old dKO mice, compared to 8-week old mdx mice.

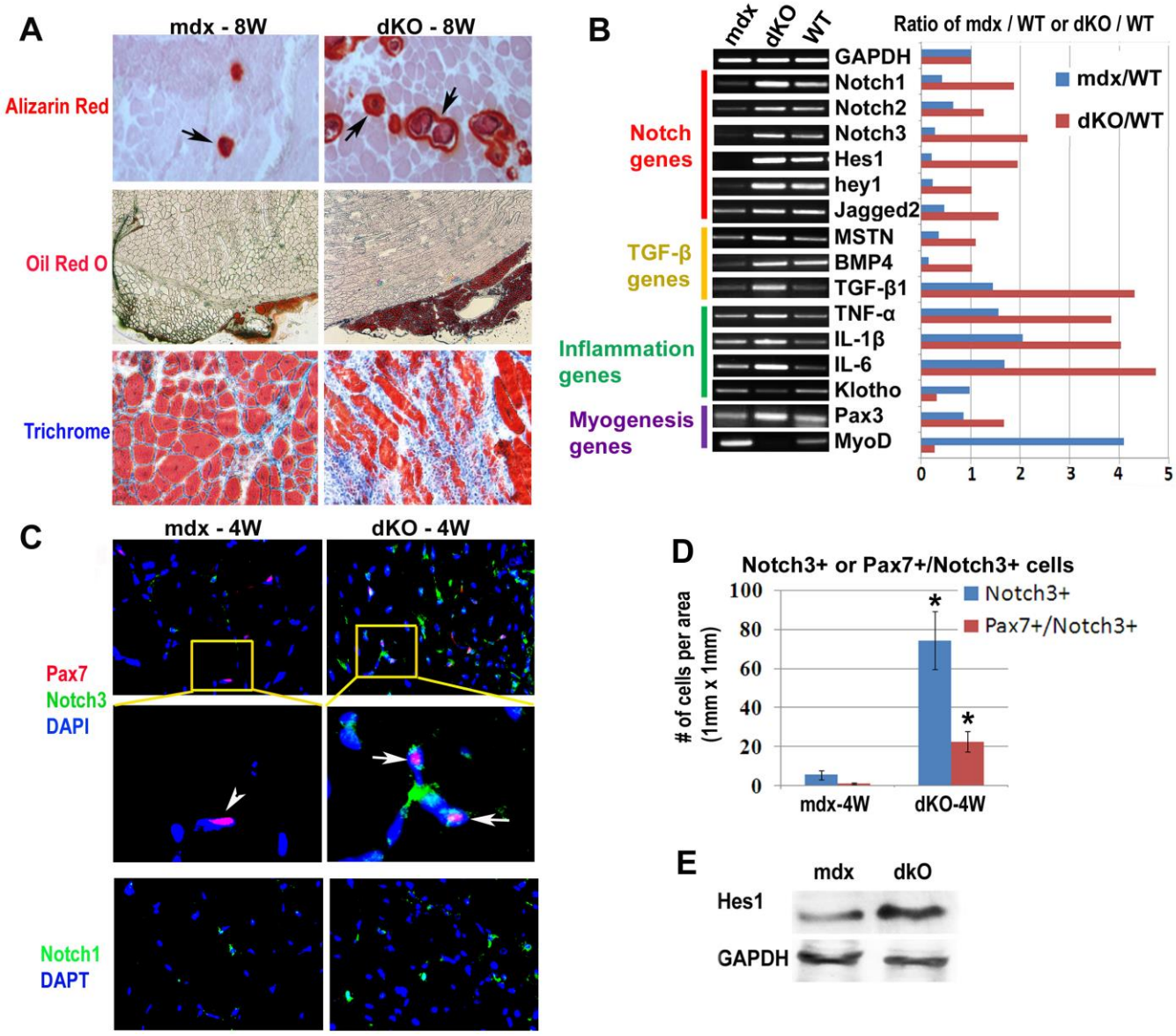

Figure 2. Increased non-muscle tissues (HO, peri-muscular adipose tissue, and fibrosis) and over-activation of Notch signaling in the skeletal muscle of dKO mice.

A. Alizarin Red staining showed extensive formation of HO (arrows) in dKO skeletal muscle; Oil Red O staining revealed extensive formation of peri-muscular adipose tissue at the surface of the dKO skeletal muscle; Trichrome staining demonstrated extensive formation of fibrotic tissue in the dKO skeletal muscle. ***B.*** Gene expression assay showed an up-regulation of Notch genes (Notch 1-3, Hes1, Hey1,

Jagged2), TGF-β genes (myostatin/MSTN, BMP4 and TGF-β1), inflammation genes (TNF-α, IL-1β and IL-6), and Pax3 (a marker of undifferentiated muscle stem cells), as well as down-regulation of Klotho (an anti-inflammation factor) and MyoD (myogenic factor) in dKO skeletal muscle, compared to both mdx and WT skeletal muscle. Bar charts show the ratio of mdx mice compared to WT mice (mdx / WT), and the ratio of dKO mice compared to WT mice (dKO / WT) for each gene. ***C.*** Immunostaining revealed more Notch3+ cells and Notch3+/Pax7+ cells (arrows) in dKO skeletal muscle, compared to mdx skeletal muscle; Pax7+ cells in mdx skeletal muscle are generally Notch3- (arrowhead). Notch1+ cells were also more abundant in dKO skeletal muscle. Red: Pax7; green: Notch3 or Notch1; blue: DAPI. ***D.*** Statistics of the number of Notch3+ and Pax7+/Notch3+ cells in the skeletal muscles of 4-week old mdx and dKO mice. "*****" indicates the p value is < 0.05. ***E.*** Western blot analysis revealed a higher level of Hes1 protein in dKO skeletal muscle.

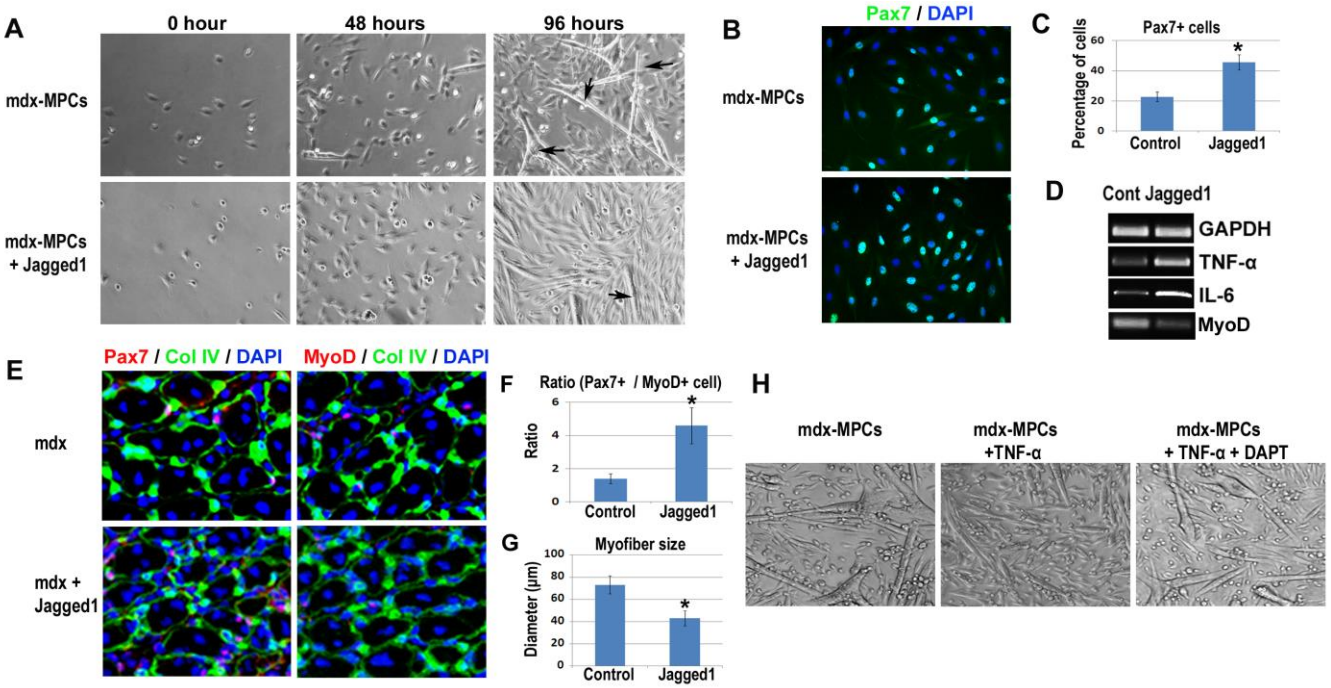

Figure 3. Effect of *in vitro* and *in vivo* manipulation of Notch signaling in MPCs and skeletal muscle of mdx mice.

A. With Jagged1 treatment (Notch activation), the proliferation of mdx MPCs was promoted while the spontaneous fusion/myotube formation was reduced compared to mdx MPCs without treatment. **Arrows:** myotubes. ***B.*** The ratio of Pax7+ cells was increased after 2 days of Jagged1 treatment. ***C.*** Statistics of the number of Pax7 + cells with and without Jagged1 treatment. "*****" indicates the p value is < 0.05. ***D.*** Gene expression assay showed that, TNF-α and IL-6 were up-regulated, and MyoD was down-regulated by Jaggged1 treatment of mdx MPCs. ***E.*** Intramuscular injection of Jagged1 peptide into the GM muscles of mdx mice lead to an elevated ratio of the number of Pax7+ cells to MyoD+ cells (Pax7/MyoD), at the site of injection; myofibers in the muscles with Jagged1 injection are also smaller in size. ***F.*** Statistics of the ratio of Pax7/MyoD with or without Jagged1 injection. "*****" indicates p < 0.05. ***G.*** Statistics of myofiber size with or without Jagged1 injection. "*****" indicates p < 0.05. ***H.*** Myogenic assay revealed that, TNF-α treatment (20 ng/mL) of mdx MPCs reduce myotube formation, while DAPT treatment (10 μM) (Notch inactivation) reduced the deleterious effect of TNF-α.

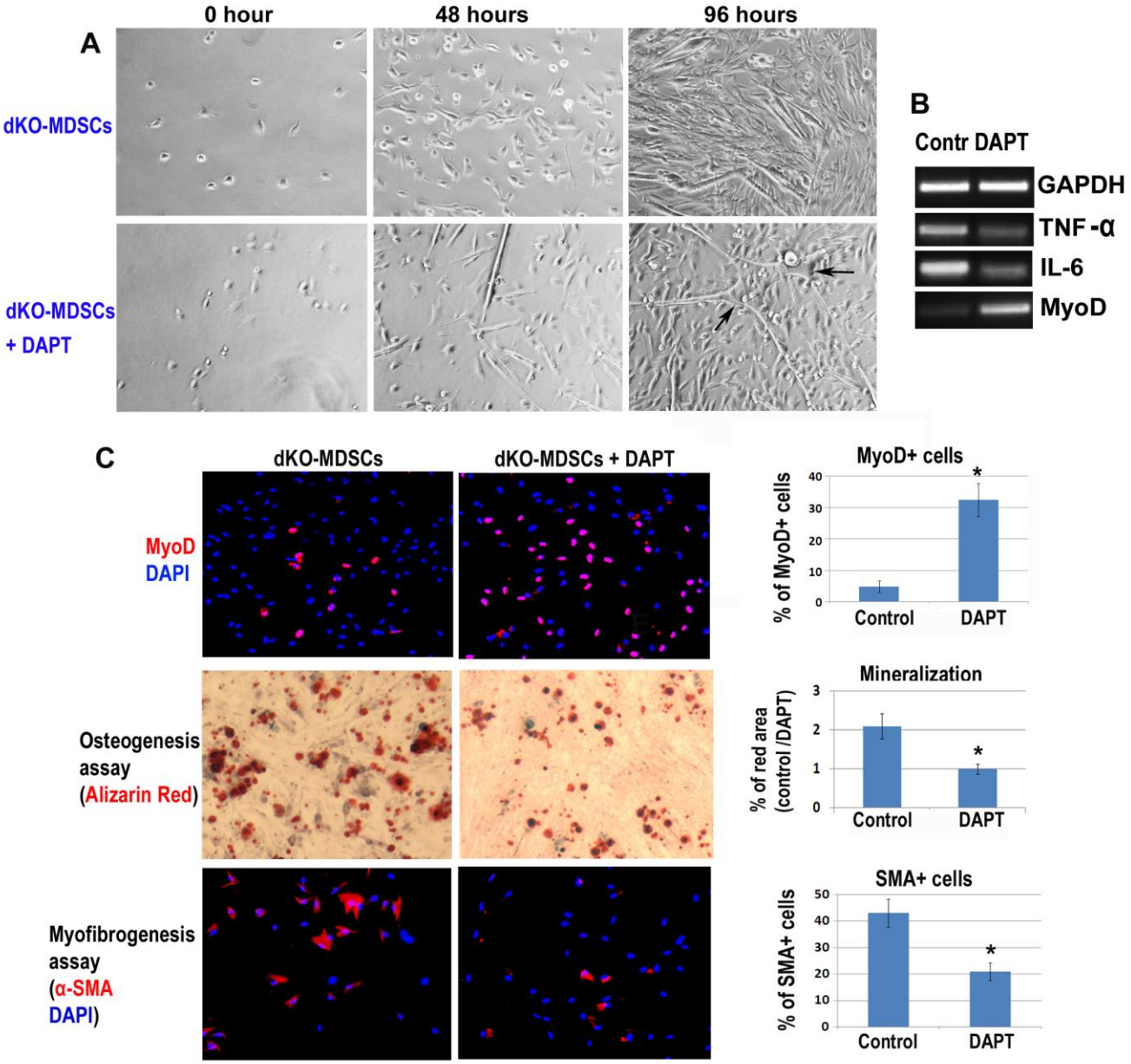

Figure 4. Effects of *in vitro* inactivation of Notch on cell proliferation, myogenic differentiation, osteogenic differentiation, and myofibroblastic differentiation of dKO MPCs.

A. With DAPT treatment (Notch inactivation), the proliferation of dKO MPCs was reduced while the spontaneous fusion/myotube formation was increase compared to dKO MPCs without treatment. **Arrows:** myotubes. ***B.*** Gene expression assay showed that, TNF-α and IL-6 were down-regulated, and MyoD was up-regulated by DAPT treatment of dKO MPCs. ***C.*** The ratio of MyoD+ cells in dKO MPCs was increased after 2 days of DAPT treatment; the osteogenic potential of dKO MPCs in osteogenic differentiation medium, which is shown as Alizarin Red staining of calcium deposition, was increased by DAPT treatment; the myofibroblastic differentiation potential of dKO MPCs, which was determined with the TGF-β1 induced production of α-Smooth Muscle Actin (SMA) by the cells, was reduced by DAPT treatment. Statistics include the comparison of MyoD+ cells in the myogenesis assay, Alizarin

Red-positive signal in the osteogenesis assay, and α-SMA+ cells in the TGF-β1 induced myofibroblastic differentiation assay. "*" indicates $p < 0.05$.

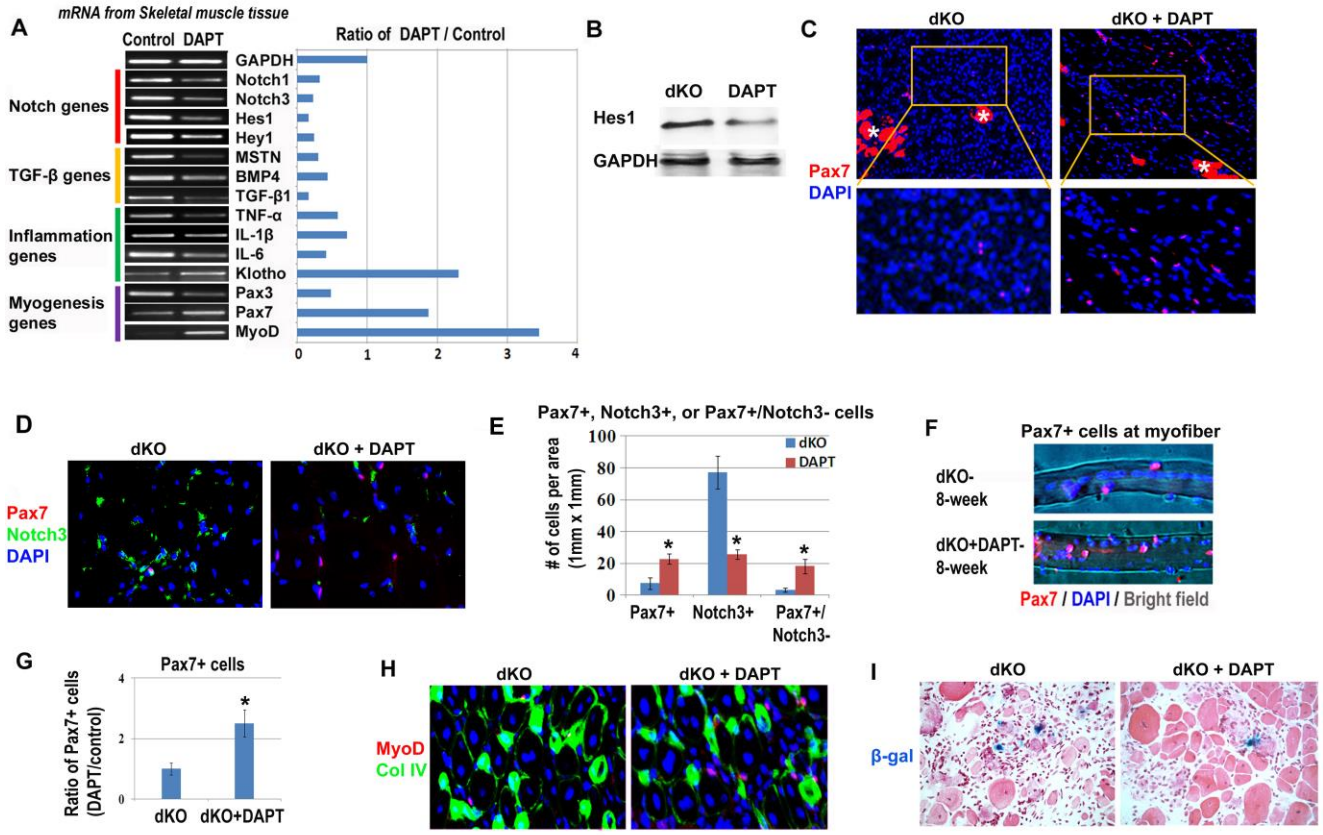

Figure 5. Effect of *in vivo* inactivation of Notch on the expression of muscle regeneration-related genes and stem cell exhaustion and senescence in the skeletal muscle of dKO mice.

A. Gene expression assay showed that compared to muscle tissue without DAPT injection (Notch inactivation), muscle tissues with DAPT injection featured a down-regulation of Notch genes (Notch 1, 3, Hes1, and Hey1), TGF-β genes (myostatin/MSTN, BMP4, and TGF-β1), inflammation genes (TNF-α, IL-1β, and IL-6) and Pax3, and an up-regulation of Klotho, Pax7, and MyoD. Bar charts show the ratio of mRNA in DAPT-injected mice to control mice for each gene. ***B.*** Western blot analysis of Hes1 validated that DAPT treatment decreased the activation of Notch signaling in dKO mice. ***C.*** Representative images of immunostaining showing that DAPT treatment increased the number of Pax7+ cells in the skeletal muscle of 8-week old dKO mice. Red: Pax7; blue: DAPI. Asterisks: necrotic myofibers. ***D.*** Immunostaining showed that DAPT treatment decreased the number of Notch3+ cells, and increased the number of Pax7+/Notch3- cells in the dKO skeletal muscle. Red: Pax7; green: Notch3; blue: DAPI. ***E.*** Statistics of the number of Pax7+, Notch3+, or Pax7+/Notch3- cells in dKO skeletal muscle with or without DAPT treatment. *"*"* indicates $p < 0.05$. ***F.*** *In vitro* cultured single myofibers isolated from 8-week old dKO mice with or without DAPT injection contain a different numbers of Pax7+ cells. Red: Pax7; blue: DAPI. ***G.*** Statistics of the number of Pax7+ at single myofibers. ***H.*** Immunostaining showed that DAPT treatment also increased the number of MyoD+ cells. Red: MyoD; green: Collagen IV; blue: DAPI. ***I.*** Cell senescence assay showed that DAPT treatment decreased the number of β-gal+ cells. H.E. staining was performed at the same slides and improved myofiber formation can be observed.

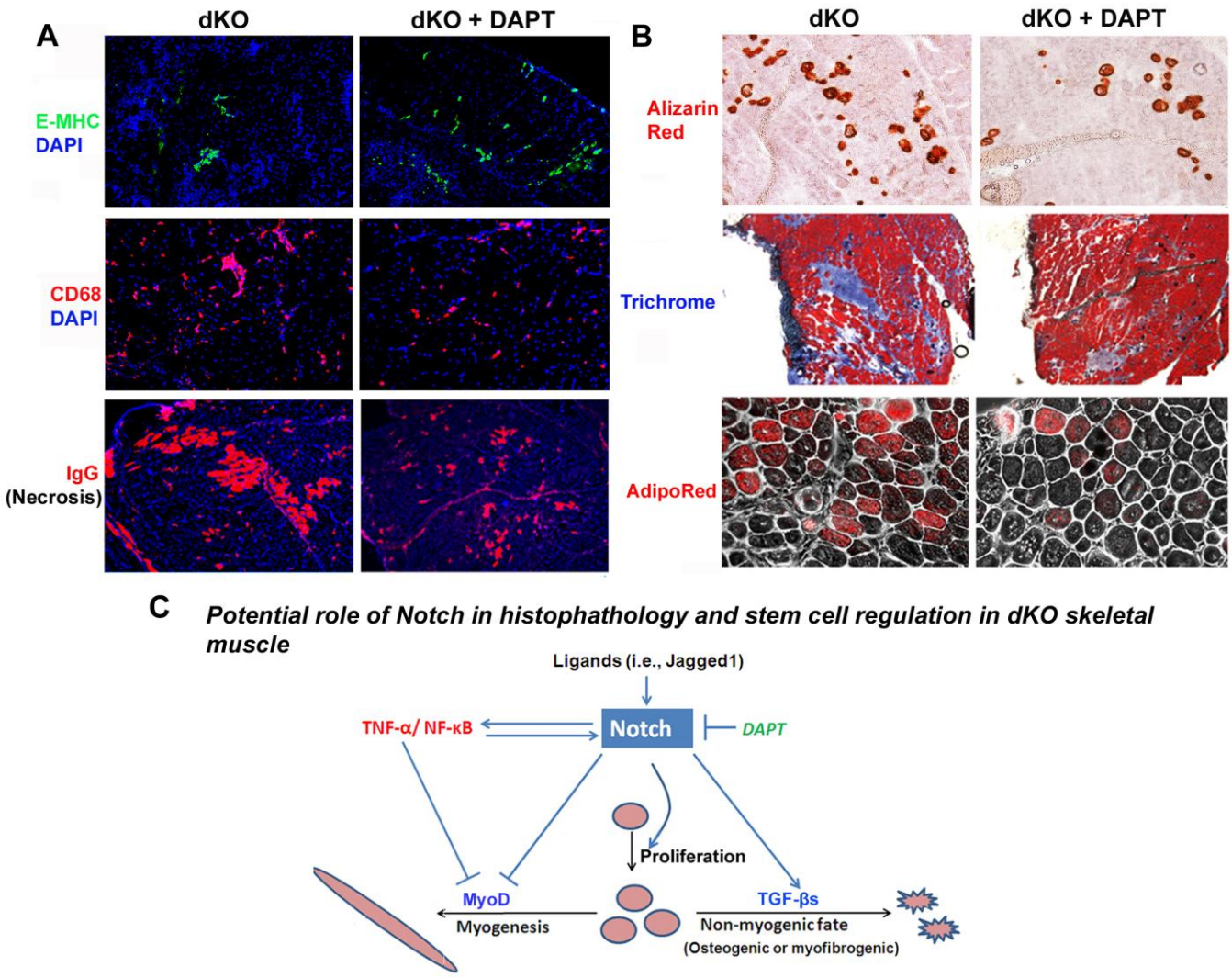

Figure 6. Effect of *in vivo* inactivation of Notch on the histopathologies of the skeletal muscle of dKO mice.

A. Histopathological changes in the GM muscles of 8-week old dKO mice with and without IP injection of DAPT include: immunostaining of embryonic Myosin Heavy Chain (E-MHC) showed an increased number of E-MHC+ cells with DAPT injection; immunostaining of CD68 showed a decreased number of CD68+ cells with DAPT injection; anti-mouse IgG staining showed reduced necrotic myofibers with DAPT injection. ***B.*** Alizarin Red staining showed reduced HO formation with DAPT injection; Trichrome staining showed reduced fibrotic tissue with DAPT injection; AdipoRed staining revealed reduced lipid accumulation in myofibers with DAPT injection. ***C.*** Schematic diagram of potential mechanism of Notch signaling in regulating stem cells in the skeletal muscle of dKO mice. Over-activated Notch signaling in muscle stem cells of dKO mice may lead to impaired muscle stem cell function.

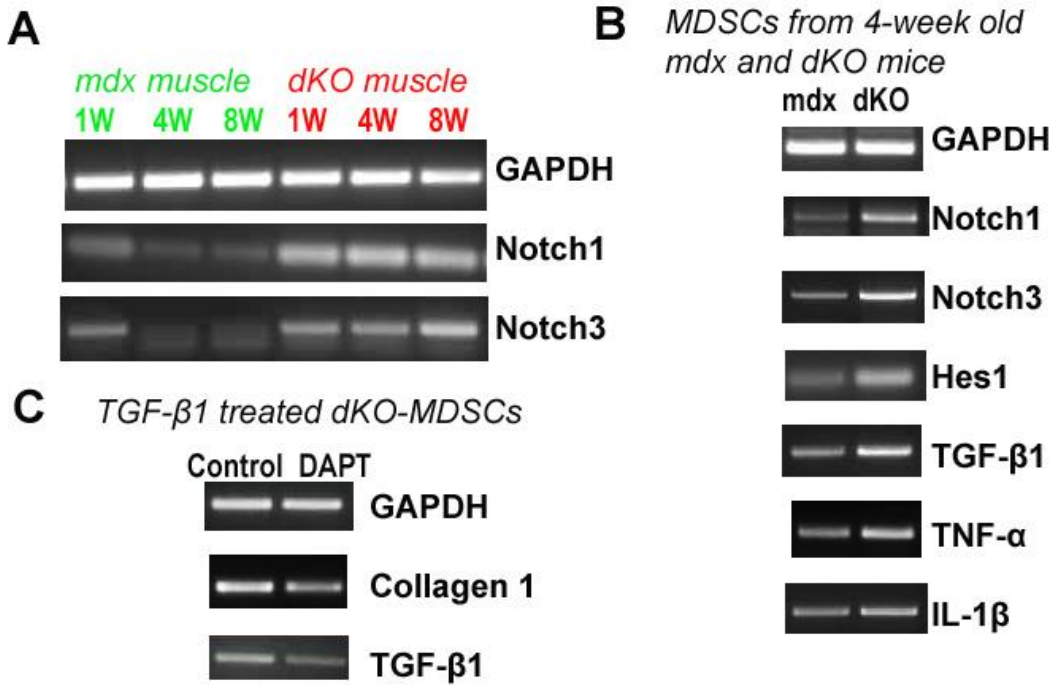

S Figure 1: Additional RT-PCR results.
A. The expression of Notch1 and 3 was consistently up-regulated in the skeletal muscle of dKO mice of different ages (1, 4 and 8-week old), compared to mdx mice. ***B.*** The expression of Notch1, Notch3, Hes1, TGF-β1, TNFα and IL-1β was up-regulated in the MPCs isolated from 4-week old dKO mice, compared to mdx mice. ***C.*** In a TGF-β1 induced myofibroblastic differentiation assay, the expression of collagen type1 and TGF-β1 was down-regulated in dKO MSDCs treated DAPT (10 μM).

Table 1: PCR primer sequences

Gene	Primer sequence
GAPDH	Forward: TCCATGACAACTTTGGCATTG Reverse: TCACGCCACAGCTTTCCA
Notch1	Forward: GCCGCAAGAGGCTTGAGAT Reverse: GGAGTCCTGGCATCGTTGG
Notch2	Forward: GAGAAAAACCGCTGTCAGAATGG Reverse: GGTGGAGTATTGGCAGTCCTC
Notch3	Forward: TGCCAGAGTTCAGTGGTGG Reverse: CACAGGCAAATCGGCCATC
Hes1	Forward: CCAGCCAGTGTCAACACGA Reverse: AATGCCGGGAGCTATCTTTCT
Hey1	Forward: CCGACGAGACCGAATCAATAAC Reverse: TCAGGTGATCCACAGTCATCTG
Jagged2	Forward: ACAGTTGTTATGGGTGGCTCT Reverse: CGGCTCCTCTCACGTTCTTTC
Myostatin	Forward: AGTGGATCTAAATGAGGGCAGT Reverse: GTTTCCAGGCGCAGCTTAC
BMP4	Forward: ATTCCTGGTAACCGAATGCTG Reverse: CCGGTCTCAGGTATCAAACTAGC
TGF-β1	Forward: GGAGAGCCCTGGATACCAAC Reverse: CAACCCAGGTCCTTCCTAAA
TNF-α	Forward: GATTATGGCTCAGGGTCCAA Reverse: CTCCCTTTGCAGAACTCAGG
IL-1β	Forward: GGAGAACCAAGCAACGACAAAATA Reverse: TGGGGAACTCTGCAGACTCAAAC
IL-6	Forward :GGAAATCGTGGAAATGAG Reverse: GCTTAGGCATAACGCACT
Klotho	Forward :CCCAAACCATCTATGAAAC Reverse: CTACCGTATTCTATGCCTTC
Pax3	Forward :CATCCGACCTGGTGCCATC Reverse: ATTTCCCAGCTAAACATGCCC
Pax7	Forward: TCTCCAAGATTCTGTGCCGAT Reverse: CGGGGTTCTCTCTCTTATACTCC
MyoD	Forward: ACAGTGGCGACTCAGATGCATC Reverse: GCTGCAGTCGATCTCTCAAAGC
Collagen I	Forward: AAGGAGTTTCATCTGGCCCT Reverse: AGCAGGTCCTTGGAAACCTT

Stem cells isolated from human dental pulp and amniotic fluid improve the dystrophic phenotype of skeletal muscle in mdx/SCID mice

[1]Alessandra Pisciotta, [1]Massimo Riccio, [1]Gianluca Carnevale, [2]Aiping Lu, [3]Giovanni B. La Sala, [4]Giacomo Bruzzesi, [5]Adriano Ferrari, [2]Johnny Huard, [1]Anto De Pol.

[1]Department of Surgical, Medical, Dental and Morphological Sciences with interest in Transplant, Oncology and Regenerative Medicine, University of Modena and Reggio Emilia, Modena, Italy; [2]Stem Cell Research Center, Department of Orthopaedic Surgery, University of Pittsburgh, Pittsburgh, PA, United States; [3]Department of Obstetrics and Gynecology, Arcispedale Santa Maria Nuova, Reggio Emilia, Italy; [4]Oro-Maxillo-Facial Department, AUSL Baggiovara, Baggiovara, Modena, Italy; [5]Department of Biomedical, Metabolic and Neuroscience, University of Modena and Reggio Emilia, Children Rehabilitation Special Unit, IRCCS Arcispedale Santa Maria Nuova, Reggio Emilia, Italy.

Running title: hDPSCs and hAFSCs improve dystrophic phenotype

Corresponding author: Dr. Alessandra Pisciotta, PhD
e-mail: alessandra.pisciotta@unimore.it
phone: +39 059 4224828
fax: +39 059 4224859

ABSTRACT

Duchenne muscular dystrophy (DMD), caused by a lack of the functional structural protein dystrophin, causes severe muscle degeneration and patients are typically wheelchair bound and die in their mid-twenties from cardiac and/or respiratory failure. Human dental pulp stem cells (hDPSCs) and amniotic fluid stem cells (hAFSCs) represent two cell populations that could potentially be utilized in cellular therapies for treating DMD patients through the repair of damaged skeletal muscle fibers and restoring dystrophin expression. Human DPSCs and AFSCs have been shown to be self-renewing, multipotent and easily accessible for isolation, from adult human dental pulp of third molars during routine extraction, and by supernumerary amniocentesis samples, respectively.

Here, we demonstrated that hDPSCs and hAFSCs commit towards a myogenic lineage *in vitro*, when directly co-cultured with C2C12 cells and when differentiated after demethylation treatment. hDPSCs and AFSCs, demethylated and pre-differentiated towards a myogenic lineage, were then injected into the dystrophic gastrocnemius muscles of *mdx*/SCID mice, which is an immune-compromised animal model of DMD. Both populations of cells achieved successful engraftment within the host muscle, promoted angiogenesis, restored dystrophin expression, and improved the dystrophic phenotype of the mice.

This study shows that hAFSCs and hDPSCs represent potential sources of stem cells for translational strategies to enhance the regeneration of injured skeletal muscle of DMD patients.

Key words: hDPSCs, hAFSCs, Duchenne muscular dystrophy, skeletal muscle regeneration, dystrophin

INTRODUCTION

Duchenne muscular dystrophy (DMD) is an X-linked recessive genetic disease, characterized by the lack of the structural protein, dystrophin, which is the primary component of the dystrophin-glycoprotein complex (DGC) that links the cytoskeleton to the extracellular matrix, thus providing stability to the sarcolemma during muscle contraction [1].

DMD is one of the most common (1 in 3500 live male births) and severe of the muscular dystrophies, presenting with severe progressive degeneration of skeletal muscle fibers and resulting in the death of the patients, typically before their third decade of life [2].

The use of corticosteroids delays the loss of muscle function in DMD patients; however, there is currently no therapy capable of preventing the progressive muscle degenerative processes associated with DMD [3], though several different therapeutic approaches have been tested over the years, including cell and gene therapies.

Cell therapy could be used to recover the lack of dystrophin in dystrophic muscles and thus repair the damaged muscle fibers and prevent future muscle degeneration. Recently, various stem cell populations have been used to treat muscular dystrophy.

Stem cells obtained from different sources, including bone marrow, adipose tissue, umbilical cord and placenta, have been investigated and could represent alternative tissue sources for obtaining adult multi-lineage progenitor cells [4-7]. Human dental pulp stem cells (hDPSCs) have been identified and can be harvested from human dental pulp during routine extraction of either deciduous teeth or third molars. hDPSCs have been widely demonstrated to be clonogenic cells capable of both self-renewal and multiple lineage differentiation [8, 9]. Human amniotic fluid stem cells (hAFSCs) have also been identified and constitute approximately 1% of the cells that could potentially be obtained from human amniocentesis backup specimens [10], samples that would otherwise be discarded. Human AFSCs have been shown to possess self-renewal and multi-

differentiation capacities, do not induce nor form teratomas, and are far less controversial than embryonic stem cells [10, 11].

In this study, we investigated the potential of human DPSCs and AFSCs to differentiate towards a skeletal myogenic lineage utilizing several different protocols in order to determine the optimal conditions for achieving myogenic commitment. The first protocol was based on the direct co-culture of the human cells with murine myoblasts in order to evaluate the capacity of both populations to fuse and form mature myotubes when directly co-cultured with mouse myoblasts.

The second protocol was based on the use of the demethylating agent 5-Aza-2'-deoxycytidine (5-Aza) and supplementation of the cultures with or without the addition of conditioned media from differentiated mouse myoblast cultures, medium that contains numerous soluble factors that can promote myogenic differentiation, including IGF-II [12]. To verify the effective differentiation of the hDPSCs and hAFSCs towards a skeletal myogenic lineage, we investigated the expression of muscle specific factors and markers including myogenin, myosin heavy chain and desmin.

It has been previously established that genes related to myogenic differentiation are controlled by DNA methylation and that the use of the demethylating agent 5-Aza was able to induce adult human bone marrow stem cells to differentiate towards a cardiomyogenic lineage [13, 14].

After treatment with 5-Aza and pre-differentiation *in vitro,* we tested the ability of the hDPSCs and hAFSCs to restore dystrophin expression and contribute in the amelioration of the pathological features associated with dystrophic skeletal muscle when intramuscularly injected into mdx/SCID mice, an immune-compromised animal model of DMD.

MATERIALS AND METHODS

Cell culture and sorting

Human dental pulp was extracted from the enclosed third molar of teenage subjects undergoing routine tooth extractions, following written informed consent from their parents. All procedures for

collecting the human samples were approved by the Provincial Ethics Committee of Santa Maria Nuova Hospital of Reggio Emilia. Human dental pulp stem cells (hDPSC) were isolated from dental pulp, as previously described by Riccio et al. [15]. The STRO-1^+ hDPSC sub-population of cells was obtained via magnetic cell sorting (MACS; Miltenyi Biotec), using a mouse anti-STRO-1 antibody (Ab; Santa Cruz).

Supernumerary amniocentesis samples were provided by Laboratorio di Genetica, Ospedale Santa Maria Nuova (Reggio Emilia, Italy). All the samples were collected after informed consent was obtained from the patients following Italian law and ethical committee guidelines. Human amniotic fluid stem cells were isolated as previously described by De Coppi et al. [10].

Briefly, human amniocentesis cultures were harvested by trypsinization, and immunoselected by MACS using a rabbit anti-c-Kit antibody (Santa Cruz). Both cell populations were expanded in culture medium containing α-MEM plus 20% Fetal Calf Serum (FCS), 2mM L-glutamine, 100 U/ml penicillin, 100 µg/ml streptomycin (Sigma Aldrich) and incubated at 37° C in an atmosphere of 5% CO_2.

The expression of STRO-1 and c-Kit antigens was assessed through immunofluorescent staining, as described below. Moreover, the expression of STRO-1 and c-Kit antigens by hDPSCs and hAFSCs, respectively, was also evaluated through FACS analysis, by indirect staining using mouse anti-STRO-1 IgM and rabbit anti-c-Kit IgG (Santa Cruz) followed by goat anti-mouse-IgG-Alexa488 and goat anti-rabbit IgG-Alexa488 (Invitrogen). Non-specific fluorescence was assessed using normal mouse IgG or IgM followed by the secondary antibody as described above. Samples were analyzed using a 16-parameters CyFlow ML flow cytometer (Partec GmbH, Munster, Germany), equipped with a 488-nm blue solid-state, a 635-nm red diode laser, a UV mercury lamp HBO, a 532-nm green solid state laser, a 405-nm violet laser, and a CCD camera. Data were acquired in list mode by using FloMax (Partec) software, and then analyzed by FlowJo 9.4.11 (Treestar Inc., Ashland, OR) under MacOS 10.

Animals

Eight to ten weeks old male B10ScSn.Cg-*Prkdc*^{scid} *Dmd*^{mdx}/J (*mdx*/SCID; Jackson Laboratory) mice were housed in the animal facility located in the Bridgeside Point II building, University of Pittsburgh, under stable conditions of humidity and temperature in a controlled vivarium on a 12:12 hour light–dark cycle with free access to food and water. All the experimental procedures were carried out according to the guidelines approved by the Institutional Animal Care and Use Committee (IACUC) of the University of Pittsburgh, Pittsburgh, PA, USA.

Myogenic differentiation in vitro

In order to evaluate the myogenic potential of the STRO-1$^+$ hDPSCs and c-kit$^+$ hAFSCs, the cells underwent distinct differentiation protocols. The first protocol required the direct co-culture of the hDPSCs or hAFSCswith the C2C12 mouse myoblast cell line as previously described by Pisciotta et al. [16]. Human stem cells and mouse myoblasts were seeded on coverslips at a ratio of 10:1 and maintained in expansion medium containing DMEM high glucose (DMEM-HG) plus 10% FCS, 2mM L-glutamine, 100 U/ml penicillin, 100 µg/ml streptomycin, until the cells reached confluency. At this point the expansion medium was replaced with fusion medium, containing DMEM-HG plus 1% FCS, 2mM L-glutamine, 100 U/ml penicillin, 100 µg/ml streptomycin, and 10nM insulin and continued to be co-cultured in fusion medium for 14 days.

The second protocol involved the myogenic differentiation of hDPSCs and hAFSCs by first treating the cells to 10 µM 5-Aza without direct co-culture. hDPSCs and hAFSCs were seeded on coverslips at a cell density of 4000 cells/cm^2 in expansion medium (DMEM-HG plus 10% FCS, 2mM L-glutamine, 100 U/ml penicillin, 100 µg/ml streptomycin) and upon reaching confluency the medium was replaced with DMEM low glucose (DMEM-LG), plus 10% horse serum, 0,5% chicken serum, 2mM L-glutamine, 100 U/ml penicillin, 100 µg/ml streptomycin, supplemented with 10µM 5-Aza for 24 hours. Subsequently, cells were rinsed twice in Phosphate Buffer Saline (PBS) and kept in myogenic medium containing DMEM-LG, plus 5% horse serum, 0.5% chicken serum, 2mM

L-glutamine, 100 U/ml penicillin, 100 µg/ml streptomycin, and 10 nM insulin for 24 hours. The following day, the horse serum concentration in the myogenic medium was reduced to 2%. Half of the cells of the hDPSCs and hAFSCs were differentiated under these conditions while the other half underwent the same treatment with the addition of conditioned medium (CM) from differentiated C2C12 mouse myoblast cells.

Western Blot

In order to further evaluate the *in vitro* differentiation capacities of the STRO-1$^+$ hDPSCs and c-kit$^+$ hAFSCs after their induction towards a myogenic lineage utilizing the protocols outlined above, western blot analysis was performed. Whole cell lysates were obtained at two weeks after initiating differentiation and processed as previously described by Pisciotta et al. [16]. Thirty µg of protein extract, quantified by a Bradford Protein Assay (Biorad), underwent SDS-polyacrylamide gel electrophoresis and were transferred to PVDF membranes. The following antibodies (abs) were used: mouse anti-myogenin and rabbit anti-desmin (Sigma Aldrich), all diluted 1:1000. Peroxidase-labelled anti-mouse (diluted 1:2000) and anti-rabbit (diluted 1:3000) secondary abs were used. Whole cell lysate obtained from C2C12 myoblasts was used as a positive control. The membranes were visualized using ECL (enhanced chemioluminescence, Amersham). Anti-actin antibody was used as control of protein loading. Densitometry of the bands was performed using Image J analysis software (NIH). Data were then normalized to values of background and the control actin band.

In vivo transplantation of the hDPSCs and hAFSCs into mdx/SCID mice

In order to evaluate whether the hDPSCs and hAFSCs were capable of contributing to the regeneration of the dystrophic skeletal muscle and restoration of dystrophin expression, both human stem cell populations demethylated with 10µM 5-Aza and pre-differentiated *in vitro* for 2 weeks in myogenic medium, with and without the addition of CM from the differentiated C2C12 cells were transplanted into the gastrocnemius muscles (GM) of *mdx*/SCID mice. Briefly, 5×10^5 pre-

differentiated hDPSCs and hAFSCs, resuspended in 30µl of PBS, were injected into the GMs of male *mdx*/SCID mice that were 8 - 10 weeks of age. Each animal received two injections: in the left GM, the cells pre-differentiated after demethylating treatment; in the right GM, the cells pre-differentiated after demethylating treatment and the addition of conditioned medium. Non-injected muscles were utilized as controls. The animals were euthanized at 7, 14, and 28 days after cell transplantation and the GMs were harvested, and snap frozen in liquid nitrogen cooled 2-methylbutane. Subsequently, transverse serial sections (8µm thick) of the frozen muscles were cut using a H525 MICROM cryostat. Sections were collected on Super Frost Plus slides (Thermo Scientific) and then stored at -80°C. A total of 30 animals were used in this study (controls n=6; treated n=24). Animal procedures were performed in compliance with the guidelines approved by the Institutional Animal Care and Use Committee (IACUC) of the University of Pittsburgh, Pittsburgh, PA, USA.

Immunofluorescent microscopy and histology

hDPSCs and hAFSCs were seeded on coverslips following magnetic cell sorting for STRO-1 and c-Kit, respectively. Once adhered the cells were fixed with 4% paraformaldehyde, blocked with 3% BSA in PBS for 30 minutes at room temperature and then incubated with mouse anti-STRO-1 and rabbit anti-c-Kit primary abs (Santa Cruz) diluted 1:50 in PBS containing 3% BSA for 1 hour at room temperature. After washing in PBS containing 3% BSA, the samples were incubated for 1 hour at room temperature with the secondary abs diluted 1:200 in PBS containing 3% BSA (goat anti-mouse Alexa546; goat anti-rabbit Alexa488; Invitrogen). After washing in PBS samples were stained with 1 µg/ml DAPI in PBS for 1 minute, and then mounted with anti-fade medium (VectaMount AQ Aqueous Mounting Medium, Vector Laboratories). Negative controls consisted of samples not incubated with the primary antibody. Immunofluorescence analysis was performed using a Nikon A1 confocal laser scanning microscope as described by Riccio et al [15]. The

confocal serial sections were processed with ImageJ software to obtain three-dimensional projections and image rendering was performed with Adobe Photoshop Software.

Fixed monolayer cells, differentiated *in vitro* on coverslips, were permeabilized with 0.1% Triton X-100 in PBS for 5 minutes and then blocked with 3% BSA in PBS for 30 minutes at room temperature. The following primary antibodies (abs) were utilized: mouse anti-human nuclei (hNu, Millipore), mouse anti-myogenin, rabbit anti-myosin heavy chain (MyHC), and rabbit anti-desmin (all from Sigma Aldrich). All the primary abs were diluted 1:50 in PBS containing 3% BSA and incubated for 1 hour at room temperature. Secondary abs were diluted 1:200 in PBS containing 3% BSA and incubated for 1 hour at room temperature (goat anti-mouse Alexa488, donkey anti-rabbit Alexa594; Invitrogen); after washing in PBS, the cells were counterstained with 1 μg/mL DAPI in PBS for 3 minutes, and then mounted with anti-fade medium (VectaMount AQ Aqueous Mounting Medium, Vector Laboratories). Negative controls consisted of samples not incubated with the primary antibody.

Histological unfixed sections from frozen muscle were processed as described above. Mouse anti-human mitochondrial protein (hMit, 1:80; Millipore), rabbit anti-human dystrophin (1:500, courtesy of Dr. Bing Wang, University of Pittsburgh, PA) and rabbit anti-human von Willebrand factor (vWill, 1:100; Millipore), were used as primary abs. The following secondary abs were utilized at a 1:200 dilution: donkey anti-mouse Alexa488, donkey anti-rabbit Alexa594, donkey anti-mouse Alexa594 and goat anti-rabbit Alexa488 (Invitrogen). Negative controls were samples not incubated with primary antibodies. Immunofluorescence analysis was performed on a Nikon Eclipse E800 microscope (Nikon) utilizing Northern Eclipse imaging software (EMPIX Imaging) to capture images. The image rendering was performed using Adobe Photoshop software.

Routine H & E staining was performed on serial cross sections (8μm) of frozen GMs in order to analyze the morphological details of the tissues. Images of the entire muscle section were captured and the number of centrally nucleated myofibers was determined and the percentage of centrally nucleated fibers to all myofibers in the entire muscle section was calculated.

The extent of fibrosis in the muscle cryosections was determined using Masson's trichrome staining to detect the collagen content of the muscles, as detailed in the manufacturer's protocol (Masson's Trichrome stain kit; IMEB, Inc.). Images of the histological samples were obtained with a Nikon Eclipse E800 microscope (Nikon).

Transmission Electron Microscopy

In order to evaluate the ultrastructure of the dystrophic skeletal muscle in the SCID/*mdx* mice, some of the GMs were processed using epoxy resin embedding and analyzed subsequently by transmission electron microscopy (TEM), as formerly described by Gibellini et al. [17]. The GMs to be analyzed for morphological changes were harvested and fixed in 1% glutaraldehyde in Sorensen's Phosphate Buffer 0.1 M pH 7,4 (PB) for 1 hour and post-fixed in 1% OsO_4 in PB 0.1 M for 2 hours. Ultrathin, 60-90 nm, were cut from the Durcupan embedded samples, collected on nickel grids, stained with uranyl acetate and lead-citrate, and then visualized using a Zeiss EM 109 Transmission Electron Microscope (Zeiss AG, Jena, Germany).

Statistical analysis

Data were expressed as the mean $\pm$ standard deviation (SD). Differences between experimental groups consisting of 5-6 samples each were analyzed by ANOVA test followed by Tukey's Multiple Comparison Test (GraphPad Prism Software version 5 Inc., San Diego, CA, USA). In all analyses, values of $p<0.05$ were considered statistically significant.

RESULTS

Cell sorting

In order to verify if hDPSCs and hAFSCs previously sorted by MACS were STRO-1^+ and c-Kit^+, respectively, immunocytochemistry and flow cytometry were performed on the cells (Fig. 1A).

Immunocytochemical analysis showed that the sorted cells were positive for their respective surface antigens (Fig. 1A, top). Moreover, flow cytometry demonstrated that almost all the sorted cells were positive for STRO-1 and c-Kit, respectively (Fig. 1A, bottom).

Myogenic differentiation in vitro

In order to test the cell populations' myogenic potential, the human DPSCs and AFSCs were induced to differentiate into a myogenic lineage *in vitro*. The immunofluorescent analysis performed on the hDPSCs and hAFSCs after 14 days of direct co-culture with C2C12 cells revealed the formation of myotubes that were positive for both anti-hNu and anti-MyHC abs, as shown in Fig. 1B. In particular, newly formed hybrid myotubes that contained both human and mouse nuclei were observed.

Immunofluorescent labeling was also carried out on the hDPSCs and hAFSCs differentiated alone and following DNA demethylation treatment with 5-Aza (Fig. 2). After 14 days of induction the hDPSCs expressed myogenin, which is an early marker for the entry of myoblasts into the differentiation pathway; moreover, they expressed myosin heavy chain and desmin, which are late-myogenic markers (Figs. 2A, 2C). The human AFSCs also underwent myogenic commitment as demonstrated by their positive staining for myogenin, myosin heavy chain and desmin, which confirmed the terminal myogenic commitment of the cells (Figs. 2B, 2D). Similar results were observed for both the hDPSCs and hAFSCs differentiated after demethylation with the addition of CM from the differentiated C2C12 cell cultures (Figs. 2E-H). After two weeks of induction no myotube formation was detected; however, after 4 weeks myotube detection could be detected in both the hDPSC and hAFSC cultures (data not shown). Human DPSCs and AFSCs cultured in myogenic induction medium, but not undergoing preliminary demethylation treatment, did not show any labeling for the myogenic specific markers myogenin, myosin heavy chain or desmin (Figs. 2I-L).

To verify the commitment and differentiation of the hDPSCs and hAFSCs towards a myogenic lineage, the expression of myogenin and desmin was also evaluated by Western Blot (WB) analysis using whole cell lysates from the hDPSCs and hAFSCs treated with 5-Aza and treated or not treated with C2C12 CM (Figure 3, top). A densitometric analysis was carried out on the WB bands to obtain a semi-quantitative analysis of the protein amount (Figure 3, bottom). Both the hDPSCs and hAFSCs expressed the muscle specific markers myogenin and desmin after two weeks of myogenic induction as revealed by the existence of the specific protein bands corresponding to 34 kDa and 50 kDa, respectively (Figure 3). Densitometric analysis revealed that in both the differentiated hDPSCs and hAFSCs, both with and without being treated with the C2C12 CM, there was a significant expression of the myogenic markers compared to the controls ($^{***}p<0,001$). In particular, a significantly higher expression of both myogenin and desmin positive cells were observed in the hDPSCs and hAFSCs cultures differentiated via 5-Aza with the addition of C2C12 CM than in the cultures not treated with C2C12 CM, respectively ($^{§§§}p<0,001$).

Engraftment evaluation and muscle regeneration after in vivo transplantation

hDPSCs and hAFSCs that were pre-differentiated towards a myogenic lineage, via 5-Aza demethylation, with and without treatment with C2C12 CM, were injected into the GMs of *mdx*/SCID mice to test their ability to regenerate the dystrophic skeletal muscle of *mdx*/SCID mice. The injected animals were sacrificed at different time points, and the GMs were flash frozen and processed for further analyses. Immunofluorescent analysis showed that as early as 7 days after injection the human DPSCs and AFSCs could be detected histologically integrated within the host muscle, as demonstrated by the positive staining of human mitochondrial protein (Fig. 4). Similar results were observed with or without culturing the cells in C2C12 CM (Figs. 4A-D). Double immunofluorescent staining, performed 7 days after cell injection using anti-hMit and anti-human vWill abs, revealed the presence of human cells positively stained as endothelial cells within the vasa walls (Fig. 5). Similar results were observed using both pre-differentiation conditions (Figs. 5A-D). Moreover, two weeks after cell injection, the immunofluorescent labelling showed a

restoration of dystrophin expression within the dystrophic skeletal muscle fibers of the transplanted mice. In particular, the fibers expressing dystrophin were also positively stained for human mitochondrial protein (Fig. 6). Similar results were observed for both pre-differentiation conditions (Figs. 6A-D). Restored expression of dystrophin by the mouse muscle fibers positively labelled for anti-human mitochondria ab was still detectable 4 weeks after cell injection (Fig. 6). Again, similar results were observed using both pre-differentiation conditions (Figs. 6E-H).

Untreated samples, consisting of non-injected GMs, did not show any positive staining against hMit, and human vWill abs (Fig. 4E, Fig. 5E).

Histological analysis

To evaluate the presence of fibrous tissue within the dystrophic skeletal muscle of the *mdx*/SCID mice after cell injection, serial sections from GMs harvested at 4 weeks after injection were stained with H&E and Masson's trichrome. Histological analysis of H&E staining revealed that the muscles injected with human stem cells contained extensive areas of muscle regeneration compared to the controls, as demonstrated by the large presence of centronucleated muscle fibers (Fig. 7A, arrows). Particularly, the percentage of centronucleated muscle fibers in the GMs treated with hDPSCs and hAFSCs were significantly higher with respect to the non-injected (control) GMs group (Fig. 7B).

At the same time, analysis of Masson's trichrome staining in Fig. 7A shows a reduction in fibrosis within the muscle fibers treated with the pre-differentiated hDPSCs and hAFSCs, compared to the controls. In particular, the GMs treated with hDPSCs and hAFSCs showed a significant reduction ($p < 0{,}01$) in fibrotic areas in comparison with the non-injected (control) GMs (Fig. 7C).

Transmission Electron Microscopy

The ultrastructure analysis performed by transmission electron microscopy (TEM) revealed that the controls showed severe damage of their myofibrils, with either alterations/lack of mitochondria and

the presence of vacuoles among the myofibrils; furthermore, their myofilaments were mostly disrupted and lost (Fig. 7D).

On the other hand, the GMs injected with pre-differentiated hDPSCs and hAFSCs showed restored arrangements of their sarcomeres within the myofibrils – given the tissue-striation pattern – with a normal display of mitochondria (Fig. 7D).

DISCUSSION

The muscular dystrophies are a diverse set of genetic myopathies characterized by progressive muscle weakness, atrophy, and the replacement of healthy myofibers with fat and scar tissue [18, 19]. Several forms of these diseases are caused by mutations in components of the dystrophin-glycoprotein complex (DGC), which links the actin cytoskeleton of the myofibers to the extracellular matrix and is a fundamental component required to maintain the contractile structure of the skeletal muscle [20, 21]. Mutations that cause disruptions in the component proteins of the DGC lead to a series of different myopathies, of which DMD is both the most severe and the most common, affecting 1 in 3500 live male births. Homologues of DMD have been identified in several animals, such as the *dy/dy* mouse, the extensively studied *mdx mouse*, the *mdx/utrn*$^{-/-}$ (dystrophin and utrophin deficient) mouse, and the muscular dystrophic Golden Retriever dog. Although there is no definitive model of DMD at this time, the variety of DMD homologues available are adequate for understanding the fundamental pathophysiology of the disease [22].

Even though satellite cells (SCs) compensate for muscle fiber loss in the early stages of DMD, the regenerated myofibers remain dystrophic since the SCs also carry the genetic defect. Moreover, as previously demonstrated by Miller et al. [23] and by Lund et al. [24], the pool of SCs becomes exhausted as a result of high demands for muscle regeneration and poor compensatory mechanisms which results in fibrous and fatty connective tissue infiltration within the functional myofibers.

Cell therapy has been considered as a potential therapeutic treatment for DMD over the years. Partridge et al. [25] originally demonstrated that donor myoblasts could fuse with host myoblasts, suggesting the possibility of functional restoration in defective muscle fibers.

The pivotal findings that donor heterologous myoblasts could restore dystrophin expression in the dystrophin deficient *mdx* mouse [26] laid the foundation for a number of human clinical trials in DMD patients in the 1990s [27]. Disappointingly, initial clinical trials with allogeneic myoblasts injection into the muscles of non-immunosuppressed DMD patients showed only a transient restoration of dystrophin positive fibers and limited improvements in muscle strength, which was soon lost [28-33].

Reasonably, the limitations of these therapeutic approaches have triggered extensive research over the years. One of the approaches attempted the transplantation of bone marrow mesenchymal stem cells (MSCs) into the dystrophic muscles of patients [4, 34, 35] which showed that the MSCs indeed possessed the capacity to differentiate into muscle tissue [36].

Besides bone marrow mesenchymal stem cells, several cell types have been identified as potential sources for muscle tissue regeneration [37, 38-40].

In the current study we evaluated the myogenic potential of STRO-1^+ enriched human dental pulp stem cells (hDPSCs) and c-Kit^+ enriched human amniotic fluid derived stem cells (hAFSCs). It has been well demonstrated that in the dental pulp, STRO-1^+ stem cells are capable of differentiating towards multilineage cell types with respect to non-sorted cells, likely due to their more homogeneous nature [41]. Similarly, as described by De Coppi et al. [10] and Baj et al. [42] c-kit^+ cells represent a group of purified MSCs newly found in amniotic fluid that have broad multipotency capacity.

Utilizing two different protocols, this study aimed to determine the optimal conditions for achieving the myogenic commitment of these two populations of human stem cells.

The results from the direct co-culture of hDPSCs and hAFSCs with C2C12 mouse myoblasts demonstrated that these human stem cells were capable of fusing with mouse myoblasts to form

new hybrid myotubes, as clearly shown by the positive staining of the myotubes with an anti-human nuclear antibody.

After being differentiated without direct co-culture, by means of DNA demethylation treatment, immunofluorescence analysis revealed that hDPSCs and hAFSCs underwent myogenic commitment even though myotube formation was not observed. Similarly, when CM from differentiated C2C12 cells was added to the myogenic medium of the demethylated cells, the expression of muscle specific markers by the hDPSCs and hAFSCs was observed, although myotube formation was not detected. In particular, both hDPSCs and hAFSCs efficiently reached myogenic commitment after 14 days of induction as confirmed by the cells' expression of muscle specific markers, which was a necessary requirement for the subsequent *in vivo* transplantation studies of the cells into *mdx*/SCID mice. Although myotube formation was not observed at the two week time point, by four weeks after the initiation of myogenic induction myotubes were detectable, with and without the addition of C2C12 conditioned media, thus demonstrating the ability of the hDPSCs and hAFSCs to undergo terminal myogenic differentiation. The induction of both hDPSCs and hAFSCs towards a myogenic lineage was further demonstrated by western blot analysis which showed that when conditioned medium from C2C12 cells was added to the hDPSC and hAFSC cultures, the cells' expression of myogenic specific markers became more pronounced. On the other hand, neither early nor late myogenic differentiation markers could be detected in the hDPSCs or hAFSCs when they were cultured in differentiation medium without first demethylating the cells.

These observations suggest that modulating the myogenic potential of these populations of cells could be achieved by combining demethylation, which triggers the expression of muscle regulatory factors necessary for the myogenic process to proceed, with the addition of the C2C12 conditioned fusion media, which contains soluble factors that promote myogenesis.

According to the results obtained *in vitro*, conditioning the cells with 5-Aza was found to be crucial for triggering the myogenic commitment of the hDPSCs and hAFSCs, when differentiating the cells

in the absence of C2C12 cells; therefore, the hDPSCs and hAFSCs with 5-Aza was performed as part of the differentiation strategy to evaluate their myogenic potential *in vivo* when injected into the dystrophic GMs of *mdx*/SCID mice.

Early engraftment was observed within the skeletal muscle fibers of the host, as confirmed by the presence of human cells in the injected muscles detected by staining for human mitochondria, which demonstrated that these cells were able to survive and integrate into the host muscle after transplantation. In particular, human DPSCs and AFSCs showed that they were capable of directly supporting the improvement of skeletal muscle by promoting neo-angiogenesis within the transplanted muscles, which is a key player in achieving good physiological repair of the tissue [43]. In fact, according to Biscetti et al. dystrophin expression is not limited to skeletal muscle cells but is also expressed by several other cell types, including endothelial cells [44], which are known to interact directly and indirectly with myoblasts and promote the proliferation of myogenic precursor cells [45]. The physiological importance of dystrophin in the vascular endothelium is demonstrated by the fact that *mdx* mice display vascular abnormalities and their muscles experience ischemic conditions [46]. Recent findings showed that increasing the vasculature in DMD patients might be capable of ameliorating the histological and functional phenotypes related to the disease and that developing an efficacious therapy for DMD would address improving both skeletal muscle regeneration and its vasculature [47]. Double positive staining for human mitochondria and human von Willebrand factor demonstrated that both the hDPSCs and hAFSCs could be localized in the endothelium of newly generated vasa after their transplantation which supports the fact that they participated in the neoangiogenesis of the transplanted muscle, a well-defined property of the cells that has been previously shown [48, 49].

The ability of the hDPSCs and hAFSCs to restore dystrophin expression within the injected host muscles, was observed as early as 14 days post-injection and continued to be detected 4 weeks after transplantation. Moreover, another important finding of the current study was that the hDPSCs and hAFSCs contributed to a reduction in the formation of fibrosis within the dystrophic muscle, which

further enhanced the regeneration process as was demonstrated by the increased presence of centronucleated muscle fibers. These observations suggest that, once engrafted within the host muscle, human DPSCs and AFSCs actively contributed to the amelioration of the dystrophic phenotype within the muscle by promoting angiogenesis, through the restoration of dystrophin expression, and by reducing the deposition of fibrosis. Qualitative details from the ultrastructure analysis of the dystrophic skeletal muscle, performed through transmission electron microscopy, showed a regular arrangement of the myofibrils from GMs treated with hDPSCs and hAFSCs, compared to the controls.

Muscle function was not tested because *mdx* mice, although representing a fully authenticated genetic model of DMD, exhibit a very mild phenotype in terms of muscle weakness and experience less seriously compromised mechanical function, compared to DMD patients [25].

The detection of human stem cells in the injected dystrophic skeletal muscle and, in particular, their presence within muscle fibers that expressed human dystrophin, demonstrated that the human DPSCs and AFSCs were capable of integrating into the muscular microenvironment, and were capable of surviving for an extended period of time, as we demonstrated via their continued expression of human dystrophin in the dystrophic GMs of the *mdx*/SCID mice over a 4 week period of time.

In light of these results, it may be reasonable to assume that human DPSCs and AFSCs underwent events that can be defined as a hybrid event where both cellular differentiation and cell fusion processes occurred. Even though no strictly new generated human muscle fibers were observed after injection of either cell type, they were involved in cell fusion with the host myoblasts giving rise to hybrid muscle fibers, some of which, notably, exhibited restored human dystrophin expression, although in a limited number of myofibers. The limited presence of dystrophin positive fibers observed after cell transplantation could be attributable in part to limitations associated to xenotransplantation. Although the recipient is a SCID mouse, human stem cells may be challenged to engraft and to functionally integrate in the host tissue, hence it could be assumed that human

stem cells exert a reduced ability to fuse with murine myofibers or that dystrophin is poorly integrated in the plasma membrane of newly formed hybrid myofibers. [50, 51].

CONCLUSIONS

In light of these results, human DPSCs and AFSCs hold promise as two potential stem cell populations that could be useful for the formation of new hybrid myofibers – some of which acquired the ability to express dystrophin - and for the improvement of pathological features of dystrophic skeletal muscle tissues, including the deposition of fibrosis and a reduction in vasculature in DMD patients. These findings are aimed to pave the way for further investigations in order to optimally characterize the contribution of human DPSCs and AFSCs to restore dystrophin expression and to improve muscle function in more severely compromised DMD animal models.

LIST OF ABBREVIATIONS

DMD: Duchenne Muscular Dystrophy

hDPSCs: human dental pulp stem cells

hAFSCs: human amniotic fluid stem cells

DGC: dystrophin-glycoprotein complex

MDSCs: muscle derived stem cells

mSP: muscle side population

5-Aza: 5-Aza-2'-deoxycytidine

IGF-II: insulin-like growth factor-II

α-MEM: Minimum Essential Medium, alpha modification

FCS: foetal calf serum

PBS: phosphate buffer saline

BSA: bovine serum albumin

DAPI: 4',6-diamidino-2-phenylindole

DMEM: Dulbecco’s modified Eagle’s Medium

GM(s): gastrocnemius muscle(s)

hNu: human Nuclei

MyHC: myosin heavy chain

hMit: human mitochondrial protein

vWill: von Willebrand factor

PB: Sorensen’s phosphate buffer

TEM: transmission electron microscopy

SCs: satellite cells

MSCs: mesenchymal stem cells

DISCLOSURE OF POTENTIAL CONFLICTS OF INTEREST

The authors declare they have no conflicts of interest.

AUTHOR CONTRIBUTIONS

AP: conception and design, cell culture and animal procedures, data collection and assembly, data analysis and interpretation, manuscript writing; MR: conception and design, data analysis and interpretation, manuscript writing; GC: data collection and assembly, data analysis and interpretation, manuscript writing; AL: animal procedures; GBLS: collection of amniotic fluids and informed consent of the patients; GB: collection of dental pulps and informed consent of the patients; AF: data analysis and interpretation; JH: data analysis and interpretation, manuscript writing; ADP: data analysis and interpretation, manuscript writing, financial support.

ACKNOWLEDGMENTS

The authors thank Dr. Gianfranco Croci (Laboratorio di Genetica, Ospedale Santa Maria Nuova, Reggio Emilia, Italy) for providing sample of amniotic fluid cells, and James H. Cummins for his editorial assistance.

FINANCIAL SUPPORT

This work was supported by grants from ‘Progetto Strategico per lo sviluppo nella sede di Reggio Emilia della Facoltà di Medicina e Chirurgia‘ (Prot: 2010 0007725), Arcispedale S. Maria Nuova di Reggio Emilia and MIUR FIRB Accordi di Programma 2010 (Prot: RBAP10Z7FS).

REFERENCES

1. Matsumura K, Ohlendieck K, Ionasescu VV, Tomé FM, Nonaka I, Burghes AH, Mora M, Kaplan JC, Fardeau M, Campbell KP: **The role of the dystrophin-glycoprotein complex**

in the molecular pathogenesis of muscular dystrophies. *Neuromuscul Disord* 1993, **3**:533-535.

2. Emery AE, Muntoni F: **Duchenne Muscular Dystrophy**. In *Oxford University Press*, 3rd edition. Oxford, UK. 2003.

3. Manzur AY, Kuntzer T, Pike M, Swan A: **Glucocorticoid corticosteroids for Duchenne muscular dystrophy**. In *Cochrane Database Syst Rev* 2008, **(1)**:CD003725.

4. Ferrari G, Cusella-De Angelis G, Coletta M, Paolucci E, Stornaiuolo A, Cossu G, Mavilio F: **Muscle regeneration by bone marrow-derived myogenic progenitors.** *Science* 1998, **281**:923.

5. Pinheiro CH, de Queiroz JC, Guimarães-Ferreira L, Vitzel KF, Nachbar RT, de Sousa LG, de Souza-Jr AL, Nunes MT, Curi R: **Local injections of adipose-derived mesenchymal stem cells modulate inflammation and increase angiogenesis ameliorating the dystrophic phenotype in dystrophin-deficient skeletal muscle.** *Stem Cell Rev* 2012, **8**:363-374.

6. Brzóska E, Grabowska I, Hoser G, Stremińska W, Wasilewska D, Machaj EK, Pojda Z, Moraczewski J, Kawiak J: **Participation of stem cells from human cord blood in skeletal muscle regeneration of SCID mice.** *Exp Hematol* 2006, **34**:1262-1270.

7. Kawamichi Y1, Cui CH, Toyoda M, Makino H, Horie A, Takahashi Y, Matsumoto K, Saito H, Ohta H, Saito K, Umezawa A: **Cells of extraembryonic mesodermal origin confer human dystrophin in the mdx model of Duchenne muscular dystrophy.** *J Cell Physiol* 2010, **223**:695-702.

8. Gronthos S, Mankani M, Brahim J, Robey PG, Shi S: **Postnatal human dental pulp stem cells (DPSCs) in vitro and in vivo.** *Proc. Natl. Acad. Sci. USA* 2000, **97**: 13625-13630.

9. Gronthos S, Brahim J, Li W, Fisher LW, Cherman N, Boyde A, DenBesten P, Robey PG, Shi S: **Stem cell properties of human dental pulp stem cells.** *J Dent Res* 2002, **81**:531-535.

10. De Coppi P, Bartsch G Jr, Siddiqui MM, Xu T, Santos CC, Perin L, Mostoslavsky G, Serre AC, Snyder EY, Yoo JJ, Furth ME, Soker S, Atala A: **Isolation of amniotic stem cell lines with potential for therapy.** *Nat Biotechnol* 2007, **25**:100-106.

11. Carnevale G, Riccio M, Pisciotta A, Beretti F, Maraldi T, Zavatti M, Cavallini GM, La Sala GB, Ferrari A, De Pol A: **In vitro differentiation into insulin-producing β-cells of stem cells isolated from human amniotic fluid and dental pulp.** *Dig Liver Dis* 2013, **45**:669-676.

12. Duan C, Ren H, Gao S: **Insulin-like growth factors (IGFs), IGF receptors, and IGF-binding proteins: roles in skeletal muscle growth and differentiation.** *Gen Comp Endocrinol* 2010, **167**:344-351.

13. Ye NS, Chen J, Luo GA, Zhang RL, Zhao YF, Wang YM: **Proteomic profiling of rat bone marrow mesenchymal stem cells induced by 5-azacytidine.** *Stem Cells Dev* 2006, **15**:665–676.

14. Antonitsis P, Ioannidou-Papagiannaki E, Kaidoglou A, Charokopos N, Kalogeridis A, Kouzi-Koliakou K, Kyriakopoulou I, Klonizakis I, Papakonstantinou C: **Cardiomyogenic potential of human adult bone marrow mesenchymal stem cells in vitro.** *Thorac Cardiovasc Surg* 2008, **56**:77–82.

15. Riccio M, Resca E, Maraldi T, Pisciotta A, Ferrari A, Bruzzesi G, De Pol A: **Human dental pulp stem cells produce mineralized matrix in 2D and 3D cultures.** *Eur J Histochem* 2010, **54**:e46.

16. Pisciotta A, Riccio M, Carnevale G, Beretti F, Gibellini L, Maraldi T, Cavallini GM, Ferrari A, Bruzzesi G, De Pol A: **Human serum promotes osteogenic differentiation of human dental pulp stem cells in vitro and in vivo.** *PLoS One* 2012, **7**:e50542.

17. Gibellini L, De Biasi S, Pinti M, Nasi M, Riccio M, Carnevale G, Cavallini GM, Sala de Oyanguren FJ, O'Connor JE, Mussini C, De Pol A, Cossarizza A: **The protease inhibitor atazanavir triggers autophagy and mitophagy in human preadipocytes.** *AIDS* 2012, **26**:2017-2026.

18. Bushby K: **Genetics and the muscular dystrophies.** *Dev Med Child Neurol* 2000, **42**:780-784.

19. Burton EA, Davies KE: **Muscular dystrophy - reason for optimism?** *Cell* 2002, **108**:5-8.

20. Watkins SC, Swartz DR, Byers TJ: **Localisation of dystrophin in skeletal, cardiac and smooth muscle.** In *Dystrophin: Gene, Protein and Cell Biology.* Edited by Brown SC and Lucy JA. Cambridge University Press; **1997**:79–104.

21. Michele DE, Campbell KP: **Dystrophin-glycoprotein complex: post-translational processing and dystroglycan function.** *J Biol Chem* 2003, **278**:15457-15460.

22. Collins CA, Morgan JE: **Duchenne's muscular dystrophy: animal models used to investigate pathogenesis and develop therapeutic strategies.** *Int J Exp Pathol* 2003, **84**:165-172.

23. Miller JB, Schaefer L, Dominov JA: **Seeking muscle stem cells.** *Curr Top Dev Biol* 1999, **43**:191-219.

24. Lund TC, Grange RW, Lowe DA: **Telomere shortening in diaphragm and tibialis anterior muscles of aged mdx mice**. *Muscle Nerve* 2007, **36**:387-390.

25. Partridge TA, Grounds M, Sloper JC: **Evidence of fusion between host and donor myoblasts in skeletal muscle grafts.** *Nature* 1978, **273**:306-308.

26. Partridge TA, Morgan JE, Coulton GR, Hoffman EP, Kunkel LM: **Conversion of mdx myofibres from dystrophin-negative to -positive by injection of normal myoblasts.** *Nature* 1989, **337**:176-179.

27. Partridge TA: **The current status of myoblast transfer.** *Neurol Sci* 2000, **21**(Suppl):S939-942.

28. Law PK: **Beneficial effects of transplanting normal limb-bud mesenchyme into dystrophic mouse muscles.** *Muscle Nerve* 1982, **5**:619-627.

29. Huard J, Bouchard JP, Roy R, Malouin F, Dansereau G, Labrecque C, Albert N, Richards CL, Lemieux B, Tremblay JP: **Human myoblast transplantation: preliminary results of 4 cases.** *Muscle Nerve* 1992;**15**:550-560.

30. Karpati G, Ajdukovic D, Arnold D, Gledhill RB, Guttmann R, Holland P, Koch PA, Shoubridge E, Spence D, Vanasse M: **Myoblast transfer in Duchenne muscular dystrophy.** *Ann Neurol* 1993, **34**:8-17.

31. Mendell JR, Kissel JT, Amato AA, King W, Signore L, Prior TW, Sahenk Z, Benson S, McAndrew PE, Rice R: **Myoblast transfer in the treatment of Duchenne's muscular dystrophy.** *N Engl J Med* 1995, **333**:832-838.

32. Gussoni E, Pavlath GK, Lanctot AM, Sharma KR, Miller RG, Steinman L, Blau HM: **Normal dystrophin transcripts detected in Duchenne muscular dystrophy patients after myoblast transplantation.** *Nature* 1992, **356**:435-438.

33. Beauchamp JR, Pagel CN, Partridge TA: **A dual-marker system for quantitative studies of myoblast transplantation in the mouse.** *Transplantation* 1997, **63**:1794-1797.

34. Saito T, Dennis JE, Lennon DP, Young RG, Caplan AI: **Myogenic expression of Mesenchymal Stem Cells within myotubes of *mdx* mice *in vitro* and *in vivo*.** *Tissue Eng* 1995, **1**:327-343.

35. Gussoni E, Soneoka Y, Strickland CD, Buzney EA, Khan MK, Flint AF, Kunkel LM, Mulligan RC: **Dystrophin expression in the mdx mouse restored by stem cell transplantation.** *Nature* 1999, **401**:390-394.

36. McIntosh K, Bartholomew A: **Stromal cell modulation of the immune system – a potential role for mesenchymal stem cells.** *Graft* 2000, **3**:324-328.

37. Torrente Y, Belicchi M, Sampaolesi M, Pisati F, Meregalli M, D'Antona G, Tonlorenzi R, Porretti L, Gavina M, Mamchaoui K, Pellegrino MA, Furling D, Mouly V, Butler-Browne GS, Bottinelli R, Cossu G, Bresolin N: **Human circulating AC133(+) stem cells restore dystrophin expression and ameliorate function in dystrophic skeletal muscle.** *J Clin Invest* 2004, **114**:182-195.

38. Huard J, Cao B, Qu-Petersen Z: **Muscle-derived stem cells: potential for muscle regeneration.** *Birth Defects Res C Embryo Today* 2003, **69**:230-237.

39. Mitchell KJ, Pannérec A, Cadot B, Parlakian A, Besson V, Gomes ER, Marazzi G, Sassoon DA: **Identification and characterization of a non-satellite cell muscle resident progenitor during postnatal development.** *Nat Cell Biol* 2010, **12**:257-266.

40. Sampaolesi M, Torrente Y, Innocenzi A, Tonlorenzi R, D'Antona G, Pellegrino MA, Barresi R, Bresolin N, De Angelis MG, Campbell KP, Bottinelli R, Cossu G: **Cell therapy of alpha-sarcoglycan null dystrophic mice through intra-arterial delivery of mesoangioblasts.** *Science* 2003, **25**: 487-492.

41. Yang X, Zhang W, van den Dolder J, Walboomers XF, Bian Z, Fan M, Jansen JA J: **Multilineage potential of STRO-1+ rat dental pulp cells in vitro.** *Tissue Eng Regen Med* 2007, **1**:128-135.

42. Bai J, Wang Y, Liu L, Chen J, Yang W, Gao L, Wang Y: Human amniotic fluid-derived c-kit(+) and c-kit (-) stem cells: growth characteristics and some differentiation potential capacities comparison. *Cytotechnology* 2012, 64:577-589.

43. Auger FA, Gibot L, Lacroix D: **The pivotal role of vascularization in tissue engineering.** *Annu Rev Biomed Eng* 2013, **15**:177-200.

44. Biscetti F, Gaetani E, Flex A, Aprahamian T, Hopkins T, Straface G, Pecorini G, Stigliano E, Smith RC, Angelini F, Castellot JJ Jr, Pola R: **Selective activation of peroxisome proliferator activated receptor (PPAR) alpha and PPAR gamma induces neoangiogenesis through a vascular endothelial growth factor-dependent mechanism.** *Diabetes* 2008, **57**: 1394-1404.

45. Sabourin LA, Girgis-Gabardo A, Seale P, Asakura A, Rudnicki MA: **Reduced differentiation potential of primary MyoD−/− myogenic cells derived from adult skeletal muscle.** *J Cell Biol* 1999, **144**: 631-643.

46. Shimizu-Motohashi Y, Asakura A: **Angiogenesis as a novel therapeutic strategy for Duchenne muscular dystrophy through decreased ischemia and increased satellite cells.** *Front Physiol* 2014, **5**:50.

47. Palladino M, Gatto I, Neri V, Straino S, Smith RC, Silver M, Gaetani E, Marcantoni M, Giarretta I, Stigliano E, Capogrossi M, Hlatky L, Landolfi R, Pola R: **Angiogenic impairment of the vascular endothelium: a novel mechanism and potential therapeutic target in muscular dystrophy.** *Arterioscler Thromb Vasc Biol* 2013, **33**: 2867-2876.

48. Hilkens P, Fanton Y, Martens W, Gervois P, Struys T, Politis C, Lambrichts I, Bronckaers A: **Pro-angiogenic impact of dental stem cells in vitro and in vivo.** *Stem Cell Res* 2014, **12**: 778-790.

49. Liu YW, Roan JN, Wang SP, Hwang SM, Tsai MS, Chen JH, Hsieh PC: **Xenografted human amniotic fluid-derived stem cell as a cell source in therapeutic angiogenesis.** *Int J Cardiol* 2013, **168**: 66-75.

50. Chirieleison SM, Feduska JM, Schugar RC, Askew Y, Deasy BM. **Human muscle-derived cell populations isolated by differential adhesion rates: phenotype and contribution to skeletal muscle regeneration in Mdx/SCID mice.** *Tissue Eng Part A* 2011, **18**:232-241.

51. Meng J, Adkin CF, Xu SW, Muntoni F, Morgan JE: **Contribution of human muscle-derived cells to skeletal muscle regeneration in dystrophic host mice.** *PLoS One* 2011, **6**:e17454.

Figure legends

Figure 1.

A: Cell characterization after magnetic cell sorting. On the top, fluorescent images of hDPSCs and hAFSCs positively labeled with anti-STRO-1 (red) and anti-c-Kit (green), respectively. Scale bar = 50 μm. At the bottom, flow cytofluorimetric analysis of hDPSCs and hAFSCs sorted by MACS; the percentage of positive cells is indicated.

B: Evaluation of *in vitro* direct co-culture of hDPSCs and hAFSCs with C2C12 mouse myoblasts. Triple immunofluorescent staining of hAFSCs and hDPSCs co-cultured with C2C12 mouse myoblasts revealed newly formed myotubes which are labeled with DAPI (blue), anti-hNu (green) and anti-MyHC (red) abs. Scale bar = 50 μm.

Figure 2. Immunofluorescent analysis of myogenic differentiation of hAFSCs and hDPSCs by means of demethylation treatment with 5-Aza. Immunofluorescent staining with anti-myogenin (green)/anti-MyHC (red) and anti-myogenin (green)/anti-desmin (red) abs. Myogenic differentiation was induced without (A-D) and with (E-H) the addition of CM from differentiated C2C12 cultures. Human DPSCs (A, C, E, G) and AFSCs (B, D, F, H) underwent myogenic commitment after 14 days of induction. Human DPSCs and AFSCs not undergoing demethylation treatment did not show any expression of muscle specific markers, after culture in myogenic induction medium (I-L). Scale bar = 50 µm.

Figure 3. Western blot (WB) analysis of myogenin and desmin expression in whole cell lysates of differentiated hDPSCs and hAFSCs, with (hDPSCs Aza + cm, hAFSCs Aza + cm) and without the addition of C2C12 CM (hDPSCs Aza, hAFSCs Aza). Whole cell lysates were collected from three plates of hDPSCs for each experimental group. Actin bands demonstrate that an equal amount of protein was loaded in each lane. Densitometric analysis of western blot bands is shown at the bottom (ANOVA followed by Tukey's test: ***$p < 0.001$ hDPSCs Aza and hDPSCs Aza + cm vs undiff hDPSCs; ***$p < 0.001$ hAFSCs Aza and hAFSCs Aza + cm vs undiff hAFSCs; $^{§§§}p < 0.001$ hDPSCs Aza + cm vs hDPSCs Aza; $^{§§§}p < 0.001$ hAFSCs Aza + cm vs hAFSCs Aza).

Figure 4. Engraftment evaluation 7 days after cell injection in *mdx*/SCID GMs. Immunofluorescent staining with DAPI (blue) and anti-hMit ab (red) shows the presence of human DPSCs (A, B) and AFSCs (C, D) within the host dystrophic muscle, after the cell injection. A, C: muscle cryosections immunostained after injection of human stem cells pre-differentiated via demethylation treatment with 5-Aza. B, D: muscle cryosections immunostained after injection of human stem cells pre-differentiated via demethylation treatment with 5-Aza and addition of CM from C2C12 cultures. E:

untreated samples, consisting of non-injected *mdx*/SCID GMs, were taken as negative controls. Scale bar = 50 μm.

Figure 5. Evaluation of angiogenesis promotion by human DPSCs and AFSCs 7 days after cell injection into *mdx*/SCID GMs. Immunofluorescent labeling with DAPI (blue), anti-vWill (green) and anti-hMit (red) abs. Green and red signals appear co-localized showing that hDPSCs (A, B) and hAFSCs (C, D) are present within the endothelium of new vasa. A, C: muscle cryosections immunostained after injection of human stem cells pre-differentiated via demethylation treatment with 5-Aza. B, D: muscle cryosections immunostained after injection of human stem cells pre-differentiated via demethylation treatment with 5-Aza and addition of conditioned fusion media from C2C12 cultures. E: untreated samples, consisting of non-injected *mdx*/SCID GMs, were used as negative controls. Scale bar = 50 μm.

Figure 6. Evaluation of muscle regeneration after cell injection in *mdx*/SCID GMs. A: immunofluorescent staining with DAPI (blue), anti-hMit (green) and anti-hDystrophin (red) abs shows the presence of human DPSCs and AFSCs within human dystrophin positive muscle fibers, as early as 14 days after cell injection. B:the restored expression of dystrophin by the muscle fibers containing human DPSCs and AFSCs was observed through the 28 day time point post-injection.

Figure 7. Histological and ultrastructural analysis after cell injection in *mdx*/SCID GMs.

A: H&E staining shows active muscle regeneration in progress within the muscles treated with human DPSCs and AFSCs, as represented by a high presence of centronucleated muscle fibers (yellow arrowheads), whereas the controls are characterized by a severe degeneration of the fibers. Comparison of fibrotic processes between controls (non-injected *mdx*/SCID GMs) and *mdx*/SCID GMs injected with human DPSCs and AFSCs. Masson's trichrome staining highlights the reduction in fibrosis within the muscles treated with human DPSCs and AFSCs, while the controls appear rich

in fibrotic tissue (blue stained collagens). Scale bar = 50μm. **B:** histograms represent the percentage of regenerating centronucleated muscle fibers. **p<0.01 *vs* control (ANOVA followed by Tukey's test). **C:** histograms represent the percentage area of fibrosis. **p<0.01 *vs* control (ANOVA followed by Tukey's test). **D:** ultrastructure analysis of *mdx*/SCID GMs through Transmission Electron Microscopy (TEM). Sections of control GMs show disruption and loss of myofilaments together with mitochondria alterations and the presence of vacuoles. On the contrary, *mdx*/SCID GMs injected with pre-differentiated hDPSCs and hAFSCs show a regular myofibril arrangement, with an intact sarcomere structure.

Isolation and characterization of non-myogenic mesenchymal stem cells that play a role in skeletal muscle pathology of utrophin/dystrophin double knockout mice

Jihee Sohn, Johnny Huard, Anthony Ascoli, Tim Hannigan, Bing Wang, Aiping Lu, Ying Tang

Abstract

The deposition of ectopic fat and fibrotic tissue in skeletal muscle is closely associated with several genetic disorders including Duchenne muscular dystrophy (DMD), which is a degenerative muscle disorder caused by mutations in the dystrophin gene; however, the origin of ectopic adipocytes and the mechanisms involved with their participation in the disease process remains unclear. Based on a previously published preplate technique, we isolated two distinct populations of muscle derived cells; rapidly adhering cells (RACs), which are Pax7 negative non-myogenic cells and slowly adhering (SAC) Pax7 positive muscle progenitor cells (MPCs) from the skeletal muscle of utrophin/dystrophin double knockout (dys-/- utro-/-, dKO) mice, which is a severely affected animal model of DMD. Previously, we showed that the rapid disease progression in the dKO model is closely associated with MPC depletion, which may contribute to the severe dystrophic phenotype observed in the dKO mice. Here, we showed that the dKO mice rapidly developed skeletal muscle abnormalities, including fibrosis, ectopic calcification and fat accumulation that worsened with age. The RACs isolated from the dKO mice were characterized as non-myogenic mesenchymal stem cells (nmMSCs) based on their multipotency capacity and their expression of PDGFRα. We observed that nmMSCs isolated from aged dKO mice displayed significantly increased proliferation and adipogenic and osteogenic potentials *in vitro* compared to age-matched C57BL/10J (WT) mice, suggesting that the activation of nmMSCs is associated with ectopic fat accumulation, calcium deposits and fibrotic tissue formation within the dystrophic dKO muscle. In addition, we found that dKO-nmMSCs hindered the terminal myogenic differentiation of dKO-MDSCs in co-cultivation experiments. Here we showed that this effect was mediated, at least in part, by secreted frizzled-related protein 1 (sFRP1) secreted by the dKO-nmMSCs. Results from this study could provide insight into new approaches to alleviate muscle weakness and wasting in DMD patients by inhibiting the proliferation of nmMSCs in dystrophic muscle.

Introduction

Adult skeletal muscle possesses a remarkable regenerative ability, which is largely dependent on satellite cells that reside beneath the basal lamina, closely juxtaposed to the muscle fibers [1-3]; however, many studies have reported that in addition to satellite cells, a variety of other stem/progenitor cells can also be found in skeletal muscle and are potential alternative cell sources for muscle repair [2, 4-6]. Despite the presence of these cell populations with exceptional regeneration potentials, skeletal muscle integrity can be debilitated by the deposition of a mix of fibrous and white adipose tissues. The deposition of these tissues is known as fatty degeneration and occurs in various pathological conditions, including Duchenne muscular dystrophy (DMD).

DMD is one of the most common childhood muscular dystrophies, with an incidence of approximately one in every 3,500 live male births. It is an x-linked, inherited disease caused by a lack of functional dystrophin, an essential transmembrane muscle protein in the dystrophin-glycoprotein complex in both

skeletal and cardiac muscle cells [7-9]. In dystrophic muscle, the damaged fibers degenerate and undergo necrosis and lose their ability to regenerate. Satellite cells are recruited to regenerate new myofibers, but this regeneration is inefficient due to the repeated degenerative-regenerative cycles that the muscle undergoes which is believed to cause an exhaustion of the satellite cell population. Progressive muscle weakness and degeneration usually leads to the loss of independent ambulation by the middle of the patient's second decade and a fatal outcome due to cardiac or respiratory failure by their third decade of life [7, 10-14].

Recent evidence has emerged implicating adult stem cell dysfunction in DMD histopathogenesis and studies have reported that the progression of muscle weakness and degeneration among DMD patients maybe a consequence of the decline in the number of functional muscle progenitor cells (MPCs) [15]. Of note, despite the lack of dystrophin at birth, the onset of the muscle weakness typically does not occur until patients reach 4-8 years of age, which coincide with the exhaustion of the MPC pool due to repeated cycles of muscle fiber necrosis over time [16, 17].

Because of these findings, we recently investigated and compared the function of MPCs isolated from *mdx*, dystrophin/utrophin double knockout (dKO), and WT mice. We found that MPCs, including both myoblast and muscle derived stem cells (MDSCs) isolated from old dKO mice (6-8wks old) have significantly reduced proliferation, resistance to oxidative stress, and multilineage differentiation potentials compared to MPCs isolated from age-matched *mdx* or WT mice, suggesting that stem cells from dKO mice are defective. Importantly, the progression of muscle weakness and degeneration in the dKO mice coincides with the depletion of the MPC pool; hence, we postulated that the decline in functional MPCs may be responsible for the progressive reduction in muscle regeneration and the rapid development of the dystrophic phenotype in the dKO mice [6].

One of the most striking pathological conditions in advanced cases of DMD is the accumulation of ectopic adipocytes with muscle being almost entirely replaced by white adipose tissue and other non-muscle tissues. The non-muscle tissue accumulates/infiltrates the skeletal muscle altering the tissue environment which affects muscle structure, function, and recovery [13, 18-20]. More importantly, even with the occurrence of MPC exhaustion, we observed the formation and accumulation of more adipose and fibrotic tissue in the skeletal muscle, heart, and diaphragm of 6-8wks old dKO mice; however, it remains unclear what cell population is responsible for the formation of these other non-skeletal muscle tissues including fibrosis, ectopic calcium and fat deposits. [6, 21].

Our research group has isolated several populations of muscle derived cells from the skeletal muscle of dKO mice utilizing a previously published preplate technique. Two distinct fractions of cells have been identified including: 1) a rapidly adhering cell (RAC) fraction and 2) a slowly adhering cell (SAC) fraction. In previous publications, we characterized SACs as a heterogeneous population of $Pax7^{+}$ cells called muscle-derived stem cells (MDSCs) which are muscle progenitor cells with high myogenic potentials, both *in vitro* and *in vivo* [22-24]. In a previous study we reported that MPCs, including MDSCs isolated from old dKO mice, are depleted and display reductions in proliferation and differentiation, both *in vitro* and *in vivo*, suggesting that MPCs may not be involved in the formation of ectopic non-muscle tissues. Until recently, we have considered RACs to be fibroblast-like cells that are highly positive for Sca-1 and

CD34 [25], two cell surface markers that are also expressed by fibro/adipogenic progenitors (FAPs) [26]; however, they have never been characterized. Therefore, we hypothesized that RACs may be responsible for the deposition of fibrotic tissue, ectopic bone formation and fat accumulation observed in the dKO mice. The current study explores and characterizes the RACs and investigates their role in establishing the dystrophic phenotype seen in the skeletal muscle of the dKO mice.

Methods

Animals: C57BL/10J (wild type; WT) mice were purchased from the Jackson laboratory (Bar Harbor, ME). Dystrophin/utrophin double knockout (dKO) mice, originally characterized by Deconinck and colleagues [27] were generated by crossing dystrophin-/-; utrophin+/- mice [28, 29]. Genotyping was performed by polymerase chain reaction (PCR) analysis of tail samples. Mice ranged in age from 5 days to 8 weeks. Specific ages for each experiment are described below. All animal protocols used for these experiments were approved by the University of Pittsburgh's Institutional Animal Care and Use Committee.

Cell Culture: Primary WT and dKO non-myogenic mesenchymal stem cells (nmMSCs) and muscle derived stem cells (MDSCs) were obtained from 1 - 8 week old WT and dKO mice using a modified preplate method previously described [6, 24, 30]. Briefly, after enzymatic digestion of skeletal muscle tissue, muscle derived cells were replated on collagen type I (C9791, Sigma-Aldrich) coated flasks over a period of days. Two hours after isolation, a rapidly adhering cell population was collected and characterized as nmMSCs. Seven days after preplating, a slowly adhering cell population was obtained, which has been described to contain the MDSC fraction of cells [22]. nmMSCs and MDSCs were cultured in proliferation medium (PM) containing 10% fetal bovine serum, 10% horse serum, 0.5% chick embryo extract and 1% Penicillin-Streptomycin in Dulbecco's modified Eagle's medium (DMEM, 11995-073, Invitrogen)

Immunophenotyping: Flow cytometry was performed on nmMSCs at the end of the second passage. One-hundred thousand WT and dKO nmMSCs were collected, washed with PBS containing 2% FBS, centrifuged, and then placed on ice. They were then re-suspended in a 1:10 dilution of mouse serum (M5905, Sigma-Aldrich) in PBS and incubated for 10 minutes. PE-conjugated rat anti-PDGFRα (12140181, eBioscience), PE-conjugated rat anti-Sca-1 (553108, BD), FITC-conjugated rat anti-CD34 (553733, BD), APC-conjugated rat anti-CD90 (553007, BD), PE-conjugated rat anti-CD105 (562759, BD), and FITC-conjugated rat anti-CD45 (553080, BD), and FITC-conjugated rat anti-ER-TR7 (73355 Santa Cruz Biotechnology) were added to each tube (1µl/100,000 cells) and incubated for 30 minutes on ice. To increase the stability of the staining, only one antibody was used in each tube. The cells were then rinsed in 300µl of cold washing buffer (2% FBS in PBS, 4 degrees). A single color antibody was used to optimize fluorescence compensation settings for multicolor analyses.

Immunofluorescence and histology: Cryosections were fixed with 5% formalin for 8 minutes and blocked with 10% donkey serum for 1 hour. Slides were then incubated with goat anti PDGFRα (1:100, R&D) and rabbit anti-mouse Ki67 (1:200, Abcam) or chicken anti mouse laminin (1:500, Abcam) in 5% donkey serum. Next, sections were incubated with secondary antibodies including 594-conjugated anti-rabbit

IgG (1:300, Invitrogen), 594-conjugated anti-chicken IgG (1:300, Invitrogen), or 488-conjugated anti-goat IgG (1:300, Invitrogen) in PBS for 45 minutes.

mRNA analysis was performed via reverse transcriptase, real-time (RT)-PCR : Total RNA was obtained from nmMSCs and MDSCs or gastrocnemius tissues isolated from 6-8 wk old WT animals using TRizol reagent (Invitrogen) and a RNeasy Mini Kit (Qiagen, Valencia, CA) according to the manufacturer's instructions. Reverse transcription was performed using a Maxima first strand cDNA synthesis kit (Fermentas) according to the manufacturer's protocol. PCR reactions were performed using an iCycler Thermal Cycler (Bio-Rad) as previously described [21]. RT-PCR was carried out using the Maxima Syber Green Assay kit (Thermo Scientific) with an iQ5 thermocycler (Bio Rad). Primers used in the study can be found in Table 1.

Gene	Forward primers	Reverse primers	Size
Desmin	AACCTGATAGACGACCTGCAG	GCTTGGACATGTCCATCTCCA	258
Pax7	GTGCCCTCAGTGAGTTCGAT	CCACATCTGAGCCCTCATCC	
Sca-1	CCTACTGTGTGCAGAAAGAGC	CAGGAAGTCTTCACGTTGACC	243
PDGFRα	GACGAGTGTCCTTCGCCAAAGTG	CAAAATCCGACCAAGCACGAGG	341
β-actin	CCACACCCGCCACCAGTTCG	TACAGCCCGGGGAGCATCGT	111
MyoD	TACCCAAGGTGGAGATCCTG	CATCATGCCATCAGAGCAGT	200
MyHC	AGGACGACTGCAGACCGAAT	CCCTCTGCAGTTCAGCCTTTACTTCC	157
Myf5	GTCAACCAAGCTTTCGAGACG	CGGAGCTTTTATCTGCAGCAC	
eMyHC	GGAGGCTGATGAACAAGCCA	GCTAGAGGTGAAGTCACGGG	
Pax3			
Myogenin			

Table 1. Primers used for RT-PCR

Differentiation Assays:

Adipogenic differentiation assays: A total of 35,000 nmMSCs were cultured in 24-well collagen type I-coated plates for 21 days in adipogenic differentiation medium (PT-3004, Lonza). When the cells reached 100% confluency, three cycles of induction/maintenance medium were applied to cells to induced optimal adipogenic differentiation. Each cycle consisted of incubating the nmMSCs with supplemented adipogenesis induction medium and cultured for 2-3 days followed by 2-3 days of culture in supplemented adipogenic maintenance medium. At the end of the third cycle, cells were incubated in adipogenic maintenance medium for an additional 5-7 days. Adipogenesis was assessed using Oil Red O (O0625, Sigma-Aldrich) to stain for intracellular lipid accumulation. For adipocyte differentiation quantification, cells were stained with AdipoRed (NC9049267, 30µl/ml, Fisher) and DAPI, and fluorescence intensities were analyzed with a spectrophotometer. The AdipoRed fluorescence emission readings were normalized to total DAPI in each well.

Osteogenic differentiation assays: A total of 35,000 nmMSCs were cultured in osteogenic medium which contains DMEM, 10% FBS, supplemented with dexamethasone (D2915, 0.1µM, Sigma-Aldrich), ascorbic-acid-2-phosphate (A8960, 50µg/ml, Sigma-Aldrich) and 10mM β-glycerophosphate (G6251, Sigma-Aldrich), and BMP2 (M11306AAB, 100ng/ml, Medtronic). Osteogenesis was assessed using a bb Fast Blue alkaline phosphatase (ALP) kit (041M4338, Sigma) and by staining mineralized matrix with alizarin

red. ALP activity was quantified with an ELISA-based assay according to the manufacturer's protocol [31].

Chondrogenic differentiation assays: A micromass culture technique was used as described by Kishimoto and colleagues [32]. One-hundred thousand cells were incubated for a week in chondrogenic induction medium (PT3003, Lonza) supplemented with 100ng/ml BMP2 and 20ng/ml TGFβ3 (PHG9305, Invitrogen). Micromass Cultured cells were fixed with 10% formalin and stained with 1% Alcian blue (pH 1.0) for 30 min. For quantification, 250,000 cells were cultured in pellets for 4 weeks in chondrogenic induction media. Sulphated glycosaminoglycans (GAGs) production was quantified using the Blyscan assay kit (Biocolor, Carrickfergus) according to the manufacturer's protocol.

Myogenic differentiation: Thirty-thousand cells were plated on 24-well plates in DMEM supplemented with 2% FBS (Fusion medium, FM) to stimulate myotube formation. Three days after differentiation, cells were fixed with 10% formalin for 8 min, and stained for fast myosin heavy chain (fMyHC) using a mouse anti-MyCHf antibody (1:250, M4276, Sigma-Aldrich) with a mouse-on-mouse (M.O.M) staining kit (Vector Labs, Burlingame, CA), according to manufacturer's directions.

Cell proliferation: To compare the proliferative potential of the dKO-nmMSCs and Wt-nmMSCs, a Live Cell Imaging system (LCI) (Kairos Instruments LLC) was used as previously described [33]. In triplicate, 5000 nmMSCs were plated in a 24 well plate and incubated in a biobox incubator that sits atop a Nikon Eclipse TE 2000 U microscope stage, which is equipped with a CCD camera. 10x bright field images were taken in fifteen minute intervals over a 72 hour period. Three locations were randomly chosen per well for imaging, giving 9 fields of view per population, per experiment. To measure the proliferation rates the LCI was used to capture images of different fields in each of the cultures over a 72 hour period. The number of cells per field of view at 12 hour intervals was determined using ImageJ software (NIH).

Co-culture experiments: dKO-MDSCs were plated in the lower compartment of Transwell Permeable Supports (Costar) in PM media at a density of 30,000 cells per well. WT/dKO-nmMSCs were seeded onto 6.5mm transwell membrane inserts at the same density in PM media and placed above the dKO-MDSCs. As a control, each plate contained wells of dKO-MDSCs without transwell membrane inserts. To measure the differentiation, the PM media was switched to FM. After 3 days, myogenic differentiation of the cells was analyzed via immunostaining for fMyHC, as described above.

Results

Accumulation of fat, calcium deposits, and fibrosis in old dKO mice

Previously, we reported that the onset of muscular dystrophy in the dKO mice occurred as early as 5 days old and the histopathology and muscular dystrophy developed more severely in older dKO mice, at the age of 6-8 wks. At this age, we also observed that the accumulation of connective tissue and ectopic calcium and fat deposits in the gastrocnemius muscles (GAS) of the dKO mice was substantially increased compared to that of age-matched WT skeletal muscle [6, 21]. To determine the age of onset

of these events, the GAS from 1-, 4- and 6-8 wk old dKO mice were examined **(Figure 1)**. Immunohistochemistry of Oil Red O, Alizarin Red, and Trichrome stain indicated that the accumulation of fat, calcium deposits and fibrosis started to occur in the GAS muscles at 4 wk of age and the severity of the histopathology increased by 6-8wk of age in dKO mice. There was a higher level of lipid accumulation observed in 4 wk old dKO-GAS compared to the of 1 wk dKO-GAS, but lipid droplets were significantly increased in the GAS of 6 wk old dKO mice compared to that of 1- or 4wks old dKO mice **(Figure 1A)**. Alizarin Red stain showed more extensive calcium deposition in the GAS of 4- and 6-8 wk old dKO mice compared to that of 1 wk old muscle **(Figure 1B)**. We observed larger areas of fibrosis between the muscle fibers of 6-8 wk old dKO-GAS compared to 1 wk old dKO muscle **(Figure 1C)**. Very little lipid, calcium deposits, and fibrosis was observed the 1wk old dKO muscle **(Figure 1)**. GAS of 1-, 4-, and 6-8wks old dKO mice were collected and analyzed for mRNA expression of adipogenic, osteogenic, and fibrosis markers by RT-PCR **(Figure 1D)**. The expression levels of the markers in the 6 wk old dKO-GAS were significantly higher than those in the 1- or 4 wk old dKO-GAS. Taken together, our results demonstrated that the dKO mice rapidly developed skeletal muscle abnormalities, including fibrosis, ectopic calcification and fat accumulation that worsened with age and exhibited a similar histopathologic phenotype to DMD patients.

Identification and characterization of non-myogenic mesenchymal stem cells (nmMSCs) isolated from the skeletal muscle of WT and dKO mice utilizing the preplate technique

Next, we sought to determine which cell population in skeletal muscle was associated with the accumulation of fat, calcium deposits and fibrosis in the dKO mice. Utilizing the preplate technique, rapidly adhering cells (RACs) were obtained within 2 hours of isolation, which is very similar to the isolation method utilized to collect bone marrow derived mesenchymal stem cells (BM-MSCs) [34]. RACs were isolated from the skeletal muscle of 6 wk old WT and dKO mice and characterized by examining their cell surface markers and stem cell functionality **(Figure 2)**. RACs had a very similar morphology to that of BM-MSCs rather than MDSCs, which are spherical and refractive under phase contrast microscopy **(Figure 2A)**. RT-PCR analysis of lineage markers in WT-MDSCs and WT-RACs clearly showed that MDSCs consisted of $Pax7^+$ and $Desmin^+$ muscle progenitor cells, and the heterogeneous RACs contained $Sca\text{-}1^+$ and $PDGFR\alpha^+$ mesenchymal stem cells **(Figure 2B)**. Immunofluorescent staining for Pax7 showed that nuclear-localized Pax7 expression was only observed in MDSCs and not in the RACs. Therefore, upon myogenic induction, only MDSCs were able to differentiate into well-developed large myotubes **(Figure 2C)**. The biological property that most uniquely identifies MSCs is their capacity for tri-lineage mesenchymal differentiation [35]. We confirmed that under appropriate induction conditions, WT-RACs exhibited evidence of adipogenic, osteogenic, and chondrogenic differentiation potentials **(Figure 2E)**.

Immunophenotyping of WT- and dKO-RACs using fluorescence-activated cell sorting (FACS) analysis with multiple mesenchymal stem cell markers indicated that the RACs were positive for PDGFRα, CD90, CD105, markers known to be expressed on mesenchymal cells, and Sca-1, a stem cell marker. More than 90% of the RACs from both WT and dKO mice were positive for CD34 and less than 1% of RACs expressed CD45, a hematopoietic cell marker **(Figure 2D top)**. Quantification of FACS analysis indicated that there was no significant difference in the percentage of positive cells between WT- and dKO-RACs

for each marker **(Figure 2D bottom)**. Based on the RACs marker profile and their tri-lineage differentiation capacities, we will hereafter refer to the RACs as non-myogenic mesenchymal stem cells (nmMSCs).

Activated proliferation and differentiation potentials of nmMSCs isolated from 6-8wks old dKO mice

Next, we compared the proliferation and differentiation potentials of nmMSCs isolated from 6-8wks old WT- and dKO mice **(Figure 3)**. Surprisingly, Live Cell Imaging (LCI) analysis of the *in vitro* proliferation rates of 6 wk old WT- and dKO- nmMSCs showed that dKO-nmMSCs displayed significantly greater proliferation rates than that of WT-nmMSCs **(Figure 3A)**. We next examined the proliferation of nmMSCs *in vivo* and performed immunohistochemistry for PDGFRα and Ki67, a proliferation marker in the GAS of 6 wk old WT and dKO mice. PDGFRα^{+} nmMSCs were localized in the interstitial space between muscle fibers of skeletal muscle **(Figure 3B Left)**. Our results indicated that the number of total PDGFRα^{+} cells in the dKO GAS was increased ~3-fold, but the number of actively proliferating Ki67^{+}PDGFRα^{+} nmMSCs was ~15-fold higher in the dKO skeletal muscle when compared to the age-matched WT muscles **(Figure 3B Right)**. We next investigated if actively proliferating dKO-nmMSCs would result in increased multi-lineage differentiation capacities. Our results indicated that there were significant increases in the adipogenic and osteogenic differentiation capacities of the nmMSCs isolated from the 6 wks old dKO mice compared to those isolated from the age-matched WT mice **(Figure 3C)**. Upon quantification, dKO-nmMSCs exhibited a 3.5-fold higher osteogenic **(Figure 3C Left)** and 4-fold higher adipogenic differentiation potentials **(Figure 3C Right)** when compared to the age-matched WT-nmMSCs. Our results demonstrated that the function of nmMSCs isolated from dKO mice are not affected, and in fact, even enhanced abnormally, showing a significant increase in number and proliferation capacities, as well as increased adipogenic and osteogenic differentiation potentials.

Proliferation and differentiation potentials of nmMSCs isolated from young dKO mice are not affected

To test whether nmMSCs become progressively activated with disease progression in the dKO mice, we isolated nmMSCs from 1-, 4-, and 6-8 wk old dKO skeletal muscle and compared their proliferation and differentiation potentials **(Figure 4)**. We observed that nmMSCs isolated from 1 wk old dKO mice displayed significantly decreased proliferation rates compared to nmMSCs isolated from 4- and 6-8 wk old dKO mice **(Figure 4A)**. The population doubling time for 1 wk old dKO-nmMSCs was about 54 hours, where it was 38 or 30 hours for 4 wk- or 6-8 wk old dKO-nmMSCs, respectively. More importantly, our results also revealed that 1 wk old dKO-nmMSCs displayed significantly decreased adipogenic and osteogenic potentials when compared to 4- and 6-8 wk old dKO-nmMSCs **(Figure 4B&C)**. In addition, immunohistochemistry for PDGFRα and laminin expressions showed that the number of PDGFRα expressing cells was significantly decreased in 1 wk old dKO GAS when compare to 4- and 6-8wk old dKO GAS **(Figure 4D)**. There were no significant differences in the number of endogenous PDGFRα^{+} nmMSCs, *in vitro* proliferation rate, and adipogenic and osteogenic potentials between the 4- and 6-8 wk dKO-nmMSCs , although small decreases were observed in each assay with the 4 wk old dKO-nmMSCs **(Figure 4)**. Our results suggest that in dKO mice, the nmMSCs increase in number and their proliferation capacity and their adipogenic and osteogenic differentiation potentials also increase with the progression of the disease. Earlier, we showed that the accumulation of lipids, calcium deposits, and

fibrotic tissue in GAS of dKO mice started mildly at 1 wk and the histopathology became more severe as the mice grew older **(Figure 1A-C)**. Taking these results together, we propose that nmMSCs become activated in their proliferation and adipogenic and osteogenic potentials as muscular dystrophy progresses and are involved in the deposition of ectopic fat, bone, and fibrotic tissue accumulation in the dKO mice.

dKO-nmMSCs isolated from old mice inhibits myofiber regeneration of dKO-MDSCs

Given that, the numbers of endogenous proliferating nmMSCs in the interstitial space of the GAS of old dKO mice were significantly increased compared to age-matched WT GAS **(Figure 3B)**, we next examined if these cells may play a role in the development of the dystrophic phenotype. We investigated the possibility of the existence of cross-talk between MDSCs and nmMSC isolated from 6wks old dKO mice to test whether nmMSCs may regulate the myogenic differentiation potential of MDSCs through a paracrine mechanism. WT-nmMSCs were used as a control. MDSCs isolated from 6-8 wk old dKO mice were co-cultured with age-matched WT/dKO-nmMSCs, using a transwell system and the fusion index of the dKO- MDSCs was monitored **(Figure 5A)**. When dKO-MDSCs were co-cultured with WT-nmMSCs, the myogenic potential of the dKO-MDSCs was significantly enhanced **(Figure 5B&C)** just as other studies have shown [26, 36-38]. Surprisingly, the limited myogenic potential of the dKO-MDSCs was further exacerbated after co-culture with the dKO-nmMSCs **(Figure 5B)**. To quantify the diminishment of myogenic differentiation potential after co-cultivation, dKO-MDSCs were collected and immune-stained for the terminal myogenic differentiation marker fMyHC. fMyHC expression was dramatically decreased when dKO-MDSCs were cultured in the presence of dKO-nmMSCs compared to the dKO-MDSCs alone **(Figure 5C)**. To rule out that the decrease in dKO-MDSC differentiation was caused by the nmMSCs and not a secondary effect of dKO-MDSC proliferation, we measured the effect of co-cultivation on the dKO-MDSCs proliferation using an MTS assay. No significant difference in proliferation was observed between dKO-MDSCs alone and dKO-MDSCs co-cultured with dKO-nmMSCS during the first 2 days of co-culture **(Figure 5D)**. Next, we further analyzed changes in expression of myogenic markers expressed by the dKO-MDSCs after 3-4 days of myogenesis with/without dKO-nmMSCs co-cultivation, using quantitative reverse transcription-PCR (qRT-PCR). We observed a significant reduction in the expression of myoblast markers, MyoD and Myogenin, and later makers, eMyHC and MyHC in the dKO-MDSCs with the presence of dKO-nmMSCs **(Figure 5E)**. These results suggest that nmMSCs isolated from old dKO mice inhibited the differentiation function of age-matched dKO-MDSCs via secreted factors.

One interesting observation from our *in vivo* studies was that the number of endogenous PDGFRα^{+} nmMSCs was almost 3 fold higher in the old dKO skeletal muscle compared to that of the age-matched WT skeletal muscle **(Figure 3C)**. To mimic the *in vivo* dKO muscle micro-environment in our co-culture assay, we repeated the co-cultivation experiments using 3:1, 1:1 and 1:6 ratios of dKO-nmMSCs to dKO-MDSCs. With a 3:1 ratio, we observed a larger effect of nmMSCs myogenic inhibition of the dKO-MDSCs compared to the 1:6 ratio. In fact, there was no significant difference in the formation of fMyHC expressing myotubes between the dKO-MDSCs only and dKO-MDSCs in the 1:6 ratio co-cultures **(Figure 5 F&G)**. Taken together, these results suggest that signals originating from nmMSCs contribute to the micro-environment's ability to limit the myogenic differentiation capacity of the MDSCs in the dKO muscle.

Secreted frizzled-related protein 1 (sFRP1) is a soluble mediator of nmMSCs and MDSCs

In search of a soluble mediator of functional interactions between nmMSCs and MDSCs from dKO mice, we considered sFRP1 as a potential candidate, as previous studies showed that sFRP1 inhibits myotube formation of C2C12 or satellite cells with no significant effect on the cell cycle or apoptosis [39]. When we compared sFRP1 mRNA expression isolated from the total GAS muscles of WT and dKO, we observed a significant increase in sFRP1 gene expression in the dKO GAS compared to that of WT GAS **(Figure 6A)**. Next, we examined if the dKO-nmMSCs expressed higher sFRP1 mRNA levels compared to that of WT-nmMSCs, and confirmed by qRT-PCR that sFRP1 gene expression was increased approximately 4.5 fold in the dKO-nmMSCs **(Figure 6B)**.

Discussion

Despite the fact that the underlying pathogenesis of DMD has been well studied, it remains a very difficult disease to treat. Traditionally available treatments for DMD patients include cell, gene, and protein-mediated therapies to restore dystrophin within the dystrophic muscle or to block inflammation; however, these technologies have major limitations [8, 12, 40]. For instance, accumulation of intramuscular fat, calcium deposits, and fibrotic tissue significantly limits the success of any traditionally available regenerative approaches in DMD patients [13, 18-20]. In the current study, we showed that the accumulation of lipid, calcium deposits, and fibrotic tissue coincide with the progressive reduction in muscle regeneration in the skeletal muscle of dKO mice. The histopathology and skeletal abnormalities start mildly by the age of 1 week, progressively worsening by 4 weeks of age and by 6-8 weeks of age the mice are severely affected and typically die by their 8th week. Severe intramuscular non-muscle tissue development may induce deregulation of muscle homeostasis, which associates with potential insulin resistance, regeneration deregulation, and physical activity dysfunction [41]. Therefore, the use of dystrophin replacement alone to treat the primary defect in DMD patients may not be successful for rescuing muscle from progressive degeneration and wasting, especially at the later stages of the disease [12, 40].

When searching for potential cell sources responsible for the accumulation of ectopic non-muscle tissues in dystrophic muscle, we considered muscle resident non-myogenic mesenchymal stem cells (nmMSCs) isolated via the preplate technique. While we previously reported that MPCs isolated from aged dKO mice progressively become defective in their proliferation and differentiation capacities, including myogenic, osteogenic, adipogenic and chondrogenic capacities [6]; the current study demonstrated that the function of the nmMSCs isolated from aged dKO mice appeared to be unaffected and even enhanced with disease progression. nmMSCs isolated from 6 week old dKO mice displayed significantly increases in cell number, *in vivo* and *in vitro* proliferation and adipogenic and osteogenic differentiation potentials compared to age-matched WT-nmMSCs. More importantly, proliferation and differentiation potentials of dKO-nmMSCs isolated from 1 week old dKO mice seemed not to be affected or yet activated, but gradually became activated by 4 weeks and started to extensively proliferate and experienced an enormous increase in their adipogenic and osteogenic differentiation capacities by 6-8

weeks of age. Taking our *in vitro* and *ex vivo* results together, the activation of the nmMSCs in the dKO mice appears to coincide with the occurrence of lipid and calcium deposition, and the formation of fibrotic tissue in the dKO muscle. Although it is not clear which event occurs first, we believe that the activation of the nmMSCs is responsible for the occurrence of fibrotic tissue, ectopic calcium deposition, and fat accumulation during disease progression in the dKO mice, and in turn, this changes the muscle micro milieu further altering the proliferation and differentiation potentials of the nmMSCs which perpetuates the entire process utterly destroying the normal phenotype of the muscle.

Furthermore, the difference in proliferation and differentiation potentials among the 1-, 4-, and 6-8 week old dKO-nmMSCs suggests that the activation of nmMSCs in the aged dKO mice may not be caused by intrinsic differences, but by the changes in their microenvironment. This result can be supported by other studies, which reported that mesenchymal progenitors isolated from injured muscle tissue showed increased adipogenic potentials, although they showed decreased osteogenic and chondrogenic potentials compared to that of BM-MSCs [31]. Therefore, the dystrophic muscle environment may influence the cells' function through characteristic muscle milieu molecules that likely play a role in determining cell fate of the nmMSCs in the dKO mice.

Recently, using a FACS-based cell isolation method, two research groups have identified resident skeletal muscle progenitor cells, which display high adipogenic or fibrogenic potentials in glycerol-injected fatty degeneration model, or *mdx* mice; fibro/adipogenic progenitors (FAPs) which express Sca-1 and CD34 and PDGFRα^+ mesenchymal stem/progenitor cells (MSCs) that are non-myogenic. However, since *mdx* mice have a relatively normal life span and exhibit virtually no clinical features of the disease [27] our group utilized dKO mice, which exhibit numerous clinically-relevant manifestations and life-threatening features similar to DMD patients, to prove that PDGFRα and Sca-1 expressing nmMSCs are in fact, highly proliferative, adipogenic and osteogenic and are associated with the deposition of lipid, calcification, and fibrosis in the dystrophic muscle of the mice.

Another group, Wosczyna et al. also reported that functionally and phenotypically similar muscle resident mesenchymal progenitor cells, expressing Tie2, PDGFRα, and Sca-1 surface markers, exhibit robust BMP-dependent osteogenic activity and mediate heterotopic ossification in mice that have experienced a traumatic injury [42]. Knowing that Tie2$^+$ cells [42], FAPs [26], PDGFRα^+ MSCs [13]and nmMSCs share the same markers, anatomical location in the muscle, and *in vitro* and possibly *in vivo* development potentials, they appear to represent the same cell population. Hence we contend that FAPs may not be the correct term to use and non-myogenic mesenchymal stem cells (nmMSCs) may be a more appropriate term for this population of cells.

Recently, a number of studies revealed that in addition to their role in muscle pathogenesis, nmMSCs play a crucial role in muscle regeneration by regulating satellite cell differentiation [13, 26, 37]. Joe et al. showed that although FAPs do not regenerate myofibers, they enhance the rate of terminal differentiation of primary myoblasts in co-cultivation experiments [26]. In addition, FAPs can facilitate the function of HDAC inhibitors to promote satellite cell-mediated regeneration at early stages of disease in *mdx* mice [37]. Conversely, Uezumi et al. demonstrated that satellite cell-derived myofibers strongly inhibit the proliferation and adipogenic potentials of nmMSCs [13], suggesting that the

interaction or balance between MPCs and nmMSCs is key to maintaining muscle integrity and homeostasis.

Contrary to these reports, our *in vitro* co-culture experiments showed that proliferating dKO-nmMSCs significantly limited the myogenic potential of the dKO-MDSCs, at least in part by, down-regulating genes that are crucial for myoblast maturation and terminal myogenic differentiation, including MyoD, myogenin, eMyHC and MyHC. Interestingly, we showed that by decreasing the number of nmMSCs co-cultured with dKO-MDSCs, we were able to rescue the MDSCs from the inhibiting effects of the nmMSCs. Therefore, knowing that dKO mice suffer from constant muscle wasting and degeneration, we contend that the extensive proliferation of the nmMSCs in the dKO mice may be a source of trophic signals for hindering muscle regeneration during the chronic disease progression of DMD and perhaps other degenerative muscle diseases. FAPs' involvement in inhibiting the MPCs myogenic potential had also been described in a study by Mozzetta et al. where they reported that FAPs isolated from old *mdx* mice repressed satellite cell-mediated myofiber regeneration. Of note, although young *mdx* mice exhibit successful muscle regeneration and very mild symptoms of DMD, old *mdx* mice (18 months and older) eventually develop muscular dystrophy, close to DMD dystrophinopathy, and exhibit severe muscle fibrosis [43] which is similar to what is seen in the dKO mice. Our results suggest that nmMSCs isolated from 6 week old dKO mice are functionally equivalent to that of 18 month old *mdx* mice, which may also support our previous findings that propose the dKO mouse as a model of accelerated aging [29].

Recent studies suggest that resident muscle fibroblasts, not FAPs or nmMSCs, maybe the main source of intramuscular adipocytes in pathological conditions, including obesity, sarcopenia, and muscular dystrophies [44] and that their interactions with satellite cells are vital for muscle regeneration [38]. Murphy et al. showed for the first time *in vivo* that during muscle regeneration after injury, $Tcf4^+$ fibroblasts extensively proliferate in close proximity to satellite cells and regenerating myofibers, and that the ablation of $Tcf4^+$ cells leads to premature satellite cell differentiation and depletion of the early satellite cell pool. In turn, ablation of $Pax7^+$ cells results in complete loss of muscle regeneration and a significant increase in connective tissue [38], suggesting that interactions between satellite cells and fibroblast are crucial for maintaining muscle homeostasis during regeneration. Another group, Agley et al. isolated TE-7^+ fibroblasts from human skeletal muscle utilizing a double immuno-magnetic sorting technique for CD56 (marker for myogenic cells) and TE-7 (marker for muscle fibroblasts), and showed that human skeletal muscle fibroblasts, but not myogenic cells, readily undergo adipogenic differentiation [44]. Interestingly, both Tcf4 and TE-7 expressing fibroblasts are rapidly adhering cells (adhering to the culture dish in 2-72 hours) and are also positive for PDGFRα antigen. When we compare the morphology, early adhering characteristics, marker profile, anatomical locations, differentiation potentials, and the role that the TE-7^+/$Tcf4^+$ fibroblasts and nmMSCs/FAPs play in muscle regeneration, it appears that the fibroblasts and mesenchymal stem cells share much more in common than previously identified, and may actually represent the same population. Further studies need to be performed to explicitly compare the relationship between fibroblasts and nmMSCs.

In order to better understand the mechanisms behind the negative effect that the nmMSCs have on the myogenesis of MPCs, we speculated that secreted frizzled-related protein 1 (sFRP1), a known inhibitor of myoblast differentiation, may be involved. sFRP1 is an antagonist of the Wnt signaling pathway and

the constitutive ectopic expression of sFRP1 in adipocytes inhibits the Wnt/β-catenin signaling pathway, resulting in the promotion of adipogenesis *in vitro* and adipose tissue expansion *in vivo* [39, 45-47]. Only weak expression has been reported in skeletal muscle [46]; yet we observed an approximate 10 fold increase in sFRP1 mRNA expression from the GAS of 6-8wk old dKO mice compared to age-matched WT mice, suggesting that sFRP1 may be associated with increased proliferation and the adipogenic potentials of the nmMSCs isolated from dKO mice. The importance of Wnt involvement in the function, differentiation, development, and proliferation of stem cells, including MSCs, has been well described [48-50]. Higher sFRP1 mRNA levels in dKO-nmMSCs compared to age-matched WT-nmMSCs indicates that sFRP1 may be responsible for the abnormally increased adipogenic potential of the nmMSCs isolated from the dKO mice. The ELISA assay results further confirmed that dKO-nmMSCs were secreting more sFRP1 protein than that of the WT-nmMSCs, further verifying our hypothesis that sFRP1 secreted from dKO-nmMSCs contributes, at least in part, to the micro-environment that inhibits the myogenic differentiation of MDSCs in dKO muscle. Furthermore, we propose that not only does the sFRP1 secreted from the dKO-nmMSCs hinder muscle regeneration, but also, sFRP1 secreted from nmMSCs may accumulate and contribute to establishing a proadipogenic muscle microenvironment which promotes fatty degeneration in dKO skeletal muscle.

Overall, our data suggests that nmMSCs isolated from old dKO mice are highly proliferative, adipogenic and osteogenic, and that the activation of nmMSCs coincides with the occurrence of fatty infiltration, ectopic calcification, and fibrotic tissue accumulation in the skeletal muscle of dKO mice. More importantly, we demonstrated that not only might the nmMSCs be a major contributor to ectopic fat, calcification, and fibrosis of skeletal muscle, but that the activation of the nmMSCs may aggravate the degeneration and wasting of the muscle fibers in dystrophic muscle. Results from this study could provide insights into new approaches to alleviate muscle weakness and wasting in DMD patients by targeting proliferating nmMSCs in the dystrophic muscle.

Reference

1. Huard, J., B. Cao, and Z. Qu-Petersen, *Muscle-derived stem cells: potential for muscle regeneration.* Birth Defects Res C Embryo Today, 2003. **69**(3): p. 230-7.
2. Judson, R.N., R.H. Zhang, and F.M. Rossi, *Tissue-resident mesenchymal stem/progenitor cells in skeletal muscle: collaborators or saboteurs?* FEBS J, 2013. **280**(17): p. 4100-8.
3. Mauro, A., *Satellite cell of skeletal muscle fibers.* J Biophys Biochem Cytol, 1961. **9**: p. 493-5.
4. Mitchell, K.J., et al., *Identification and characterization of a non-satellite cell muscle resident progenitor during postnatal development.* Nat Cell Biol, 2010. **12**(3): p. 257-66.
5. Pannerec, A., et al., *Defining skeletal muscle resident progenitors and their cell fate potentials.* Development, 2013. **140**(14): p. 2879-91.
6. Lu, A., et al., *Rapid depletion of muscle progenitor cells in dystrophic mdx/utrophin-/- mice.* Hum Mol Genet, 2014.
7. Mendell, J.R., et al., *Dystrophin immunity in Duchenne's muscular dystrophy.* N Engl J Med, 2010. **363**(15): p. 1429-37.
8. Hayes, J., F. Veyckemans, and B. Bissonnette, *Duchenne muscular dystrophy: an old anesthesia problem revisited.* Paediatr Anaesth, 2008. **18**(2): p. 100-6.
9. Hoffman, E.P., et al., *Conservation of the Duchenne muscular dystrophy gene in mice and humans.* Science, 1987. **238**(4825): p. 347-50.
10. Brack, A.S., et al., *Increased Wnt signaling during aging alters muscle stem cell fate and increases fibrosis.* Science, 2007. **317**(5839): p. 807-10.
11. Miranda, A.F., et al., *Dystrophin immunocytochemistry in muscle culture: detection of a carrier of Duchenne muscular dystrophy.* Am J Med Genet, 1989. **32**(2): p. 268-73.
12. Bonilla, E., et al., *Duchenne muscular dystrophy: deficiency of dystrophin at the muscle cell surface.* Cell, 1988. **54**(4): p. 447-52.
13. Uezumi, A., et al., *Mesenchymal progenitors distinct from satellite cells contribute to ectopic fat cell formation in skeletal muscle.* Nat Cell Biol, 2010. **12**(2): p. 143-52.
14. Luz, M.A., M.J. Marques, and H. Santo Neto, *Impaired regeneration of dystrophin-deficient muscle fibers is caused by exhaustion of myogenic cells.* Braz J Med Biol Res, 2002. **35**(6): p. 691-5.
15. Sacco, A., et al., *Short telomeres and stem cell exhaustion model Duchenne muscular dystrophy in mdx/mTR mice.* Cell, 2010. **143**(7): p. 1059-71.
16. Blau, H.M., C. Webster, and G.K. Pavlath, *Defective myoblasts identified in Duchenne muscular dystrophy.* Proc Natl Acad Sci U S A, 1983. **80**(15): p. 4856-60.
17. Webster, C. and H.M. Blau, *Accelerated age-related decline in replicative life-span of Duchenne muscular dystrophy myoblasts: implications for cell and gene therapy.* Somat Cell Mol Genet, 1990. **16**(6): p. 557-65.
18. Uezumi, A., et al., *Fibrosis and adipogenesis originate from a common mesenchymal progenitor in skeletal muscle.* J Cell Sci, 2011. **124**(Pt 21): p. 3654-64.
19. Sussman, M., *Duchenne muscular dystrophy.* J Am Acad Orthop Surg, 2002. **10**(2): p. 138-51.
20. Uezumi, A., M. Ikemoto-Uezumi, and K. Tsuchida, *Roles of nonmyogenic mesenchymal progenitors in pathogenesis and regeneration of skeletal muscle.* Front Physiol, 2014. **5**: p. 68.
21. Mu, X., et al., *RhoA mediates defective stem cell function and heterotopic ossification in dystrophic muscle of mice.* FASEB J, 2013. **27**(9): p. 3619-31.
22. Qu-Petersen, Z., et al., *Identification of a novel population of muscle stem cells in mice: potential for muscle regeneration.* J Cell Biol, 2002. **157**(5): p. 851-64.
23. Deasy, B.M., et al., *Long-term self-renewal of postnatal muscle-derived stem cells.* Mol Biol Cell, 2005. **16**(7): p. 3323-33.

24. Gharaibeh, B., et al., *Isolation of a slowly adhering cell fraction containing stem cells from murine skeletal muscle by the preplate technique.* Nat Protoc, 2008. **3**(9): p. 1501-9.
25. Jankowski, R.J., et al., *Flow cytometric characterization of myogenic cell populations obtained via the preplate technique: potential for rapid isolation of muscle-derived stem cells.* Hum Gene Ther, 2001. **12**(6): p. 619-28.
26. Joe, A.W., et al., *Muscle injury activates resident fibro/adipogenic progenitors that facilitate myogenesis.* Nat Cell Biol, 2010. **12**(2): p. 153-63.
27. Deconinck, A.E., et al., *Utrophin-dystrophin-deficient mice as a model for Duchenne muscular dystrophy.* Cell, 1997. **90**(4): p. 717-27.
28. Wang, B., et al., *Systemic human minidystrophin gene transfer improves functions and life span of dystrophin and dystrophin/utrophin-deficient mice.* J Orthop Res, 2009. **27**(4): p. 421-6.
29. Isaac, C., et al., *Dystrophin and utrophin "double knockout" dystrophic mice exhibit a spectrum of degenerative musculoskeletal abnormalities.* J Orthop Res, 2013. **31**(3): p. 343-9.
30. Lavasani, M., et al., *Isolation of muscle-derived stem/progenitor cells based on adhesion characteristics to collagen-coated surfaces.* Methods Mol Biol, 2013. **976**: p. 53-65.
31. Jackson, W.M., et al., *Differentiation and regeneration potential of mesenchymal progenitor cells derived from traumatized muscle tissue.* J Cell Mol Med, 2011. **15**(11): p. 2377-88.
32. Kishimoto, K.N., C.L. Oxford, and A.H. Reddi, *Stimulation of the side population fraction of ATDC5 chondroprogenitors by hypoxia.* Cell Biol Int, 2009. **33**(12): p. 1222-9.
33. Deasy, B.M., et al., *Modeling stem cell population growth: incorporating terms for proliferative heterogeneity.* Stem Cells, 2003. **21**(5): p. 536-45.
34. Soleimani, M. and S. Nadri, *A protocol for isolation and culture of mesenchymal stem cells from mouse bone marrow.* Nat Protoc, 2009. **4**(1): p. 102-6.
35. Dominici, M., et al., *Minimal criteria for defining multipotent mesenchymal stromal cells. The International Society for Cellular Therapy position statement.* Cytotherapy, 2006. **8**(4): p. 315-7.
36. Heredia, J.E., et al., *Type 2 innate signals stimulate fibro/adipogenic progenitors to facilitate muscle regeneration.* Cell, 2013. **153**(2): p. 376-88.
37. Mozzetta, C., et al., *Fibroadipogenic progenitors mediate the ability of HDAC inhibitors to promote regeneration in dystrophic muscles of young, but not old Mdx mice.* EMBO Mol Med, 2013. **5**(4): p. 626-39.
38. Murphy, M.M., et al., *Satellite cells, connective tissue fibroblasts and their interactions are crucial for muscle regeneration.* Development, 2011. **138**(17): p. 3625-37.
39. Descamps, S., et al., *Inhibition of myoblast differentiation by Sfrp1 and Sfrp2.* Cell Tissue Res, 2008. **332**(2): p. 299-306.
40. Cossu, G. and M. Sampaolesi, *New therapies for Duchenne muscular dystrophy: challenges, prospects and clinical trials.* Trends Mol Med, 2007. **13**(12): p. 520-6.
41. Tuttle, L.J., D.R. Sinacore, and M.J. Mueller, *Intermuscular adipose tissue is muscle specific and associated with poor functional performance.* J Aging Res, 2012. **2012**: p. 172957.
42. Wosczyna, M.N., et al., *Multipotent progenitors resident in the skeletal muscle interstitium exhibit robust BMP-dependent osteogenic activity and mediate heterotopic ossification.* J Bone Miner Res, 2012. **27**(5): p. 1004-17.
43. Lefaucheur, J.P., C. Pastoret, and A. Sebille, *Phenotype of dystrophinopathy in old mdx mice.* Anat Rec, 1995. **242**(1): p. 70-6.
44. Agley, C.C., et al., *Human skeletal muscle fibroblasts, but not myogenic cells, readily undergo adipogenic differentiation.* J Cell Sci, 2013. **126**(Pt 24): p. 5610-25.
45. Kawano, Y. and R. Kypta, *Secreted antagonists of the Wnt signalling pathway.* J Cell Sci, 2003. **116**(Pt 13): p. 2627-34.

46. Svensson, A., et al., *Secreted frizzled related protein 1 (Sfrp1) and Wnt signaling in innervated and denervated skeletal muscle.* J Mol Histol, 2008. **39**(3): p. 329-37.
47. Lagathu, C., et al., *Secreted frizzled-related protein 1 regulates adipose tissue expansion and is dysregulated in severe obesity.* Int J Obes (Lond), 2010. **34**(12): p. 1695-705.
48. Christodoulides, C., et al., *Adipogenesis and WNT signalling.* Trends Endocrinol Metab, 2009. **20**(1): p. 16-24.
49. Baksh, D., G.M. Boland, and R.S. Tuan, *Cross-talk between Wnt signaling pathways in human mesenchymal stem cells leads to functional antagonism during osteogenic differentiation.* J Cell Biochem, 2007. **101**(5): p. 1109-24.
50. Sethi, J.K. and A. Vidal-Puig, *Wnt signalling and the control of cellular metabolism.* Biochem J, 2010. **427**(1): p. 1-17.

Figures

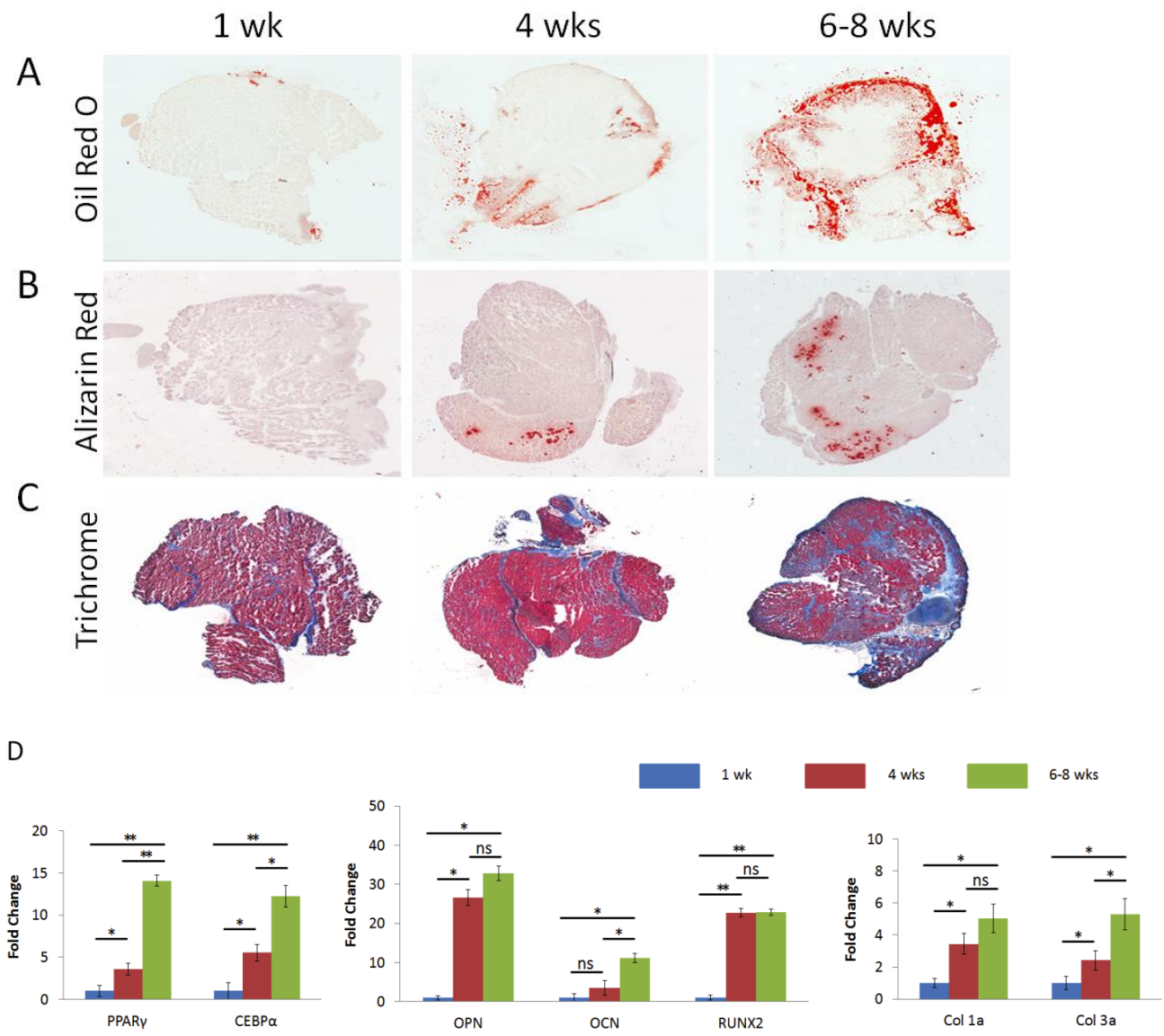

Figure 1. Severe skeletal muscle abnormalities, including lipid infiltration/accumulation, ectopic calcification, and fibrosis, were observed in old dKO mice. (A) Oil Red O stain revealed amounts of lipid droplets infiltrated/accumulated in gastrocnemius of 1-, 4-, 6wk old dKO mice. Severe lipid accumulation was observed in old dKO muscle (n>4). (B) Alizarin Red stain visualized calcium deposits in dKO muscle sections. More extensive calcium deposits were detected in old dKO muscle (n>4) (C) Trichrome stain was performed to identify fibrotic regions of the gastrocnemius of dKO mice. Increased fibrotic area was observed in old dKO muscle (n>4). (D) RNA was extracted from freshly collected muscle tissues of 1-, 4-, and 6-8wk old dKO mice and real RT-PCR was performed (n>4). Error bars indicate 'mean ± SD'. * p <0.005, ** p <0.0001.

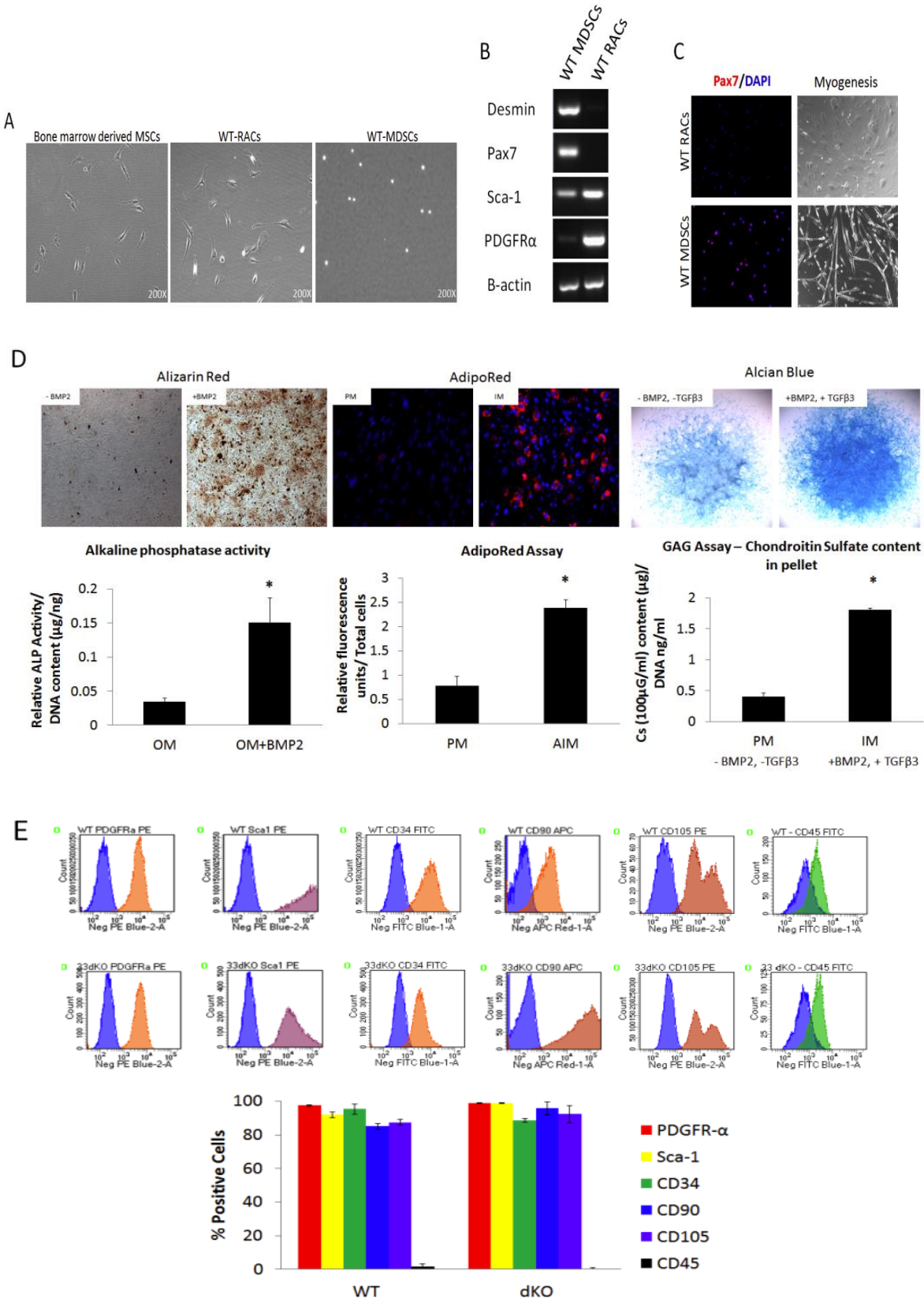
A
Bone marrow derived MSCs
WT-RACs
WT-MDSCs
200X
B
WT MDSCs
WT RACs
Desmin
Pax7
Sca-1
PDGFRα
B-actin
C
Pax7/DAPI
Myogenesis
WT RACs
WT MDSCs
D
Alizarin Red
- BMP2
+BMP2
AdipoRed
PM
IM
Alcian Blue
- BMP2, -TGFβ3
+BMP2, + TGFβ3
Alkaline phosphatase activity
Relative ALP Activity/ DNA content (µg/ng)
OM
OM+BMP2
AdipoRed Assay
Relative fluorescence units/ Total cells
PM
AIM
GAG Assay – Chondroitin Sulfate content in pellet
Cs (100µG/ml) content (µg)/ DNA ng/ml
PM
IM
- BMP2, -TGFβ3
+BMP2, + TGFβ3
E
WT PDGFRa PE
WT Sca1 PE
WT CD34 FITC
WT CD90 APC
WT CD105 PE
WT - CD45 FITC
33dKO PDGFRa PE
33dKO Sca1 PE
33dKO CD34 FITC
33dKO CD90 APC
33dKO CD105 PE
33 dKO - CD45 FITC
% Positive Cells
WT
dKO
PDGFR-α
Sca-1
CD34
CD90
CD105
CD45

Figure 2. Non-myogenic mesenchymal stem cells (nmMSCs) were isolated from age-matched WT and dKO mice, utilizing preplate technique. (A) Phase contrast microscopy images of bone marrow derived MSCs (left), WT-RACs (middle), and WT-MDSCs (right). (B) RT-PCR analysis of lineage markers in freshly isolated WT-MDSCs and WT-RACs. (C) Immunohistochemistry stain of Pax7 indicated that WT-RACs are Pax7 negative cells and are unable to differentiate into myotubes, while WT-MDSCs are Pax7 positive cells and are highly myogenic. (D) Tri-lineage differentiation capacities of WT-RACs were verified. WT-RACs were able to undergo osteogenic (left), adipogenic (middle), and chondrogenic (right) differentiation upon appropriate induction (n>4). Error bars indicate 'mean ± SD'. * p <0.005. (E) Freshly isolated WT- and dKO-RACs were analyzed for multiple mesenchymal stem cell markers, PDGFRα, CD90, and CD105, a hematopoietic stem cell marker, CD45 and FAPs markers, Sca-1 and CD34. No statistical significant differences were observed in percentage of marker expressions between WT and dKO cells (n=4). Error bars indicate 'mean ± SD'.

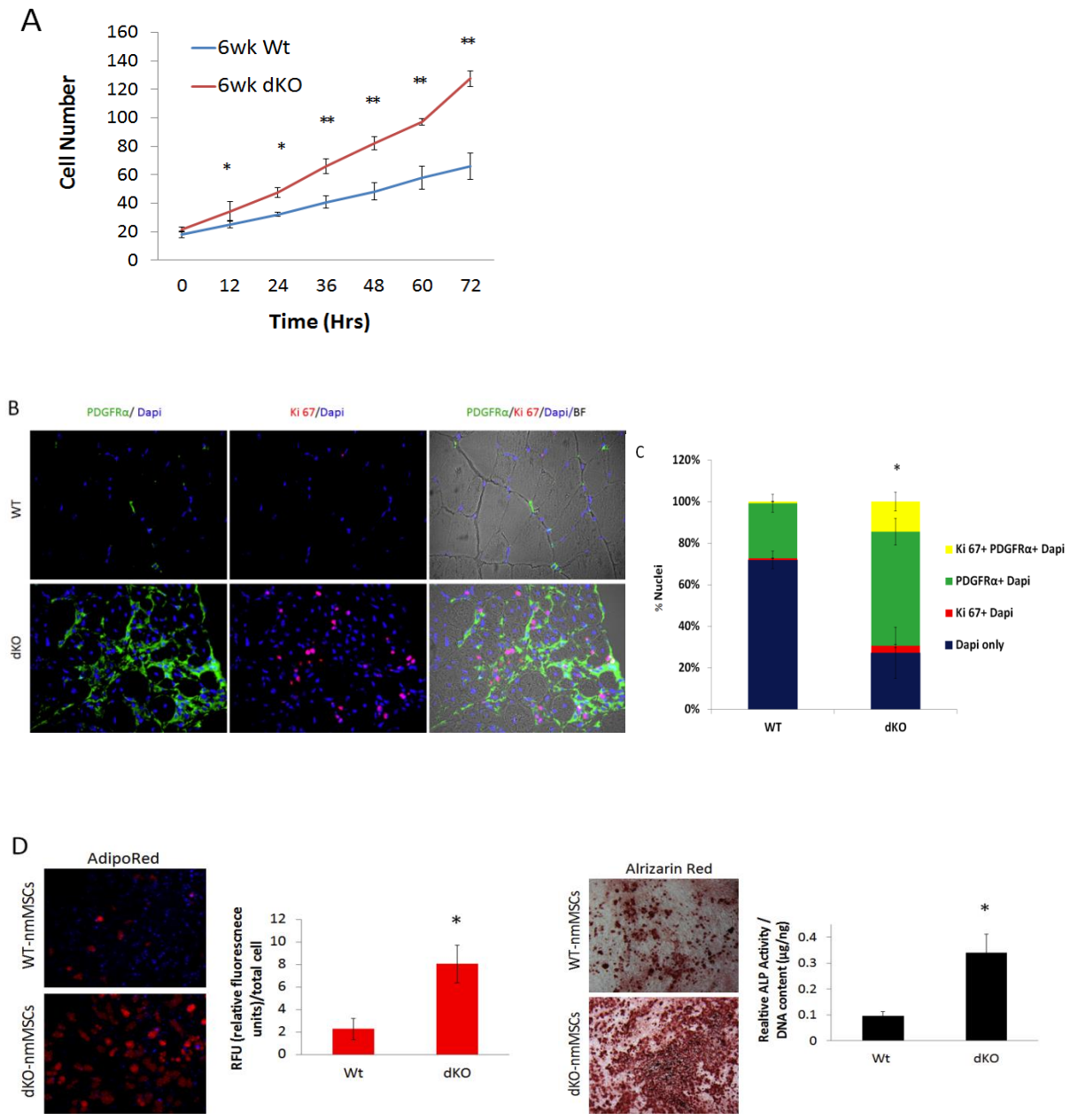

Figure 3. nmMSCs do not become progressively defective with the disease progression in dKO mice. (A) Comparison of cell proliferation rates of WT- and dKO-nmMSCs isolated from skeletal muscle of 6 wks old mice investigated using a live cell imaging system (n=4). Error bars indicate 'mean ± SD'. * $p < 0.005$, ** $p < 0.0001$. (B) Immunohistochemistry for PDGFRα (green) expression and Ki67 (Red) in the skeletal muscle of 6wks old WT and dKO mice. Immunofluorescent images were merged with bright field images (n=4).. (C) Quantification indicating percentage of cells that were expressing PDGFRα only, PDGFRα and Ki67, Ki67 only, and dapi only. Error bars indicate 'mean ± SD'. * $p < 0.005$ (D) Comparison of adipogenic (left) and osteogenic (right) differentiation potentials of WT- and dKO-nmMSCs isolated from 6 wks old mice (n=4). Error bars indicate 'mean ± SD'. * $p < 0.005$.

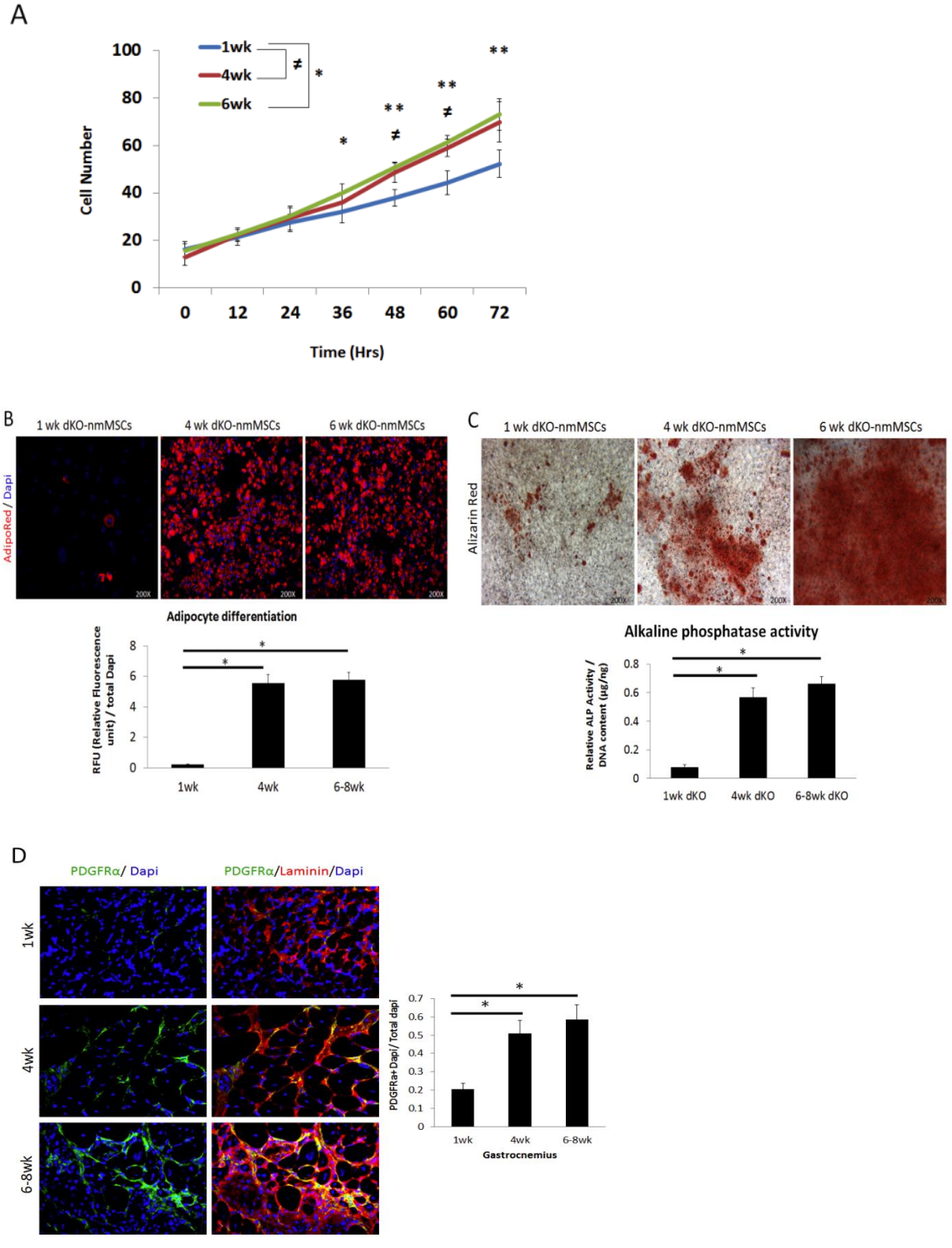
A
1wk
4wk
6wk
Cell Number
Time (Hrs)
B
1 wk dKO-nmMSCs
4 wk dKO-nmMSCs
6 wk dKO-nmMSCs
AdipoRed / Dapi
Adipocyte differentiation
RFU (Relative Fluorescence unit) / total Dapi
1wk
4wk
6-8wk
C
1 wk dKO-nmMSCs
4 wk dKO-nmMSCs
6 wk dKO-nmMSCs
Alizarin Red
Alkaline phosphatase activity
Relative ALP Activity / DNA content (μg/ng)
1wk dKO
4wk dKO
6-8wk dKO
D
PDGFRα/ Dapi
PDGFRα/Laminin/Dapi
1wk
4wk
6-8wk
PDGFRa+ Dapi/ Total dapi
Gastrocnemius

Figure 4. Proliferation and differentiation potentials of dKO-nmMSCs are progressively activated as disease progress. (A) Comparison of proliferation rates of nmMSCs isolated from 1-, 4-, 6 wk old dKO mice (n=4). Error bars indicate 'mean ± SD'. * $p < 0.005$, ** $p < 0.0001$, ≠ < 0.005. (B) Adipogenic differentiation potentials of dKO-nmMSCs from different aged mice were compared. AdipoRed staining was performed for detection of lipid accumulation in the cells (n>3). Error bars indicate 'mean ± SD'. * $p < 0.005$. (C) Osteogenic differentiation potentials of dKO-nmMSCs from different aged mice were compared. Alizarin Red staining was performed for detection of calcium deposits formation (n>3). Error bars indicate 'mean ± SD'. * $p < 0.005$. (D) Immunohistochemistry for PDGFRα expression (green) and laminin (Red) in the skeletal muscle of 1-, 4-, 6wk old dKO mice (n=4). Error bars indicate 'mean ± SD'. * $p < 0.005$.

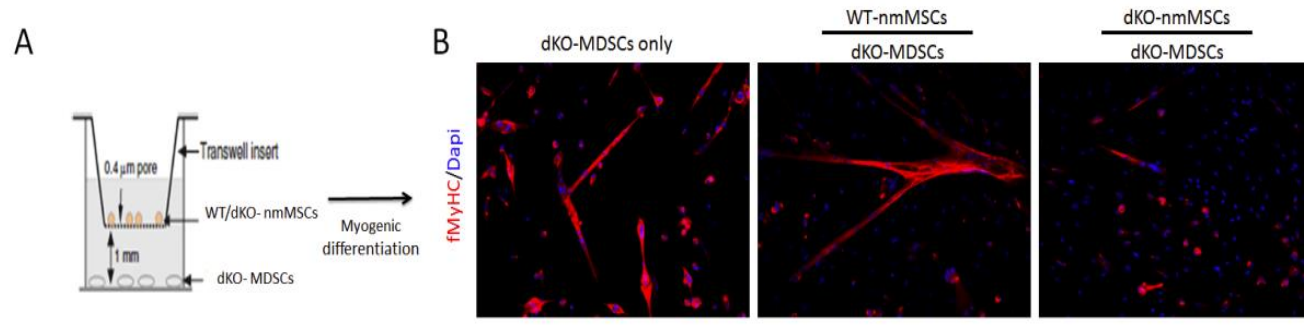
A
0.4 μm pore
Transwell insert
WT/dKO- nmMSCs
1 mm
dKO- MDSCs
Myogenic differentiation
B
dKO-MDSCs only
WT-nmMSCs
dKO-MDSCs
dKO-nmMSCs
dKO-MDSCs
fMyHC/Dapi

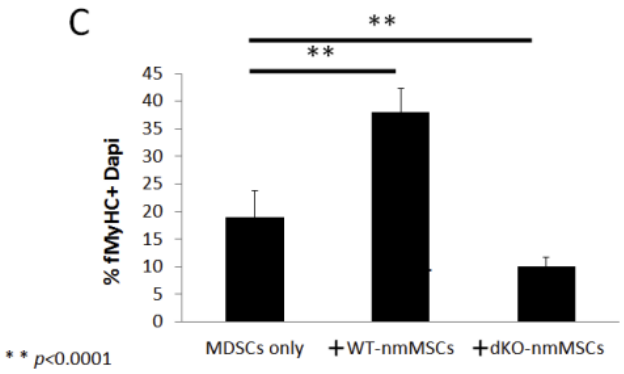
C
**
**
% fMyHC+ Dapi
MDSCs only
+WT-nmMSCs
+dKO-nmMSCs
* * p<0.0001

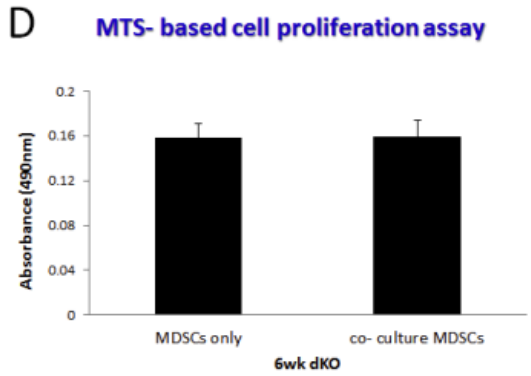
D
MTS- based cell proliferation assay
Absorbance (490nm)
MDSCs only
co- culture MDSCs
6wk dKO

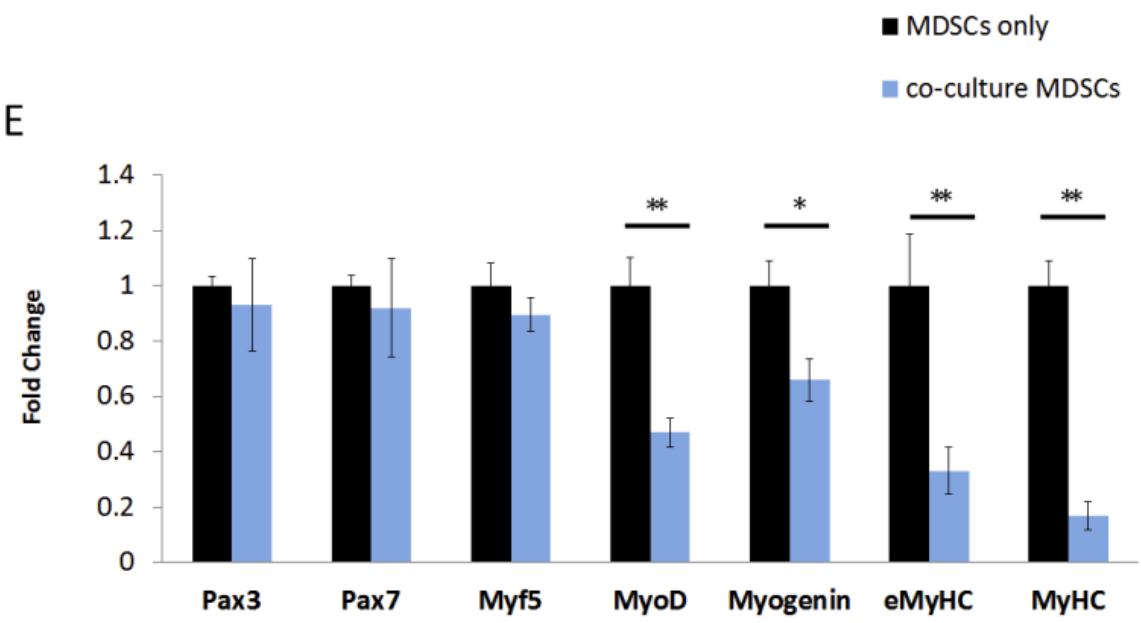
E
MDSCs only
co-culture MDSCs
Fold Change
Pax3
Pax7
Myf5
MyoD
Myogenin
eMyHC
MyHC

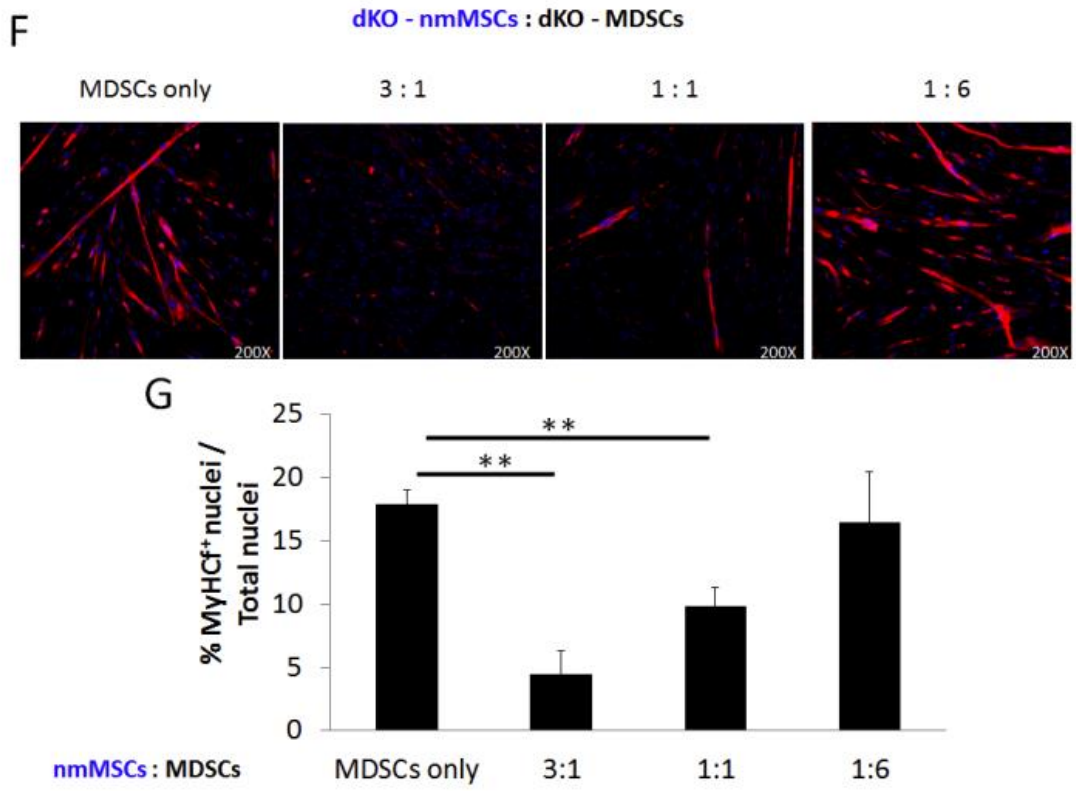

Figure 5. Limited myogenic potential of 6wk old dKO-MDSCs was further exacerbated by co-culturing them with 6wk old dKO-nmMSCs. (A) WT- or dKO-nmMSCs were co-cultivated with dKO-MDSCs using collagen type I coated transwell insert for myogenic differentiation. (B) Immunohistochemistry of fMyHC was performed for detection of myotube formation. Dapi was used for counterstaining. (C) Quantification of percentage myotube formation of dKO-MDSCs after 3 days of myogenic differentiation with/without nmMSCs co-cultivation (n>4). Error bars indicate 'mean ± SD'. ** $p < 0.0001$. (D) MTS-based cell proliferation assay of dKO-MDSCs during first 48 hours of co-cultivation with/without dKO-nmMSCs. (E) Real time RT-PCR analysis was performed and the myogenic gene expression was compared from dKO-MDSCs co-cultivated with/without dKO-nmMSCs (n>4). Error bars indicate 'mean ± SD'. * $p < 0.005$, ** $p < 0.0001$. (F) Co-culture myogenic differentiation experiments were done using 3:1, 1:1 and 1:6 ratios of dKO-nmMSCs to dKO-MDSCs. (G) Quantification of percentage myotube formation of dKO-MDSCs after 3 days of myogenic differentiation with 3:1, 1:1 and 1:6 ratios of dKO-nmMSCs to dKO-MDSCs co-cultivation (n=3). Error bars indicate 'mean ± SD'. ** $p < 0.0001$.

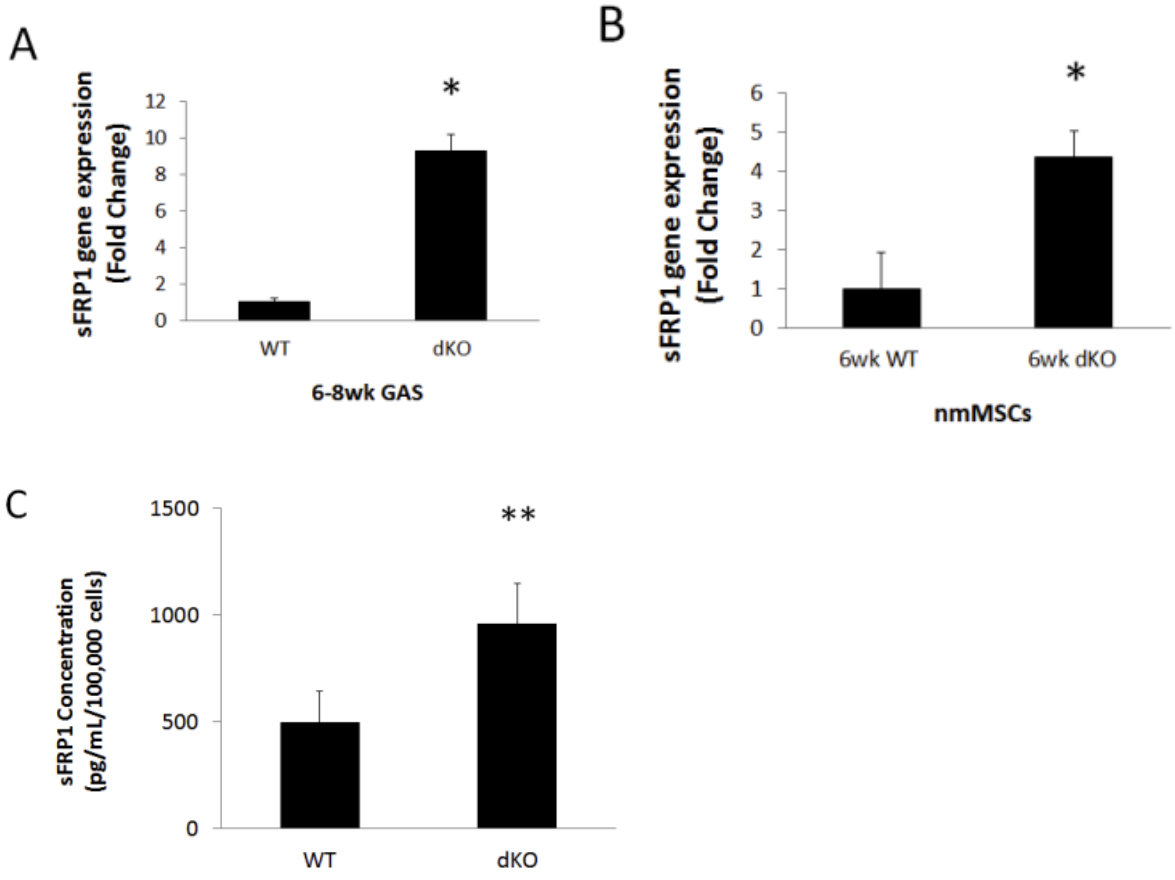

Figure 6. Higher sFRP1 expression in dKO skeletal muscle and dKO-nmMSCs. RNA was extracted from frozen muscle tissue and real time RT-PCR was performed. Higher sFRP1 gene expression was observed from (A) dKO-GAS compared to age-matched WT-GAS (n>4) and (B) 6wk old dKO-nmMSCs compared to age-matched WT-nmMSCs (n>4). Error bars indicate 'mean ± SD'. * $p < 0.005$. (C) Concentration of secreted sFRP1 from WT- or dKO-nmMSCs was measured with mouse sFRP1 ELISA kit. The graph represents sFRP1 concentration per every 100,000 WT- or dKO-nmMSCs (n=6). Error bars indicate 'mean ± SD'. * $p < 0.005$

Sexual dimorphism in skeletal muscle and muscle stem cells

Jihee Sohn and Johnny Huard

Abstract

Musculoskeletal health is one of the areas of medicine in which the differences between males and females are most striking. Differences in injury mechanism, pain sensation, drug handling, and healing response have known biologic bases; however, how these biologic processes are affected by sex is not yet clear. In skeletal muscle, stem and progenitor cells are known to persist throughout life and contribute to repair and regeneration. Therefore, understanding sexual dimorphism and sex related differences in skeletal muscle and muscle stem cells will greatly enhance our knowledge about the differences that exist between males and females in regard to muscle diseases and healing. Currently, literature describing sex-related differences in satellite cells and other muscle stem cells is scarce and sexual dimorphism is an under-investigated variable in cell therapy approaches for regenerative medicine. In this review, we provide a discussion about sexual dimorphism in skeletal muscle stem cells and regeneration. Significant efforts to prioritize research to include sexual dimorphism in stem and progenitor cells could be imperative to improving patient care and healthcare delivery approaches as it relates to regenerative medicine.

Introduction

Stem cell therapy for muscle disease has been extensively investigated by many research groups in the context of muscular dystrophy, a muscle disease characterized by continuous muscle weakness and degeneration due to the lack of functional dystrophin at the sarcolemma of muscle fibers [1]. Skeletal muscle is favorable to cell transplantation since the mode of muscle repair and fiber formation is via the fusion of mononuclear cells, and transplanted donor stem cells can participate in this process [2]. In addition, applications of stem cell technology can simultaneously aid in reducing inflammation, which may slow the progress of the disease and increase the survival of the transplanted donor cells [3]. In 1989, Partridge et al. first showed that myoblast transplantation could give rise to dystrophin-expressing myofibers in *mdx* mice, a murine model of Duchenne muscular dystrophy (DMD) [4]. This led to several clinical trials in the 1990s where researchers transplanted normal muscle cells into DMD patients, and recently a Phase I clinical trial has been completed [5-11]. These important studies showed that cell transplantation into dystrophin-deficient muscle resulted in dystrophin delivery and that cell therapy may be a viable option for other skeletal muscle disorders that have no attractive therapeutic choices. According to clinicaltrials.gov, there are currently 3198 federally approved clinical trials using stem cells, and thousands of research articles published exploring the identification, characterization and therapeutic applications of stem cells. However, with each research group attempting to find a "better" cell for tissue regeneration, sex-related differences in stem cells are a rarely examined variable. Our previous finding that female stem cells have higher muscle regeneration capacity compared to male stem cells urged us to review the sexual dimorphism of skeletal muscle cells and skeletal muscle. Our striking results emphasize the necessity of controlling of differentiation and identifying sex-based differences and individual stem cell differences for the safe and efficacious use of stem cells for the development of personalized medicine approaches.

In this review, we discuss sex-related differences in skeletal muscle regeneration. We describe sexual differences in skeletal muscle structure, and review currently available articles that demonstrate sex-related differences in satellite cells and other muscle stem cells. Finally, we discuss the role of host sex in the *in vivo* microenvironment and sexual dimorphism in determining how skeletal muscle responds to stress and the role that sex hormones play in response to skeletal muscle damage and oxidative stress.

Recently, Nakada et al. showed that mouse haematopoietic stem cells (HSCs) exhibit sex differences in cell cycle regulation by estrogen, suggesting that other stem cell types exhibit sex-related differences as well [12]. Better understanding of potential innate cellular sex differences in stem and progenitor cells will greatly influence the way stem cells are utilized in biomedical research as well as in regenerative medicine for the treatment of musculoskeletal diseases.

Sexual dimorphism and sex differences in aging and disease

Sex refers to the intrinsic characteristics that distinguish males from females, and is known to influence birth survival, life expectancy, and response to disease in many species, including *Homo sapiens*. Sexual dimorphism is most evident as differences in body size and composition. Most adult mammals exhibit physiologic and morphologic differences, with males generally being larger and having shorter life expectances [13, 14]. According to the 2010 U.S. Census, of 308.7 million people in the United States, 157 million were female (50.8%) and 151.8 million were males (49.2%). Life expectancy for a woman is currently 81.2 years, while life expectancy for men is 75.9 years; however, the human life expectancy at birth for women (80 years) in more developed countries is nearly 8 years longer than that of men (72 years) [15]. Studies also have shown distinct sexual dimorphism in the incidence, disease presentation, and progression of arthritic, autoimmune, cardiovascular, and central nervous system diseases – e.g. systemic lupus erythematosus (SLE), thyroid disease, and multiple sclerosis (MS) have an increased incidence and prevalence in females [16, 17], while end-stage renal disease, coronary heart disease, and Parkinson's disease predominantly affect males [18-20]. More interestingly, sexual dimorphism can be observed from differences in age of disease onset as well; for instance, males in their 40s are more susceptible to stroke than females; however, after the age of 80, women have a higher incidence of stroke [21]. Despite the obvious relevance of these sex differences in human, studies reflecting the differences between men and women at the cellular and molecular levels, have only recently been reported.

Sexual dimorphism in skeletal muscle

A. Skeletal muscle mass and muscle development

In many animal groups, sexual size dimorphism is widespread and tends to be more pronounced in species with large body size. Generally in mammals and birds, males are larger [22, 23], probably due to sexual selection through male-male competition within groups [24]. Humans show significant average sex differences in body size; however, unlike in many animal species, humans also show significant average sex differences in body composition of muscle mass, fat mass, and bone mineral mass. Sexual dimorphism in human body composition is evident from fetal life, with males possessing a similar fat mass to females but are larger and have greater muscle mass; however, with the onset of puberty, females undergo a rapid transition and cease to continue to grow at a younger age than males. During adolescence, girls gain considerable amounts of fat but relatively little muscle, and boys present with the opposite strategy. After puberty, adult males have greater arm muscle mass, larger and stronger bones, and reduced limb and central abdominal fat. Females generally have more peripheral fat in early adulthood; however, greater parity and menopause induce more android fat distribution with increasing age [25]. In general, male muscles generate faster and have a higher maximum power output than female muscles; however, women have the advantage of recovering faster from muscle injury and being more fatigue-resistant than men [26]. Estrogen-B and testosterone seem to play important roles in the differential capacities of muscle-building and producing efficient power between men and women and will be explored in detail later.

B. Skeletal muscle structure and fiber composition

Although the literature that describes sex-related differences in muscle fiber cross-sectional area (CSA) in animal models is surprisingly scarce [27, 28], several studies have reported sex differences in skeletal muscle CSA in humans. Recent development of technologies such as ultrasonography, computerized tomography (CT) and magnetic resonance imaging (MRI) have made possible the measurement of CSA of both fat and muscle tissues in intact healthy individuals [29-31]. Utilizing the latter techniques, several studies indicated that men generally have larger and stronger muscles of both upper and lower limbs than women and those differences tend to be more pronounced in muscles of the upper limbs. Although comparisons among studies are complicated by the fact that there are a number of different muscle groups that are studied, some studies clearly showed that in general, muscle CSA is smaller in women compared with men in the biceps branchii (BB) [32, 33], gastrocnemius (GAS) [34], sartorius [30], vastus lateralis (VL) [32, 35], and multifidius [36]. For example, Kanehis et al. [30] examined the CSA of sartorius by ultrasound on the thigh from untrained men (n=27) and women (n=26) aged 18-25 years and found that the mean CSA of men was 63.2% larger than that of women. In addition, Miller et al. [32] compared muscle characteristics of BB and VL from eight men and women and reported that the men had 67% and 65% larger mean muscle CSA for the BB and VL, respectively. Finally, Abe et al. [31] investigated sex differences in whole body skeletal muscle mass in 10 female and 10 male college students in Japan using MRI and found that men had a greater skeletal muscle CSA at the shoulder, chest, and lower gluteus regions compared with women. Other studies on sex differences in skeletal muscle CSAs of physically trained athletes also reported similar results, showing men had larger muscle CSA than women [34, 35] after training. Costill et al. [34] and Alway et al. [37] demonstrated that male athletes have larger fiber CSA in GAS and BB muscles, respectively compared to female athletes.

Sexual dimorphism in muscle tissue can exist in muscle fiber composition as well. The skeletal muscle contains two types of muscle fibers: fast-twitch and slow-twitch, and muscle fiber type reflects the myoglobin and mitochondrial content, its expression of a specific myosin heavy chain isoform, and its glycolytic and oxidative capacities. The fast-twitch and slow-twitch muscle fibers are composed of three distinct types. Slow-twitch fibers contain type I muscle fibers, while the fast twitch fibers contain both Type IIa and Type IIb. The percentage of each muscle fiber differs among individuals, between males and females and from one muscle to another in the same individual [38]. Type I muscle fibers are slow-twitch fibers, which have high oxidative, low glycolytic capacities, a very low force output, and are highly resistant to fatigue and utilize the aerobic pathway; these fibers are designated by their expression of the myosin heavy chain (MHC) type I isoform. Type I fibers are dominantly used in prolonged low-intensity exercise such as Marathoning and once the exercise intensity is increased, Type 2 fibers will gradually be recruited. Type IIa muscle fibers are intermediate fast twitch fibers and produce high force output for longer periods of time, meaning Type IIa fibers can use both the aerobic and anaerobic pathways. Type IIb muscle fibers are fast twitch fibers and have low oxidative capacities, strictly utilize the anaerobic pathway, have high glycolotyic capacities, are prone to fatigue, and express the MHC type II isoform. Type IIb fibers are recruited for activities involving very short-duration with high-intensity burst of power such as sprints or near-maximal lifts [39-41]. Different muscles have different muscle fiber compositions, and sex-related muscle differences vary with each particular muscle. For example,

Brook et al. showed that men have a larger percentage of type II fibers compared to women, who have more type I fibers in the BB, which is why men are stronger and women are more fatigue-resistant. On the other hand, women (0.9) have higher a Type I to Type II fiber ratio compared with men (0.6) [33]. In addition, Simoneau et al. reported that in VL, females (51%) have a higher percentage of type I fibers than males (46%), while males have higher Type IIa (39%) and IIb (15%) fibers than females (37% and 12%, respectively) when they compared 203 females and 215 males [35]. A greater ratio of Type I/Type II fibers in the BB [32] and VL [32, 33] in females compared with males has been shown by many other studies. However, some studies, including Costill et al. reported reverse findings, showing higher a Type I/Type II ratio in GAS of men [34] while other reports have found no sex-related differences in muscle fiber types [32, 40], clearly showing that there is a need for additional research in this area.

Sex differences have been described for physiologic differences in response to physical exercise or aging. A number of studies show that men and women generally respond the same way to training; however, women are more fatigue-resistant and consistently demonstrate greater endurance compared with men [42-44]. For examples, studies comparing sustained submaximal contractions of the knee extensors, elbow flexors, handgrip muscles, and adductor pollicis muscle performance, significantly slower muscle fatigue and faster recovery in women compared to men have reported [43-45]. In addition, sex differences in skeletal muscle strength and function have been reported. According to Glenmark et al. since men have more skeletal muscle mass compared to women, men tend to generate a larger force and power output faster than women [26]; however, once total whole muscle CSA is accounted for the analysis, many studies find no sex differences in force generation [26, 46]. Aging is generally associated with muscle mass loss and decline in the number of precursor satellite cells. Some studies regarding the skeletal muscle fiber quality in older men and women have reported that larger areas of slow-twitch fibers are observed in older women and fast-twitch fibers represent a larger area in older men; however, a number of other studies have shown that there is no difference in the muscle fiber composition of older men and women [46, 47]. In addition, Phillips et al. show that muscle weakness in women occurs at an earlier age than in men due to age-related changes in estrogen levels [48].

Understanding sexual dimorphism in skeletal muscle development and structure is not sufficient to explain how these biologic processes are affected by differences in men and women. An important question is whether the muscle stem cells also exhibit sex differences in physiological function and muscle mass and structure? In adult skeletal muscle, the satellite cells are responsible for the growth and maintenance of skeletal muscle [49, 50]. Recently, many studies have reported that in addition to satellite cells, a variety of other stem and progenitor cells residing in the interstitial spaces may be derived from the vasculature could be potential alternative cells sources for muscle repair [50-52]. Next, we will review current literature describing sex-related differences in these stem and progenitor cells and examine their contribution to skeletal muscle growth and regeneration.

Sexual dimorphism in muscle stem cells

To date, only a few studies have investigated the influence of sex-related differences in tissue or organ regeneration with stem or progenitor cells. Blankenhorn et al. reported that sex plays a significant role in the closure of wounded tissue in autoimmune mice, showing regrowth of hair follicles, sebaceous

glands, and cartilage in female mice is faster and more complete than male mice [53]. Another study shows that female mice exhibit more efficient liver regeneration than their male counterparts [54], while another group reported that male rats show significantly more tissue growth than female rats after nephroctomy [55]. Clinical trials done in recent years demonstrate that stem cells isolated from various sources have shown improved outcomes as compared to committed cells [56-60]. In particular, stem cell therapy for muscle disorders has been extensively investigated; however, understanding the developmental origins of muscle stem cells, the regulation of the mechanisms of differentiation and identifying optimal cell populations for skeletal muscle regeneration are crucial. Muscle stem cells in cell therapeutics or tissue engineering strategies require control of differentiation and identification of sex-based differences for the safe use of stem cells; however, sex-related differences in muscle stem cells has only recently been reported to play a role in cell therapy studies for skeletal muscle regeneration.

A. Satellite cells

From the time of their initial description in 1961, satellite cells, located between the sarcolemma and basal lamina of the muscle fiber, are responsible for the maintenance and regeneration of the adult skeletal muscle [61]. Satellite cells are considered to be mitotically quiescent; however, upon activation, satellite cells will migrate, rapidly undergo extensive proliferation, differentiate into myoblasts, and finally fuse with existing muscle fibers to form new multinucleated myofibers [62, 63]. Cell surface markers associated with satellite cells include M-cadherin, Pax7, Myf5, neural cell adhesion molecule-1 (NCAM), CD34, and Pax3 and Pax7 transcription factors, which are known to play essential roles in the early specification, migration, and myogenic differentiation of satellite cells [50, 64, 65]. Myoblasts, which are activated satellite cells, have been described as multipotent cells, but are mainly committed to the myogenic lineage [66] and have been examined as candidates for cell therapy for treating muscular dystrophies and other skeletal muscle disorders [4, 59, 67, 68].

There are a few studies that have examined sexual dimorphism in human satellite cells. Roth et al. assessed satellite cell populations in VL biopsies obtained from healthy men and women and found that the frequency of satellite cells in male muscle (2.8% ± 0.5%) was slightly higher than that in female muscle (1.7% ± 0.6%), although women demonstrated significantly larger satellite cell and satellite cell nucleus areas than men [69]. On the other hand, in another study done by Kadi et al., they found no significant difference in the number of satellite cells per muscle fiber from the TA muscles of young and elderly women and men, although they observed significantly more myonuclei per muscle fiber in both young and elderly men compared to that in young and elderly women [70]. Similarly, Petrella et al. reported no sex-related differences in the percentage of CD56/NCAM$^+$ satellite cells per 100 myofibers in VL muscles of young and old men and women, before and after training [71]. Lastly, a study was performed to determine if the sex of the cell influences human myoblast cell yield, proliferation, and differentiation rates, and Bonavaud et al. found that the sex of donor did not influence muscle culture parameters and also observed no significant differences in the number of cells isolated per gram of male and female biopsied tensor fasciae muscle tissues [72].

In a study done by Salimena et al., GAS muscle from male and female 6 week old C57BL/10J mice were used to investigate if sexual dimorphism influenced the regenerative capacities and numbers of

myogenic progenitors. They reported that both male and female mice showed similar expression levels of stem cell antigen-1 (Sca-1) and the satellite cell marker (NCAM). Interestingly, they observed increased numbers of activated myoblasts (NCAM expressing cells) in the GAS of female *mdx* mice compared to that of male mice [73]. In contrast, a more recent study on sex-related differences in satellite cells in developing and adult mouse muscle demonstrated that the satellite cell numbers are increased in growing, compared to adult mice, and in male compared to female adult mice. But they observed no difference in engraftment efficiency between male and female donor cells or between male and female host muscle environments [74]. Niel et al. isolated satellite cells from the levator ani (LA) muscle of rats and found a greater number of satellite cells in the male compared to female muscles [75].

Two groups have studied sex-related differences of satellite cells isolated from turkeys. Velleman et al. investigated the effects of gender-related differences on proliferation and differentiation of satellite cells isolated from the pectoralis major (PM) muscle of turkeys and reported that compared to female myoblasts, the male cells showed increased differentiation potential as measured by creatine kinase, myotube length, and the percentage of multinucleated myotubes formed in culture [76]. Contrary to this study, Doumit et al. reported that fusion percentages of female and male myogenic satellite cells isolated from the PM and latissimus dorsi (ALD) muscles showed no differences in culture [77]; however, no further studies on turkey cell lines have confirmed either set of results. To summarize, very little literature is available to understand sex-related differences in satellite cells and myoblasts, although currently available studies suggest that differences may not exist.

B. Muscle-derived stem cells (MDSCs) and non-myogenic mesenchymal stem cells (nmMSCs) isolated by the preplate technique

Our research group has isolated several populations of muscle derived cells from skeletal muscle utilizing a previously published preplate technique [57, 78]. Two distinct fractions of cells can be identified: 1) A slow adhering fraction of cells that are highly myogenic called muscle derived stem cells (MDSCs) with stem cell-like characteristics, including multi-lineage differentiation and self-renewal [57, 78, 79] . 2) A rapidly adhering fraction of cells that are non-myogenic and expressed a variety of mesenchymal stem cell (MSC) markers, called non-myogenic mesenchymal stem cells (nmMSCs). Evidence already exists that human MDSCs have the potential for clinical use, since they are currently undergoing clinical trials for the treatment of urinary incontinence [80] and new findings and ongoing work have shown that human MDSCs contribute to the repair of skeletal muscle and cardiac tissue [79]. Therefore, it is important to determine how sex-differences may affect their behavior in order to optimize their successful use for regenerative medicine approaches.

i) Muscle derived stem cells (MDSCs)

The MDSCs are characterized by slow cycling, long term self-renewing cells, as MDSCs can divide for more than 30 passages in proliferation medium with an average division time of 15.1hours. MDSCs express both stem (Sca-1, CD34), myogenic (desmin, MyoD), and endothelial (CD31, CD144) cell surface markers, distinguishing them from satellite cells [78, 81]. It was previously reported that when

compared to committed muscle precursor cells (myoblast), MDSCs demonstrated a higher intramuscular engraftment capability in both skeletal and cardiac muscle [32, 82]. The exact mechanism involved in the improved regenerative potential of MDSCs remains unclear; however, current evidence from animal studies suggests that their elevated resistance to stress is critical [30, 83, 84] as well as their release of soluble factors such as vascular endothelial growth factor (VEGF) [33, 35, 85, 86]. More importantly, our group recently found that cell sex, a rarely considered variable, has a significant effect on *in vivo* outcome of cell transplantation of MDSCs into diseased muscle. We previously reported that the transplantation of MDSCs into diseased skeletal muscle of *mdx* mice, which is a mouse model of DMD, results in a large number of regenerated myofibers [57, 79]. More recently, our group reported that female MDSCs (F-MDSCs) regenerate skeletal muscle more efficiently that male MDSCs (M-MDSCs). We examined 25 populations of male and female MDSCs and observed that M- and F-MDSCs demonstrated similar *in vitro* stem cell characteristics, including similar morphologies, multilineage differentiation potentials, long and short term proliferation kinetics, and marker profiles. However, in a side by side comparison study, we reported that the transplantation of F-MDSCs resulted in significantly better skeletal muscle regeneration in the skeletal muscle of *mdx* mice, as determined by calculating each population's mean regeneration index, RI (the ratio of dystrophin$^+$ fibers per 10^5 donor cells implanted). Implanted F-MDSCs regenerated about twice as many dystrophin$^+$ myofibers (n=15 F-MDSCs; 2-6 muscles per population; RI=230±52) than the implanted M-MDSCs (n=10 M-MDSCs; 2-6 muscles per population; RI=95±20). In addition, after transplantation into the skeletal muscle of dystrophic mice, F-MDSCs transplanted into a host of either sex consistently regenerated more dystrophin$^+$ myofibers than did the M-MDSCs transplanted into hosts of either sex. We further reported that a higher immune response at the site of cell delivery after sex-crossed transplantations was observed compared to sex-matched transplantations by measuring the total CSA of CD4 expression [87].

Finally, this study suggested that differential myogenic differentiation potentials response to cell oxidative stress and reactive oxygen species (ROS) were responsible for the *in vivo* sex-related differences at the skeletal muscle delivery site. Following cell transplantation, inflammatory cytokines released at the delivery site can contribute to increases in the presence of ROS, which are small free radicals such as hydrogen peroxide (H_2O_2) that cause oxidative damage of DNA, RNA, proteins and lipids due to reactive unpaired electrons [88, 89]. Previously, Piao et al. described that ROS may also function as secondary messengers in muscle differentiation, and in particular H_2O_2 has been proposed as the most likely ROS that would function physiologically as a secondary messenger [90]. Interestingly, we previously reported that M-MDSCs, but not F-MDSCs, respond to H_2O_2-induced oxidative stress by increasing myogenic markers, including desmin and myogenic differentiation determined by increased MHC expression [36]. F-MDSCs appeared to respond to cell stress by maintaining a low level of proliferation, whereas M-MDSCs showed increased myogenic differentiation under low oxygen or oxidative stress [87]. It may be possible that the increased myogenic differentiation of M-MDSCs under cell stressful conditions could result in the rapid depletion of the transplanted M-MDSCs as cells undergo transient expansion followed by differentiation and fusion to form mature myofibers. On the other hand, F-MDSCs may remain quiescent post-transplantation until acute inflammation subsides, and then undergo cell proliferation. The tendency of F-MDSCs to maintain an undifferentiated phenotype during early time points post transplantation allows more cells available for expansion and

differentiation at later time points, resulting in better long term muscle regeneration. Another possible explanation for the differential myogenic differentiation capacities between the F- and M-MDSCs could be due to differences in glutathione (GSH) expression in the cells. According to Ardite et al., depletion of GSH, a thiol mediator of free radicals can significantly impair myogenic differentiation of C2C12 cells mediated through NFkB activation [91]. Interestingly, we have found strikingly higher levels of GSH in M-MDSCs compared to F-MDSCs [87], which may explain the greater propensity for male cells to undergo myogenesis. The underlying mechanism of GSH signaling during myogenic differentiation is still not well understood, and particularly, sex-related differences in this signaling pathway need to be investigated.

Other than myogenic differentiation potential, a few studies provide a comparison of sex-related differences in osteogenic and chondrogenic potentials of the MDSCs. Adipogenic and osteogenic potentials of the MDSCs have been reported by Sarig et al. [58] and Lee et al. [60]; however, neither study discusses anything about sex-related differences. Our previous study on the influence of sex on MDSCs in cardiac repair demonstrated that donor MDSCs or the recipient's sex had no significant effect on the efficiency of MDSC-triggered myocardial engraftment or regeneration [92]. Lastly, we showed that MDSCs exhibited sex-based differences for bone and cartilage repair, with M-MDSCs demonstrating superior osteogenic potentials both *in vitro* and *in vivo* [93] and higher chondrogenic differentiation capacities in a micromass culture system *in vitro* and were better at repairing osteochondral defects created in the calvarium of mice [94].

ii) Non-myogenic mesenchymal stem cells (nmMSCs)

Recently, several publications have identified non-myogenic muscle stem/progenitor cells in the skeletal muscle of both mice and humans that highly express the mesenchymal stem cell marker PDGFRα [95-97] . It has reported that, of the muscle-derived cell populations, only PDGFRα^+ cells display efficient *in vitro* and *in vivo* adipogenic differentiation potentials, and can participate in ectopic adipoctye formation when transplanted into fatty degenerating muscle [95]. Although adult skeletal muscle possesses remarkable regeneration ability in several pathological conditions; where there is a loss of muscle cells without efficient regeneration, ectopic adipocytes accumulate in fascicles. For example, in DMD, one of the most common childhood muscular dystrophies with an incidence rate of approximately one in 3500 live male birth, a striking accumulation of fat cells is observed. Dystrophic muscle is characterized with lack of functional dystrophin and therefore, muscle fibers are damaged during muscle contraction. Damaged muscle fibers degenerate and the satellite cells are recruited to regenerate new muscle fibers; however, this regeneration is inefficient and successive rounds of degeneration leads to the gradual replacement of muscle with connective tissue and fatty deposits [98-101]. Uezumi et al. showed that PDGFRα^+ cells are the major contributor to ectopic fat cell and/or collagen type-I-producing cells, which contribute to the formation of fibrosis, observed in the diseased skeletal muscle of *mdx* mice. They suggested that interactions between muscle stem and PDGFRα^+ cells are important in maintaining muscle homeostasis [95, 96]. Another group also identified cells with high adipogenic potentials that expression Sca-1 and CD34 cell surface markers and refer them as fibro/adipogenic porgenitors (FAPs), since they have the potential to differentiate into both adipocytes and fibroblasts *in vivo* [102]. Finally, Wosczyna et al. demonstrated that Tie2$^+$PDGFRa$^+$Sca-1$^+$ muscle resident progenitor cells exhibit robust BMP-dependent osteogenic potentials and are major

contributors to heterotopic ossification in skeletal muscle under pathological conditions [103]. All three cell types seem to represent the same cell population both functionally and phenotypically because the PDGFRα$^+$ cells also express Sca-1 and Tie2 [95] and FAPs express PDGFRα [102]. Furthermore, the role of PDGFRα$^+$ cells in muscle regeneration was illustrated by Joe et al. where they showed that muscle injury activates muscle resident PDGFRα$^+$ cells /FAPs that facilitate satellite cell-dependent myogenesis in co-culture experiments [102]. A recent study done by Mozzetta et al. also demonstrated that FAPs can mediate the ability of histone deacetylase (HDAC) inhibitors to promote muscle regeneration and young *mdx* FAPs promote satellite cell-mediated regeneration of myotubes in *mdx* mice [104]. Knowing that non-myogenic PDGFRα$^+$ cells are the major contributors of fat infiltration, fibrosis, and heterotopic ossification in the pathogenesis of the skeletal muscle, and because they play a pivotal role in muscle regeneration through the regulation of satellite cell differentiation potential, understating the nature of PDGFRα$^+$ cells will provide new insights into therapeutic strategies to treat muscle diseases. However, none of the above studies or any literature to date, has discussed sex-related differences in non-myogeic PDGFRα$^+$ mesenchymal stem/progenitor cells. In the studies done thus far, the sex of the donor cells is unknown and the role of host sex has not been examined. There is an urgent need for more studies investigating sex-related differences in adipogenic, osteogenic, and fibrogenic potentials of non-myogenic PDGFRα$^+$ cells, both in *in vitro* and *in vivo,* and their developmental potentials in sex-matched and sex-crossed host.

Previous studies and ongoing work in our lab provide the perception of sex-related differences in non-myogenic mesenchymal stem/progenitor cells. Utilizing the preplate technique, we isolated non-myogenic mesenchymal stem cells (nmMSCs) that adhere within minutes to two hours of isolation and express multiple mesenchymal stem cell markers and demonstrate functional characteristics of multipotency. These cells express Sca-1 and CD34 [105], makers for FAPs, as well as PDGFRα, but lack expression of Pax7 and desmin, markers of muscle progenitor cells **(Figure 1A)**. We have performed immunohistochemistry for PDGFRα expression and laminin in the skeletal muscle tissue of 6 week old C57BL/10J mice and confirmed the anatomical localization of nmMSCs is the muscle interstitum **(Figure 1B)**, whereas satellite cells are located beneath the basement membrane, which indicates that nmMSCs and satellite cells represent distinct cell populations. These cells are distinct from pericytes as well since PDGFRα$^+$ cells reside outside the vessel wall and outside the capillary basement membrane [95]. Upon appropriate induction conditions, nmMSCs exhibit evidence of adipogenic, osteogenic, and chondrogenic, but not myogenic differentiation potentials *in vitro.* Interestingly, when we compared adipogenic differentiation potentials of age-matched female nmMSCs (F-nmMSCs) and male nmMSCs (M-nmMSCs), we observed significantly increased adipogenesis with F-nmMSCs **(Figure 1C)**.

Although we do not understand the exact mechanism behind the increased adipogenic potential of F-nmMSCs compared to M-nmMSCs, we hypothesize that sex steroid hormones may play a role in proliferation and differentiation in nmMSCs. The indirect or direct role of sex hormones in proliferation and differentiation potentials of various stem/progenitor cells, including preadipocytes, bone marrow derived mesenchymal stem cells (BM-MSCs), hematopoietic stem cells have been studied [12, 106-108]. The role played by sex hormones in adipogenesis is still poorly understood; however, it is known that in human adipocytes, estrogen modulate *in vitro* adipogenesis by increasing a preadipocyte replication

process [109]. Dieudonne et al. reported that rat preadipocytes from ovariectomized female rats showed significantly increased adipogenic differentiation and peroxisome proliferator-activated receptor γ2 (PPAR γ2) expression upon exposure to 17β-estradiol, but showed no difference under androgen stimulation, suggesting that only estrogen acts as a proadipogenic hormone [106]. Therefore, increased adipogenic potential of the F-nmMSCs may be associated to the higher level of estrogen in female compared to male mice; however, further studies are needed to confirm the actual effect that estrogen has on the differential potential of nmMSCs *in vivo* and *in vitro*.

Sexual dimorphism in BM-MSCs has been described in several studies. Crisostomo et al. studied sex-related differences in BM-MSCs' paracrine response to acute injury and reported that endotoxin treatment of female and male BM-MSCs provoked significantly more VEGF production in female BM-MSCs compared to male BM-MSCs. In addition, female BM-MSCs expressed significantly less tumor necrosis factor-α (TNF-α) than male BM-MSCs after one hour of hypoxia and hydrogen peroxide exposure [107]. Another study done by Tan et al. demonstrated that upon transplantation of female and male BM-MSCs into pulmonary arterial hypertensive C57BL/6J mice, female BM-MSCs displayed superior efficacy, showing a greater decrease in muscularization of pulmonary vessels, than male BM-MSCs [110]. Previous and current studies suggest that sexual dimorphism exists within MSCs derived from both bone marrow and muscle. Although it is known that PDGFRα^{+} nmMSCs do not originate from bone marrow [95], similarities in morphology, surface marker profiles, and multilineage differentiation property between muscle resident and bone marrow derived MSCs suggest that more sex-related differences, other than just adipogenic potential, may exist within the nmMSCs populations. Therefore, studies examining sex differences of MSCs in muscle and bone marrow and the understanding of underlying mechanisms become necessary for developing better tissue or disease specific therapeutic strategies.

C. Other muscle stem cells

Many studies have identified other non-satellite stem cell populations from skeletal muscle including side population (SP) cells, pericytes, mesoangioblasts, PW1^{+} interstitial cells (PICs), and circulating AC133^{+} cells. Recently additional studies have been performed to characterize these cell populations; however, no studies comparing sex-related differences *in vitro* and/or *in vivo* are available. For example, two recently published studies describe pericytes that they contribute to muscle regeneration *in vivo*, and this contribution increases significantly during acute injury or in dystrophic muscle [111, 112]. This study suggests an important point that non-myogenic cells may also contribute to muscle regeneration; however, both of these studies were performed without distinguishing male and female cells. Other studies discuss the therapeutic potential of murine mesoangioblasts, vessel-associated stem cells, to treat muscular dystrophy in α-sarcoglycan null [113] or *mdx/utrn*$^{-/-}$ mice [114] which successfully showed that mesoangioblasts injected systemically or intramuscularly have the ability to contribute to the muscle regeneration; however, no sex-related differences were described. Recently, Pannérec et al. identified a non-satellite cell population from the skeletal muscle interstitium, referred to as PICs, which display myogenic potential and participated in the generation of new myofibers and SCs [115]. Because of the relatively new characterization of PICs, there are no studies addressing sex-related differences in this cell population. Based on current findings on sex-related differences in total cell number or

regeneration capacities of SCs and MDSCs, there may be sexual dimorphism in other muscle stem cells as well, and therefore, further research is warranted.

Sexual dimorphism in muscle microenvironment in respond to oxidative stress and damage

The production of reactive oxygen species (ROS), small free radicals and reactive nitrogen species (RNS) in skeletal muscle increases during endurance training and prolonged exercise and it is associated with muscle fatigue, oxidative damage, lipid peroxidation, and muscle aging [116-119]. The ROS including, superoxide, hydroxyl, alkoxyl, peroxyl radicals, are the major internal threats to cellular homeostasis of aerobic organisms arising from reactive oxygen intermediates and the byproducts generated from normal oxygen metabolism. These free radicals, although in a small quantity, react with many molecules in muscle cells, including proteins, lipids, nucleic acids, and carbohydrates to damage the tissue. Since the skeletal muscles are constituted with postmitotic cells and use a large amount of oxygen, they are particularly vulnerable to the accumulation of oxidative stress and damage over time. Many studies show that the slow buildup of ROS and RNS over the years is thought to be a factor in aging as well [112, 120]. As a defense system against oxidative threats, our body's generate antioxidants capable of scavenging ROS and RNS to neutralize their potential ill effects, including superoxide dismutases, catalase, GSH peroxidase/reductase, vitamine C and E, glucose, uric acid, and estrogen [112, 121].

A. Effect of sex hormones in the skeletal muscle

i) Estrogens

Estrogens, including estrone (E1), 17β-estradiol (E2) and estriol (E3) are known to be antioxidants, gene regulators and membrane stabilizers, and they confer many protective effects on post-exercise muscle damage. First, estrogens, especially E2 and E3, which possess a phenolic hydroxyl groups, can donate hydrogen atoms to free radicals to suppress peroxidation chain reactions [122, 123], and thus serve as antioxidants themselves. Secondly, it is known that estrogens may have a direct effect on genes that are involved in lipid or lipoprotein metabolism, for example, the low density lipoprotein receptor [123]. Estrogen receptors, ERα and ERβ are identified in skeletal muscle, and both acute and chronic changes in circulating E2 may also positively regulate the ERα gene expression in skeletal muscle [124]. Lastly, estrogens bind to estrogen receptors and up-regulate expression of the genes encoding other antioxidants, such as glutathione peroxidase via intracellular signaling pathways [125]. In addition, estrogens are known to exert a non-genomic effect on lipid metabolism that affects the membrane fluidity as a cell protective mechanism. The sex hormones are known to intercalate into the muscle membrane bilayer and interact with the phospholipid molecules. Estrogen, a fat-soluble hormone may protect membranes from peroxidative damage by decreasing membrane fluidity and increasing membrane stability in ways similar to the stabilizing mechanisms of cholesterol [126]. While estrogen increases the fluidity of the sarcoplasmic reticulum, which in turn, increases the activity of Ca^{2+}ATPase activity and regulates calcium storage and muscle contraction [127], it decreased the membrane fluidity of liposomes [126]. Knowing that estrogens have potentials to protect cells from oxidative stress and damage, we would expect to see sex-related differences in their abilities to respond to muscle damage, since females have much higher level of estrogen than males.

Estrogens have been shown to improve muscle's resistance to mechanical and biochemical injuries and the lack of estrogens may impair specific muscle force and recovery from disuse atrophy [128]. In addition, the effect of estrogens on muscle is associated with the induction of heat shock proteins (HSP), which are molecular chaperones that provide a means of coping with many cellular stresses, including exercise. It had been reported that the expression of most HSPs was generally greater in the skeletal muscle of males compared to female animals [128], and one study demonstrated that upon exercise, even greater HSP70 induction was observed in males than females. Because HSP70 is stress inducible, the lower induction observed in females compared to males suggested that estrogen has a protective role in postexercise HSP70 expression in the skeletal muscle [129].

There have been many reports of sex-related differences in postexercise-induced muscle injury in humans and animal models [130, 131] Creatine kinase (CK) activity, inflammatory response, and leukocyte infiltration are commonly measured as markers of muscle damage, and are generally reported to be lower in females than in males [130, 132]. After both endurance and resistance eccentric exercise, females show much less CK efflux compared to males, and this large difference in CK activity has been attributed to the effects of circulating estrogen on skeletal muscle [133]. For example, Amelink et al. showed increased muscle damage in ovariectomized female rats and this could be prevented by the administration of E2 before exercise. In addition, they reported lower CK activity with male animals treated with estrogen after exercise [133]. Investigations into the effect of estrogen on muscle damage have explored the possible protective role that estrogen may play by minimizing inflammation and leukocyte infiltration. The inflammatory response is necessary for the removal of damaged tissue; however, factors associated with inflammation can also increase secondary muscle injury. Previously, Komulainen et al. reported that they observed sex-related differences in histopathological changes after downhill running exercise. For example, myofiber swelling occurred more slowly and the necrosis and macrophage invasion occurred to a lesser extent in females than in male rats [134]. In addition, other studies reported that estrogen can attenuate neutrophil and leucocyte infiltration into the skeletal muscle and prevent elevated macrophage concentration in blood vessels after exercise [132, 135]. Furthermore, Jovaovi et al. demonstrated that low levels of E2 may provide resistance to female, cardiomyocytes against intracellular Ca^{2+} loading, which can lead into cell injury, through an estrogen receptor-mediated mechanism. This protective property of E2 contributed to cardiomyocyte protection in females only [136]. Lastly, some studies reported that low physiological levels of estrogen can inhibit IL-6 production or can finely regulated TNFα release by macrophages upon muscle damage [137, 138]. Interestingly, Tiidus et al. showed that estrogen can also enhance post-exercise injury muscle satellite cell activation and proliferation, possibly by activating the *c-fos* and *egr-1* genes, which are involved in the induction of myoblasts [139]. Although the exact mechanisms behind its action are not entirely clear, these studies provide evidence that estrogen can positively influence the rate of muscle repair while simultaneously limiting the inflammatory response **(Figure 2)**.

ii) Effect of pregnancy

Recently many studies have shown that one of the benefits of pregnancy is the increased regenerative ability in the mother. Although underlying mechanisms might not be revealed fully, several studies demonstrated that during pregnancy, fetal stem cells can repair the mother's brain [140], liver [141],

heart [142] and help increase blood volume [12]. For the first time, Tan et al. demonstrated that fetal cells can enter the maternal brain during pregnancy. Mice expressing enhanced green fluorescent protein (eGFP) were crossed with female wild type C57BL/6 mice. During pregnancy, an excitotoxic lesion was made to the brain which led to the translocation of fetal cells to the injured region, which was detected by quantitative real-time PCR for Y chromosomes. They showed that $eGFP^+$ fetal cells were found to be neuron-, astrocyte-, and oligodendrocyte-like cell types [140]. In addition, Gielchinsky et al. reported that pregnancy could restore liver regeneration capacity of the aged mice. They showed that 2 days after two-thirds partial hepatectomy, the liver regenerated to only 46% in the aged mice, while liver regeneration in aged pregnant mice was significantly increased to 96% ± 3%. They also found that the restored capacity of the aged liver for regeneration during pregnancy was due to a function of cell growth rather than cell proliferation and suggested that the activation of the Akt/mTORC1 pathway mediated this hypertrophy in the regenerating livers of pregnant mice [141]. Kara et al. also reported that when a pregnant mouse had cardiomyopathy, the fetus donated some of its stem cells to help rebuild the damaged heart tissue. They utilized eGFP-tagged fetuses and demonstrated engraftment of multipotent $eGFP^+$ fetal cells in the injury area of the maternal hearts. Engrafted $eGFP^+$ fetal cells were differentiated into endothelial cells, smooth muscle cells, and cardiomyocytes [142]. Most recently, Nakada et al. observed that during pregnancy, haematopoietic stem cell division, cell frequency, cellularity and erythropoiesis in the spleen significantly increased and they proposed that activation of E2Fs via estradio-ERα signaling was responsible for those actions in the female mice [12]. Estrogen levels significantly increase during ovulation and pregnancy, and increased cellularity, erthropoiesis and myelopoiesis in the spleen and increased haematopoietic stem cells in the bone marrow and spleen which would be a possible mechanism to maintain the mother and fetus(es) with a sufficient volume of blood throughout the pregnancy. ERα and ERβ are also known to be highly expressed in skeletal muscle and muscle stem cells, including satellite cells and possibly MDSCs [143]. Knowing that estrogen levels can affect satellite cell proliferation [139], pregnancy may have some effects on muscle repair and regeneration and the frequency of muscle stem cells in females, though no studies have been performed in this area. In fact, estrogens, and high peaks of estrogen during pregnancy, are suggested to be responsible for the longer longevity of females compared to males due to the many beneficial effects that estrogens have as antioxidants as well as regulating longevity-related genes, including mitogen-activated protein kinases (MAPKs) and nuclear factor kappa B (NF_kB) [125]. Based on currently available studies showing that somatic cells and/or stem cells from the fetus(es) can contribute to the regeneration or repair tissue of the mother, accumulation and rejuvenation of stem/progenitor cells during pregnancy by the fetus may account for the sex-related differences seen in skeletal muscle and muscle stem cells, as well as increased longevity.

B. Sex-related differences in gene expression in skeletal muscle

The sexual dimorphism of skeletal muscle may be most obvious in males since they generally have larger muscles than females. Although the molecular basis for this difference has not been clearly identified, several studies provide sex-related differences in gene expression in skeletal muscle. For example, Pas et al. reported that the muscle regulatory factors (MRF) gene family, which includes myogenin, myf-5, MyoD1, and myf-6, showed sex-related differences in their mRNA levels. Interestingly, they investigated

anterior tibial muscles of rats and demonstrated that myogenin, myf-5 and myf-6 mRNA levels were significantly increased in females compared to male rats. This result was unexpected as MRFs regulate skeletal muscle formation and postnatal muscle growth and muscle mass is typically greater in males; however, when they treated the muscle with dexamethasone, they observed increased levels of MyoD1, myogenin and myf-5 in the male rats, while they observed significantly decreased expression of myf-6 in female rats. These results suggest that dexamethasone increases satellite cell-specific MRFs activity and is responsible for muscle hypertrophy (Henning, 1999, gender related). Another study done by McMahon et al. group reported that sexual dimorphism is associated with decreased myostatin protein in skeletal muscle of male mice compared to female mice. Although there was no differences in mRNA levels, western blot analysis showed 40-60% lower expression of processed myostatin in males compared to females, which correlated with 40% heavier body and muscle mass in males (Bass, 2003, sexual dimorphism). A more recent study performed by Welle et al. also identified genes that might contribute to the sexual dimorphism of skeletal muscle size and mass. They showed that expression of growth factor receptor-bound 10 (GRB10), which encodes a protein that inhibits insulin-like growth factor-1 (IGF-1) signaling and activin A receptor IIB (ACV2B), which encodes a myostatin receptor, were more than 2 fold increase in females compared to males. This result suggests that reduced IGF-1 signaling and increased myostatin activity may contribute to the sexual dimorphism in skeletal muscle size (Thornton, 2007, sex-related differences).

Conclusion

In skeletal muscle, stem and progenitor cells are known to persist throughout life and contribute to repair and regeneration. Therefore, understanding sexual dimorphism and sex related differences in skeletal muscle and muscle stem cells will greatly enhance our knowledge in understanding the differences between males and females in their presentation of various muscle diseases and healing differences. Currently, literature describing sex-related differences in satellite cells and other muscle stem cells is scarce and sexual dimorphism remains an under-investigated variable that could affect cell therapy approaches for regenerative medicine. Recent studies demonstrating sexual dimorphism in stem and progenitor cells, including hematopoietic stem cells and MDSCs suggest that cell sex may provide insight to stem cell biology. Musculoskeletal health is one of the areas of medicine in which the differences between males and females are most striking; however, sex-related differences of the cells have rarely been examined. Significant efforts to prioritize research to include sexual dimorphism in stem and progenitor cells may be imperative to improve basic science research as well as patient care for healthcare delivery.

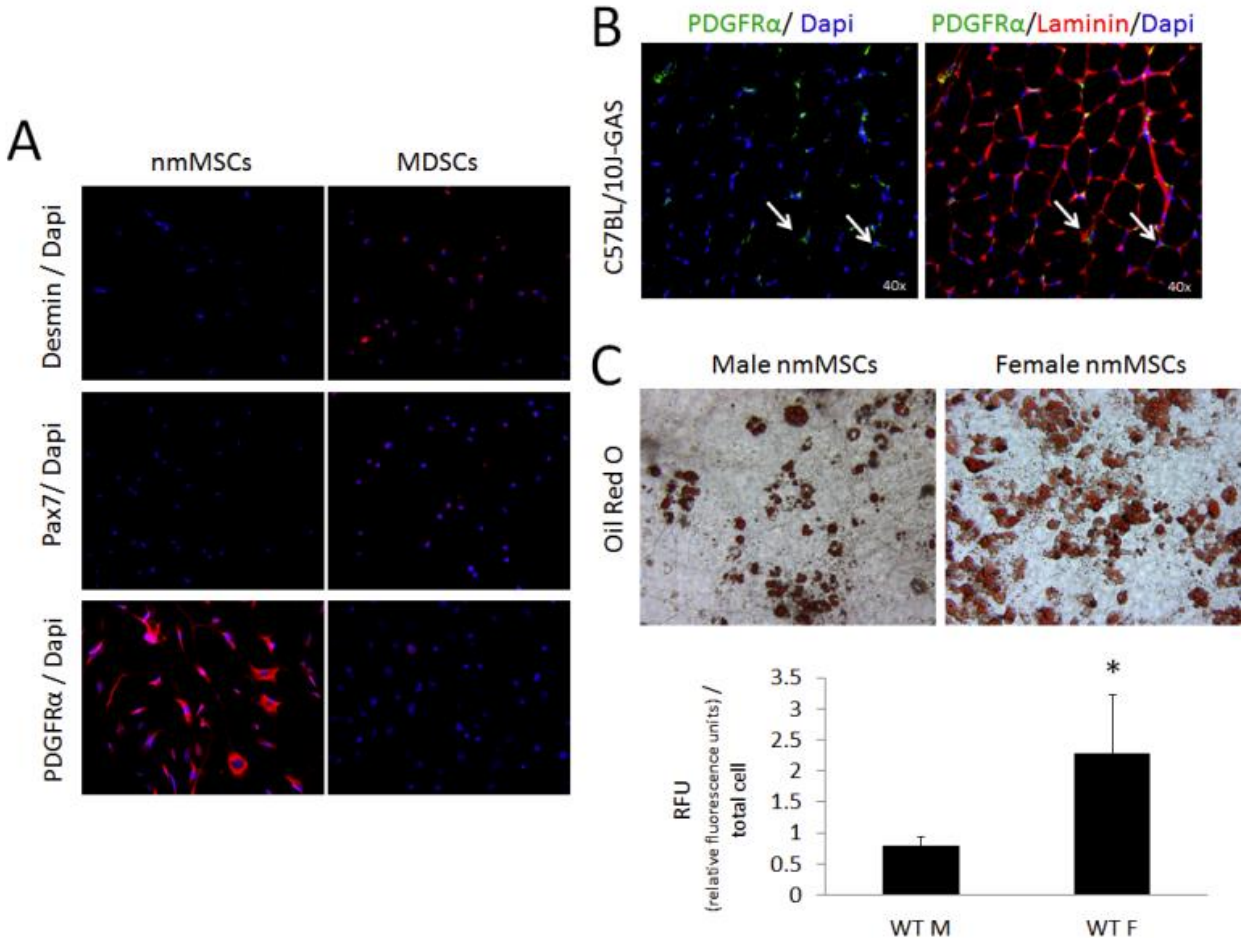

Figure 1. Muscle resident non-myogenic mesenchymal stem cells (nmMSCs) demonstrate sex-related difference in adipogenic differentiation. (A) Immunohistochemistry stain of Pax7 and Desmin indicated that MDScs are myogenic progenitor cells, while nmMSCs are PDGFRα expressing mesenchymal stem cells. (B) Immunohistochemistry for PDGFRα (green) and laminin (Red) in the gastrocnemius of 4wk old C57BL/10J mice. The anatomical location of PDGFRα expressing nmMSCs is skeletal muscle interstitium. (C) Adipogenic differentiation potential of male-nmMSCs and female-nmMSCs were examined. Female-nmMSCs displayed significantly increased adipogenic potential compared to male-nmMSCs (n=5). Error bars indicate 'mean ± SD'. * $p < 0.005$.

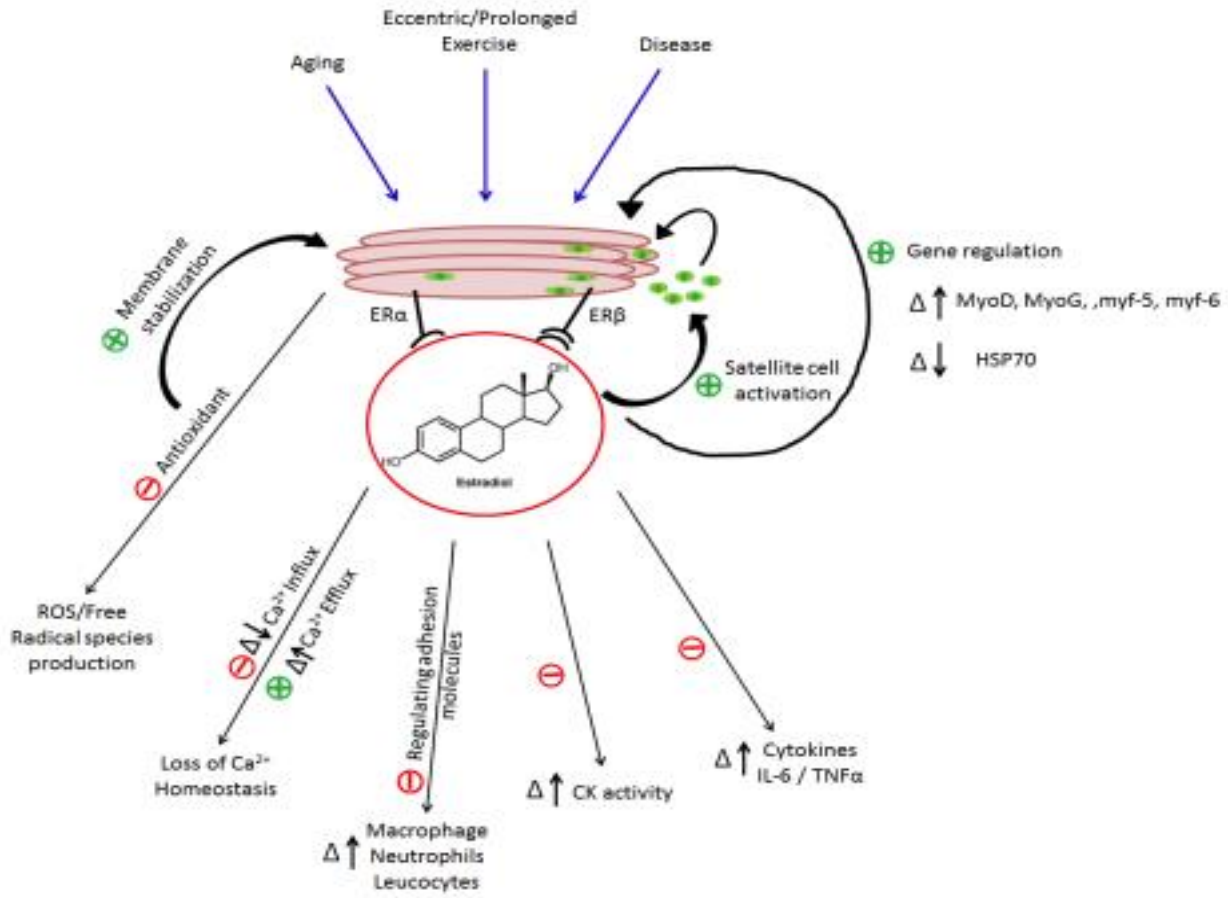

Figure 2. Skeletal muscle damage and the potential protective role of estrogen. Eccentric or prolonged exercise, disease, or age-related changes may induce skeletal muscle damage and estrogen has an apparent protective effect against skeletal muscle damage. As a result of skeletal muscle damage, ROS or free radical species are produced, intracellular $Ca2^{+}$ homeostasis may be lost, inflammatory and immune response triggers cytokines and macrophage, neutrophils and leucocytes are recruited, creatine kinase (CK) activity is elevated. Estrogen is known to act as an antioxidant, regulator of $Ca2^{+}$ influx/efflux and adhesion molecules via estrogen receptor (ERα and ERβ) binding. Estrogen plays an important role in lowering CK activity and stabilizing the membrane in damaged muscle. In addition, estrogen can enhance post-exercise injury muscle satellite cell activation and proliferation and regulate myogenic muscle regulatory genes.

References

1. Hoffman, E.P., R.H. Brown, Jr., and L.M. Kunkel, *Dystrophin: the protein product of the Duchenne muscular dystrophy locus.* Cell, 1987. **51**(6): p. 919-28.
2. Deasy, B.M. and J. Huard, *Gene therapy and tissue engineering based on muscle-derived stem cells.* Curr Opin Mol Ther, 2002. **4**(4): p. 382-9.
3. Singer, N.G. and A.I. Caplan, *Mesenchymal stem cells: mechanisms of inflammation.* Annu Rev Pathol, 2011. **6**: p. 457-78.
4. Partridge, T.A., et al., *Conversion of mdx myofibres from dystrophin-negative to -positive by injection of normal myoblasts.* Nature, 1989. **337**(6203): p. 176-9.
5. Huard, J., et al., *Myoblast transplantation produced dystrophin-positive muscle fibres in a 16-year-old patient with Duchenne muscular dystrophy.* Clin Sci (Lond), 1991. **81**(2): p. 287-8.
6. Huard, J., et al., *Human myoblast transplantation: preliminary results of 4 cases.* Muscle Nerve, 1992. **15**(5): p. 550-60.
7. Karpati, G., P. Holland, and R.G. Worton, *Myoblast transfer in DMD: problems in the interpretation of efficiency.* Muscle Nerve, 1992. **15**(10): p. 1209-10.
8. Tremblay, J.P., et al., *Results of a triple blind clinical study of myoblast transplantations without immunosuppressive treatment in young boys with Duchenne muscular dystrophy.* Cell Transplant, 1993. **2**(2): p. 99-112.
9. Miller, R.G., et al., *Myoblast implantation in Duchenne muscular dystrophy: the San Francisco study.* Muscle Nerve, 1997. **20**(4): p. 469-78.
10. Mendell, J.R., et al., *Myoblast transfer in the treatment of Duchenne's muscular dystrophy.* N Engl J Med, 1995. **333**(13): p. 832-8.
11. Gussoni, E., H.M. Blau, and L.M. Kunkel, *The fate of individual myoblasts after transplantation into muscles of DMD patients.* Nat Med, 1997. **3**(9): p. 970-7.
12. Nakada, D., et al., *Oestrogen increases haematopoietic stem-cell self-renewal in females and during pregnancy.* Nature, 2014. **505**(7484): p. 555-8.
13. Carey, J.R. and D.S. Judge, *Longevity records : life spans of mammals, birds, amphibians, reptiles, and fish*. Monographs on population aging,. 2000, Odense: Odense University Press. 241 p.
14. Stindl, R., *Tying it all together: telomeres, sexual size dimorphism and the gender gap in life expectancy.* Med Hypotheses, 2004. **62**(1): p. 151-4.
15. Gutierrez-Adan, A., et al., *Differential expression of two genes located on the X chromosome between male and female in vitro-produced bovine embryos at the blastocyst stage.* Molecular Reproduction and Development, 2000. **55**(2): p. 146-151.
16. McCombe, P.A., J.M. Greer, and I.R. Mackay, *Sexual Dimorphism in Autoimmune Disease.* Current Molecular Medicine, 2009. **9**(9): p. 1058-1079.
17. Nikezic-Ardolic, M., et al., *Gender differences in cellular response.* Lupus, 1999. **8**(5): p. 375-379.
18. Mayeux, R., et al., *The Frequency of Idiopathic Parkinsons-Disease by Age, Ethnic-Group, and Sex in Northern Manhattan, 1988-1993.* American Journal of Epidemiology, 1995. **142**(8): p. 820-827.
19. Erdely, A., et al., *Sexual dimorphism in the aging kidney: Effects on injury and nitric oxide system.* Kidney Int, 2003. **63**(3): p. 1021-6.
20. Van Den Eeden, S.K., et al., *Incidence of Parkinson's disease: variation by age, gender, and race/ethnicity.* Am J Epidemiol, 2003. **157**(11): p. 1015-22.
21. in *Sex Differences and Implications for Translational Neuroscience Research: Workshop Summary*. 2011: Washington (DC).
22. Andersson, M. and Y. Iwasa, *Sexual selection.* Trends Ecol Evol, 1996. **11**(2): p. 53-8.

23. Abouheif, E. and D.J. Fairbairn, *A comparative analysis of allometry for sexual size dimorphism: Assessing Rensch's rule.* American Naturalist, 1997. **149**(3): p. 540-562.
24. Gustafsson, A. and P. Lindenfors, *Human size evolution: no evolutionary allometric relationship between male and female stature.* J Hum Evol, 2004. **47**(4): p. 253-66.
25. Wells, J.C.K., *Sexual dimorphism of body composition.* Best Practice & Research Clinical Endocrinology & Metabolism, 2007. **21**(3): p. 415-430.
26. Glenmark, B., et al., *Difference in skeletal muscle function in males vs. females: role of estrogen receptor-beta.* Am J Physiol Endocrinol Metab, 2004. **287**(6): p. E1125-31.
27. Ustunel, I. and R. Demir, *A histochemical, morphometric and ultrastructural study of gastrocnemius and soleus muscle fiber type composition in male and female rats.* Acta Anat (Basel), 1997. **158**(4): p. 279-86.
28. Fox, J., et al., *Morphological characteristics of skeletal muscles in relation to gender.* Aging Clin Exp Res, 2003. **15**(3): p. 264-9.
29. Kanehisa, H., et al., *Cross-sectional areas of fat and muscle in limbs during growth and middle age.* Int J Sports Med, 1994. **15**(7): p. 420-5.
30. Kanehisa, H., S. Ikegawa, and T. Fukunaga, *Comparison of muscle cross-sectional area and strength between untrained women and men.* Eur J Appl Physiol Occup Physiol, 1994. **68**(2): p. 148-54.
31. Abe, T., C.F. Kearns, and T. Fukunaga, *Sex differences in whole body skeletal muscle mass measured by magnetic resonance imaging and its distribution in young Japanese adults.* Br J Sports Med, 2003. **37**(5): p. 436-40.
32. Miller, A.E., et al., *Gender differences in strength and muscle fiber characteristics.* Eur J Appl Physiol Occup Physiol, 1993. **66**(3): p. 254-62.
33. Brooke, M.H. and W.K. Engel, *The histographic analysis of human muscle biopsies with regard to fiber types. 1. Adult male and female.* Neurology, 1969. **19**(3): p. 221-33.
34. Costill, D.L., et al., *Skeletal muscle enzymes and fiber composition in male and female track athletes.* J Appl Physiol, 1976. **40**(2): p. 149-54.
35. Simoneau, J.A. and C. Bouchard, *Human variation in skeletal muscle fiber-type proportion and enzyme activities.* Am J Physiol, 1989. **257**(4 Pt 1): p. E567-72.
36. Rantanen, J., A. Rissanen, and H. Kalimo, *Lumbar muscle fiber size and type distribution in normal subjects.* Eur Spine J, 1994. **3**(6): p. 331-5.
37. Alway, S.E., et al., *Contrasts in muscle and myofibers of elite male and female bodybuilders.* J Appl Physiol (1985), 1989. **67**(1): p. 24-31.
38. Herbison, G.J., M.M. Jaweed, and J.F. Ditunno, *Muscle fiber types.* Arch Phys Med Rehabil, 1982. **63**(5): p. 227-30.
39. Pette, D. and R.S. Staron, *Myosin isoforms, muscle fiber types, and transitions.* Microsc Res Tech, 2000. **50**(6): p. 500-9.
40. Komi, P.V. and J. Karlsson, *Skeletal muscle fibre types, enzyme activities and physical performance in young males and females.* Acta Physiol Scand, 1978. **103**(2): p. 210-8.
41. Scott, W., J. Stevens, and S.A. Binder-Macleod, *Human skeletal muscle fiber type classifications.* Phys Ther, 2001. **81**(11): p. 1810-6.
42. Wust, R.C., et al., *Sex differences in contractile properties and fatigue resistance of human skeletal muscle.* Exp Physiol, 2008. **93**(7): p. 843-50.
43. Hicks, A.L., J. Kent-Braun, and D.S. Ditor, *Sex differences in human skeletal muscle fatigue.* Exerc Sport Sci Rev, 2001. **29**(3): p. 109-12.
44. Fulco, C.S., et al., *Slower fatigue and faster recovery of the adductor pollicis muscle in women matched for strength with men.* Acta Physiol Scand, 1999. **167**(3): p. 233-9.

45. Benbadis, S.R., et al., *The influence of the full moon on seizure frequency: myth or reality?* Epilepsy Behav, 2004. **5**(4): p. 596-7.
46. Frontera, W.R., et al., *Skeletal muscle fiber quality in older men and women.* Am J Physiol Cell Physiol, 2000. **279**(3): p. C611-8.
47. Essen-Gustavsson, B. and O. Borges, *Histochemical and metabolic characteristics of human skeletal muscle in relation to age.* Acta Physiol Scand, 1986. **126**(1): p. 107-14.
48. Phillips, S.K., et al., *Muscle weakness in women occurs at an earlier age than in men, but strength is preserved by hormone replacement therapy.* Clin Sci (Lond), 1993. **84**(1): p. 95-8.
49. Huard, J., B. Cao, and Z. Qu-Petersen, *Muscle-derived stem cells: potential for muscle regeneration.* Birth Defects Res C Embryo Today, 2003. **69**(3): p. 230-7.
50. Peault, B., et al., *Stem and progenitor cells in skeletal muscle development, maintenance, and therapy.* Mol Ther, 2007. **15**(5): p. 867-77.
51. Shi, X. and D.J. Garry, *Muscle stem cells in development, regeneration, and disease.* Genes Dev, 2006. **20**(13): p. 1692-708.
52. Mitchell, K.J., et al., *Identification and characterization of a non-satellite cell muscle resident progenitor during postnatal development.* Nat Cell Biol, 2010. **12**(3): p. 257-66.
53. Blankenhorn, E.P., et al., *Sexually dimorphic genes regulate healing and regeneration in MRL mice.* Mamm Genome, 2003. **14**(4): p. 250-60.
54. Harada, H., et al., *Sexual dimorphism in reduced-size liver ischemia and reperfusion injury in mice: role of endothelial cell nitric oxide synthase.* Proc Natl Acad Sci U S A, 2003. **100**(2): p. 739-44.
55. Mulroney, S.E., et al., *Gender differences in renal growth and function after uninephrectomy in adult rats.* Kidney Int, 1999. **56**(3): p. 944-53.
56. Carr, L.K., et al., *1-year follow-up of autologous muscle-derived stem cell injection pilot study to treat stress urinary incontinence.* Int Urogynecol J Pelvic Floor Dysfunct, 2008. **19**(6): p. 881-3.
57. Qu-Petersen, Z., et al., *Identification of a novel population of muscle stem cells in mice: potential for muscle regeneration.* J Cell Biol, 2002. **157**(5): p. 851-64.
58. Sarig, R., et al., *Regeneration and transdifferentiation potential of muscle-derived stem cells propagated as myospheres.* Stem Cells, 2006. **24**(7): p. 1769-78.
59. Gussoni, E., et al., *Dystrophin expression in the mdx mouse restored by stem cell transplantation.* Nature, 1999. **401**(6751): p. 390-4.
60. Lee, J.Y., et al., *Clonal isolation of muscle-derived cells capable of enhancing muscle regeneration and bone healing.* J Cell Biol, 2000. **150**(5): p. 1085-100.
61. Mauro, A., *Satellite cell of skeletal muscle fibers.* J Biophys Biochem Cytol, 1961. **9**: p. 493-5.
62. Collins, C.A., et al., *Stem cell function, self-renewal, and behavioral heterogeneity of cells from the adult muscle satellite cell niche.* Cell, 2005. **122**(2): p. 289-301.
63. Cossu, G., et al., *In vitro differentiation of satellite cells isolated from normal and dystrophic mammalian muscles. A comparison with embryonic myogenic cells.* Cell Differ, 1980. **9**(6): p. 357-68.
64. Beauchamp, J.R., et al., *Expression of CD34 and Myf5 defines the majority of quiescent adult skeletal muscle satellite cells.* J Cell Biol, 2000. **151**(6): p. 1221-34.
65. Yoshida, N., et al., *Cell heterogeneity upon myogenic differentiation: down-regulation of MyoD and Myf-5 generates 'reserve cells'.* J Cell Sci, 1998. **111 (Pt 6)**: p. 769-79.
66. Asakura, A., M. Komaki, and M. Rudnicki, *Muscle satellite cells are multipotential stem cells that exhibit myogenic, osteogenic, and adipogenic differentiation.* Differentiation, 2001. **68**(4-5): p. 245-53.
67. Huard, J., et al., *Gene transfer into skeletal muscles by isogenic myoblasts.* Hum Gene Ther, 1994. **5**(8): p. 949-58.

68. Kinoshita, I., et al., *Very efficient myoblast allotransplantation in mice under FK506 immunosuppression.* Muscle Nerve, 1994. **17**(12): p. 1407-15.
69. Roth, S.M., et al., *Skeletal muscle satellite cell populations in healthy young and older men and women.* Anat Rec, 2000. **260**(4): p. 351-8.
70. Kadi, F., et al., *Satellite cells and myonuclei in young and elderly women and men.* Muscle Nerve, 2004. **29**(1): p. 120-7.
71. Petrella, J.K., et al., *Efficacy of myonuclear addition may explain differential myofiber growth among resistance-trained young and older men and women.* Am J Physiol Endocrinol Metab, 2006. **291**(5): p. E937-46.
72. Bonavaud, S., et al., *Primary human muscle satellite cell culture: variations of cell yield, proliferation and differentiation rates according to age and sex of donors, site of muscle biopsy, and delay before processing.* Biol Cell, 1997. **89**(3): p. 233-40.
73. Salimena, M.C., J. Lagrota-Candido, and T. Quirico-Santos, *Gender dimorphism influences extracellular matrix expression and regeneration of muscular tissue in mdx dystrophic mice.* Histochem Cell Biol, 2004. **122**(5): p. 435-44.
74. Neal, A., L. Boldrin, and J.E. Morgan, *The satellite cell in male and female, developing and adult mouse muscle: distinct stem cells for growth and regeneration.* PLoS One, 2012. **7**(5): p. e37950.
75. Niel, L., et al., *Sexual dimorphism and androgen regulation of satellite cell population in differentiating rat levator ani muscle.* Dev Neurobiol, 2008. **68**(1): p. 115-22.
76. Velleman, S.G., et al., *Heterogeneity in growth and differentiation characteristics in male and female satellite cells isolated from turkey lines with different growth rates.* Comp Biochem Physiol A Mol Integr Physiol, 2000. **125**(4): p. 503-9.
77. Doumit, M.E., D.C. McFarland, and R.D. Minshall, *Satellite cells of growing turkeys: influence of donor age and sex on proliferation and differentiation in vitro.* Exp Cell Res, 1990. **189**(1): p. 81-6.
78. Gharaibeh, B., et al., *Isolation of a slowly adhering cell fraction containing stem cells from murine skeletal muscle by the preplate technique.* Nat Protoc, 2008. **3**(9): p. 1501-9.
79. Deasy, B.M., et al., *Long-term self-renewal of postnatal muscle-derived stem cells.* Mol Biol Cell, 2005. **16**(7): p. 3323-33.
80. Anderson, W.A., et al., *A biomarker approach to measuring human dietary exposure to certain phthalate diesters.* Food Addit Contam, 2001. **18**(12): p. 1068-74.
81. Wu, X., et al., *Muscle-derived stem cells: isolation, characterization, differentiation, and application in cell and gene therapy.* Cell Tissue Res, 2010. **340**(3): p. 549-67.
82. Jankowski, R.J., et al., *The role of CD34 expression and cellular fusion in the regeneration capacity of myogenic progenitor cells.* J Cell Sci, 2002. **115**(Pt 22): p. 4361-74.
83. Kanehisa, H., et al., *Strength and cross-sectional area of knee extensor muscles in children.* Eur J Appl Physiol Occup Physiol, 1994. **68**(5): p. 402-5.
84. Brooke, M.H. and W.K. Engel, *The histographic analysis of human muscle biopsies with regard to fiber types. 4. Children's biopsies.* Neurology, 1969. **19**(6): p. 591-605.
85. Hood, D.A. and J.A. Simoneau, *Rapid isolation of total RNA from small mammal and human skeletal muscle.* Am J Physiol, 1989. **256**(5 Pt 1): p. C1092-6.
86. Brooke, M.H. and W.K. Engel, *The histographic analysis of human muscle biopsies with regard to fiber types. 3. Myotonias, myasthenia gravis, and hypokalemic periodic paralysis.* Neurology, 1969. **19**(5): p. 469-77.
87. Deasy, B.M., et al., *A role for cell sex in stem cell-mediated skeletal muscle regeneration: female cells have higher muscle regeneration efficiency.* J Cell Biol, 2007. **177**(1): p. 73-86.

88. Sharif-Askari, E., et al., *Direct cleavage of the human DNA fragmentation factor-45 by granzyme B induces caspase-activated DNase release and DNA fragmentation.* EMBO J, 2001. **20**(12): p. 3101-13.
89. Nedelec, B., et al., *Myofibroblasts and apoptosis in human hypertrophic scars: the effect of interferon-alpha2b.* Surgery, 2001. **130**(5): p. 798-808.
90. Piao, Y.J., et al., *Nox 2 stimulates muscle differentiation via NF-kappaB/iNOS pathway.* Free Radic Biol Med, 2005. **38**(8): p. 989-1001.
91. Ardite, E., et al., *Glutathione depletion impairs myogenic differentiation of murine skeletal muscle C2C12 cells through sustained NF-kappaB activation.* Am J Pathol, 2004. **165**(3): p. 719-28.
92. Drowley, L., et al., *Sex of muscle stem cells does not influence potency for cardiac cell therapy.* Cell Transplant, 2009. **18**(10): p. 1137-46.
93. Corsi, K.A., et al., *Osteogenic potential of postnatal skeletal muscle-derived stem cells is influenced by donor sex.* J Bone Miner Res, 2007. **22**(10): p. 1592-602.
94. Matsumoto, T., et al., *The influence of sex on the chondrogenic potential of muscle-derived stem cells: implications for cartilage regeneration and repair.* Arthritis Rheum, 2008. **58**(12): p. 3809-19.
95. Uezumi, A., et al., *Mesenchymal progenitors distinct from satellite cells contribute to ectopic fat cell formation in skeletal muscle.* Nat Cell Biol, 2010. **12**(2): p. 143-52.
96. Uezumi, A., et al., *Fibrosis and adipogenesis originate from a common mesenchymal progenitor in skeletal muscle.* J Cell Sci, 2011. **124**(Pt 21): p. 3654-64.
97. Uezumi, A., et al., *Identification and characterization of PDGFRalpha+ mesenchymal progenitors in human skeletal muscle.* Cell Death Dis, 2014. **5**: p. e1186.
98. Lapidos, K.A., R. Kakkar, and E.M. McNally, *The dystrophin glycoprotein complex: signaling strength and integrity for the sarcolemma.* Circ Res, 2004. **94**(8): p. 1023-31.
99. Cossu, G. and M. Sampaolesi, *New therapies for Duchenne muscular dystrophy: challenges, prospects and clinical trials.* Trends Mol Med, 2007. **13**(12): p. 520-6.
100. Bonilla, E., et al., *Duchenne muscular dystrophy: deficiency of dystrophin at the muscle cell surface.* Cell, 1988. **54**(4): p. 447-52.
101. Miranda, A.F., et al., *Dystrophin immunocytochemistry in muscle culture: detection of a carrier of Duchenne muscular dystrophy.* American Journal of Medical Genetics, 1989. **32**(2): p. 268-73.
102. Joe, A.W., et al., *Muscle injury activates resident fibro/adipogenic progenitors that facilitate myogenesis.* Nat Cell Biol, 2010. **12**(2): p. 153-63.
103. Wosczyna, M.N., et al., *Multipotent progenitors resident in the skeletal muscle interstitium exhibit robust BMP-dependent osteogenic activity and mediate heterotopic ossification.* J Bone Miner Res, 2012. **27**(5): p. 1004-17.
104. Mozzetta, C., et al., *Fibroadipogenic progenitors mediate the ability of HDAC inhibitors to promote regeneration in dystrophic muscles of young, but not old Mdx mice.* EMBO Mol Med, 2013. **5**(4): p. 626-39.
105. Jankowski, R.J., et al., *Flow cytometric characterization of myogenic cell populations obtained via the preplate technique: potential for rapid isolation of muscle-derived stem cells.* Hum Gene Ther, 2001. **12**(6): p. 619-28.
106. Dieudonne, M.N., et al., *Opposite effects of androgens and estrogens on adipogenesis in rat preadipocytes: evidence for sex and site-related specificities and possible involvement of insulin-like growth factor 1 receptor and peroxisome proliferator-activated receptor gamma2.* Endocrinology, 2000. **141**(2): p. 649-56.
107. Crisostomo, P.R., et al., *Sex dimorphisms in activated mesenchymal stem cell function.* Shock, 2006. **26**(6): p. 571-4.

108. Lee, D.M., et al., *Effects of gender-specific adult bovine serum on myogenic satellite cell proliferation, differentiation and lipid accumulation.* In Vitro Cell Dev Biol Anim, 2011. **47**(7): p. 438-44.
109. Hauner, H., P. Schmid, and E.F. Pfeiffer, *Glucocorticoids and insulin promote the differentiation of human adipocyte precursor cells into fat cells.* J Clin Endocrinol Metab, 1987. **64**(4): p. 832-5.
110. Tan, R., et al., *GAPDH is critical for superior efficacy of female bone marrow-derived mesenchymal stem cells on pulmonary hypertension.* Cardiovasc Res, 2013. **100**(1): p. 19-27.
111. Birbrair, A., et al., *Role of pericytes in skeletal muscle regeneration and fat accumulation.* Stem Cells Dev, 2013. **22**(16): p. 2298-314.
112. Dellavalle, A., et al., *Pericytes resident in postnatal skeletal muscle differentiate into muscle fibres and generate satellite cells.* Nat Commun, 2011. **2**: p. 499.
113. Sampaolesi, M., et al., *Cell therapy of alpha-sarcoglycan null dystrophic mice through intra-arterial delivery of mesoangioblasts.* Science, 2003. **301**(5632): p. 487-92.
114. Berry, S.E., et al., *Multipotential mesoangioblast stem cell therapy in the mdx/utrn-/- mouse model for Duchenne muscular dystrophy.* Regen Med, 2007. **2**(3): p. 275-88.
115. Pannerec, A., et al., *Defining skeletal muscle resident progenitors and their cell fate potentials.* Development, 2013. **140**(14): p. 2879-91.
116. Yu, B.P., *Cellular defenses against damage from reactive oxygen species.* Physiol Rev, 1994. **74**(1): p. 139-62.
117. O'Neill, C.A., et al., *Production of hydroxyl radicals in contracting skeletal muscle of cats.* J Appl Physiol (1985), 1996. **81**(3): p. 1197-206.
118. Reid, M.B., et al., *Reactive oxygen in skeletal muscle. II. Extracellular release of free radicals.* J Appl Physiol (1985), 1992. **73**(5): p. 1805-9.
119. Davies, K.J., et al., *Free radicals and tissue damage produced by exercise.* Biochem Biophys Res Commun, 1982. **107**(4): p. 1198-205.
120. Tiidus, P.M., et al., *Biochemistry primer for exercise science*. 4th ed. 2012, Champaign, IL: Human Kinetics. p.
121. Clarkson, P.M. and H.S. Thompson, *Antioxidants: what role do they play in physical activity and health?* Am J Clin Nutr, 2000. **72**(2 Suppl): p. 637S-46S.
122. Sugioka, K., Y. Shimosegawa, and M. Nakano, *Estrogens as natural antioxidants of membrane phospholipid peroxidation.* FEBS Lett, 1987. **210**(1): p. 37-9.
123. Santanam, N., et al., *Estradiol as an antioxidant: incompatible with its physiological concentrations and function.* J Lipid Res, 1998. **39**(11): p. 2111-8.
124. Baltgalvis, K.A., et al., *Estrogen regulates estrogen receptors and antioxidant gene expression in mouse skeletal muscle.* PLoS One, 2010. **5**(4): p. e10164.
125. Vina, J., et al., *Why females live longer than males: control of longevity by sex hormones.* Sci Aging Knowledge Environ, 2005. **2005**(23): p. pe17.
126. Wiseman, H., P. Quinn, and B. Halliwell, *Tamoxifen and related compounds decrease membrane fluidity in liposomes. Mechanism for the antioxidant action of tamoxifen and relevance to its anticancer and cardioprotective actions?* FEBS Lett, 1993. **330**(1): p. 53-6.
127. Whiting, K.P., C.J. Restall, and P.F. Brain, *Steroid hormone-induced effects on membrane fluidity and their potential roles in non-genomic mechanisms.* Life Sci, 2000. **67**(7): p. 743-57.
128. Romani, W.A. and D.W. Russ, *Acute effects of sex-specific sex hormones on heat shock proteins in fast muscle of male and female rats.* Eur J Appl Physiol, 2013. **113**(10): p. 2503-10.
129. Paroo, Z., E.S. Dipchand, and E.G. Noble, *Estrogen attenuates postexercise HSP70 expression in skeletal muscle.* Am J Physiol Cell Physiol, 2002. **282**(2): p. C245-51.
130. Amelink, G.J., H.H. Kamp, and P.R. Bar, *Creatine kinase isoenzyme profiles after exercise in the rat: sex-linked differences in leakage of CK-MM.* Pflugers Arch, 1988. **412**(4): p. 417-21.

131. Magal, M., et al., *Relationship between serum creatine kinase activity following exercise-induced muscle damage and muscle fibre composition.* J Sports Sci, 2010. **28**(3): p. 257-66.
132. St Pierre Schneider, B., L.A. Correia, and J.G. Cannon, *Sex differences in leukocyte invasion in injured murine skeletal muscle.* Res Nurs Health, 1999. **22**(3): p. 243-50.
133. Amelink, G.J. and P.R. Bar, *Exercise-induced muscle protein leakage in the rat. Effects of hormonal manipulation.* J Neurol Sci, 1986. **76**(1): p. 61-8.
134. Agley, C.C., et al., *Human skeletal muscle fibroblasts, but not myogenic cells, readily undergo adipogenic differentiation.* J Cell Sci, 2013. **126**(Pt 24): p. 5610-25.
135. Tiidus, P.M., *Can oestrogen influence skeletal muscle damage, inflammation, and repair?* Br J Sports Med, 2005. **39**(5): p. 251-3.
136. Jovanovic, S., et al., *Low concentrations of 17beta-estradiol protect single cardiac cells against metabolic stress-induced Ca2+ loading.* J Am Coll Cardiol, 2000. **36**(3): p. 948-52.
137. Chao, T.C., et al., *Steroid sex hormones regulate the release of tumor necrosis factor by macrophages.* Cell Immunol, 1995. **160**(1): p. 43-9.
138. Pottratz, S.T., et al., *17 beta-Estradiol inhibits expression of human interleukin-6 promoter-reporter constructs by a receptor-dependent mechanism.* J Clin Invest, 1994. **93**(3): p. 944-50.
139. Tiidus, P.M. and D.L. Enns, *Point:Counterpoint: Estrogen and sex do/do not influence post-exercise indexes of muscle damage, inflammation, and repair.* J Appl Physiol (1985), 2009. **106**(3): p. 1010-2; discussion 1014-15, 1021.
140. Tan, X.W., et al., *Fetal microchimerism in the maternal mouse brain: a novel population of fetal progenitor or stem cells able to cross the blood-brain barrier?* Stem Cells, 2005. **23**(10): p. 1443-52.
141. Gielchinsky, Y., et al., *Pregnancy restores the regenerative capacity of the aged liver via activation of an mTORC1-controlled hyperplasia/hypertrophy switch.* Genes Dev, 2010. **24**(6): p. 543-8.
142. Kara, R.J., et al., *Fetal cells traffic to injured maternal myocardium and undergo cardiac differentiation.* Circ Res, 2012. **110**(1): p. 82-93.
143. Wiik, A., et al., *Expression of oestrogen receptor alpha and beta is higher in skeletal muscle of highly endurance-trained than of moderately active men.* Acta Physiol Scand, 2005. **184**(2): p. 105-12.

Science
AAAS

Use of differentiated pluripotent stem cells as replacement therapy for treating disease
Ira J. Fox *et al.*
Science **345**, (2014);
DOI: 10.1126/science.1247391

Appendix 23

REVIEW SUMMARY

STEM CELL THERAPY

Use of differentiated pluripotent stem cells in replacement therapy for treating disease

Ira J. Fox,* George Q. Daley, Steven A. Goldman, Johnny Huard, Timothy J. Kamp, Massimo Trucco

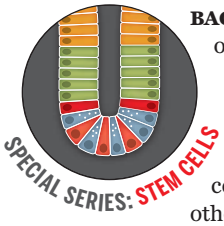

BACKGROUND: Decades of laboratory and clinical investigation have led to successful therapies using hematopoietic stem cells (HSCs), but few other cell therapies have transitioned from experimental to standard clinical care. Providing patients with autologous rather than allogeneic HSCs reduces morbidity and mortality, and in some circumstances broader use could expand the range of conditions amenable to HSC transplantation. The availability of a homogeneous supply of mature blood cells would also be advantageous. An unlimited supply of pluripotent stem cells (PSCs) directed to various cell fates holds great promise as source material for cell transplantation and minimally invasive therapies to treat a variety of disorders. In this Review, we discuss past experience and challenges ahead and examine the extent to which hematopoietic stem cell transplantation and cell therapy for diabetes, liver disease, muscular dystrophies, neurodegenerative disorders, and heart disease would be affected by the availability of precisely differentiated PSCs.

ON OUR WEB SITE

Read the full article at http://dx.doi.org/10.1126/science.1247391

ADVANCES: Although it is not yet possible to differentiate PSCs to cells with characteristics identical to those in the many organs that need replacement, it is likely a matter of time before these "engineering" problems can be overcome. Experience with cell therapies, both in the laboratory and the clinic, however, indicate that many challenges remain for treatment of diseases other than those involving the hematopoietic system. There are issues of immunity, separate from controlling graft rejection, and identifying the optimal cell type for treatment in the case of muscular dystrophies and heart disease. Optimization is also needed for the transplant site, as in diabetes, or when dealing with disruption of the extracellular matrix in treating degenerative diseases, such as chronic liver and heart disease. Finally, when the pathologic process is diffuse and migration of transplanted cells is limited, as is the case with Alzheimer's disease, amyotrophic lateral sclerosis, and the muscular dystrophies, identifying the best means and location for cell delivery will require further study.

OUTLOOK: Considering the pace of progress in generating transplantable cells with a mature phenotype, and the availability of PSC-derived lineages in sufficient mass to treat some patients already, the challenges to scaling up production and eliminating cells with tumor-forming potential are probably within reach. However, generation of enough cells to treat an individual patient requires time for expansion, differentiation, selection, and testing to exclude contamination by tumorigenic precursors. Current methods are far too long and costly to address the treatment of acute organ injury or decompensated function. Immune rejection of engrafted cells, however, is likely to be overcome through transplantation of autologous cells from patient-derived PSCs. Availability of PSC-derived cell populations will have a dramatic effect on blood cell transfusion and the use of hematopoietic stem cell transplantation, and it will likely facilitate treatment of diabetes, some forms of liver disease and neurologic disorders, retinal diseases, and possibly heart disease. Close collaboration between scientists and clinicians—including surgeons and interventional radiologists—and between academia and industry will be critical to overcoming challenges and to bringing new therapies to patients in need. ■

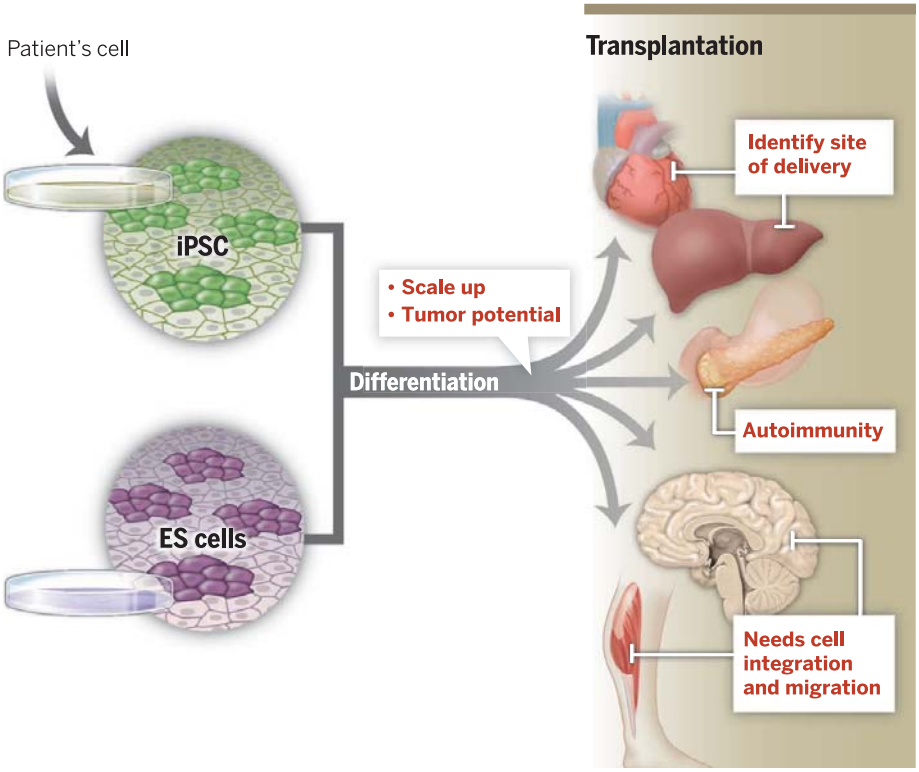

Unlimited populations of differentiated PSCs should facilitate blood therapies and hematopoietic stem cell transplantation, as well as the treatment of heart, pancreas, liver, muscle, and neurologic disorders. However, successful cell transplantation will require optimizing the best cell type and site for engraftment, overcoming limitations to cell migration and tissue integration, and possibly needing to control immunologic reactivity (challenges indicated in red). iPSC, induced PSC; ES cells, embryonic stem cells.

The list of author affiliations is available in the full article online.
*Corresponding author. E-mail: foxi@upmc.edu
Cite this article as I. J. Fox *et al.*, *Science* 345, 1247391 (2014); DOI: 10.1126/science.1247391

REVIEW

STEM CELL THERAPY

Use of differentiated pluripotent stem cells in replacement therapy for treating disease

Ira J. Fox,[1]* George Q. Daley,[2,3,4] Steven A. Goldman,[5,6] Johnny Huard,[7] Timothy J. Kamp,[8] Massimo Trucco[9]

Pluripotent stem cells (PSCs) directed to various cell fates holds promise as source material for treating numerous disorders. The availability of precisely differentiated PSC-derived cells will dramatically affect blood component and hematopoietic stem cell therapies and should facilitate treatment of diabetes, some forms of liver disease and neurologic disorders, retinal diseases, and possibly heart disease. Although an unlimited supply of specific cell types is needed, other barriers must be overcome. This review of the state of cell therapies highlights important challenges. Successful cell transplantation will require optimizing the best cell type and site for engraftment, overcoming limitations to cell migration and tissue integration, and occasionally needing to control immunologic reactivity, as well as a number of other challenges. Collaboration among scientists, clinicians, and industry is critical for generating new stem cell–based therapies.

Induced pluripotent stem cells (PSCs) are generated by reprogramming somatic cells to a pluripotent state by transient expression of pluripotency factors. These cells can self-renew indefinitely and are able to differentiate into any cell lineage (*1*, *2*). The ability to generate PSCs from individual patients and differentiate them into an unlimited supply of tissue and organ-specific cells capable of circumventing immunologic rejection after transplantation could facilitate development of cell-based therapies for the treatment of a variety of debilitating disorders and dramatically change the practice of medicine.

Before these cells can be used in the clinic, a variety of barriers must be overcome. For many diseases, it is not yet possible to differentiate PSCs to cells with characteristics identical to those in the organs that need replacement. There are also challenges like scaling up production, eliminating cells with tumor-forming potential, and decreasing the time needed for expansion, differentiation, selection, and testing. Furthermore, treatment of a genetic mutation using autologous cells will often require genetic manipulation, which might result in changes that could increase cancer risk.

Some form of immune suppression may also be required to control cell loss after transplantation, whether due to rejection, an immune response to a genetically corrected protein, or recurrence of autoimmunity, with destruction of the transplant, as might be the case for diabetes. The standard signs of rejection used in solid organ transplantation are not likely to be useful because the sensitivity of functional changes has been shown, after islet transplantation, to be inadequate to diagnose rejection before damage to the engrafted cells is irreversible (*3*). Of course, it might be possible to engineer PSC-derived grafts, with the usual caveats concerning activating oncogenes, so that they would be immunologically inert and identifiable by an array of imaging strategies.

Although decades of laboratory and clinical investigation have led to successful therapies using hematopoietic cells, few other cell therapies have transitioned from experimental to standard clinical care. Here, we discuss the present state of cell therapy in the context of having available differentiated PSC-derived cells. The "gold standard," blood and hematopoietic stem cell (HSC) transplantation, is highlighted first, followed by an examination of cell therapy for diabetes, liver disease, neurologic and retinal disorders, muscular dystrophies, and heart disease.

Hematopoietic cell-based therapies

Many of the principles of cell transplantation derive from our long experience with transfusion of blood products. Infused red blood cells (RBCs), platelets, and HSCs are the most widely employed cellular therapies in use today. The relative ease of HSC transplantation (HSCT) derives in large part from the intrinsic potential of HSCs to home to and integrate into native niches, give rise to differentiated progeny, and thereafter to egress into the circulation. Thus, HSCT avoids the challenges of restoring integrity and function of more anatomically complex organs like the lung, heart, liver, and brain.

Despite the successes of HSCT, isolated HSCs cannot be expanded to the degree needed, although there has been limited success with cord blood. Furthermore, allogeneic HSCT is associated with considerable treatment-related morbidity and mortality. Thus, transplantation with autologous HSCs for the same indications would eliminate the major morbidities of immune mismatch and could potentially expand the range of conditions, including cancers, amenable to HSCT. One of the most promising applications of somatic cell reprogramming is the production of customized pluripotent stem cells followed by gene correction (*4*), differentiation into HSCs, and autotransplant with intention to cure any one of dozens of inherited genetic disorders of the blood-forming system. Such a proof of principle has been achieved for treating murine models of severe combined immune deficiency and sickle cell anemia (*4*, *5*). HSCs have been derived from murine embryonic stem cells that manifest the cardinal features of clonal self-renewal and multilineage lymphoid-myeloid engraftment in primary and secondary irradiated hosts (*6*, *7*). The derivation of HSCs from human PSCs has proven elusive, although several examples of low-level engraftment have been reported (*8*–*10*). Although true HSCs are not yet available, methods exist to produce RBCs (*11*, *12*) and platelets (*13*) in vitro that are suitable for transfusion. To eliminate the costly and sometimes unreliable system of volunteer blood supply, as well as the risk of transmission of infectious agents, a reliable method for generating an inexhaustible, uniform supply of pathogen-free blood products has tremendous appeal. Ultimately, advances in in vitro cell manufacture should soon be able to reduce costs and enable an off-the-shelf supply.

Diabetes

One of several approaches to resolving the long-term complications associated with diabetes has been beta cell replacement by allogeneic whole-pancreas or isolated pancreatic islet transplantation, using immune suppression in an attempt to control rejection and recurrent autoimmune destruction of the transplanted tissue. Cadaver pancreas transplantation has been

[1]Department of Surgery, Children's Hospital of Pittsburgh and McGowan Institute for Regenerative Medicine, University of Pittsburgh, Pittsburgh, PA, USA. [2]Boston Children's Hospital and Dana Farber Cancer Institute, Boston, MA, USA. [3]Department of Biological Chemistry and Molecular Pharmacology, Harvard Medical School Broad Institute, Cambridge, MA, USA. [4]Howard Hughes Medical Institute, Chevy Chase, MD, USA. [5]Center for Translational Neuromedicine, The University of Rochester Medical Center, Rochester, NY, USA. [6]Center for Basic and Translational Neuroscience, University of Copenhagen, Denmark. [7]Stem Cell Research Center, Department of Orthopaedic Surgery, University of Pittsburgh, School of Medicine, Pittsburgh, PA, USA. [8]Stem Cell and Regenerative Medicine Center, Cellular and Molecular Arrhythmia Research Program, Department of Medicine, School of Medicine and Public Health, University of Wisconsin, Madison, WI, USA. [9]Division of Immunogenetics, Children's Hospital of Pittsburgh, University of Pittsburgh, Pittsburgh, PA, USA.
*Corresponding author. E-mail: foxi@upmc.edu

shown to reduce the complications associated with type 1 diabetes. However, it is a complex surgical procedure associated with morbidity and measureable mortality (*14*). An important lesson from this experience, however, is that conventional immune suppression is able to inhibit recurrent destruction of insulin-producing cells while controlling allograft rejection.

After years of laboratory and clinical investigation, islet transplantation has become a realistic alternative therapy, which, over the past several decades has become increasingly more successful (*15*–*17*). Experience with autologous islet transplantation after total or near-total pancreatic resection for severe chronic pancreatitis and allogeneic islet transplantation for type 1 diabetes have both been instructive (*18*). The preferred site for implantation is the liver, and engraftment is accomplished by minimally invasive transcutaneous catheter infusion through the liver into the portal vein. This approach is associated with a small but measureable risk of hemorrhage and partial portal vein thrombosis. More important, an immediate blood-mediated inflammatory response and pathologic activation of the coagulation system results in a large loss of the infused islets as soon as they come into direct contact with blood (*19*). As the yield of islets from a chronically injured pancreas is already reduced, this constitutes a limiting factor in trying to reach an islet mass sufficient for insulin independence after autologous islet transplantation. It is also a serious issue after islet allotransplantation, where success often requires multiple infusions from different donors and transplantation of a much greater islet mass to achieve insulin independence. Although it is not completely understood why so many more islets are required for initial success in allo- than for autotransplants, this barrier to successful insulin replacement by cell therapy should be resolvable with an inexhaustible supply of donor beta cells.

Failure to achieve long-term insulin independence is more problematic. Five-year insulin independence rates after islet allotransplantation in selected centers are approaching 50% (*17*, *20*). These improved outcomes have resulted from the transplantation of a larger islet mass and more effective control of rejection and autoimmunity, with late graft loss being attributed to toxicity to beta cells arising from medications that suppress immunity and an inability to diagnose or treat recurrent disease or rejection. Advances in donor cell imaging by genetic engineering of PSCs and the development of new strategies for controlling the immune response should resolve some of these issues.

However, experience with islet autotransplantation indicates a more serious problem for long-term function of engrafted islet cells, independent of the need to control rejection or recurrent autoimmune destruction (*21*). Although short-term insulin independence has been accomplished, almost all patients are back on insulin therapy after 5 years. This loss of graft function may be attributable to chronic stimulation of an initially marginal intrahepatic beta cell mass that produces metabolic deterioration and loss of beta cells (*18*). Transplantation of a larger mass of islets may alleviate this problem and result in indefinite graft function. However, the site of engraftment in the liver may also be responsible for poor long-term survival. Islets ectopically engrafted in the liver are known to produce a number of pathologic histologic abnormalities, including extensive amyloid deposition within the islets (*22*). Thus, it remains unclear whether whole islets can remain functionally intact in the liver over time.

The use of PSC-derived beta cells could resolve many of the above issues. Beta cells that have been dissociated and isolated from intact islets successfully engraft within the liver lobule. This is in contrast to how intact islets engraft, which is by partially remaining within the portal circulation (Fig. 1) and requiring neovascularization. Isolated cells may not be as susceptible to forming amyloid deposits, and transplantation of a large mass of individual beta cells might avoid metabolic exhaustion and apoptosis. Dissociated cells do not, however, engraft when infused as individual beta cells but require reaggregation (*23*). In addition, individual beta cells function less well when isolated. It has been reported that more insulin by a factor of 30 is released from beta cells within intact islets as compared with that released from purified single beta cells, and reaggregated beta cells and beta cells aggregated with alpha cells respond better to glucose challenge by a factor of 4 than do single beta cells alone (*24*). Thus, to treat type 1 diabetes, it may be necessary to transplant PSC-derived beta cells as aggregates or possibly to transplant them with PSC-derived non–beta cells.

Whether PSC–derived surrogate beta cells will have the same capacity to engraft in the liver-like primary beta cells is not known. Because they are small, they might pass through the liver into the lungs, as has been described after hepatocyte transplantation. Other sites of transplantation, like the gastric submucosal space, might offer some advantages over the portal vein (Fig. 2).

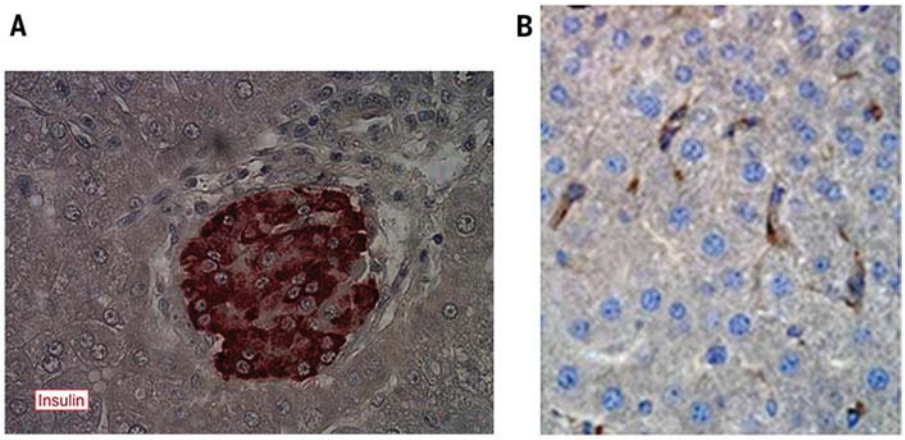

Fig. 1. Comparison of intrahepatic engraftment of intact islets versus isolated beta cells after intraportal transplantation. (**A**) Transplanted islet (in brown) within the blood vessel of the liver after intraportal transplantation [From (*28*), with permission]. (**B**) Induced PSC-derived beta cells (in brown) engraft as cells scattered throughout the liver parenchyma [From (*150*), with permission].

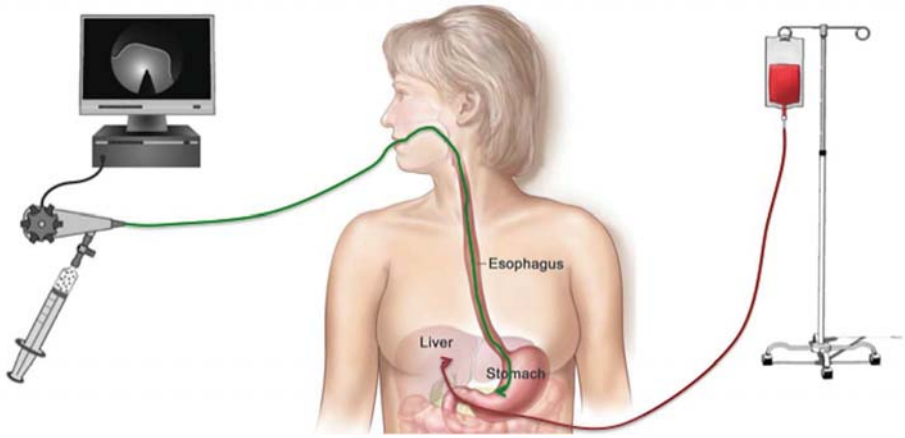

Fig. 2. Transplantation of insulin-producing cells. Illustration of traditional portal-vein infusion of insulin-producing cells for engraftment in the liver versus endoscopic placement of transplanted cells in the gastric submucosal space.

Surrogate beta cells could be implanted in the gastic submucosal space endoscopically, where they would be accessible for biopsy to monitor the graft status (*25*).

Without concomitant use of immune suppression, autoimmunity will mediate destruction of grafts composed of even autologous cells (*26*). Whether autoimmunity can be suppressed in a way that is less detrimental to the insulin-producing cells than conventional drug-based allogeneic protection is as yet unknown. Strategies for potentially controlling this process by inducing tolerance are in development (*27*). To modulate immunologically mediated problems, transgenes might help confer long-term function and reduce early loss of the graft in diabetic recipients. Candidates for this approach are like the ones targeting the tissue factor and coagulation cascade, or exerting anti-inflammatory activity, that have already been tested in cloned pigs (*28*). An alternative approach is to encapsulate the PSC-derived insulin-producing surrogates, providing a protective barrier from immune rejection and autoimmunity while allowing free exchange of nutrients, waste, and, most important, insulin and glucose. Unfortunately, thus far these approaches have shown mixed results, at least after transplantation of intact islets in diabetic patients with low levels of circulating C-peptide, and rarely achieve full and lasting insulin independence (*29*). A variation on this encapsulation and transplant strategy, using PSC-derived beta cells, will soon be tested in clinical trials for the treatment of type 1 diabetes (*30*).

Liver Disease

Hepatocyte transplantation holds great promise as a therapy for individuals with life-threatening liver diseases, where organ transplantation is often the only available treatment option. Patients with both acute liver failure and liver-based inborn errors of metabolism, leading to life-threatening extrahepatic complications, are ideal candidates for cell therapy. Numerous studies in rodents have shown that hepatocyte transplantation can reverse acute fulminant hepatic failure (*31*) and correct liver-based metabolic deficiencies (*32*–*37*). Because the native architecture of the liver is intact in these diseases, the transplant procedure involves simple injection of hepatocytes through the portal vein into the liver, where the cells integrate into the host liver and are indistinguishable from the native liver cells (*38*, *39*). Infusion of hepatocytes is a minimally invasive procedure, so it can be performed on severely ill patients with relatively low risk. Because the native liver is not removed, the transplanted hepatocytes only need to improve liver function enough to stabilize a patient with acute liver failure until their own liver is able to regenerate or to replace the enzyme deficiency that is missing in liver-based metabolic disorders, a goal similar to that of gene therapy.

Clinical trials of hepatocyte transplantation have only demonstrated the long-term safety of the procedure (*40*–*46*). Transplanted hepatocytes have not restored liver function enough to circumvent the need for organ replacement in patients with liver failure, and transplantation has only resulted in partial correction of metabolic disorders (*47*). Efficacy has been limited by relatively poor initial and long-term engraftment and an inability to monitor graft function in real time, which makes diagnosing and treating rejection nearly impossible. In acute liver failure, the severity of liver dysfunction requires that the transplanted hepatocytes function immediately, and the lack of a clinically relevant disease model means that the number of cells that need to engraft to reverse hepatic failure is essentially unknown (*48*, *49*). Although animal models of metabolic liver disease recapitulate the human processes better, achieving an adequate level of engraftment is still a problem because the number of donor cells that can be safely transplanted into the liver at any one time is small, usually less than 1% of the liver mass (*50*). Transplantation of a larger number of cells can lead to severe portal hypertension and translocation of cells into the systemic circulation with embolization to the lungs. Liver-directed radiation has been proposed as a way to facilitate repopulation of the native liver by transplanted hepatocytes, whose viability is relatively short once isolated (*51*). Preparative radiation inhibits host hepatocyte proliferation and induces postmitotic hepatocyte death, allowing donor hepatocytes to preferentially proliferate and repopulate the irradiated host liver. This strategy has been employed to completely correct a rodent model of Crigler-Najjar syndrome (*52*).

An immediately available, inexhaustible supply of functioning donor hepatocytes would allow early intervention in patients with hepatic failure and would allow hepatocytes to be infused over a longer period of time. It is possible that daily large-scale portal-vein PSC-derived hepatocyte infusions could provide the hepatocyte mass necessary to normalize the encephalopathy, coagulation defects, and other life-threatening consequences of hepatic failure and completely correct liver-based enzyme deficiencies. In addition, unrestricted availability of donor hepatocytes could allow treatment of patients with less severe, but debilitating, liver-based metabolic disorders, which are not now considered candidates for organ transplantation, such as phenylketonuria and partial urea cycle disorders. Whether acute hepatic failure is associated with changes in the local microenvironment that might interfere with engraftment and function of transplanted hepatocytes is not yet known and will need to be addressed with further clinical experience.

Although PSC-derived hepatocytes may help advance cell therapies for acute liver failure and metabolic liver diseases, the vast majority of patients who are in need of life-saving intervention are patients with end-stage cirrhosis and chronic hepatic failure. After infusion through the portal vein, hepatocytes have a difficult time entering the hepatic cords through the pathologically expanded extracellular matrix (Fig. 3) present in advanced cirrhosis (*53*). As a result, transplantation by this route generates severe portal hypertension and may produce portal thrombosis. Animal studies suggest that transplantation by direct injection into an extrahepatic site, such as the spleen, can circumvent this engraftment difficulty, improve liver function, and prolong survival in end-stage cirrhosis (*43*, *54*, *55*). Even then, however, transplanted hepatocytes

Fig. 3. Cirrhosis and chronic liver failure. Normal control liver (behind) and liver with advanced cirrhosis (in front), highlighting the structural differences that make liver failure from cirrhosis difficult to treat by intrahepatic cell therapy [Images courtesy of R. Markin, University of Nebraska Medical Center].

provide function for only a period of months. Because it is not clear that transplanted cells can function for any sustained period of time in the abnormal environment produced by hepatic failure and portal hypertension, the same fate may await hepatocytes transplanted into other extra-anatomic locations, such as the lymph node (*56*), although diversion of the portal circulation may be able to enhance survival (*55*, *57*). For a variety of reasons, anecdotal reports of hepatocyte transplantation in humans with end-stage cirrhosis has not produced any measurable level of success (*58*). Treatment of chronic liver failure might benefit from transplantation of a large mass of hepatocytes into a decellularized human or animal liver scaffold (*59*). When repopulated with donor hepatocytes and nonparenchymal cells, the biohybrid graft might then be vascularized through the portal circulation as an engineered internal auxiliary liver graft. Because this strategy would leave the native cirrhotic liver in place, it would still leave unresolved the management of coexisting portal hypertension and the risk of developing hepatocellular carcinoma in the native liver.

Neurologic and retinal diseases

The brain is arguably the most difficult of organs in which to employ stem cell–based therapeutics; the myriad connections of its neurons and their complex interdependency with macroglia, including astrocytes, oligodendrocytes, and glial progenitor cells, defy precise structural reconstitution. Neurodegenerative disorders, in particular, include diseases of both single and multiple phenotypes, the heterogeneity of which can dictate how amenable each might be to cell-based therapeutics. Some prototypic degenerative dementias, such as Alzheimer's disease and Lewy body disease, involve a multitude of neuronal phenotypes—and in some cases glial as well, in multisystem atrophy. These multiphenotypic disorders span anatomic and functional domains and may exhibit both contiguous and transsynaptic patterns of spread. For these reasons, they remain poor targets for neuronal replacement strategies, at least for the near future.

However, many diseases of the brain involve single cell types, and these conditions lend themselves to phenotype-specific cell replacement, whether by transplantation or by the induction of endogenous neural stem or progenitor cells (*60*) (Fig. 4). Degenerative disorders in which the loss of single phenotypes predominate, especially those in which a single region is differentially affected—such as Parkinson's disease (PD), in which nigrostriatal neurons are lost before other neurons, and Huntington's disease (HD), in which medium spiny neuronal loss and striatal atrophy become apparent long before the onset of cortical neuronal loss—have proven more amenable to phenotype-specific cell replacement (*61*, *62*). Memory disorders, which can involve loss of the basal forebrain cholinergic neurons projecting to the hippocampus, have responded to PSC-derived cholinergic neuronal replacement in rodents (*63*). Yet the memory loss of early Alzheimer's and frontotemporal dementia typically heralds

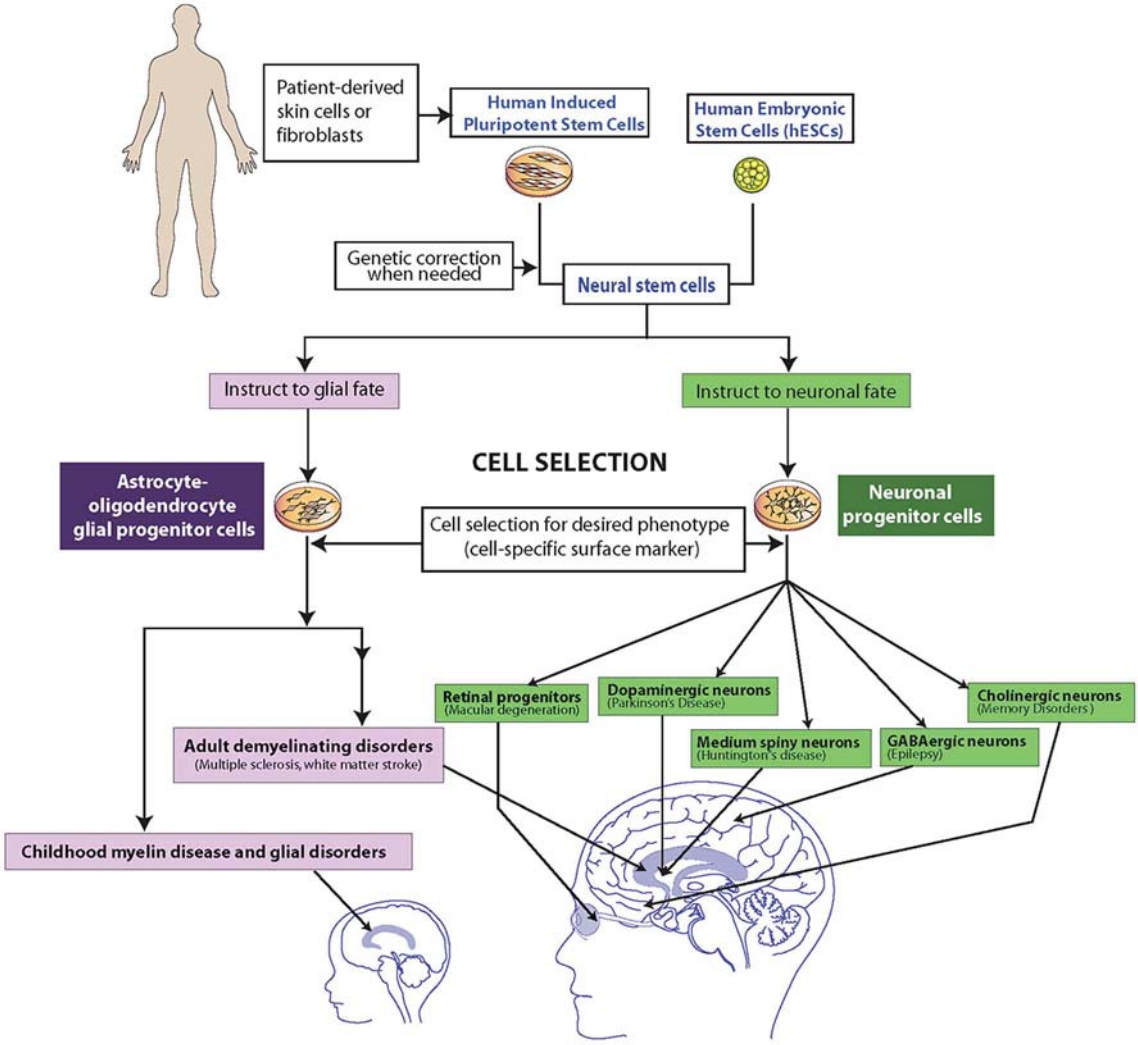

Fig. 4. PSC-derived glial and neural cells. Schematic representation of how PSC-derived glial and neural cells populations might be employed to treat a vast array of neurologic and retinal diseases.

deterioration across all cognitive modalities; thus, isolated replacement of cholinergic neurons is likely to prove effective in only very selected cases of memory loss, which remain difficult to identify at the onset. Nonetheless, for each of these subcortical neuronal phenotypes, animal studies have proven sufficiently promising to justify both the production of cells appropriate for clinical transplantation and the design of clinical trials by which to evaluate their safety and efficacy.

Clinical trials of cell transplantation have already been performed in PD and HD (*61*, *62*). These trials used fetal tissue dissected from the regions of interest, so that the specific cell types needed comprised but a fraction of the cells delivered. Perhaps as a result, these early trials yielded largely disappointing results with considerable variability in outcome and frequent untoward side effects, the most prominent being refractory dyskinesias after fetal mesencephalic tissue grafts in PD. Nonetheless, some transplanted PD patients did experience durable benefit, providing at least a proof of principle in favor of dopaminergic neuronal transplantation. The generation of midbrain dopaminergic neurons (*64*, *65*) and medium spiny neurons (*66*, *67*) from human PSCs (*64*–*67*) thus permit a leap forward in the availability of well-defined engraftable neurons of relative phenotypic homogeneity. This advance should enable a new generation of therapeutic trials less compromised by donor variability and compositional heterogeneity.

Some disorders affect single neuronal types but are so dispersed throughout the central nervous system (CNS) as to present problems of delivery. Several primary epilepsies may derive from deficits in γ-aminobutyric acid (GABAergic) interneuron numbers and function. A number of groups have asked whether transplantation of healthy, migration-competent interneurons into epileptic cortex may provide benefit to patients with medication-refractory epilepsy. The production of GABAergic interneurons from PSCs (*68*) has permitted assessment of this promising approach to epileptic therapy. That said, GABAergic neurons comprise a plethora of functionally distinct phenotypes, thus rendering the effects of their transplantation on host neural circuits unpredictable.

Phenotype-specific disorders of the eye may prove more straightforward targets for cell therapy. Loss of the retinal pigment epithelium (RPE) in age-related macular degeneration has been a particular target of interest in that efficient protocols for generating RPE cells from PSCs have been developed (*69*, *70*). PSC-derived RPEs are now in trials for macular degeneration. As more efficient protocols are developed for producing specific retinal phenotypes from PSCs, a broad variety of both intrinsic retinal disorders and optic neuropathies may prove appropriate targets for cell replacement.

Other disorders of single phenotype are not attractive as targets for cell-based therapy because of their multicentric pathology, the nonmigratory nature of potential replacement cells, or both. The motor neuronopathies, such as amyotrophic lateral sclerosis (ALS) and spinal muscular atrophy, are examples. Spinal motor neurons may be generated from PSCs (*71*–*73*), and yet their clinical utility has been limited by the multisegmental nature of motor neuron loss in these diseases and by our current inability to direct long-distance axonal regrowth and target reinnervation. Cell-based treatment approaches for ALS have thus shifted away from neuronal replacement toward the delivery of astrocytes, with the goal of correcting underlying glial metabolic deficiencies that may contribute to disease progression in ALS (*74*). If successful, such studies may herald the use of PSC-derived glia for ALS and related disorders, in which neurons may be the paracrine victims of glial dysfunction.

Diseases of glia may prove especially accessible targets for cell-based therapy. The myelin diseases, which involve the loss or dysfunction of oligodendrocytes, are among the most prevalent and disabling conditions in neurology and may be particularly appropriate targets for replacement (*75*). They include multiple sclerosis and white matter stroke, the cerebral palsies, and the hereditary pediatric leukodystrophies. As a result, oligodendrocyte progenitor cells (OPCs), which can give rise to myelinogenic oligodendrocytes, have become of great interest as potential therapeutic agents (*76*–*78*). Recently, transplantation of OPCs derived from human PSCs rescued otherwise lethally hypomyelinated shiverer mice (*79*). As such, one might expect that efforts under way using tissue-derived cells to treat myelin disorders, such as childhood Pelizaeus-Merzbacher disease (*80*) and adult progressive multiple sclerosis, may be supplanted by PSC-derived OPCs.

Because OPCs produce astrocytes as well as oligodendrocytes and are highly migratory, they might prove useful in rectifying the demyelination-associated enzymatic deficiencies of the lysosomal storage disorders, such as Krabbe disease, metachromatic leukodystrophy, and Tay-Sachs disease, as well as the astrocytic pathology of vanishing white matter disease (*81*). In particular, transcription activator-like effector nuclease (TALEN) and clustered regularly interspaced short pallendromic repeats (CRISPR)/Cas gene editing technologies (*82*) may allow correction of mutations in PSCs, thus allowing autologous and allogeneic therapy to be assessed across the entire range of hereditary leukodystrophies.

Their promise notwithstanding, introducing PSC-derived cells into the postnatal and mature CNS has its own set of risks, which include immune rejection, the induction of neuroepithelial neoplasms and teratomas (*65*, *80*, *83*), heterotopic neuronal differentiation and epileptogenesis, and the mass effect that may accompany exuberant cell expansion. Neural stem cells have been reported to have escaped to the ventricular system and subarachnoid space, adventitious growths that may present a risk of hydrocephalus, syringomyelia, or surface venous compression, as well as disruption of cerebrospinal fluid flow and waste clearance. The list goes on and serves to highlight the degree to which we must always be concerned that any cell therapeutic not result in unintended consequences.

Muscular Dystrophies

Duchenne muscular dystrophy (DMD) is a devastating, heritable X-linked muscle disease characterized by progressive muscle weakness due to the lack of dystrophin expression at the sarcolemma of muscle fibers (*84*–*87*). Although various approaches have been investigated for delivering dystrophin to dystrophic muscle, there is still no effective treatment that alleviates progression of the disease. Satellite cells play a key role in development of skeletal muscle during embryogenesis and in regeneration of muscle fibers during postnatal life. Upon isolation and culturing, satellite cells re-enter the cell cycle as myoblasts and eventually fuse to form myotubes in vitro (*88*). Transplantation of normal myoblasts into dystrophin-deficient muscle can create a reservoir of normal myoblasts capable of fusing with one another and with dystrophic muscle fibers, restoring dystrophin to the muscle (*89*–*97*).

Myoblast transplantation in animal models and DMD patients can transiently deliver dystrophin and improve the strength of injected dystrophic muscle, but this approach is hindered by poor cell survival and limited migration of injected cells from the original injection site (*89*–*97*). Researchers have used preparative irradiation or injection of myonecrotic agents into the transplantation site to improve efficiency (*89*–*98*), and although these approaches have led to an improvement in restoration of dystrophin in *mdx* mice, success remains limited.

Many scientists consider satellite cells to be the only myogenic cells responsible for muscle growth, regeneration, and repair; however, reports suggest that other cell populations may be able to support muscle regeneration, making them a potential alternative source of cells (*99*–*103*). Cells from bone marrow (*101*, *103*), blood vessels (*100*, *104*–*106*), the neuronal compartment (*99*, *102*), and connective tissue can differentiate toward a myogenic lineage, suggesting that transplantation of these nonsatellite cell populations could be effective in improving muscle regeneration (*107*). Animal studies have shown that many have a very limited capacity to enhance muscle regeneration after transplantation; however, mesoangioblasts, pericytes, and muscle-derived stem cells (MDSCs) survive postimplantation (Fig. 5) and repair skeletal muscle after injury and disease (*96*, *100*, *104*–*106*, *108*). As a result, their human counterparts have been isolated and are undergoing clinical trials for the treatment of stress urinary incontinence (*108*, *109*).

Most cell therapies for treating DMD employ an intramuscular route of administration; however, systemic delivery would be a far superior method because it is the heart, intercostal muscles, and diaphragm that are involved in the early death of DMD patients and are almost impossible to reach by intramuscular injection. Systemic delivery of stem cells can achieve widespread delivery and leads to dystrophin expression in various muscle groups, although with varying

levels of success (*110*). This technology is still under development and is technically challenging, especially when using small-animal models (*110*, *111*).

Although most cell transplant studies for DMD have focused on the use of postnatal stem cells, the progeny of PSCs may eventually be useful for muscle regeneration and repair. A number of stem cell lineages can be easily generated in vitro, but differentiation into skeletal muscle has proven to be difficult (*112*–*116*). PSCs transfected with myogenic regulatory factors, in particular Pax3 and Pax7, undergo partial myogenic differentiation and participate in skeletal muscle regeneration (*117*, *118*), whereas MyoD and Myf5 have also been used to produce myoblasts from normal and dystrophic human PSCs (*119*). Intramuscular transplantation of human skeletal myogenic progenitors derived from PSCs results in durable engraftment, contributing to the satellite cell pool (*120*). Furthermore, PSCs derived from patients with muscular dystrophies, differentiated into satellite and mesoangioblast-like cells, have been genetically corrected and, after reintroduction into dystrophic mice, ameliorate their dystrophic phenotype (*121*, *122*). Although PSCs have the potential to create an inexhaustible source of therapeutic cells for muscle repair, the availability of large numbers of muscle progenitor cells has not been a major limitation. Poor cell survival and the limited ability of the cells to migrate from their initial site of injection remain the two major hurdles to muscle cell–based therapies, even using PSC-derived cell populations.

Finally, despite the lack of dystrophin at birth, the initiation of acute, severe muscle weakness does not occur in DMD patients until they have reached the age of 4 to 8 years, which coincides with gradual exhaustion of their muscle progenitor cells (MPCs). Impairment in the myogenic potential of the MPCs isolated from DMD muscle in various animal models has been described (*123*–*125*), and recent studies indicate that sparing of the extraocular muscles in DMD patients may be related to the existence of a subpopulation of MPCs that that do not become exhausted with age, indicating that muscle weakness in DMD patients is related to MPC exhaustion during disease progression (*126*). These findings, taken together, suggest that a relationship likely exists between the rapid progression of muscular dystrophy and stem cell exhaustion, and the development of cell therapeutic approaches to delay the exhaustion of MPCs may represent an important alternative avenue to explore for delaying the onset of pathologies associated with muscular dystrophies.

Heart Disease

Heart disease is the most common cause of death worldwide. Because the disease can result in the replacement of contractile cardiomyocytes (CMs) with scar tissue, cellular and regenerative therapies hold great promise. A wide variety of cell types have been investigated for their ability to repair the heart. These include skeletal myoblasts, bone marrow–derived cells, cardiac stem cells, and mesenchymal stem cells (*127*). Most effort has focused on treating ischemic heart disease by infusing cells intravascularly (intravenous, intracoronary, or retrograde coronary sinus), by intramyocardial injection (transendocardial catheter–based injection or epicardial injection), or by scaffold or patch-based epicardial delivery to the myocardium (*127*).

When skeletal myoblasts are transplanted by direct epicardial injection into the heart, they form stable skeletal muscle grafts that do not couple to the native cardiac muscle (*128*), and clinical experience in the setting of coronary artery bypass surgery has not demonstrated significant benefit (*129*). Initial studies in a post–myocardial infarction (MI) mouse model showed that injection of bone marrow–derived c-kit$^+$ and lineage negative (lin$^-$) cells dramatically regenerated myocardium and improved cardiac function (*130*). Subsequent studies, however, failed to demonstrate myocardial regeneration using this approach (*131*, *132*). Nevertheless, clinical trials evaluating the ability of bone marrow mononuclear cells (BMNCs) to repair the myocardium were initiated, and phase 1 trials of intracoronary BMNC delivery via the reperfused infarct-related artery hinted at efficacy. Larger phase 2 trials, however, have produced mixed results, ranging from no effect to a modest improvement in ejection fraction (*133*). In small phase 1 trials, mesenchymal stem cells, autologous cardiac stem cells, and cardiosphere-derived cells have similarly shown possible benefit with respect to left ventricular structure and function in patients post-MI with ischemic cardiomyopathy (*133*).

Cell survival and engraftment have been major limitations with adult stem cell sources, and the vast majority of transplanted cells are lost within days in most investigations (*134*). Thus, robust myocardial regeneration has not been observed, and the beneficial effects on cardiac function and structure have been attributed to other mechanisms, largely acting by paracrine signaling to preserve the border zone around the infarction, reduce apoptosis, blunt adverse remodeling, potentially stimulate endogenous stem cells, modulate inflammation, and promote angiogenesis.

PSCs can differentiate into a range of cell types relevant for cardiac repair, including CMs

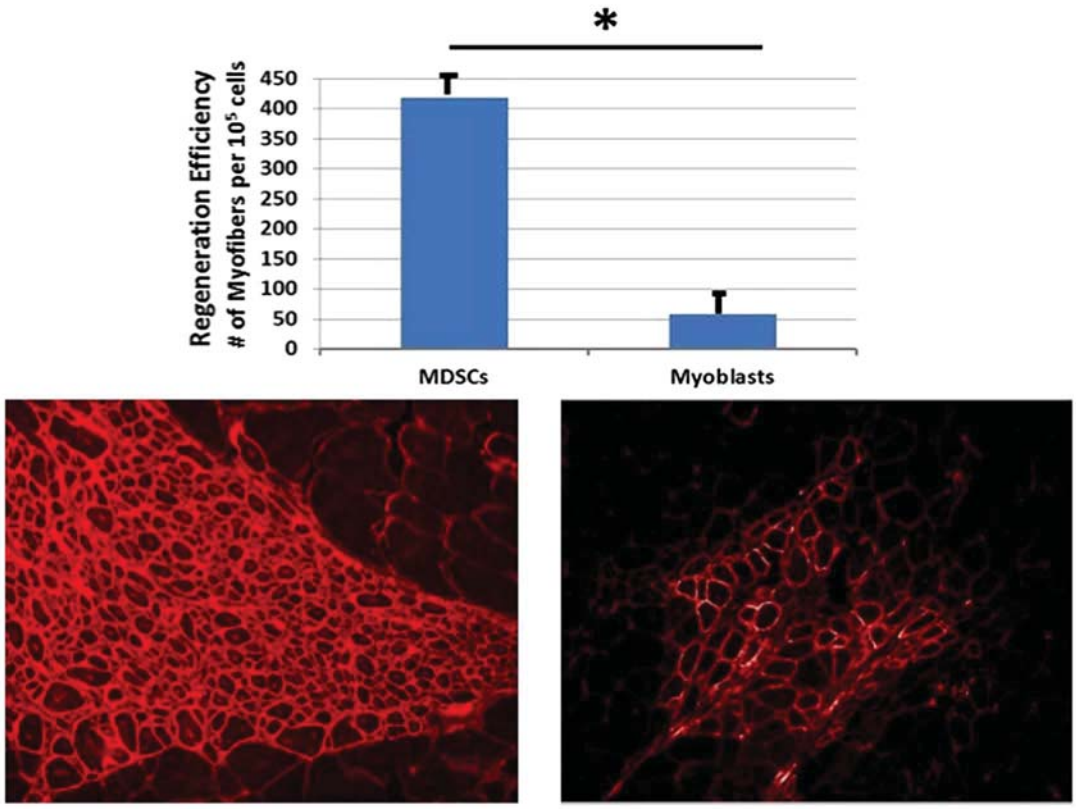

Fig. 5. Importance of cell type for restoration of dystrophin-expressing myofibers. Engraftment efficiency for muscle-derived stem cells (**left**) and myoblasts (**right**) after transplant.

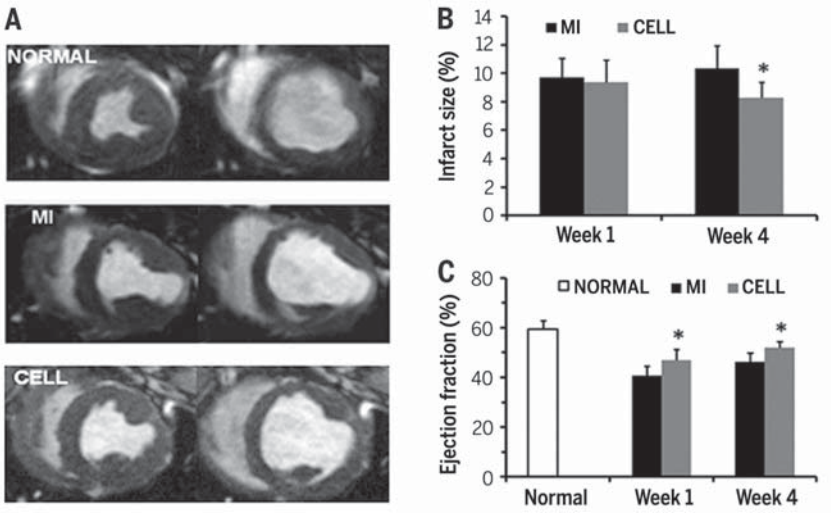

Fig. 6. Fibrin patch–based delivery of human PSC–derived ECs and SMCs. (**A**) Cardiac magnetic resonance image (MRI) from normal, MI, and cell-treatment groups at end systole (left) and end diastole (right). (**B**) After infarction, the cell treatment produced significantly smaller infarct size (delayed-enhancement MRI) and (**C**) improved ejection fraction compared with MI alone. *$P < 0.05$ versus MI alone. Modified from (*147*), with permission.

(*135*), cardiac progenitors (*136*, *137*), endothelial cells (ECs) (*138*), and smooth muscle cells (SMCs) (*138*), which have been tested in small-animal models. Protocols for efficient generation of CMs from human PSCs have been developed (*139*), and purification of CMs has been accomplished using cell surface markers or glucose-free culture conditions optimized for survival of CMs (*140*, *141*). However, PSC-derived CMs are, in general, a mixture of nodal-like, atrial-like and ventricular-like cells (*142*) that have limited proliferative capacity and have a relatively immature phenotype based on electrophysiological characteristics, contractile performance, and metabolic profile. Despite these limitations, mouse PSC–derived CMs are capable of integration into the mouse myocardium, but this is an extremely rare event (*113*). Survival of transplanted PSC-derived CMs has been a limitation, but by modulating multiple cellular processes a prosurvival cocktail was developed, which enabled the survival of human PSC-derived CMs as islands in athymic rat hearts post-MI, improving cardiac function (*143*). Transplanted mouse PSC–derived cardiac progenitors improve the function of infarcted mouse hearts (*144*), and, in guinea pigs, where the heart exhibits an intrinsic heart rate closer to that in man, human PSC–derived CMs engraft and functionally couple to host CMs to improve left ventricular function and reduce ventricular arrhythmias (*145*).

Preclinical studies are beginning to test PSC cell therapy in large-animal models of heart disease. Epicardial delivery of cell sheets composed of PSC-derived CMs in post-MI pig hearts has shown encouraging results (*146*), and epicardial application of human PSC–derived ECs and SMCs, incorporated into a fibrin-based patch, post-MI, to the hearts of immune-suppressed pigs has reduced infarction size and improved left ventricular function (Fig. 6) (*147*). In addition, direct intramyocardial injection of human PSC–derived CMs in immune-suppressed nonhuman primate hearts post-MI has produced large areas of engraftment and electrical coupling, but no clear improvement in cardiac function has been observed (*148*). However, a transient increase in ventricular arrhythmias has occurred, raising a potential safety concern. Transplantation of human PSC–derived cardiac progenitors has been associated with multilineage regeneration in the immunosuppressed rhesus monkey heart post-MI (*149*). Thus, large-animal studies are beginning to define which cell preparations and delivery strategies hold promise.

Overall, clinical studies using adult cell sources have not yet demonstrated robust clinical benefits. Animal studies using PSC-derived cardiac cells, however, have shown promising results, with some evidence of improvement in left ventricular function and structure. Strategies that combine cells with bioengineered patches or decellularized cardiac matrices are now also being explored, especially for use in congenital heart disease. At this time, however, the mechanisms by which different cell populations and delivery strategies affect the various cardiac disease states remain poorly understood, and the optimal cell populations to use and the best delivery strategies for clinical translation have not yet been defined. Further research is required.

Conclusions

As discussed above, the generation of an unlimited supply of specific cell types is crucial for cell and regenerative therapies, because they offer great hope for the treatment of a wide spectrum of diseases. However, numerous challenges remain. Recurrent autoimmunity will probably require immune suppression for some diseases, and it is still unclear which specific cell type will be useful for the treatment of disorders such as DMD and heart disease. Optimization will also be needed for the transplant site, as in diabetes, or when dealing with disruption of the extracellular matrix in treating degenerative diseases, as in chronic liver and heart disease. Finally, when the pathologic process is diffuse and migration of transplanted cells is limited, as is the case with Alzheimer's disease, ALS, and the muscular dystrophies, identifying the best means and location for cell delivery will require further study in many cases. Using autologous cells and genetic engineering should help control rejection and autoimmunity and improve monitoring of short- and long-term engraftment. Despite existing challenges, the availability of an unlimited supply of clinically useful PSC-derived cell populations will facilitate studies into the biology of those cells and will likely assist in the treatment of diabetes, acute hepatic failure, metabolic liver diseases, retinal diseases, PD, HD, and possibly heart disease. Close collaboration between scientists and clinicians, and between academia and industry, will be critical to overcoming remaining challenges to bringing novel therapies to patients in need.

REFERENCES AND NOTES

1. K. Takahashi *et al*., Induction of pluripotent stem cells from adult human fibroblasts by defined factors. *Cell* **131**, 861–872 (2007). doi: 10.1016/j.cell.2007.11.019; pmid: 18035408
2. J. A. Thomson *et al*., Embryonic stem cell lines derived from human blastocysts. *Science* **282**, 1145–1147 (1998). doi: 10.1126/science.282.5391.1145; pmid: 9804556
3. S. Lacotte, T. Berney, A. J. Shapiro, C. Toso, Immune monitoring of pancreatic islet graft: Towards a better understanding, detection and treatment of harmful events. *Expert Opin. Biol. Ther.* **11**, 55–66 (2011). doi: 10.1517/14712598.2011.536530; pmid: 21073277
4. J. Hanna *et al*., Treatment of sickle cell anemia mouse model with iPS cells generated from autologous skin. *Science* **318**, 1920–1923 (2007). doi: 10.1126/science.1152092; pmid: 18063756
5. W. M. Rideout 3rd, K. Hochedlinger, M. Kyba, G. Q. Daley, R. Jaenisch, Correction of a genetic defect by nuclear transplantation and combined cell and gene therapy. *Cell* **109**, 17–27 (2002). doi: 10.1016/S0092-8674(02)00681-5; pmid: 11955443
6. M. Kyba, R. C. Perlingeiro, G. Q. Daley, HoxB4 confers definitive lymphoid-myeloid engraftment potential on embryonic stem cell and yolk sac hematopoietic progenitors. *Cell* **109**, 29–37 (2002). doi: 10.1016/S0092-8674(02)00680-3; pmid: 11955444
7. S. L. McKinney-Freeman *et al*., Surface antigen phenotypes of hematopoietic stem cells from embryos and murine embryonic stem cells. *Blood* **114**, 268–278 (2009). doi: 10.1182/blood-2008-12-193888; pmid: 19420357
8. M. H. Ledran *et al*., Efficient hematopoietic differentiation of human embryonic stem cells on stromal cells derived from hematopoietic niches. *Cell Stem Cell* **3**, 85–98 (2008). doi: 10.1016/j.stem.2008.06.001; pmid: 18593561
9. X. Tian, P. S. Woll, J. K. Morris, J. L. Linehan, D. S. Kaufman, Hematopoietic engraftment of human embryonic stem cell-derived cells is regulated by recipient innate immunity. *Stem Cells* **24**, 1370–1380 (2006). doi: 10.1634/stemcells.2005-0340; pmid: 16456127
10. L. Wang, P. Menendez, C. Cerdan, M. Bhatia, Hematopoietic development from human embryonic stem cell lines. *Exp. Hematol.* **33**, 987–996 (2005). doi: 10.1016/j.exphem.2005.06.002; pmid: 16140146
11. C. Mazurier, L. Douay, H. Lapillonne, Red blood cells from induced pluripotent stem cells: Hurdles and developments. *Curr. Opin. Hematol.* **18**, 249–253 (2011). doi: 10.1097/MOH.0b013e3283476129; pmid: 21519239
12. G. F. Rousseau, M. C. Giarratana, L. Douay, Large-scale production of red blood cells from stem cells: What are the technical challenges ahead? *Biotechnol. J.* **9**, 28–38 (2014). doi: 10.1002/biot.201200368; pmid: 24408610
13. S. Nakamura *et al*., Expandable megakaryocyte cell lines enable clinically applicable generation of platelets from

human induced pluripotent stem cells. *Cell Stem Cell* **14**, 535–548 (2014). doi: 10.1016/j.stem.2014.01.011; pmid: 24529595

14. R. Bottino, M. Trucco, A. N. Balamurugan, T. E. Starzl, Pancreas and islet cell transplantation. *Best Pract. Res. Clin. Gastroenterol.* **16**, 457–474 (2002). doi: 10.1053/bega.2002.0318; pmid: 12079269
15. C. B. Kemp, M. J. Knight, D. W. Scharp, P. E. Lacy, W. F. Ballinger, Transplantation of isolated pancreatic islets into the portal vein of diabetic rats. *Nature* **244**, 447 (1973). doi: 10.1038/244447a0; pmid: 4200461
16. C. Ricordi, P. E. Lacy, E. H. Finke, B. J. Olack, D. W. Scharp, Automated method for isolation of human pancreatic islets. *Diabetes* **37**, 413–420 (1988). doi: 10.2337/diab.37.4.413; pmid: 3288530
17. E. A. Ryan *et al*., Five-year follow-up after clinical islet transplantation. *Diabetes* **54**, 2060–2069 (2005). doi: 10.2337/diabetes.54.7.2060; pmid: 15983207
18. R. Alejandro *et al*., Natural history of intrahepatic canine islet cell autografts. *J. Clin. Invest.* **78**, 1339–1348 (1986). doi: 10.1172/JCI112720; pmid: 3095376
19. B. Nilsson, K. N. Ekdahl, O. Korsgren, Control of instant blood-mediated inflammatory reaction to improve islets of Langerhans engraftment. *Curr. Opin. Organ Transplant.* **16**, 620–626 (2011). doi: 10.1097/MOT.0b013e32834c2393; pmid: 21971510
20. F. B. Barton *et al*., Improvement in outcomes of clinical islet transplantation: 1999-2010. *Diabetes Care* **35**, 1436–1445 (2012). doi: 10.2337/dc12-0063; pmid: 22723582
21. D. E. Sutherland *et al*., Total pancreatectomy and islet autotransplantation for chronic pancreatitis. *J. Am. Coll. Surg.* **214**, 409–424, discussion 424–426 (2012). doi: 10.1016/j.jamcollsurg.2011.12.040; pmid: 22397977
22. G. T. Westermark, P. Westermark, C. Berne, O. Korsgren; Nordic Network for Clinical Islet Transplantation, Widespread amyloid deposition in transplanted human pancreatic islets. *N. Engl. J. Med.* **359**, 977–979 (2008). doi: 10.1056/NEJMc0802893; pmid: 18753660
23. M. E. De Paepe, B. Keymeulen, D. Pipeleers, G. Klöppel, Proliferation and hypertrophy of liver cells surrounding islet grafts in diabetic recipient rats. *Hepatology* **21**, 1144–1153 (1995). doi: 10.1002/hep.1840210438; pmid: 7705790
24. D. G. Pipeleers *et al*., Transplantation of purified islet cells in diabetic rats. I. Standardization of islet cell grafts. *Diabetes* **40**, 908–919 (1991). doi: 10.2337/diab.40.7.908; pmid: 2060727
25. G. J. Echeverri *et al*., Endoscopic gastric submucosal transplantation of islets (ENDO-STI): Technique and initial results in diabetic pigs. *Am. J. Transplant.* **9**, 2485–2496 (2009). doi: 10.1111/j.1600-6143.2009.02815.x; pmid: 19775318
26. Worcester Human Islet Transplantation Group, Autoimmunity after islet-cell allotransplantation. *N. Engl. J. Med.* **355**, 1397–1399 (2006). doi: 10.1056/NEJMc061530; pmid: 17005967
27. R. J. Creusot, N. Giannoukakis, M. Trucco, M. J. Clare-Salzler, C. G. Fathman, It's time to bring dendritic cell therapy to type 1 diabetes. *Diabetes* **63**, 20–30 (2014). doi: 10.2337/db13-0886; pmid: 24357690
28. D. J. van der Windt *et al*., Long-term controlled normoglycemia in diabetic non-human primates after transplantation with hCD46 transgenic porcine islets. *Am. J. Transplant.* **9**, 2716–2726 (2009). doi: 10.1111/j.1600-6143.2009.02850.x; pmid: 19845582
29. S. W. Liao *et al*., Maintaining functional islets through encapsulation in an injectable saccharide-peptide hydrogel. *Biomaterials* **34**, 3984–3991 (2013). doi: 10.1016/j.biomaterials.2013.02.007; pmid: 23465491
30. T. C. Schulz *et al*., A scalable system for production of functional pancreatic progenitors from human embryonic stem cells. *PLOS ONE* **7**, e37004 (2012). doi: 10.1371/journal.pone.0037004; pmid: 22623968
31. A. A. Demetriou *et al*., Transplantation of microcarrier-attached hepatocytes into 90% partially hepatectomized rats. *Hepatology* **8**, 1006–1009 (1988). doi: 10.1002/hep.1840080505; pmid: 3047034
32. J. M. De Vree *et al*., Correction of liver disease by hepatocyte transplantation in a mouse model of progressive familial intrahepatic cholestasis. *Gastroenterology* **119**, 1720–1730 (2000). doi: 10.1053/gast.2000.20222; pmid: 11113093
33. C. G. Groth, B. Arborgh, C. Björkén, B. Sundberg, G. Lundgren, Correction of hyperbilirubinemia in the glucuronyltransferase-deficient rat by intraportal hepatocyte transplantation. *Transplant. Proc.* **9**, 313–316 (1977). pmid: 405772
34. A. J. Matas *et al*., Hepatocellular transplantation for metabolic deficiencies: Decrease of plasms bilirubin in Gunn rats. *Science* **192**, 892–894 (1976). doi: 10.1126/science.818706; pmid: 818706
35. H. E. Rugstad, S. H. Robinson, C. Yannoni, A. H. Tashjian Jr., Transfer of bilirubin uridine diphosphate-glucuronyltransferase to enzyme-deficient rats. *Science* **170**, 553–555 (1970). doi: 10.1126/science.170.3957.553; pmid: 4319199
36. J. C. Wiederkehr, G. T. Kondos, R. Pollak, Hepatocyte transplantation for the low-density lipoprotein receptor-deficient state. A study in the Watanabe rabbit. *Transplantation* **50**, 466–471 (1990). doi: 10.1097/00007890-199009000-00021; pmid: 2144923
37. Y. Yoshida, Y. Tokusashi, G. H. Lee, K. Ogawa, Intrahepatic transplantation of normal hepatocytes prevents Wilson's disease in Long-Evans cinnamon rats. *Gastroenterology* **111**, 1654–1660 (1996). doi: 10.1016/S0016-5085(96)70029-X; pmid: 8942746
38. S. Gupta *et al*., Entry and integration of transplanted hepatocytes in rat liver plates occur by disruption of hepatic sinusoidal endothelium. *Hepatology* **29**, 509–519 (1999). doi: 10.1002/hep.510290213; pmid: 9918929
39. K. P. Ponder *et al*., Mouse hepatocytes migrate to liver parenchyma and function indefinitely after intrasplenic transplantation. *Proc. Natl. Acad. Sci. U.S.A.* **88**, 1217–1221 (1991). doi: 10.1073/pnas.88.4.1217; pmid: 1899924
40. A. Dhawan, J. Puppi, R. D. Hughes, R. R. Mitry, Human hepatocyte transplantation: Current experience and future challenges. *Nat. Rev. Gastroenterol. Hepatol.* **7**, 288–298 (2010). doi: 10.1038/nrgastro.2010.44; pmid: 20368738
41. C. M. Habibullah, I. H. Syed, A. Qamar, Z. Taher-Uz, Human fetal hepatocyte transplantation in patients with fulminant hepatic failure. *Transplantation* **58**, 951–952 (1994). doi: 10.1097/00007890-199410270-00016; pmid: 7940741
42. S. P. Horslen *et al*., Isolated hepatocyte transplantation in an infant with a severe urea cycle disorder. *Pediatrics* **111**, 1262–1267 (2003). doi: 10.1542/peds.111.6.1262; pmid: 12777539
43. M. Mito *et al*., Morphology and function of isolated hepatocytes transplanted into rat spleen. *Transplantation* **28**, 499–505 (1979). doi: 10.1097/00007890-197912000-00013; pmid: 516133
44. M. Mito, M. Kusano, Y. Kawaura, Hepatocyte transplantation in man. *Transplant. Proc.* **24**, 3052–3053 (1992). pmid: 1466053
45. M. Muraca *et al*., Hepatocyte transplantation as a treatment for glycogen storage disease type 1a. *Lancet* **359**, 317–318 (2002). doi: 10.1016/S0140-6736(02)07529-3; pmid: 11830200
46. E. M. Sokal *et al*., Hepatocyte transplantation in a 4-year-old girl with peroxisomal biogenesis disease: Technique, safety, and metabolic follow-up. *Transplantation* **76**, 735–738 (2003). doi: 10.1097/01.TP.0000077420.81365.53; pmid: 12973120
47. I. J. Fox *et al*., Treatment of the Crigler-Najjar syndrome type I with hepatocyte transplantation. *N. Engl. J. Med.* **338**, 1422–1427 (1998). doi: 10.1056/NEJM199805143382004; pmid: 9580649
48. P. N. Newsome, J. N. Plevris, L. J. Nelson, P. C. Hayes, Animal models of fulminant hepatic failure: A critical evaluation. *Liver Transpl.* **6**, 21–31 (2000).pmid: 10648574
49. J. Terblanche, R. Hickman, Animal models of fulminant hepatic failure. *Dig. Dis. Sci.* **36**, 770–774 (1991). doi: 10.1007/BF01311235; pmid: 2032519
50. B. M. Bilir *et al*., Hepatocyte transplantation in acute liver failure. *Liver Transpl.* **6**, 32–40 (2000). doi: 10.1002/lt.500060113; pmid: 10648575
51. H. Zhou *et al*., Repopulation of individual liver lobes by transplanted hepatocytes using regiospecific hepatic irradiation cures jaundice in the Gunn rat model of Crigler-Najjar Syndrome type I. *Hepatology* **50**, 303A (2009).
52. C. Guha *et al*., Normal hepatocytes correct serum bilirubin after repopulation of Gunn rat liver subjected to irradiation/partial resection. *Hepatology* **36**, 354–362 (2002). doi: 10.1053/jhep.2002.34516; pmid: 12143043
53. S. Gagandeep *et al*., Transplanted hepatocytes engraft, survive, and proliferate in the liver of rats with carbon tetrachloride-induced cirrhosis. *J. Pathol.* **191**, 78–85 (2000). doi: 10.1002/(SICI)1096-9896(200005)191:1<78::AID-PATH587>3.0.CO;2-P; pmid: 10767723
54. N. Kobayashi *et al*., Hepatocyte transplantation in rats with decompensated cirrhosis. *Hepatology* **31**, 851–857 (2000). doi: 10.1053/he.2000.5636; pmid: 10733539
55. J. Ribeiro *et al*., Intrasplenic hepatocellular transplantation corrects hepatic encephalopathy in portacaval-shunted rats. *Hepatology* **15**, 12–18 (1992). doi: 10.1002/hep.1840150104; pmid: 1727787
56. T. Hoppo, J. Komori, R. Manohar, D. B. Stolz, E. Lagasse, Rescue of lethal hepatic failure by hepatized lymph nodes in mice. *Gastroenterology* **140**, 656–666.e2 (2011). doi: 10.1053/j.gastro.2010.11.006; pmid: 21070777
57. I. K. Schumacher *et al*., Transplantation of conditionally immortalized hepatocytes to treat hepatic encephalopathy. *Hepatology* **24**, 337–343 (1996). doi: 10.1002/hep.510240209; pmid: 8690402
58. K. A. Soltys *et al*., Barriers to the successful treatment of liver disease by hepatocyte transplantation. *J. Hepatol.* **53**, 769–774 (2010). doi: 10.1016/j.jhep.2010.05.010; pmid: 20667616
59. B. E. Uygun *et al*., Organ reengineering through development of a transplantable recellularized liver graft using decellularized liver matrix. *Nat. Med.* **16**, 814–820 (2010). doi: 10.1038/nm.2170; pmid: 20543851
60. A. Benraiss *et al*., Sustained mobilization of endogenous neural progenitors delays disease progression in a transgenic model of Huntington's disease. *Cell Stem Cell* **12**, 787–799 (2013). doi: 10.1016/j.stem.2013.04.014; pmid: 23746982
61. A. Benraiss, S. A. Goldman, Cellular therapy and induced neuronal replacement for Huntington's disease. *Neurotherapeutics* **8**, 577–590 (2011). doi: 10.1007/s13311-011-0075-8; pmid: 21971961
62. O. Lindvall, Dopaminergic neurons for Parkinson's therapy. *Nat. Biotechnol.* **30**, 56–58 (2012). doi: 10.1038/nbt.2077; pmid: 22231097
63. Y. Liu *et al*., Medial ganglionic eminence-like cells derived from human embryonic stem cells correct learning and memory deficits. *Nat. Biotechnol.* **31**, 440–447 (2013). doi: 10.1038/nbt.2565; pmid: 23604284
64. S. Kriks *et al*., Dopamine neurons derived from human ES cells efficiently engraft in animal models of Parkinson's disease. *Nature* **480**, 547–551 (2011).pmid: 22056989
65. N. S. Roy *et al*., Functional engraftment of human ES cell-derived dopaminergic neurons enriched by coculture with telomerase-immortalized midbrain astrocytes. *Nat. Med.* **12**, 1259–1268 (2006). doi: 10.1038/nm1495; pmid: 17057709
66. A. D. Carri *et al*., Developmentally coordinated extrinsic signals drive human pluripotent stem cell differentiation toward authentic DARPP-32+ medium-sized spiny neurons. *Development* **140**, 301–312 (2013). doi: 10.1242/dev.084608; pmid: 23250204
67. The HD iPSC Consortium, Induced pluripotent stem cells from patients with Huntington's disease show CAG-repeat-expansion-associated phenotypes. *Cell Stem Cell* **11**, 264–278 (2012). doi: 10.1016/j.stem.2012.04.027; pmid: 22748968
68. C. R. Nicholas *et al*., Functional maturation of hPSC-derived forebrain interneurons requires an extended timeline and mimics human neural development. *Cell Stem Cell* **12**, 573–586 (2013). doi: 10.1016/j.stem.2013.04.005; pmid: 23642366
69. D. E. Buchholz *et al*., Rapid and efficient directed differentiation of human pluripotent stem cells into retinal pigmented epithelium. *Stem Cells Transl. Med.* **2**, 384–393 (2013). doi: 10.5966/sctm.2012-0163; pmid: 23599499
70. J. H. Stern, S. Temple, Stem cells for retinal replacement therapy. *Neurotherapeutics* **8**, 736–743 (2011). doi: 10.1007/s13311-011-0077-6; pmid: 21948217
71. N. Singh Roy *et al*., Enhancer-specified GFP-based FACS purification of human spinal motor neurons from embryonic stem cells. *Exp. Neurol.* **196**, 224–234 (2005). doi: 10.1016/j.expneurol.2005.06.021; pmid: 16198339
72. S. Karumbayaram *et al*., Directed differentiation of human-induced pluripotent stem cells generates active motor neurons. *Stem Cells* **27**, 806–811 (2009). doi: 10.1002/stem.31; pmid: 19350680
73. X. J. Li *et al*., Specification of motoneurons from human embryonic stem cells. *Nat. Biotechnol.* **23**, 215–221 (2005). doi: 10.1038/nbt1063; pmid: 15685164
74. A. C. Lepore *et al*., Human glial-restricted progenitor transplantation into cervical spinal cord of the SOD1 mouse model of ALS. *PLOS ONE* **6**, e25968 (2011). doi: 10.1371/journal.pone.0025968; pmid: 21998733
75. S. A. Goldman, M. Nedergaard, M. S. Windrem, Glial progenitor cell-based treatment and modeling of neurological disease. *Science* **338**, 491–495 (2012). doi: 10.1126/science.1218071; pmid: 23112326
76. D. R. Archer, P. A. Cuddon, D. Lipsitz, I. D. Duncan, Myelination of the canine central nervous system by glial cell transplantation: A model for repair of human myelin disease. *Nat. Med.* **3**, 54–59 (1997). doi: 10.1038/nm0197-54; pmid: 8986741
77. M. S. Windrem *et al*., Fetal and adult human oligodendrocyte progenitor cell isolates myelinate the congenitally dysmyelinated

brain. *Nat. Med.* **10**, 93–97 (2004). doi: 10.1038/nm974; pmid: 14702638
78. M. S. Windrem *et al*., Neonatal chimerization with human glial progenitor cells can both remyelinate and rescue the otherwise lethally hypomyelinated shiverer mouse. *Cell Stem Cell* **2**, 553–565 (2008). doi: 10.1016/j.stem.2008.03.020; pmid: 18522848
79. S. Wang *et al*., Human iPSC-derived oligodendrocyte progenitor cells can myelinate and rescue a mouse model of congenital hypomyelination. *Cell Stem Cell* **12**, 252–264 (2013). doi: 10.1016/j.stem.2012.12.002; pmid: 23395447
80. N. Gupta *et al*., Neural stem cell engraftment and myelination in the human brain. *Sci. Transl. Med.* **4**, 155ra137 (2012). doi: 10.1126/scitranslmed.3004373; pmid: 23052294
81. S. A. Goldman, Progenitor cell-based treatment of the pediatric myelin disorders. *Arch. Neurol.* **68**, 848–856 (2011). doi: 10.1001/archneurol.2011.46; pmid: 21403006
82. M. Li, K. Suzuki, N. Y. Kim, G. H. Liu, J. C. Izpisua Belmonte, A cut above the rest: Targeted genome editing technologies in human pluripotent stem cells. *J. Biol. Chem.* **289**, 4594–4599 (2014). doi: 10.1074/jbc.R113.488247; pmid: 24362028
83. M. H. Tuszynski *et al*., Neural stem cell dissemination after grafting to CNS injury sites. *Cell* **156**, 388–389 (2014). doi: 10.1016/j.cell.2014.01.016; pmid: 24485445
84. E. P. Hoffman, R. H. Brown Jr., L. M. Kunkel, Dystrophin: The protein product of the Duchenne muscular dystrophy locus. *Cell* **51**, 919–928 (1987). doi: 10.1016/0092-8674(87)90579-4; pmid: 3319190
85. S. C. Watkins, E. P. Hoffman, H. S. Slayter, L. M. Kunkel, Immunoelectron microscopic localization of dystrophin in myofibres. *Nature* **333**, 863–866 (1988). doi: 10.1038/333863a0; pmid: 3290684
86. K. Arahata *et al*., Immunostaining of skeletal and cardiac muscle surface membrane with antibody against Duchenne muscular dystrophy peptide. *Nature* **333**, 861–863 (1988). doi: 10.1038/333861a0; pmid: 3290683
87. E. E. Zubrzycka-Gaarn *et al*., The Duchenne muscular dystrophy gene product is localized in sarcolemma of human skeletal muscle. *Nature* **333**, 466–469 (1988). doi: 10.1038/333466a0; pmid: 3287171
88. R. Bischoff, Proliferation of muscle satellite cells on intact myofibers in culture. *Dev. Biol.* **115**, 129–139 (1986). doi: 10.1016/0012-1606(86)90234-4; pmid: 3516758
89. J. R. Beauchamp, J. E. Morgan, C. N. Pagel, T. A. Partridge, Dynamics of myoblast transplantation reveal a discrete minority of precursors with stem cell-like properties as the myogenic source. *J. Cell Biol.* **144**, 1113–1122 (1999). doi: 10.1083/jcb.144.6.1113; pmid: 10087257
90. Y. Fan, M. Maley, M. Beilharz, M. Grounds, Rapid death of injected myoblasts in myoblast transfer therapy. *Muscle Nerve* **19**, 853–860 (1996). doi: 10.1002/(SICI)1097-4598(199607)19:7<853::AID-MUS7>3.0.CO;2-8; pmid: 8965839
91. E. Gussoni *et al*., Normal dystrophin transcripts detected in Duchenne muscular dystrophy patients after myoblast transplantation. *Nature* **356**, 435–438 (1992). doi: 10.1038/356435a0; pmid: 1557125
92. J. Huard *et al*., Human myoblast transplantation: Preliminary results of 4 cases. *Muscle Nerve* **15**, 550–560 (1992). doi: 10.1002/mus.880150504; pmid: 1584246
93. G. Karpati *et al*., Dystrophin is expressed in mdx skeletal muscle fibers after normal myoblast implantation. *Am. J. Pathol.* **135**, 27–32 (1989). pmid: 2672825
94. J. R. Mendell *et al*., Myoblast transfer in the treatment of Duchenne's muscular dystrophy. *N. Engl. J. Med.* **333**, 832–838 (1995). doi: 10.1056/NEJM199509283331303; pmid: 7651473
95. J. E. Morgan, E. P. Hoffman, T. A. Partridge, Normal myogenic cells from newborn mice restore normal histology to degenerating muscles of the mdx mouse. *J. Cell Biol.* **111**, 2437–2449 (1990). doi: 10.1083/jcb.111.6.2437; pmid: 2277066
96. Z. Qu *et al*., Development of approaches to improve cell survival in myoblast transfer therapy. *J. Cell Biol.* **142**, 1257–1267 (1998). doi: 10.1083/jcb.142.5.1257; pmid: 9732286
97. J. T. Vilquin, E. Wagner, I. Kinoshita, R. Roy, J. P. Tremblay, Successful histocompatible myoblast transplantation in dystrophin-deficient mdx mouse despite the production of antibodies against dystrophin. *J. Cell Biol.* **131**, 975–988 (1995). doi: 10.1083/jcb.131.4.975; pmid: 7490298
98. Y. Torrente, E. El Fahime, N. J. Caron, N. Bresolin, J. P. Tremblay, Intramuscular migration of myoblasts transplanted after muscle pretreatment with metalloproteinases. *Cell Transplant.* **9**, 539–549 (2000). pmid: 11038070
99. D. L. Clarke *et al*., Generalized potential of adult neural stem cells. *Science* **288**, 1660–1663 (2000). doi: 10.1126/science.288.5471.1660; pmid: 10834848
100. L. De Angelis *et al*., Skeletal myogenic progenitors originating from embryonic dorsal aorta coexpress endothelial and myogenic markers and contribute to postnatal muscle growth and regeneration. *J. Cell Biol.* **147**, 869–878 (1999). doi: 10.1083/jcb.147.4.869; pmid: 10562287
101. G. Ferrari *et al*., Muscle regeneration by bone marrow–derived myogenic progenitors. *Science* **279**, 1528–1530 (1998). doi: 10.1126/science.279.5356.1528; pmid: 9488650
102. R. Galli *et al*., Skeletal myogenic potential of human and mouse neural stem cells. *Nat. Neurosci.* **3**, 986–991 (2000). doi: 10.1038/79924; pmid: 11017170
103. M. F. Pittenger *et al*., Multilineage potential of adult human mesenchymal stem cells. *Science* **284**, 143–147 (1999). doi: 10.1126/science.284.5411.143; pmid: 10102814
104. M. Crisan *et al*., A perivascular origin for mesenchymal stem cells in multiple human organs. *Cell Stem Cell* **3**, 301–313 (2008). doi: 10.1016/j.stem.2008.07.003; pmid: 18786417
105. A. Dellavalle *et al*., Pericytes of human skeletal muscle are myogenic precursors distinct from satellite cells. *Nat. Cell Biol.* **9**, 255–267 (2007). doi: 10.1038/ncb1542; pmid: 17293855
106. B. Zheng *et al*., Prospective identification of myogenic endothelial cells in human skeletal muscle. *Nat. Biotechnol.* **25**, 1025–1034 (2007). doi: 10.1038/nbt1334; pmid: 17767154
107. H. M. Blau, T. R. Brazelton, J. M. Weimann, The evolving concept of a stem cell: Entity or function? *Cell* **105**, 829–841 (2001). doi: 10.1016/S0092-8674(01)00409-3; pmid: 11439179
108. B. Péault *et al*., Stem and progenitor cells in skeletal muscle development, maintenance, and therapy. *Mol. Ther.* **15**, 867–877 (2007). doi: 10.1038/mt.sj.6300145; pmid: 17387336
109. L. K. Carr *et al*., 1-year follow-up of autologous muscle-derived stem cell injection pilot study to treat stress urinary incontinence. *Int. Urogynecol. J. Pelvic Floor Dysfunct.* **19**, 881–883 (2008). doi: 10.1007/s00192-007-0553-z; pmid: 18204978
110. M. Sampaolesi *et al*., Mesoangioblast stem cells ameliorate muscle function in dystrophic dogs. *Nature* **444**, 574–579 (2006). doi: 10.1038/nature05282; pmid: 17108972
111. E. Bachrach *et al*., Systemic delivery of human microdystrophin to regenerating mouse dystrophic muscle by muscle progenitor cells. *Proc. Natl. Acad. Sci. U.S.A.* **101**, 3581–3586 (2004). doi: 10.1073/pnas.0400373101; pmid: 14993597
112. M. Kennedy *et al*., A common precursor for primitive erythropoiesis and definitive haematopoiesis. *Nature* **386**, 488–493 (1997). doi: 10.1038/386488a0; pmid: 9087406
113. M. G. Klug, M. H. Soonpaa, G. Y. Koh, L. J. Field, Genetically selected cardiomyocytes from differentiating embronic stem cells form stable intracardiac grafts. *J. Clin. Invest.* **98**, 216–224 (1996). doi: 10.1172/JCI118769; pmid: 8690796
114. M. Müller *et al*., Selection of ventricular-like cardiomyocytes from ES cells in vitro. *FASEB J.* **14**, 2540–2548 (2000). doi: 10.1096/fj.00-0002com; pmid: 11099473
115. F. Rinaldi, R. C. Perlingeiro, Stem cells for skeletal muscle regeneration: Therapeutic potential and roadblocks. *Transl. Res.* **163**, 409–417 (2014). doi: 10.1016/j.trsl.2013.11.006; pmid: 24299739
116. D. Vittet *et al*., Embryonic stem cells differentiate in vitro to endothelial cells through successive maturation steps. *Blood* **88**, 3424–3431 (1996). pmid: 8896407
117. T. Barberi *et al*., Derivation of engraftable skeletal myoblasts from human embryonic stem cells. *Nat. Med.* **13**, 642–648 (2007). doi: 10.1038/nm1533; pmid: 17417652
118. J. Rohwedel *et al*., Muscle cell differentiation of embryonic stem cells reflects myogenesis in vivo: Developmentally regulated expression of myogenic determination genes and functional expression of ionic currents. *Dev. Biol.* **164**, 87–101 (1994). doi: 10.1006/dbio.1994.1182; pmid: 8026639
119. S. Goudenege *et al*., Myoblasts derived from normal hESCs and dystrophic hiPSCs efficiently fuse with existing muscle fibers following transplantation. *Mol. Ther.* **20**, 2153–2167 (2012). doi: 10.1038/mt.2012.188; pmid: 22990676
120. R. Darabi *et al*., Human ES- and iPS-derived myogenic progenitors restore DYSTROPHIN and improve contractility upon transplantation in dystrophic mice. *Cell Stem Cell* **10**, 610–619 (2012). doi: 10.1016/j.stem.2012.02.015; pmid: 22560081
121. A. Filareto *et al*., An ex vivo gene therapy approach to treat muscular dystrophy using inducible pluripotent stem cells. *Nat. Commun.* **4**, 1549 (2013). doi: 10.1038/ncomms2550; pmid: 23462992
122. F. S. Tedesco *et al*., Transplantation of genetically corrected human iPSC-derived progenitors in mice with limb-girdle muscular dystrophy. *Sci. Transl. Med.* **4**, 140ra89 (2012). doi: 10.1126/scitranslmed.3003541; pmid: 22745439
123. G. Jasmin, C. Tautu, M. Vanasse, P. Brochu, R. Simoneau, Impaired muscle differentiation in explant cultures of Duchenne muscular dystrophy. *Lab. Invest.* **50**, 197–207 (1984). pmid: 6694359
124. S. Liechti-Gallati, H. Moser, H. P. Siegrist, U. Wiesmann, N. N. Herschkowitz, Abnormal growth kinetics and 5′-nucleotidase activities in cultured skin fibroblasts from patients with Duchenne muscular dystrophy. *Pediatr. Res.* **15**, 1411–1414 (1981). doi: 10.1203/00006450-198111000-00004; pmid: 6272184
125. A. Sacco *et al*., Short telomeres and stem cell exhaustion model Duchenne muscular dystrophy in mdx/mTR mice. *Cell* **143**, 1059–1071 (2010). doi: 10.1016/j.cell.2010.11.039; pmid: 21145579
126. K. M. Kallestad *et al*., Sparing of extraocular muscle in aging and muscular dystrophies: A myogenic precursor cell hypothesis. *Exp. Cell Res.* **317**, 873–885 (2011). doi: 10.1016/j.yexcr.2011.01.018; pmid: 21277300
127. S. K. Sanganalmath, R. Bolli, Cell therapy for heart failure: A comprehensive overview of experimental and clinical studies, current challenges, and future directions. *Circ. Res.* **113**, 810–834 (2013). doi: 10.1161/CIRCRESAHA.113.300219; pmid: 23989721
128. B. Leobon *et al*., Myoblasts transplanted into rat infarcted myocardium are functionally isolated from their host. *Proc. Natl. Acad. Sci. U.S.A.* **100**, 7808–7811 (2003). doi: 10.1073/pnas.1232447100; pmid: 12805561
129. P. Menasché *et al*., The Myoblast Autologous Grafting in Ischemic Cardiomyopathy (MAGIC) trial: First randomized placebo-controlled study of myoblast transplantation. *Circulation* **117**, 1189–1200 (2008). doi: 10.1161/CIRCULATIONAHA.107.734103; pmid: 18285565
130. D. Orlic *et al*., Bone marrow cells regenerate infarcted myocardium. *Nature* **410**, 701–705 (2001). doi: 10.1038/35070587; pmid: 11287958
131. L. B. Balsam *et al*., Haematopoietic stem cells adopt mature haematopoietic fates in ischaemic myocardium. *Nature* **428**, 668–673 (2004). doi: 10.1038/nature02460 pmid: 15034594
132. C. E. Murry *et al*., Haematopoietic stem cells do not transdifferentiate into cardiac myocytes in myocardial infarcts. *Nature* **428**, 664–668 (2004). doi: 10.1038/nature02446; pmid: 15034593
133. S. A. Fisher *et al*., Stem cell therapy for chronic ischaemic heart disease and congestive heart failure. *Cochrane Database Syst. Rev.* **4**, CD007888 (2014). pmid: 24777540
134. P. K. Nguyen, F. Lan, Y. Wang, J. C. Wu, Imaging: Guiding the clinical translation of cardiac stem cell therapy. *Circ. Res.* **109**, 962–979 (2011). doi: 10.1161/CIRCRESAHA.111.242909; pmid: 21960727
135. O. Caspi *et al*., Transplantation of human embryonic stem cell-derived cardiomyocytes improves myocardial performance in infarcted rat hearts. *J. Am. Coll. Cardiol.* **50**, 1884–1893 (2007). doi: 10.1016/j.jacc.2007.07.054; pmid: 17980256
136. A. Moretti *et al*., Multipotent embryonic isl1+ progenitor cells lead to cardiac, smooth muscle, and endothelial cell diversification. *Cell* **127**, 1151–1165 (2006). doi: 10.1016/j.cell.2006.10.029; pmid: 17123592
137. L. Yang *et al*., Human cardiovascular progenitor cells develop from a KDR+ embryonic-stem-cell-derived population. *Nature* **453**, 524–528 (2008). doi: 10.1038/nature06894; pmid: 18432194
138. L. S. Ferreira *et al*., Vascular progenitor cells isolated from human embryonic stem cells give rise to endothelial and smooth muscle like cells and form vascular networks in vivo. *Circ. Res.* **101**, 286–294 (2007). doi: 10.1161/CIRCRESAHA.107.150201; pmid: 17569886
139. C. L. Mummery *et al*., Differentiation of human embryonic stem cells and induced pluripotent stem cells to cardiomyocytes: A methods overview. *Circ. Res.* **111**, 344–358 (2012). doi: 10.1161/CIRCRESAHA.110.227512; pmid: 22821908
140. N. C. Dubois *et al*., SIRPA is a specific cell-surface marker for isolating cardiomyocytes derived from human pluripotent stem cells. *Nat. Biotechnol.* **29**, 1011–1018 (2011). doi: 10.1038/nbt.2005; pmid: 22020386
141. S. Tohyama *et al*., Distinct metabolic flow enables large-scale purification of mouse and human pluripotent

stem cell-derived cardiomyocytes. *Cell Stem Cell* **12**, 127–137 (2013). doi: 10.1016/j.stem.2012.09.013; pmid: 23168164
142. J. Q. He, Y. Ma, Y. Lee, J. A. Thomson, T. J. Kamp, Human embryonic stem cells develop into multiple types of cardiac myocytes: Action potential characterization. *Circ. Res.* **93**, 32–39 (2003). doi: 10.1161/01.RES.0000080317.92718.99; pmid: 12791707
143. M. A. Laflamme *et al*., Cardiomyocytes derived from human embryonic stem cells in pro-survival factors enhance function of infarcted rat hearts. *Nat. Biotechnol.* **25**, 1015–1024 (2007). doi: 10.1038/nbt1327; pmid: 17721512
144. N. Christoforou *et al*., Implantation of mouse embryonic stem cell-derived cardiac progenitor cells preserves function of infarcted murine hearts. *PLOS ONE* **5**, e11536 (2010). doi: 10.1371/journal.pone.0011536; pmid: 20634944
145. Y. Shiba *et al*., Human ES-cell-derived cardiomyocytes electrically couple and suppress arrhythmias in injured hearts. *Nature* **489**, 322–325 (2012). doi: 10.1038/nature11317; pmid: 22864415
146. M. Kawamura *et al*., Feasibility, safety, and therapeutic efficacy of human induced pluripotent stem cell-derived cardiomyocyte sheets in a porcine ischemic cardiomyopathy model. *Circulation* **126** (suppl. 1), S29–S37 (2012). doi: 10.1161/CIRCULATIONAHA.111.084343; pmid: 22965990
147. Q. Xiong *et al*., Functional consequences of human induced pluripotent stem cell therapy: Myocardial ATP turnover rate in the in vivo swine heart with postinfarction remodeling. *Circulation* **127**, 997–1008 (2013). doi: 10.1161/CIRCULATIONAHA.112.000641; pmid: 23371930
148. J. J. H. Chong *et al*., Human embryonic-stem-cell-derived cardiomyocytes regenerate non-human primate hearts. *Nature* **510**, 273–277 (2014). doi: 10.1038/nature13233; pmid: 24776797
149. G. Blin *et al*., A purified population of multipotent cardiovascular progenitors derived from primate pluripotent stem cells engrafts in postmyocardial infarcted nonhuman primates. *J. Clin. Invest.* **120**, 1125–1139 (2010). doi: 10.1172/JCI40120; pmid: 20335662
150. Z. Alipio *et al*., Reversal of hyperglycemia in diabetic mouse models using induced-pluripotent stem (iPS)-derived pancreatic beta-like cells. *Proc. Natl. Acad. Sci. U.S.A.* **107**, 13426–13431 (2010). doi: 10.1073/pnas.1007884107; pmid: 20616080

ACKNOWLEDGMENTS

We thank E. Tafaleng, N. Giannoukakis, and J. H. Cummins for providing figures and for text editing. This work was supported in part by NIH R01DK48794, P01DK096990, and R01DK099320 (I.J.F.); National Institute of Neurological Disorders and Stroke, National Institute of Mental Health, the Mathers Charitable Foundation, the National Multiple Sclerosis Society, the Adelson Medical Research Foundation, Child Health and Development Institute, and the New York Stem Cell Research Program (S.A.G.); NIH 1P01AG043376 (J.H.); U01HL099773 (T.J.K.); and DOD W81XWH-10-1-1055 (M.T.). I.J.F. is a member of the Scientific Advisory Board of Regenerative Medicine Solutions, Inc.; G.Q.D. is a member of the Senior Advisory Board of MPM Capital, Inc.; S.A.G. is a consultant for Biogen Idec; T.J.K. is a founding shareholder in Cellular Dynamics International; and J.H. is a consultant for Cook Myosite. S.A.G. is an inventor on patents owned by the University of Rochester and Cornell University concerning the use of tissue- and iPSC-derived glial progenitor cells.

10.1126/science.1247391